

PL-TR-96-2038  
Special Reports, No. 277

**PROCEEDINGS OF AIR FORCE OFFICE OF  
SCIENTIFIC RESEARCH AND  
PHILLIPS LABORATORY WORKSHOP  
ON SPRITES AND BLUE JETS**

**Editor:  
L. Jeong**

**30 January 1996**


**APPROVED FOR PUBLIC RELEASE; DISTRIBUTION UNLIMITED**

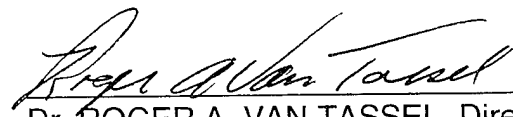


**PHILLIPS LABORATORY  
Directorate of Geophysics  
AIR FORCE MATERIEL COMMAND  
HANSCOM AFB, MA 01731-3010**

19960220 077

"This technical report has been reviewed and is approved for publication"

  
Dr. WILLIAM A.M. BLUMBERG, Chief  
Simulation Branch  
Optical Environment Division

  
Dr. ROGER A. VAN TASSEL, Director  
Optical Environment Division

This report has been reviewed by the ESC Public Affairs Office (PA) and is releasable to the National Technical Information Service (NTIS).

Qualified requesters may obtain additional copies from the Defense Technical Information Center (DTIC). All others should apply to the National Technical Information Service (NTIS).

If your address has changed, if you wish to be removed from the mailing list, or if the addressee is no longer employed by your organization, please notify PL/IM, 29 Randolph Road, Hanscom AFB, MA 01731-3010. This will assist us in maintaining a current mailing list.

Do not return copies of this report unless contractual obligations or notices on a specific document require that it be returned.

| REPORT DOCUMENTATION PAGE  |  |  | Form Approved<br>OMB No. 0704-0188 |  |
|--|--|--|------------------------------------|--|
| Public reporting burden for this collection of information is estimated to average 1 hour per response, including the time for reviewing instructions, searching existing data sources, gathering and maintaining the data needed, and completing and reviewing the collection of information. Send comments regarding this burden estimate or any other aspect of this collection of information, including suggestions for reducing this burden, to Washington Headquarters Services, Directorate for Information Operations and Reports, 1215 Jefferson Davis Highway, Suite 1204, Arlington, VA 22202-4302, and to the Office of Management and Budget, Paperwork Reduction Project (0704-0188), Washington, DC 20503. |  |  |                                    |  |
| 1. AGENCY USE ONLY (Leave blank)   | 2. REPORT DATE<br>30 January 1996                        | 3. REPORT TYPE AND DATES COVERED<br>Scientific Interim                   |                                    |  |
| 4. TITLE AND SUBTITLE<br>Proceedings of Air Force Office of Scientific Research and Phillips Laboratory Workshop on Sprites and Blue Jets  |  | 5. FUNDING NUMBERS<br>PR 3054<br>TA GD<br>WU 01                          |                                    |  |
| 6. AUTHOR(S)<br>Editor, L.S. Jeong   |  |  |                                    |  |
| 7. PERFORMING ORGANIZATION NAME(S) AND ADDRESS(ES)<br>Phillips Laboratory/GPOS<br>Geophysics Directorate<br>29 Randolph Road<br>Hanscom AFB, MA 01731-3010   |  | 8. PERFORMING ORGANIZATION REPORT NUMBER<br>PL-TR-96-2038<br>SR, No. 277 |                                    |  |
| 9. SPONSORING/MONITORING AGENCY NAME(S) AND ADDRESS(ES)  |  | 10. SPONSORING/MONITORING AGENCY REPORT NUMBER                           |                                    |  |
| 11. SUPPLEMENTARY NOTES  |  |  |                                    |  |
| 12a. DISTRIBUTION / AVAILABILITY STATEMENT<br>Approved for public release; distribution unlimited  |  | 12b. DISTRIBUTION CODE   |                                    |  |
| 13. ABSTRACT (Maximum 200 words)<br>This report contains the viewgraphs presented at the AFOSR-PL Workshop on Sprites and Blue Jets held at the Phillips Laboratory, Geophysics Directorate, Hanscom AFB, MA, 18-19 October 1995.  |  |  |                                    |  |
| 14. SUBJECT TERMS<br>Sprites; Upward Lightning   |  |  | 15. NUMBER OF PAGES<br>412         |  |
|  |  |  | 16. PRICE CODE                     |  |
| 17. SECURITY CLASSIFICATION OF REPORT<br>UNCLASSIFIED  | 18. SECURITY CLASSIFICATION OF THIS PAGE<br>UNCLASSIFIED | 19. SECURITY CLASSIFICATION OF ABSTRACT<br>UNCLASSIFIED                  | 20. LIMITATION OF ABSTRACT<br>SAR  |  |

**Air Force Office of Scientific Research  
and  
Phillips Laboratory  
Workshop on Sprites and Blue Jets  
18-19 October 1995  
Hanscom Air Force Base, MA**

**Agenda**

Wednesday, 18 October

- |                     |   |
|---------------------|---|
| 8:30 AM - 8:40 AM   | Welcome<br>Dr. Herb Carlson, Deputy Chief Scientist<br>Geophysics Directorate, Phillips Laboratory  |
| 8:40 AM - 8:50 AM   | Opening Remarks<br>Major J. Kroll, AFOSR<br>L. Jeong, Phillips Laboratory   |
| 8:50 AM - 9:10 AM   | The Colorado SPRITES '95 Campaign: Initial Results<br>W.A. Lyons, ASTER Division, Mission Research Corp.  |
| 9:10 AM - 9:30 AM   | Red Sprite and Blue Jet Campaigns of the University of Alaska<br>D. Sentman and E. Westcott, University of Alaska   |
| 9:30 AM - 9:50 AM   | Spectral and Spatial Properties of Sprites<br>S.B. Mende, Lockheed Martin Palo Alto Research Laboratory   |
| 9:50 AM - 10:05 AM  | Evidence for Ionization in Sprites - $N_2^+$ 427.8 First Negative Emission<br>Measured in SPRITES '95 Campaign<br>R.A. Armstrong and J. Shorter, Mission Research Corp.<br>W.A. Lyons, ASTER Division, Mission Research Corp.                       |
| 10:05 AM - 10:20 AM | Fast Imaging of High Altitude Atmospheric Flashes (Sprites)<br>J.D. Molitoris, Lawrence Livermore National Laboratory<br>J.F. Arens, University of CA Berkeley<br>C. Price, Tel Aviv University<br>W. Lyons, ASTER Division, Mission Research Corp. |
| 10:20 AM - 10:40 AM | Break   |
| 10:40 AM - 10:50 AM | Short Wavelength Infrared Images of Sprites<br>P.A. Bernhardt and J.A. Antoniadis, Naval Research Laboratory  |



- 10:50 AM - 11:05 AM Topside Views of Lightning and Sprites  
W.L. Boeck, Niagara University  
O.H. Vaughan, Jr. and R. Blakeslee, NASA Marshall Space Flight Center
- 11:05 AM - 11:20 AM Observations of Electric Field and X-Rays Above Thunderstorms:  
Relevant to Optical Sprites?  
K.B. Eack, W.H. Beasley, and M. Stolzenburg, University of Oklahoma  
W.D. Rust, National Severe Storms Laboratory  
T.C. Marshall, University of Mississippi
- 11:20 AM - 11:30 AM US/Russian Joint Lightning Experiments  
S. Voss and E. Symbalisty, Los Alamos National Laboratory
- 11:30 AM - 11:40 AM Measurements of Lightning-Generated Electric Fields in the Nighttime D-Region  
C.L. Siefring, Naval Research Laboratory
- 11:40 AM - 12:00 AM Space-Borne Observations of Intense Gamma-Ray Flashes Above Thunderstorms  
G.J. Fishman, NASA Space Flight Center
- 12:00 AM - 1:00 PM Lunch
- 1:00 PM - 1:15 PM Electromagnetic Fields of Red Sprites  
L.Hale and L. Marshall, Penn State University
- 1:15 PM - 1:35 PM Mesoscale Origin of Sprites and Schumann Resonance Methods for their Location on a Global Scale  
E. Williams, Massachusetts Institute of Technology
- 1:35 PM - 1:55 PM Sprites, Blue Jets, and High Altitude Optical Flashes Produced by Quasi-Electrostatic Thundercloud Fields and Lightning EMP  
U.S. Inan, Stanford University
- 1:55 PM - 2:05 PM VLF Observations of the Ionospheric Effects of Lightning in East Coast Summer Storms  
J.V. Rodriguez and K.M. Groves, Phillips Laboratory
- 2:05 PM - 2:25 PM Measurements of Sprites and Blue Jets with High-Frequency Diagnostics  
F. T. Djuth, Geospace Research Inc.
- 2:25 PM - 2:40 PM RF Measurements of Lightning-Induced Ionospheric Effects  
K.M. Groves, J.V. Rodrriguez, P.J. Erickson, J.M. Quinn, T. Arce, and M. Cox, Phillips Laboratory
- 2:40 PM - 3:00 PM Break

- 3:00 PM - 3:15 PM Pulsed Radar Investigations of Red Sprites  
R.T.Tsunoda, SRI International
- 3:15 PM - 3:35 PM On Runaway Breakdown and Upward Propagating Discharges  
R. Roussel-Dupre and Y. Taranenko, Los Alamos National Laboratory  
A.V. Gurevich, Lebedev Institute of Physics
- 3:35 PM - 3:50 PM Numerical Simulations of Lower Ionospheric Breakdown Caused by Lightning-Generated Electric Fields  
H.L. Rowland, R.F. Fernsler, C.L. Sieftring, and P.A. Bernhardt, Naval Research Laboratory
- 3:50 PM - 4:00 PM Runaway Breakdown in the Presence of a Magnetic Field  
G.M. Milikh, K. Papadopoulos, and J. Valdivia, University of Maryland  
A.V. Gurevich, Lebedev Institute of Physics
- 4:00 PM - 4:10 PM On the Fine Structure of the Red Sprites  
K. Papadopoulos, G.M. Milikh, and J. Valdivia, University of Maryland
- 4:10 PM - 4:30 PM Nonequilibrium Infrared Radiative Modeling - Application to Sprites  
R.H. Picard, J.R. Winick, Phillips Laboratory  
P.P. Wintersteiner, ARCON Corp.  
R.A. Armstrong and J. Shorter, Mission Research Corp.

Thursday, 19 October

- 8:30 AM - 9:00 AM Overview of Air Force Program Plans  
Major J. Kroll, AFOSR  
L. Jeong, Phillips Laboratory
- 9:00 AM - 9:30 AM Overview of NASA Sprite Activities  
R. Howard, NASA Headquarters
- 9:30 AM - 10:00 AM Overview of Air Force ARES Aircraft Program  
P. Kupferman, Aerospace Corp.
- 10:00 AM - 12:00 AM Summary and Discussion of Major Research Issues
- 12:00 AM - 1:00 PM Lunch

|                   |   |
|-------------------|---|
| 1:00 PM - 5:00 PM | Discussion of Major Research Issues (continued)<br>Discussion of Experiments for SPRITES '96 Campaign |
| 5:00 PM           | End of Meeting  |

**PROCEEDINGS OF  
AIR FORCE OFFICE OF SCIENTIFIC RESEARCH  
AND  
PHILLIPS LABORATORY  
WORKSHOP ON SPRITES AND BLUE JETS  
18-19 OCTOBER 1995  
HANSCOM AIR FORCE BASE, MA**

# THE SPRITES'95 CAMPAIGN

## Our Guiding Principles.....

Cooperation

Coordination

Correlation

ASTeR, Inc.

Yucca Ridge Field Station

46050 Weld County Road 13

Ft. Collins, CO 80524

(voice) 970-568-7664

(fax) 970-482-8627

(e-mail) [lyonsccm@csn.org](mailto:lyonsccm@csn.org)

# SPRITES'95

§ § § § § §

A Large Scale  
Multi-Agency, Multi-Disciplinary  
Research Effort Seeded by the  
NASA KSC SBIR Phase II Project

= = = = =

18 Teams of Investigators  
(US, Japan, New Zealand)

46 Scientists and Support Staff

45 Day Intensive Field Program [CO]

Optical

[visible, infrared, ultraviolet, all sky OH and narrow band]

Spectra (Narrow and Broad-Band)

In-situ Electric Field Measurements

ELF, VLF

VHF

Radar

Acoustic (Infrasound)

Satellite

## ASTER, Inc. SPRITE-RELATED PUBLICATIONS/PRESENTATIONS

### Publications

- Lyons, W.A., 1996: The SPRITES'95 field campaign: Initial results - characteristics of sprites and the mesoscale convective systems that produce them, Preprints, 18th Conf. on Severe Local Storms, AMS, San Francisco, 5 pp.
- Lyons, W.A. and T.E. Nelson, 1996: Processing, integrating and displaying disparate data sources from the SPRITES'95 field program. Preprints, 12th IIIPS for Meteor., Oceanog. and Hydrol., AMS, Atlanta, 6 pp.
- Fukunishi, H., Y. Takahashi, M. Kubota, K. Sakanoi, U.S. Inan and W.A. Lyons, 1996: Elves: Lightning-induced transient luminous events in the lower ionosphere. Nature (in press).
- Dowden, R.L., J.B. Brundell and W.A. Lyons, 1996: Are VLF RORDs and optical sprites produced by the same cloud-to-ionosphere discharge? J. Geophys. Res., (in preparation).
- Mende, S.B., R.L. Rairden, G.R. Swenson and W.A. Lyons, 1995: Sprite spectra: N<sub>2</sub> First Positive Band Identification. Geophys. Res. Lett., 22, 2633-2636.
- Winckler, J.R., W.A. Lyons, T. E. Nelson and R.J. Nemzek, 1995: New high-resolution ground based studies of sprites. J. Geophysical Res. (submitted).
- Inan, U.S., T.F. Bell, V. Pasko, D. Sentman, E. Wescott and W. Lyons, 1995: VLF signatures of red sprites. Geophys. Res. Lett. (submitted).
- Boccippio, D.J., E.R. Williams, W.A. Lyons, I. Baker and R. Boldi, 1995: Sprites, ELF transients and positive ground strokes. Science, 269, 1088-1091.
- Lyons, W.A., 1995: The relationship of large luminous stratospheric events to the anvil structure and cloud-to-ground discharges of their parent mesoscale convective system. Preprints, Conf. on Cloud Physics, AMS, Dallas, 541-546.
- Lyons, W.A., 1994: Characteristics of luminous structures in the stratosphere above thunderstorms as imaged by low-light video. Geophysical Research Letters, 21, 875-878.
- Lyons, W.A. and E.R. Williams, 1994: Some characteristics of cloud-to-stratosphere "lightning" and consideration for its detection. Preprints, Symposium on the Global Electrical Circuit, Global Change and the Meteorological Applications of Lightning Information, AMS, Nashville, 8 pp.
- Lyons, W.A., 1994: Low-light video observations of frequent luminous structures in the stratosphere above thunderstorms. Mon. Wea. Rev., 122, 1940-1946.
- Lyons, W.A. and E.R. Williams, 1993: Preliminary investigations of the phenomenology of cloud-to-stratosphere lightning discharges. Preprints, Conference on Atmospheric Electricity, American Meteorological Society, St. Louis, 8 pp.

## Presentations

- Lyons, W.A., 1996: Coordinated RF and optical measurements of sprites, jets and elves in the Colorado SPRITES'95 campaign. National Radio Science Meeting, Boulder, CO. (abstract only).
- Armstrong, R.A., J. Shorter, W.A. Lyons, L. Jeong and W.A.M. Blumberg, 1995: Evidence for ionization in sprites -  $N_2^+$  478.8 first negative emission measured in SPRITES'95 campaign. AGU winter meeting, San Francisco, EOS (abstract only).
- Lyons, W.A. and T.E. Nelson, 1995: The Colorado SPRITES'95 Campaign: Initial results. AGU winter meeting, San Francisco, EOS (abstract only).
- Rairden, R.L., S.B. Mende G.R. Swenson and W.A. Lyons, 1995: Ground based observations of airglow above thunderstorms. AGU winter meeting, San Francisco, EOS (abstract only).
- Takahashi, Y., M. Kubota, K. Sakanoi, H. Fukunishi, U.S. Inan, and W.A. Lyons, 1995: Spatial and temporal relationships between lower ionospheric flashes and sprites. AGU winter meeting, San Francisco, EOS (abstract only).
- Dowden, R.L., J. Brundell, W.A. Lyons and T. Nelson, 1995: RORDs and sprites. AGU winter meeting, San Francisco, EOS (abstract only).
- Williams, E., D. Boccippio, C. Wong, W. Lyons, M. Ishii and W. Koshak, 1995: The physical origin of Schumann resonance excitation. AGU winter meeting, San Francisco, EOS (abstract only).
- Inan, U.S., S.C. Reising, V.P. Pasko and W.A. Lyons, 1995: VLF signatures of ionospheric disturbances associated with sprites. AGU winter meeting, San Francisco, EOS (abstract only).
- Lyons, W.A., I.T. Baker, T.E. Nelson, R. Armstrong, J. Shorter, J. R. Winckler, R.J. Nemzek, P. R. Malcolm and E.R. Williams, 1995: Sprite Observations above the U.S. High Plains. Preprints, IUGG, Boulder, CO (poster, abstract only).
- Lyons, W.A., 1995: Observations of sprites above intense thunderstorms during the 1994 Colorado Sprite Campaign. URSI, National Radio Science Meeting. (abstract only)
- Lyons, W.A., I.T. Baker, T.E. Nelson, J.R. Winckler, R.J. Nemzek, P.R. Malcolm, E.R. Williams and D. Boccippio, 1994: The 1994 Colorado SPRITE Campaign (abstract), EOS, 75, vol. 44, p. 108.
- Lyons, W.A., I.T. Baker, T.E. Nelson, J.R. Winckler, R.J. Nemzek, E.R. Williams, D. Boccippio and P.R. Malcolm, 1994: New observations of luminous stratospheric and ionospheric events above intense thunderstorms (abstract). EOS, 75, vol. 44, p. 108.
- Winckler, J.R., W.A. Lyons, T. Nelson and R.J. Nemzek, 1994: New high-resolution ground-based studies of cloud-ionosphere discharges (abstract). EOS, 75, vol. 44, p. 107.
- Boccippio, D., E. Williams, W. A. Lyons, I. T. Baker and R. Boldi, 1994: Sprites, Q-bursts and positive ground flashes (abstract). EOS, 75, vol. 44, p. 108.



# 1995 COLORADO SPRITE CAMPAIGN

## DATES (UTC) WITH IMAGED SPRITES

§ § § § §

19 June

20 June

21 June

23 June

25 June

27 June

04 July

07 July

08 July

12 July

13 July

15 July

16 July

20 July

21 July

22 July

23 July

24 July

25 July

26 July

27 July

31 July

3 August

4 August

6 August

## THE YUCCA RIDGE FIELD STATION

- 24 hour operation; 80 acres for deployment
- 1000 km radius of operations for optical (areal coverage 400,000 km<sup>2</sup>)
- 3 year sprite archive
- available now
- culturally quiet for RF
- can "guarantee" sprites 25-50 nights per warm season (ideal storms and viewing conditions)
- have meteorological data acquisition infrastructure in place
- convenient to other related facilities
- low overhead

FROM THE YUCCA RIDGE FIELD STATION...

## SOME INITIAL ACCOMPLISHMENTS

NAS10-12113 and Cooperating Groups

- Confirmed high frequency of sprites above high plains MCSs
- Relationship of sprites to large positive CGs
- Relationships between Sprites, +CGs and Q-bursts
- Multi-channel high speed photometry identified lower ionospheric flash as separate entity (ELVES)
- Stereo imaging confirms sprites/+CG proximity
- More evidence for "blue" jets
- Developed sprite forecasting tools for mesoscale convective systems
- Coordinated optical and RF measurements of specific sprite events
- Confirmed presence of "VLF sprites"
- Multiple ELF Q-burst measurements, confirmed relationship w/ sprites
- Obtained numerous spectra
- Evidence of significant ionization in sprites and or elves
- Initial calculations of impact upon upper atmospheric chemistry
- High speed infrared optical and infrared measurements (IROCS)
- Active probing of sprites using radar
- Vectored balloon-borne electric-field measurements above Kansas
- Imaged gravity waves emanating from sprite producing storm system and evidence of other luminous phenomena

# EMERGING SCIENTIFIC QUESTIONS

- How are sprites, elves and jets different from each other?
- What is the entire spectrum of each phenomena [UV-visible-IR] ?
- What other phenomena are present above thunderstorms?
- What don't large negative CG apparently produce sprites?
- Why do only some large positive CGs produce sprites and elves?
- What actually triggers a sprite, jet or elve?
- What is the cause of the fine structure/tendrils in sprites?
- So sprites illuminate pre-existing atmospheric structure?
- What role, if any, do storm-generated gravity waves play in sprite structure?
- What is the direction of propagation for sprites and elves?
- Why do some mature storms wait several hours before generating sprites?
- Do sprites, jet and elves also occur during the day?
- Are sprites induced by large "spider" lightning discharges?
- Relationship to x-rays, gamma rays and TIPPS/SIPPS?
- What is the structure of the ENTIRE lightning discharge producing sprites?
- Can sprites generate acoustic waves?
- What is the electric field above the parent thunderstorms?
- Can we use ELF/VLF measurements for global detection and location?
- What are their roles in the global circuit?
- Relationship to whistlers/trimpis ?
- What is the global temporal and spatial climatology of sprites, jets and elves?
- What are the atmospheric chemistry impacts of sprites, elves and jets?
- Do they pose a hazard to aerospace navigation between 20 -110 km altitude?

# CREATURES IN THE MESOSPHERIC ZOO....

SPRITES

BLUE JETS

ELVES

AIRGLOW WAVES

GNOMES

# SPRITES

Stratospheric/ mesospheric

Perturbations

Resulting from

Intense

Thunderstorm

Electrification

# ELVES

Emissions of

Light and

VLF perturbations from

EMP

Events

(Singular: ELVE ?)

# GNOMES

Goofy

Nocturnal

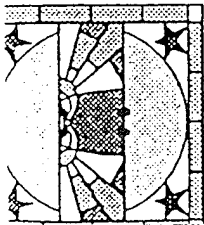
Optical

Mesospheric

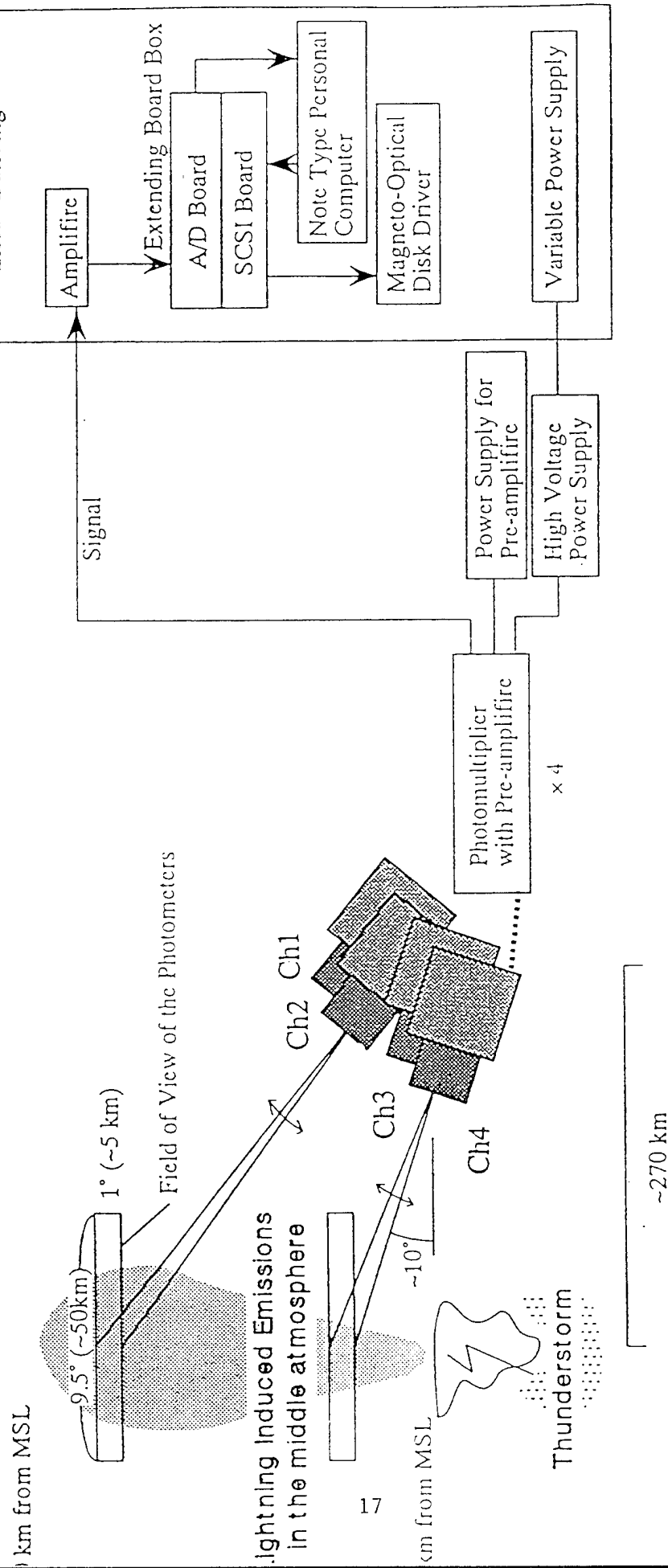
EmissionS

This is a “holding category” for the various other phenomena which are yet to be identified and named. It is not proposed to be used in formal publications.





# Tohoku University Lightning Photometer



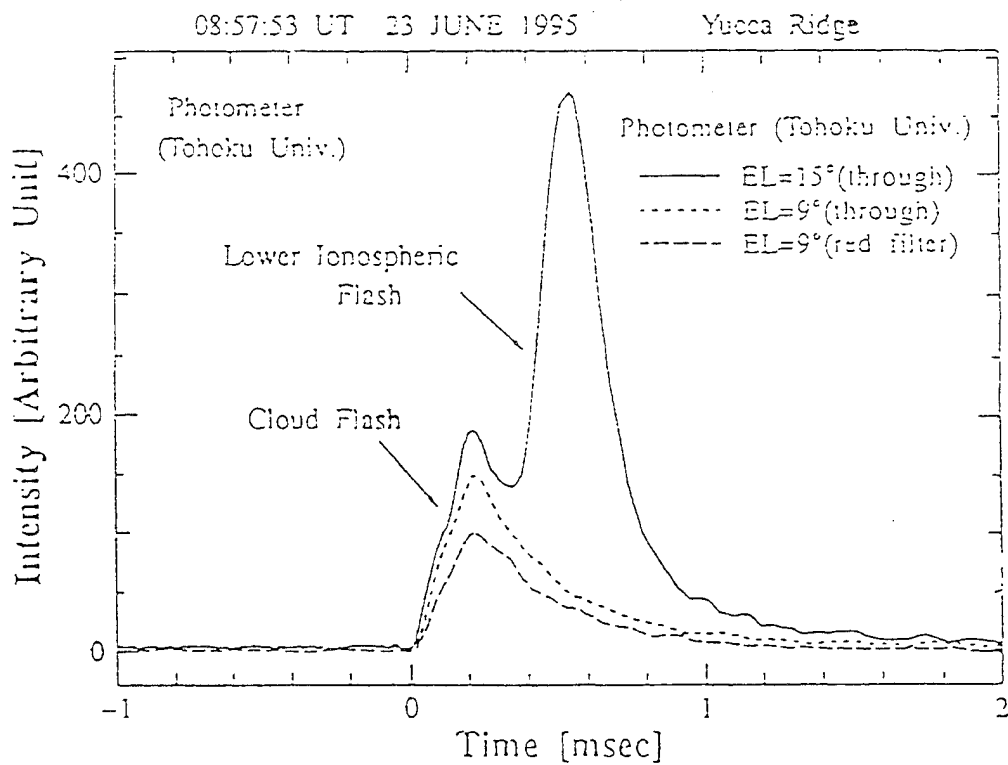
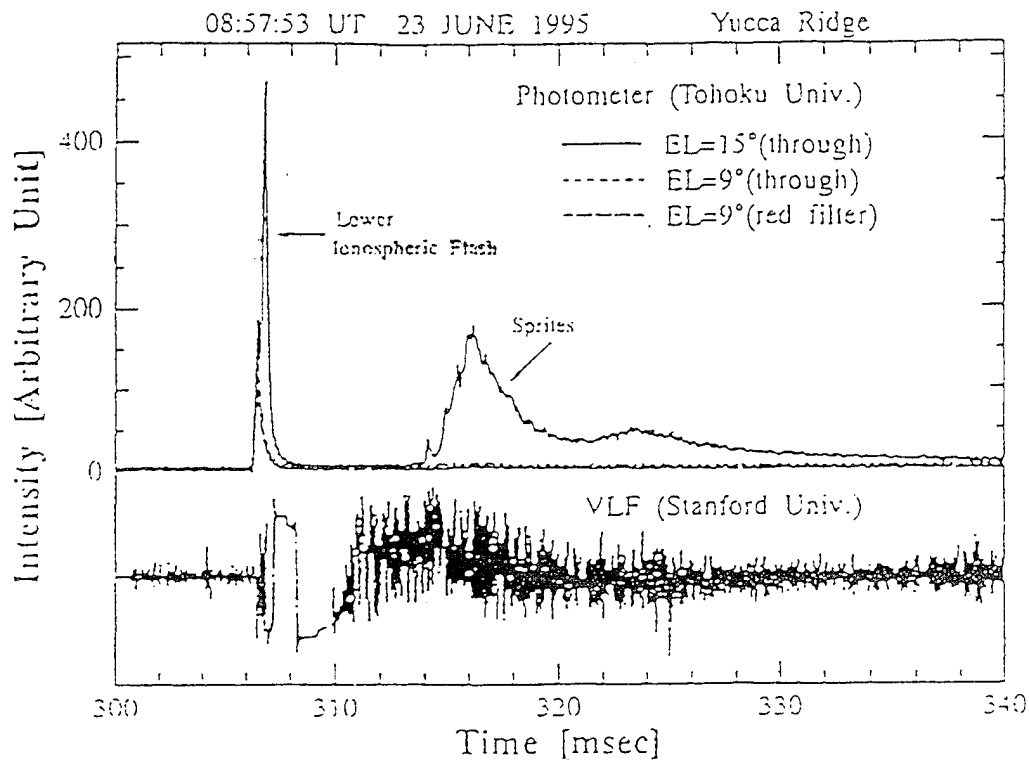


Fig. 1

Aster, Inc.

APPARENT LOWER IONOSPHERIC FLASH ASSOCIATED WITH A 213 KILOAMP POSITIVE CG IN NORTHEASTERN NEW MEXICO. NO SPRITE WAS IMAGED WITH THIS EVENT. 25 JUNE 1995.

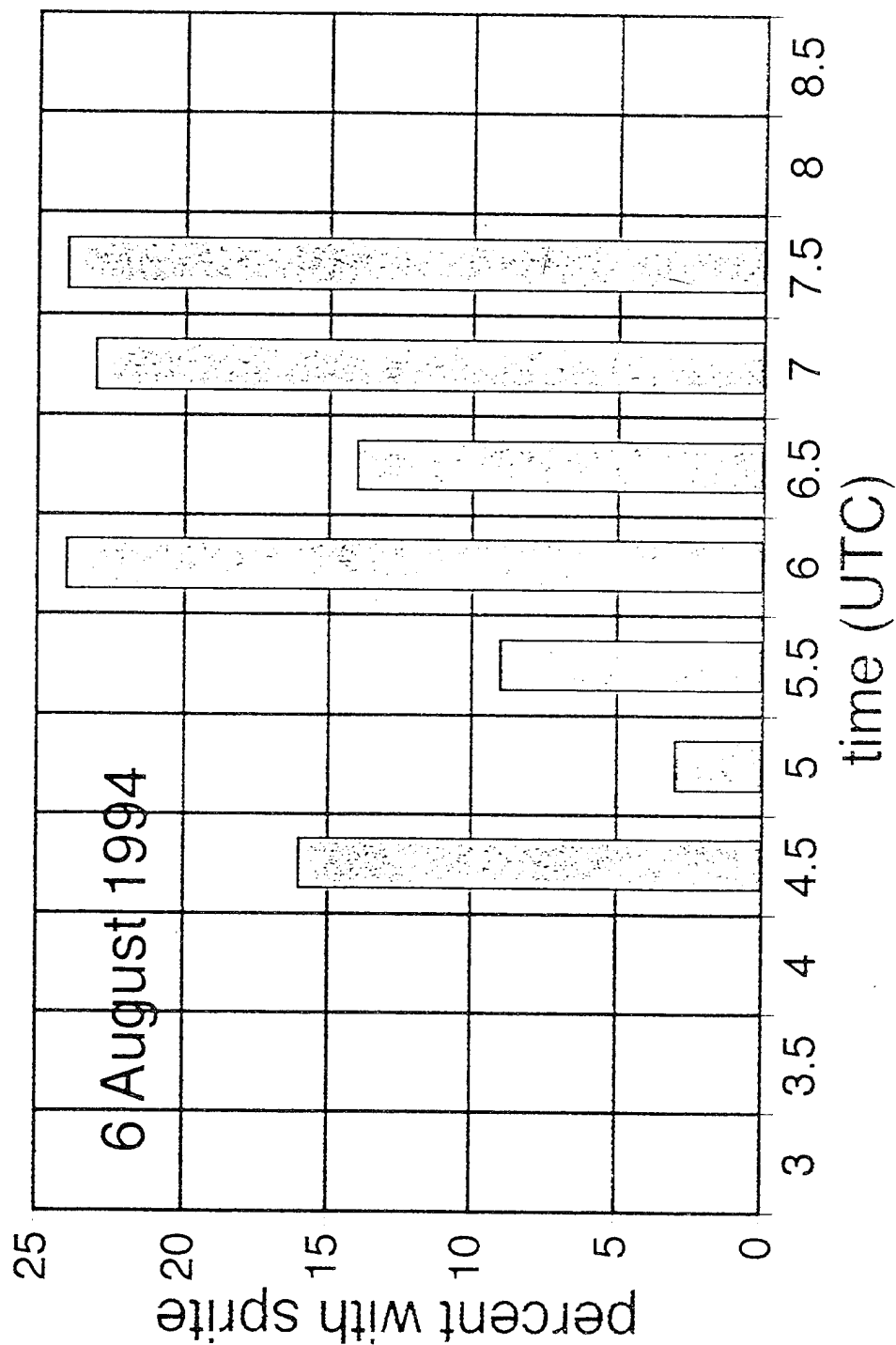


# 24 July 1995

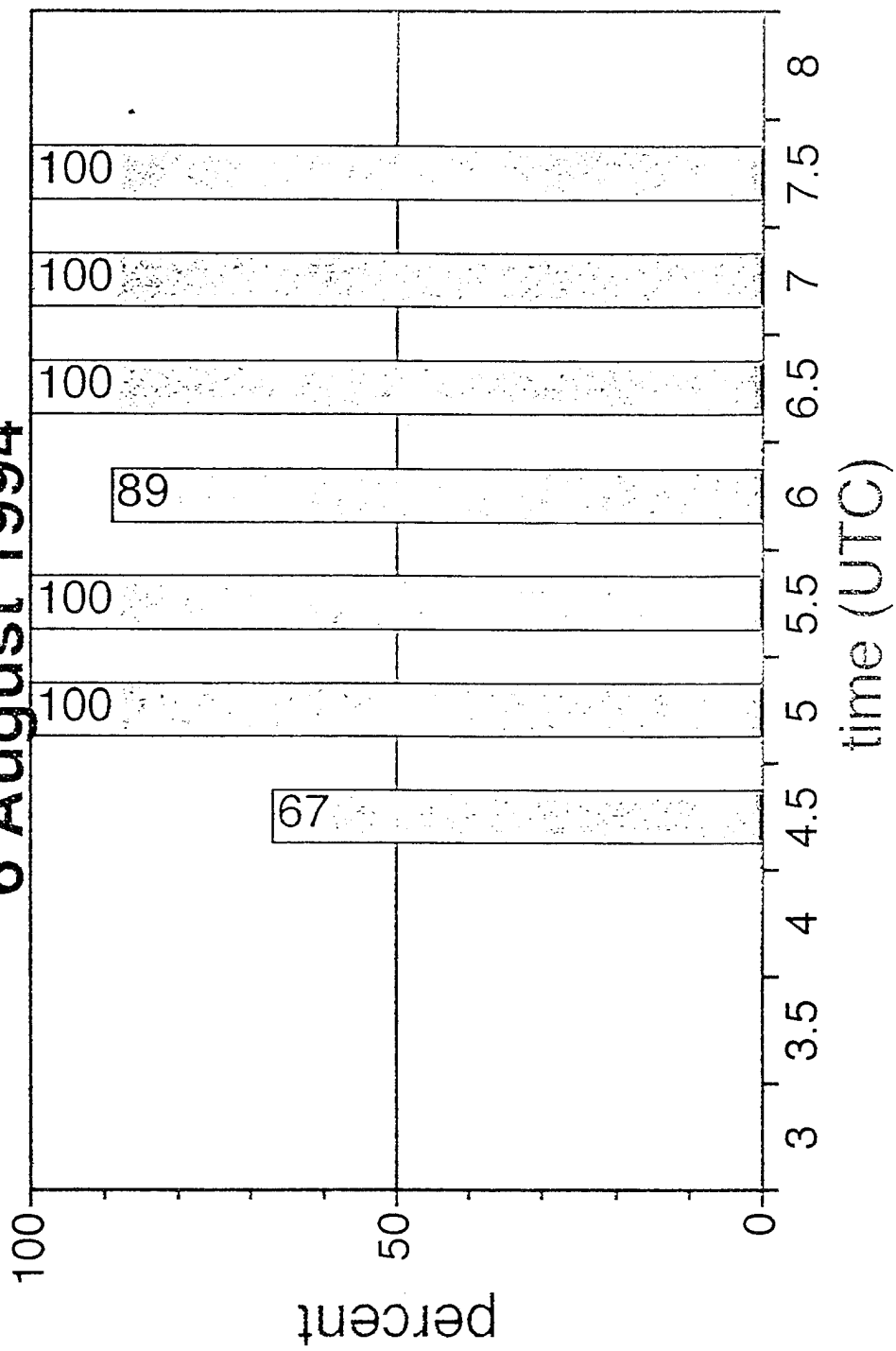
Sprites and elves both result from large positive CG events - but elves seem to be associated with the largest of the +CG flashes.

| <u>Phenomena</u> | <u>Number</u> | <u>Avg Peak Current</u> | <u>Largest</u> |
|------------------|---------------|-------------------------|----------------|
| SPRITES          | 68            | 58 kamp                 | 113 kamp       |
| ELVES            | 14            | 104 kamp                | 200 kamp       |

# % positive CGs with sprites

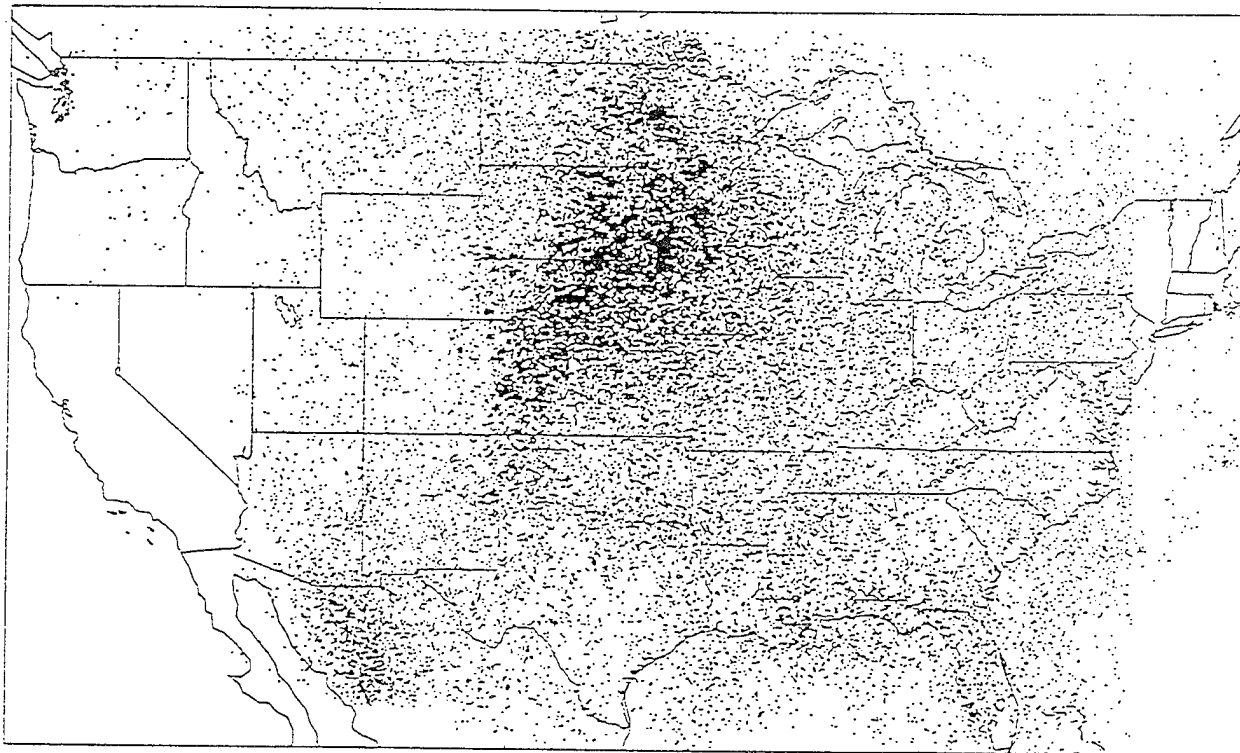


# % of sprites with positive flashes 6 August 1994



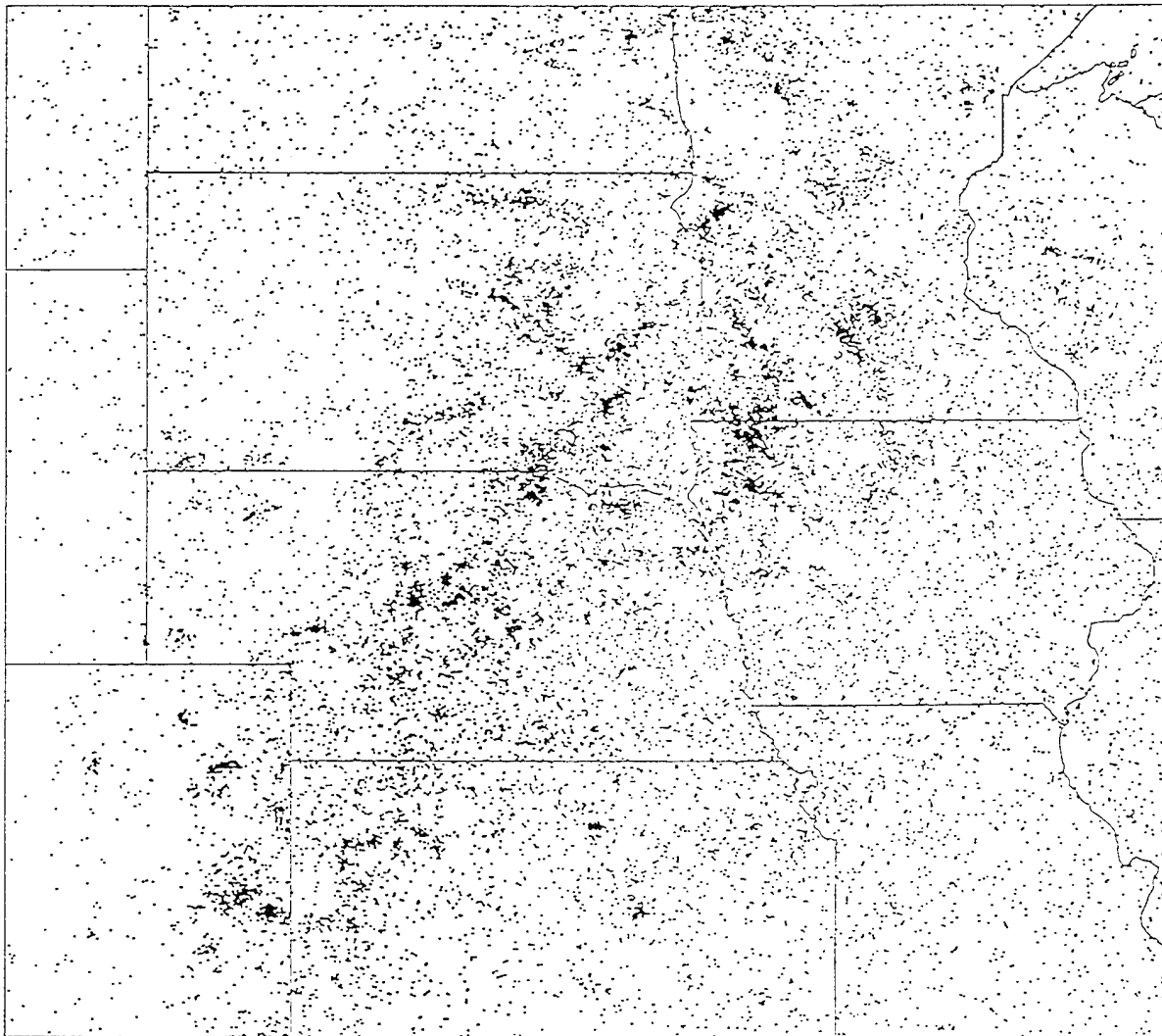
# CLIMATOLOGY OF LARGE POSTIVES

JUL-AUG 93, JUN-SEP 94



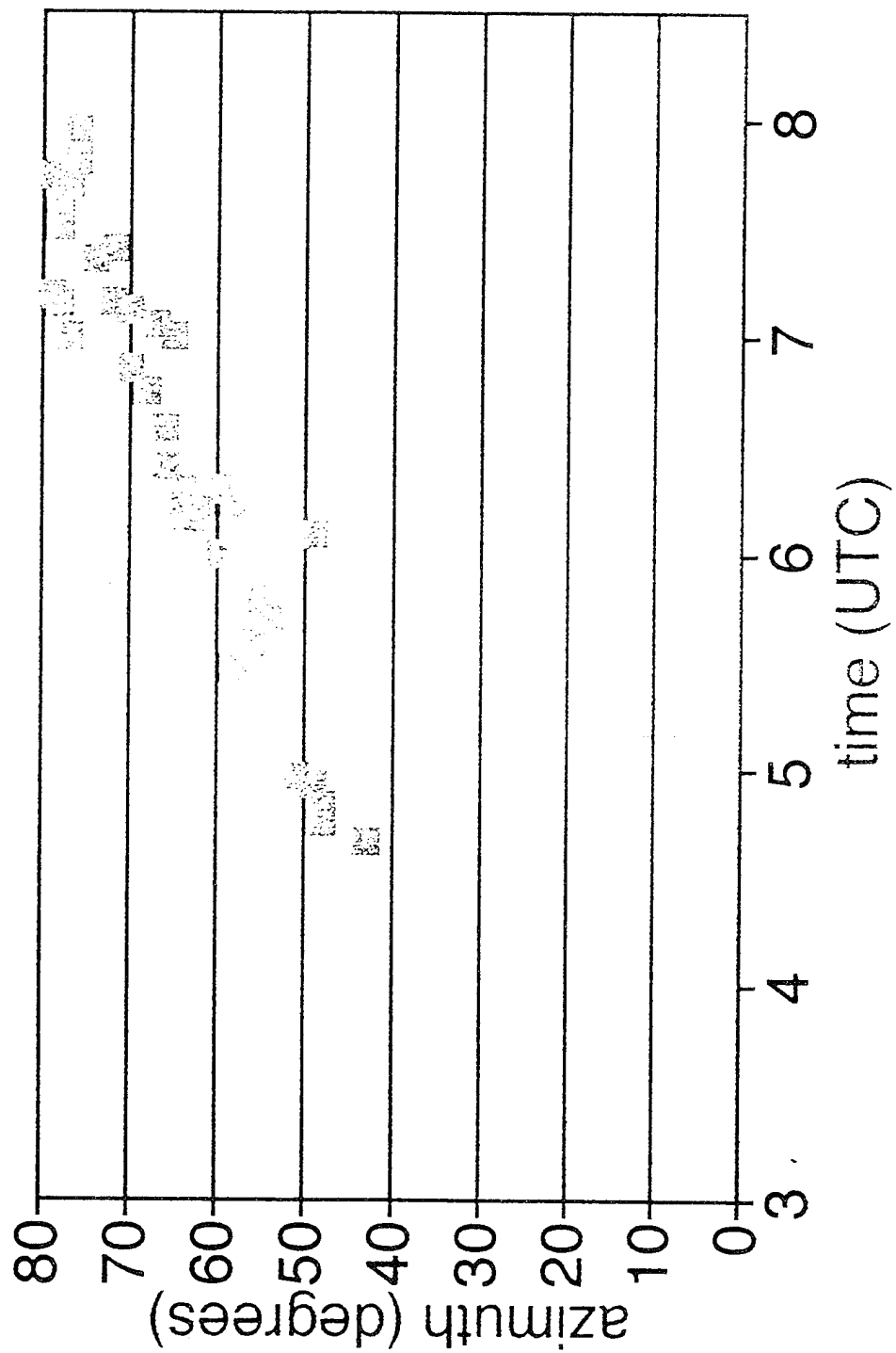


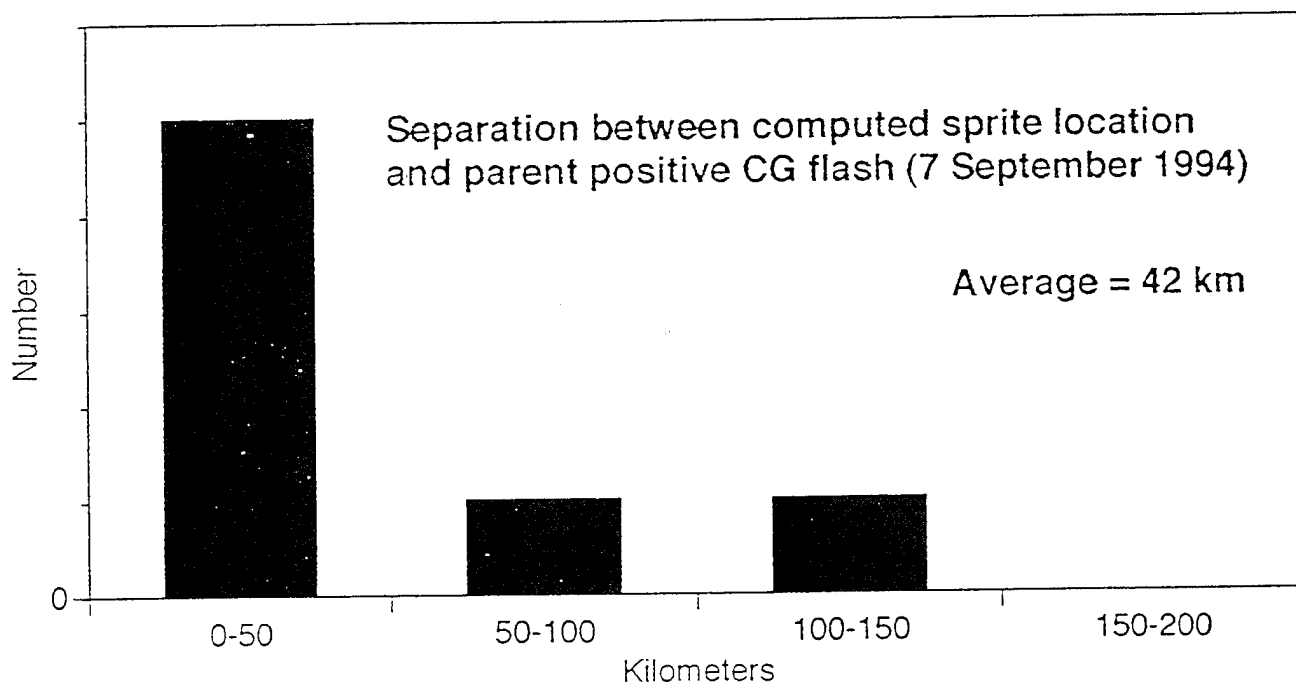
## CLIMATOLOGY OF LARGE POSTIVES

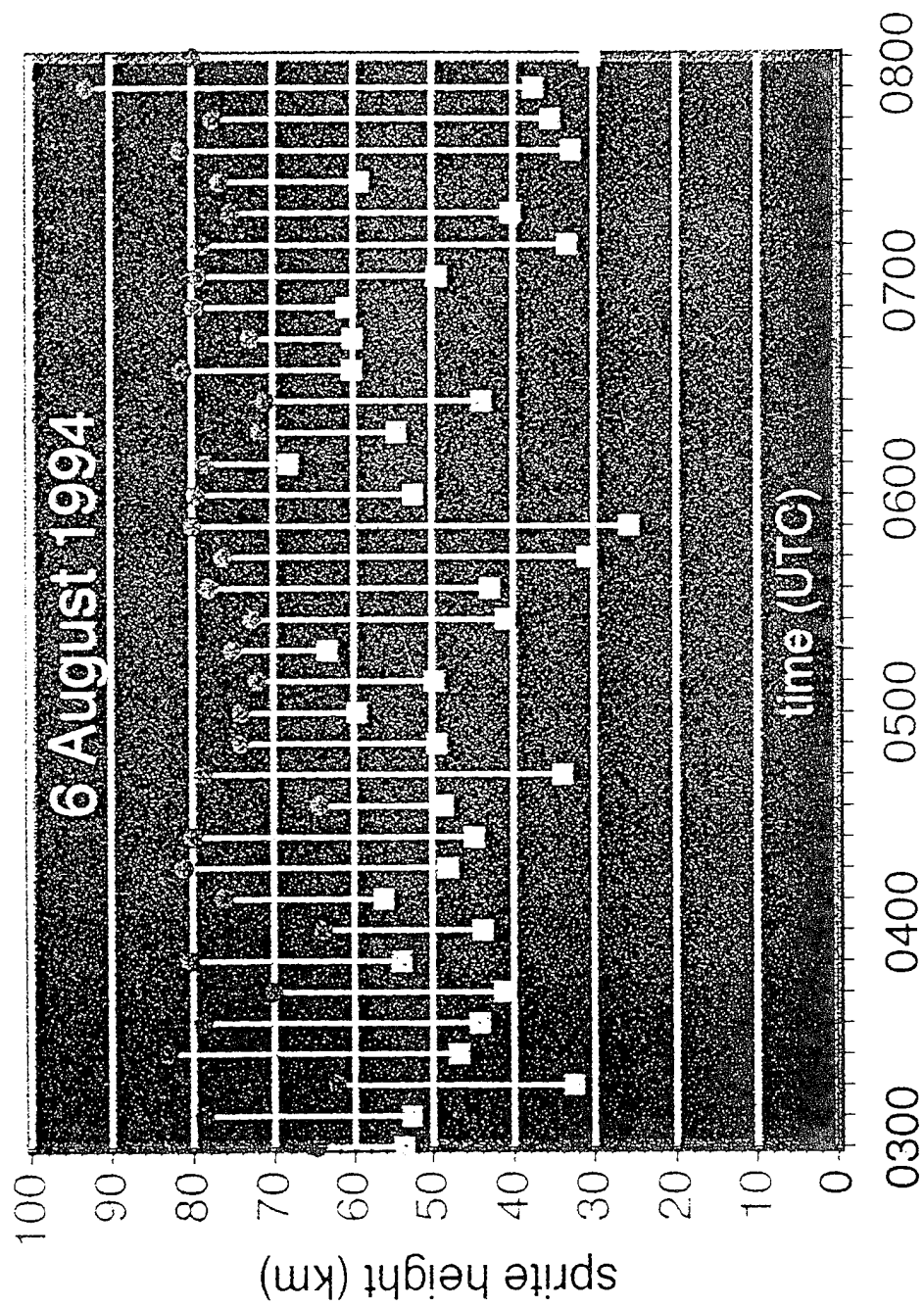


JUL-AUG 1993, JUN-SEP 1994  
All strikes larger than 100kA

# sprite azimuth, 6 August 1994







# LIGHTNING STRIKES - RADAR SPRITES

Box represents calculated sprite location

08 06 94

0700 TO 0705 UTC



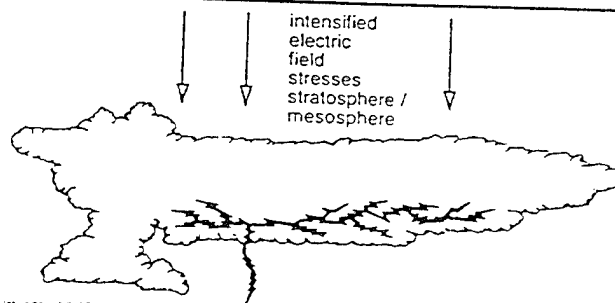
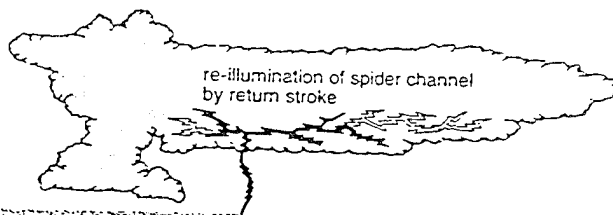
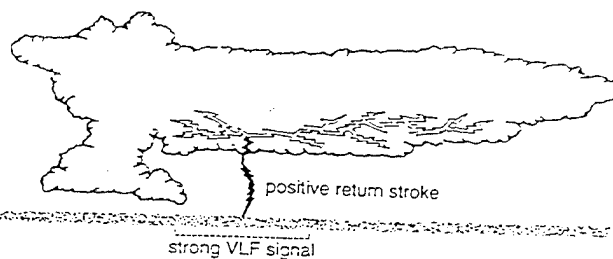
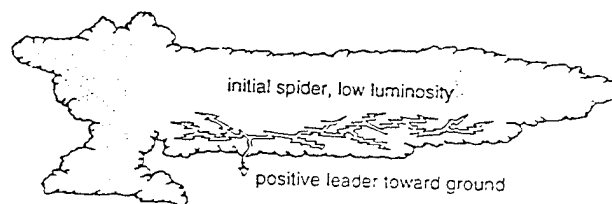
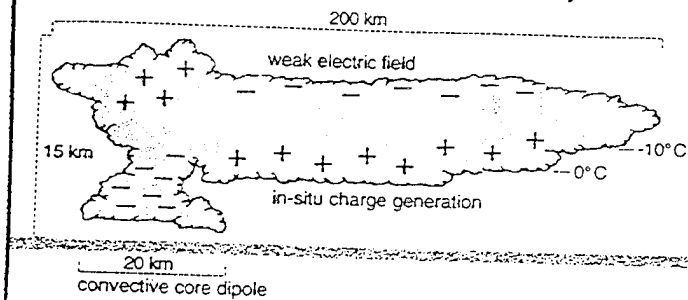
CAMERA AZIMUTH 076.0 DEGREES

SPRITE AZIMUTH 072.5 TO 084.0 DEGREES

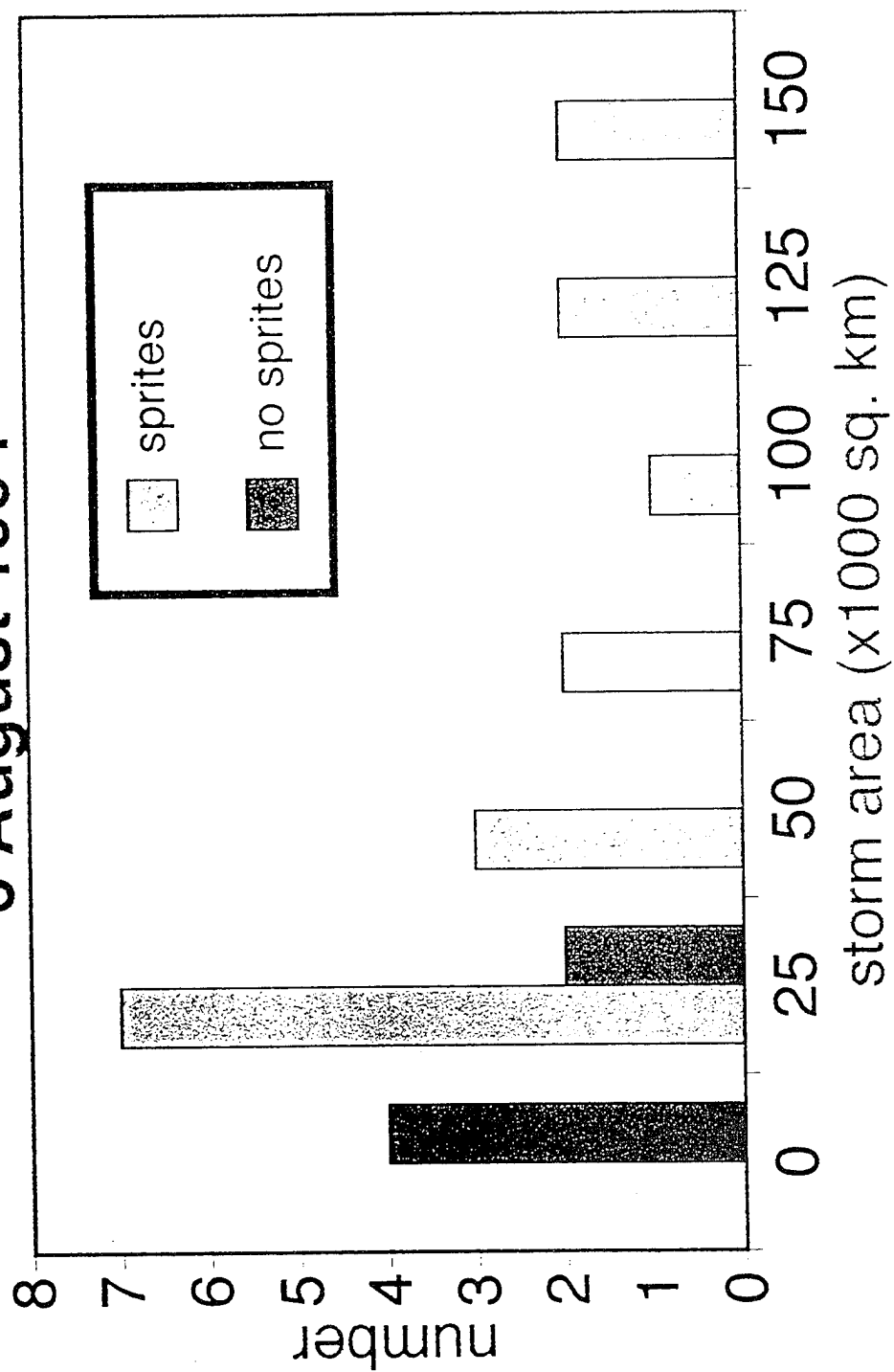
SPRITE RANGE 425.0 TO 465.0 KILOMETERS

positive strikes (+)                      0 negative strikes (-)

# Typical Great Plains Sprite-Generating Mesoscale Convective System



# areas of selected 1994 storms 6 August 1994



# **(HIGH PLAINS) FORECAST ACCURACY**

1995

**25 Sprite Nights**

**100% Correctly Forecasted**



**\* ASTeR, Inc.**

Atmospheric Simulation, Testing &amp; Research

46050 Weld County Road 13 • Ft. Collins, CO 80522 • 970-568-7664

DATE: 31 October 1995  
FROM: Walt Lyons  
RE: SPRITES '95 Project Participants

The following is the updated roster of direct and indirect participants for the SPRITES '95 Campaign in Colorado. Please inform us if there are any errors in this information and/or you wish to provide additional information.

**ASTeR, Inc.**

Participants: Walt Lyons, Tom Nelson, Liv Lyons  
Yucca Ridge Field Station  
46050 Weld County Road 13  
Ft. Collins, CO 80524

970-568-7664

970-482-8627

lyonsccm@csn.org

voice

fax

e-mail

**Mission Research Corporation**

Participants: Dr. Russ Armstrong, Dr. Jeff Shorter  
One Tara Blvd., Suite 302  
Nashua, NH 03062-2801

603-891-0070, x203

603-891-0088

@lanl.gov:rarmstrong@mrcnh.com

voice

fax

e-mail

**Lawrence Livermore National Lab**

Participants: Dr. John Molitoris/Dr. Colin Price  
Regional Atmospheric Sciences Div.  
7000 East Avenue  
PO Box 808, MS/L-262

510-423-3496

510-423-2300

520-422-5844

molitoris1@llnl.gov

voice (JM)

voice (CP)

fax

e-mail

**STAR Lab, Stanford University**

Participants: Prof. Umrn Inan, Steve Reising,  
Bill Trabucco, Alexander Slingeland  
Durand 321, MC-4055  
Stanford University  
Stanford CA 94305

415-723-4994

415-723-1461

415-723-9251

inan@nova.stanford.edu

scr@nova.stanford.edu

trabucco@nova.stanford.edu

voice

voice

fax

e-mail

e-mail

e-mail

**Tohoku University**

Participants: Profs. Yukihiro Takahashi, M. Kubota and  
Prof. Hiroshi Fukunish  
Dept. of Astrophysics & Geophysics  
Sendai, Miyagi 980-77, Japan

011+81 22 217 6537

011+81 22 217 6739

yukihiro@stpp2.geophys.tohoku.ac.jp

voice

fax

e-mail

**University of Otago**

Participant: Prof. Richard L. Dowden  
Department of Physics  
PO Box 56  
Dunedin, New Zealand

011+64 03 479 7752

011+64 03 479 0964

dowden@newton.otago.ac.nz

voice

fax

e-mail

**Utah State University**

Participants: Prof. Michael Taylor, Peter Mace  
Space Dynamics Laboratory  
Logan, Utah 84322-4145

801-797-0491 (PM), 797-3919 (MT)

801-797-4044

petermace@cc.usu.edu

taylor@psi.sci.sdl.usu.edu

voice

fax

e-mail

e-mail

**Lockheed Space and Missile**

Participants: Stephen Mende, Rick Rairden  
Dept. 91-20, Building 252  
3251 Hanover Street  
Palo Alto, CA 94304

415-424-3282

415-424-3333

rairden@lockhd.space.lockheed.com

mende@sag.space.lockheed.com

voice

fax

e-mail

e-mail

**Pennsylvania State University**

Participants: Les Hale, Lee Marshall  
780 Suzanne Ave.  
Las Cruces, NM 88005

505-647-0104  
505-642-1906  
814-863-8457  
814-867-8077

voice (LH)  
voice (LH)  
fax(LM)  
voice [LM]

**SRI International**

Participant: Dr. Roland T. Tsunoda, John Buonacore  
Geoscience & Engineering Center  
333 Ravenswood Avenue  
Menlo Park, CA 94025

415-859-3124  
415-322-2318  
tsunoda@unix.sri.com

voice  
fax  
e-mail

**Massachusetts Institute of Technology**

Participants: Dr. Earle Williams, Charles Wong  
Lincoln Lab, Group 43, Weather Systems  
Cambridge, MA

617-253-2459  
617-981-7430  
617-253-4689  
617-981-  
401-397-8982

voice (MIT)  
voice (LL)  
voice (CW)  
fax  
(V-RI SR site)

**Los Alamos National Laboratory**

Participant: Dr. Robert Franz, Dave Smith  
LANL  
MS D466  
Los Alamos NM 87545

505-665-3331  
505-667-1055  
505-665-2483  
rfranz@lanl.gov  
smithda@lanl.gov.  
505-665-7395

voice(RF)  
voice (DS)  
fax  
e-mail  
e-mail  
fax(DS)

**University of Minnesota**

Participant: Prof. John Winckler  
2012 Irving Avenue South  
Minneapolis, MN 55405

612-374-5722

voice

**Dr. Robert Nemzek**

4226 C Alabama Avenue  
Los Alamos, NM 87544

505-662-7621  
nemzek@delphi.com

(home)  
e-mail

**National Severe Storms Laboratory**

Participants: Dr. W. David Rust,  
Dr. Thomas Marshall (U of Miss)  
1313 Halley Circle  
Norman, OK 73069

405-366-0404  
405-366-0472  
rust@nssl.uoknor.edu  
405-498-3735

voice  
fax  
e-mail  
pager

**GeoSpace Research, Inc.**

Participants: Frank T. Djuth, Matthew Cox, Ken Williams  
550 N. Continenrtal Blvd.  
Suite 110  
El Segundo, CA 90245

310-322-1160  
310--322-2596  
djuth@netcom.com

voice  
fax  
e-mail

**US Air Force Academy**

Participants: Maj. Perry Malcolm,  
Maj. Geoff McHarg, Maj. Scott Dudley  
HQ USAFA/DFP  
2354 Fairchild Drive, Suite 2A42  
USAF Academy, CO 80840-6254

719-472-2579  
malcolmpr%dfp%usafa@dfmail.usafa.af.mil  
719-472-3055  
719-481-8543  
grahm@nord.usafa.af.mil  
719-472-3055  
dudleysc%dfp%usafa@dfmail.usafa.af.mil

voice (PM)  
e-mail  
voice (GM)  
voice (GM) (home)  
e-mail (GM)  
voice (SD)  
e-mail

7 September 1994, 07:04:29.332 UTC

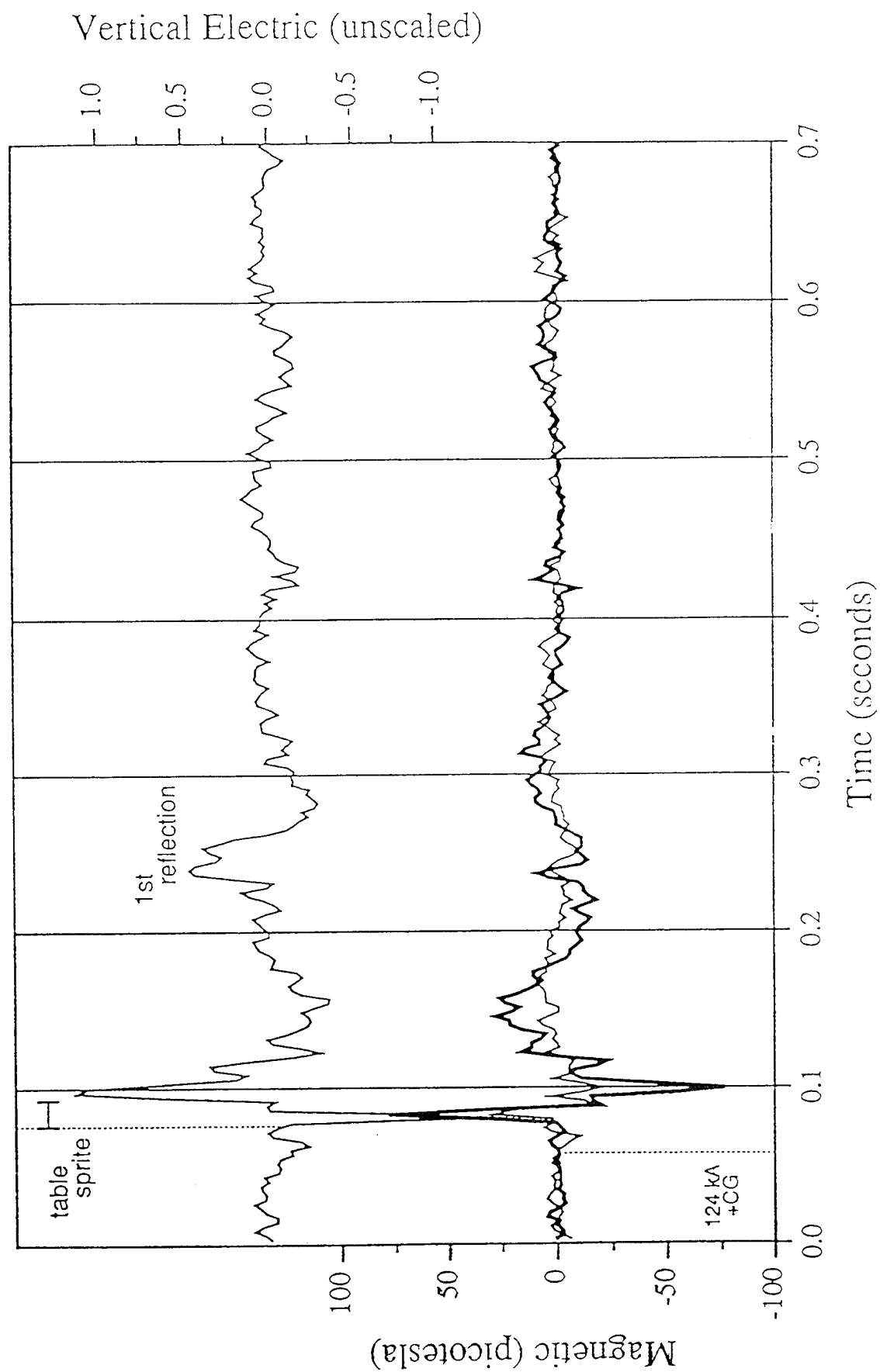


Figure 3

## THE SPRITES '95 FIELD CAMPAIGN: INITIAL RESULTS - CHARACTERISTICS OF SPRITES AND THE MESOSCALE CONVECTIVE SYSTEMS THAT PRODUCE THEM

Walter A. Lyons

ASTeR, Inc.  
Ft. Collins, CO 80524

### 1. INTRODUCTION

Anecdotal reports of unusual "lightning" discharging upward into the stratosphere or beyond have been reported for over a century (Toynbee and Mackenzie 1886) and were theoretically postulated by Wilson (1956). Little import was accorded such "cloud-to-space" lightning reports until 1989 when a chance observation from a low-light video system documented a transient (<33 ms) luminous structure extending 30-40 km above a thunderstorm top (Franz et al. 1990) ignited interest in this subject. Subsequently, similar features were discovered in low-light video images of storm systems taken onboard the Space Shuttle (Boeck et al. 1995). Low-light video imaging from the Yucca Ridge Field Station (YRFS) in Colorado since 1993 (Lyons 1994 a,b) have confirmed over 1500 of these large, luminous structures, now called sprites, in the stratosphere and mesosphere above mesoscale convective systems (MCS). Sprite rates as high as once per two minutes have been found with the most active systems. Sprites can extend from above the cloud tops to almost 100 km altitude and can be many tens of kilometers wide (Fig. 1). The detectable optical emissions may last 20 to 200 ms. They clearly appear to be related to electrical discharges within the storm. Concern that such a potentially energetic event occurs within portions of the upper atmosphere routinely traversed by aerospace vehicles, in particular the Space Shuttle, led NASA to fund a multi-year research effort. Among the goals of this current program are to determine the predictability of such events. This implies understanding the characteristics of the parent thunderstorms and their lightning discharges which result in sprites.

### 2. THE SPRITES'95 CAMPAIGN

A NASA-KSC funded field program was conducted at the Yucca Ridge Field Station, located some 20 km northeast of Ft. Collins, CO during the summer of 1995 (10 June - 6 August). This site has a panoramic view of the nocturnal thunderstorms which form over the High Plains. Low-light video systems have detected sprites at ranges up to 1000 km from YRFS. In addition to ASTeR's base experiments of low-light video

-----  
*Corresponding author address:* Walter A. Lyons, CCM, ASTeR, Inc., 46050 Weld County Road 13, Ft. Collins, CO 80524, (Voice) 970-568-7664; (Fax) 970-482-8627; e-mail: lyonsccm@csn.org

monitoring and coincident VLF and ELF measurements, coordinated observations were made by numerous organizations in 1995 (Table 1). Additional optical measurements using special CCD sensors and photometers were made by Lawrence Livermore National Lab, Tohoku University, the University of Alaska and Mission Research Corporation. Coordination of measurements allowed for Mende et al. (1995) to obtain optical spectra indicating the presence of the N<sub>2</sub> 1 PG bands, confirmatory of the red coloration of the sprites reported by Sentman et al. (1995). A suite of ELF and VLF measurements during sprite events were taken by MIT, Stanford University (STAR Labs) and the University of Otago (New Zealand). Other VHF propagation data were collected by GeoSpace Research, Inc. The National Severe Storms Laboratory and the University of Mississippi (Dave Rust and Tom Marshall) deployed an instrumented van (video, electric field) beneath the MCS anvils and made balloon soundings of electric fields in the stratosphere above anvils of sprite-producing MCS.



Fig. 1 Large sprite cluster, some 325 km NNE of the YRFS low-light camera site (0620 UTC 26 July 1995). The glow above the distant storm top is the from the parent lightning. The vertical striping is an artifact of the imager. (Courtesy of Steve Mende and Rick Rairden, Lockheed Space and Missile).

Table 1. Participants in SPRITES'95

|   |
|---|
| <p><u>ASTeR, Inc., Fort Collins, Colorado</u><br/> Walter Lyons, Project Director; Tom Nelson<br/> dual Xybion ISS-255 low light imagers • ELF and VLF<br/> measurements • photometer • meteorological data</p>   |
| <p><u>Tohoku University, Sendai, Japan</u><br/> Hiroshi Fukunishi, Yukihiro Takahashi,<br/> Minoru Kubota<br/> multiple (4) high speed <math>1^\circ \times 10^\circ</math> FOV photometers</p>   |
| <p><u>University of Otago, Dunedin, New Zealand</u><br/> Richard Dowden - OMNIPAL VLF interferometry (3 sites)</p>  |
| <p><u>STAR Laboratory, Stanford University</u><br/> Umran Inan, Steve Reising, Bill Trabucco, Alex Slingeland<br/> narrowband VLF from mobile van • VLF narrowband<br/> and broadband (0-30 kHz) VLF at YR • VLF<br/> observations in conjugate region (Palmer station)</p> |
| <p><u>GeoSpace Research, Inc.</u><br/> Frank Djuth, Matt Cox, Ken Williams - bi-static<br/> propagation (WWV at 2.5, 5, 10, 15 and 20 mHz and 28<br/> mHz transmissions)</p>  |
| <p><u>Utah State University, Space Dynamics Lab</u><br/> Michael Taylor, Peter Mace<br/> all sky airglow camera • highly sensitive low-light<br/> vidicon and SIT cameras (filtered)</p>  |
| <p><u>Lawrence Livermore National Laboratory</u><br/> John Molitoris, Colin Price<br/> IROCS - infrared optical camera system • fast optical<br/> imager • large format optical imager</p>  |
| <p><u>Massachusetts Institute of Technology</u><br/> Earle Williams, Charles Wong, Bob Boldi<br/> Schumann Resonance/Q-bursts at<br/> Rhode Island and YR sites</p>   |
| <p><u>NOAA, National Severe Storms Laboratory</u><br/> David Rust, Thomas Marshall<br/> lightning video and balloon-borne electric field mill</p>   |
| <p><u>Pennsylvania State University</u><br/> Les Hale, Lee Marshall<br/> ELF and VLF measurements</p>   |
| <p><u>Los Alamos National Laboratory</u><br/> Robert Franz, Dave Smith<br/> measurements of TIPPS and SIPPS</p>   |
| <p><u>Mission Research Corporation, Nashua, NH</u><br/> Russ Armstrong, Jeff Shorter<br/> CCD cameras system and photometer</p>   |
| <p><u>Lockheed Space and Missile</u><br/> Steve Mende, Rick Rairden<br/> imaging spectrometer and low-light video</p>   |
| <p><u>SRI International</u><br/> Roland Tsunoda, John Buonocore<br/> tunable radar system (2-30 mHz)</p>  |
| <p><u>NASA Kennedy Space Center &amp; MSFC</u><br/> Carl Lennon, Launa Maier, Otha Vaughan, Jr.<br/> LDAR • ELF/Q-burst measurements • OTD</p>  |

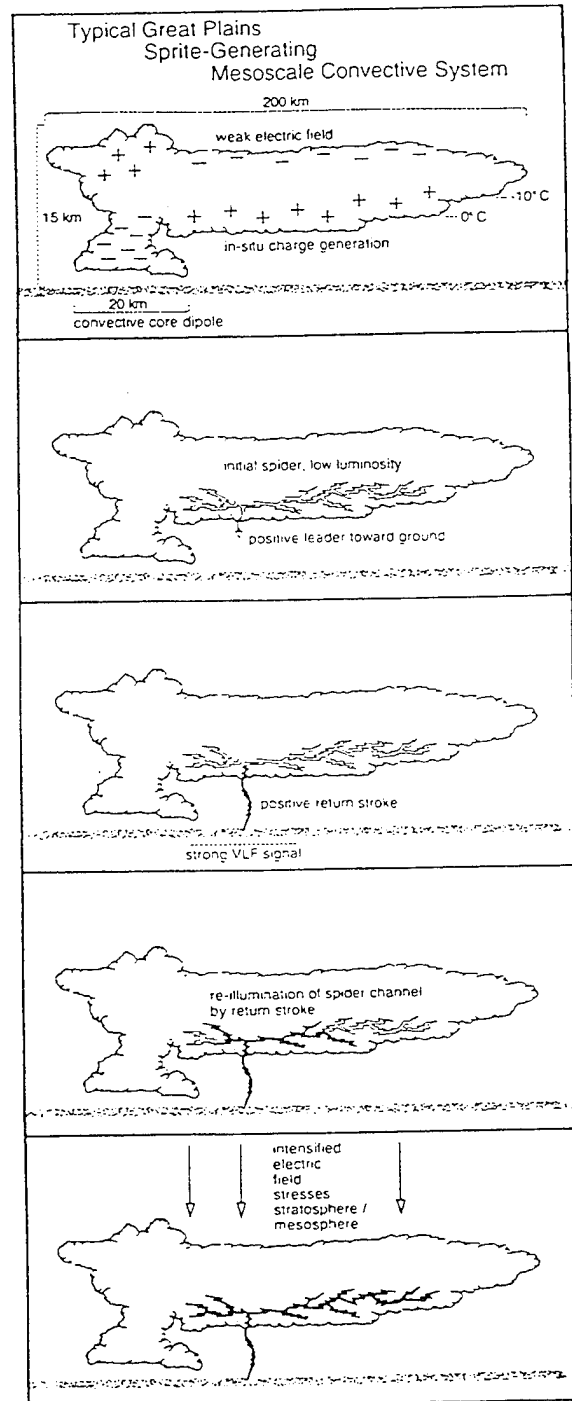


Fig. 2. A schematic of the hypothesized cloud morphology and electrical discharge mechanisms believed to be responsible for the sprite phenomenon in the stratosphere and mesosphere due to the quasi-electrostatic mechanism. This model is appropriate for midwestern mesoscale convective systems but may not be globally valid.

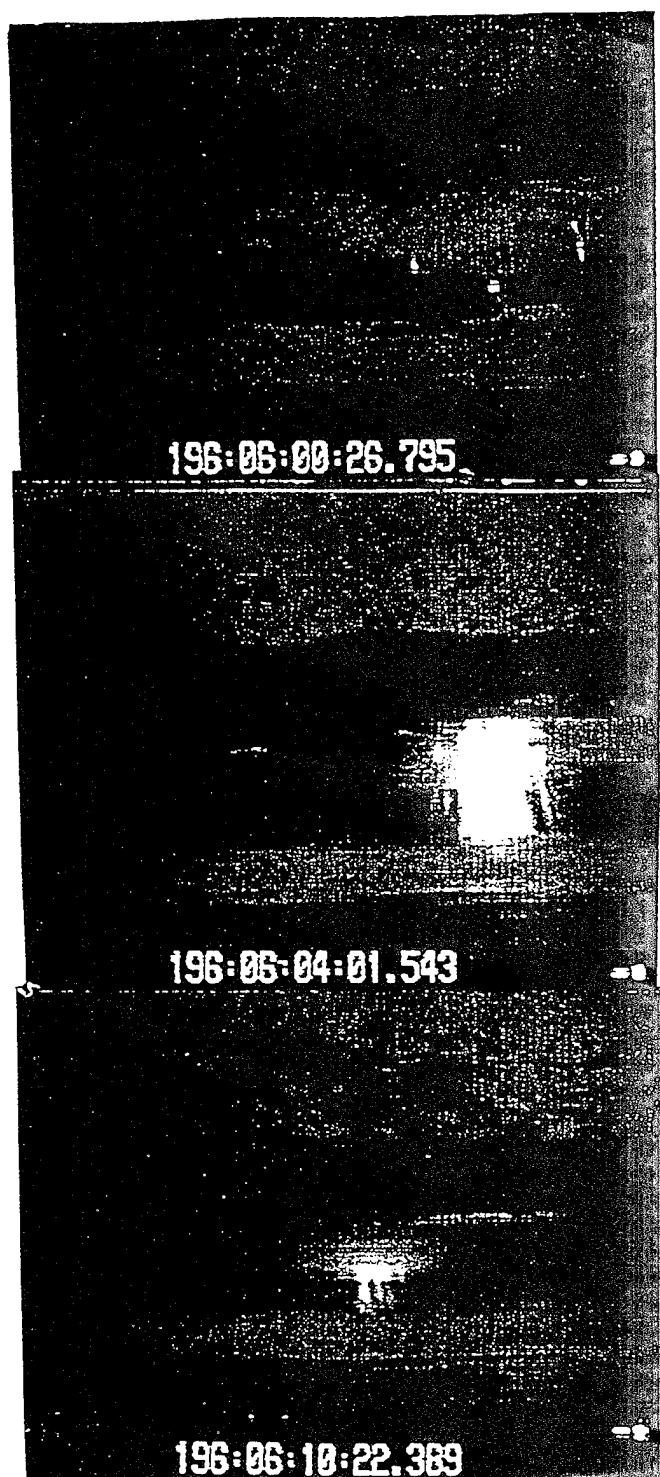


Figure 3. Xybion low-light camera views, 48 degree horizontal field of view, looking east from YRFS, 15 July 1995 (a) 06:00:26.795 UTC showing apparent blue jet (center) surrounded by ring of several small sprites, (b) 06:04:01.543 UTC, large sprite partially obscured by clouds, and (c) 06:10:22.383, elve (horizontal glow) and sprite (vertical tendrils) occurring during same 117 ms video field.

The focus of this paper is to begin quantification of the types of storms that generate sprites above the U.S. High Plains. Previous experience (Lyons 1995) has suggested that only the larger MCS (radar precipitation area  $>25,000 \text{ km}^2$ ) generate sprites, and only if they also possess significant numbers of high peak current, positive polarity cloud-to-ground (CG) discharges detected by the National Lightning Detection Network (NLDN), preferably in a bi-polar pattern. During 1995, we monitored a wide variety of convective storm types demonstrating a variety of CG lightning characteristics in order to confirm or revise our working hypothesis. Initial results suggest that the above criteria were essentially correct, though some slightly smaller systems (on the order of  $20,000 \text{ km}^2$ ) could also generate a few sprites. On 25 nights during the 1995 experiment, both storm characteristics and viewing conditions were deemed conducive to sprite observations. On all of these 25 nights, at least one sprite was detected. Numerous smaller (sometimes severe) convective storms were also monitored, but without evidence of sprites. It has been previously demonstrated that sprites are uniquely associated with powerful cloud-to-ground (CG) flashes having positive polarity (Lyons 1995; Boccippio et al. 1995). Do sprites occur systematically over any special type(s) of convective systems? A working hypothesis (Fig. 2) suggests that an extensive mesoscale stratiform precipitation region is required. This allows for horizontally extensive in-cloud lightning discharges (sometimes called dendritic or "spider" lightning) in association with a large +CG flash. Balloon-borne field mills have demonstrated the presence of large regions of positively charged anvil cloud (Marshall et al. 1995). It is suspected that the transfer of large quantities of charge within the broad anvil in association with the +CG event is a critical aspect of the sprite formation process.

A large MCS developed over eastern Colorado and Kansas after 0100 UTC 15 July 1995. Low clouds along the Front Range prevented viewing until shortly before 0600 UTC. However, as clouds cleared, in one eleven minute period, three distinct types of mesospheric luminous transient events were noted. A "blue jet," first identified by Wescott et al. (1995) rose upwards from behind a cloud bank over a six video field period (100 ms). It was characterized by a bright leading front and a glowing trail (rather like a roman candle). It was oriented about 25 degrees off the vertical, and subtended an angle of approximately 10 degrees. During the forth video field (50-67 ms into the event) a "ring" of small sprites appeared around the ascending jet (Fig. 3a). These sprites lasted only for one video field. The event was most likely related to a 36 kAmp +CG flash at 0600.26.650 UTC at  $89^\circ$  azimuth and 326 km from YRFS. At 0604.01 UTC a very large and bright sprite, displaying downward diverging tendrils, was imaged (Fig. 3b). It was most likely associated with a 116 kAmp +CG occurring at 0604.01.526 UTC at a  $93^\circ$  azimuth and 290 km range. The next event (Fig. 3c), at 0610.22 UTC, included an example of another recently identified phenomena called "elves." This is most likely the bright, very transient disk-shaped enhancement of the airglow layer seen in Space Shuttle video reported by Boeck et al. (1992). Similar disk-shaped glows were noted by Lyons et al. (1994). Fukunishi et al. (1995) confirmed that elves and sprites were distinct phenomena using a fast response (15  $\mu\text{s}$ ) photometer operated in conjunction with the low-light video

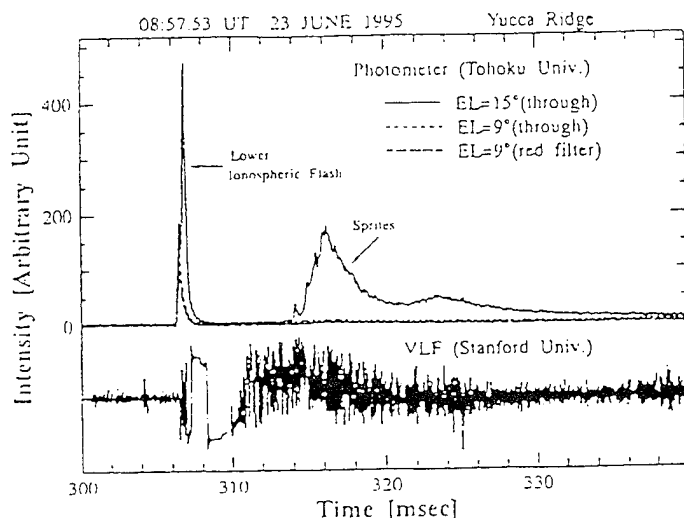
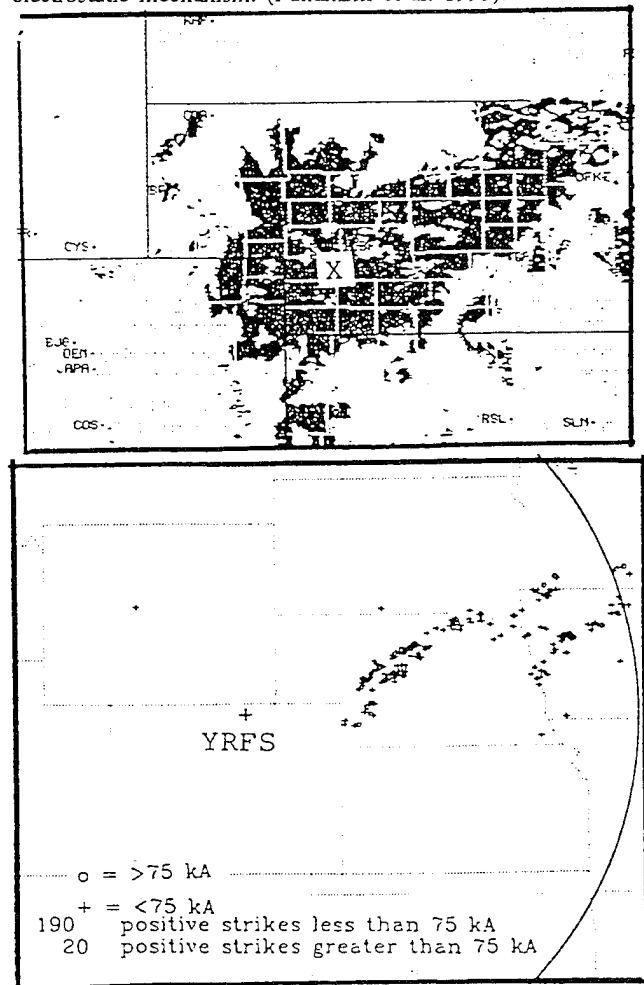


Fig. 4. High speed photometer traces revealing that a broad disk shaped glowing region and vertically oriented sprite-like tendrils were two separate events. The first (an elfe) lasted less than 1 ms and was likely a response to the lightning CG's EMP whereas the dimmer but much longer lasting sprite occurred roughly 10 ms later, possibly in response to a quasi-electrostatic mechanism. (Fukunishi et al. 1995).



systems at YRFS (Fig. 4). Numerous cases of a broad, disk-shaped glows at altitudes (85-105 km) slightly higher than the sprites lasting less than 1 ms were noted, some with and many without associated sprites (the sprites generally occurring 5 to 30 ms after the elfe). The +CG associated with the sprite/elfe combination occurring at 0610.22.387 UTC, was located at 83° azimuth and 325 km range, and had a very high peak current of 185 kAmp.

By 0600 UTC, the MCS had developed a region of radar reflectivity of 140,000 km<sup>2</sup> (Fig. 5). NLDN data revealed a large number of large +CG events within the system (Fig. 6). Many more sprites may have occurred than were detected by the YRFS cameras due to the patchy intervening cloud cover. During the 660 seconds spanning the three events shown here, there were a total of 282 CGs (26 flash/min rate). Of these, 24 CGs (8.5%) were positive in polarity. The average peak current for -CGs was 27 kAmp, for +CGs (without sprites or elves) was 37 kAmp, and for the 3 +CGs having sprites, jets or elves, 112 kAmp. The tendency of sprite-related +CGs to have substantially higher reported peak currents as detected by the NLDN was noted by Boccippio et al. (1995). For the night of 24 July 1995, preliminary analysis shows that +CGs associated with sprites (64 cases) averaged 58 kAmp, whereas those associated with elves or elves and sprites combined were even stronger, averaging 104 kAmp for 14 cases (Earle Williams, personal communication). Thus very preliminary analysis suggests that jets, sprites and elves all are associated with +CG events, but that those producing elves may have, on the average, the strongest peak currents. The "X" in Fig. 5 marks the approximate location of the three +CGs apparently involved in the events shown in Fig. 3. As has been noted in previous analyses, these electrical discharges are located within the large stratiform region rather than directly above the high reflectivity core of the MCS. Stereo sprite images from Yucca Ridge and the USAF Academy 250 km to the south indicated that sprites were typically centered within  $\pm 25$  km of their parent +CG event (Perry Malcolm, personal communication). This allows reasonable estimates of the vertical and horizontal sprite dimensions using single image photogrammetry using the NLDN-provided range to the sprite as well as relating sprites to the underlying storm structure. It is hypothesized that the sprite is in some way induced by extremely large and complex electrical discharges within the MCS anvil. Such horizontal anvil discharges are known to extend for over 100 km. The +CG may be part of this complex discharge. On a number of occasions sprites have been noted "dancing" in sync with cloud flashes propagating within extensive anvil canopies. All of the hard physical data obtained during SPRITES'95 are being assembled in part to begin testing the various theoretical models of sprites and elves of which Pasko et al. (1995) is an example.

Fig. 5 (left middle) Radar reflectivity chart (6 DVIP levels) from the national composite radar map at 0600 UTC 15 July 1995. "X" marks the general location of the several events shown in Fig. 3

Fig. 6. (left lower) NLDN lighting flash data from 0600-0700 UTC 15 July showing only positive CG events, with peak current amplitudes of greater than and less than 75 kAmp indicated.

#### 4. FUTURE RESEARCH REQUIREMENTS

Future activities should in part center of establishing the relationship between the in-cloud electrical processes and the sprite, jet and elve phenomena. This would include the coordination of ground-based and airborne remote sensing using a variety of optical and RF sensors, using the fixed base installation to guide aircraft reconnaissance. Ideally such a program would include the deployment of a system, such as the LDAR developed at the Kennedy Space Center, which is capable of three-dimensional mapping of the entire electrical discharge within the MCS. Coordination of such measurements with overflights of the Optical Transient Detector (OTD) now being tested by NASA would further assist in obtaining an integrated picture of the interrelationship of sprites and the electrical discharges within their parent cloud. Finally, a combination of low stratospheric balloon-borne field mills (and other sensors), along with a station-keeping instrumented UAV (unmanned aerospace vehicle) would complete the sensing suite for an ideal experiment.

#### 5. ACKNOWLEDGMENTS

This work was supported under an SBIR Phase II contract (NAS10-12113) from the NASA Kennedy Space Center. We acknowledge the contributions of many including Carl Lennon, Launa Maier and Ron Benti (NASA KSC), O. H. Vaughan, Jr. (NASA MSFC), John R. Winckler (University of Minnesota), Robert J. Nemzek (Los Alamos, NM), Perry R. Malcolm (U.S. Air Force Academy), Earle Williams, Charles Wong, Robert Boldi and Dennis Boccippio (MIT), William Sturz (Xyber Electronics Corp.), John Molitoris and Colin Price (Lawrence Livermore National Lab), Russ Armstrong, Ian Baker and Jeff Shorter (Mission Research Corp.), Michael Taylor and Peter Mace (Utah State Univ.), David Rust and Thomas Marshall (NSSL/Univ. of Mississippi), Umrin Inan, Bill Trabucco, Alex Slingeland and Steve Reising (STAR Lab, Stanford University), Y. Fukunishi, Y. Takahashi and M. Kubota (Tohoku University), Richard Dowden (University of Otago), Stephen Mende and Rick Rairden (Lockheed), Les Hale and Lee Marshall (Pennsylvania State Univ.), Frank Djuth (GeoScience, Inc.), Roland Tsunoda (SRI International), Davis Sentman and Eugene Wescott (University of Alaska) and especially Thomas Nelson and Liv Lyons (ASTeR).

#### 6. REFERENCES

- Boccippio, D.J., E.R. Williams, W.A. Lyons, I. Baker and R. Boldi, 1995: Sprites, Q-bursts and positive ground strokes. Science, **269**, 1088-1091.
- Boeck, W.L., O.H. Vaughan, Jr., R.J. Blakeslee, B. Vonnegut and M. Brook, 1992: Lightning induced brightening of the airglow layer. Geophys. Res. Lett., **19**, 99-102.
- Boeck, W.L., O.H. Vaughan, Jr., R.L. Blakeslee, B. Vonnegut, M. Brook and J. McKune 1995: Observations of lightning in the stratosphere. J. Geophys. Res., **100**, 11465-1475.
- Franz, R.C., R. J. Nemzek and J.R. Winckler, 1990: Television image of a large upward electrical discharge above a thunderstorm system. Science, **249**, 48-51.
- Fukunishi, H., Y. Takahashi, M. Kubota, K. Sakanai, U.S. Inan and W.A. Lyons, 1996: Elves: Lightning-induced transient luminous events in the lower ionosphere. Nature (in press).
- Inan, U.S., T.F. Bell, V. Pasko, D.D. Sentman, E.M. Wescott, and W.A. Lyons, 1995: VLF signatures of ionospheric disturbances associated with sprites. Geophys. Res. Lett., (in press).
- Lyons, W.A., 1995: The relationship of large luminous stratospheric events to the anvil structure and cloud-to-ground discharges of their parent mesoscale convective system. Preprints, Conf. on Cloud Physics, AMS, Dallas, 541-546.
- Lyons, W.A., I.T. Baker, T.E. Nelson, J.R. Winckler, R.J. Nemzek, P.R. Malcolm, E.R. Williams and D. Boccippio, 1994: The 1994 Colorado SPRITE Campaign (abstract), EOS, **75**, vol. 44, p. 108. Also a 20 minute video tape, available from ASTeR, Inc.
- Lyons, W.A., 1994: Characteristics of luminous structures in the stratosphere above thunderstorms as imaged by low-light video. Geophysical Research Letters, **21**, 875-878.
- Lyons, W.A. and E.R. Williams, 1994: Some characteristics of cloud-to-stratosphere "lightning" and consideration for its detection. Preprints, Symposium on the Global Electrical Circuit, Global Change and the Meteorological Applications of Lightning Information, AMS, Nashville, 8 pp.
- Lyons, W.A., 1994: Low-light video observations of frequent luminous structures in the stratosphere above thunderstorms. Mon. Wea. Rev., **122**, 1940-1946.
- Marshall, T.C., W.D. Rust and M. Stolzenburg, 1995: Electrical structure and updraft speeds in thunderstorms over the southern Great Plains. J. Geophys. Res., **100**, 1001-1015.
- Mende, S.B., R.L. Rairden, G.R. Swenson and W.A. Lyons, 1995: Sprite spectra: N<sub>2</sub> first positive band identification. Geophys. Res. Lett., **22**, 2633-2636.
- Pasko, V. P., U.S. Inan, Y. N. Taranenko and T.F. Bell, 1995: Heating, ionization and upward discharges in the mesosphere due to intense quasi-electrostatic thunderstorm fields. Geophys. Res. Letts., **22**, 365-368.
- Toynbee, H. and T. Mackenzie, 1886: title unknown. Nature, **33**, p. 245.
- Sentman, D.D., E.M. Wescott, D. L. Osborne, D. L. Hampton and M.J. Heavner, 1995: Preliminary results from the Sprites94 aircraft campaign 1. Red sprites. Geophys. Res. Lett., **22**, 1205-1208.
- Wescott, E.M., D. Sentman, D. Osborne, D. Hampton and M. Heavner, 1995: Preliminary results from the Sprites94 aircraft campaign: 2. Blue jets. Geophys. Res. Lett., **22**, 1209-1212.
- Wilson, C.T.R., 1956: A theory of thundercloud electricity, Proc. Royal Soc. London, **236**, 297-317.
- Winckler, J.R., W.A. Lyons, T. E. Nelson and R.J. Nemzek, 1995: New high-resolution ground based studies of sprites. J. Geophysical Res. (submitted).



## PROCESSING, INTEGRATING AND DISPLAYING DISPARATE DATA SOURCES FROM THE SPRITES '95 FIELD PROGRAM

Walter A. Lyons and Thomas E. Nelson

ASTeR, Inc./FMA, Inc.  
Ft. Collins, CO 80524

### 1. INTRODUCTION

Rarely during a career is one in the position of designing and conducting a major field measurement program for a phenomenon the existence of which was suspect, its characteristics unknown, and for which no proper names even yet existed. The SPRITES'95 field campaign was indeed the culmination of such an endeavor. While anecdotal reports of unusual "lightning" discharging upward into the stratosphere or beyond have been reported for over a century (Toynbee and Mackenzie 1886) and were theoretically postulated by Wilson (1956), little import was accorded such "cloud-to-space" lightning reports. Indeed, if known at all to atmospheric scientists, it was through Corliss (1977) who also included tales of turtles encased in hailstones and half-meter wide snowflakes, not to mention accounts of spontaneous human combustion. But the atmospheric science community was galvanized by a chance 1989 observation from a low-light video system which documented a huge, transient (<33 ms) luminous structure extending 30-40 km above a thunderstorm top (Franz et al. 1990). Subsequently, similar features were suspected after reviews of low-light video images of distant storm systems taken onboard the Space Shuttle (Vaughan et al., 1992). These new observations, combined with a detailed literature search (Lyons and Williams, 1993 and 1994) suggested these luminous events, now generally called sprites (Fig. 1), occur with some regularity and were not a totally rare or "freak" event. Concern that such a potentially energetic event occurs within layers of the upper atmosphere routinely traversed by aerospace vehicles, in particular the Space Shuttle, led to NASA funding a multi-year research effort. The goal was to document how frequently such sprites occurred, how they might be detected, and thereafter what their potential impacts might be. The initial observation phase of the study was conducted at the Yucca Ridge Field Station, located 20 km northeast of Ft. Collins, CO. This site has a panoramic view of the deep convection which develops over the U.S. High Plains, often during the night hours (Fig. 2). The challenge of the project: how to study a phenomenon only a few fleeting glimpses of which had

ever been obtained and about which virtually no information existed as to its frequency, phenomenology or physical characteristics. The initial approach selected (Lyons, 1994 a,b) deployed low-light video camera systems which, it has proven, can detect sprite events to distances approaching 1000 km. On a single night (7 July 1993) as many as 240 sprites were detected from the Yucca Ridge site. Far from being rare, at least over the U.S. High Plains, the sprite is a common event above mesoscale convective systems (MCS).

### 2. THE 1995 SPRITE CAMPAIGN

Given that the sprite was a frequent summer occurrence above the central U.S., how best to characterize its structure and its impacts? Do sprites occur systematically over any special type(s) of convective systems? Can they be predicted? What are their optical spectra? Do they have signatures in the UV and infrared? Were they associated with perturbations in RF signals at various frequencies?

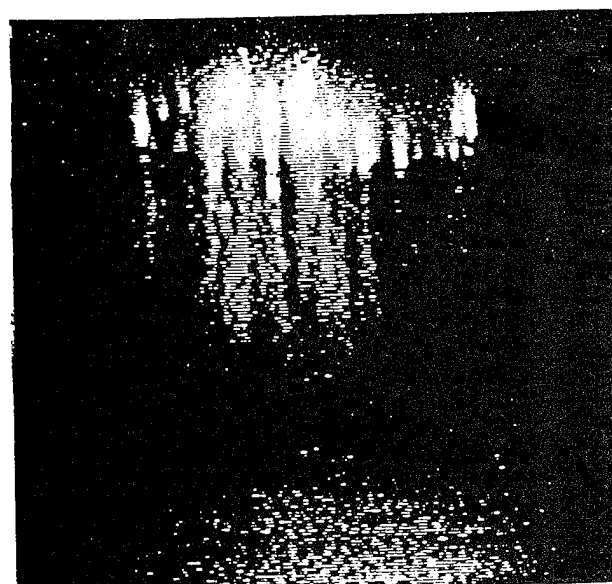


Fig. 1 A large sprite extending to 92 km altitude, 400 km east of the low-light camera site. The glow above the horizon is the parent CG lightning in the distant storm.

Corresponding author address: Walter A. Lyons, CCM, ASTeR, Inc./FMA Inc., 46050 Weld County Road 13, Ft. Collins, CO 80524, (Voice) 970-568-7664; (Fax) 970-482-8627; e-mail: lyonsccm@csn.org

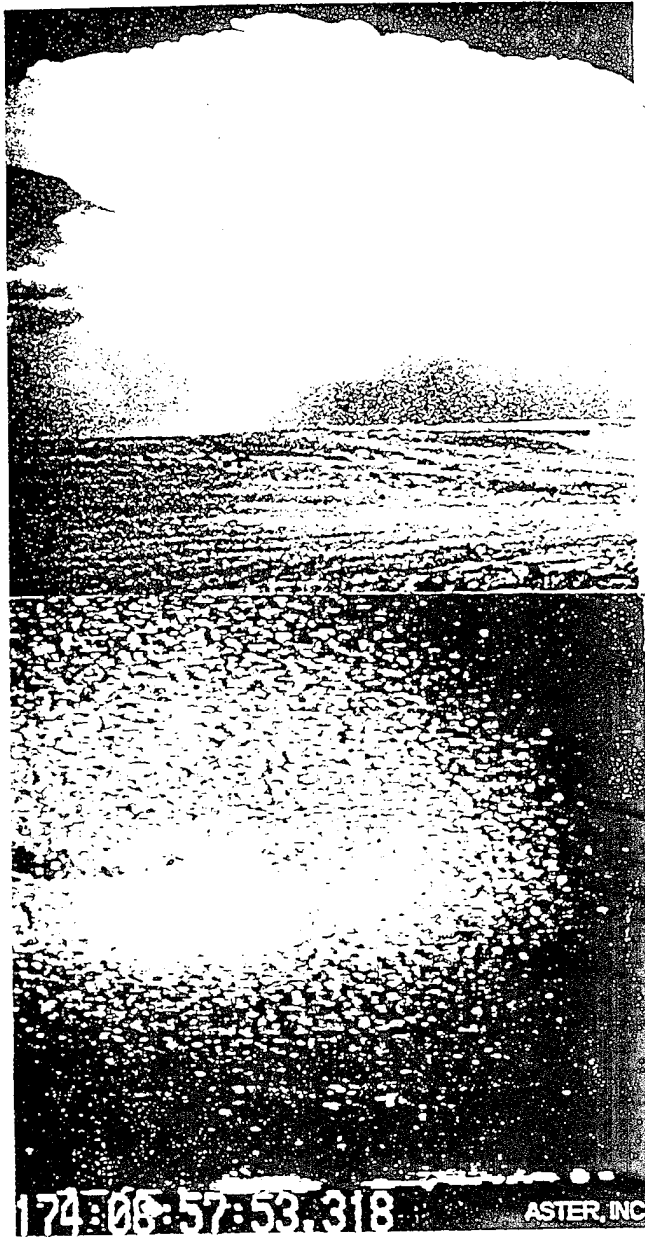
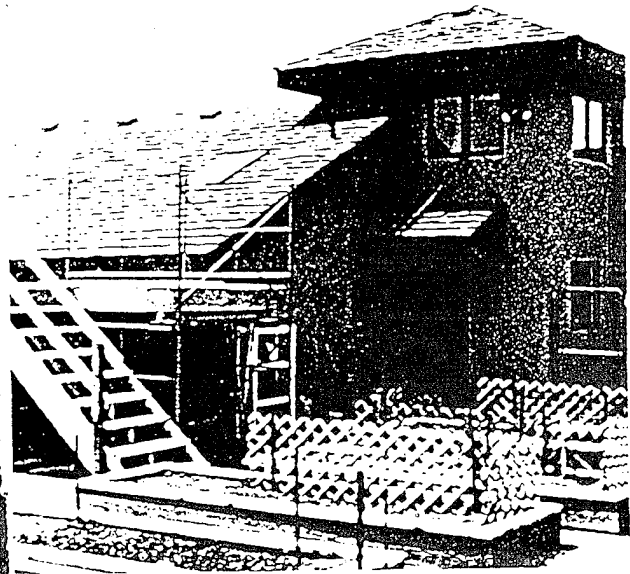


Fig. 2 (top) Panoramic view of mesoscale convective systems as viewed from Yucca Ridge Field Station near Ft. Collins, CO and the instrumentation platform built at the site to collocate the various cameras and optical systems.

Fig. 3. (bottom) Single video field (16.7 ms) from Xybion low-light camera showing both a sprite (bright spot) and the brightening of the airglow layer, an amorphous ionospheric glow, now tentatively called elves.

Can they be detected by radar? These are some of the questions that needed to be addressed in order to assess their potential impact on the middle and atmosphere. The SFRITES'95 campaign was designed to deploy as many different types of passive and active remote sensing



systems as possible in a coordinated study of individual sprite events as well as their parent storms. Table 1 summarizes the participating organizations and sensors deployed during a two month period (June through early August) at Yucca Ridge. A key objective was to coordinate observations in space and time. Since preliminary studies (Winckler et al. 1995) had shown the sprite time scales to be on the order of 10-100 ms, precise time coordination was a requisite. This was accomplished by use of GPS time (2  $\mu$ s nominal accuracy) for all systems. When possible, video cameras were further electronically synched so each 17 ms video field record would be temporally coincident. Selected RF signals were continuously recorded on the four-channel audio of the SVHS tapes, and also digitally sampled at 40 kHz and 200 kHz using LabView on a Pentium-based PC in 1500 ms segments coincident with sprites. RF receivers included a 1-10 MHz system suitable for whistler detection, broader bandwidth VLF systems (1-50 and 1-100 kHz), and narrow band receivers at selected frequencies. In addition, coordinated measurements of ELF signals (3-30 Hz) were made at the Rhode Island Schumann resonance station of the Massachusetts Institute of Technology (Williams 1992). Initial results from 1994 tests and the full 1995 field program, in which large and disparate data sets were collected and integrated, have already begun to yield significant results. In addition to sprites, we have confirmed from ground-based sensors the presence of brief ( $\approx$  1 ms) brightenings of the airglow layer (tentatively called "elves") as a distinct phenomenon (Fig. 3). This was made possible by the use of high speed pointing photometers with 15  $\mu$ sec resolution. A video field (Fig 3) shows a sprite which is surrounded by a broad amorphous glowing region. The high temporal resolution photometer traces revealed that this single 17 ms video

Table 1. Participants in SPRITES'95

|  |
|--|
| <p><u>ASTeR, Inc., Fort Collins, Colorado</u><br/> Walter Lyons, Project Director; Tom Nelson<br/> dual Xybion ISS-255 low light imagers • ELF and VLF measurements • photometer • meteorological data</p> <p><u>Tohoku University, Sendai, Japan</u><br/> Hiroshi Fukunishi, Yukihiro Takahashi,<br/> Minoru Kubota<br/> multiple (4) high speed 1°x10° FOV photometers</p> <p><u>University of Otago, Dunedin, New Zealand</u><br/> Richard Dowden - OMNIPAL VLF interferometry (3 sites)</p> <p><u>STAR Laboratory, Stanford University</u><br/> Umrhan Inan, Steve Reising, Bill Trabucco, Alex Slingeland<br/> narrowband VLF from mobile van • VLF narrowband and broadband (0-30 kHz) VLF at YR • VLF observations in conjugate region (Palmer station)</p> <p><u>GeoSpace Research, Inc.</u><br/> Frank Djuth, Matt Cox, Ken Williams - bi-static propagation (WWV at 2.5, 5, 10, 15 and 20 mHz and 28 mHz transmissions)</p> <p><u>Utah State University, Space Dynamics Lab</u><br/> Michael Taylor, Peter Mace<br/> all sky airglow camera • highly sensitive low-light vidicon and SIT cameras (filtered)</p> <p><u>Lawrence Livermore National Laboratory</u><br/> John Molitoris, Colin Price<br/> IROCS - infrared optical camera system • fast optical imager • large format optical imager</p> <p><u>Massachusetts Institute of Technology</u><br/> Earle Williams, Charles Wong, Bob Boldi<br/> Schumann Resonance/Q-bursts at Rhode Island and YR sites</p> <p><u>NOAA, National Severe Storms Laboratory</u><br/> David Rust, Thomas Marshall<br/> lightning video and balloon-borne electric field mill</p> <p><u>Pennsylvania State University</u><br/> Les Hale, Lee Marshall<br/> ELF and VLF measurements</p> <p><u>Los Alamos National Laboratory</u><br/> Robert Franz, Dave Smith<br/> measurements of TIPPS and SIPPS</p> <p><u>Mission Research Corporation, Nashua, NH</u><br/> Russ Armstrong, Jeff Shorter<br/> CCD cameras system and photometer</p> <p><u>Lockheed Space and Missile</u><br/> Steve Mende, Rick Rairden<br/> imaging spectrometer and low-light video</p> <p><u>SRI International</u><br/> Roland Tsunoda, John Buonocore<br/> tunable radar system (2-30 mHz)</p> <p><u>NASA Kennedy Space Center &amp; MSFC</u><br/> Carl Lennon, Launa Maier, Otha Vaughan, Jr.<br/> LDAR • ELF/Q-burst measurements • OTD</p> |
|--|

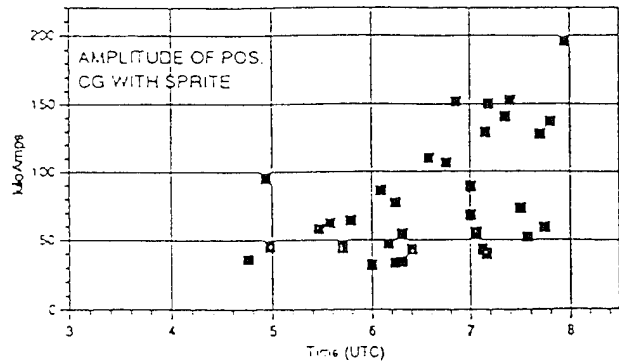


Fig. 4. The peak current (kiloamps) of each +CG associated with a sprite plotted versus time for the night of 6 August 1994.

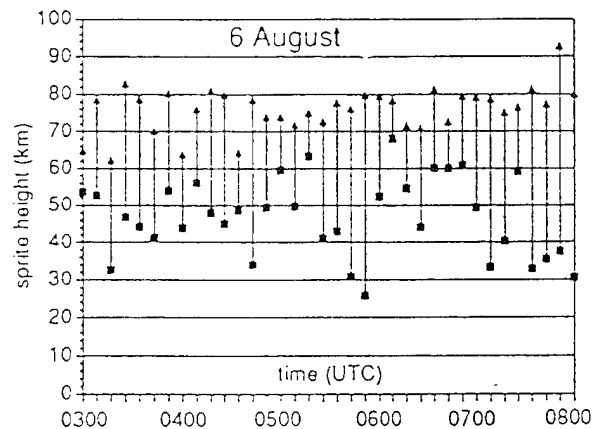


Fig. 5. Estimated altitude of the top and base of the sprite as a function of time. Single image photogrammetry assumes that the sprite is centered above its parent +CG.

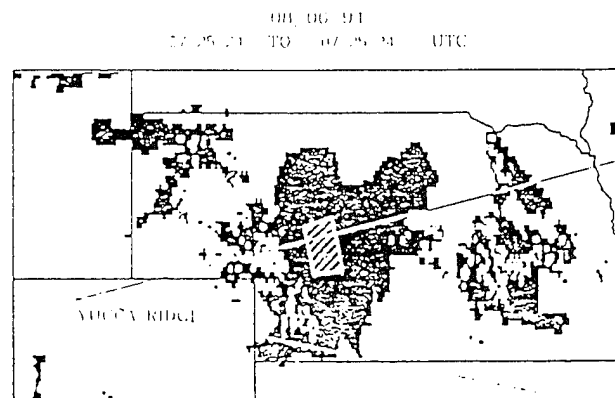


Fig. 6. Combined workstation display showing radar reflectivity, the field-of-view of the low-light camera and the estimated location of the sprite based upon its observed azimuth (video) and range (assumed the same as the associated +CG flash).

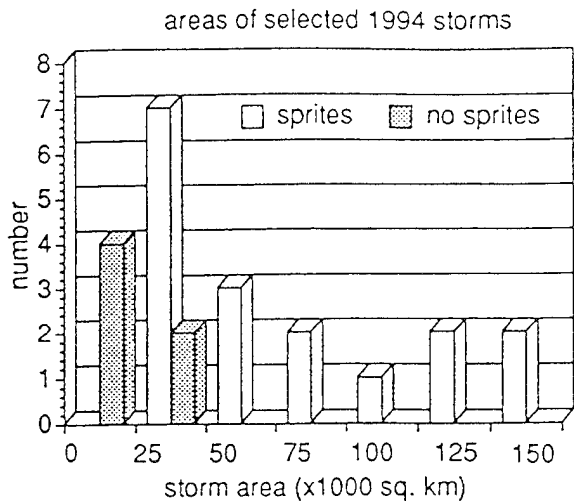


Fig. 7. Areas of storms that did and did not generate sprites, based upon areal reflectivity from composite digital national radar, suggesting a minimum critical anvil size for a sprite-producing storm.

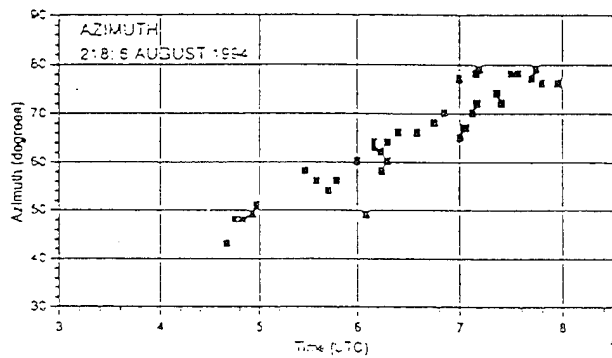


Fig. 8. The azimuth (degrees) of the center of each sprite observed on a given night plotted as a function of time, illustrating the clustering of sprites in a relatively small portion of the anvil.

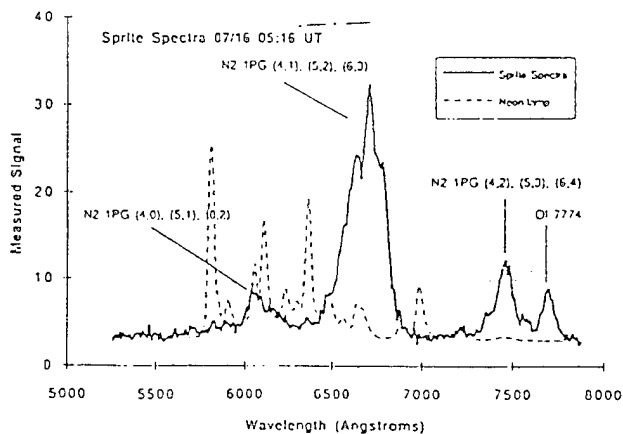


Fig. 9. Optical spectra of a sprite showing the N<sub>2</sub> first positive bands (Mende et al., 1995), an observation made possible by coordinating low-light video imagers and pointing spectrometers.

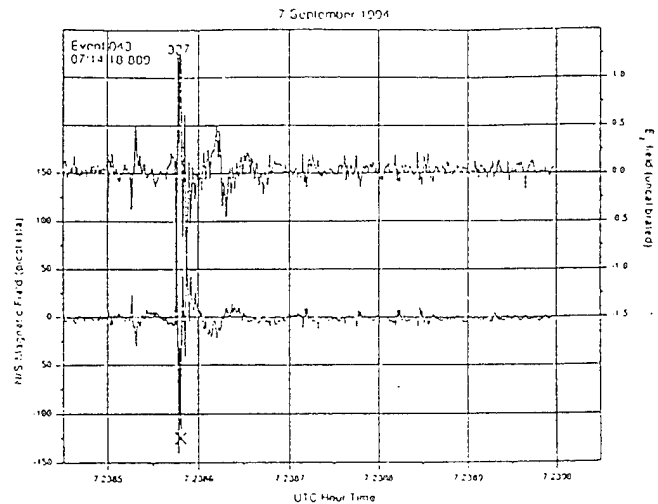


Fig. 10. Q-bursts signature in the ELF Schumann resonance bands which is coincident with the occurrence of a very large +CG flash measured by the NLDN (Boccippio et al., 1995). This pattern suggests Q-bursts serve as a diagnostic for sprite events.

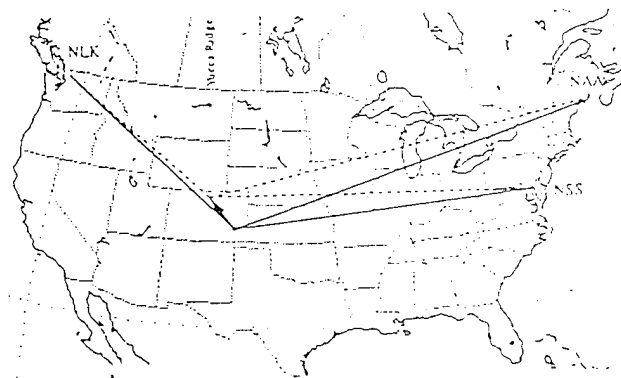


Fig. 11. Location of three VLF transmitters, the Yucca Ridge Omnipal receiver (point of arrow) and the sprite (small circle, 300 km SE), the same event as shown in Fig. 3. (Dowden, personal communication).

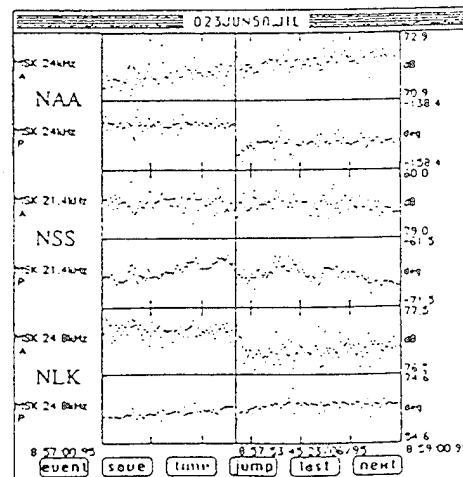


Fig. 12. Changes in phase and amplitude of Navy VLF transmissions due to the sprite discussed in Figs. 3 and 11. (Dowden, personal communication).

field contains two distinct phenomena: the 1 ms elve event followed about 10 ms later by the onset of the sprite, which then lasted for several more video fields. Cloud-to-ground (CG) flash data from the National Lightning Detection Network (NLDN) were compared (using millisecond timing coincidences) with the sprite events. It was immediately discovered (Lyons, 1995) that sprites were almost uniquely correlated with positive CG events, often with amplitudes substantially larger than the average for such events (Fig. 4). Stereo sprite images from Yucca Ridge and the USAF Academy 250 km to the south indicated that sprites were typically centered within  $\pm 25$  km of their parent +CG event. This allows reasonable estimates of the vertical and horizontal sprite dimensions using single image photogrammetry using the NLDN-provided range to the sprite (Fig. 5). Combining the NLDN CG data, the estimated sprite locations and regional radar reflectivity composites at 4 km resolution (from Kavouras, Inc.) revealed that the sprite occurred not over the high reflectivity core but rather in the large stratiform precipitation region associated with the MCS anvil. This was accomplished by integrating and displaying these data using an IBM RS/6000 workstation and NCAR graphics (Fig. 6). Successive case studies showed that not only were sprites associated with unusually energetic +CG events, but that the parent storm required a precipitation area generally  $>20,000$  km<sup>2</sup> (Fig. 7). These two simple forecast rules resulted in a virtual 100% forecast accuracy for sprite storms during the 1995 campaign. Detailed study of the sprite location in the video images also revealed that the sprites tended to concentrate in relatively small portions of the MCS anvil. The tight clustering of sprite azimuths viewed by the Yucca Ridge cameras (Fig. 8) typifies this behavior. Aside from raising interesting questions about the sprite-generating mechanism itself, it also suggests that once sprites are detected, close-up views can be attained by pointing telescopic systems at distant storms. This allowed us to acquire numerous optical spectra (Fig. 9) from storms as distant as 500-600 km (Mende et al. 1995). The ability to detect sprites and associate them with their parent CG lightning has resulted in a variety of discoveries relating sprites to VLF and ELF radio propagation. Boccippio et al. (1995) found a strong correlation between sprites, large +CGs and a global ELF phenomenon called the Q-burst. It has long been assumed that the background "hum" of natural radio at frequencies below 100 Hz was due to the integrated effect of all the planet's lightning discharges. Occasional large excursions (Fig. 10) called Q-bursts remained something of a mystery. Apparently the intense RF emissions from sprite-producing +CGs are the source of this ringing of the earth-ionospheric cavity on a global scale. At higher frequencies (20 kHz), researchers from the University of Otago (New Zealand) have found that continuous VLF transmissions from several U.S. Navy sites are distorted both in phase and amplitude as shown in Figs. 11 and 12 (R. Dowden, personal communication, 1995). By comparing these time-tagged perturbations with the corresponding low-light videos, it will be possible to verify whether this effect can be used as the basis of an automated sprite detection system that would work during cloudy conditions and daylight, when low-light video systems are unsuitable.

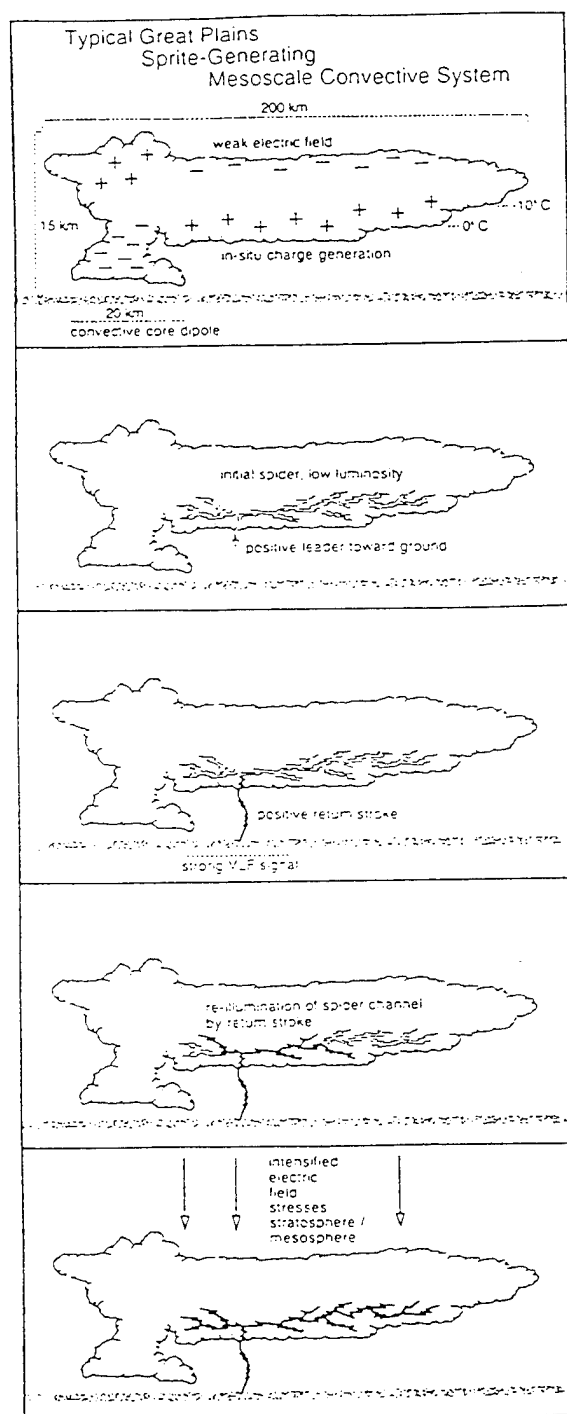


Fig. 13. A schematic of the hypothesized cloud morphology and electrical discharge mechanisms believed to be responsible for the sprite phenomenon in the stratosphere and mesosphere above midwestern mesoscale convective systems.

### 3. CONCLUSIONS

The collection of various optical and RF data types using common GPS-time bases has already yielded extensive results. The use of a common precision time base may also allow for coordination with other field programs operating at the same time, such as mountain-top measurements similar to those described by Sentman et al. (1995). The variety of coordinated observations has already permitted a physical model of the sprite-generating mechanism in large MCS storms to emerge (Lyons, 1995) (Fig. 13). The sprites appear associated spatially and temporally with positive CG events, often of much larger than average peak current amplitude and multiplicity. It is hypothesized that the sprite is in some way induced by extremely large and complex electrical discharges within the MCS anvil. Such horizontal anvil discharges are known to extend for over 100 km. The +CG may be part of this complex discharge. On a number of occasions sprites have been noted "dancing" in sync with cloud flashes propagating within extensive anvil canopies. Hard physical data are being assembled against which various theoretical models of sprites can be tested (Pasko et al., 1995). Future activities may include the coordination of ground-based and airborne sprite imaging (Sentman et al., 1995). Ongoing analyses will continue integrating NLDN lightning, digital radar and GOES data for comprehensive studies of sprite storms. The morphology of sprites and elves are being investigated using new digital, non-linear video editing systems which allow motion studies while maintaining perfect synch with the simultaneously recorded 4-channel audio of the various VLF signals.

### 4. ACKNOWLEDGMENTS

This work was supported under an SBIR Phase II contract (NAS10-12113) from the NASA Kennedy Space Center. We acknowledge the contributions of many including Carl Lennon, Laura Maier and Ron Benti (NASA KSC), O. H. Vaughan, Jr. (NASA MSFC), John R. Winckler (University of Minnesota), Robert J. Nemzek (Los Alamos, NM), Perry R. Malcolm (U.S. Air Force Academy), Earle Williams, Charles Wong, Robert Boldi and Dennis Boccippio (MIT), William Sturz (Xyberon Electronics Corp.), John Molitoris and Colin Price (Lawrence Livermore National Lab), Russ Armstrong, Ian Baker and Jeff Shorter (Mission Research Corp.), Michael Taylor and Peter Mace (Utah State Univ.), David Rust and Thomas Marshall (NSSL/Univ. of Mississippi), Umrin Inan, Bill Trabucco, Alex Slingeland and Steve Reising (STAR Lab, Stanford University), Y. Fukunishi, Y. Takahashi and M. Kubota (Tohoku University), Richard Dowden (University of Otago), Stephen Mende and Rick Rairden (Lockheed), Les Hale and Lee Marshall (Pennsylvania State Univ.), Frank Djuth (GeoScience, Inc.), Roland Tsunoda (SRI International), and Liv Lyons (ASTeR).

### 5. REFERENCES

Boccippio, D.J., E.R. Williams, W.A. Lyons, I. Baker and R. Boldi, 1995: Sprites, Q-bursts and positive ground strokes. Science, in press.

Corliss, W.L., 1977: Handbook of Unusual Natural Phenomena. The Source Book Project, Glen Arm, MD 21057.

Franz, R.C., R. J. Nemzek and J.R. Winckler, 1990: Television image of a large upward electrical discharge above a thunderstorm system. Science, **249**, 48-51.

Lyons, W.A., 1995: The relationship of large luminous stratospheric events to the anvil structure and cloud-to-ground discharges of their parent mesoscale convective system. Preprints, Conf. on Cloud Physics, AMS, Dallas, 541-546.

Lyons, W.A., 1994: Characteristics of luminous structures in the stratosphere above thunderstorms as imaged by low-light video. Geophysical Research Letters, **21**, 875-878.

Lyons, W.A. and E.R. Williams, 1994: Some characteristics of cloud-to-stratosphere "lightning" and consideration for its detection. Preprints, Symposium on the Global Electrical Circuit, Global Change and the Meteorological Applications of Lightning Information, AMS, Nashville, 8 pp.

Lyons, W.A., 1994: Low-light video observations of frequent luminous structures in the stratosphere above thunderstorms. Mon. Wea. Rev., **122**, 1940-1946.

Lyons, W.A. and E.R. Williams, 1993: Preliminary investigations of the phenomenology of cloud-to-stratosphere lightning discharges. Preprints, Conference on Atmospheric Electricity, American Meteorological Society, St. Louis, 8 pp.

Mende, S.B., R.L. Rairden, G.R. Swenson and W.A. Lyons, 1995: Sprite spectra: N<sub>2</sub> first positive band identification. Geophys. Res. Lett. (submitted).

Pasko, V. P., U.S. Inan, Y. N. Taranenko and T.F. Bell, 1995: Heating, ionization and upward discharges in the mesosphere due to intense quasi-electrostatic thunderstorm fields. Geophys. Res. Lett., **22**, 365-368.

Toynbee, H. and T. Mackenzie, 1886: title unknown. Nature, **33**, p. 245.

Sentman, D.D., E.M. Wescott, D. L. Osborne, D. L. Hampton and M.J. Heavner, 1995: Preliminary results from the Sprites94 aircraft campaign 1. Red sprites. Geophys. Res. Lett., **22**, 1205-1208.

Williams, E.R., 1992: The Schumann Resonance: A global tropical thermometer. Science, **256**, 1184-1187.

Wilson, C.T.R., 1956: A theory of thundercloud electricity. Proc. Royal Soc. London, **236**, 297-317.

Winckler, J.R., W.A. Lyons, T. E. Nelson and R.J. Nemzek, 1995: New high-resolution ground based studies of sprites. J. Geophysical Res. (submitted).



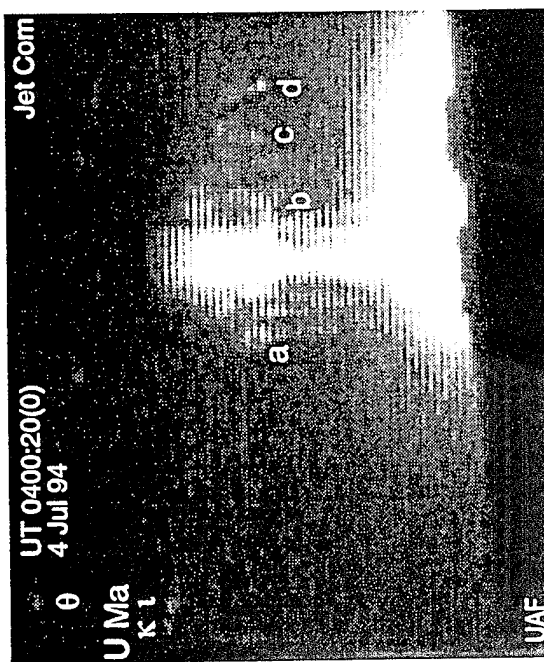
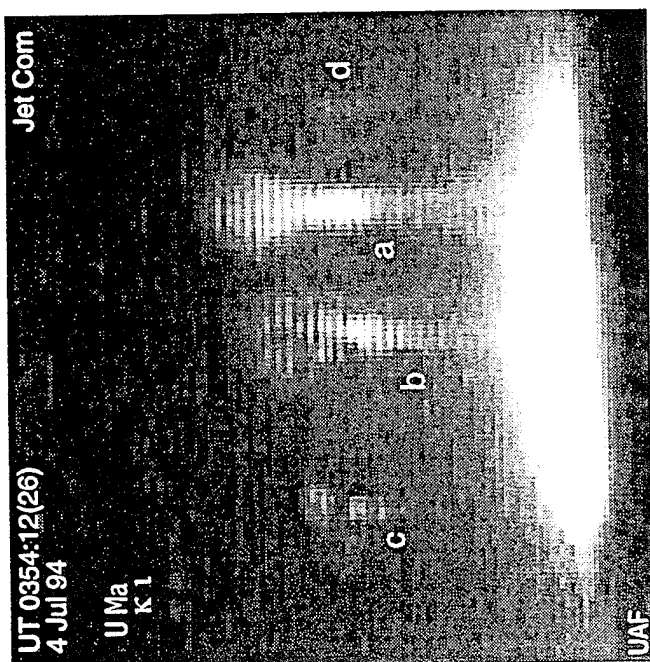
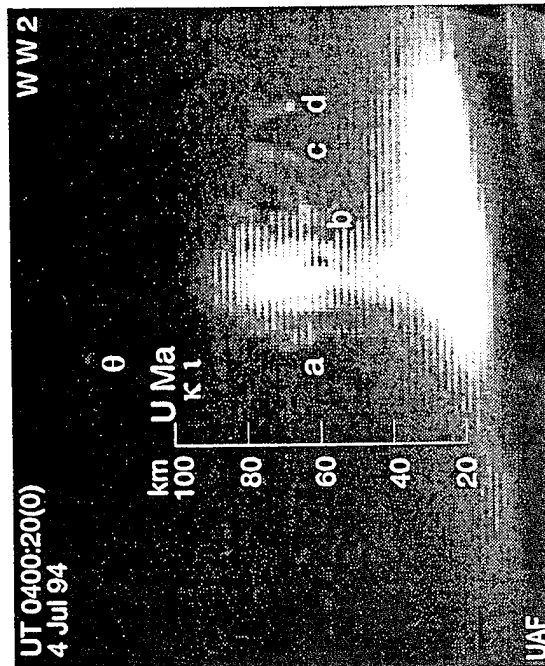
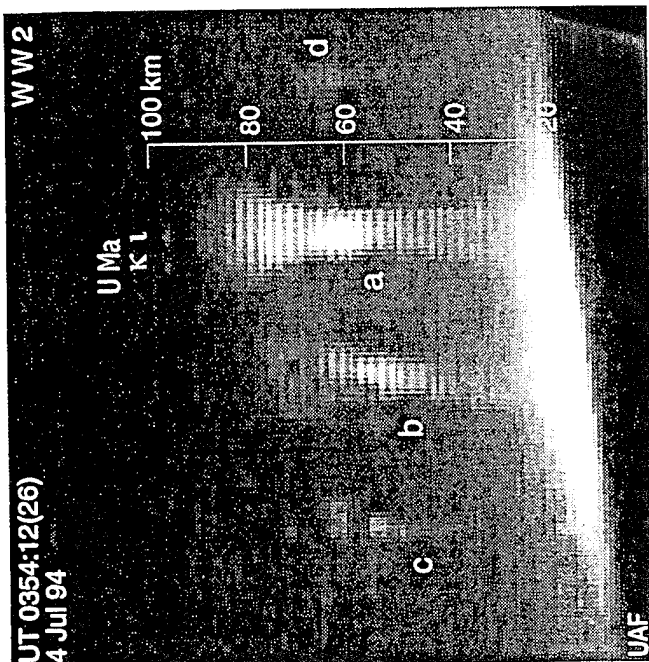
# University of Alaska Aircraft and Ground Campaigns to Observe Red Sprites and Blue Jets

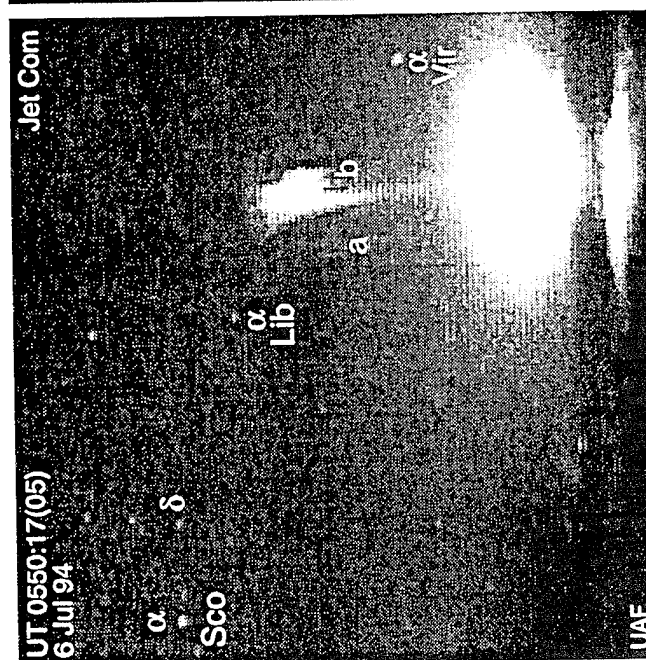
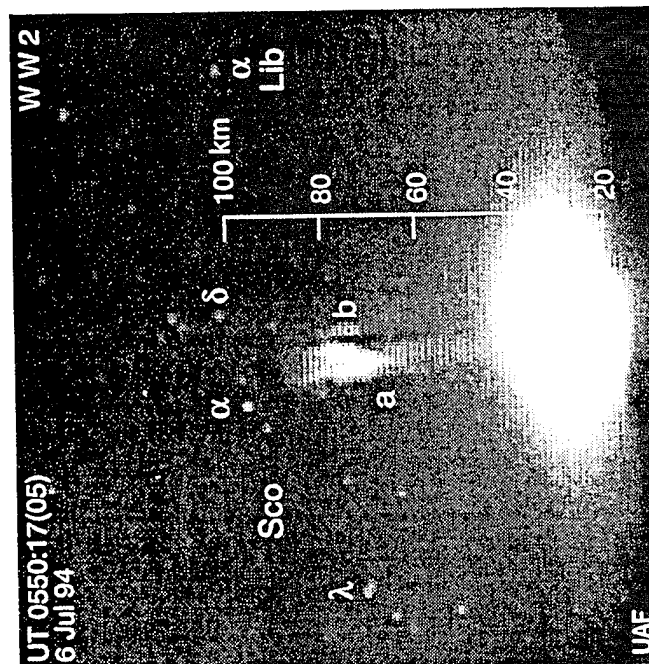
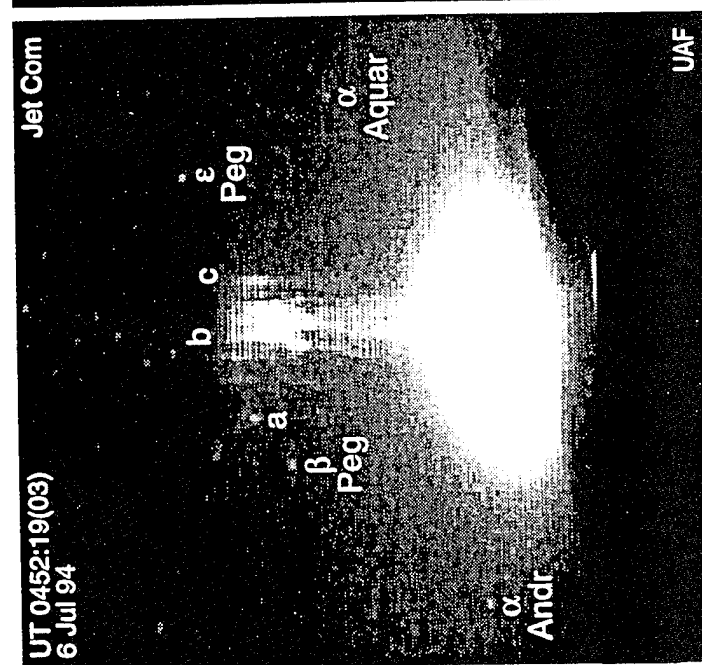
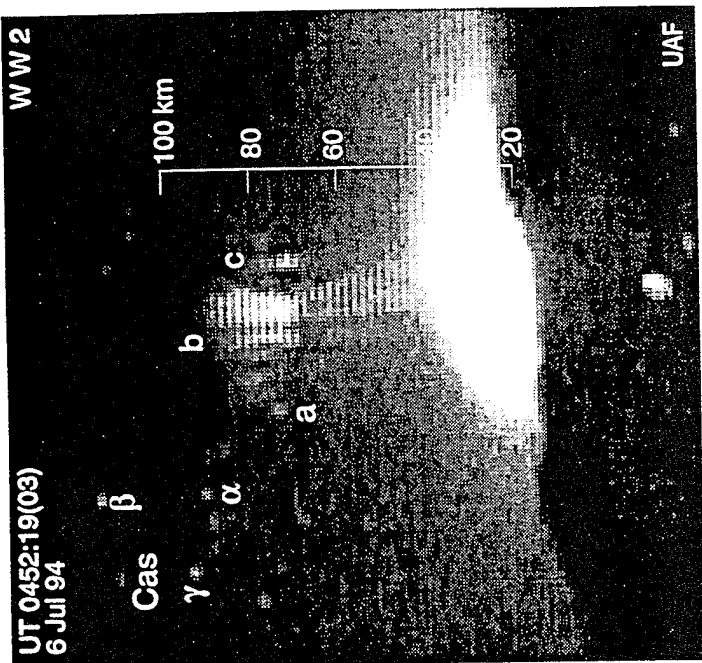
D.D. Sentman and E.M Wescott

- Brazil93 A/C Campaign: Andes/Amazon
- Sprites94 A/C Campaign: Midwest Low/High Plains
- Peru95 A/C Campaign: Peru, Brazil, Bolivia
- Panama95 A/C Campaign: Central America, Colombia
- Gasp95 Ground Campaign: Colorado, High Plains



# Sprites94 Aircraft Campaign





100 — km

80

60

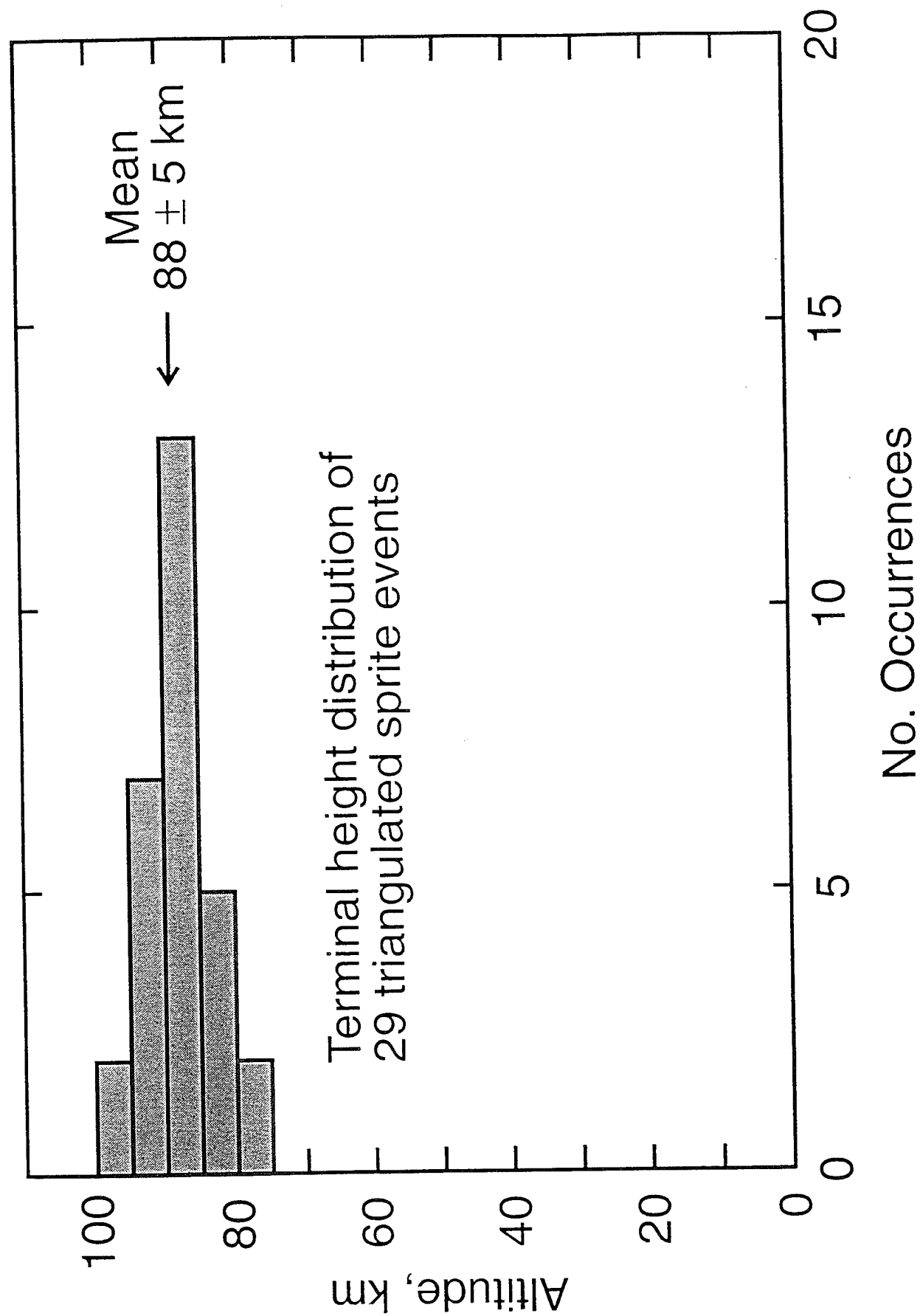
40

20

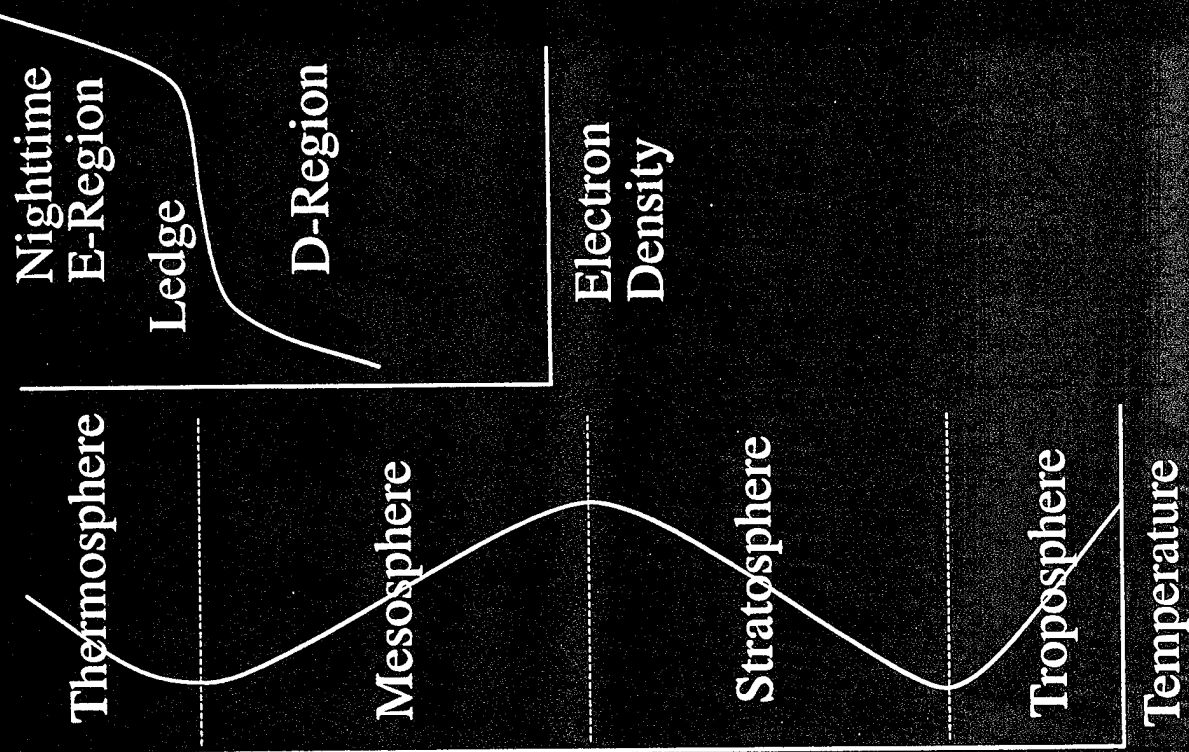
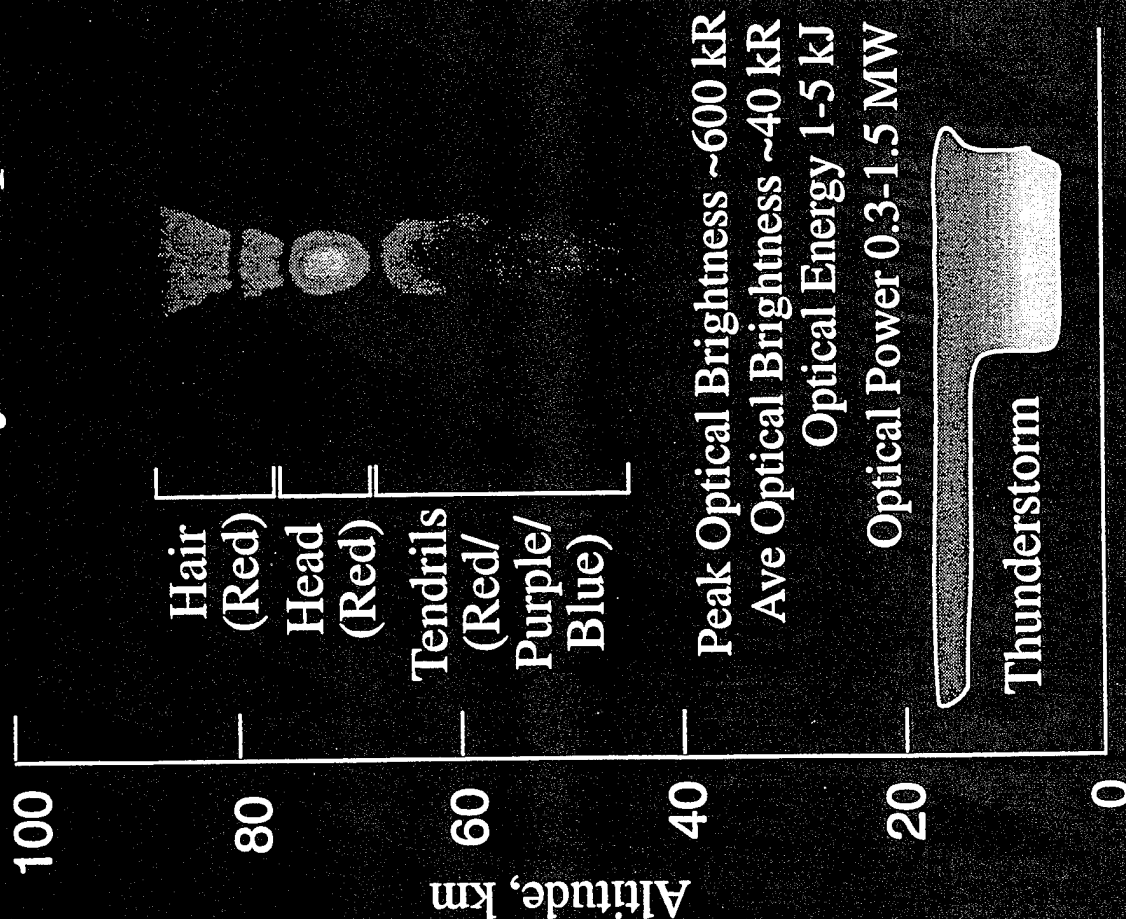
UT 0400:20(0)  
4 Jul 94

W W 2

UAF

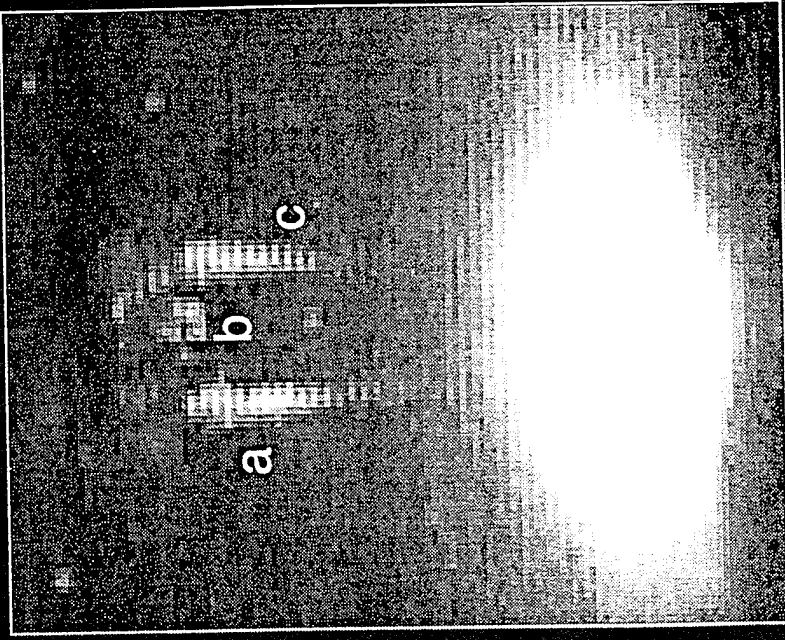


# Anatomy of a Sprite



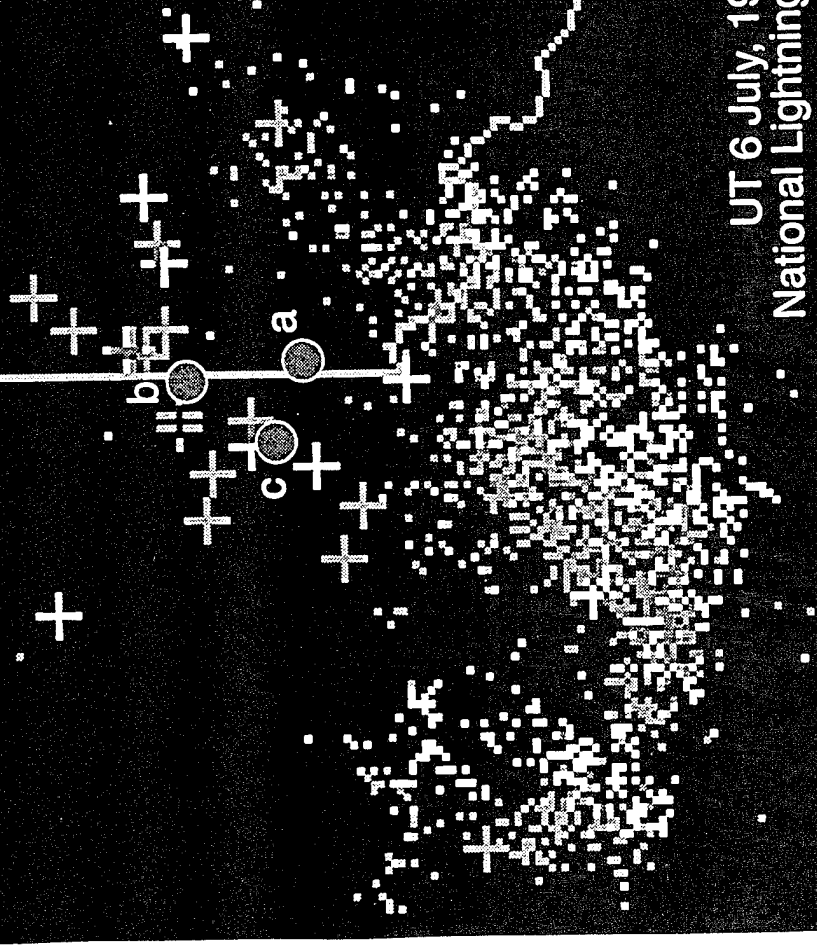


UT 0529:52(25)



Oklahoma

Texas



UT 6 July, 1994 0440-0540  
National Lightning Detection Network

# Perú95

Aircraft Observations of Sprites Over Western Amazonia

University of Alaska Sprite Observation Campaign



## Rationale for the Peru95 Sprites Campaign

Using low light level television systems, more than 1000 instances of upper atmospheric optical emissions (red sprites and blue jets) were recorded above thunderstorms in the American plains states in the summers of 1993 and 1994. Each observation of sprites and jets was accompanied by simultaneous intense lightning activity in a thunderstorm below. However, it is believed the bulk of Earth's atmospheric lightning takes place in equatorial thunderstorm systems, principally in the Amazon basin, the Congo basin, and the extreme western Pacific. Given the differences in the manner in which storm systems evolve in equatorial and midlatitude regions, it is therefore of interest to know if equatorial storms are also the globally dominant sources of sprites and blue jets.

During the Peru95 Aircraft Campaign we investigated sprites over storms in the thunderstorm region believed to be globally dominant. The goals of the Peru95 Aircraft Campaign were to:

- Investigate the occurrence of sprites and blue jets (upper and middle atmospheric optical emissions) above equatorial thunderstorm systems.
- Determine the optical structure and color of sprites and blue jets, and compare with midlatitude observations.
- Obtain optical spectra.
- Investigate their correlation with size and height of thunderstorm systems.
- Investigate possible effects of the equatorial ionospheric magnetic field.

## Peru95 Sprites Campaign

- Observing Platform

Westwind 2 corporate jet aircraft, operated by Aero Air, Inc., Hillsboro, OR  
Typical operating altitude: 39,000-45,000 ft

Cruise speed: 425 knots

Modifications to accommodate instruments

Factory new plastic windows for left/right side viewing ports, aircraft equipment racks, 400-60 Hz power converters, lightning strike finder

- Instruments

Wide angle low light level monochrome television camera system

Dage Model MTI VE-1000 SIT camera  
92 x 68 deg field of view

Intensified color television camera system

Ikegami Model HL-51S, 3 separate red, green and blue SIT subsystems  
Intensified slit spectrograph television camera system

## Peru95 Sprites Campaign Summary

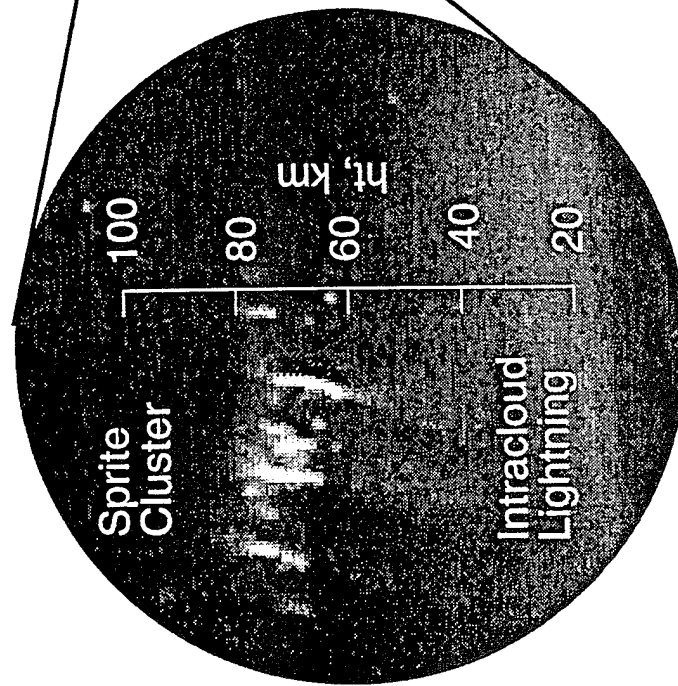
### Data Flights (evenings, Local Time)

- 18 Feb 95 In transit from Brownsville, TX to Lima, Peru. Desultory lightning observed 1 hr north of Lima over Andes. No sprites detected.
- 20 Feb 95 Storms along Andes spine north and south of Lima. No sprites detected.
- 21 Feb 95 Storms in Amazon basin near Iquitos, Peru. No sprites detected.
- 24 Feb 95 Storms between Lima, Peru and Chilean border. No sprites detected.
- 25 Feb 95 Storms in Amazon basin in north-eastern Peru near Ecuador. Three groups of sprites observed.
- 26 Feb 95 Storms over Amazon basin in Peru, Colombia and Brazil. No sprites detected.
- 28 Feb 95 Storms over central Peru north of Lima. Fourteen groups of sprites observed.
- 1 Mar 95 Storms over Amazon basin in Peru and Brazil. No sprites detected.
- 2 Mar 95 Storms over central Bolivia. Three groups of sprites observed.

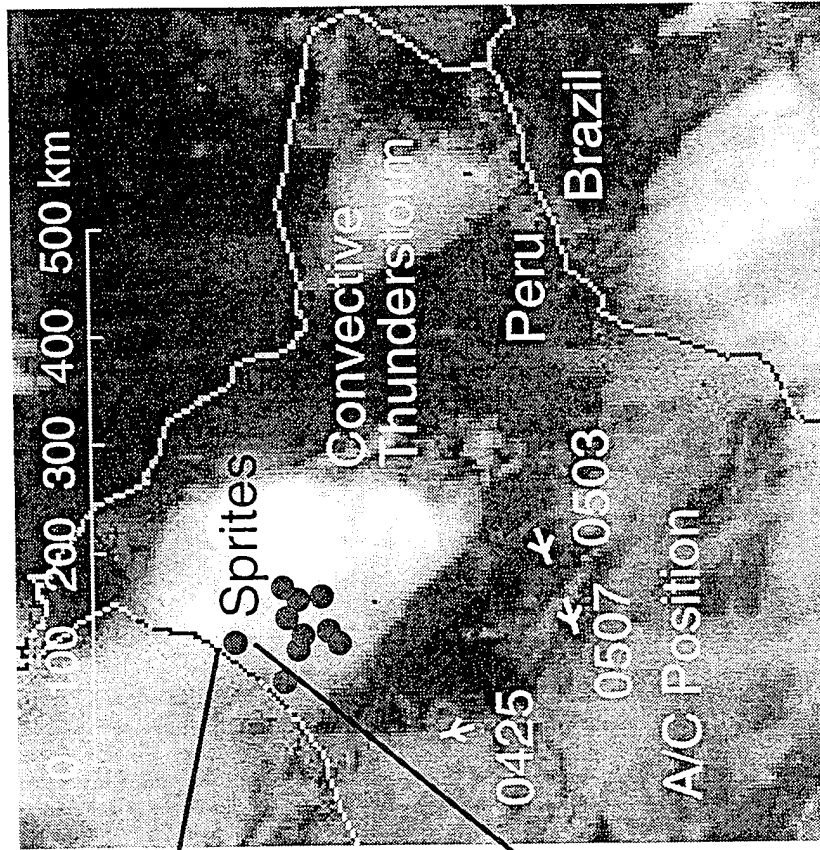
26 February 1995

- The right hand figure shows the region of aircraft operation during an interval when images of 3 groups of sprites were captured, superimposed on a GOES 8 11 micron temperature map of storms in the area, on the first night sprites were observed during the Peru95 aircraft campaign. Dark blue corresponds to +25 C, and white to the approximately -70 C temperature of cloud tops. Regions of thunderstorm activity show up as white blobs. The positions of the sprites, assuming their terminal altitude to be 88 km, are indicated by red dots. The sprites were associated with a moderate sized convective storm system about 200 km diameter in northeast Peru near the border with Ecuador.
- The left hand figure shows a single frame from the low light level TV sequence that captured a cluster of sprites. . The cluster of sprites has a spatial distribution reminiscent of similar clusters of sprites observed over the American midwestern states. Here, the altitude scale has been set to correspond to previously triangulated sprites. Note that the horizontal extent of the cluster is about 50 km.

Aircraft View  
UT 0425:53(16)



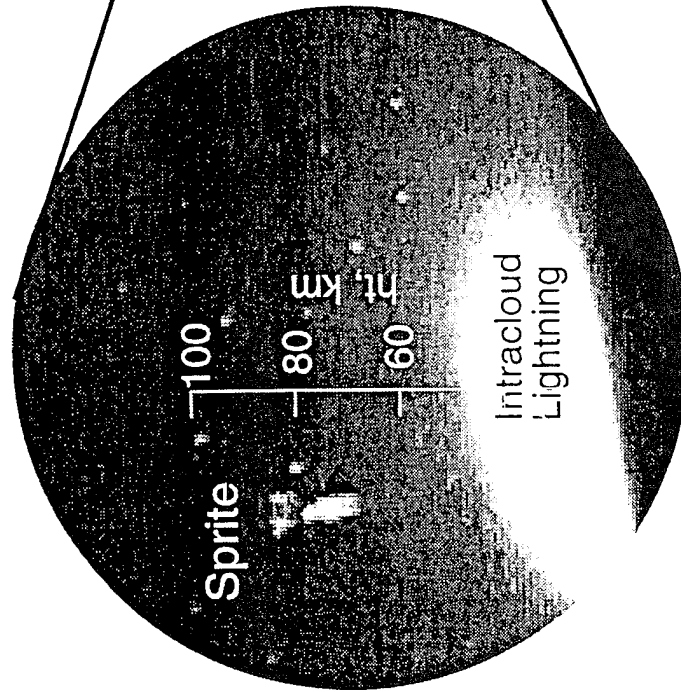
Goes 8 View  
0344 UT, 26 Feb 95  
11 micron IR Temperature



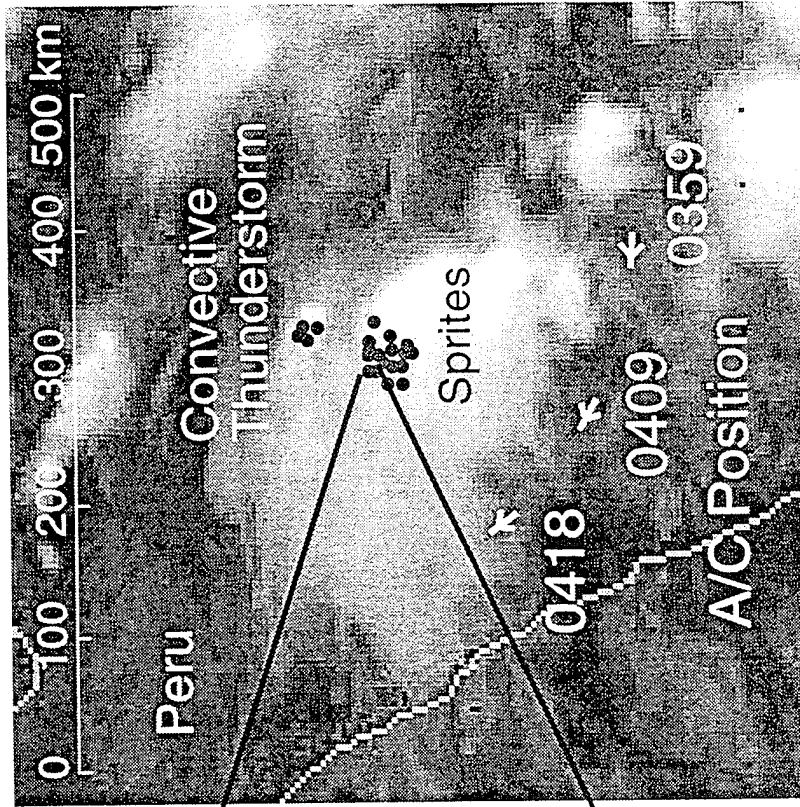
1 March 1995

- The figure on the right shows the region of aircraft operation north of Lima during an interval when sprite images were captured. The image is from GOES 8 11 micron temperature data. Dark blue corresponds to +25 C, and white to the approximately -70 C temperature of cloud tops. Regions of thunderstorm activity show up as white blobs. The positions of the sprites are indicated by red dots. The sprites were observed from two separate regions. The larger region is a convective system about 100-150 km diameter. The smaller convection region has a diameter of about 50 km, much smaller than the minimum size previously thought to be a necessary condition for sprites to occur.
- The figure on the left shows an expanded portion of a single TV sequence that captured a sprite. Note the bright lower part separated from the upper part by a dark band. The altitude scale has been set in the same fashion as in the previous figure.

Aircraft View  
UT 0405:58(13)



Goes 8 View  
0344 UT, 1 Mar 95  
11 micron IR Temperature

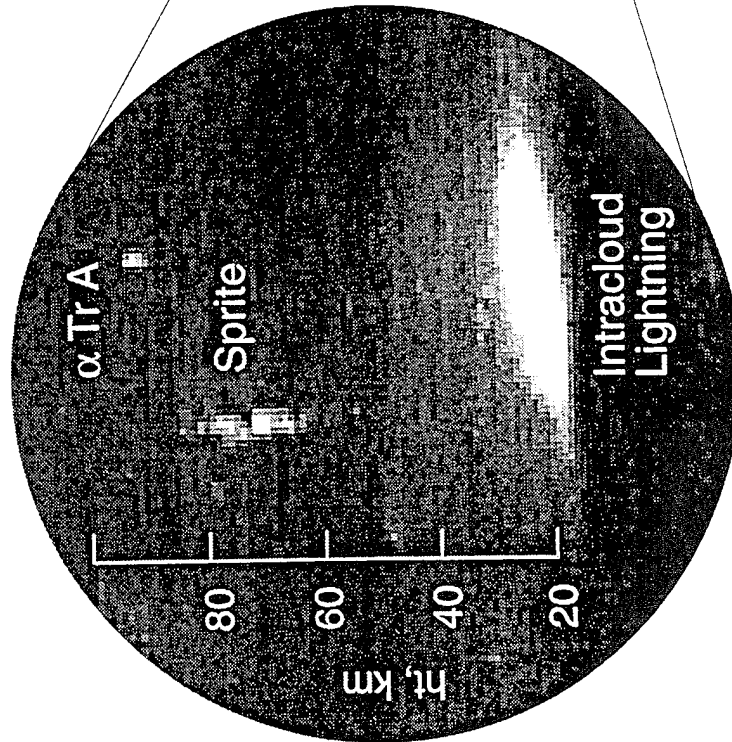


3 March 1995

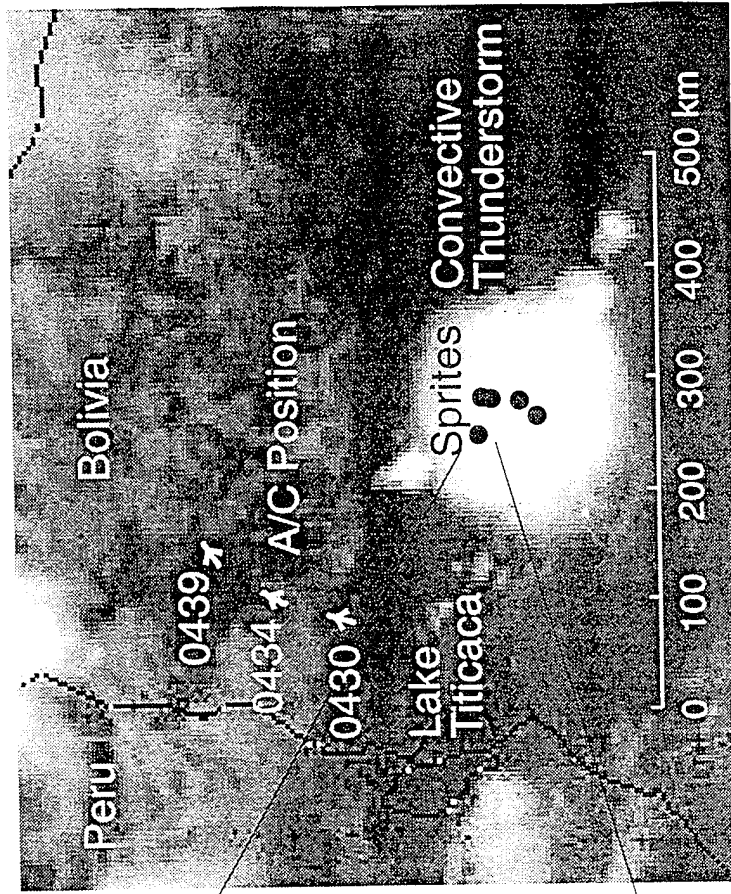
- The right hand figure shows a scan from the GOES 8 11 micron infrared channel that covered southern Peru and west-central Bolivia for the indicated scan time. Coincidentally, we studied the single convective storm system present in this image. The storm system was stationary and nearly circular, with a diameter of approximately 200 km. Here we show the region of aircraft operation superimposed on the infrared weather image. The positions of the sprites are indicated by red dots and are approximately centered on the storm.
- The left hand figure shows a frame from the low light level TV sequence that captured a very tight cluster of sprites. The star labeled here is Alpha Triangulum Australus. The altitude scale has been set in the same fashion as in the previous figures.



Aircraft View  
UT 0439:13(28)



Goes 8 View  
0400 UT, 3 Mar 95  
11 micron IR Temperature



## Conclusions - Peru95 Campaign

- Sprites occur over tropical-equatorial convective thunderstorms, which may be as small as ~50 km in diameter. The sprites appear in coincidence with large lightning discharges in the thunderstorm below.
- South American sprites resemble in color, shape, duration and probable altitude structure the sprites observed over summer thunderstorm systems in the continental U.S. They are also similar in average brightness for the storms studied during Peru95, but none were as bright as some of the very large, tight clusters seen over the continental U.S.
- There does not seem to be any readily apparent effect of the quasi-horizontal orientation of the magnetic field on the vertical structure of the sprites.
- No sprites were detected during five of the eight research flights launched from Lima, although there was lightning in the storms investigated. The rate of sprite occurrence seemed to be much less, relative to the background lightning flash rate, than midwestern thunderstorms.
- No blue jets were detected.

## The University of Alaska Gasp95 Sprite Observation Campaign

- Purpose was to measure optical line spectra of sprites.
- Operated slit spectrograph and high resolution, low light level scene camera from top of Mt. Evans, Colorado.
- Principal results: In late June, obtained first sprite spectra. High quality spectra were measured for about a dozen events. The red color of sprites comes from the 1st positive bands of neutral N<sub>2</sub>.

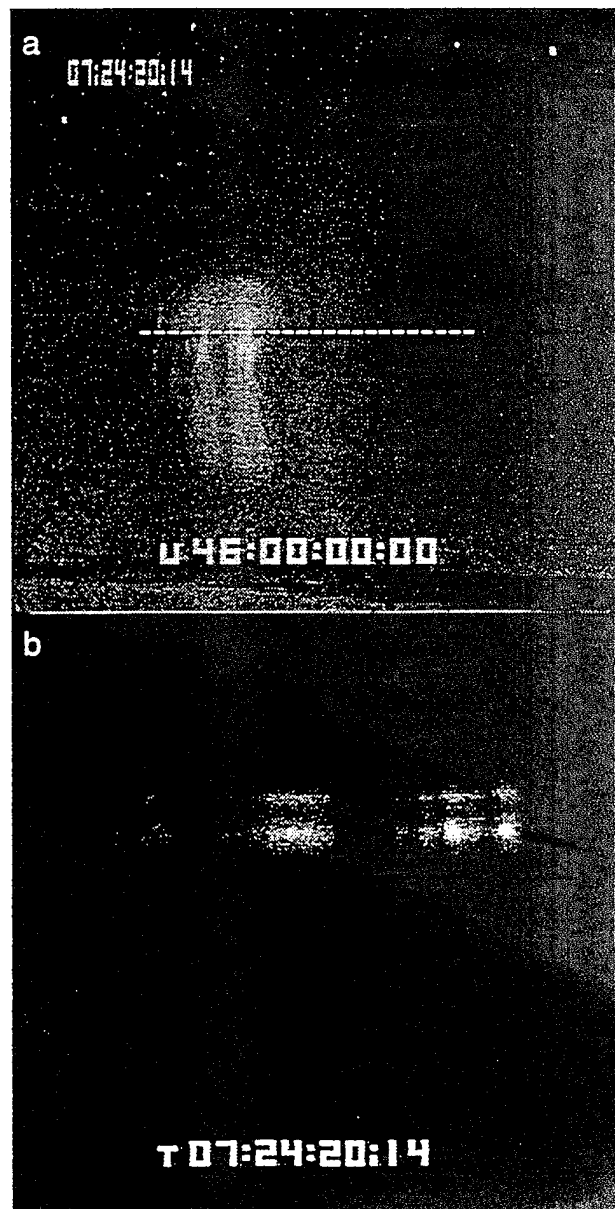


Figure 2. Raw digitized video images of (a) the scene camera and (b) the spectrograph. Note the spectrograph image is rotated, in that the slit direction is vertical.

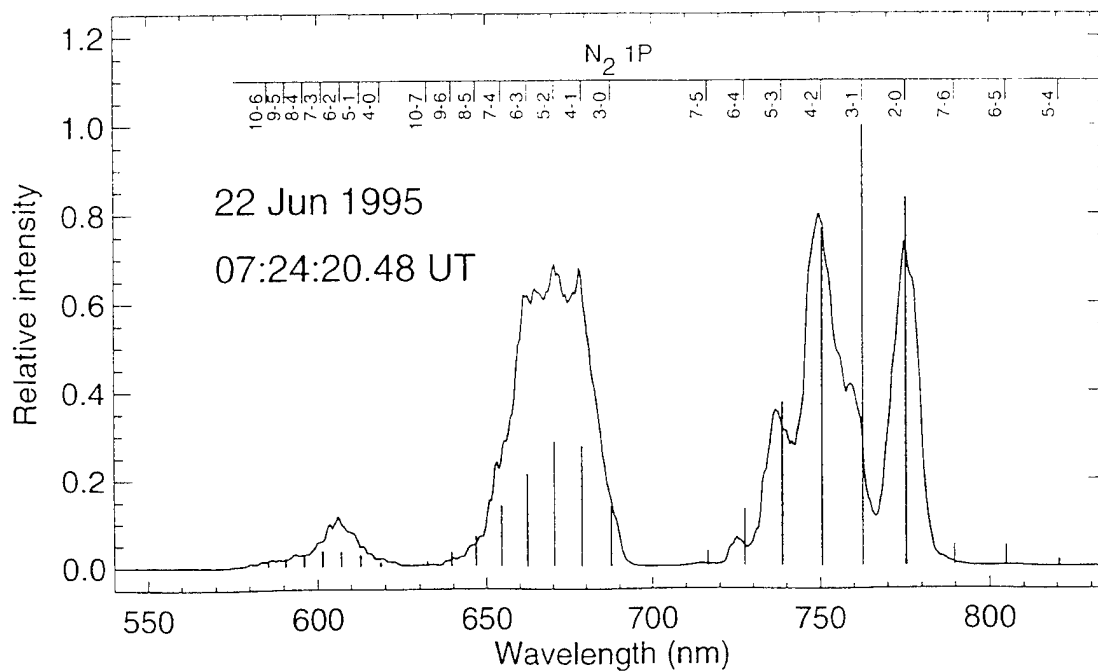


Figure 3. Reduced spectrum from 07:24:20;14 UT. The wavelengths for the band heads for different transitions of the first positive bands of  $N_2$  are marked at top. The vertical lines show the auroral intensities of these transitions

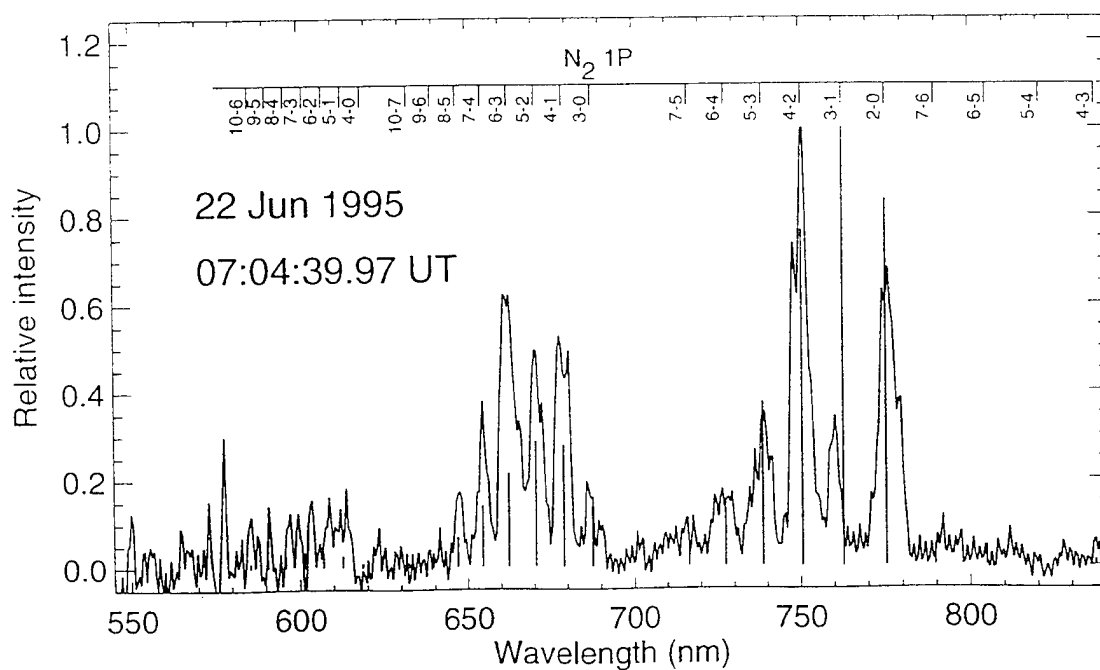
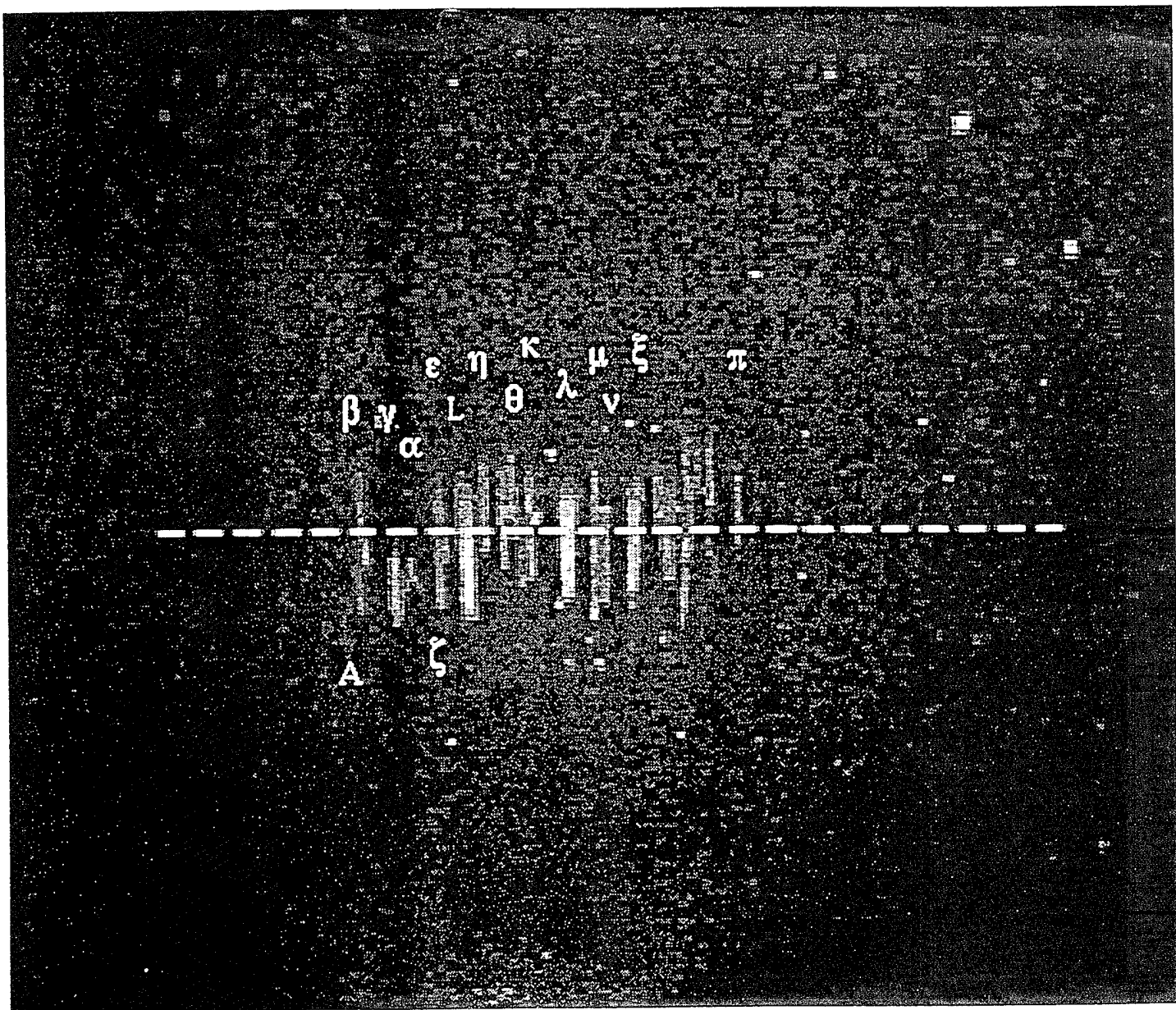


Figure 4. Reduced spectrum from 07:04:39;29 UT. The format is the same as that in Figure 3.



High resolution TV picture, June 19, 1995 from Mount Evans, Colorado showing a group of a different type of sprite. The sprites appear to be very thin (less than 1 km horizontal cross section), and generally seem to be higher than the classic sprite. Tops are at  $86.4 \pm 1.9$  km and the bottoms are at  $76.14 \pm 1.4$  km from 14 triangulated elements.

07:52:45:22

W9E:00:39:34

High resolution TV picture of a large group of sprites which show very clearly that the tendrils show fine dendritic structures, branching downwards. This is proof that the sprites propagate downwards from the core. There is no way that the dendritic structures would start from below and join together as they propagated upward.



07:04:40:10

U49:00:00:00

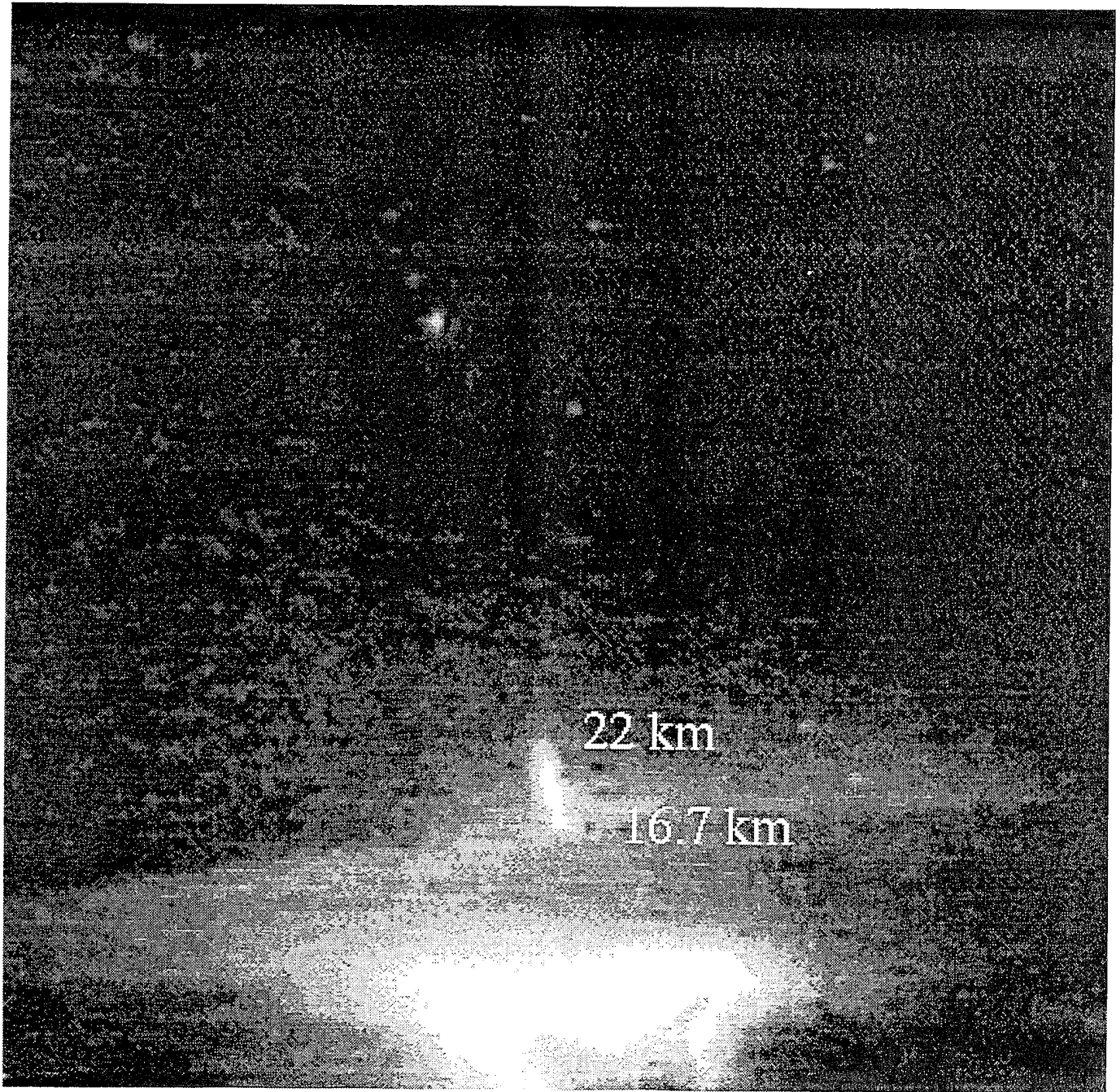
Another high resolution TV picture of a large group of sprites which show very clearly that the tendrils show fine dendritic structures, branching downwards.



# Blue Jets and Blue Starters

Twenty-seven events were recorded from both aircraft during the five minute period 03:04:16.47 to 03:09:29.97 UT. Many were just barely visible above the apparent cloud. The locations of thirteen of the blue starters have been triangulated. Twelve of them arose from one small area near 33.670N, 94.453W with a  $\sigma$  of radius about 3.7 km. The other triangulated blue starter occurred within 1 km of Texarkana.

None of the blue starters was associated with a positive stroke as measured by the lightning network. There were no simultaneous or close in time negative cloud to ground strokes associated with the blue starters either. We have examined this possibility by comparing the distance from the blue starter to the nearest previous stroke in time.



This shows a  $46^\circ$  by  $35^\circ$  portion of a monochrome SIT TV frame at 03:07:55.27 UT of a blue starter which extended upward to 22 km (72,000 ft). The pillar of light is  $7.5^\circ$  off the vertical.

## Blue Jets

- Color: primarily blue.
- Narrowly collimated ( $\sim 15 \pm 7.5^\circ$ ) with an apparent fan out near the top (40 to 50 km).
- Apparent vertical propagation speed:  $\sim 100$  km/s.
- The angle of propagation varies slightly from the vertical, and does not correspond to the magnetic field direction.
- Their apparent source duration is  $\sim 200$  ms at the base of the jet.
- The overall brightness decays simultaneously along the jet beginning at about 200 to 300 ms.
- The estimated brightness near the base ranges up to near 800 kR assuming emissions from the first negative bands of  $N_2^+$  and from the second positive bands of  $N_2$ .
- They are often observed to follow blue starters.
- There is a faint hemispherical "shock" observed beyond the terminus of some jets travelling at the same speed as the earlier rising portion of the jet. If it were a sonic shock it would be at Mach 300.
- The average occurrence rate was  $\sim 2.8/\text{min}$  in the July 1, 1994 storm during the first 22 minutes of observation.
- The estimated energy deposited is about 30 MJ.
- They are not associated with positive cloud to ground strokes, they occur with negative cloud to ground strokes.
- During the Arkansas storm hail 2.75 inches in diameter was observed in the area of the blue starters and jets during the 22 minutes.

## Blue Jets

### Outstanding questions

- What are the actual spectral emissions, optical, IR and UV?
- Is there any detailed structure to the jets not evident in the wide angle images available?
- What is the production mechanism?
  - Cloud to cloud, cloud to ground, d.c. field effect?
  - Particle (electron, ion) beam?
  - Ion fountain?
  - Optical bleaching?
- What is the nature and energetics of the "shock wave"?
- Are there associated ULF/ELF/VLF emissions?
- Are blue jets associated with gamma rays and TIPPS detected from satellites?
- Secondary effects:
  - Stratospheric chemistry?
  - Danger to aircraft?
- Are Blue jets related to the VHS radar echoes reported by *Rumi* [1957]?
- What are the meteorological conditions for creating blue jets, and what is the occurrence rate of blue jets compared to red sprites?

## VHF radar echoes from blue jets.

*Rumi* [1956,1957] described VHF echoes whose characteristics are similar to the optical observations of blue jets. He was operating a 27.85 MHz radar pointed north from Cornell, in a study of auroras, meteors and lightning funded by the U. S. Signal Corps. His observations were limited to the Fall of 1955. Detailed analysis of amplitude vs time displays led him to dissociate many of the echoes from meteors or auroras. He attributed these echoes to "upward discharges" although no correlation with thunderstorms or lightning strokes was made. *Rumi*, [1956] was also operating a 106.6 Mhz radar which was used to deal with lightning strokes. He could clearly distinguish lightning strokes separately. *Rumi*[private communication, 1995] wrote that there was considerable lightning activity north of Ithaca during the Fall of 1955.

*Rumi* [1957] listed the characteristics of the 27.85 MHz echoes as:

1. They are discrete and generally last less than 500 ms.
2. They show no preferred range, the maximum in the absence of aurora was around 900 km.
3. They sometime rise from noise level to maximum in two repetition periods of the radar, or 40 ms. Calculations of the velocity to produce the first Fresnell zone of a column of ionization gives values in some cases greater than 100 km/s. (Meteors with their origin within the solar system have a maximum velocity of 72 km/s.)
4. They usually decay very rapidly in 100 ms. The decay is not exponential (as expected from meteors).
5. They sometimes show a tendency to repeat themselves at the same range.
6. They generally occurred for two hours around midnight, but did not occur every night. During the months of September, October, and November, 1955, they occurred on more than half the nights. Very few were observed during December. As many as 400 echoes in one hour were seen.
7. The columns of ionization do not present a preferred direction (indeed they do not show a preferred range) and disappear at a height of about 50 km.
8. The peak of activity was in October, but there was no correlation with any meteor showers.
9. The appearance of the echoes was not a regular one; nights of complete absence were randomly alternated with very active nights.

University of Alaska campaign results reported to date include:

Sentman, D.D., and E.M. Wescott, Video observations of upper atmospheric optical flashes recorded from an aircraft, *Geophys. Res. Lett.*, **20**, 2857, 1993.

Sentman, D.D., E.M. Wescott, D.L Osborne, D.L. Hampton, and M.J. Heavner, Preliminary results from the Sprites94 aircraft campaign: 1. Red sprites,

*Geophys. Res. Lett.*, **22**, 1205, 1995.

Sentman, D. D. and E.M., Wescott, Red sprites and blue jets: Thunderstorm-excited optical emissions in the stratosphere, mesosphere, and ionosphere, *Phys. Plasmas*, **2**, 2415, 1995.

Wescott, E.M., D.D. Sentman, , D.L Osborne, D.L. Hampton, and M.J. Heavner, Preliminary results from the Sprites94 aircraft campaign: 2. Blue jets, *Geophys. Res. Lett.*, **22**, 1205, 1995.

Hampton, D.L., M.J. Heavner, E.M. Wescott, and D.D. Sentman, Optical spectra of sprites, *Geophys. Res. Lett.*, (in press), 1995.

Inan, U.S., T.F. Bell, V.P Pasko, D.D. Sentman, E.M. Wescott, and W.A. Lyons, VLF signatures of ionospheric disturbances associated with sprites, *Geophys. Res. Lett.*, (in press), 1995.

# Spectral and spatial properties of SPRITE-s

S. B. Mende

*Lockheed*

## Abstract

S. B. Mende, (Lockheed Martin Palo Alto Research Laboratory, 3251 Hanover St., Palo Alto CA 94304; 415-424-3282; MENDE@SAG.SPACE.LOCKHEED.COM)

Imagery and spectra of high altitude luminous flashes, otherwise known as Sprites, occurring in the stratosphere/mesosphere above electrically active cumulonimbus clouds were acquired in the month of July, 1995 from an observation site near Ft. Collins, CO. The spectra, resolved from ~4500-8000 included four spectral features in the 6000-7600 region which have been identified as N2 1PG system with  $dv=2,3$ , and 4 from the  $v=2,4,5,6$  vibrational levels of the  $B^3\Pi_g$  state. The spectra were lacking in other features such as the N2<sup>+</sup> Meinel or the N2<sup>+</sup> 1st neg system indicating that the electron energy causing the excitation is quite low. The absence of other emissions and the spectral profile of the N2 first positive emissions suggests that the observed Sprite did not produce hard electrons. This observation therefore does not support the explanation that Sprites are responsible for generating energetic electrons above thunderstorms. Our spectral observations confirm the previous reports that the Sprites appear red in color. During these experiments images of several sprites were recorded with the wide field imaging camera. Most of the sprites exhibited multiple columns or channels. Light entering the CCD-s frame transfer register showed artifacts on the images which could be used in measuring the temporal behavior of the observed sprites. Evidence was also obtained for short lived broad diffuse airglow enhancements above thunderstorms. The duration of the observed enhancements are less than a single television frame. The enhancements sometimes occur simultaneously with SPRITES detected from the same site. These enhancements are expected to be the same phenomena that was reported from the space shuttle camera observations. Planned future ground aircraft and spacecraft based observations will also be reviewed.

# Spectral and spatial properties of SPRITE-s

S. B. Mende

*Lockheed*

- Lockheed has participated in the Sprites 95 campaign.
- Images were recorded with high detail. Narrow channels seemingly connecting adjacent sprites. Triangulation is needed
- Spectra were recorded and published. The energy content of the sprites are low. Agrees with theoretical predictions of electric field excited discharge.
- High time resolution imaging paper was submitted. Measurements of time interval between lightning and sprite. Duration and timing of adjacent columns.
- Airglow enhancements are being studies. What are the connections between airglow enhancements and sprites?

Space based measurements.

Reasons for space based measurements:

- Latitude longitude survey association with thunderstorm types.
- Wide spectral range UV/IR
- Accelerated particles, X rays etc.

Tether Optical Phenomena (TOP) experiment flight in February 1996  
Repeat are proposed flights. These flights are somewhat similar to the Philips Lab sponsored APE shuttle experiments

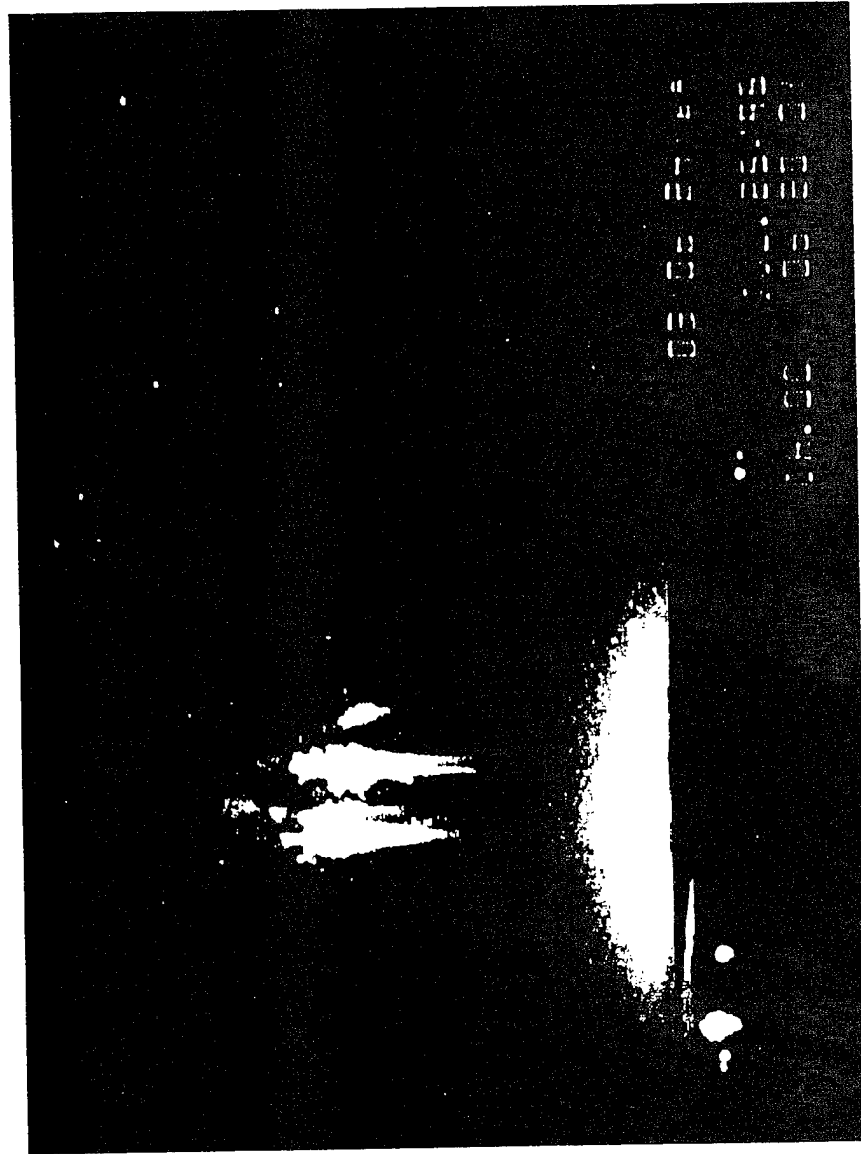


# Spectral and spatial properties of SPRITE-s

Lockheed

S. B. Mende

Image showing the narrow filamentary structure of some Sprites

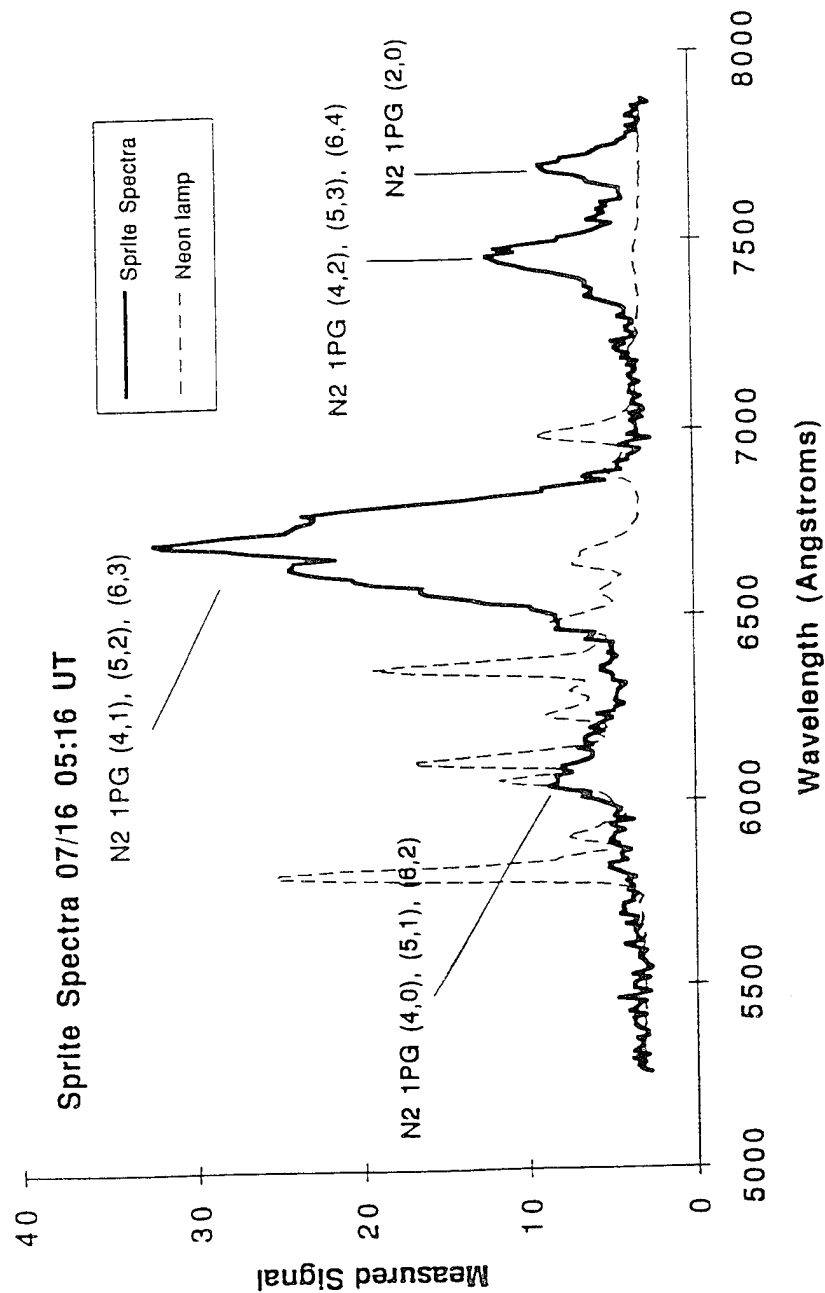


# Spectral and spatial properties of SPRITE-s

S. B. Mende

Lockheed

Spectrum of the Sprite showing enhancement in the N<sub>2</sub> 1 PG system only



# Spectral and spatial properties of SPRITE-s

S. B. Mende

Lockheed

One of the cameras during the Sprites 95 campaign had a light leak into the transfer registers. From the measurement of the resulting ghost streaks the timing of the sprites could be derived.

The following conclusions were derived from this study.

1. The onset of the Sprites occurs 1.5 - 4 ms after the positive lightning flash pre-cursor
2. Each element of a Sprite cluster is initiated within 1 ms of each other.
3. The brightest "core" gains full intensity strength within a period of .3 msec. It generally lasts for 5-10 msec with a decay which is also 5-10 msec.

Tasks ahead:

- Analyze current data
- Repeat observations with improvements:
  - "Tune up" spectrometer
  - Bore sight photometer
  - Triangulated data multiple sights
  - Measurement of altitude propagation
  - Obtain temperature of N2 1st positive
  - Observe in N2 2nd positive

# Spectral and spatial properties of SPRITE-s

Lockheed

S. B. Mende

---

Space based measurements.

Reasons for space based measurements:

Latitude longitude survey association with thunderstorm types.

Wide spectral range UV/IR

Accelerated particles, X rays etc.

Tether Optical Phenomena (TOP) experiment flight in February 1996

Repeat flights which are specifically optimized for studying sprite phenomena are proposed.

## Sprite Spectra; N<sub>2</sub> 1 PG band identification

S. B. Mende, R. L. Rairden, and G. R. Swenson  
Lockheed Martin Palo Alto Research Laboratory, Palo Alto, California

W. A. Lyons  
ASTeR, Inc., Fort Collins, Colorado

**Abstract.** Imagery and spectra of high altitude luminous flashes, otherwise known as sprites, occurring in the stratosphere/mesosphere above electrically active cumulonimbus clouds were acquired on July 16, 1995 from an observation site near Ft. Collins, Colorado. The spectra, resolved from ~4500-8000 Å included four spectral features in the 6000-7600 Å region which have been identified as N<sub>2</sub> 1PG system with  $\Delta v=2,3$ , and 4 from the  $v=2,4,5,6$  vibrational levels of the B<sup>3</sup>π<sub>g</sub> state. The spectra were lacking in other features such as the N<sub>2</sub><sup>+</sup> Meinel or the N<sub>2</sub><sup>+</sup> 1st neg system indicating that the electron energy causing the excitation is quite low.

### Introduction

Direct evidence for coupling from lightning events to the upper atmosphere is found in the optical observation and recording of cloud-ionosphere (CI) discharges or sprites from thunderstorm regions [Franz et al., 1990; Winckler et al., 1993; Sentman and Wescott, 1993; Lyons, 1994; Sentman et al., 1995]. The images of these CI discharges were obtained by ground and aircraft-based, low light level television systems. Morphologically there are probably several distinct types of upward luminous phenomena associated with thunderstorms, the most common of which are the so-called red sprites [Sentman et al., 1995] which have been observed by red sensitive low light level television cameras from the ground and from aircraft. A second class of phenomena, "blue jets", which do not propagate beyond the stratosphere [Wescott et al., 1995] have also been identified. There are however no published spectral measurement of these type of events. Spectral measurements are exceedingly important because they can provide a remote sensing characterization of the physical and chemical processes resulting in the emission. In this paper we are reporting one of the first sets of spectral observations of upward discharge phenomena.

### Observations

The instrument used in our observation is illustrated schematically in Figure 1 from a top view. It consisted of two channel bore sighted intensified CCD video camera system. The optics of the spectrometer channel is a copy of the transmission grating spectrometers used in the shuttle borne

aurora and airglow investigations e.g. Mende et al., [1993]. The spectrograph consisted of an objective lens L1 (f=85 mm F/1.4) which projected the image of the scene on a plate which had a 25 mm long vertically oriented open slit. The slit was widened for the sprite observations and the slit width was approximately 0.3 mm producing an equivalent spectral resolution of about 9 nm. The light from the lens was collimated by L2, a 50 mm F/1.2 lens and diffracted by a transmission grating mounted on the back side of the prism. The prism grating combination (Grism) split the light into divergent beams into a horizontal fan according to wavelength. In Figure 1 three different monochromatic wavelength regions are illustrated as being focused at different part of the detector as  $\lambda_1$ ,  $\lambda_2$  and  $\lambda_3$ . An imaging lens L3 (50 mm F/1.2), focused parallel light rays on the intensifier photo cathode, therefore a given wavelength of light, appeared along a vertical line on the image intensifier photo cathode. The prism was used mainly to steer the light beam back to the center so that the center wavelength of the first order spectra appeared in the center of the image. Note, that the system is an imaging spectrometer and the distribution of luminosity of the image in the direction parallel to the vertical slit is preserved providing true vertical intensity profiles of the observed phenomena. The second optical channel the imaging camera was a simple low light level intensified CCD camera with a 50 mm F/1.4 photographic lens producing an approximately 20x15 degree field of view image on a 25 mm image intensifier. Both cameras had second generation image intensifiers with extended red S-20 photo cathodes. The image intensifiers were fiber optically coupled to the CCD-s. Both video cameras were scanned at standard video rates at 30 frames per second. The video signals were recorded on VHS video tape with suitable time codes marked on each video frame. The spectral responses of both channels were determined through calibration using light sources of known spectral profile. The imager sensitivity peaked at 490 nm dropping off uniformly and quite rapidly towards the blue/UV region to reach 25% sensitivity at about 400 nm. Towards the red it dropped off more gradually reaching the 25% sensitivity point at around 800 nm. The spectrometer had a similar S-20 detector but the grating blaze favored the red region putting the overall sensitivity peak at around 630 nm. The response dropped off quite symmetrically in either direction reaching 25% of peak sensitivity at 450 and 760 nm.

Both instruments were mounted on an azimuth and elevation mount. The bore sighting of the camera and spectrograph were pre calibrated using star images. This allowed the precise determination of the spatial position of the spectrograph slit in the imaging camera field of view and accurate real time pointing of the spectrometer through the imaging camera. This technique also permitted the recording of the two

Copyright 1995 by the American Geophysical Union.

Paper number 95GL02827  
0094-8534/95/95GL-02827\$03.00

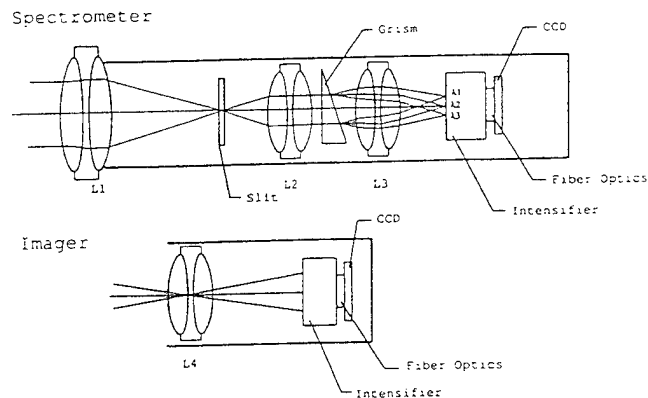


Figure 1. Instrument block diagram of the boresighted imager and spectrograph for Sprite Observations.

dimensional image of the sprite simultaneously with the sprite spectra.

The system was operated at the Yucca Ridge Field Station, operated by ASTeR, Inc. 20 km northeast of Ft. Collins, Colorado. This site provides for nearly unobstructed viewing of sprites and related phenomena to distances as great as 1000 km over the U. S. High Plains (approximately from northwest clockwise through directly south). Several sprite events were detected. On July 16, 1995 conditions were favorable for the observation of sprites although the storms were at some distance from Yucca Ridge. A sprite occurred at 05:16:48.534 UT and a sequence of video frames depicting the sprite is shown on Figure 2. To minimize unwanted backgrounds and nonuniformities a common background frame taken prior to each sprite set was subtracted from each image presented here. The onset of the sprite luminosity was coincident with the start of the underlying cloud illumination and continued for 3 video frames (33 msec each). The first two frames were the brightest with rapid decay in the third frame. The data shows an apparent motion of the luminosity in the westerly direction (towards the left). The far left feature for example on the third frame is actually brighter on the third frame than on the first two.

The storm under surveillance was located near Rapid City, SD, on an azimuth of roughly 25 degrees, and spanned a range from about 400 to 450 km. The radar derived precipitation area associated with the cell was approximately 25,000 km<sup>2</sup>. Given the storm's size, and the presence of positive cloud to ground (CG) lightning flashes, it met the criteria found by Lyons [1995] for mesoscale convective systems over the US High Plains to begin generating sprites.

The sprite morphology was typical of the many observed during the campaign. It exhibited a curtain of smaller vertical striations (8-10) with the brightest portion near the top of the structure with less intense tendrils extending downward. From the star field present in the raw images the angular extent of the sprite could be measured accurately. The horizontal extent was 6.5 degrees, and at the estimated range of 450 km (based on the location of the parent positive CG) this implies a horizontal dimension of 51 km. The upper portion of the sprite extended to about 9.2 degree elevation, and locating the sprite within 25 km of the parent positive CG implies the highest extent to be 90 km. The bottom end of the same sprite was at 74 km. No indication of vertical propagation could be obtained from our low-light level video system operating at 16.7 ms field rate.

The spectral slit was vertical and located very close to the brightest event near the center of the image. On Figure 3 we present the spectrum which was observed simultaneously with the imager of Figure 2. Figure 3 is a spectrum in which the left edge of the image represents the 850 nm infrared region and the right edge corresponds to the blue cut off of the instrument at approximately at 430 nm. In the entire spectral range there were only four features. It is important to note that outside of these features there were no other discernible enhancements in the entire spectral range covered by the instrument. The region, which contained some discernible signal, was digitized. In Figure 3 a white frame marks this region. A spectral plot (Figure 4) was produced by summing vertically across the luminous features of Figure 3 and plotting the results along a horizontal (wavelength) axis. To facilitate wavelength calibration we have superimposed the spectra of a neon calibration light source taken while the instrument was still in position at the field site. Using the features of the neon gas a wavelength scale was determined and added to the figure. The wavelength scale permits the recognition of the major features of the sprite spectra.

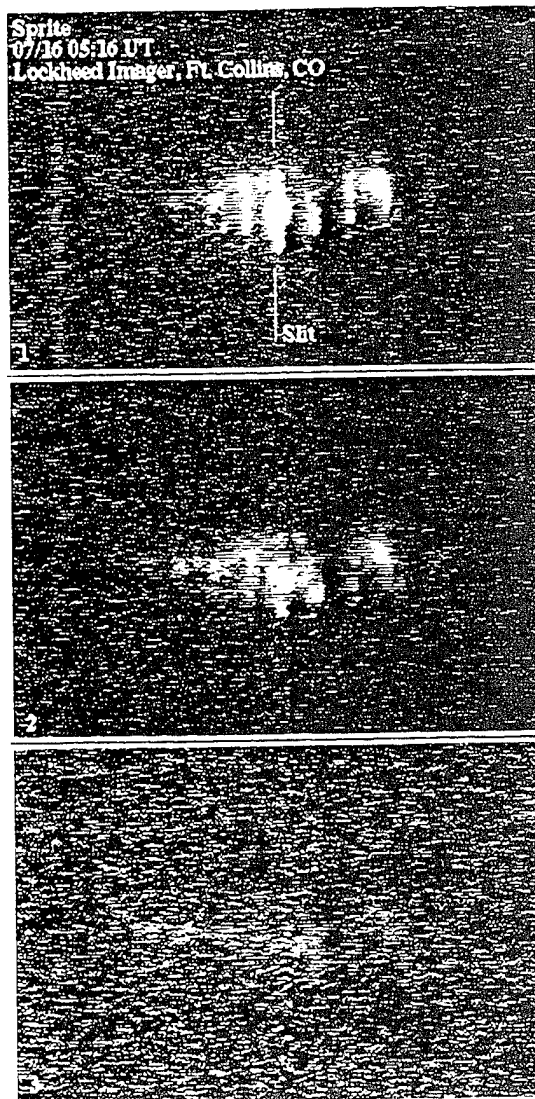


Figure 2. Three consecutive TV frames of the sprite observed with the imaging camera on the 16th of July at 05:16:48.534 UT.

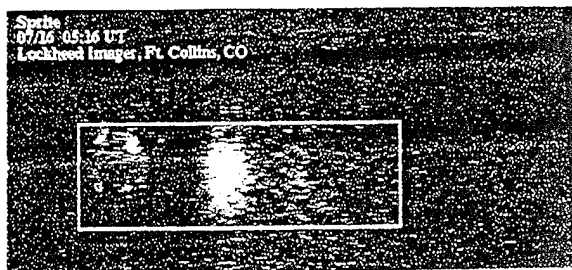


Figure 3. Spectral image or spectrogram of the Sprite event occurring at 05:16 UT. The image covers the wavelength range from 850 nm (left) to 430 nm (right). White frame shows area of detectable signal selected for display on Figure 4.

## Discussion

The processes leading to emissions in the atmosphere by energetic electrons accelerated by electric fields in thunderstorms should be greatly similar to auroral light production. Auroras however do not generally penetrate to 90 km and light in sprites is generally produced at this altitude or lower. Although the atmospheric composition is not drastically different at these lower altitudes increased collision frequencies will quench long lifetime auroral emissions. Thus we expect to see only the fast, permitted transitions. The theory of optical excitation of the atmosphere above thunderstorms and the generation of sprites by quasi electrostatic fields has been discussed by Taranenko et al., [1993] and by Pasko et al., [1995] respectively. Taranenko et al. [1993] have predicted that the  $N_2$  1PG system is the brightest emission feature to occur in lightning stimulated upper atmospheric emissions.

The  $N_2$  1PG system was been positively identified in our sprite spectrum and is shown in Figure 4. Between 760 and 770 the (3,1) component of  $N_2$  1PG is strongly attenuated due to absorption by  $O_2$  at 762 nm at slant path. It should be noted that the instrumental spectral response was not applied to the data presented in Figure 4. The  $N_2$  1PG system is a well investigated emission associated with electron bombardment of the atmosphere by auroral electrons is largely the result of secondary electron impact on atmospheric  $N_2$  as described by Vallance Jones [1974] and Strickland [1976]. Chutjian et al.

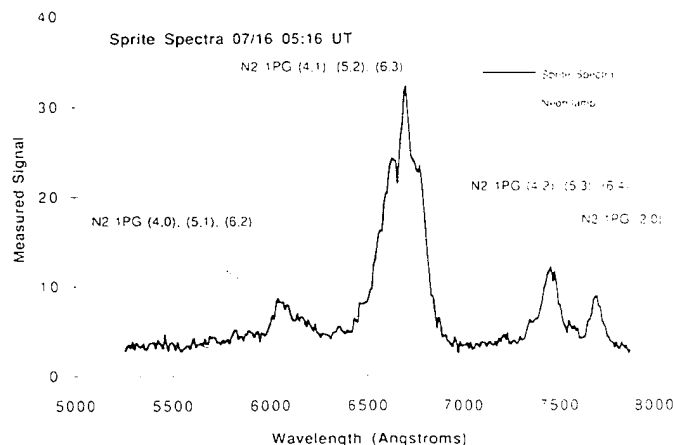


Figure 4. Spectral scan of the image shown in Figure 3. The thick trace represents the spectra of the sprite while the thin trace shows the spectra of a calibration neon light.

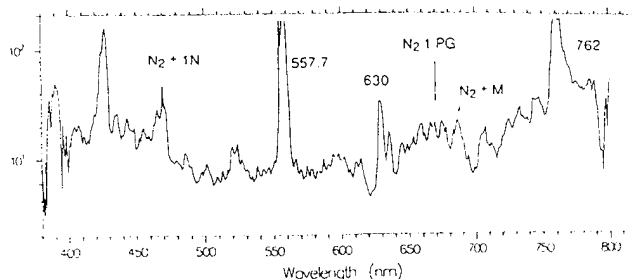


Figure 5. Auroral spectrum taken from the space shuttle. The spectrum was taken with a similar transmission grating image intensified instrument system.

shown the peak of excitation to be near 10 eV with a fast drop off to higher energy with the cross section decreasing by a factor of 15 at 100 eV. In the aurora, it is the large population of secondary electrons produced by primary (keV) electrons which produces the  $N_2$  1PG emission. It is well established that the lifetime is 6-8  $\mu s$  [Nicholls, 1969], and that with known quenching rates, the emission is not visible below ~50 km as a result of the collisional frequency with known quenching species [Vallance Jones, 1974].

In the case of the sprite spectra, the  $N_2$  1PG system was the only emission detected. In the spectral range of the instrument (430 - 850 nm) no other features were detected above instrument noise background. If electrons with energies higher than 20 eV had been produced by the sprite, then  $N_2^+$  emissions would have been present. For example in aurora where higher energy electrons are available several  $N_2^+$  emissions features are significant. Some of these emissions have very short lifetimes and would not be quenched significantly at sprite altitudes down to 50-60 km. In auroral spectra at about 690 nm there is a strong contribution of the  $N_2^+$  (3,0) Meinel band (See for example spectra presented by Vallance Jones [1974 page 83]). This feature is missing from the spectra presented in Figure 4. The absence of this feature indicates that the electrons in the sprite had insufficient energy to efficiently ionize the nitrogen. Several other features were also missing from the sprite spectra which are characteristic of normal auroral spectra. The same type of instrument was flown on the space shuttle and several auroral spectra had been taken for example on mission STS-45. We have included one of these spectra for comparison as Figure 5. These spectra give us direct one to one comparison between the Sprite spectra and the auroral spectra as observed by the same instrument type. If the sprite had contained hard electrons of several keV then we would expect some of the auroral fast transitions to take place. The shuttle based instrument detected strong 427.8 and 470.9  $N_2^+$  emissions. Although 427.8 nm emissions was just outside of the wavelength range of the ground based instrument one would have expected to see  $N_2^+$  first negative at 470.9 nm which, when observed in aurora is stronger than the  $N_2$  1PG bands in the 650 and 680 nm range. In Figure 5, apart from the well known auroral features such as 427.8, 557.7, 630 and 636.4 and the 762 airglow band, we can distinguish four peaks between 650 and 700 nm. The three on the left are the  $N_2$  1PG (4.1), (5.2) and (6.3) components. The fourth peak is a combination of the  $N_2$  1PG (3.0) and the  $N_2^+$  Meinel (3.0) where most of the intensity is produced by the ionized Meinel contribution in aurora suggesting the absence of such emission in the sprite. Note that the  $O_2$  atmospheric (0,0)

band at 762 nm is a strong emission band in the topside auroral spectra whereas it is a dark absorption feature in the ground based sprite spectra. The relatively poor signal to noise ratio of our measured spectra coupled with the decreasing sensitivity of the instrument and the larger scattering of the slant range atmosphere in the blue spectral region probably accounts for the absence of the  $N_2$  2nd positive bands in our spectra. Our observations therefore could be consistent with the intensity ratio of 7 between the two bands as predicted by Taranenko et al. [1993]. There remain a number of controversial issues regarding the details of  $N_2$  1PG excitation in sprites. Just as in auroras these emissions can be produced from possible interactions with other  $N_2$  states or  $N(^4S)$  [see Partridge et al. 1988 and Vallance Jones, 1974]. These issues may be enlightened regarding the excitation in sprites through spectral observations in the UV and IR, but the likeliest conclusion is that the electrons in the sprite discharge have energies  $<100$  eV.

## Conclusions

During these experiments several sprite images were recorded with the wide field imaging camera. These sprites were quite similar in appearance to the one described above. Most of the observed sprites exhibited multiple columns or channels similar to the image presented in Figure 2. It should be also noted that there appeared to be a spatial drift of the Sprite phenomena. Most sprites observed by our instrument showed that after the first bright frame the images in the weaker frames were seen to be substantially displaced spatially. Assuming that the range was 450 km the event shown on Figure 2 appears to be displaced by a distance of about 50 km in 1 or 2 TV frames. Thus the speed of propagation of this phenomena was of the order of about 1500 km/sec in the plane normal to the viewing direction.

A bore sighted imaging camera and imaging spectrograph observed sprite events and recorded their spectra. The spectra contains  $N_2$  first positive bands without any discernible contribution from other emissions. The observed spectrum is consistent with predictions of Taranenko et al. [1993] regarding the relative intensity of optical emissions created in this altitude regime. The absence of other emissions in the sensitivity range of the instrument and the spectral profile of the  $N_2$  first positive emissions suggest that the efficiency of hard electron production in the observed Sprite was low. This observation therefore does not support the attempt of Chang and Price [1995] in explaining the observations of energetic electrons above thunderstorms [Fishman et al., 1994]. Our spectral observations confirm the previous reports that the sprites appear red in color.

**Acknowledgments.** The authors are indebted to R. Armstrong of Mission Research for valuable discussions and for assistance in the operation of the instrument during the observation of the reported sprites. The authors are also grateful to Mr. T. Nelson of ASTeR Inc. for providing assistance during the field operations. The Lockheed observations and data handling were supported by a Lockheed Independent Research Program. ASTeR's coordination of the SPRITE'95 project was funded by NASA Kennedy Space Center, SBIR Phase II Contract NAS10-12113.

## References

- Chang B., and C. Price, Can gamma radiation be produced in the electrical environment above thunderstorms?, *Geophys. Res. Lett.*, 22, 1117-1120, 1995.
- Chuijian, A., D. C. Cartwright, and S. Trajmar, Excitation of the  $W^3\Delta_u$ ,  $w^1\Delta_u$ ,  $B^3\Sigma_u^-$ , and  $a^1\Sigma_u^-$  states of  $N_2$  by electron impact, *Phys. Rev. Lett.*, 30, 195, 1973.
- Fishman, et al., Discovery of intense gamma-ray flashes of atmospheric origin, *Science*, 264, 1313-1316, 1994.
- Franz, R. C., R. J. Nemzek, R. J. Winckler, Television image of a large upward electrical discharge above a thunderstorm system, *Science*, 249, 48-51, 1990.
- Lyons, W. A., Characteristics of luminous structures in the stratosphere above thunderstorms as imaged by low-light video, *Geophys. Res. Lett.*, 21, 875-878, 1994.
- Lyons, W. A., The relationship of large, luminous stratospheric events to the anvil structure and cloud to ground discharges of their mesoscale convective system. *Conference on Cloud Physics*, American Meteorological Society, Dallas, Tex., 1995.
- Mende, S.B., G.R. Swenson, S.P. Geller, R.A. Viereck, E. Murad, and C.P. Pike, Limb view spectrum of the earth airglow, *J. Geophys. Res.*, 98, 19,117-19,125, 1993.
- Nicholls, R. W., Aeronomically important Transition Probability Data, *Can. J. Chem.*, 47, 1847, 1969.
- Partridge, H., S. R. Langhoff, C. W. Bauschlicher, Jr., and D. W. Schwenke, Theoretical study of the  $A^5\Sigma_g^+$  and  $C^5\Pi_u$  states of  $N_2$ : Implications of Afterglow, *J. Chem. Phys.*, 88, 3174-3186, 1988.
- Pasko, V. P., U. S. Inan, Y. N. Taranenko, T. F. Bell, Heating, ionization and upward discharges in the mesosphere due to intense quasi-electrostatic thundercloud fields, *Geophys. Res. Lett.*, 22, 365-368, 1995.
- Sentman, D. D., E. Westcott, Observations of upper atmospheric optical flashes recorded from an aircraft, *Geophys. Res. Lett.*, 20, 2857, 1993.
- Sentman, D. D., E. M. Westcott, D. L. Osborne, D. L. Hampton and M. J. Heavner, Preliminary results from the sprites 94 aircraft campaign. 1. Red sprites, *Geophys. Res. Lett.*, 22, 1205-1208, 1995.
- Strickland, D. J., Transport equation techniques for the deposition of auroral electrons, *J. Geophys. Res.*, 81, 2755-2764, 1976.
- Taranenko, Y. N., U. S. Inan, and T. F. Bell, The interaction with lower ionosphere electromagnetic pulses from lightning: excitation of optical emissions, *Geophys. Res. Lett.*, 20, 2675, 1993.
- Vallance Jones, Alistair, *Aurora*, D. Reidel, Hingham, Mass., 1974.
- Westcott, E. M., D. Sentman, D. Osborne, D. Hampton and M. Heavner, Preliminary results from the sprites 94 aircraft campaign: 2. Blue jets, *Geophys. Res. Lett.*, 22, 1209-1212, 1995.
- Winckler, J. R., R. C. Franz, R. J. Nemzek, Fast low-level light pulses from the night sky observed with the SKYFLASH program, *J. Geophys. Res.*, 98, 8775, 1993.

W.A. Lyons, ASTeR, Inc, 46050 Weld County Road 13, Fort Collins, CO 80524.

S.B. Mende, R.L. Rairden and G.R. Swenson, Lockheed Martin Palo Alto Research Laboratory, Dept. 91-20, Bldg. 252, 3251 Hanover Street, Palo Alto, CA 94304. (email: internet: mende@sag.space.lockheed.com; rairden@lockhd.span.nasa.gov; swenson@lockhd.span.nasa.gov)

(Received July 31, 1995; revised September 1, 1995; accepted September 8, 1995.)



**EVIDENCE FOR IONIZATION IN SPRITES**

**$N_2^+(1N)$  4278A EMISSION IN SPRITES '95 CAMPAIGN**

**IMPLICATIONS FOR CHEMICAL DYNAMICS AND RADIANCE**

---

RUSS ARMSTRONG, JEFF SHORTER  
MISSION RESEARCH CORPORATION, NASHUA, NH

WALT LYONS  
MRC/AS<sub>Te</sub>R DIVISION, FORT COLLINS, CO

BILL BLUMBERG, LAILA JEONG  
PHILLIPS LABORATORY, HANSCOM AFB, MA

PRESENTATION AT THE WORKSHOP ON SPRITES AND BLUE JETS

PHILLIPS LABORATORY, HANSCOM AFB, MA

18-19 OCTOBER 1995



Mission Research Corporation

## CHARACTERISTICS OF SPRITES

### ARE SPRITES IMPORTANT FOR CHEMICAL DYNAMICS AND RADIANCE IN THE MIDDLE ATMOSPHERE?

- EMISSION FROM  $N_2^+(1N)$  DETERMINES IONIZATION LEVELS AND RESULTING CHEMICAL DYNAMICS
- CHEMICAL DYNAMICS DETERMINES LEVEL AND PERSISTENCE OF STRUCTURED RADIANCE
- PHOTOMETRIC CHARACTERIZATION ALONG WITH SPECTRAL/SPATIAL INFORMATION REQUIRED
- "QUICK-LOOK" IN SPRITES '95 CAMPAIGN IS THE FIRST PHOTOMETRIC EVIDENCE OF IONIZATION
- RESULTS HAVE IMPLICATIONS FOR INTERPRETATION OF OTHER EXPERIMENTAL FINDINGS
- PRESENTATION OF PRELIMINARY FINDINGS - ANALYSIS IN PROGRESS - SUGGESTIONS WELCOME



Mission Research Corporation

# SOURCES OF OPTICAL EMISSION IN ELECTRIC FIELD INDUCED CS EVENTS

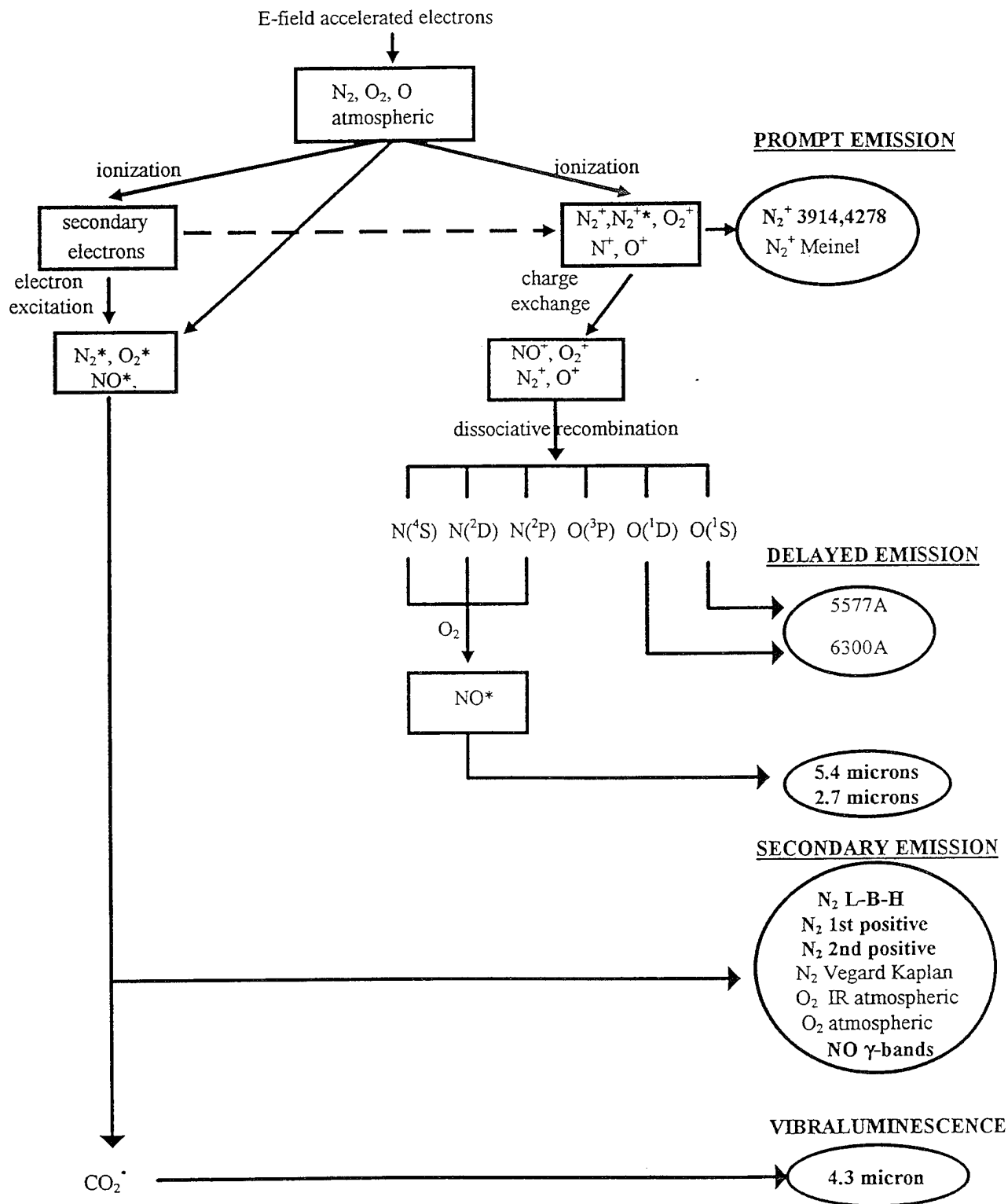


Table 1.  
Characteristic Emission Features for Energized Atmosphere  
(Molecular Band Characteristic Wavelength Refers to ( $v', v''=0,0$ ) band origin)

| Species System  | Characteristic Transition         | Characteristic Wavelength | Radiative Lifetime (s) |
|---|-----------------------------------|---------------------------|------------------------|
| O( $^1D$ ) Red Line                                     | $^1D \rightarrow ^3P$             | 6300A                     | 148                    |
| O( $^1S$ ) Green Line                                   | $^1S \rightarrow ^1D$             | 5577A                     | 0.8                    |
| O <sub>2</sub> ( $^1\Sigma$ ) Atmospheric               | $b^1\Sigma \rightarrow X^3\Sigma$ | 7619A                     | 11.76                  |
| O <sub>2</sub> ( $^1\Delta$ ) IR Atmospheric            | $a^1\Delta \rightarrow X^3\Sigma$ | 1.269 $\mu$ m             | 3.9x10 <sup>3</sup>    |
| O <sub>2</sub> ( $^3\Sigma$ ) Herzberg                  | $A^3\Sigma \rightarrow X^3\Sigma$ | 2856A                     | 3.0x10 <sup>-2</sup>   |
| O <sub>2</sub> ( $^3\Sigma$ ) Schumann-Runge            | $B^3\Sigma \rightarrow X^3\Sigma$ | 2030A                     | 4.2x10 <sup>-8</sup>   |
| N <sub>2</sub> <sup>+</sup> ( $^2\Sigma$ ) 1st Negative | $B^2\Sigma \rightarrow X^2\Sigma$ | 3914A, 4278A(0,1)         | 7.1x10 <sup>-8</sup>   |
| N <sub>2</sub> <sup>+</sup> ( $^2\Pi$ ) Meinel          | $A^2\Pi \rightarrow X^2\Sigma$    | 7200A                     | 1.7x10 <sup>-5</sup>   |
| N <sub>2</sub> ( $^3\Sigma$ ) Vegard Kaplan             | $A^3\Sigma \rightarrow X^1\Sigma$ | 2600A                     | 1.9                    |
| N <sub>2</sub> ( $^3\Pi$ ) First Positive               | $B^3\Pi \rightarrow A^3\Sigma$    | 6700A                     | 8.9x10 <sup>-6</sup>   |
| N <sub>2</sub> ( $^3\Pi$ ) Second Positive              | $C^3\Pi \rightarrow B^3\Pi$       | 4000A                     | 3.7x10 <sup>-8</sup>   |
| N <sub>2</sub> ( $a^1\Pi$ ) L-B-H                       | $a^1\Pi \rightarrow X^1\Sigma$    | 2000A                     | 1.5x10 <sup>-4</sup>   |
| NO( $A^2\Sigma$ ) $\gamma$ -bands                       | $A^2\Sigma \rightarrow X^2\Pi$    | 2275A                     | 2.0x10 <sup>-7</sup>   |

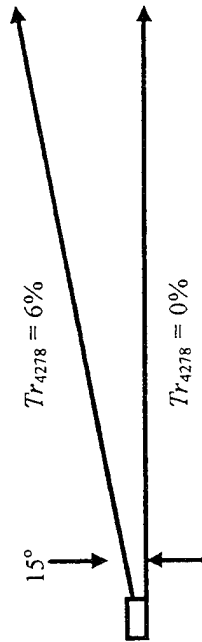


Mission Research Corporation

(BACK-UP)

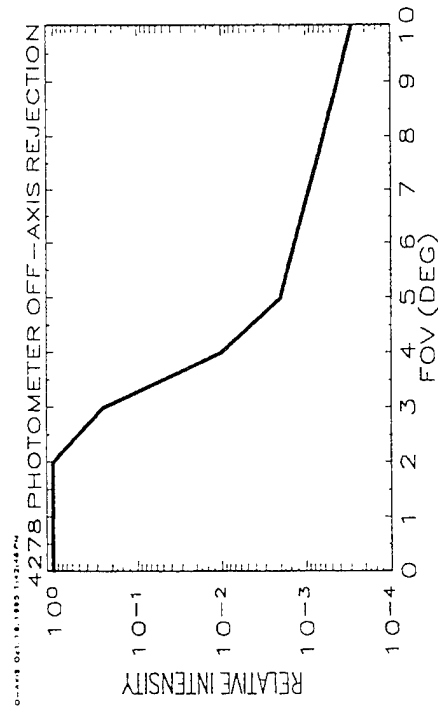
## CHARACTERISTICS OF SPRITES

### DESCRIPTION OF PHOTOMETER MEASUREMENTS



ELEVATION ANGLE PUTS C/L AT  $\approx 80$  KM FOR 300 KM RANGE

PHOTOMETER FOV= $6^\circ$  - FOOTPRINT  $\approx 10$  KM PER 100 KM RANGE



- PHOTOMETER DESIGNED FOR PL EXCEDE III
- APERTURE =  $4.458 \text{ CM}^2$ ,  $A\Omega = 8.559 \times 10^{-5} \text{ CM}^2\text{-SR}$
- DETECTOR RESPONSE N, TIME CONSTANT 80 nS
- DARK NOISE 10 COUNTS  $\text{S}^{-1}$
- QUANTUM EFFICIENCY @ 4278A  $\approx 17\%$
- FILTER 4317A CENTER AT  $\approx 50\%$ , FWHM 106A
- SAMPLE FREQUENCY - 700 Hz

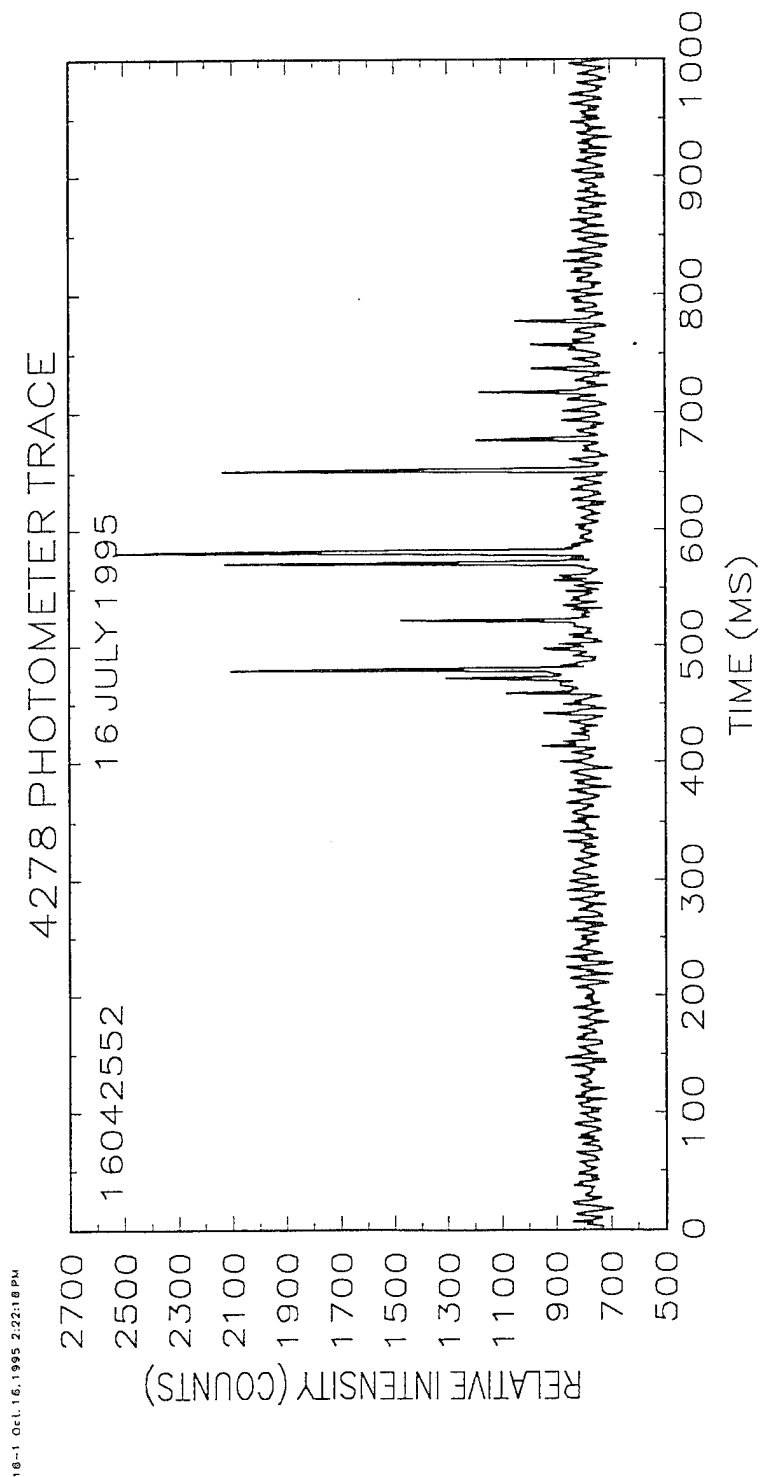


Mission Research Corporation

# CHARACTERISTICS OF SPRITES

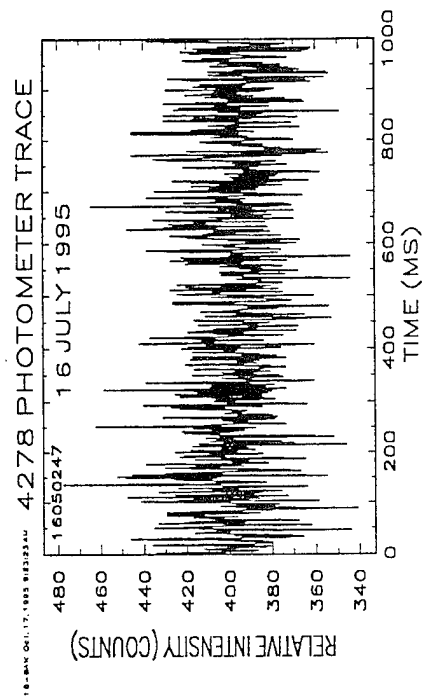
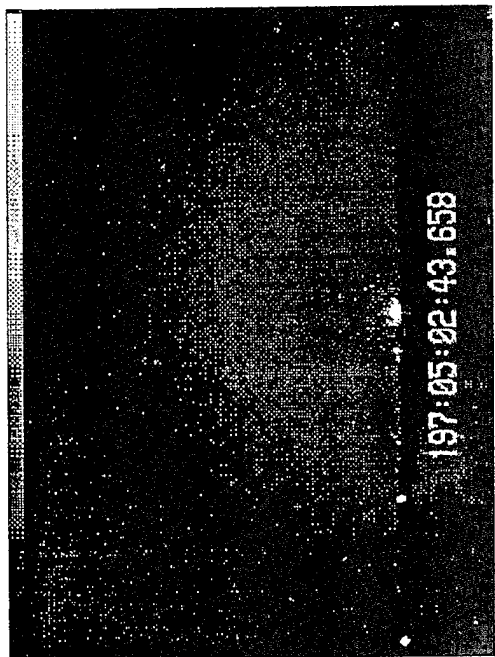
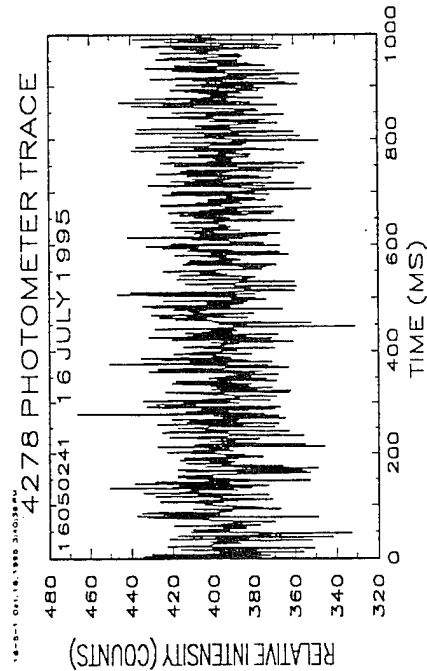
4278A PHOTOMETER RESULTS FOR SPRITES

NORMAL CG/CC LIGHTNING TO SOUTH



Mission Research Corporation

# CHARACTERISTICS OF SPRITES 4278A PHOTOMETER RESULTS FOR SPRITES

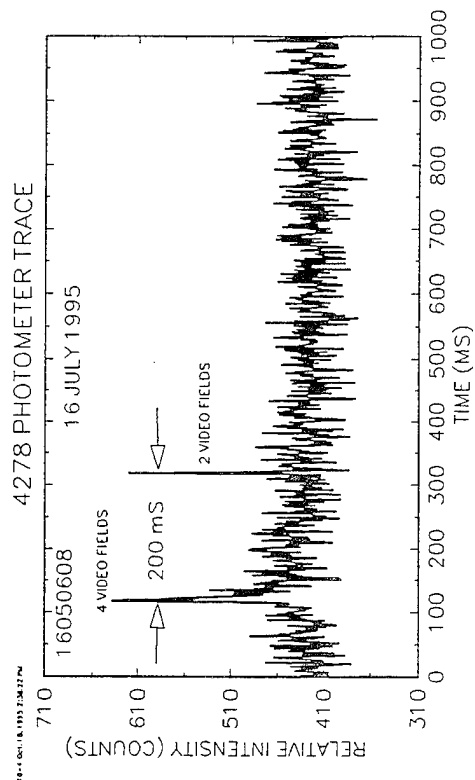


BACKGROUND LIGHTNING DOES NOT YIELD SIGNAL



Mission Research Corporation

# CHARACTERISTICS OF SPRITES 4278A PHOTOMETER RESULTS FOR SPRITES



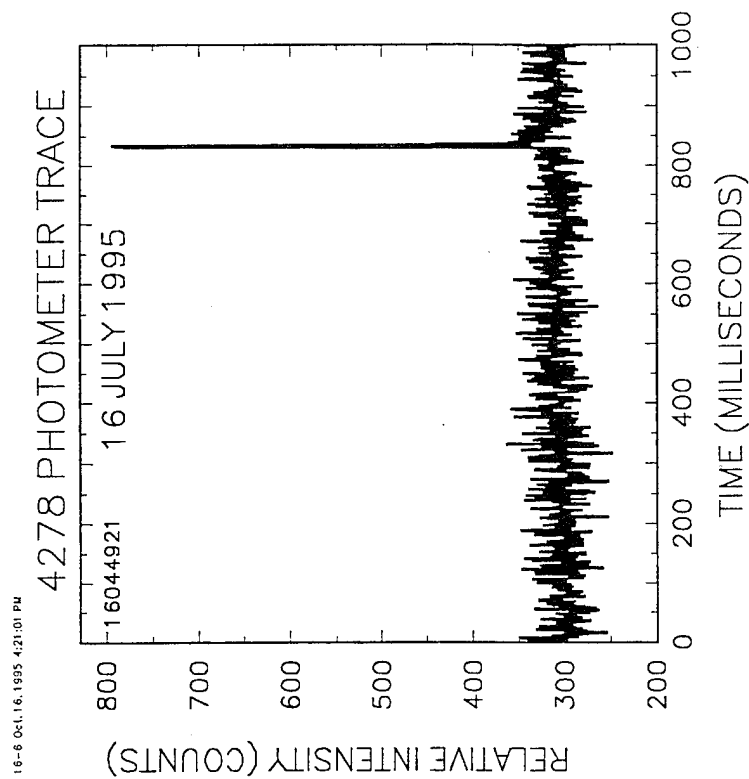
TYPICAL SIGNATURE FROM SPRITE WITHOUT WELL-DEVELOPED TENDRIL STRUCTURE



Mission Research Corporation



**CHARACTERISTICS OF SPRITES**  
**4278A PHOTOMETER RESULTS FOR SPRITES**



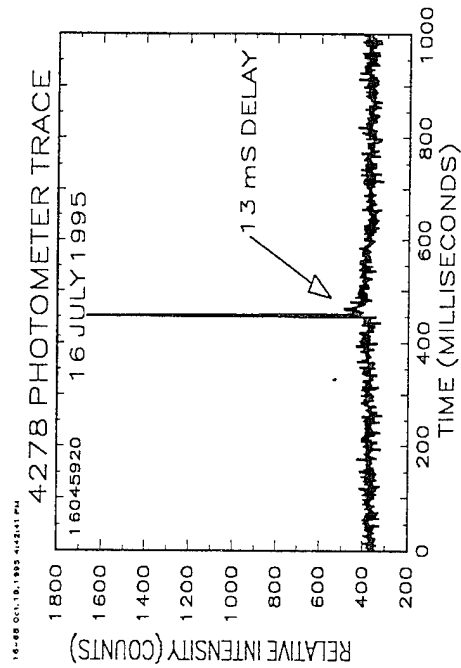
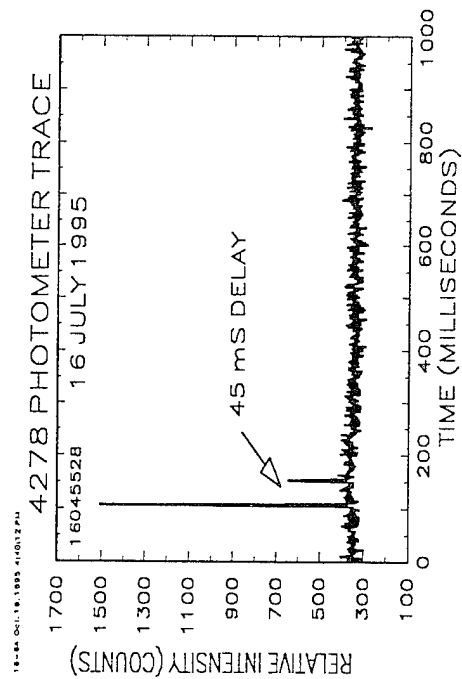
TYPICAL SIGNAL FROM SPRITE WITH WELL-DEVELOPED TENDRIL STRUCTURE



Mission Research Corporation

# CHARACTERISTICS OF SPRITES

## 4278A PHOTOMETER RESULTS FOR SPRITES



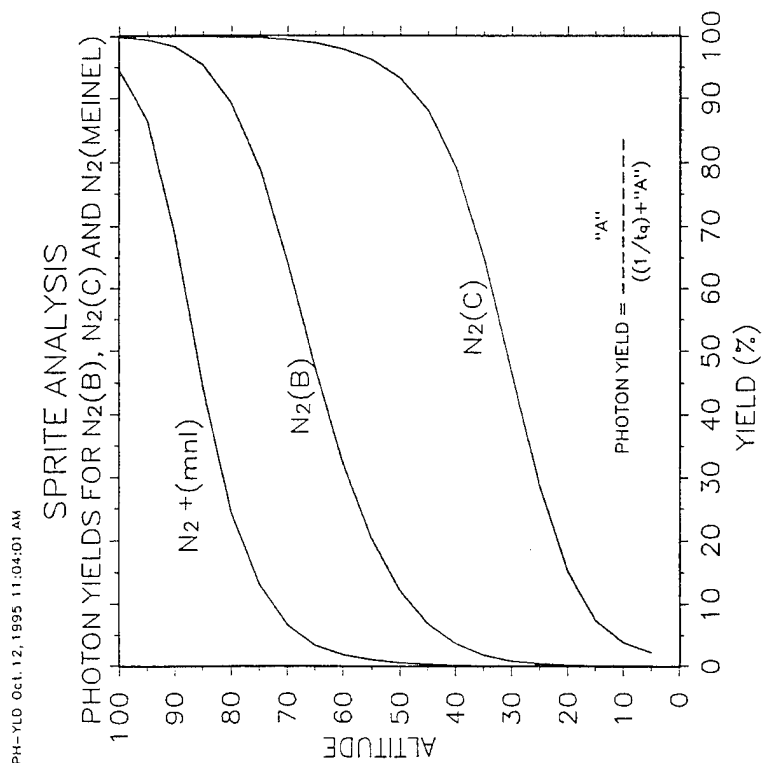
TYPICAL SIGNAL FROM SPRITE WITH WELL-DEVELOPED TENDRIL STRUCTURE AND ELF



Mission Research Corporation

## CHARACTERISTICS OF SPRITES

ATMOSPHERIC QUENCHING CAN BE IMPORTANT



ANALYSIS BY ANALOGY WITH AURORA HELPFUL

BUT

ATMOSPHERIC QUENCHING AND SCATTERING CAN  
PLAY AN IMPORTANT ROLE

THIS MAY EXPLAIN WHY N<sub>2</sub>(1P) NOT DOMINANT AT  
LOWER ALTITUDES

BUT

THIS DOES NOT EXPLAIN WHY N<sub>2</sub>(2P) NOT  
IMPORTANT AT HIGHER ALTITUDES

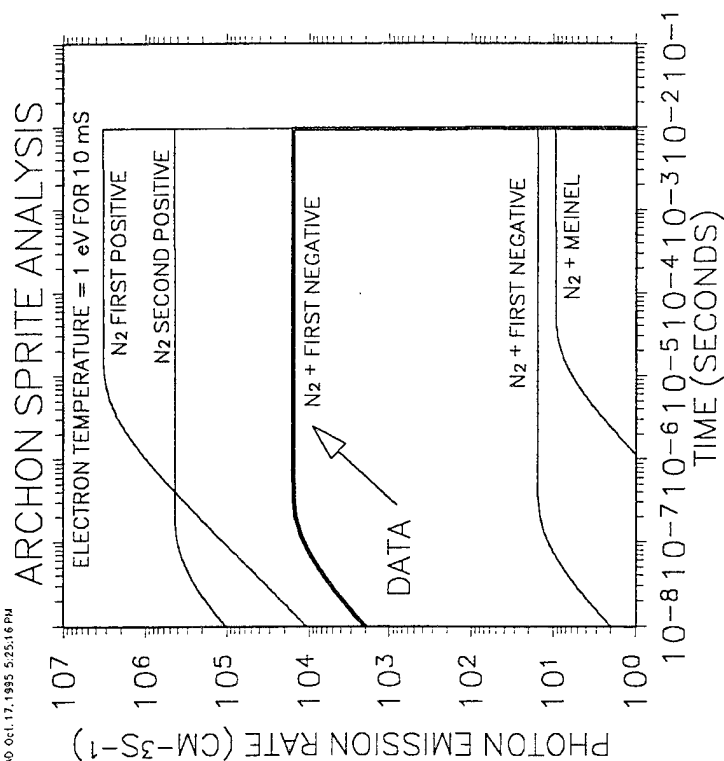


Mission Research Corporation

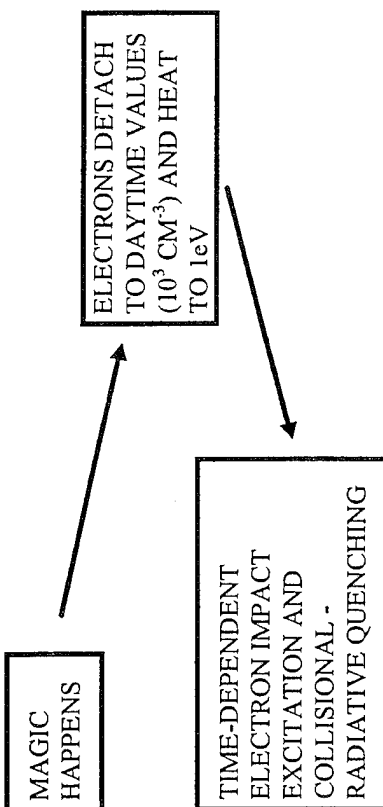
# CHARACTERISTICS OF SPRITES

## ANALYSIS OF "RED" PART OF SPRITE

112\_R40 Oct 17, 1995 5:25:16 PM



QUESTION: CAN LOW ENERGY ELECTRONS MAKE 600 kR N<sub>2</sub>(1P)?



ANSWER: YES - BUT THIS MODEL DOESN'T MAKE PHYSICAL SENSE  
REALITY IS MORE COMPLEX

CAVEATS:

- (1) IGNORES ENERGY INPUT
- (2) E- SPECTRUM NOT LIKELY MAXWELLIAN
- (3) E- "BITE-OUT"



Mission Research Corporation

## CHARACTERISTICS OF SPRITES

### SPRITE MORPHOLOGY (ÁLA SENTMAN)



- ELF - LOWER IONOSPHERIC HEATING - FEW ms PULSE, MEGA-RALEIGH (FUKUNISHI) HIGHLY ENERGETIC APPARENTLY RED AND BLUE
- UPPER PART OF SPRITE (RED) IDENTIFIED AS  $N_2(1^{st} \text{ POSITIVE})$  (MENDE, SENTMAN) CAN POSSIBLY (?) BE EXPLAINED WITH LOW ENERGY/LOW DENSITY ELECTRON IMPACT EXCITATION
- LOWER PART OF SPRITE, BLUE TENDRILS, NOT SPECTRALLY IDENTIFIED - HIGHER ENERGY (PERHAPS "DISCHARGE") - INTENSITY NOT YET DETERMINED
- BLUE JETS IN THIS REGION HIGHLY ENERGETIC ESTIMATED TO BE 500 KR  $N_2(1^{st} \text{ NEGATIVE})$  (WESCOTT)

### IMPLICATIONS FOR CHEMISTRY

THIS SUGGESTS MOST ENERGETIC PROCESSES AT LOWER ALTITUDES WITH RELATED BUT SEPARATE IONOSPHERIC HEATING (TARANENKO, INAN, et. al.)

(Lyons - 1993)

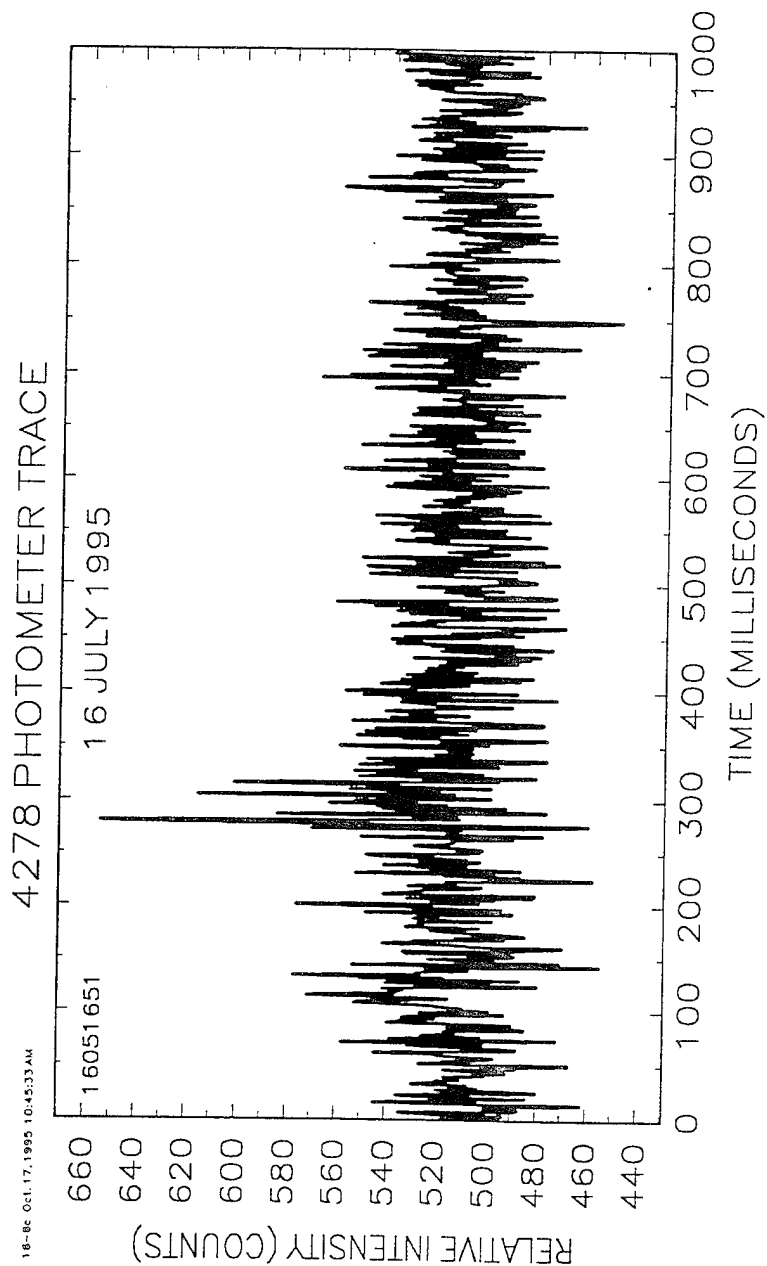


Mission Research Corporation

## CHARACTERISTICS OF SPRITES

### 4278A PHOTOMETER RESULTS FOR SPRITES

#### PHOTOMETER SIGNAL CORRESPONDING TO MENDE'S SPECTRUM



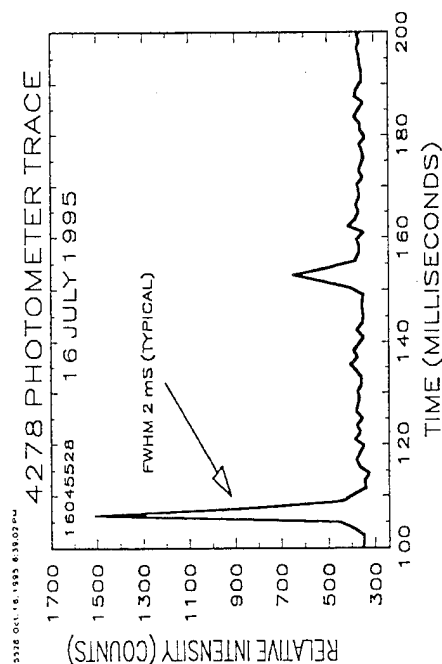
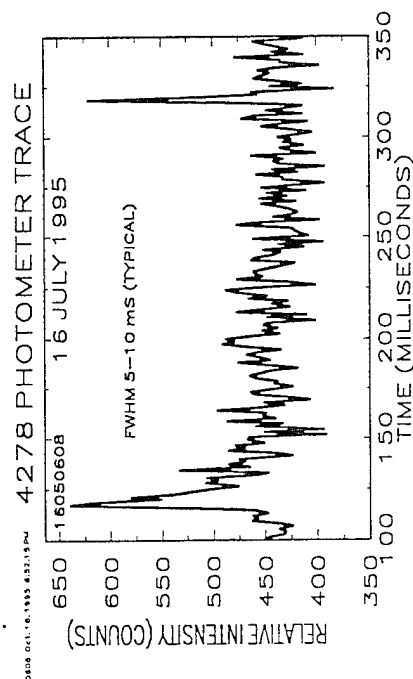
PHOTOMETER POINTING SLIGHTLY TO NORTH - PICKED UP "EDGE" OF SPRITE



Mission Research Corporation

## CHARACTERISTICS OF SPRITES

### SUMMARY OF 4278A PHOTOMETER RESULTS FOR SPRITES



- FIRST DIRECT EVIDENCE OF IONIZATION IN SPRITES
- SUMMARY OF FINDINGS:
  - SPRITES WITHOUT TENDRILS  $\approx$  200-400 COUNTS
  - SPRITES WITH DEVELOPED TENDRILS  $\approx$  800 COUNTS
  - "ELVES" SIGNATURE CHARACTERISTICS CONSISTENT WITH FINDINGS OF FUKUNISHI, 1200-2000 COUNTS
  - OPTICAL SCATTERING AND QUENCHING IMPORTANT
- WHAT'S NEXT?
  - CO-ALIGNED PHOTOMETER WITH VIDEO
  - SPECTRAL IDENTIFICATION REQUIRED



Mission Research Corporation



## *Plasma Physics Division*

# **Optical Instruments Available From NRL**

Carl L. Sieftring, Paul A. Bernhardt, John A. Antoniades

The NRL Plasma Physics Division has two low-light level optical systems that may be of use in ground based studies of Sprite, Elves, and Blue Jets.

- 1) Is a low-light level Near-IR imager ideally suited for monitoring OH emissions. This camera can be used to monitor atmospheric density and temperature changes due to gravity waves and Sprites.
- 2) Is a modular low-light level spectral imager (PHILLS) which covers the entire visible range plus a portion of the NIR and UV. This camera can be used as either a spectrograph or as a streak camera.



NEAR INFRARED CAMERA AVAILABLE FOR OBSERVING  
SPRITES AND RELATED PHENOMENA

P.A. Bernhardt, J.A. Antoniadis, and C. Siefring  
Plasma Physics Division  
Naval Research Laboratory  
Washington, DC 20375-5320

Air Force Workshop on Sprites and Blue Jets  
18-19 October 1995  
Hanscom Air Force Base, MA

## **OBSERVATION OBJECTIVES**

- Modulation of OH ( $\Delta v = 2$ ) Nightglow During Lightning  
Atmospheric Heating  
Gravity Waves
- Excitation of Stratospheric and Mesospheric OH During Sprite  
Events
- Survey of Near Infrared in the Stratosphere/Mesosphere Over Storms

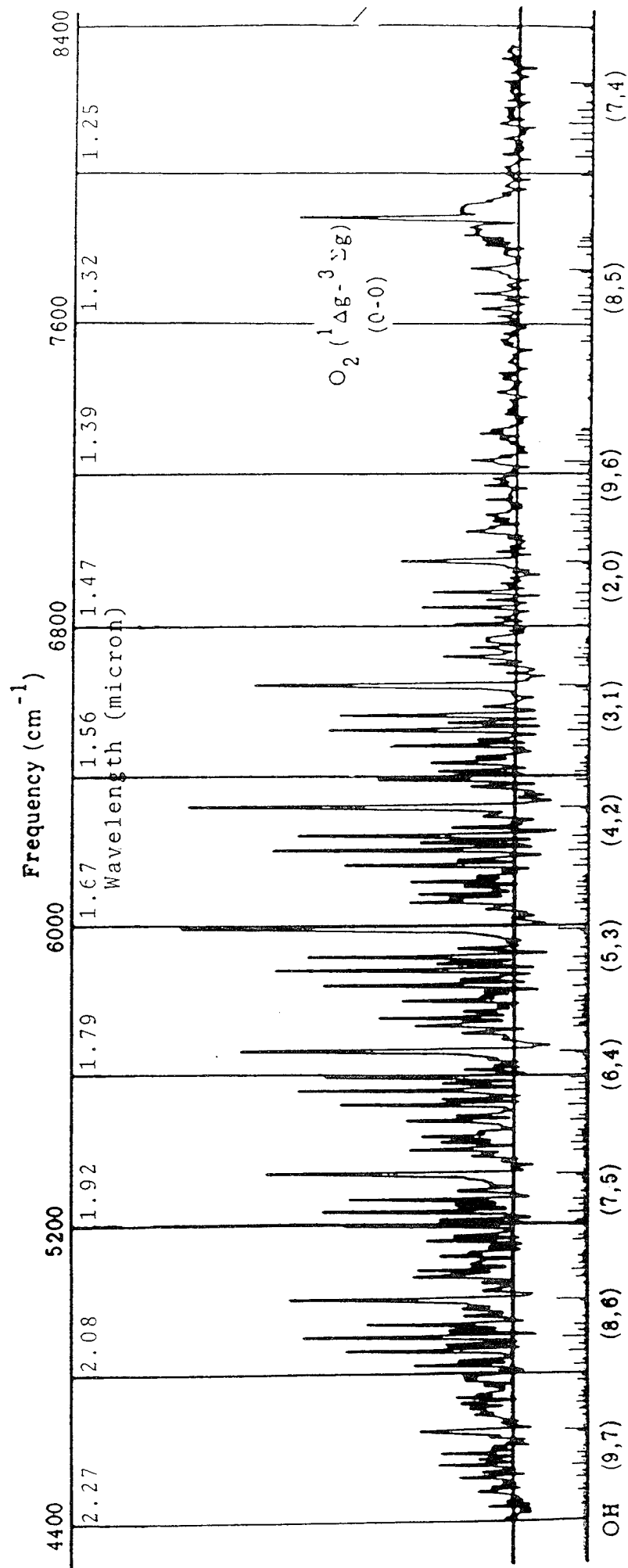
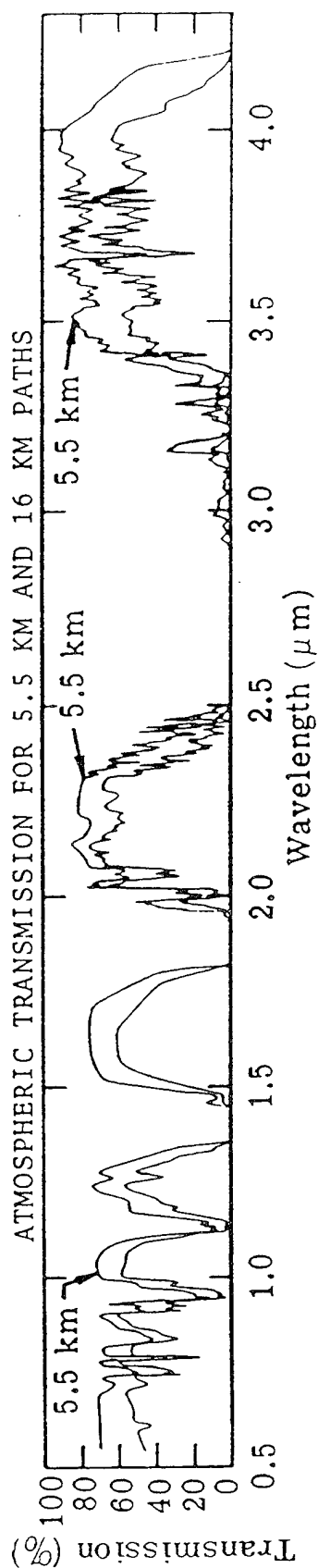
## OH MOLECULAR BAND EMISSIONS



Peak Emission Altitude 85 to 90 km (Mesosphere)

Strong 100 kR band near  $1.5 \mu\text{m}$

Spatial and Temporal Variations from Acoustic Gravity Waves



Spectrum of night airglow observed from an altitude of about 80,000 feet.

# **InGaAs Focal Plane Array Camera (IFPAC)**

Unique Capabilities

1 to 1.7  $\mu\text{m}$  Near Infrared Sensitivity

Room Temperature Operation

Small, Portable System Available for Aircraft

Both Imaging and Spectroscopy Configurations

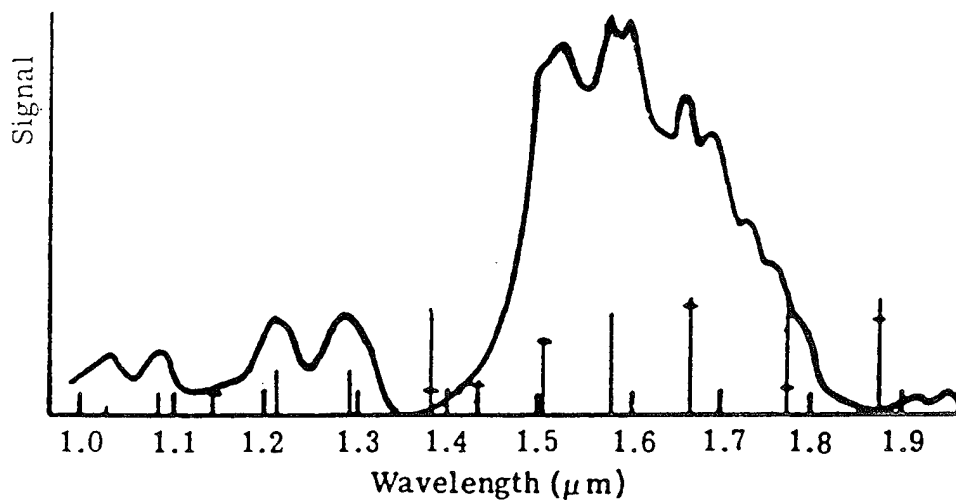
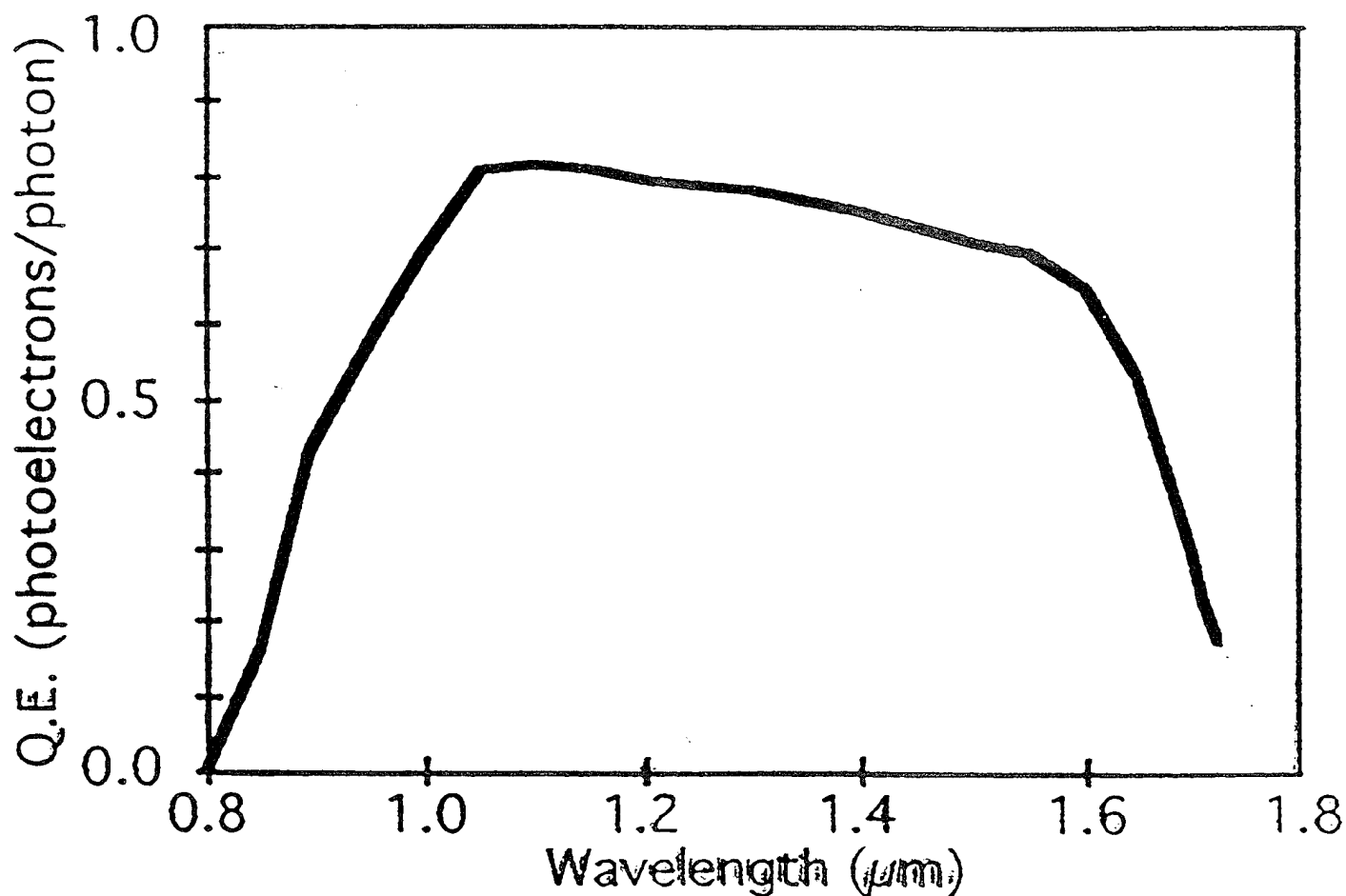


**Fig. 3.41** Nightglow spectrum. It is obtained with a scanning spectrometer (projecting slit width of 200 Å). The origins and expected intensities of OH bands are shown by vertical lines; the horizontal strokes indicate the reduction due to water vapor.<sup>80</sup>





SHORT WAVELENGTH INFRARED CAMERA  
InGaAs Photodiode Array (128 by 128)  
Thermoelectrically Cooled to -30 C  
200 Images/s 12 bits/pixel



## *Plasma Physics Division*

# PHILLS

Carl L. Siefiring, John A. Antoniades

PHILLS is a modular low-light level spectral imager which covers the entire visible range plus a portion of the NIR and UV.

The camera can be used as a spectrograph to measure the optical spectra of Sprites and Blue Jets.

Or like a streak camera to measure the time/altitude history of the Sprite optical emissions.

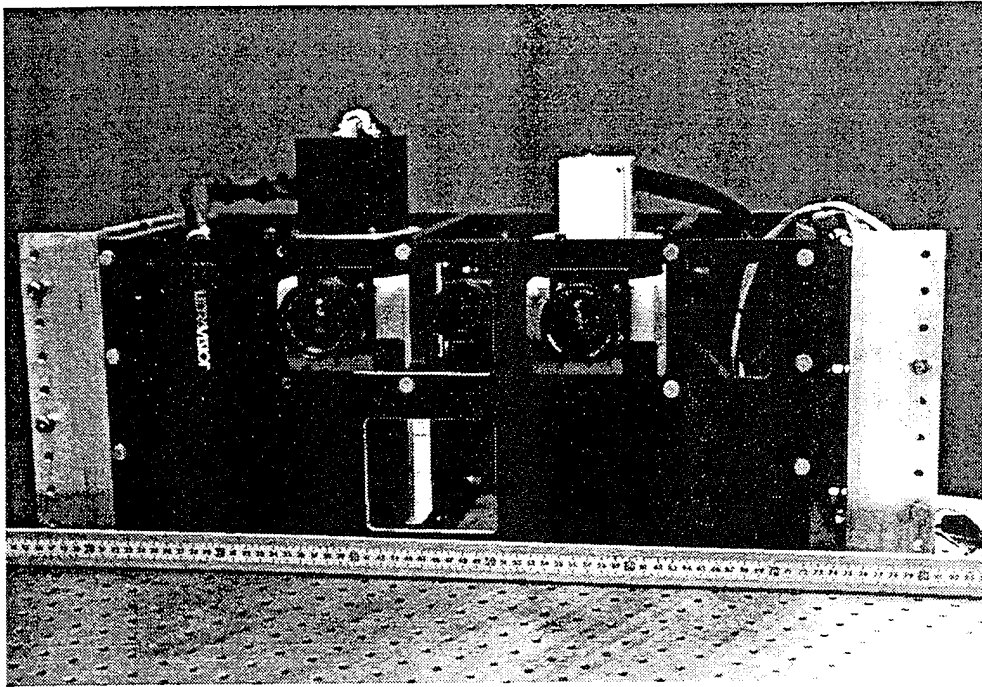




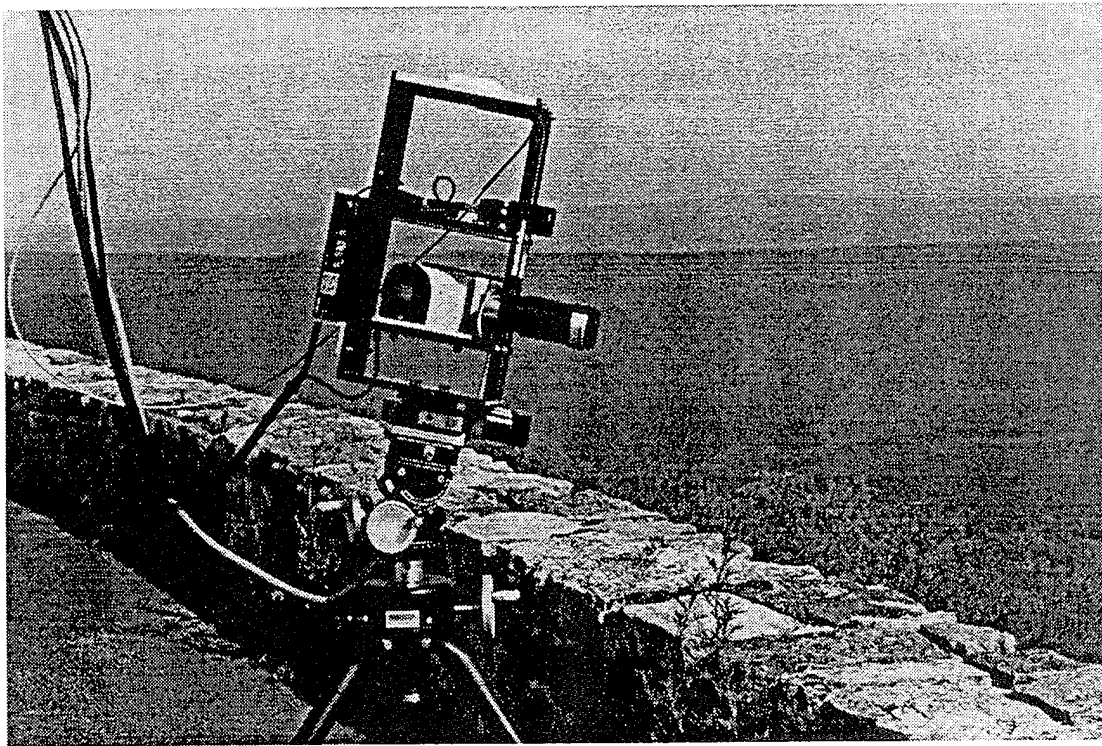
## PHILLS Sensor Modules

- Light, Compact Device Ruggedized for Airborne or Field Operation
- Modular Design for Customized Sensor Configuration
- $\geq 0.2$  nm Resolution,  $\geq 500$  bands / module, 1-72 deg Field of View
- Integrated Video Viewfinder for Precise Pointing
- Integrated GPS Tracking and Recording
- Multiple Modules
  - Analog: RS-170 Tape Output, up to 10 bits/pixel, 2hr Continuous Recording, Multiple Cameras, 300-950 nm intensified
  - High Speed Digital: (12 bits or 16 bits/pixel, up to 200 frames/sec with 256000 pixels/frame)
- Intensified modules for Low Light Operation

## NRL PHILLS Sensor Assemblies

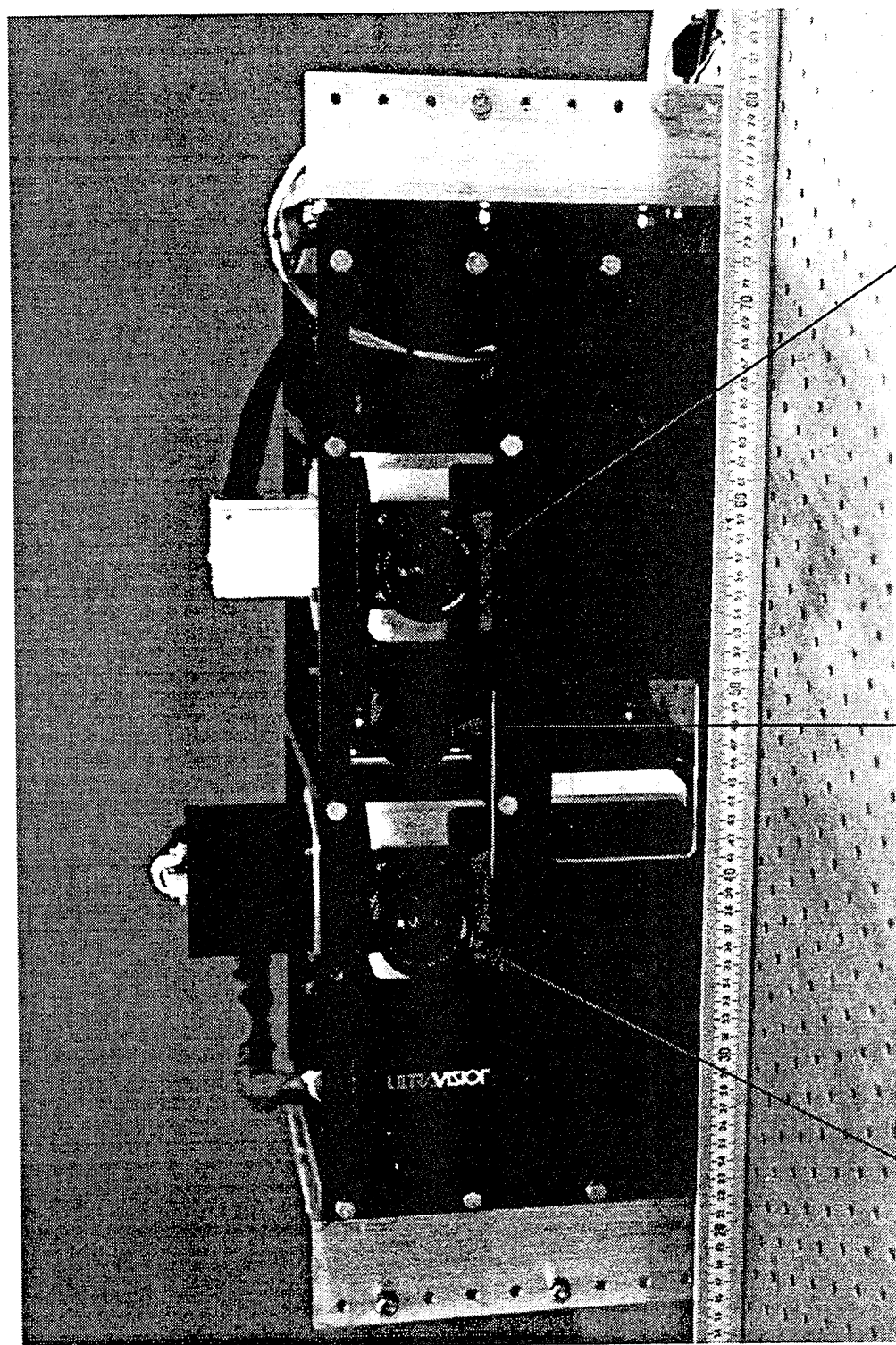


PHILLS sensor assembly deployed on NRL's P-3 589 for the Florida Keys Mapping expedition in October, 1994. The sensor assembly includes the intensified UV/VIS CCD and the VIS/NIR intensified hyperspectral imaging modules and the color CCD viewfinder.



PHILLS ground based deployment at Skyline Drive, Virginia. The photograph depicts the 16 bit digital, UV-NIR module. The sensor assembly includes the hyperspectral imager, the 3-CCD color viewfinder camera, the GPS antenna and the computerized scanning mount (360 degree rotation in 50  $\mu$ rad steps).

# Portable Hyperspectral Imager for Low Light Spectroscopy (PHILLS)



Near Infrared (NIR)  
Spectrometer (500nm  
to 950nm, 420 bands)

3-CCD Color  
Viewfinder  
Camera

Visible Wavelength  
Spectrometer (330nm  
to 670nm, 610 bands)

# Hyperspectral Imaging System

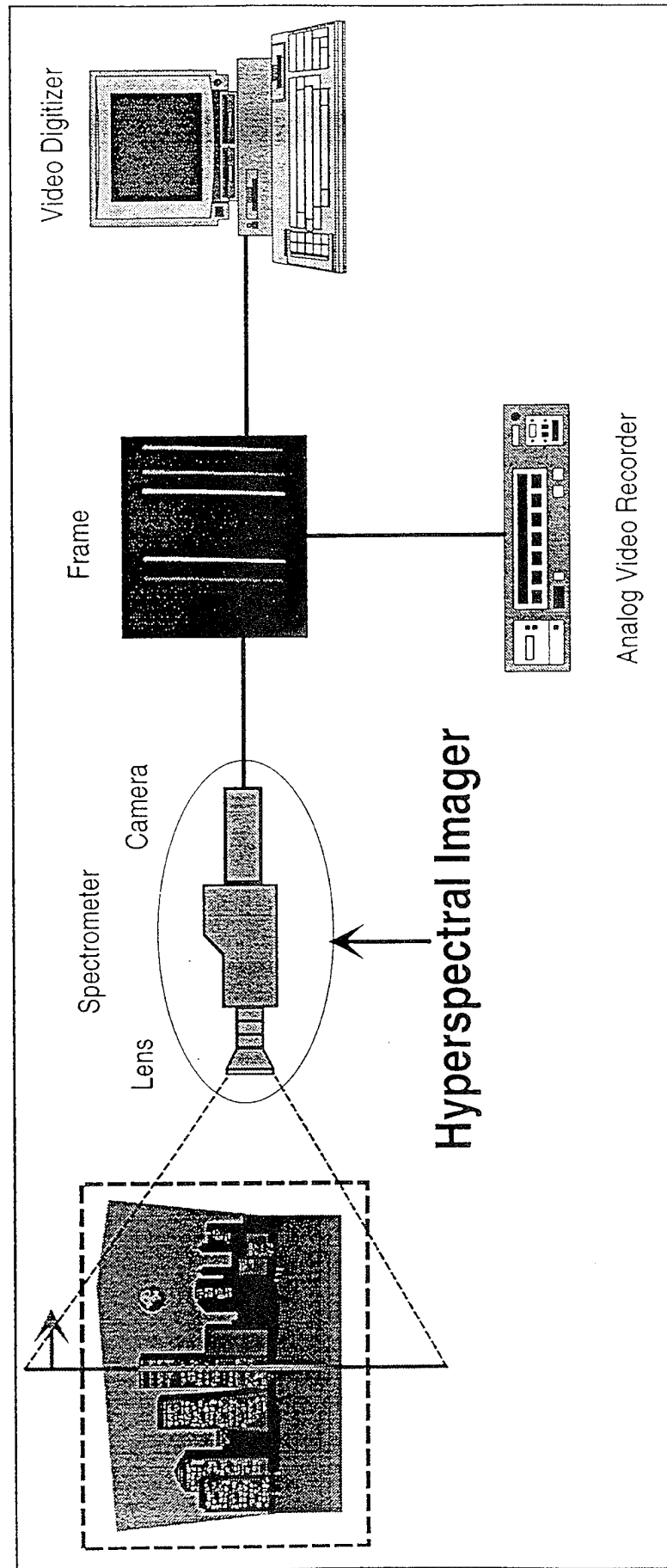


Figure 3. Basic components of a Hyperspectral Imaging System

# Sample Analysis of 2-D Spatially Resolved Hyperspectral Images

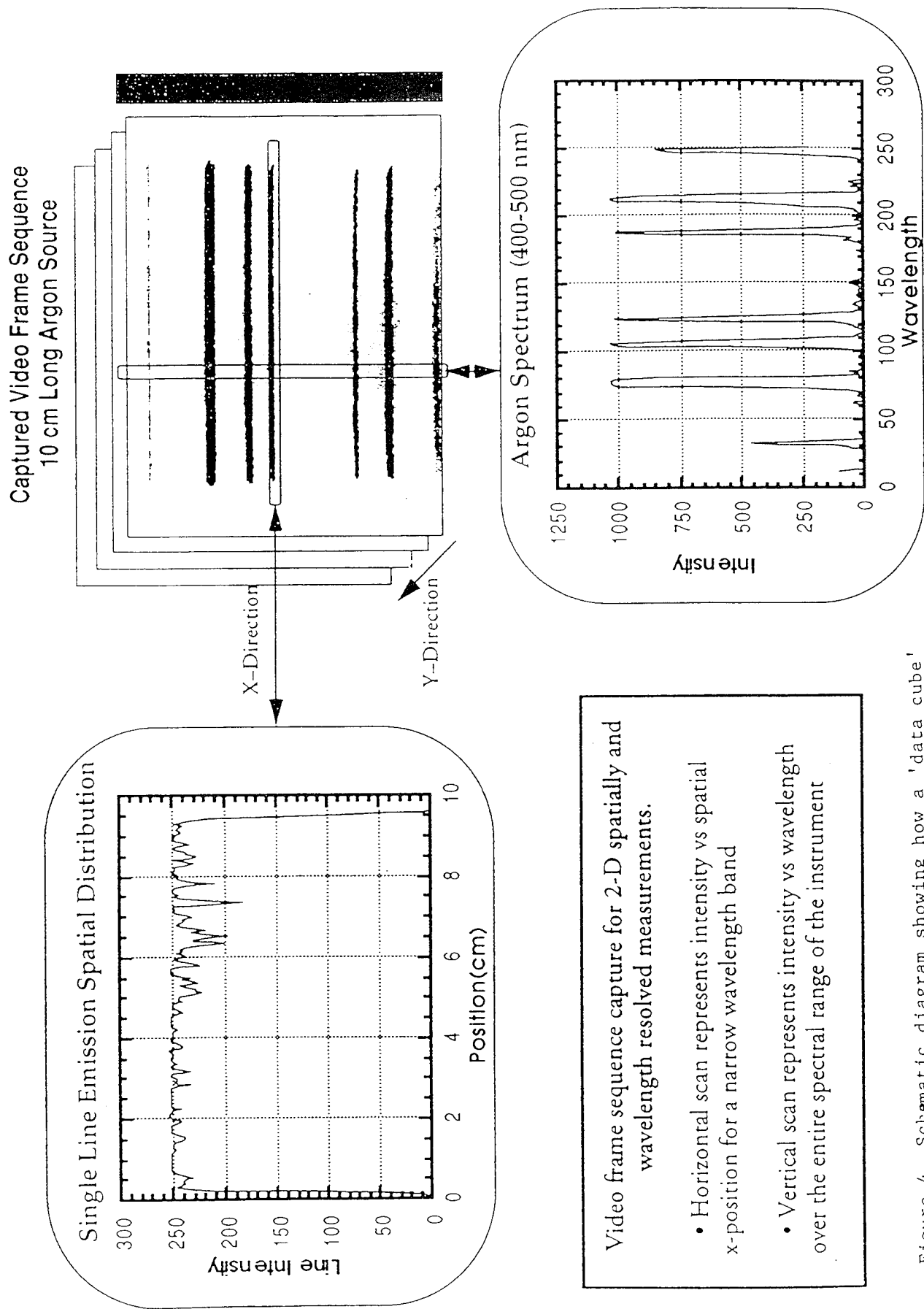


Figure 4. Schematic diagram showing how a 'data cube' is formed from video frames.



# PHILLS

## Portable Hyperspectral Imager for Low Light Spectroscopy

### Instrument Capabilities

Modular Multisensor Imaging Instrument  
Highly Intensified CCD Detectors(<10 R\*sec min  
Illumination for S/N=1,  $10^{-8}$  fc sensitivity)  
Auto or Manual Gain, Gate and Iris ( $>10^{11}$  total  
dynamic range)  
5.5-700 mm Focal Length Input Optics  
Remote Iris, Focus and Zoom Lens control  
High Throughput (f2.8 spectrograph)  
300-1050 nm Coverage in  $>1100$  Spectral Bands  
 $\geq 0.3$  nm Resolution with intensification  
275 Spatial bands for UV/VIS, 488 for VIS/NIR  
15 min max operation with real time (30 fps) full  
frame digital acquisition  
2 hrs continuous acquisition with Hi8 tape  
8-bit gray scale arbitrarily extensible with built-in  
frame accumulation operation  
RS-170 Output, 30 fps for Hi8 or SVHS tape  
Real Time Digital Frame Capture with up to 3  
cameras  
SMPTE, RC or GPS Time and position tagging

### Instrument Components

Standard TV (C-mount) or 35 mm Input Optics  
Flat Field Holographic Grating Spectrographs  
with Interchangeable Gratings  
Extended Red GEN III ICCD Camera(VIS/NIR  
module)  
GEN II ICCD Camera (UV/VIS)  
Integrated Computer Controlled Programmable  
Scanning Mount (6 arc\*sec resolution)  
PentiumPC based Real Time Image Acquisition  
and Processing  
Real Time Frame Grabber for Digital Capture  
Hi8 Tape Recorders  
Color or Monochrome Viewfinder Video Camera

### Spectrograph Specifications

Concave Holographic Flat Field Spectrograph  
(200 mm fl, 25x8 mm image) with  
Interchangeable Gratings  
Interchangeable Slits (25-1000  $\mu$ m wide x 8 mm  
high)  
24-70 nm/mm Dispersion

### ICCD Camera Specifications

Gated ICCD Camera ( $\geq 100$  ns gate)  
25 mm GEN III Intensifier  
18 mm GEN II Intensifier  
16-bit Digital Slow Scan CCD Camera  
600 TV Line Resolution, RS 170 output  
Remote Operation via Camera Controller

Genlock Sync

### Scanning Mount Specifications<sup>1</sup>

Stepper Motor Controlled Rotary Table  
55 lbs load, 6 arcsec Resolution, 72 deg/sec max  
Computer Programmable Controller with up to  
99 program memory+Hand Held Terminal  
RS-232 Mount Control Interface

### Digital Frame Acquisition<sup>1</sup>

EISA Bus Frame Grabber  
30 fps full frame Real Time Acquisition,  
Processing and Display  
On-Board Graphics Accelerator  
40 MPixel/sec Monochrome Data Acquisition  
Simultaneous Grab of up to 3 Synchronized  
Monochrome Inputs

### Digital Data Acquisition System<sup>1</sup>

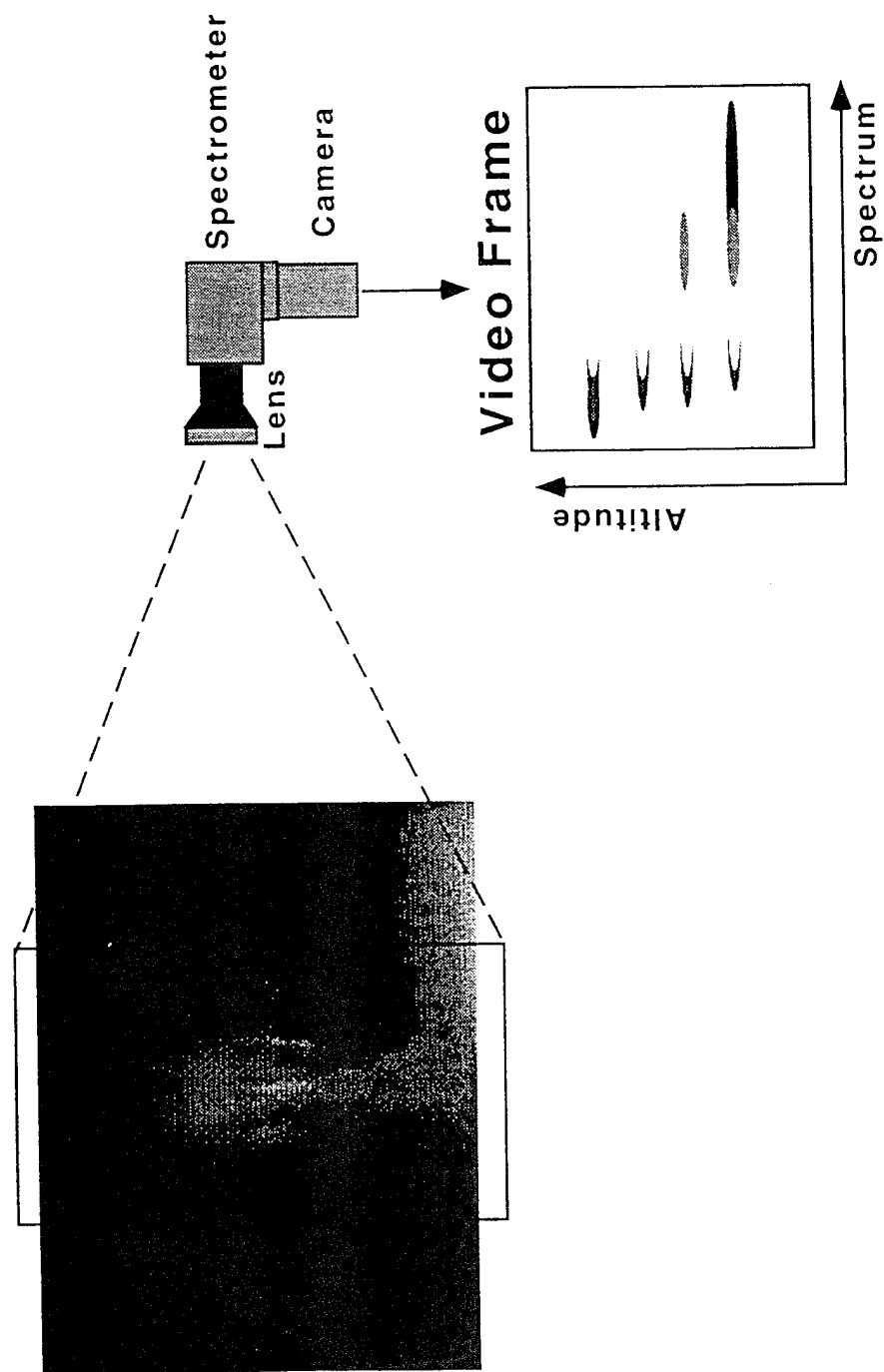
90 MHz Pentium Multi-processor System  
6 GB Fast and Wide SCSI-2 Disk Array  
96 MB Memory  
Fast Ethernet Adapter

### Modes of Operation

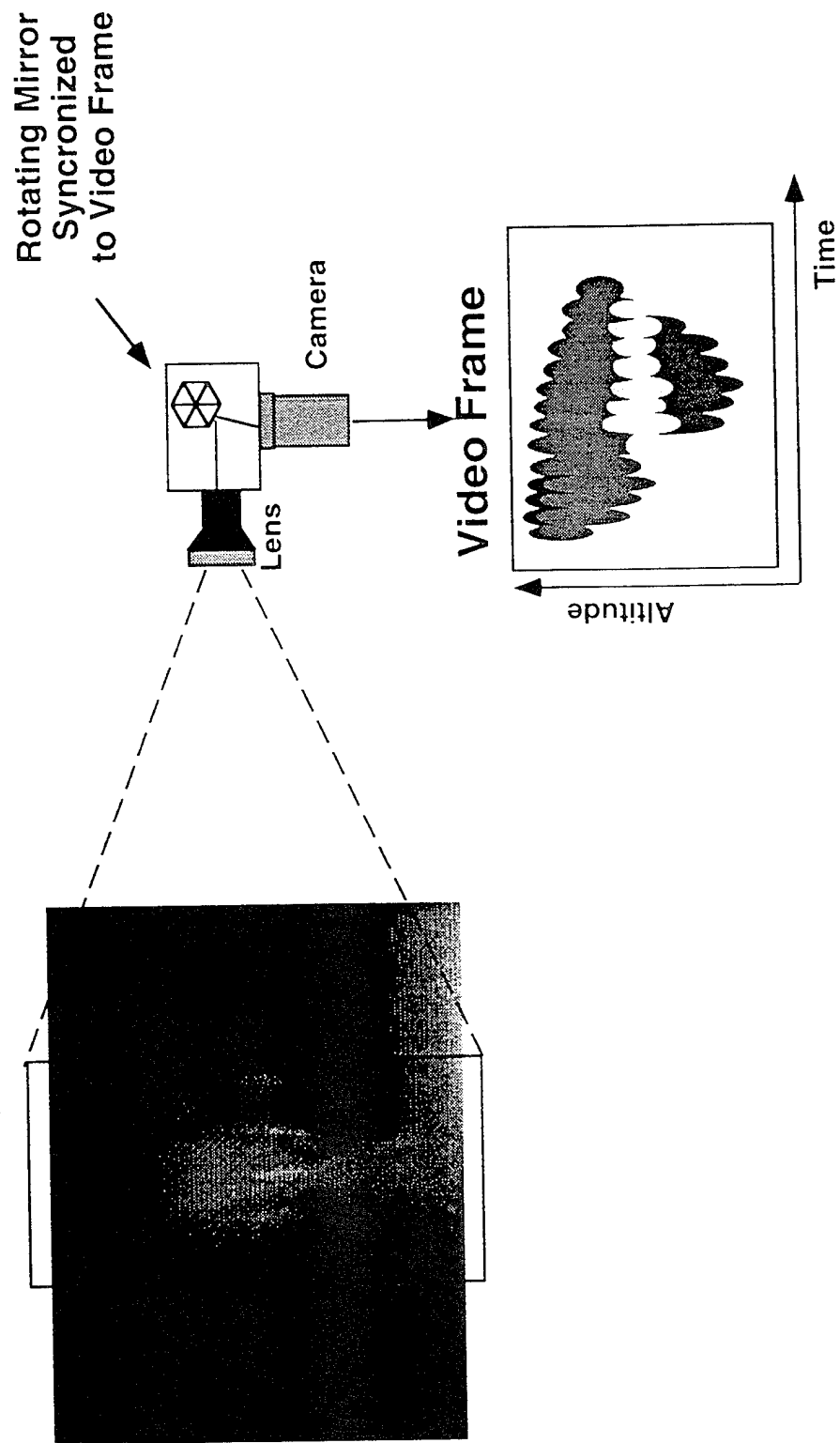
1. Analog Tape Acquisition  
**Hi8 Tape Format (2 hrs/tape  
maximum)**
2. Real-time Fast-Scan Digital Acquisition  
**30 fps Acquisition Limited By Disk  
Space and Memory (15 MB/sec  
max)**  
**8-bits/pixel**
3. Extended Dynamic Range Mode  
**Real-time Frame Accumulation for  
Extended Sensitivity and  
Dynamic Range**
4. Ultra High Sensitivity, Reduced Resolution  
Mode  
**Arbitrary Pixel Binning in both  
directions**  
**Non-Contiguous, Variable Width  
Band Selection**

Table 1. Specifications for PHILLS Instrument as presently configured.

# PHILLS Module used as a Sprite Spectrometer



# PHILLS Module used Like a Streak Camera





## TOPSIDE VIEWS OF LIGHTNING AND SPRITES

W. L. Boeck  
Niagara University  
and

O. H. Vaughan Jr. and R. Blakeslee  
NASA Marshall Space Flight Center

For many years Vaughan and Vonnegut have gathered and published pilots reports of unusual sightings above lightning storms. The first video image of a sprite by Winckler showed the sprite but not the causative lightning flash. Trees in the foreground blocked the view of the horizon and the storm. Images obtained from space platforms view these phenomena from the topside.

In the following years, 17 images of sprites were found in the MLE video archives of lightning storm observations from the Space Shuttle. These images established: a strong causal link between a very bright lightning flash under a cloud anvil and a sprite in the mesosphere above the anvil; a fraction of a second time delay between the onset of cloud lightning activity and the appearance of the sprite; that the cloud source of the sprite is characterized by a low lightning flash rate( a few flashes /min) and that sprites are found over North and South America, Africa and Australia, the Atlantic and Pacific Oceans.

The one North American sprite was associated with a positive cloud to ground strike. The other lightning flashes in the scene were associated with negative CG and TRIMPI events. Measurements in the American Mid West demonstrated that the early estimated of height and frequency were much too small.

MLE also recorded the first images of rocket lightning a.k.a. "Blue Jet" on October 21, 1989. The Australian storm differed in several ways from a typical sprite producing storm. The most notable characteristic is the high lightning flash rate (greater than 50/min) and an optically thick anvil cloud. There is some evidence that an overshooting cloud turret is present when "jets" are observed.

In addition to luminous phenomena in the stratosphere and mesosphere, there is the first observation of a lightning flash simultaneous with a flash at the airglow layer. This phenomena is distinguished by the absence of a sprite or other visible event in the clear air below the airglow layer. The example was found during the STS-41 mission on October 7, 1990. The causal storm was over the Atlantic Ocean off the coast of South America. The cloud had a flash rate of less than 1 per minute. The airglow flash appear promptly along with the causal flash. Theories explain this observation as the prompt heating of the ionosphere due to the EMP produced by lightning. Other observations of this phenomena confirm that the production of a luminous disc of several hundred kilometers diameter occurs within 1 ms of the lightning discharge and well before any sprite activity.

## Observations of Electric Field and X-rays Above Thunderstorms: Relevant to Optical Sprites?

K.B. Eack, Department of Physics and Astronomy, University of Oklahoma, Norman, OK.

W.H. Beasley, School of Meteorology, University of Oklahoma, Norman, OK.

W.D. Rust, NOAA - National Severe Storms Laboratory (NSSL), Norman, OK.

M. Stolzenburg, Cooperative Institute for Mesoscale Meteorology / NSSL, Norman, OK.

T.C. Marshall, Department of Physics and Astronomy, University of Mississippi, University, MS.

During the Spring of 1995, X-ray detectors were flown on four balloon flights into the stratiform regions of four mesoscale convective systems (MCS). The X-ray instrument uses a sodium iodide scintillation detector. A three-channel (30 to 60, 60 to 90 and 90 to 120 keV) X-ray spectrum is acquired every 0.25 seconds. In addition to the X-ray detector, an electric-field mill and a meteorological radiosonde are also flown on the balloon (Figure 1).

The original motivation for this work was to verify the hypothesis of C.T.R Wilson (1925) that thunderstorm electric fields should be able to produce energetic electrons, and to extend the measurements made by Parks et. al. (1981) and McCarthy and Parks (1985) of X-ray production in thunderstorms. In two of the four flights made, we did observe X-rays associated with the strong electric field region inside the cloud. The fourth and final flight of the season was made on June 29, 1995 from a launch site east of Guymon in the Oklahoma Panhandle. The detector was modified from the previous three flights in that it looked up rather than down. The complete X-ray and electric-field soundings for this flight are shown in Figure 2. Although no X-ray events were detected in the cloud, three pulses with a duration of about 1 second were observed above the cloud near 15 km MSL with a measured atmospheric pressure of 127 mb (Figure 3). Each step in Figure 3 is 0.25 seconds wide. The electric field strength measured at the balloon at the time of the pulses was about -0.5 kV/m (negative meaning the field lines directed downward).

The pulses occurred at 06:54:50, 06:55:24 and 06:55:26 UTC. From the NLDN (National Lightning Detection Network) ground-strike data, no cloud-to-ground lightning occurred at these times within 50 miles of the launch point. However during a period of 5 minutes on either side of the pulses there were 5 flashes within the 50 mile radius, all but one were positive, with one of the positives having a reported current of 103 kA. Expanding the search radius, we found that there were two positive flashes that occurred two seconds apart, but according to NLDN, were offset two seconds earlier than the observed X-ray pulses. A systematic timing error of 2 seconds is possible given the methods used to synchronize the time to a satellite clock, but would probably be on the outer edge of the error margin. The flashes occurred at 06:55:22 and 06:55:24 with currents of 73 kA and 74 kA. The first flash was 100 miles from the balloon's position, while the second was 64 miles distant. In addition, at the time of the X-ray pulses, we observed a large horizontal lightning discharge from the launch site.

## References

- Wilson, C.T.R., *Proc. Cambr. Phil. Soc.*, **22**, 534-538, 1925.  
Parks, G.K. B.H. Mauk, R. Spiger, and J. Chin, *Geophys. Res. Lett.*, **8**, 1176-1179, 1981.  
McCarthy, M., and G.K. Parks, *Geophys. Res. Lett.*, **12**, 393-396, 1985.

## Acknowledgements

This work was supported by grant ATM-9414122 from the Physical Meteorology Program of the NSF. Field work was supported in part by NOAA/NSSL.

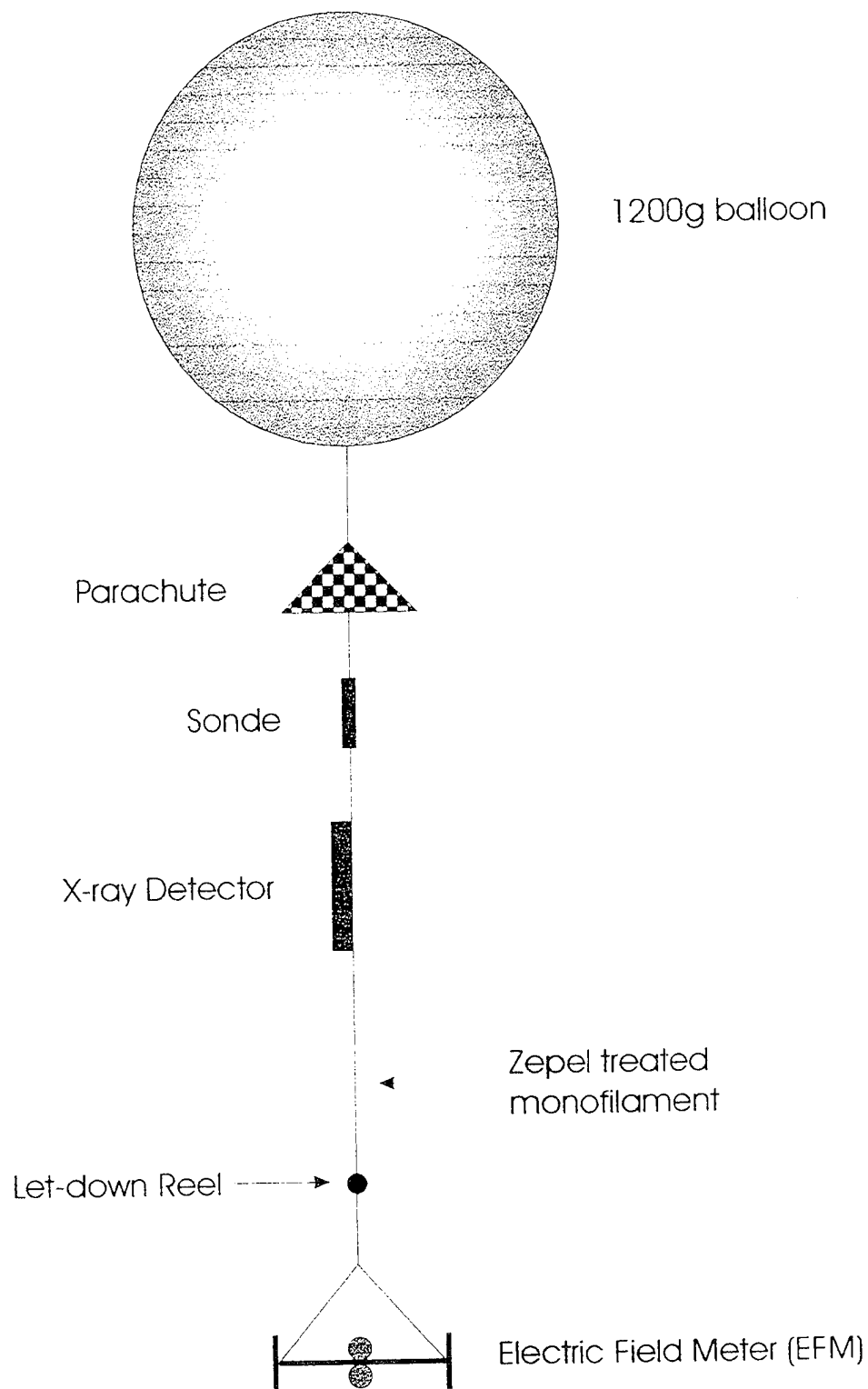


Figure 1. Typical configuration of balloon instrumentation for X-ray measurements.

Figure 2. X-ray and electric-field soundings 29 June 1995

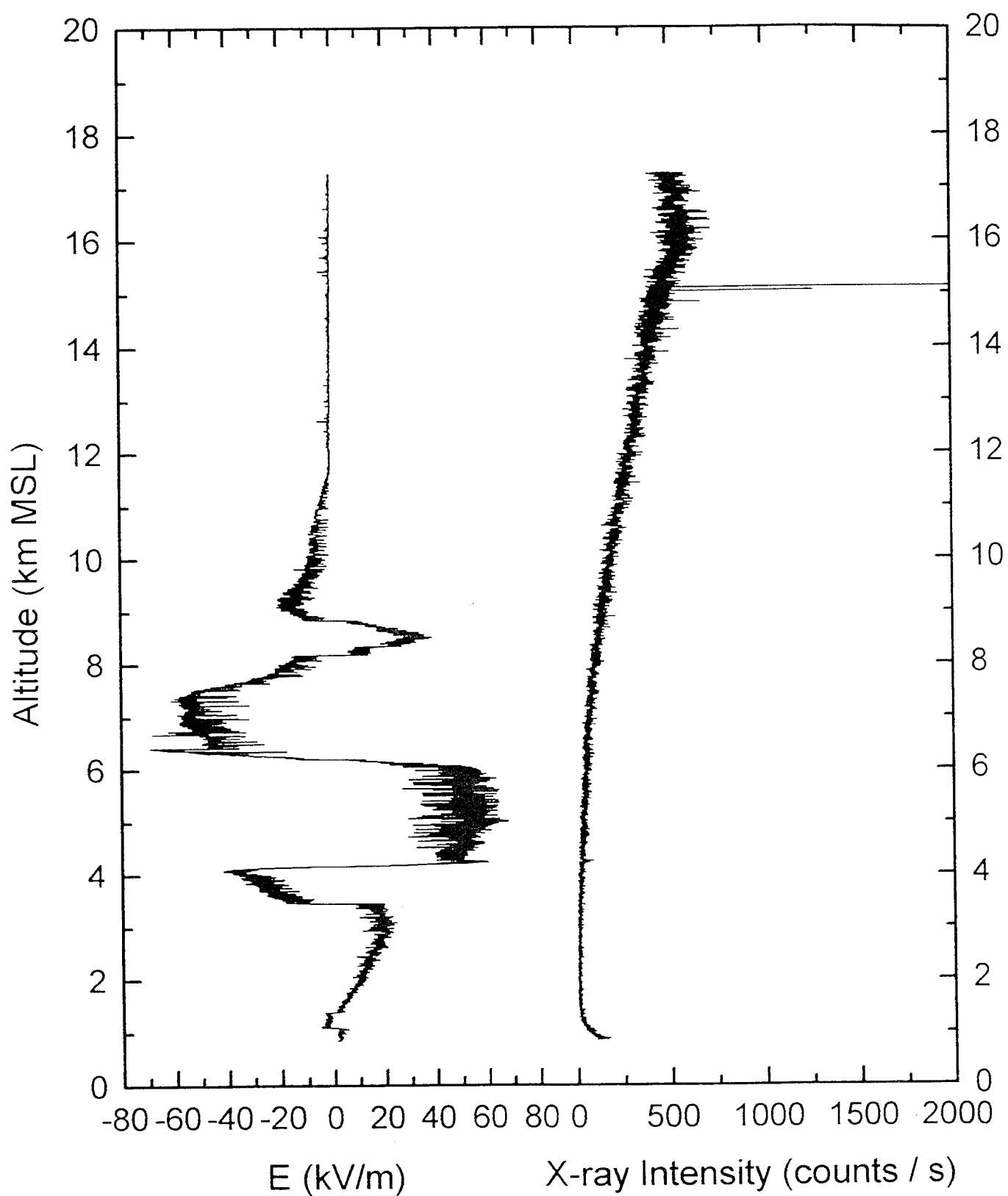
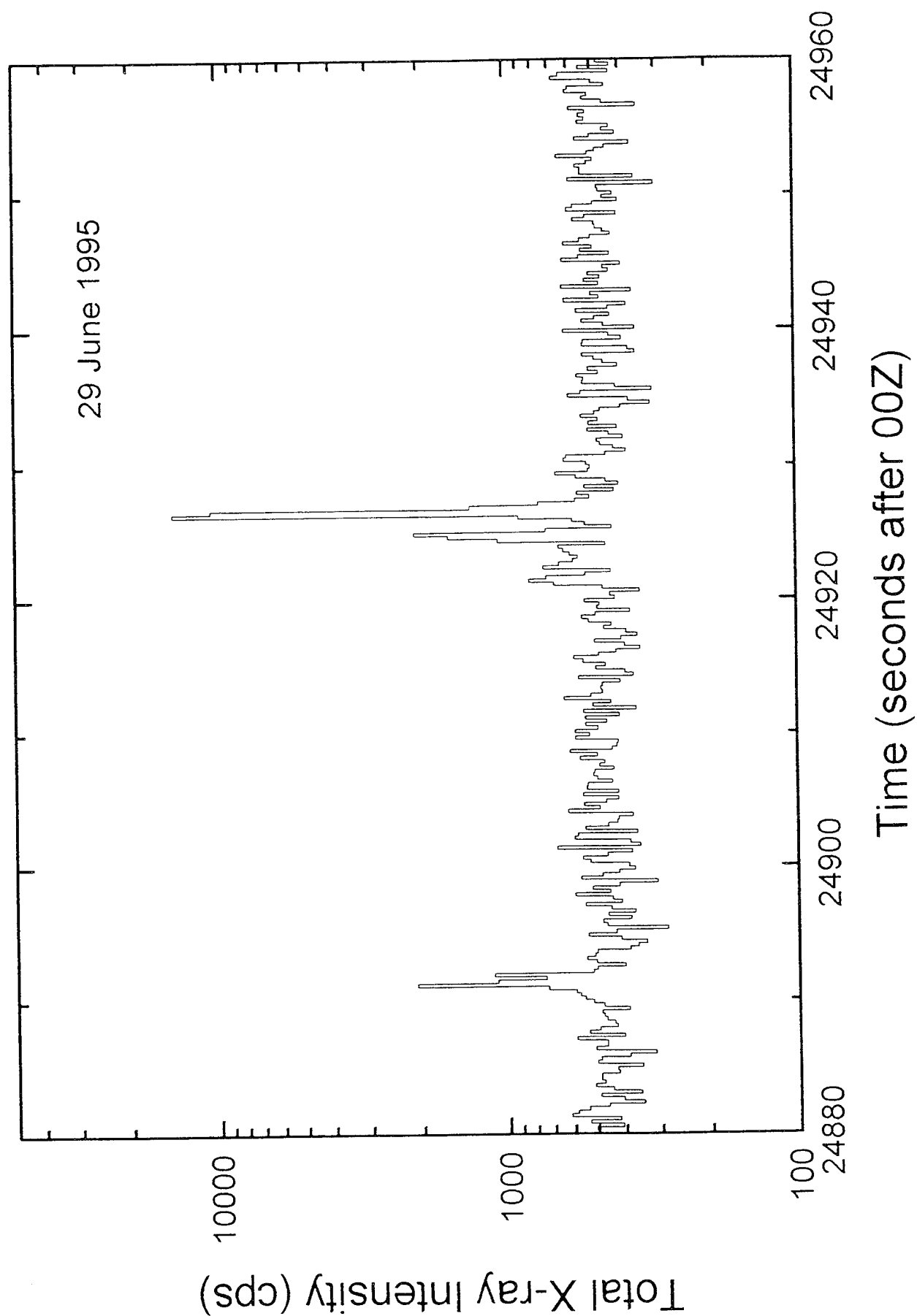


Figure 3. Detail of X-ray pulses at 15km MSL.



# Joint US/Russian Lightning Experiments

Susan Voss and Eugene Symbalisky  
Los Alamos National Laboratory  
Space and Atmospheric Group

Presented at:

Phillips Laboratory Workshop on Sprites  
and Blue Jets  
October 18, 1995  
Hanscom AFB, MA

## Project Overview

- Los Alamos, in conjunction with two Russian Institutes, Arzamas-16 and Lebedev, are proposing to conduct joint experiments to obtain a better understanding of upward lightning.
- Four experiments have been proposed - the first of which was completed at the end of FY95 with the support of the AFPL Balloon Operations group in Albuquerque.
- US funding for FY95 was obtained in-house at Los Alamos and the Phillips Laboratory. A request has been submitted to DOE for FY96 project funds.
- Russian funding has been requested from the International Science and Technology Center (ISTC) in Moscow.



# Test Objectives

The four primary objectives and their corresponding experiment are presented:

1. Determine if Trans-Ionospheric Pulse Pairs (TIPPs) could be caused by the reflection of RF off the ground.  
  
The experiment was completed September 28, 1995 with the support of the AFPL balloon experiments group. A Marx generator was used to produce RF pulses on a high altitude balloon. Data is currently being analyzed.
2. Determine if there is the predicted correlation between the optical signal produced by upward lightning, gamma-ray bursts and TIPPs. Compare to the predicted signals from the proposed theoretical relativistic-electron breakdown avalanche (Rousel-Dupre and Gurivich).  
  
Diagnostics to be carried on a high-altitude balloon (25 km) or the manned Odyssey flight during the summer of 1996.  
Payload: gamma detectors, digital cameras, RF receivers and field mills.

# Test Objectives -

3. Generate an electric field in the absence of thunderstorm activity to test the proposed theoretical relativistic-electron breakdown avalanche (Roussel-Dupre and Gurivich).  
Fly an electron or ion generator on a low altitude (~5 km) tethered balloon to produce a uniform electric field.  
Diagnostic on the balloon: gamma detector and electric field mills. Diagnostic on the ground: gamma detectors, digital cameras, RF receivers and field mills.
4. Study the upward lightning tie to the ionosphere (preliminary planning stages). Experiment to be performed in Russia.  
Two options currently being examined are a Russian high-altitude balloon launch or a suborbital launch on a Russian SS-19. A magnetocumulative generator (MCG) is being considered as the primary payload.

# Progress

- Developed a US and Russian team. Definition of roles and responsibilities.
- Developing our goals/objectives, experiment configuration and diagnostic requirements.
- Expansion of theoretical basis to experimental requirements.
- Requests for US and Russian funding.
- AFPL support - completion of the first proposed experiment.
- Examining Russian options for FY97 experiment.

**Measurements of Lightning-Generated  
Electric Fields  
in the Nighttime D-Region**

**Dr. Carl L. Siefring**

**Naval Research Laboratory  
Plasma Physics Division**

# **The NASA 1981 Thunderstorm Campaign**

**Led By Cornell University**

**Designed to Study the Upward Coupling of  
of Lightning Generated-Electric Fields**

**Three Sounding Rockets,  
a Balloon  
and  
Ground Based Instrumentation**

**Published Results:**

Siefring, C. L. and M. C. Kelley, Lightning transients in the ionosphere, mesosphere, stratosphere and on the ground, Paper 3.6, **Seventh International Conference on Atmospheric Electricity**, American Meteorological Society, Boston, MA, 1984.

Holzworth, R. H., M. C. Kelley, C. L. Siefring, L. C. Hale, and J. D. Mitchell, Electrical measurements in the atmosphere and ionosphere above a thunderstorm: 2. Direct Current electric fields and conductivity, *J. Geophys. Res.*, 90, 9824, 1985.

Kelley, M. C., C. L. Siefring, R. F. Pfaff, P. M. Kintner, M. Larsen, R. Green, R. H. Holzworth, L. C. Hale, J. D. Mitchell, and D. LeVine, Electrical measurements in the atmosphere and ionosphere above a thunderstorm: 1. Campaign overview and initial ionospheric results, *J. Geophys. Res.*, 90, 9815, 1985.

Siefring, C. L., Upward Propagating Electric Fields from Thunderstorms and VLF Transmitters, PH.D. thesis, Cornell University, Ithaca, N.Y. (Available: Univ. Microfilms Intl., Ann Arbor, MI), 1987.

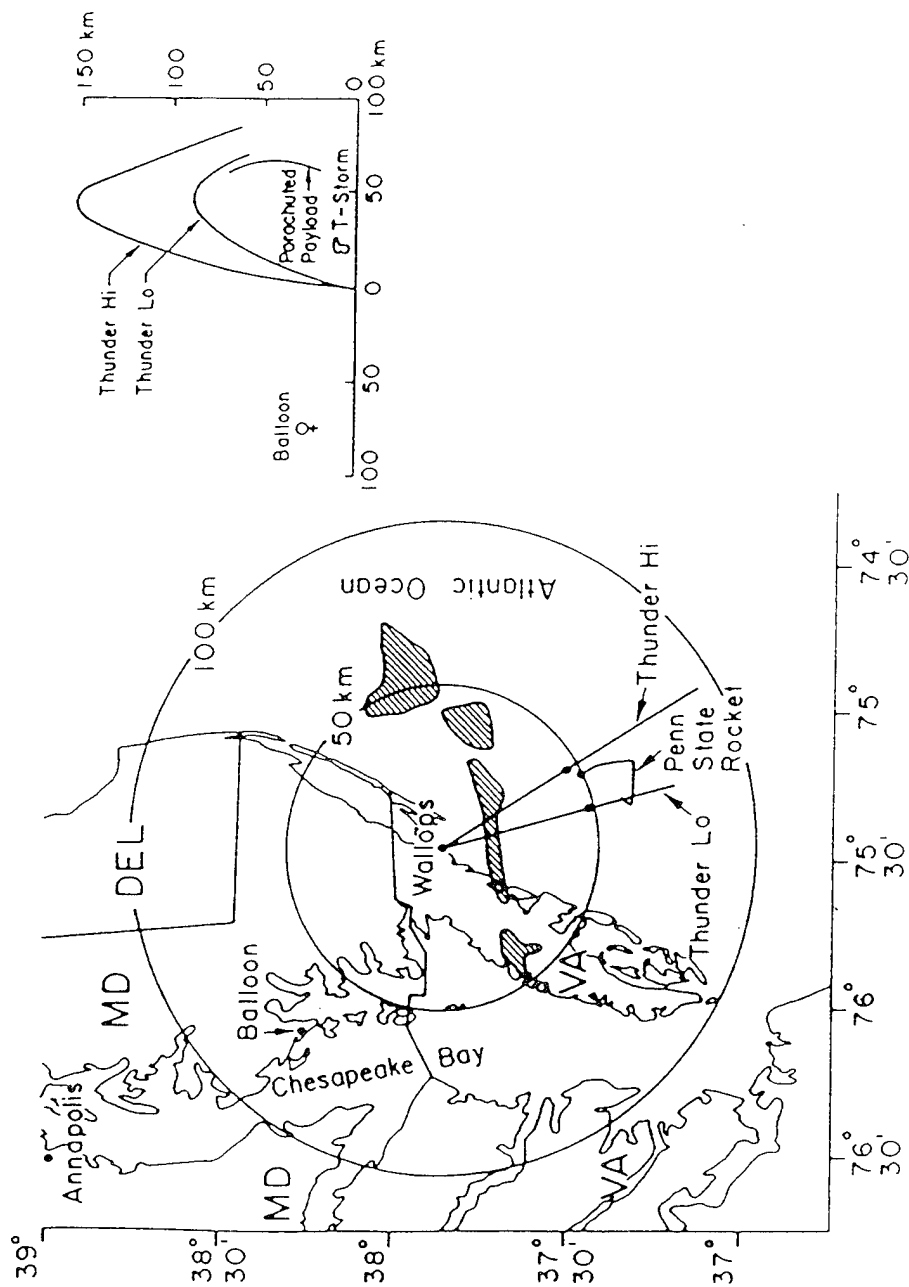
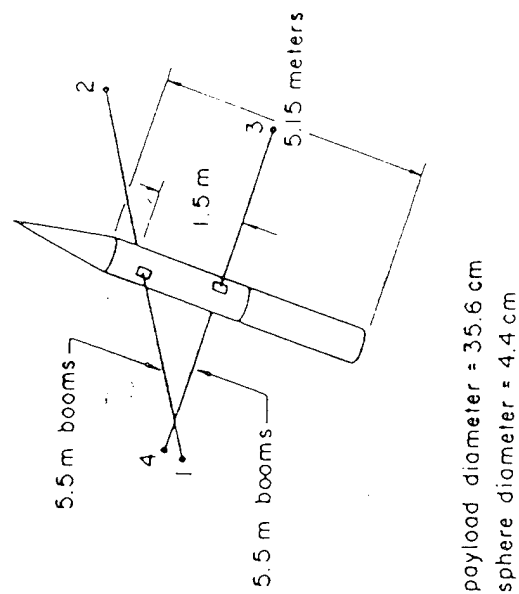


Figure 2.2 Map showing the location of the four thunderstorm cells and the balloon at the launch time of Thunder Lo. The ground tracks of the rocket payloads are also indicated. A vertical schematic of the thunderstorm and experiment trajectories is shown on the right-hand side.

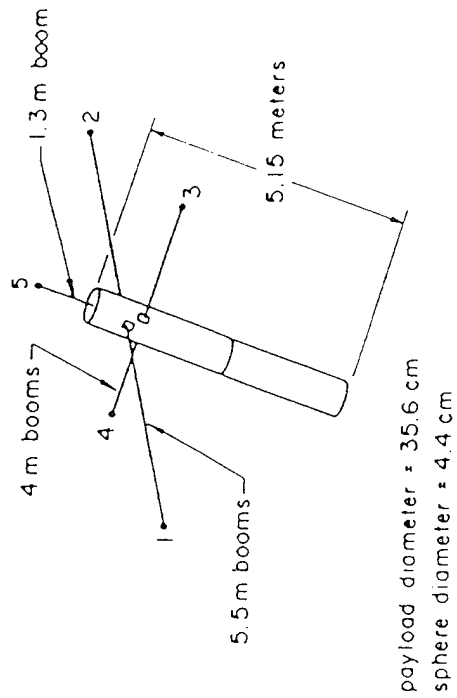
Table 2.1: The instrumentation used during the thunderstorm electric field campaign, with the altitude ranges and operating institutions.

| <u>Experiment</u>                          | <u>Altitude Range</u> | <u>Institution</u>                  |
|--|-----------------------|-------------------------------------|
| Ionospheric Rocket<br>(Thunder Hi)         | 85 km - 154 km        | Cornell University                  |
| Mesospheric Rocket<br>(Thunder Lo)         | 60 km - 88 km         | Cornell University                  |
| Rocket Released<br>Parachute-Borne Payload | 25 km - 75 km         | Pennsylvania State<br>University    |
| Stratospheric Balloon                      | 24 km - 30 km         | University of<br>Washington         |
| Flat Plate Antenna                         | Ground Based          | NASA/Goddard Space<br>Flight Center |
| Meteorological Radar<br>(SPANDAR)          | Ground Based          | NASA/Wallops Flight<br>Facility     |
| Lightning Locating<br>System (LDAR)        | Ground Based          | NASA/Wallops Flight<br>Facility     |
| Ionosonde                                  | Ground Based          | NASA/Wallops Flight<br>Facility     |

Thunderstorm Electric Field Campaign  
 Wallops Island, Virginia  
 August 9, 1981



Thunder - Hi  
 154 km Apogee  
 Taurus - Orion



Thunder - Lo  
 89 km Apogee  
 Nike - Orion

Figure 2.1 Electric field measurement configuration for Thunder Hi (33.022) and Thunder Lo (31.022).



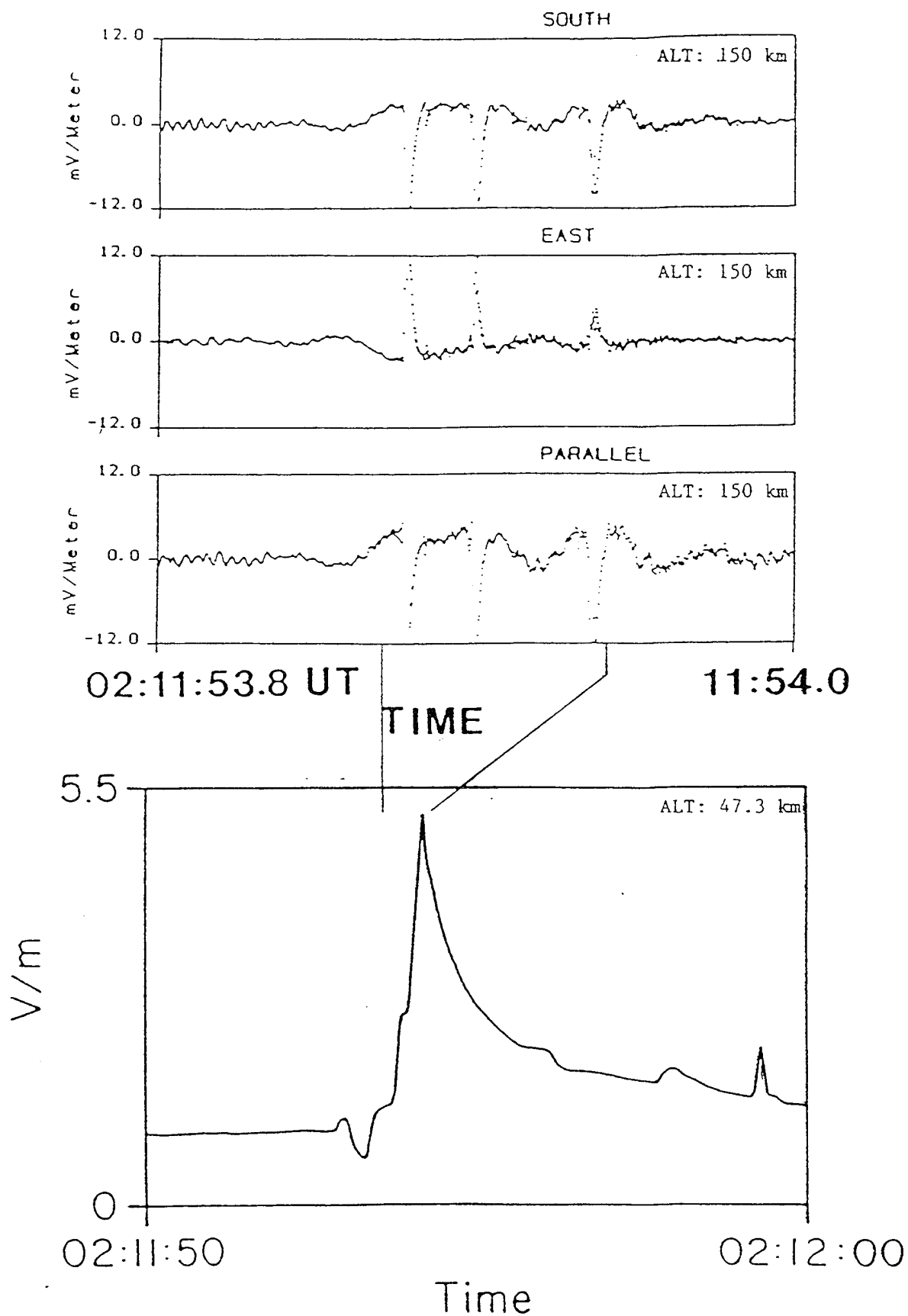


Figure 1. Lightning Induced Electric Fields in the Mesosphere and Ionosphere.

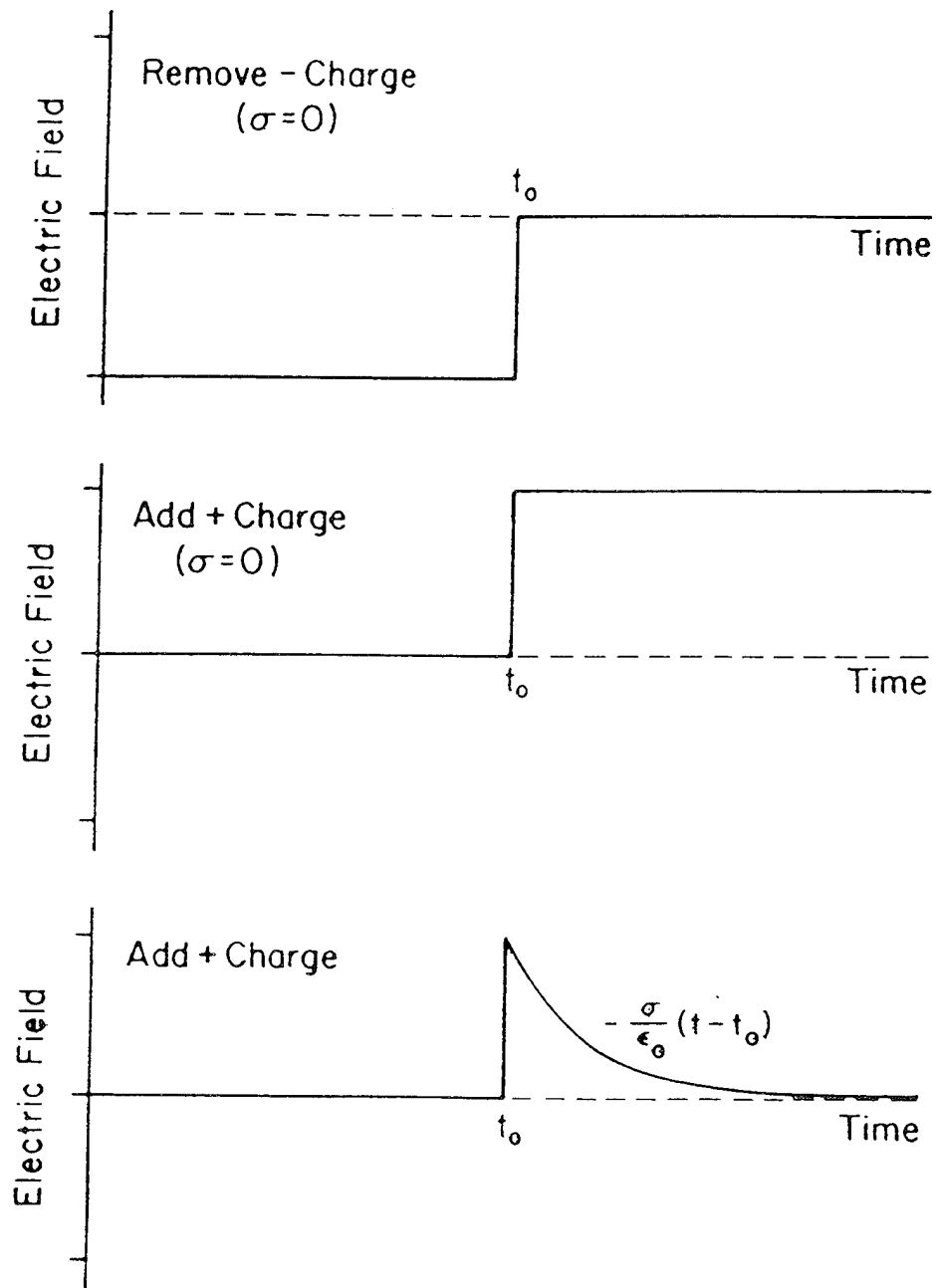


Figure 4.11 Electric field changes produced by: a) removing a negative charge from a perfect dielectric; b) adding a positive charge to a perfect dielectric; c) adding a positive charge to a conductor.

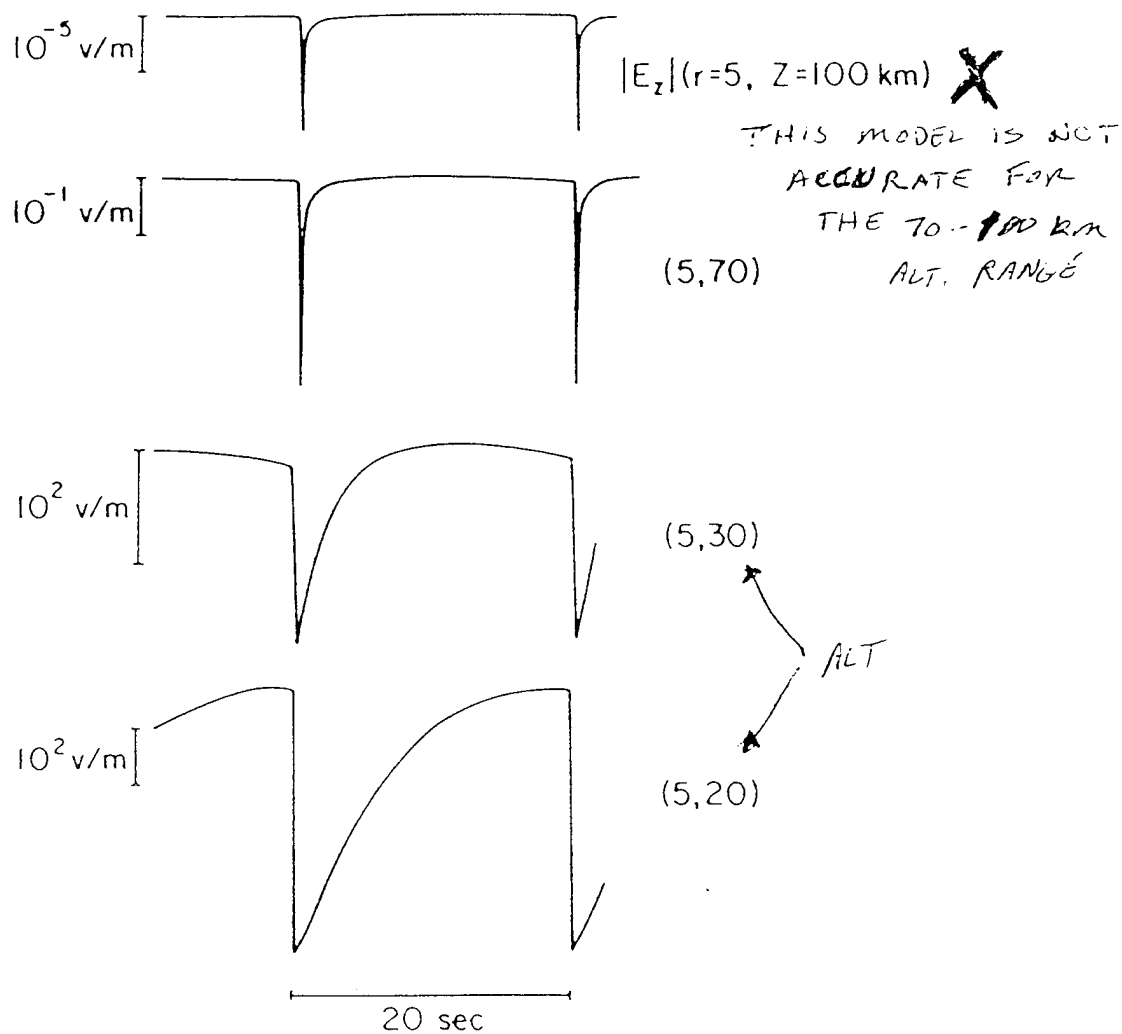


Figure 4.13 Plots of the vertical electric field ( $E_z$ ) for a lightning flash as modelled by Dejnakintra and Park [1974] at a horizontal distance  $r=5$  km and selected altitudes ( $z$ ).

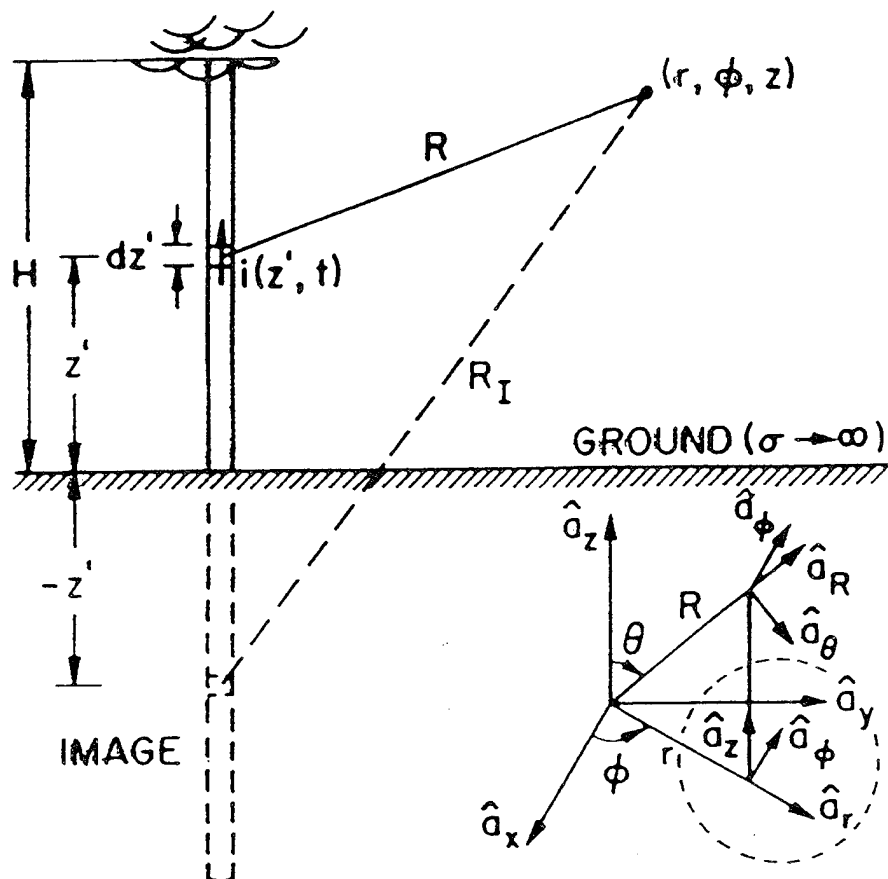


Figure 4.10 Geometry of the travelling-wave antenna model for lightning return strokes. Note: the fields are calculated in a cylindrical coordinate system.

the relationship between the currents and the electric fields they produce.

$$\begin{aligned}
 d\mathbf{E}(r, \phi, z, t) = & \frac{dz'}{4\pi\epsilon_0} \left[ \overbrace{\left( \frac{3r(z-z')}{R^5} \int_0^t i(z', r-R/c) dr \right)}^{(1) \text{ ELECTROSTATIC SOURCE TERM}} \right. \\
 & + \overbrace{\left( \frac{3r(z-z')}{cR^4} i(z', t-R/c) \right)}^{(2) \text{ INDUCTIVE}} + \overbrace{\left( \frac{r(z-z')}{c^2 R^3} \frac{\partial i(z', t-R/c)}{\partial t} \right)}^{(3) \text{ RADIATIVE}} \left. \right] \hat{\mathbf{a}}_r \\
 & + \frac{dz'}{4\pi\epsilon_0} \left[ \overbrace{\left( \frac{2(z-z')^2 - r^2}{R^5} \int_0^t i(z', r-R/c) dr \right)}^{(1)} \right. \\
 & + \overbrace{\left( \frac{2(z-z')^2 - r^2}{cR^4} i(z', t-R/c) \right)}^{(2)} - \overbrace{\left( \frac{r^2}{c^2 R^3} \frac{\partial i(z', t-R/c)}{\partial t} \right)}^{(3)} \left. \right] \hat{\mathbf{a}}_z
 \end{aligned} \tag{4.5}$$

$$d\mathbf{B}(r, \phi, z, t) = \frac{\mu_0 dz'}{4\pi} \left[ \overbrace{\left( \frac{r}{R^3} i(z', t-R/c) \right)}^{(2)} + \overbrace{\left( \frac{r}{c R^2} \frac{\partial i(z', t-R/c)}{\partial t} \right)}^{(3)} \right] \hat{\mathbf{a}}_\phi \tag{4.6}$$

There are three source terms in Equation (4.5) for the electric field produced by the travelling-wave antenna, while there are only two source terms in the magnetic field equation. We have labelled these terms in Equations (4.5) and (4.6) and will discuss each of them separately.

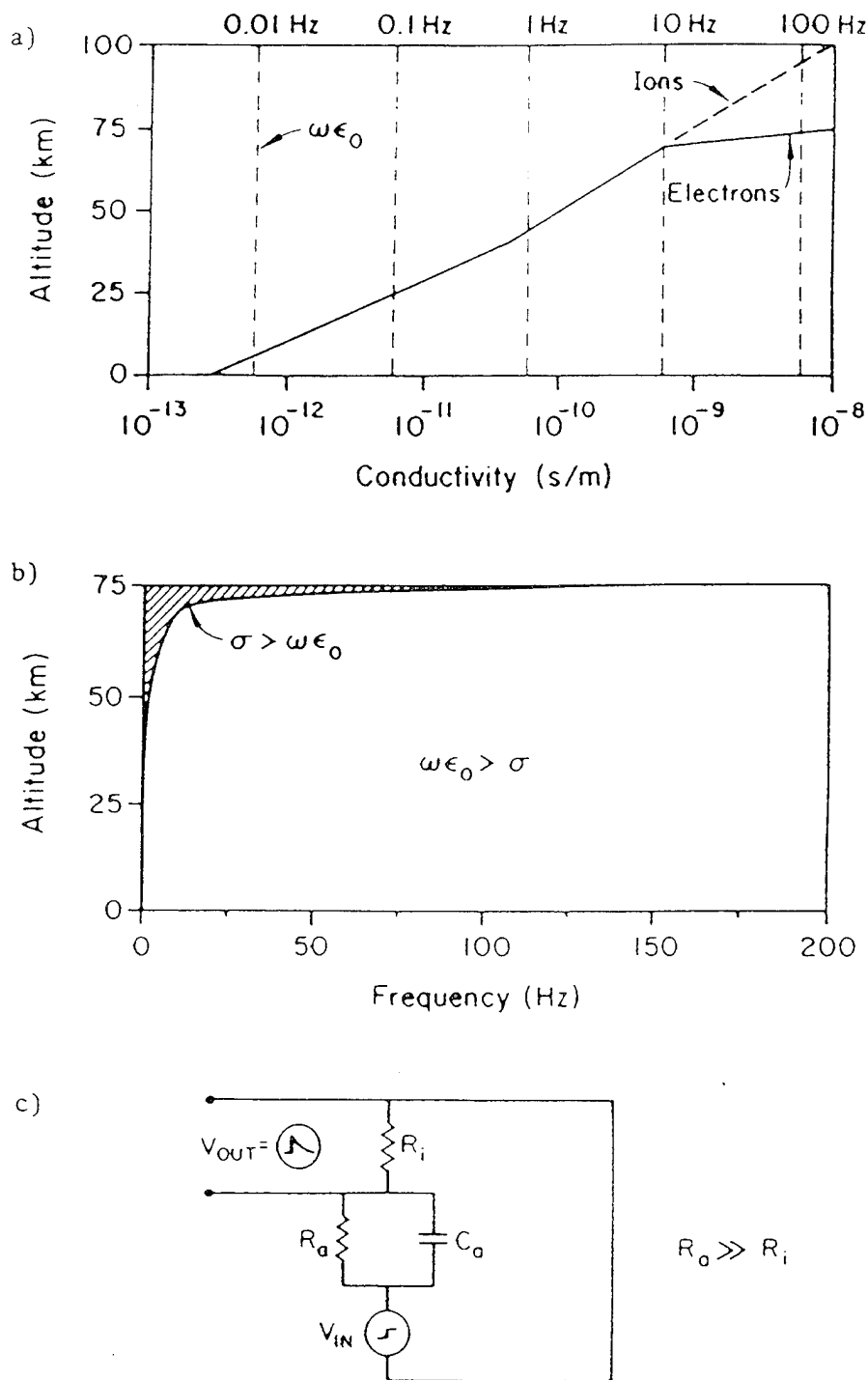


Figure 4.14 a) Conductivity profile derived from measurements shown in Figure 3.1. Conductivity is estimated above 75 km. b) Altitude where the conduction current equals the displacement current ( $\sigma = \omega\epsilon_0$ ). In the shaded region the atmosphere can be considered a resistive medium. c) Equivalent circuit for the stratified atmosphere.

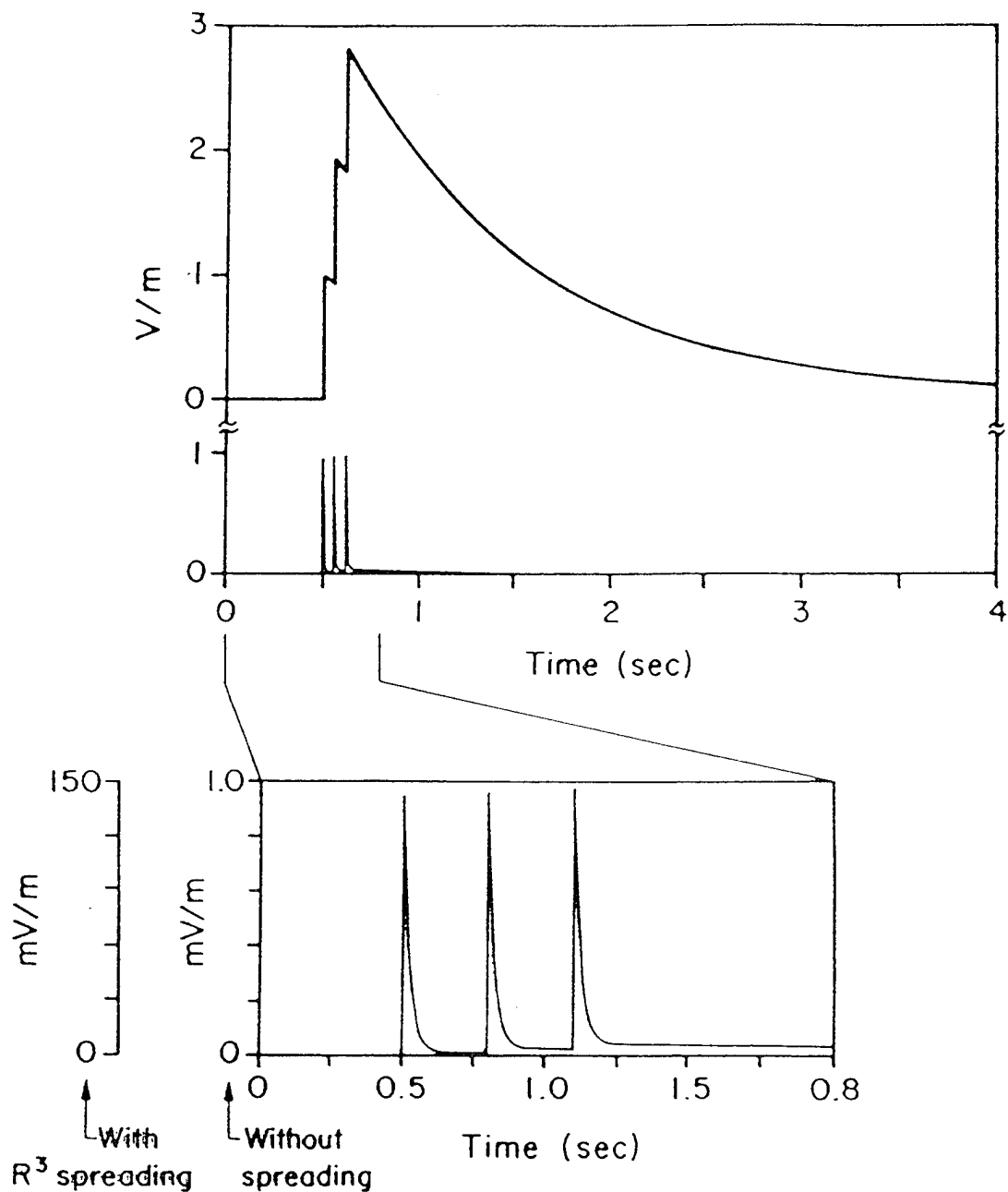
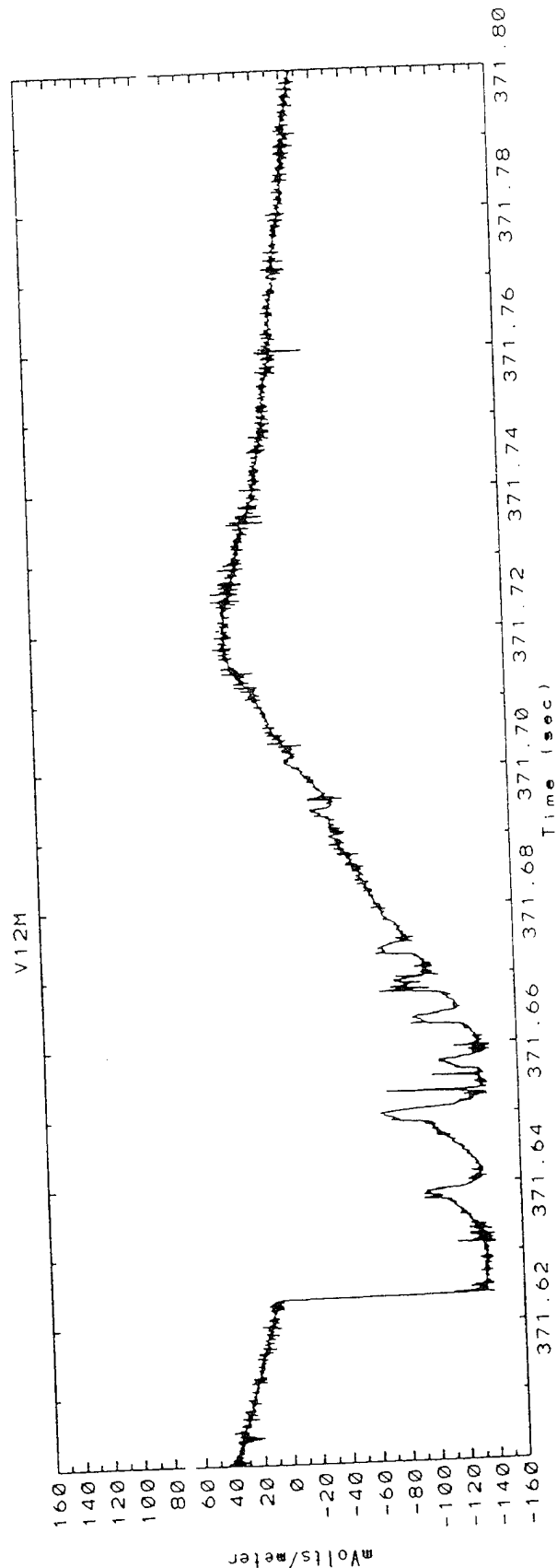
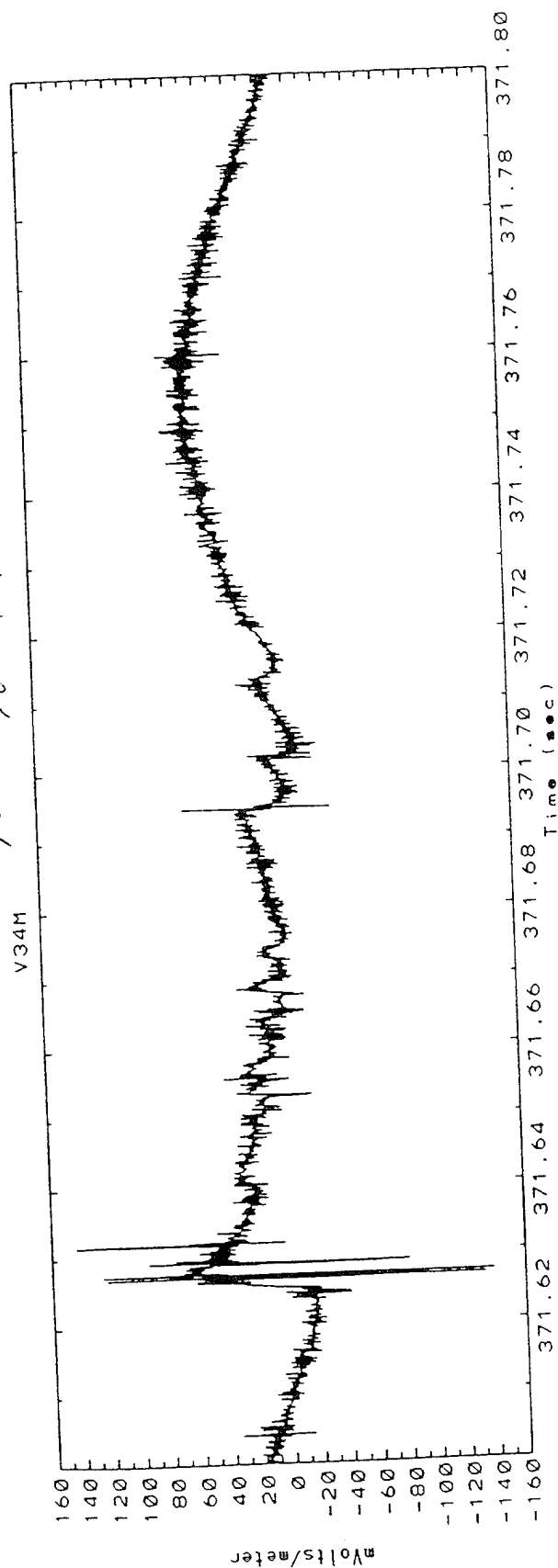


Figure 4.16 (Top panel) Model of electric fields measured in the upper atmosphere due to a lightning flash consisting of three return strokes and the result when the transfer function (with no spreading) is applied. (Cutout) Expanded section shows the expected up-going electric fields at 75 km. Two scales are given for the case with no spreading and for the case with  $R^3$  spreading.

# A SERIES OF ELECTRIC FIELD MEASUREMENTS FROM THE 1987

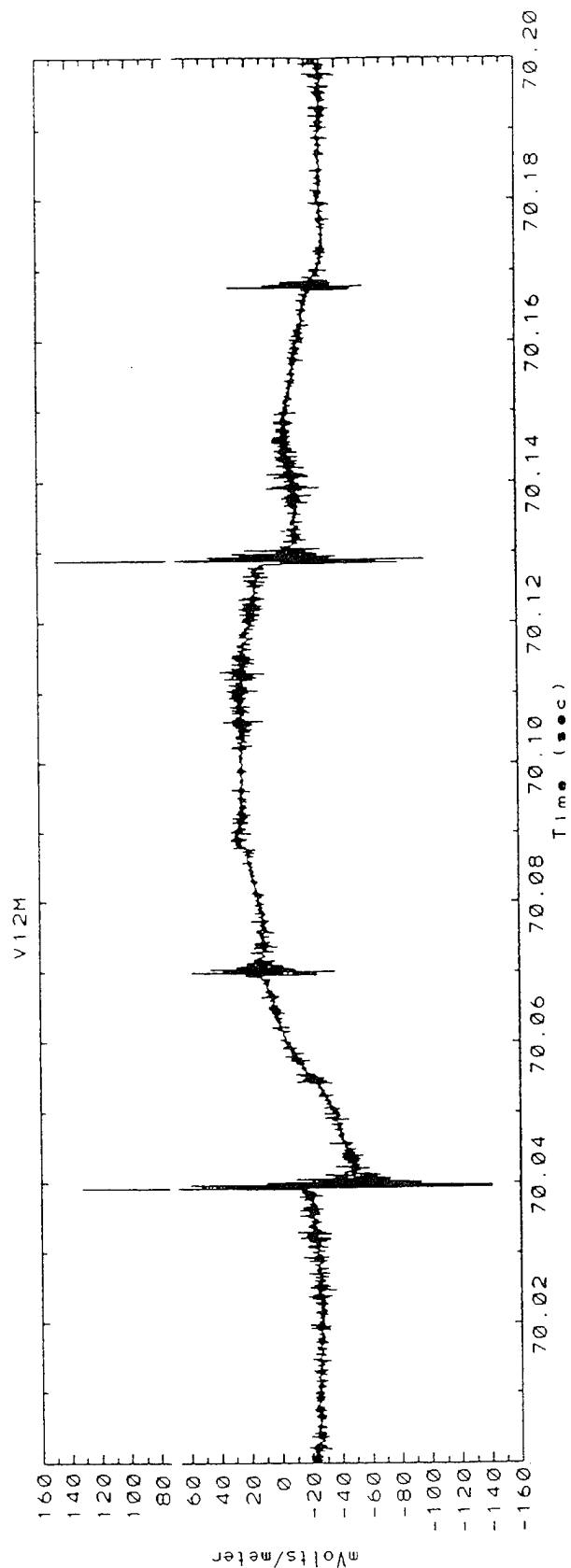
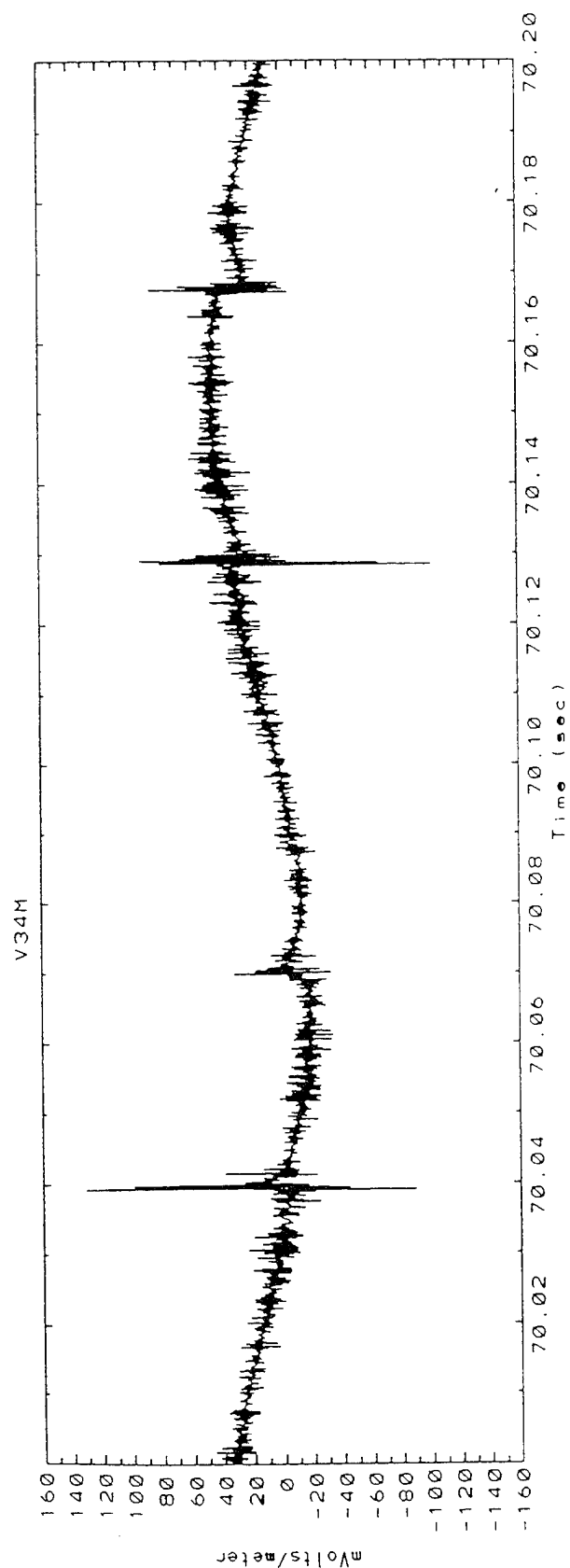
## WIPP Campaign Rocket 33.053 -- Alt=73.0 km

NOTE: DECAY TIME VERSUS ALTITUDE

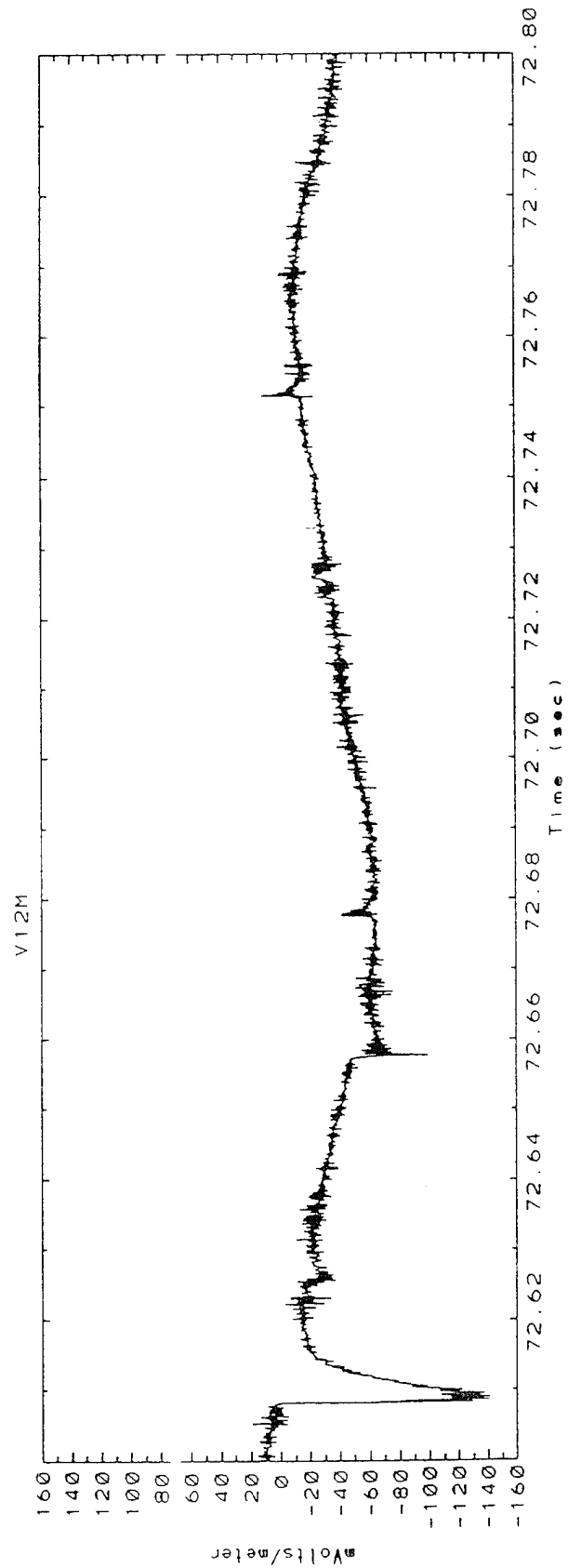
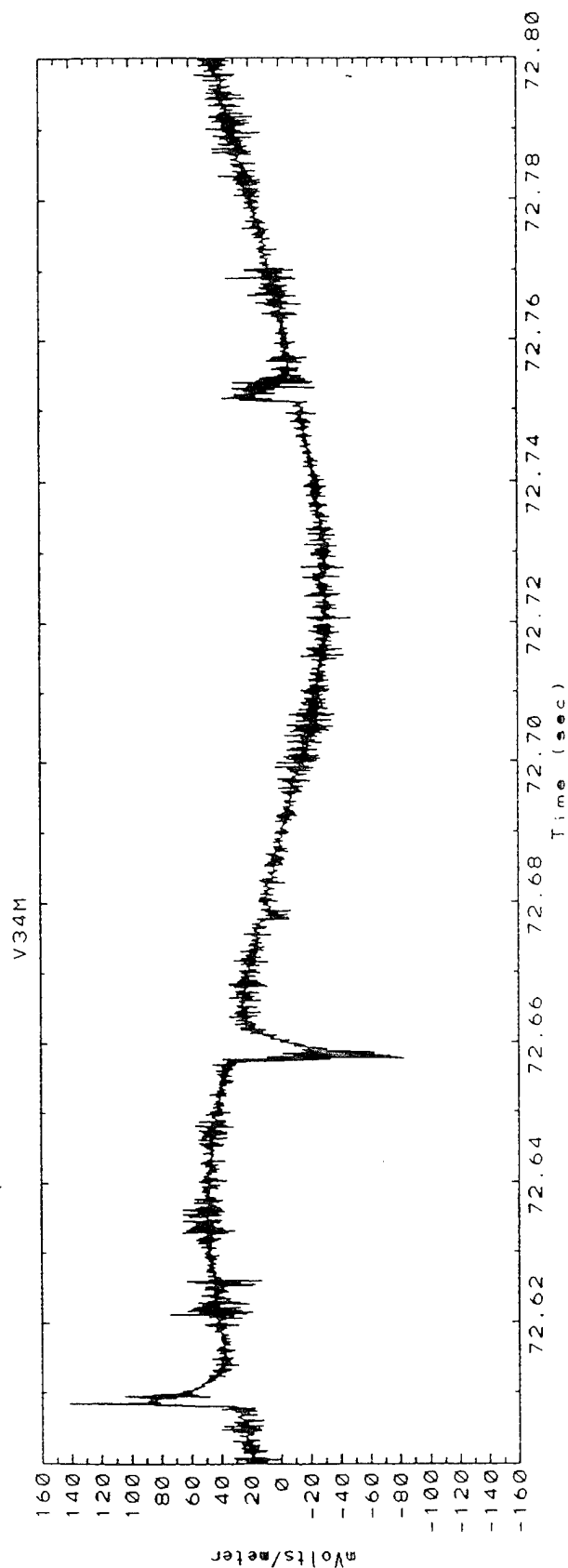




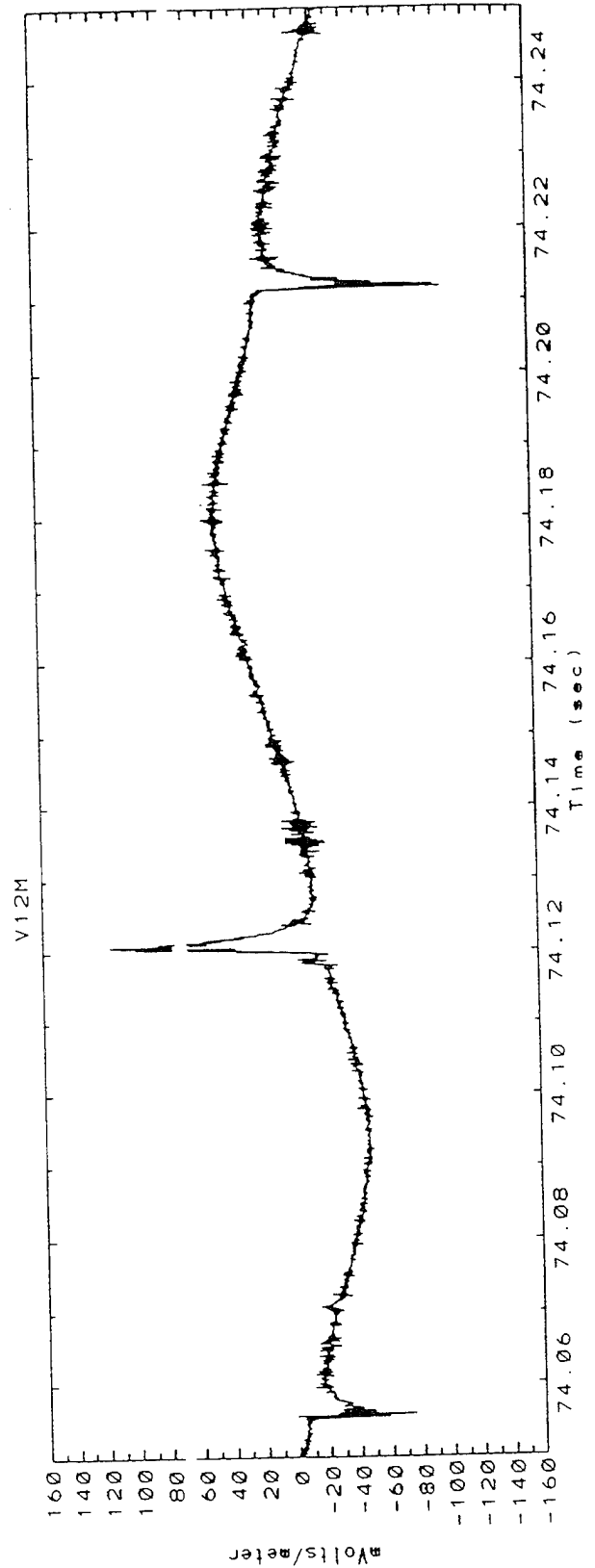
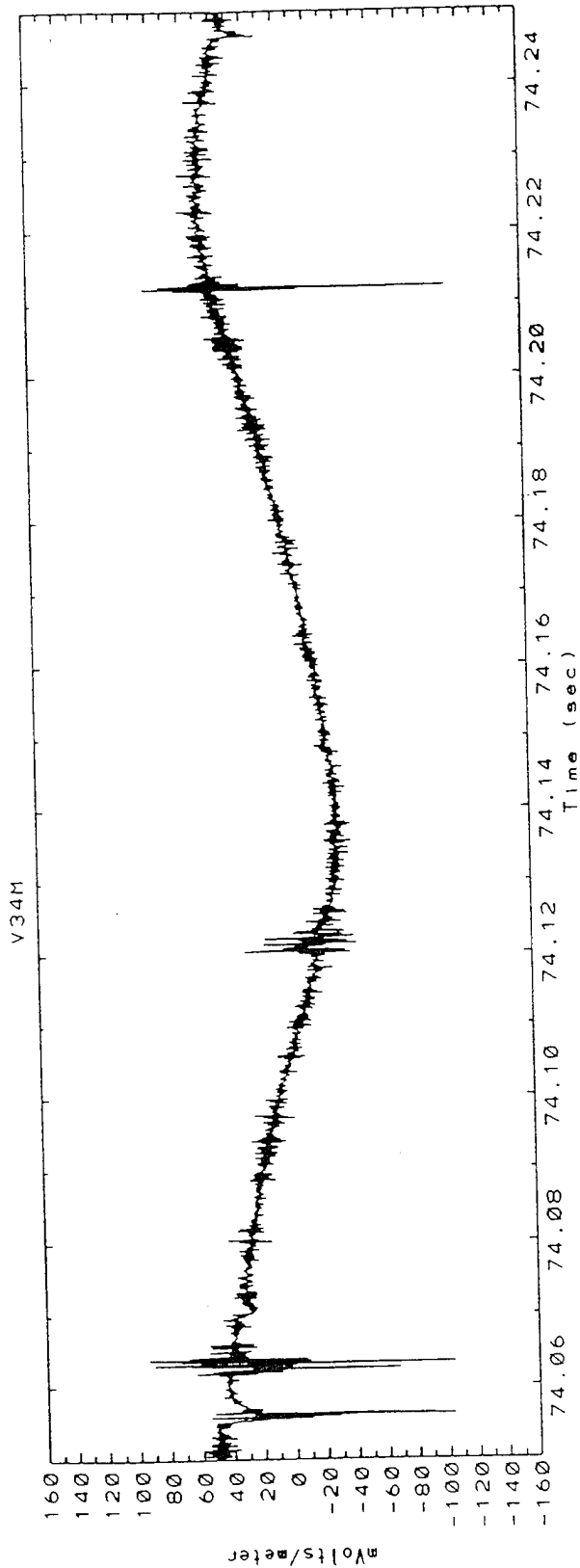
WIPP Campaign Rocket 33.053 -- Alt=84.1 km



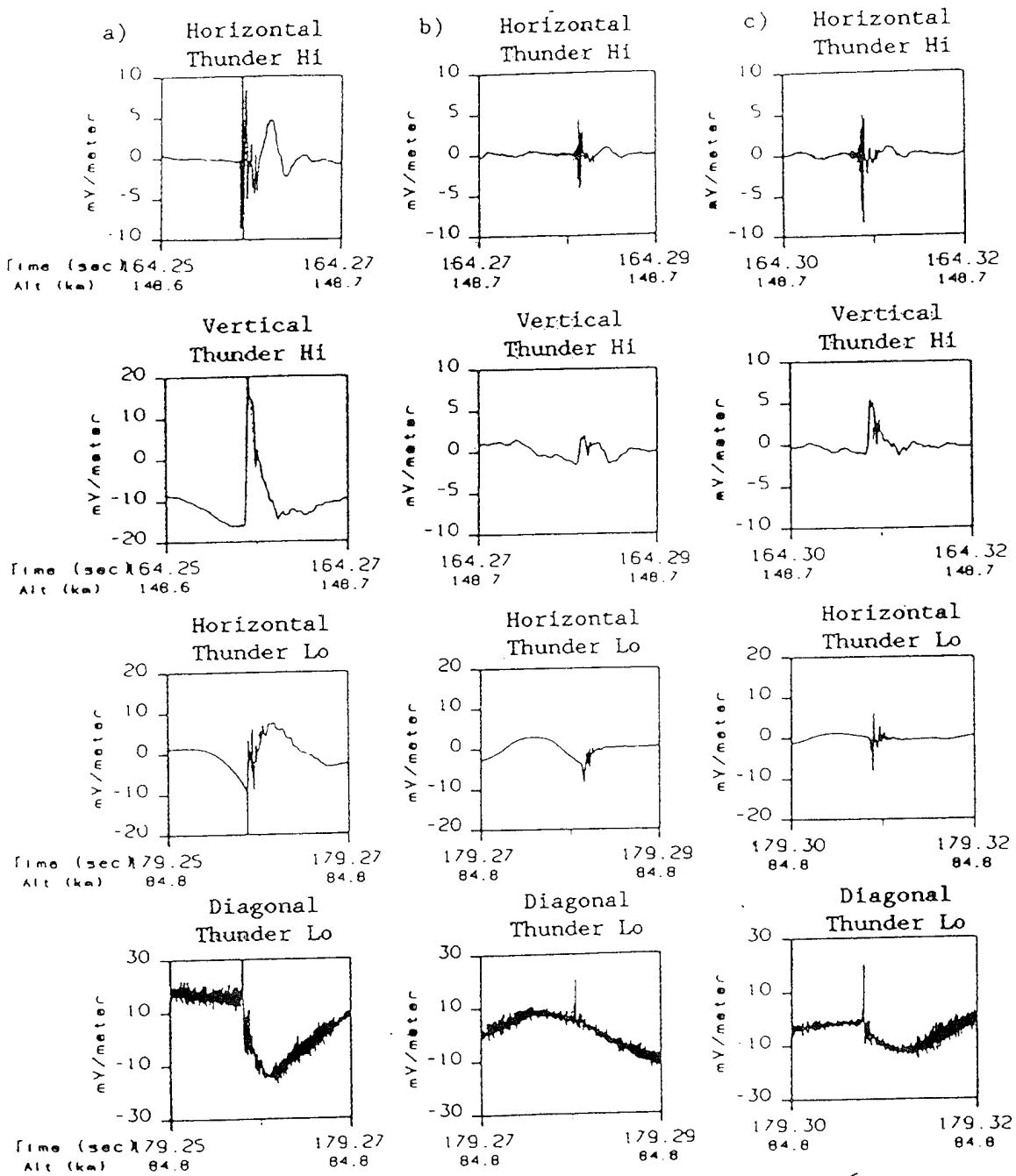
# WIPP Campaign Rocket 33.053 -- Alt=87.6 km



# WIPP Campaign Rocket 33.053 -- Alt=89.6 km



AUGUST 9, 1981



IN TROPOSPHERE      IN MESOSPHERE  
↓                                      ↓

Figure 4.6 Electric field data from both Thunder Hi and Thunder Lo. The data is for three strokes of the same lightning flash.

# COMPARISON OF TIME SCALES FOR TYPICAL MESOSPHERIC E-FIELD AND SPRITE OPTICAL INTENSITY

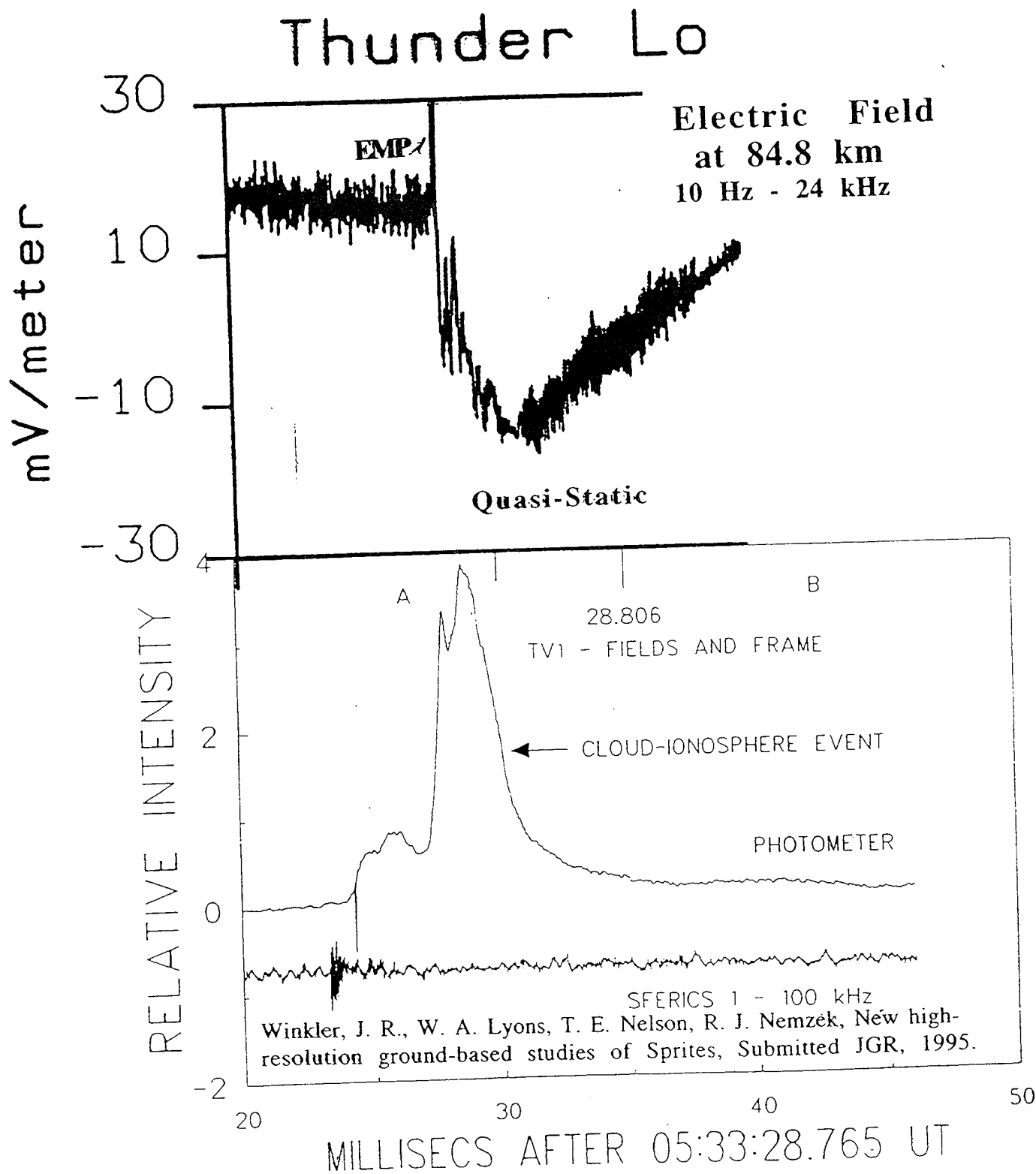


Table 4.1 Statistics for lightning-induced electric field transients.

| Instrument              | Number of Transients                  | Length of Data Period | Average Amplitude    | Rise Time            | Decay Time                  |
|-------------------------|---------------------------------------|-----------------------|----------------------|----------------------|-----------------------------|
| Flat-Plate Antenna      | 11 <sup>1</sup>                       | 300 s                 | * <sup>4</sup>       | * <sup>4</sup>       | ~10 s                       |
| Balloon                 | 13 <sup>1</sup><br>(721) <sup>1</sup> | 300 s<br>(3 hr)       | ~100mV/m             | 0.1 s <sup>5</sup>   | ~10 s                       |
| Parachute-Borne Payload | 2 <sup>1</sup><br>(8) <sup>1</sup>    | 300 s<br>(11 min)     | ~5V/m                | 0.1 s <sup>5,6</sup> | 1-2 s <sup>8</sup><br>5-7 s |
| Thunder Lo              | 35 <sup>2</sup>                       | 120 s                 | ~40mV/m              | * <sup>7</sup>       | 30 ms <sup>7,9</sup>        |
| Thunder Hi              | 70 <sup>2</sup>                       | 300 s                 | ~15mV/m              | 0.2 ms <sup>5</sup>  | 3-5ms                       |
| 33.050                  |                                       |                       |                      |                      |                             |
| Below 150 km            | 45 <sup>1</sup>                       | 124 s                 | ~35mV/m              | 0.2 ms <sup>5</sup>  | >3 ms                       |
| Above 150 km            | 19 <sup>1,3</sup>                     | 179 s                 | ~25mV/m <sup>3</sup> | 0.2 ms <sup>5</sup>  | >3 ms                       |

<sup>1</sup>Corresponds to the number of lightning flashes that induced a transient.

<sup>2</sup>Corresponds to the number of lightning strokes that induced a transient.

<sup>3</sup>Signal-to-Noise ratio limited resolution to signals >10 mV/m.

<sup>4</sup>Instrument calibration not available.

<sup>5</sup>Measurement is limited by frequency response of instrument.

<sup>6</sup>Measurement somewhat limited by telemetry degradation due to lightning.

<sup>7</sup>Signals did not show a clear rise-time and decay.

<sup>8</sup>Data is fit best by two time constants. A fast time constant for the first portion of the transient (1 to 2 e-folds) and a 'tail' with a slower decay.

<sup>9</sup>Signals did not show a clear decay-time. The time given corresponds to the duration of the lightning induced signals.

## D-Region Electric Field Measurements and Sprites

- Lightning-generated electric fields have been measured directly over thunderstorms in the nighttime D-region (although not many cases published).
- Field strengths are much lower than required for local breakdown 10-100 mV/m versus a few V/m (at 90 km) or 100 V/m (at 70 km).
- In the past entire field (EMP and Quasi-Static) has not been measured.
- Highest frequency response limited to about 24kHz, thus a large fraction of the EMP fields are unmeasured.
- Time scale of the Quasi-static field ~10 ms is close to Sprite duration while the EMP is consistent with short duration large area airglow.
- Previous measurements are from average sized east coast thunderstorms.
- There are no indications that large lightning discharges or positive cloud-to-ground discharges have ever been measured.

The upward coupling of the 'quasi-static' fields in the 70 -100 km altitude range is not well understood.

$$\sigma = \begin{pmatrix} \sigma_P & \sigma_H & 0 \\ -\sigma_H & \sigma_P & 0 \\ 0 & 0 & \sigma_{\parallel} \end{pmatrix}$$

$\sigma_{\parallel} = \text{parallel}, \sigma_P = \text{Pedersen}, \sigma_H = \text{Hall}$

Parallel fields ( $E \parallel B$ ) should couple as at lower altitudes with  $E \propto \sigma_{\parallel}^{-1}$ .

Perpendicular fields are more complicated.

The 'quasi-static' electric field is driving currents in the atmosphere which are then converting to electromagnetic waves.

The Hall term in the conductivity allows the fields to penetrate much further in a whistler mode (i.e.,  $J \perp E$  is energy not absorbed in the medium).

Picture is further complicated by wave reflection and destructive interference in this region.

Most models have ignored Hall term.



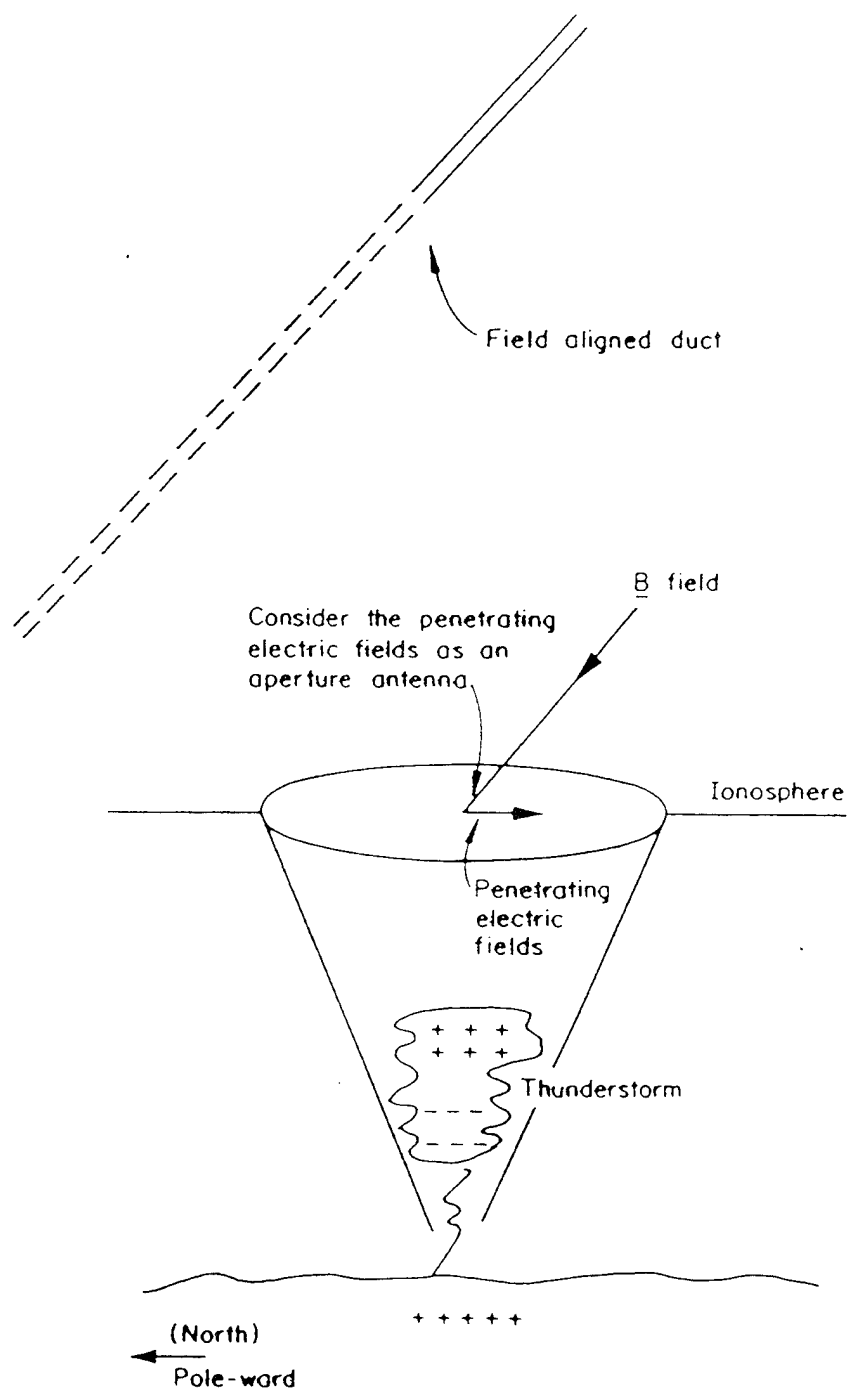


Figure 4.17 Schematic diagram of a new whistler generation model.

## **What to do next?**

**Fly rockets over a large storm that is producing both positive and negative cloud-to-ground flashes.**

**Wallops Island is not a good location.  
White Sands Missile Range, New Mexico?  
Eglin AFB, Florida?  
Puerto Rico in 1997?  
Others?**

**Measure full vector electric field (EMP and Quasi-Static) with high frequency response 0 - 100 KHz (? MHz).**

**Have high time resolution ground-based measurements to determine  $Q$ ,  $I$ ,  $\delta I/\delta t$  so we can scale fields for the largest of lightning strokes.**

**Measure the response of the D-region to the applied fields (electron energy distribution, density enhancements, etc.).**

*Sprites Workshop*  
Phillips Laboratories  
Hanscom AFB  
Bedford, Mass.  
October 18-19, 1995

## SPACE-BORNE OBSERVATIONS OF GAMMA-RAY FLASHES ABOVE THUNDERSTORMS

G.J. Fishman, R. Mallozzi<sup>1</sup>, J.M. Horack  
Space Sciences Laboratory  
NASA- Marshall Space Flight Center  
Huntsville, AL 35812

### Abstract

Intense flashes of MeV photons have been observed with space-borne detectors above thunderstorms. These flashes must originate at altitudes above 30 km, in order to be observable by orbiting detectors. At least fifty events have been detected over the past four years by the Burst and Transient Source Experiment (BATSE) aboard the Compton Gamma-Ray Observatory (CGRO). The most likely origin of these high-energy photons is bremsstrahlung from electrons, presumably from high altitude electrical discharges above thunderstorm regions. As a discharge phenomenon they are likely related to jets and sprites, although a coincident event has not yet been observed due to sporadic global coverage of both phenomena.

<sup>1</sup>also University of Alabama, Huntsville

## Introduction

The Compton Gamma-Ray Observatory (CGRO) was launched in April 1991 to perform observations of celestial gamma-ray sources. The Burst and Transient Source Experiment (BATSE) is one of four experiments on the observatory. It serves as an all-sky monitor, detecting cosmic gamma-ray bursts, hard x-ray transients, persistent x-ray sources and solar flares. In addition to these celestial sources, on rare occasions BATSE has seen gamma-ray flashes from the earth's atmosphere.

The terrestrial gamma-ray flashes discovered by BATSE must originate at altitudes above at least 30 km in order to be observable by orbiting detectors. At least fifty events have been detected over the past four and a half years. Several of the events are seen to come from the direction of large weather systems, although concurrent weather images are not available in most cases. The energy spectra from the events are consistent with bremsstrahlung from energetic (MeV) electrons.

## The BATSE Detector System

BATSE consists of an array of eight detector modules located at the corners of the observatory, arranged to provide maximum unobstructed sky coverage (Figure 1). The scintillation detectors are sensitive to photons with energies above 20 keV. The geometry of the array results in sources being usually observed by four detectors. Data from the detectors are processed on-board by a data system which sorts the data into several data types with differing temporal and spectral resolution.

The BATSE data type with high time resolution used to study the gamma-ray flashes reported here is the time-tagged event (TTE) data. These data are usually recorded whenever the on-board trigger system is enabled. However, sometimes these data are overwritten or otherwise unavailable due to telemetry gaps. In these cases, only data with 64 ms time resolution are available. The TTE data consist of up to 32,000 individual scintillation detector events that are identified by the detector module that recorded it, the energy channel (one of four channels) and the arrival time (recorded to 2 $\mu$ s relative accuracy). The four energy channels are approximately 20-50 keV, 50-100 keV, 100-300 keV and >300 keV. A continuously operating ring buffer allows the recording of approximately 8,000 events prior to the time of the trigger recognition. These "pre-trigger" data have been essential in these studies of short timescale phenomena such as these events.

## Observations

The initial paper describing twelve of over fifty of these events was published last year (Ref. 1). A world map of the spacecraft location at the time of these twelve events, along

with the global distribution of thunderstorms is shown in Figure 2 (from Ref. 1). Note that the 28.5 degree inclination of the spacecraft orbit confines the observatory primarily to tropical regions. The general similarity of the two distributions is apparent, along with the scarcity of events over the large ocean regions of the world, where few mesoscale thunderstorms form.

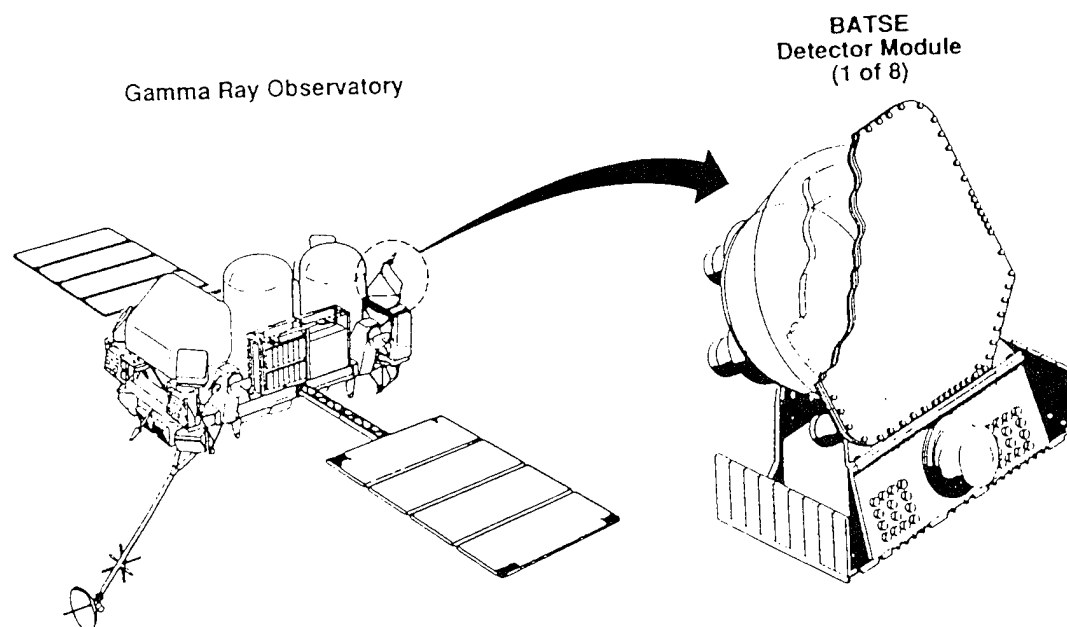


Figure 1. The BATSE experiment on the Compton Gamma-Ray Observatory

Two unique characteristics of these events are their extremely hard spectra and their short duration. These features are very distinct from other events which have triggered the BATSE detectors such as gamma-ray bursts, solar flares, fluctuations of other known hard x-ray and gamma-ray sources, and bremsstrahlung from precipitating magnetospheric electrons. Most of these events are seen by more than four detectors, as there is considerable scattering of photons in the spacecraft and transmission through the rear of the detector modules. However, the observed counting rate ratios of the detectors are consistent with the source of these events originating from a large distance relative to the spacecraft dimensions. Furthermore, these events are located by the BATSE detectors as emanating from below the local horizon. Other, independent detectors from another experiment on the Compton Observatory confirm these events. It is likely that many other, weaker events of similar origin go undetected due to the trigger criteria implemented by BATSE. In particular, the minimum sampling time for triggering the BATSE burst mode is 64ms, over ten times longer than the duration of most of these events. Estimates of the direction to the sources of the flashes can be made by comparing the relative responses of the eight BATSE detectors which view different directions.

However, the directions thus derived are rather imprecise due to the penetrating nature of these photons. Typically, the azimuth and elevation direction sectors are derived with uncertainties of from 30 to 60 degrees.

It is believed that prior instrumentation and experiments were incapable of detecting the events reported here for various reasons, or these events were overlooked as being

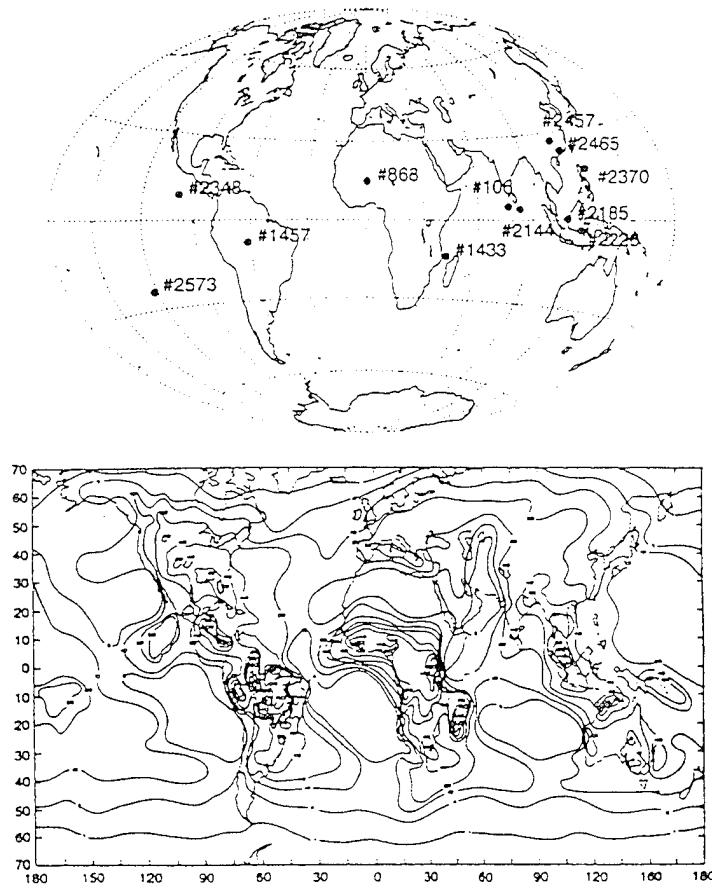


Figure 2. The global distribution of 12 of the events compared with that of thunderstorm regions.

spurious. The temporal resolution of most experiments would not have been able to respond to these very brief events and/or would have had poor signal to noise when sampled with coarser time resolution.

Many of the events have multiple pulses and, in a few events, the pulses seem to overlap. Durations of the majority of events are from 1ms to 6ms, although durations as short as 0.5ms and as long as 10ms have been seen. The time profile of an event detected on September 22, 1995 is shown in Figure 3. Here the detected photons in two detectors are

plotted in 100 $\mu$ s bins. The event duration was about 5ms and consisted of multiple of peaks, some of which are unresolved in the later stages of the event. All of the peaks have characteristic rise-times and fall-times of 100-200 $\mu$ s.

No prior references to gamma radiation from atmospheric electrical discharges or from electrons precipitating from the magnetosphere have been found in the literature. Because of the new and unique nature of these events, the lack of correlated observations in other spectral regions, and the paucity of concurrent weather data, the exact cause of the

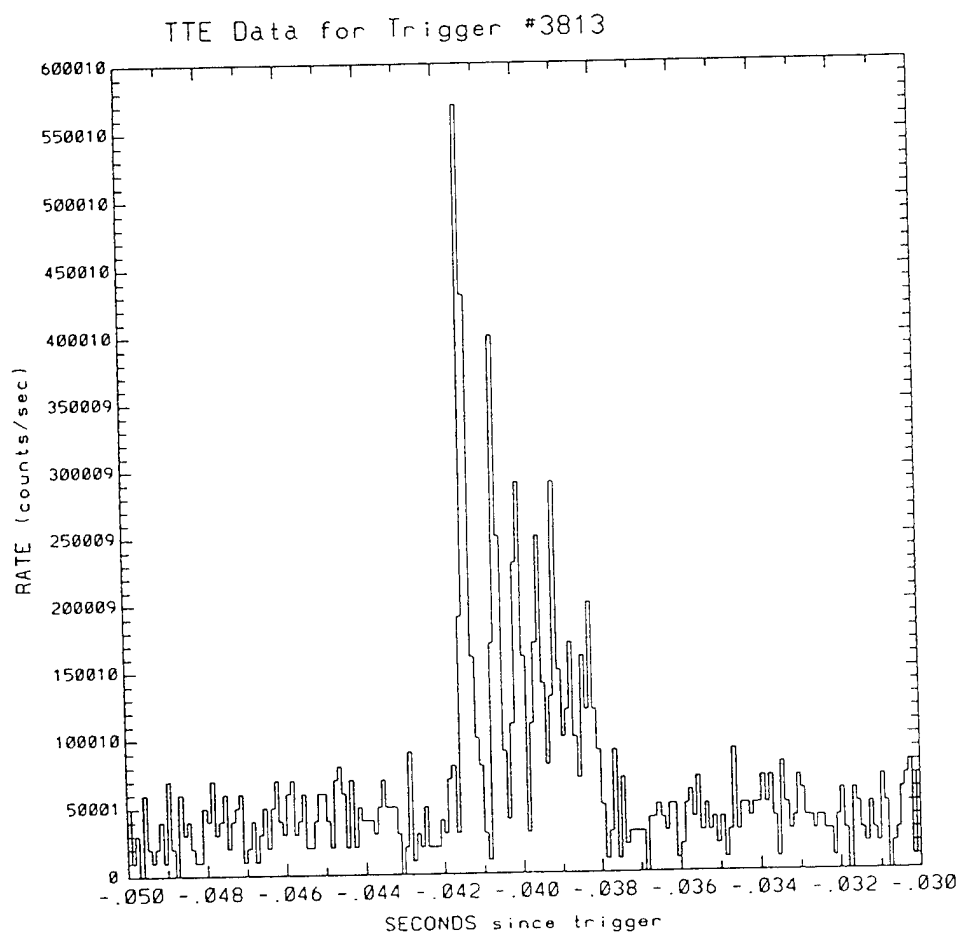


Figure 3. The time profile of a recent event (see text).

phenomenon must await further study. However, recent observations by Inan, et al. (priv. comm.) show evidence for at least one of these events being associated with intense spherics from thunderstorms off the western coast of Mexico.

## Spectral Characteristics of the Terrestrial Gamma-ray Flashes

The terrestrial gamma-ray flashes (TGF's) seen by the BATSE experiment all have characteristic hard spectra that are unlike any other spectra observed by BATSE from either a geophysical or an astrophysical source. For example, the spectra produced by precipitating geomagnetically-trapped electrons are often seen by BATSE in the geomagnetic regions above  $L=1.0$ . These photons have a relatively soft spectra, with few observed photons above 300 keV. Most galactic neutron star and black hole sources observed by BATSE have spectra that are characteristic of radiation produced by optically-thin thermal bremsstrahlung (OTTB), with typical characteristic temperatures between 10 keV and 50 keV.

It has been difficult to deconvolve the spectra of the TGF's due to: 1) The penetrating nature of their spectra makes a unique deconvolution difficult, since only partial energy losses from the photons are usually recorded in the detectors and 2) The TGF's produce only a limited number of detected photons during the brief appearance of the event.

In Figure 4, we show a plot of individual photons (or, more correctly, counts) from one of the TGF events. Plotted here are the detected energy deposits of single photons in the eight BATSE spectroscopy detectors (SD's). Each photon is indicated by its arrival time and energy loss in the detector. The cluster of photons around 0.019s before the trigger of the on-board burst system clearly distinguishes the TGF from the isolated background events (mainly secondary cosmic-ray photons). The detectors are operated at different

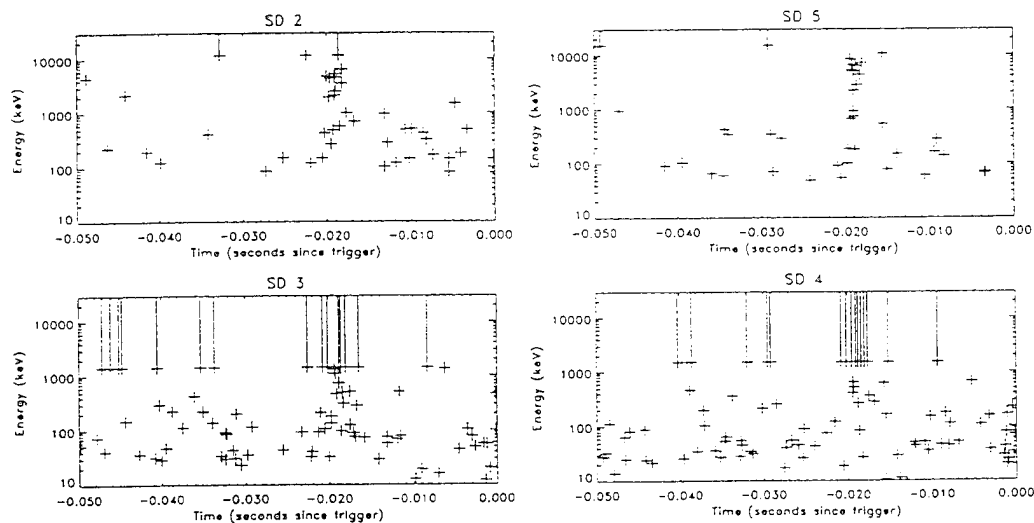


Figure 4. A plot of the arrival time and energy of photons from four of the eight BATSE spectroscopy detectors (SD's), from event #868, detected on October 5, 1991.



gains and thus have different energy ranges. Many of the events in the BATSE spectroscopy detectors no. 3 and 4 are above the upper range of the detectors (about 1.5 MeV), as indicated by an upward line from the cross at each event. The incident photon energies of these events are likely to be considerably higher than this lower limit.

#### Future Work

The Compton Gamma Ray Observatory will continue observations for at least another five years. The current interest in Sprite observations should allow numerous opportunities for coordinated observations of the gamma-ray phenomena and high-altitude discharges above thunderstorms. Work is currently in progress to improve the determination of the spectra of these events.

#### Reference

1. Fishman, G.J.; Bhat, P.N.; Mallozzi, R.; Horack, J.M., et al., "Discovery of Intense Gamma-ray Flashes of Atmospheric Origin", *Science*, 27 May 1994, Vol. **264**, (no. 5163): 1313-16.

## ELECTROMAGNETIC FIELDS OF RED SPRITES

Les Hale and Lee Marshall

Communications and Space Sciences Laboratory

Penn State University, University Park, PA 16802

Tel: (814) 865-2361; FAX: (814) 863-8457; e-mail: Les Hale@PSU.EDU

The time-dependent electromagnetic (E and H) fields of several dozen "red sprites" (visually identified by Walt Lyons of Ft. Collins, CO) were measured in Central Pennsylvania. Battery-powered equipment at a low-noise site away from power lines was used to avoid 60 Hz and harmonics, although a 60 Hz notch filter was still necessary for the magnetic field data.

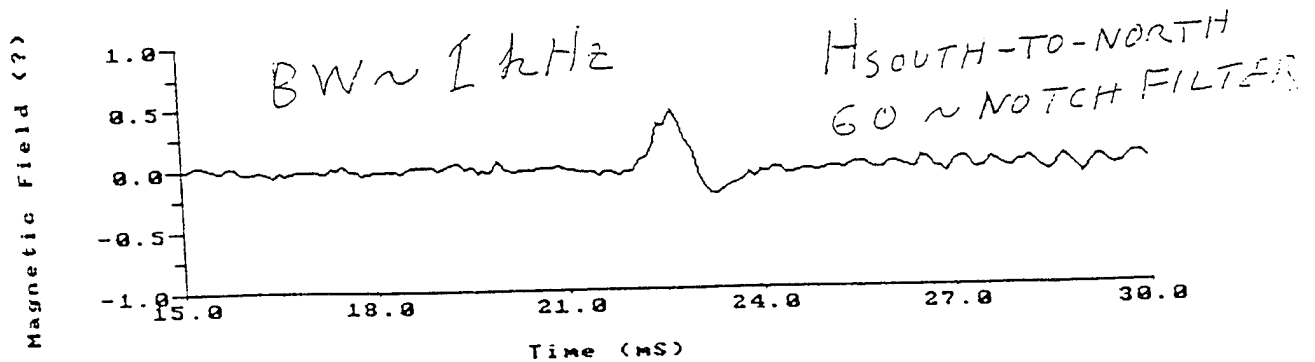
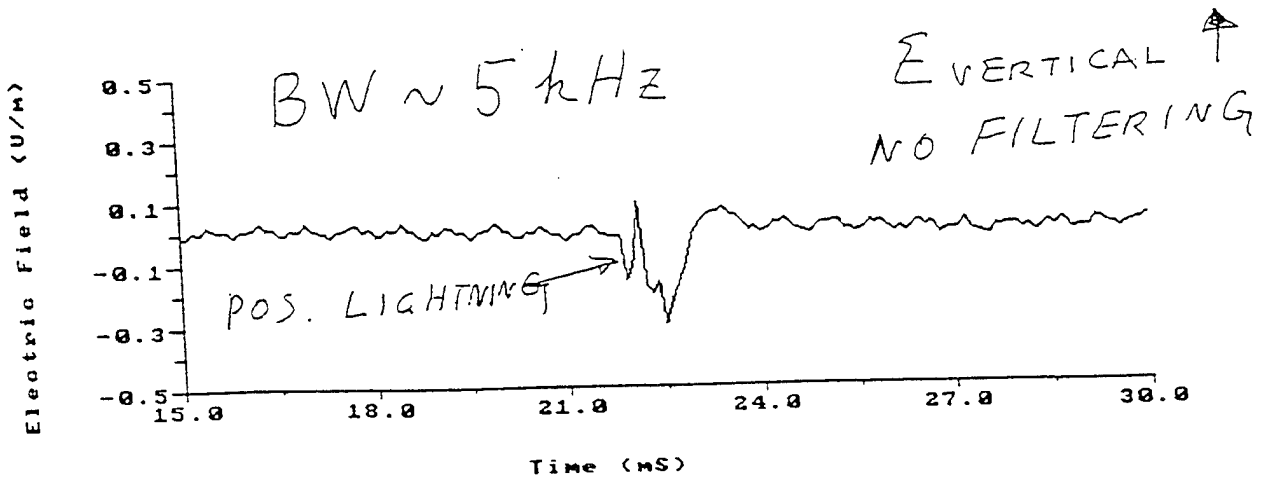
Unexpectedly, the sprites-related data were easily distinguishable from other events, which occurred much more frequently. This was due to a characteristic polarity (related to "positive" lightning), a greater pulse width, and other characteristics, including detailed structure related to the "visual" sprite. The power spectra of the sprites were primarily at ELF above the Schumann resonance range, at about 100-300 Hz. However, the EM energy was so large (about a megajoule) that they could be detected over a broader range of frequencies, and are probably large IR sources.

The characteristic shape of the waveforms was such that it would appear to be possible to build an electronic "sprite detector," which in conjunction with lightning locator data could provide a "sprite mapper" which would function independently of visual observations.

The original abstract is above. What was presented at the workshop follows below:

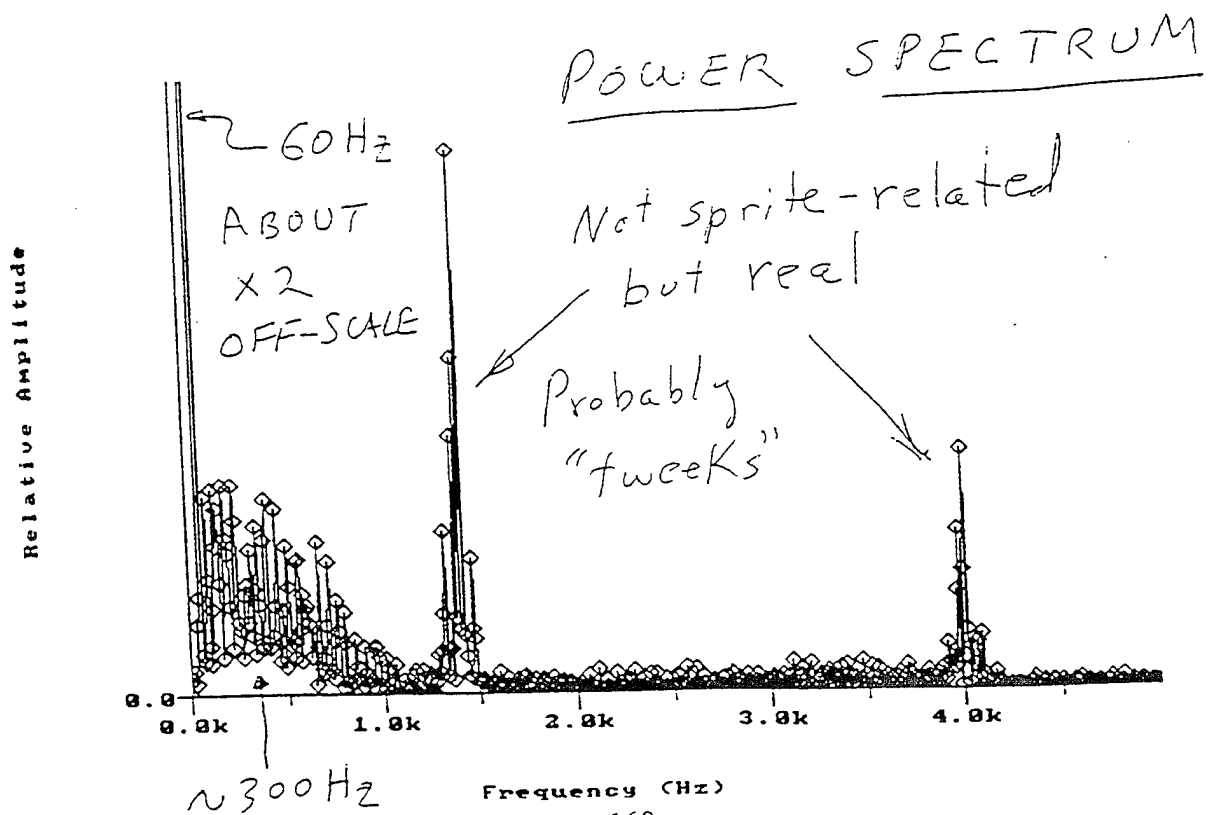
We show in the following figures electric and magnetic field data related to "sprites" and "airglow events identified by Walt Lyons on the date of July 24, 1995. The magnetic field has not yet been accurately calibrated but is believed to be related to the electric field by  $E_z = 377H_\phi$ , which is consistent with the "radial TEM" or zero mode of propagation. The bandwidth of the electric field measurement was about 5 kHz and the magnetic field about 1 kHz. Note that the electric field consequently shows much more structure due to faster events but the lower frequency "filtered" magnetic field, which could also be generated by filtering of the electric field, shows a more consistent structure. This indicates that the ELF signal in the roughly 100 Hz to 1 kHz range could be used in constructing a "sprite monitor" with a range of thousands of kilometers (but ~5 Hz to ~50 kHz should be used to study basic physical processes, in conjunction with optical measurements, in future campaigns).

# "SPRITE"

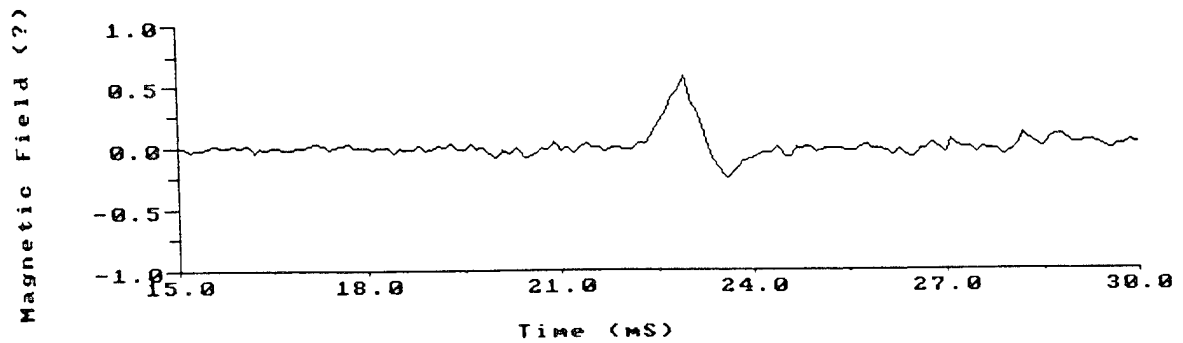
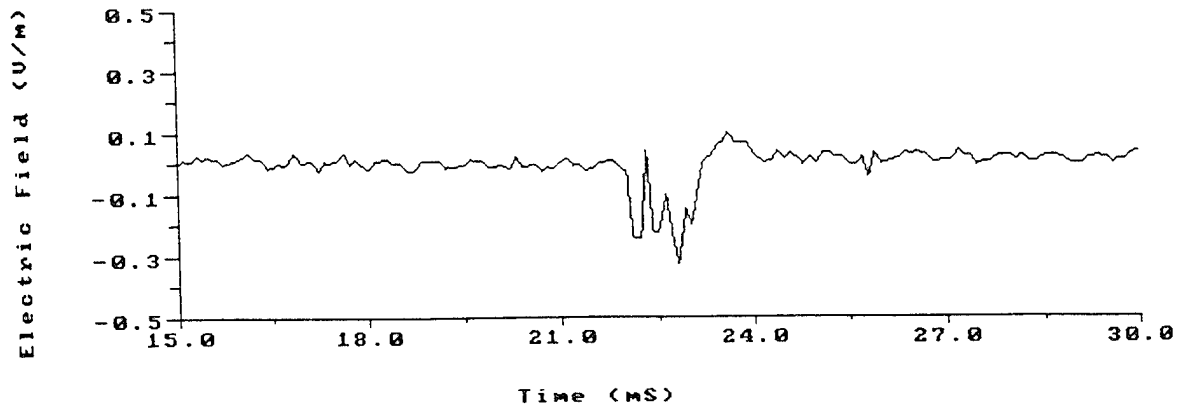


d:\rs724\064040.DAT

## ELECTRIC PSD

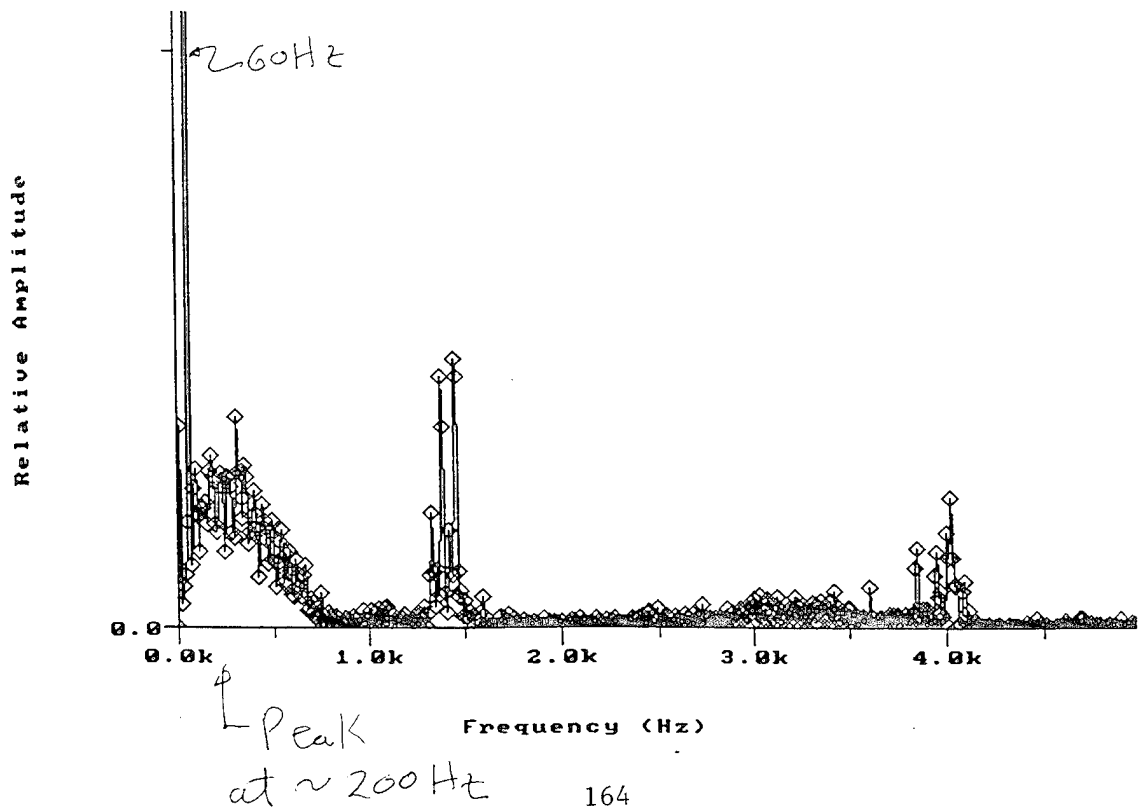


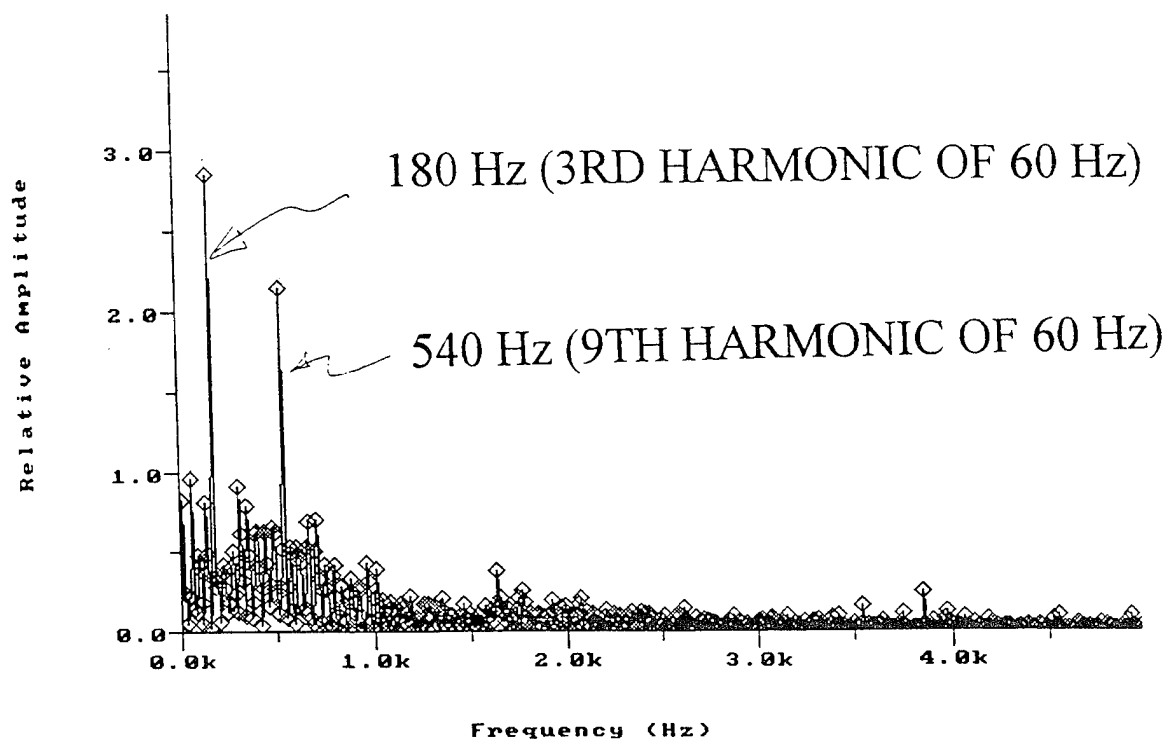
# "SPRITE"



d:\rs724\065138.DAT

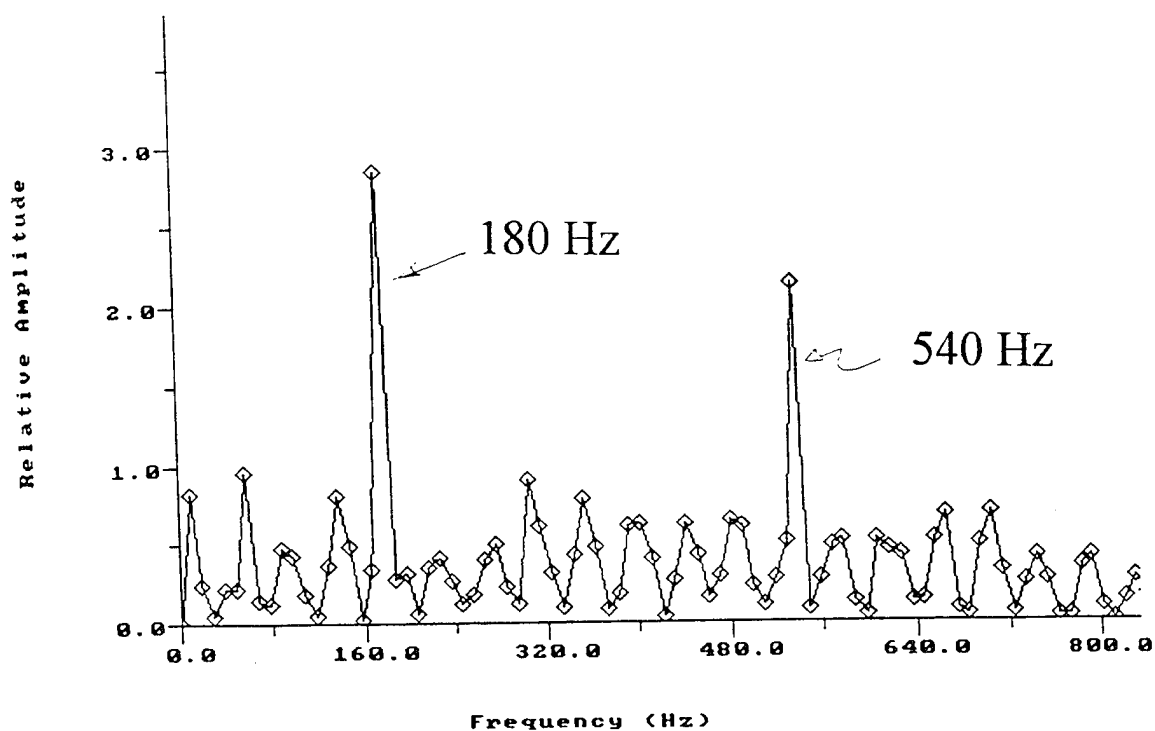
ELECTRIC PSD



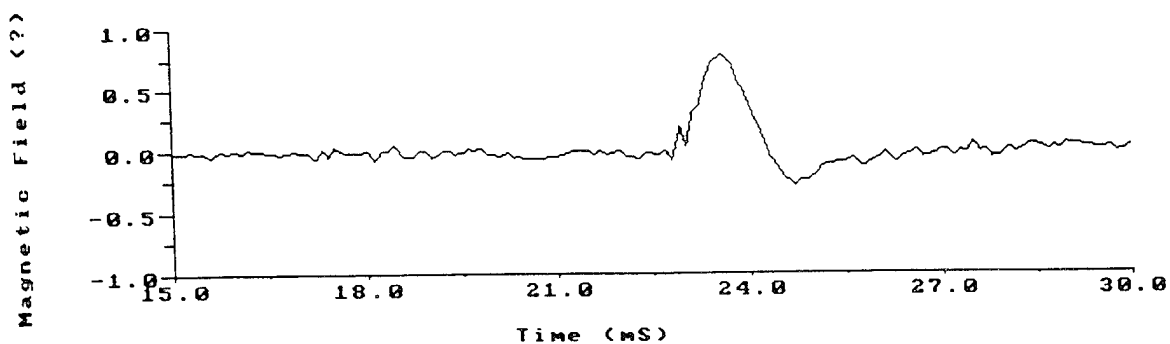
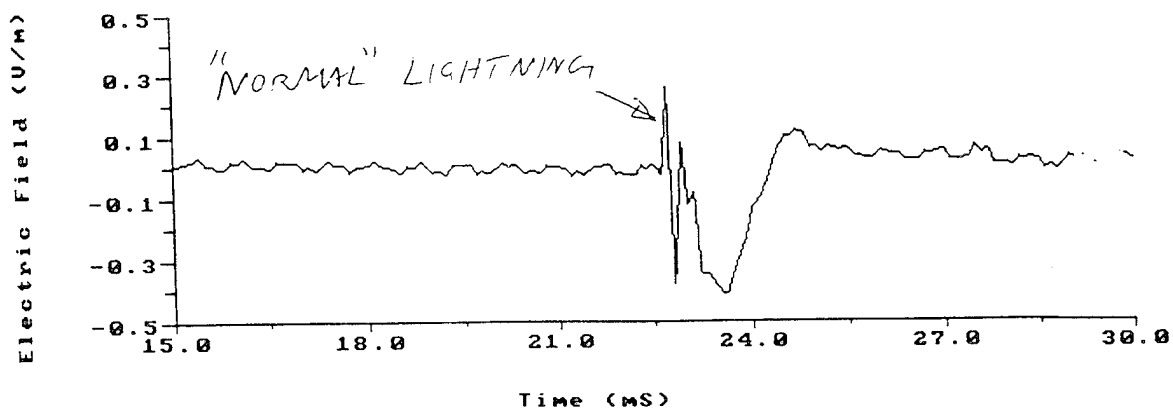


d:\rs724\065138.DAT

MAGNETIC PSD

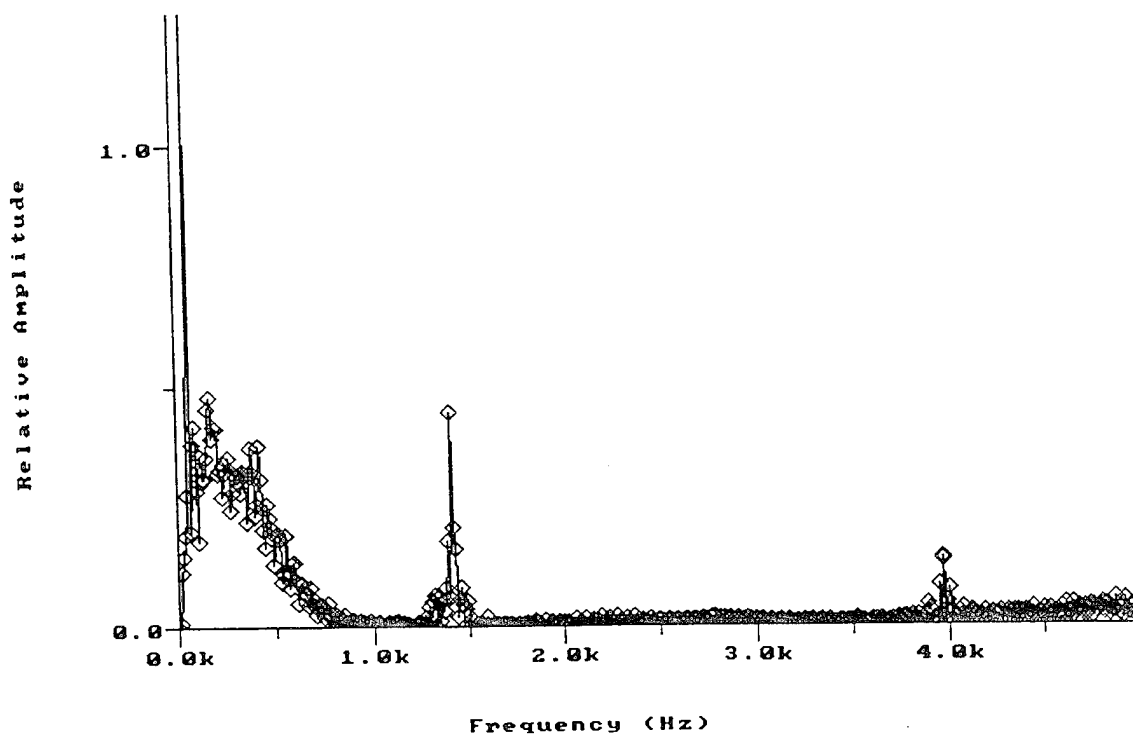


# "AIRGLOW EVENT"

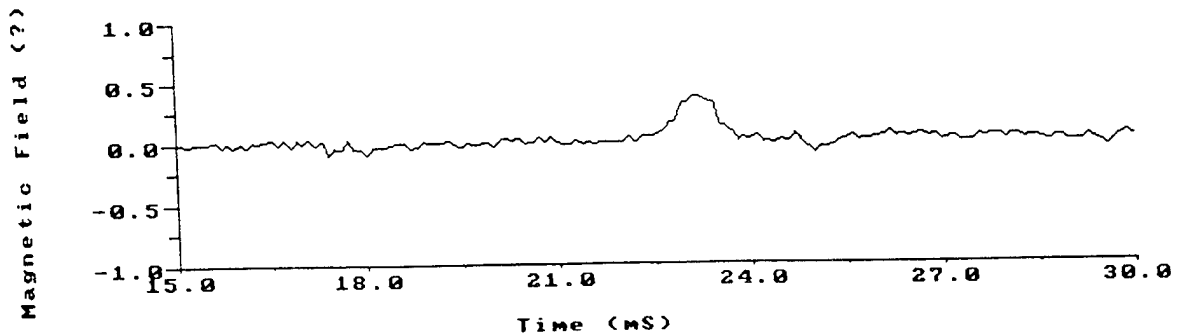
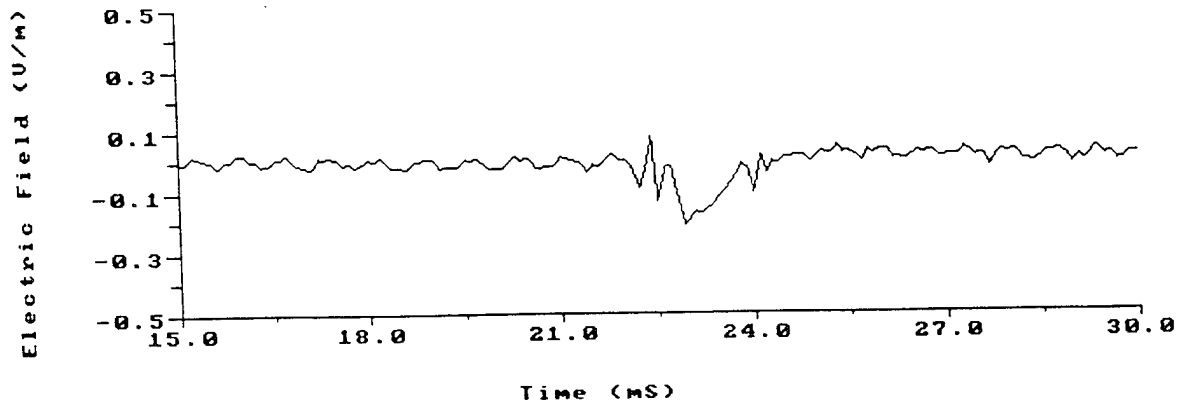


d:\rs724\065753.DAT

## ELECTRIC PSD

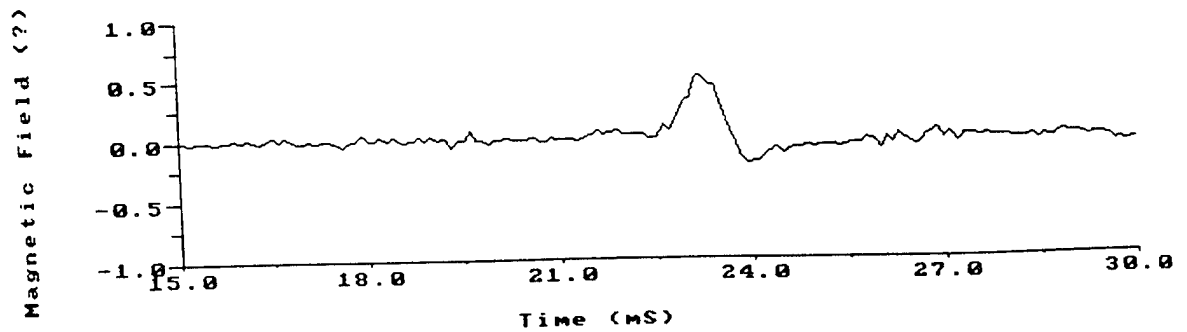
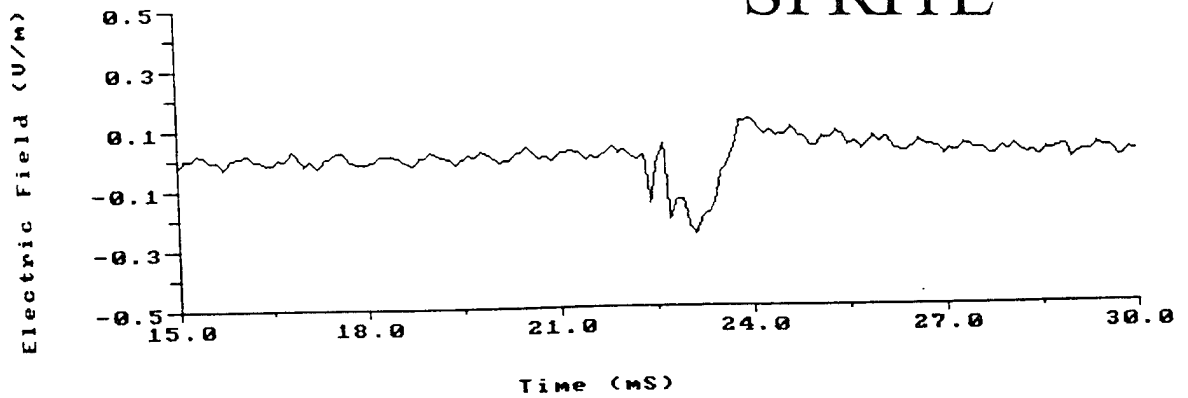


# "SPRITE"

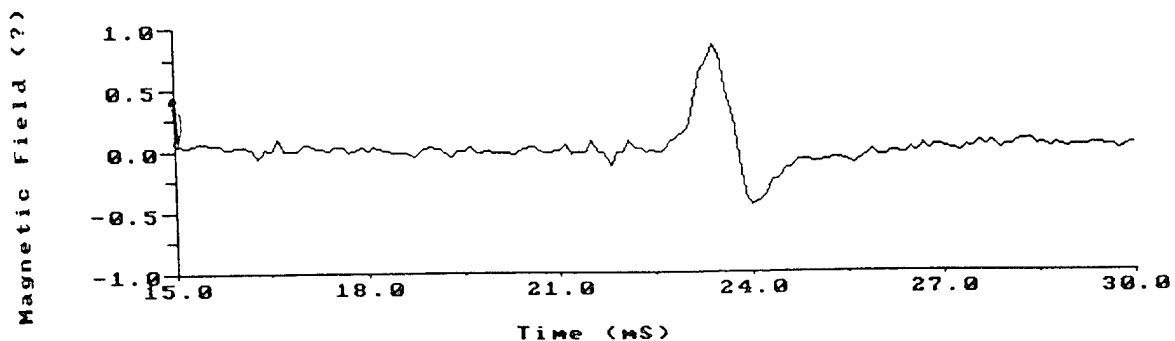
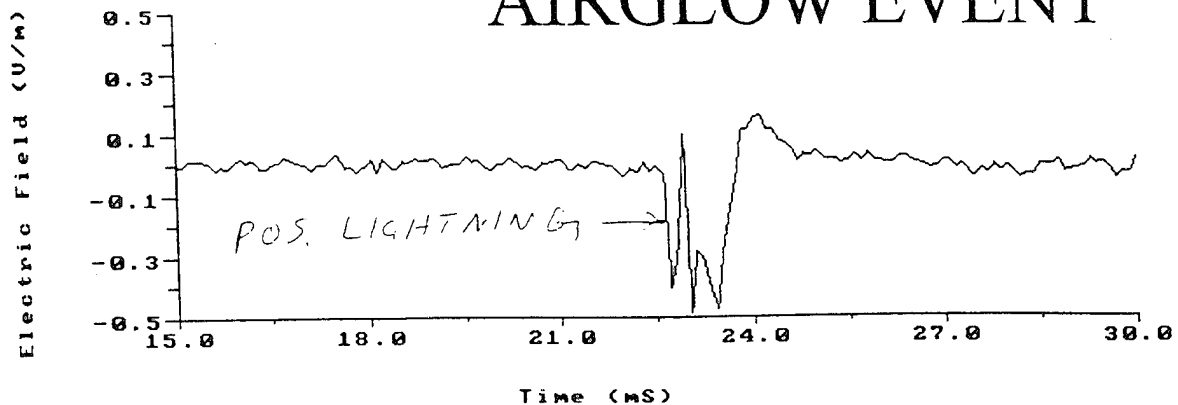


d:\rs724\071632.DAT

# "SPRITE"

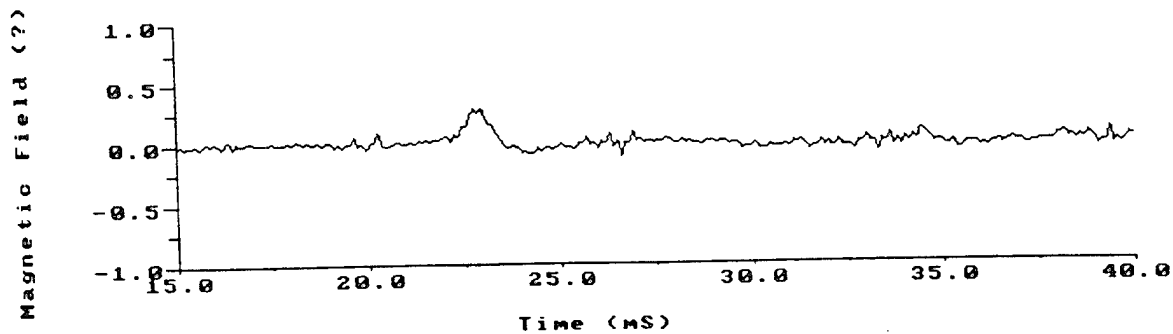
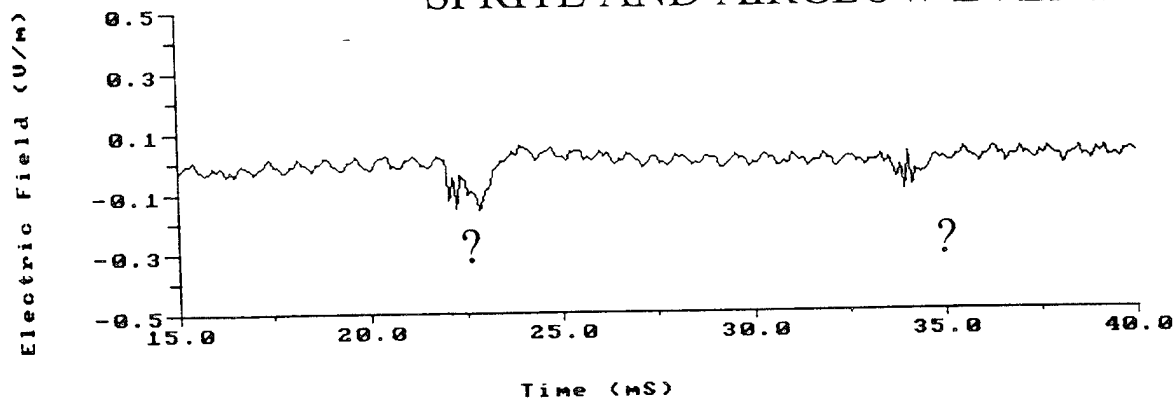


# "AIRGLOW EVENT"



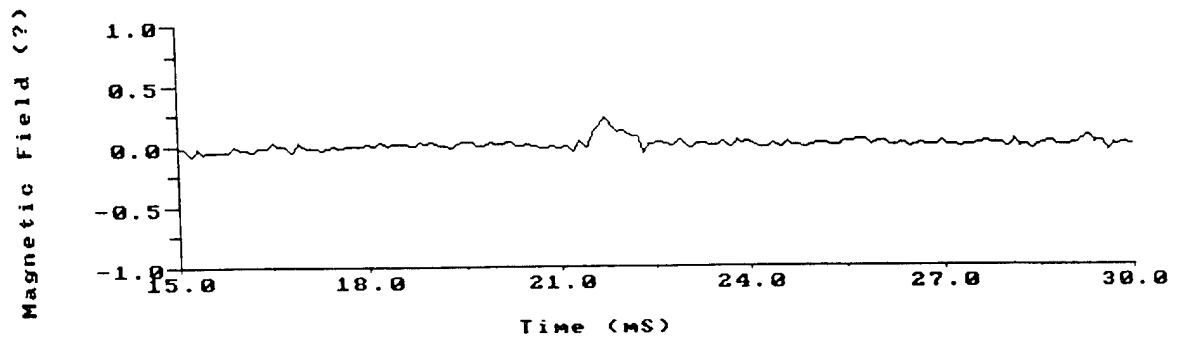
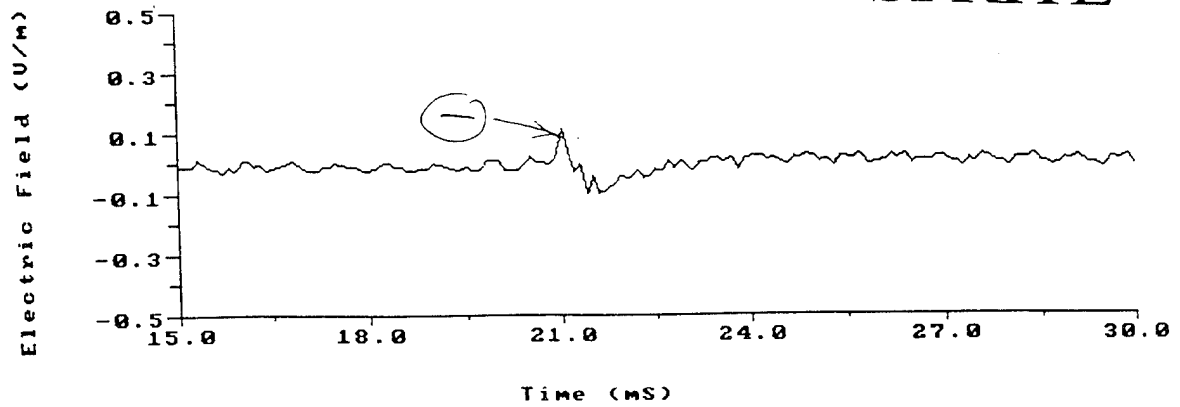
d:\Nrs724\070546.DAT

# "SPRITE AND AIRGLOW EVENT"



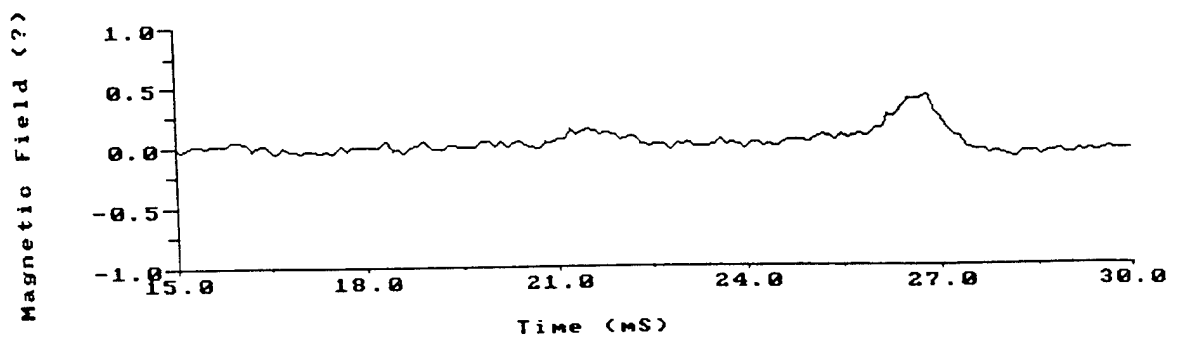
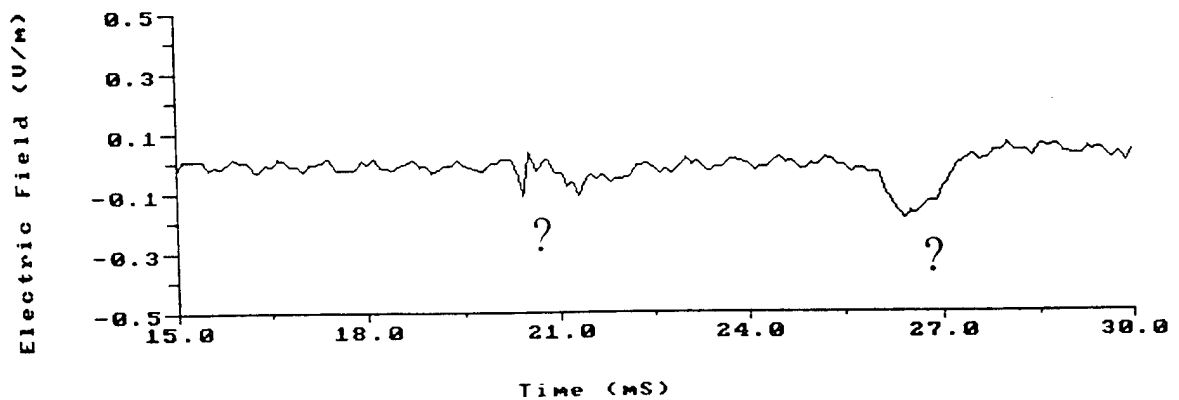


# "SPRITE"

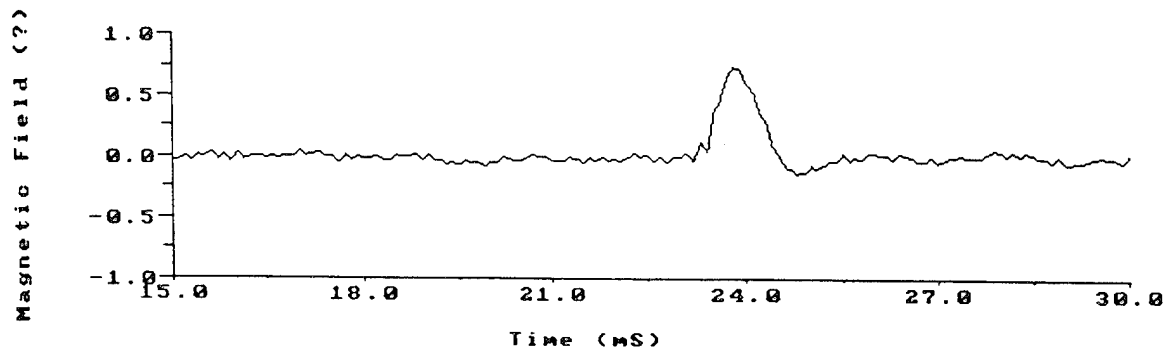
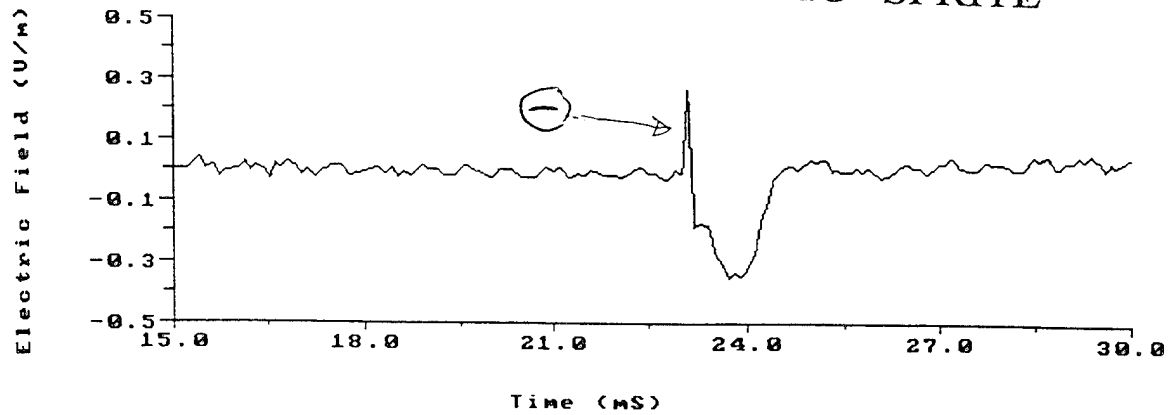


d:\rs724\080034.DAT

# "SPRITE"

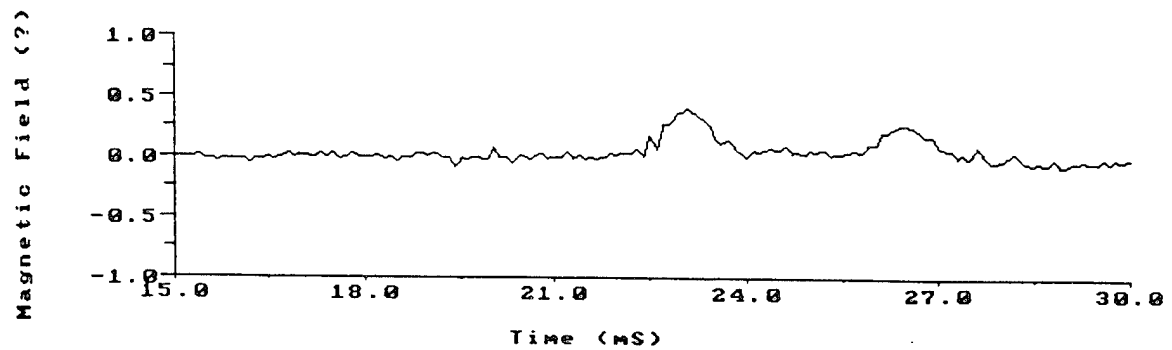
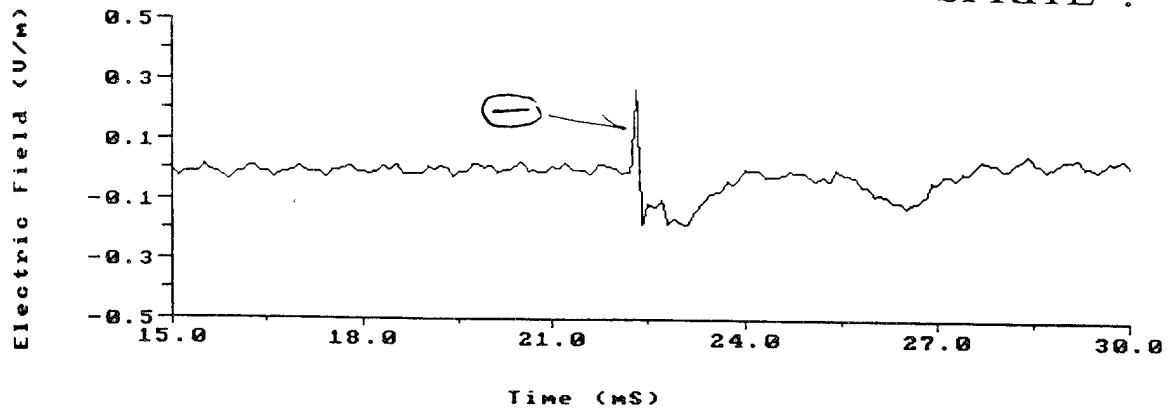


## BIG "SPRITE"

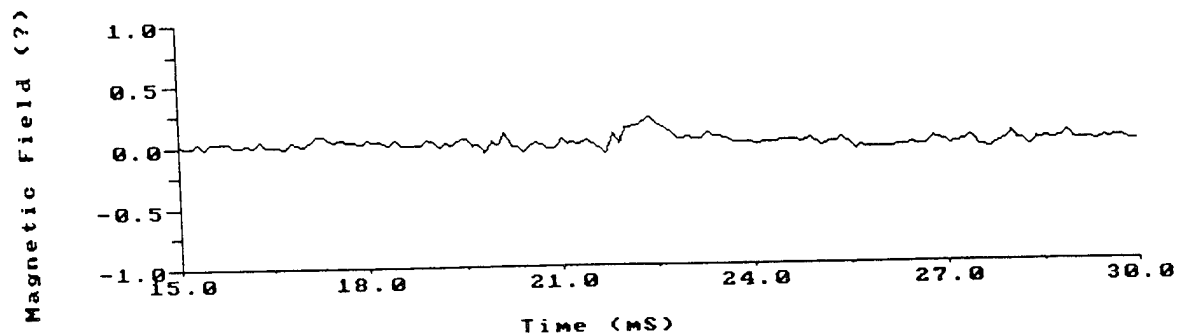
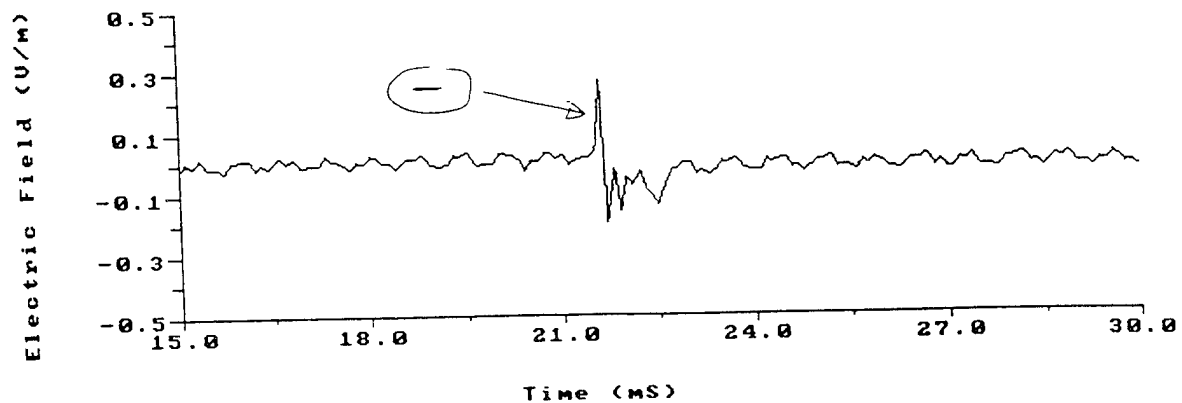


d:\rs724\081549.DAT

## DOUBLE "SPRITE"?

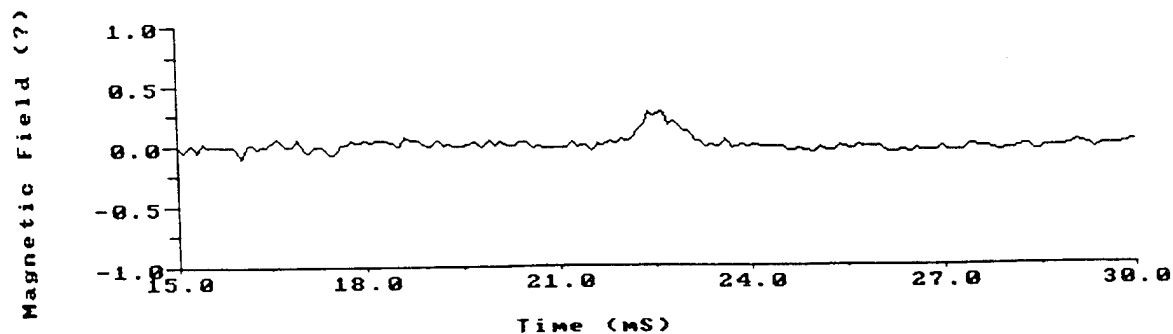
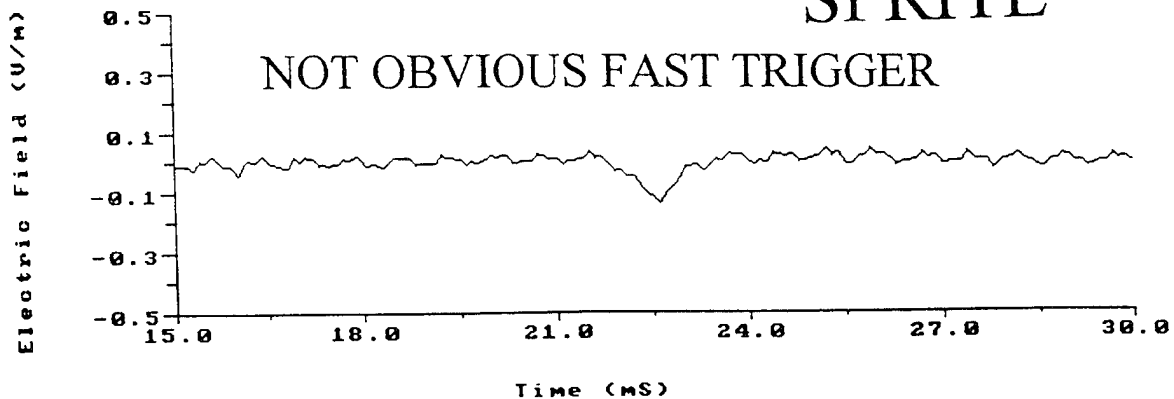


# "SPRITE"

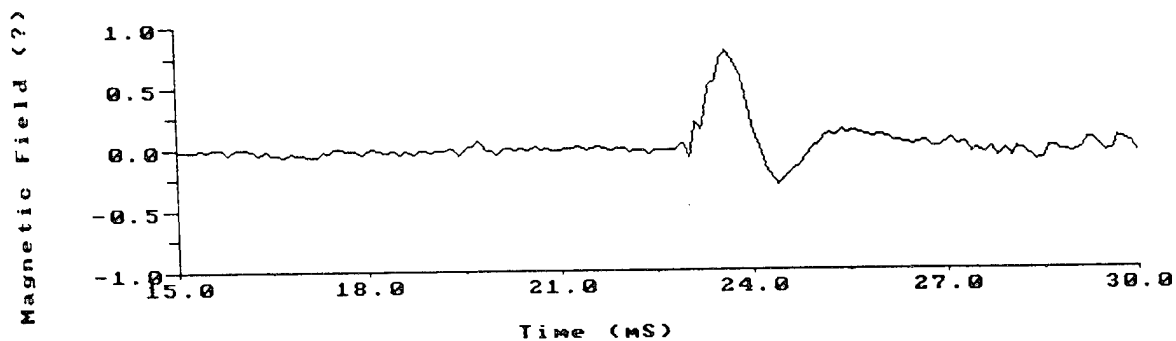
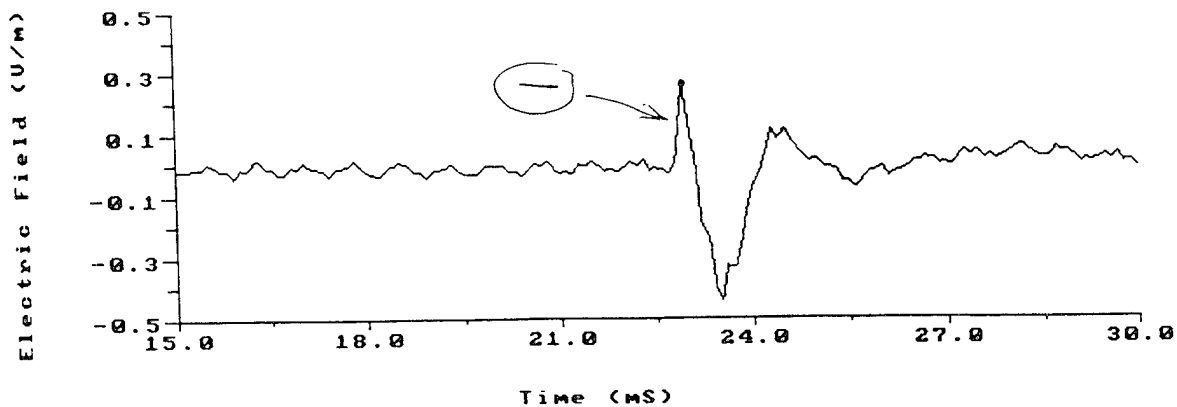


# "SPRITE"

NOT OBVIOUS FAST TRIGGER

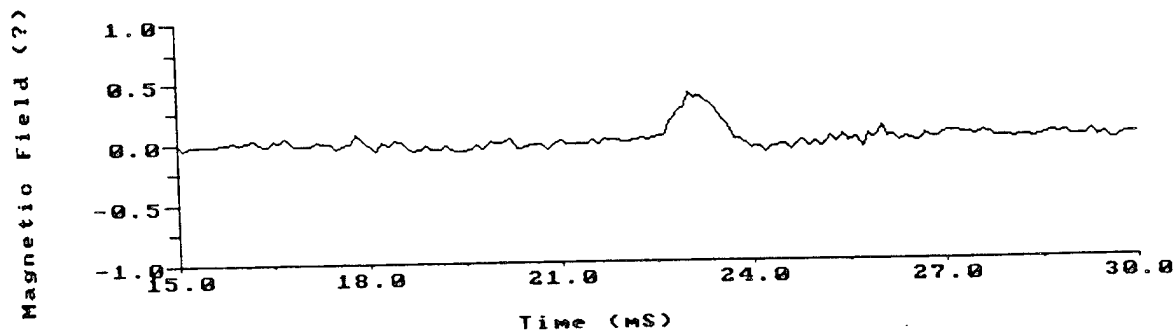
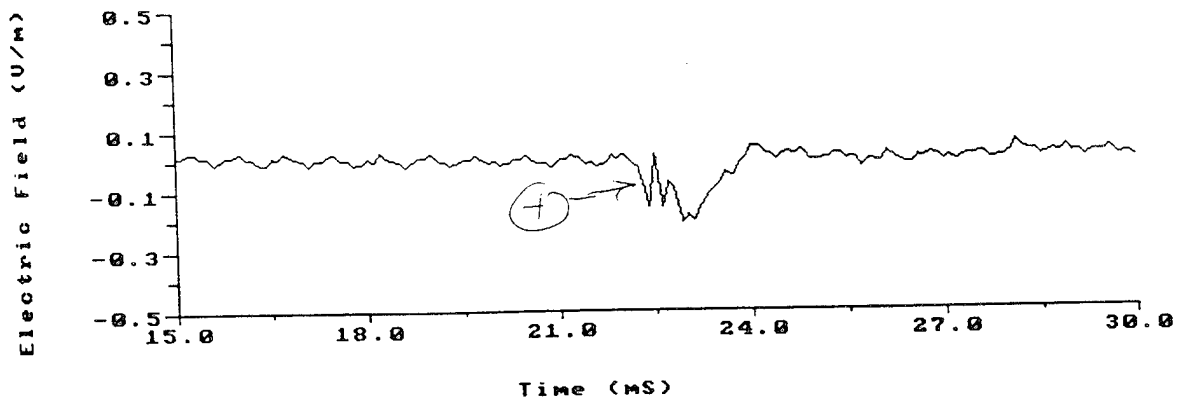


# "SPRITE"

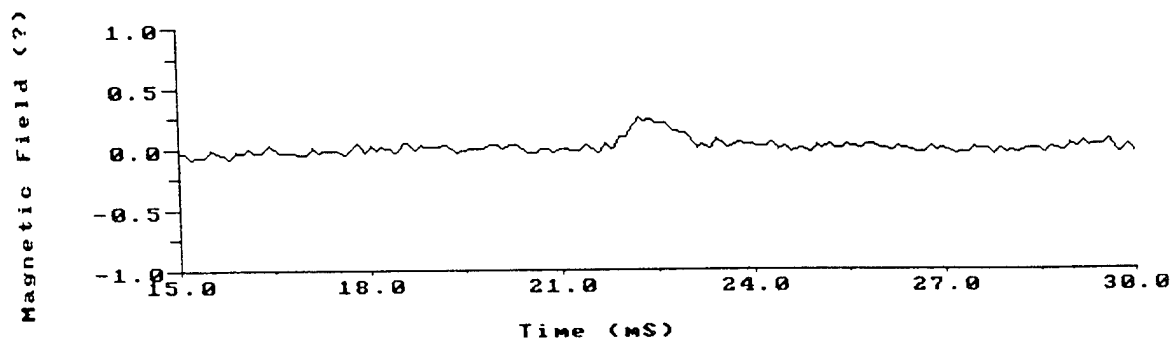
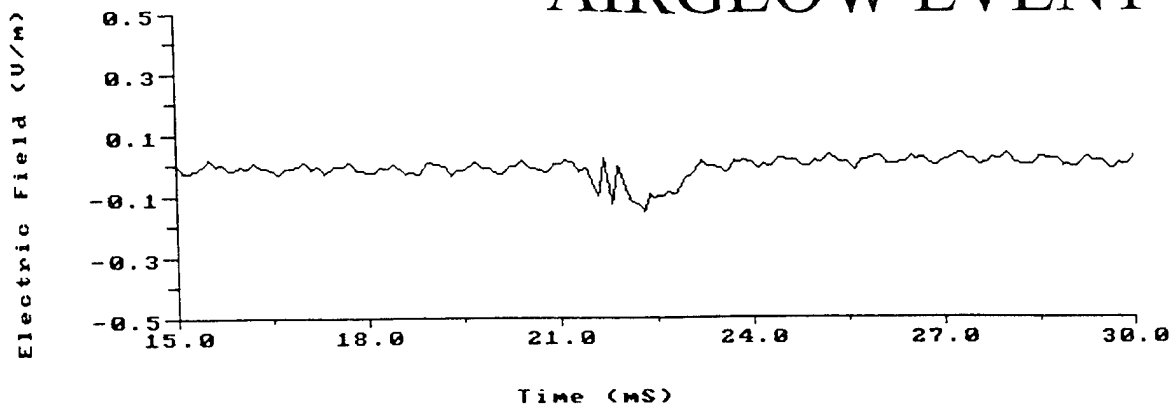


d:\rs724\083334.DAT

# "SPRITE"

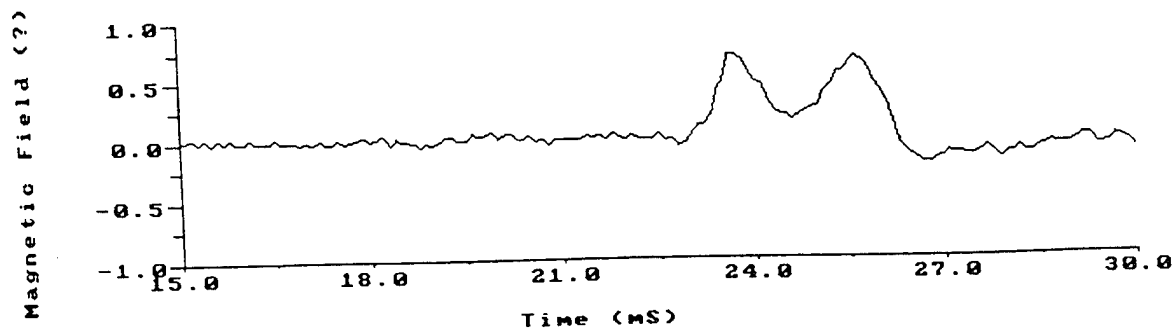
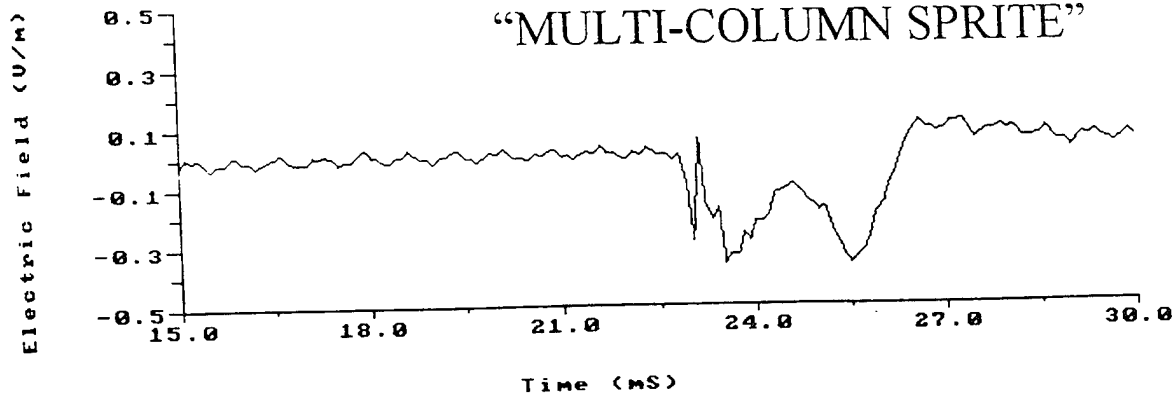


# "AIRGLOW EVENT"

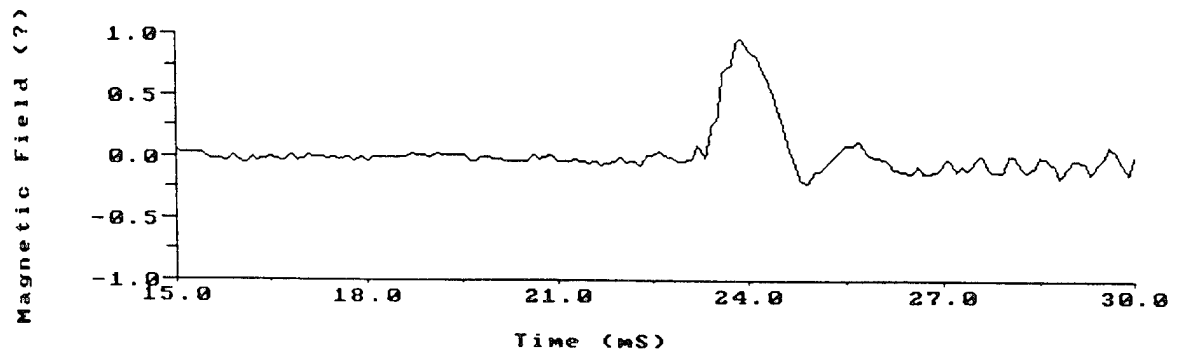
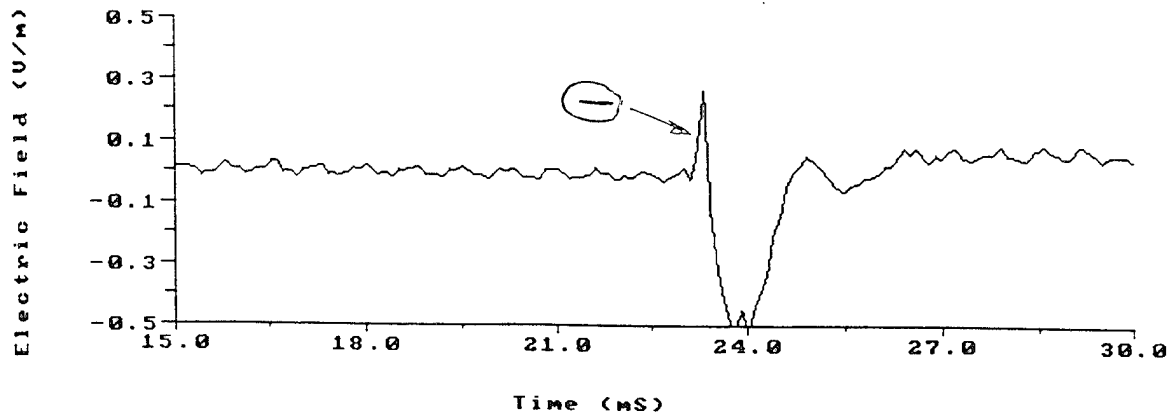


d:\rs724\081844.DAT

# "MULTI-COLUMN SPRITE"

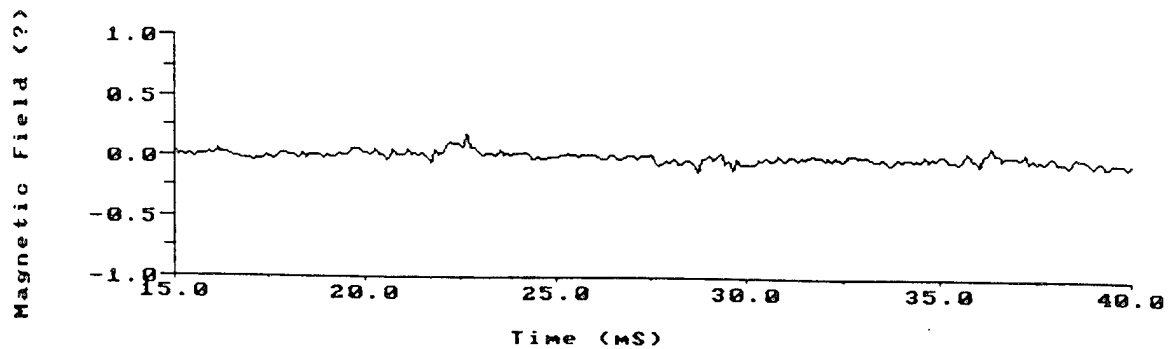
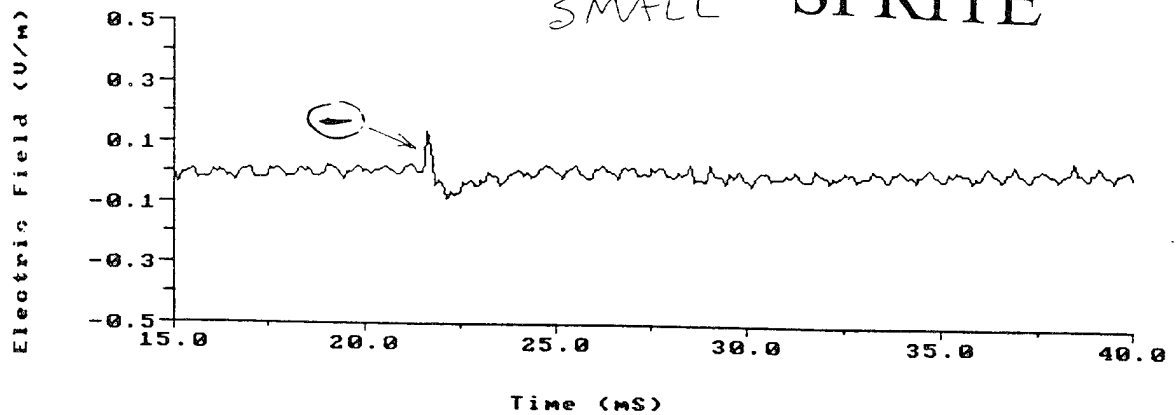


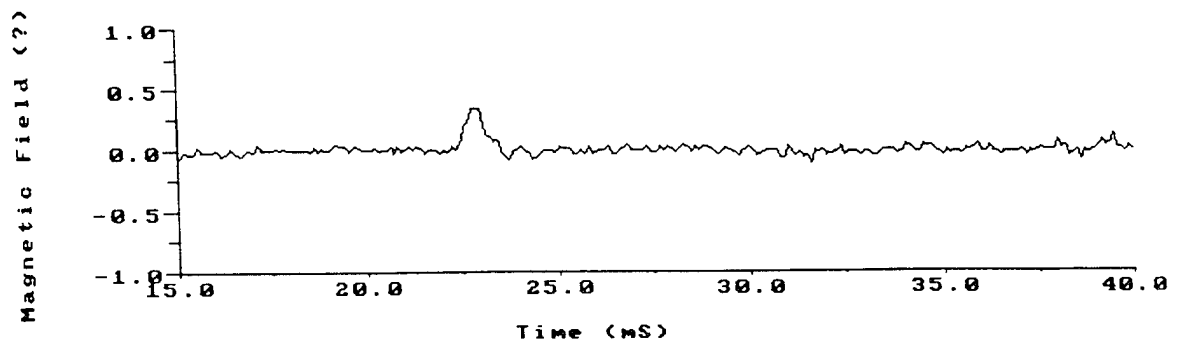
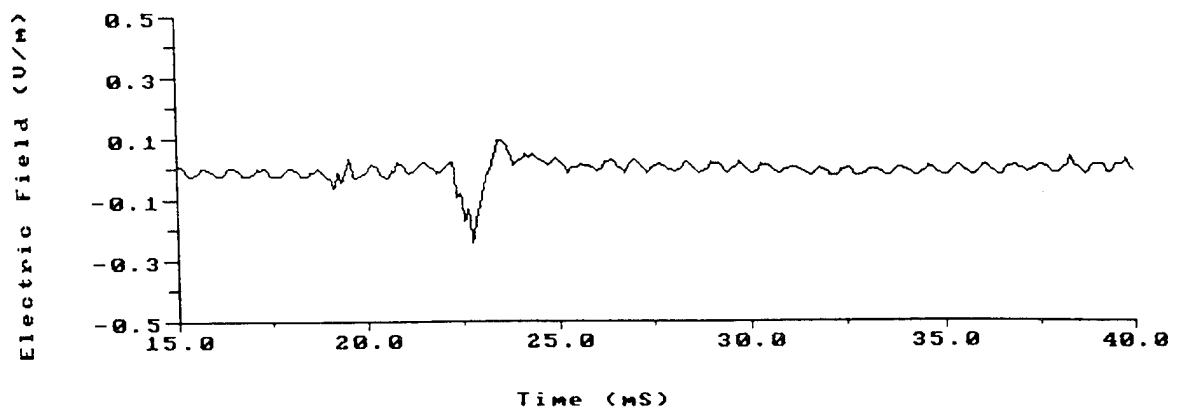
# BIG "SPRITE"



d:\nrs724\084111.DAT

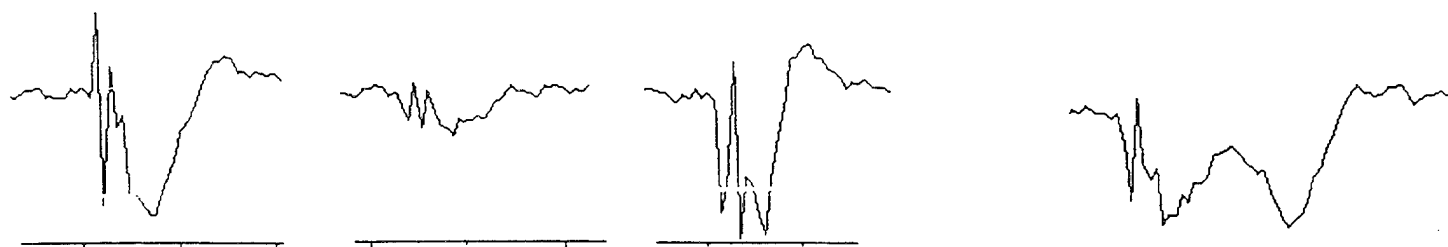
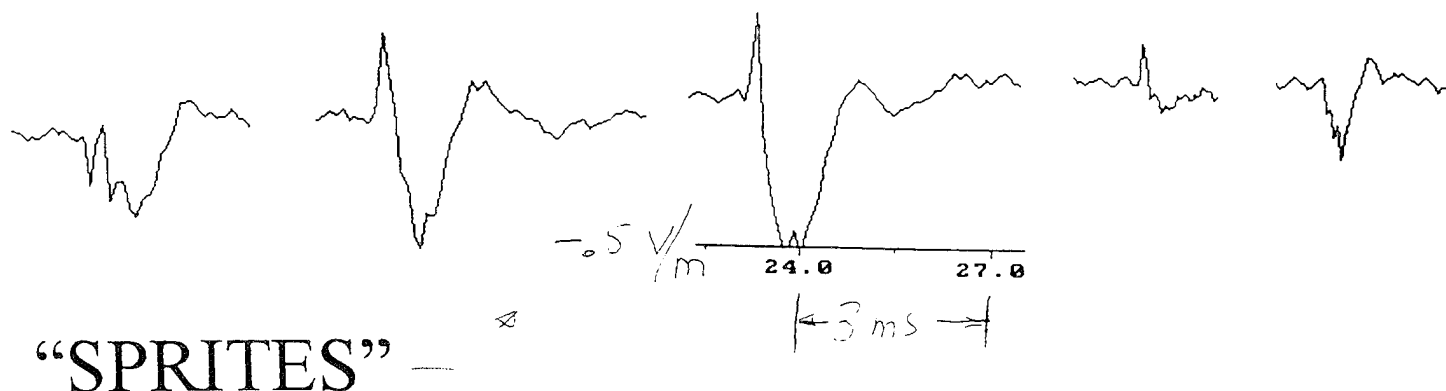
# SMALL "SPRITE"





LAST SPRITE OF DAY IN E & M OBSERVATION IN PA.

ELECTRIC FIELD WAVEFORMS OF EVENTS IDENTIFIED  
BY WALT LYONS IN COLORADO - OBSERVED IN  
PENNSYLVANIA 24 JULY 1995 0640UT - 0910UT



"AIRGLOW EVENTS"

"MULTI-COLUMN  
SPRITE"



"SPRITE AND AIRGLOW EVENT"

BANDWIDTH  $\sim 5 \text{ kHz}$  (RETURN STROKES IDENTIFIED BUT  
NOT RESOLVED)



## CONCLUSIONS

- 1) VARIETY OF E & M SIGNALS FROM "SPRITES" AND "AIRGLOW EVENTS" WITH AND WITHOUT "FAST" EVENTS OF BOTH POLARITIES.
- 2) COMMON FEATURE: NEGATIVE GOING ELF WAVEFORM - POSSIBILITY TO COMBINE WITH LIGHTNING LOCATOR DATA FOR "SPRITE MAPPER".
- 3) ENERGY OF ELF SPRITE  $\sim 10^6$  JOULES  $\gg$  VISIBLE SPRITE.
- 4) ADVANTAGES OF E-FIELD MEASUREMENTS:
  - ◆ EASIER TO FIND QUIET LOCATION
  - ◆ EASIER TO MEASURE WIDE-BAND
  - ◆ OMNI-DIRECTIONAL
- 5) ADVANTAGES OF H-FIELD MEASUREMENTS:
  - ◆ POSSIBILITY OF DIRECTION-FINDING
  - ◆ LESS SENSITIVE TO LOCAL WEATHER
- 6) NEXT TIME: AT LEAST TWO LOCATIONS, ONE WITH OPTICS. 5 Hz TO 25kHz BANDWIDTH. COMPLETELY DIGITAL WITH TAPE BACKUP.

POSSIBLY UNPOPULAR CONCLUSION:

CONSISTENT "POSITIVE" LIGHTNING SIGNAL MAY BE FROM THE SPRITE ITSELF.

NOTE: This material was not considered sufficiently "new" to be published as a letter by a couple of journals, but may be of interest to some people not intimately familiar with the literature in this "field." Comments, including violent disagreement, are welcomed with enthusiasm. L.H.

## ON THE COUPLING OF FIELDS, CURRENTS, AN ENERGY FROM LIGHTNING TO THE UPPER ATMOSPHERE AND IONOSPHERE: A "CURRENT" STATEMENT

Les Hale, CSSL/Penn State  
University Park, PA 16802-2707  
Tel: (814) 865-2361 e-mail: Les Hale@PSU.EDU

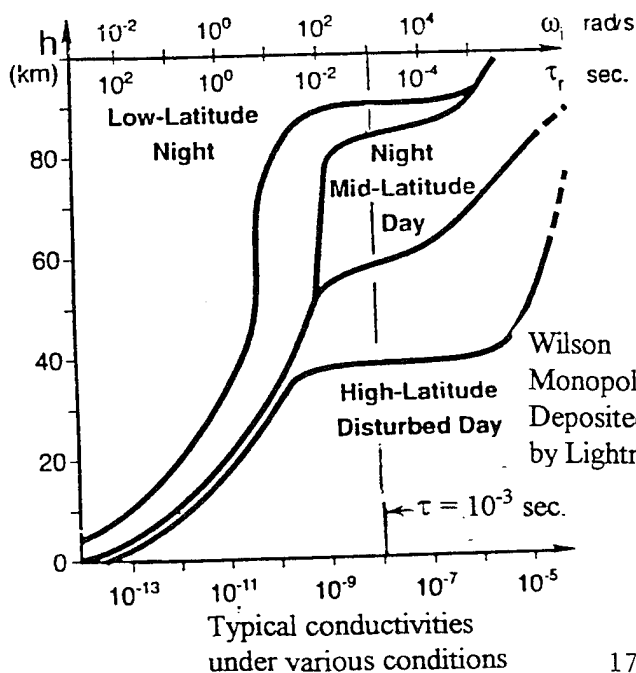
Stimulated by the "red-sprites" phenomenon, there has been a resurgence of interest in the coupling of E & M fields from tropospheric lightning to the "ionosphere." Many workers have concluded that the fields calculated using free space dipole moments (or, using superposition, multipole moments), e.g. radiation, induction or intermediate, and electrostatic, are inadequate to explain the mesospheric phenomenon of "red sprites." This communication is intended to collect some ideas which, while generally not new, may be relevant to the problem. While there appear to be some good theoretical treatments, for example the recent work of Sukorukov, such work tends to be somewhat mathematical, which is avoided in this discussion.

Free space dipole moments are not generally valid for lightning fields which are confined between the conducting earth and the generally more "fuzzy" ionospheric boundary. However, for a lightning return stroke current  $i_L(t)$  which flows in less than about a millisecond, the "induction" and "radiation" fields incident on the upper atmosphere, due to  $i_L$  and  $di_L/dt$ , are valid as long as ground reflection is considered. This is not true for the "electrostatic" component, which is quite different from the free-space case. In the case of cloud-to-earth strokes this is usually handled by considering the effects of "Wilson monopoles," which are charge centers created by the time integral of the lightning currents. ("Dipoles" and more complex situations can be considered using the superposed fields of two or more such monopoles.) At large distances the monopoles can generally be considered to be point charges, persisting for the tens of seconds "relaxation time" of their tropospheric deposition altitude. They provide sources for calculating the time dependent "quasi-static" fields associated with the lightning. Although this is a very complex problem in an atmosphere with continuously varying conductivity, generally requiring a computer solution of the complete Maxwell's equations, in some cases simplifying assumptions may enable estimation of the fields and currents. In particular, in the "quiet" nighttime mesosphere, there are essentially zero free electrons and the electrical conductivity  $\sigma$  remains as low as  $10^{-10}$  to  $10^{-9}$  S/m up to a "ledge" at 80 to 85 km, which defines the effective height of the transient solution which persists for a time  $\epsilon_0/\sigma$  of up to tens of milliseconds after a lightning stroke. This gives rise to a virtually free-space "electrostatic" solution for the fields involving upper and lower conducting boundaries and a Wilson monopole following a cloud-to-earth return stroke. The solution of this electrostatic problem is well known, and involves an infinite Bessel series. A result of interest to the sprites problem is that the electric field just below the "ledge" directly above the monopole is nearly double that calculated without considering the presence of the ionospheric boundary. Thus whatever lightning charge would be necessary to initiate "breakdown" just below the ledge (generally estimated at over 200 C using the "free-space-monopole-plus-earth-image" model) can be reduced by about half.

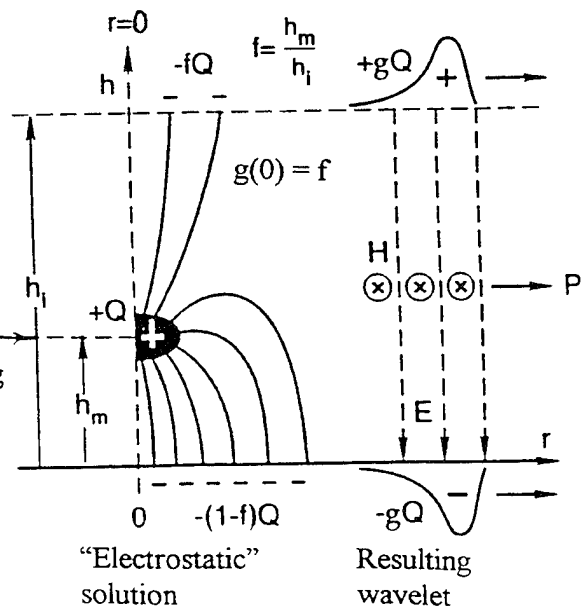
Although sufficient to create the electric fields that initiate breakdown, a purely "electrostatic" solution couples little energy and cannot sustain the discharge for the observed duration of several milliseconds. This requires substantial current in the discharge region, which can be generated in different ways. The first is direct excitation by a portion of the source lightning current  $i_L(t)$ . Although the electric fields are complex, the ratio of the electric flux is given by a fraction  $f$  (typically  $\sim 0.1$ ) equal to the simple distance ratio  $h_m/h_i$ , where  $h_m$  is the altitude of the monopole and  $h_i$  is the effective height of the ionosphere. This means that for current pulses of milliseconds or longer, for which a quasi-static solution is valid a current of  $fi_L(t)$  is coupled directly to the ionosphere. As the width of the current pulse is decreased to the millisecond range and below, it is found by a computer solution of the complete Maxwell's equation that the current pulse to the ionosphere does not continue to decrease accordingly, but remains about a millisecond. This is interpreted as the time required to establish the initial "quasi-static" solution, which is controlled by the round-trip propagation delay between the lightning and the upper boundary. In this limit the peak current is found to be several hundred amperes per coulomb of lightning-separated charge [Hale and Baginski, Nature 329, 814, 1987], and the writer believes that this is the most likely candidate for producing the brightest portion of the sprite discharge (which may be what is currently being called an elf).

Another mechanism which produces a current to the ionosphere is due to the conductivity gradient  $\nabla\sigma$ . This mechanism was suggested by C. and P. Greifinger [JGR 81, 2237, 1976], who also gave an interesting physical interpretation, a post-stroke downward moving boundary between regions dominated by conduction current (above) and displacement current (below), which has been termed a "variable capacitor" model by Sukorukov. This mechanism dominates at ULF frequencies, but is much weaker than the "millisecond" ELF pulse, which has been shown by computer modelling to be dominant even in situations where the conductivity varies continuously, with no obvious "ledge." This mechanism could be important to the sprites situation if the discharge originated at or more likely propagated rapidly to very much lower altitudes (with a velocity of  $10^7$  m/sec or greater), causing a substantial change in the ionospheric boundary height on the millisecond time scale.

These post-stroke currents to the ionosphere give rise to radial TEM (zero mode) wavelets which are easily observed at a distance of thousands of kilometers as slow tails, although their waveshape will appear modified, both by local effects of the earth's magnetic field [Hale, JGR 99, 21089, 1994] and dispersion and attenuation, which will be much greater in the daytime than nighttime. The best diagnostics will probably be done by E & M measurements extending from about 5 Hz to 50 kHz to pass all of the highest energy parts of the E & M signal. The principal unknown quantity continues to be the actual pre-existing conductivity profile associated with "red sprites."



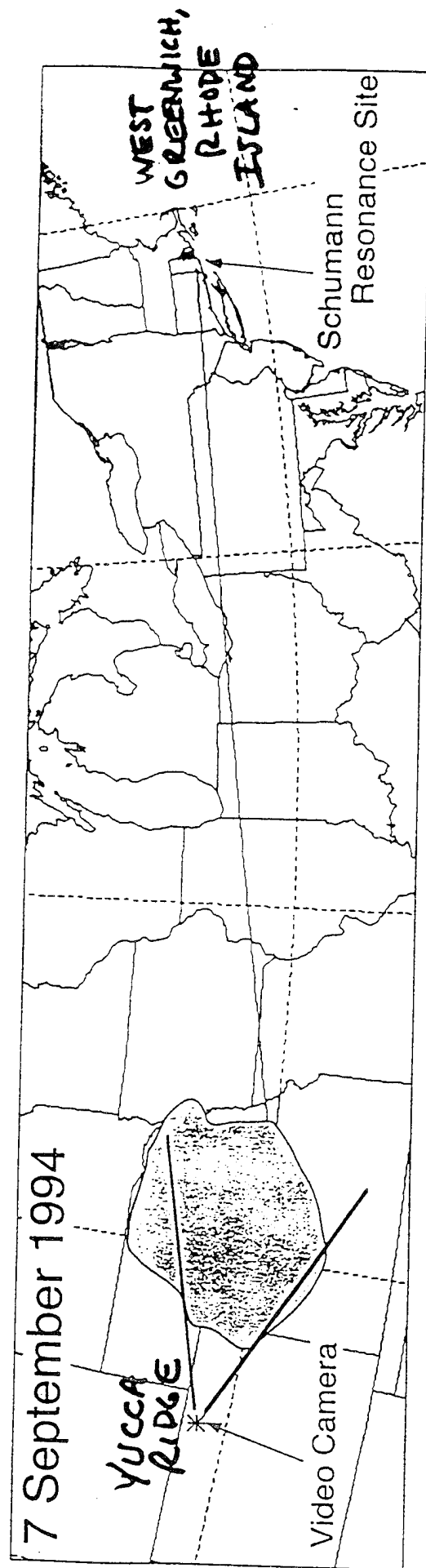
Radial TEM Wavelet Launched to Satisfy Post-stroke Electrostatic Boundary Conditions:



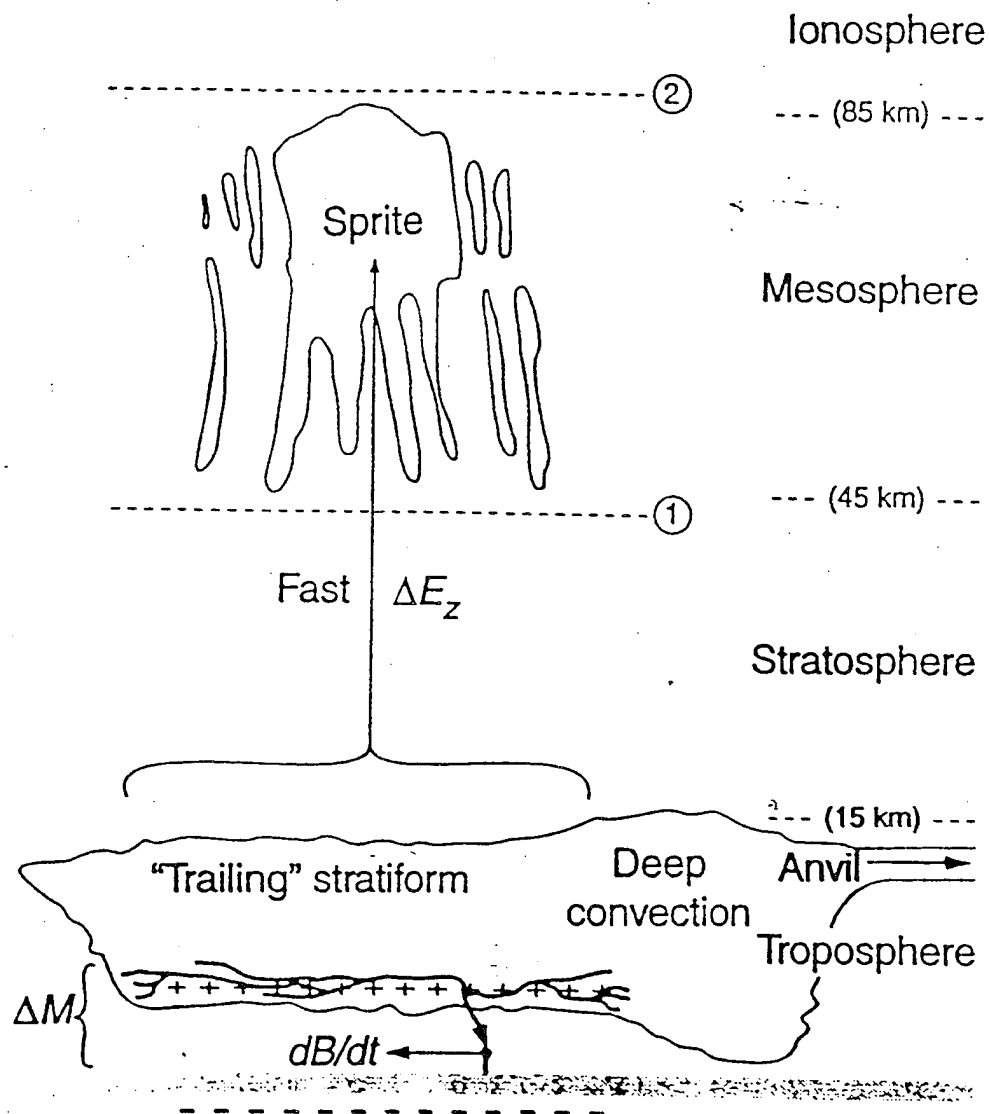
**Mesoscale Origin of Sprites  
and  
Schumann Resonance Methods for their  
Location on a Global Scale**

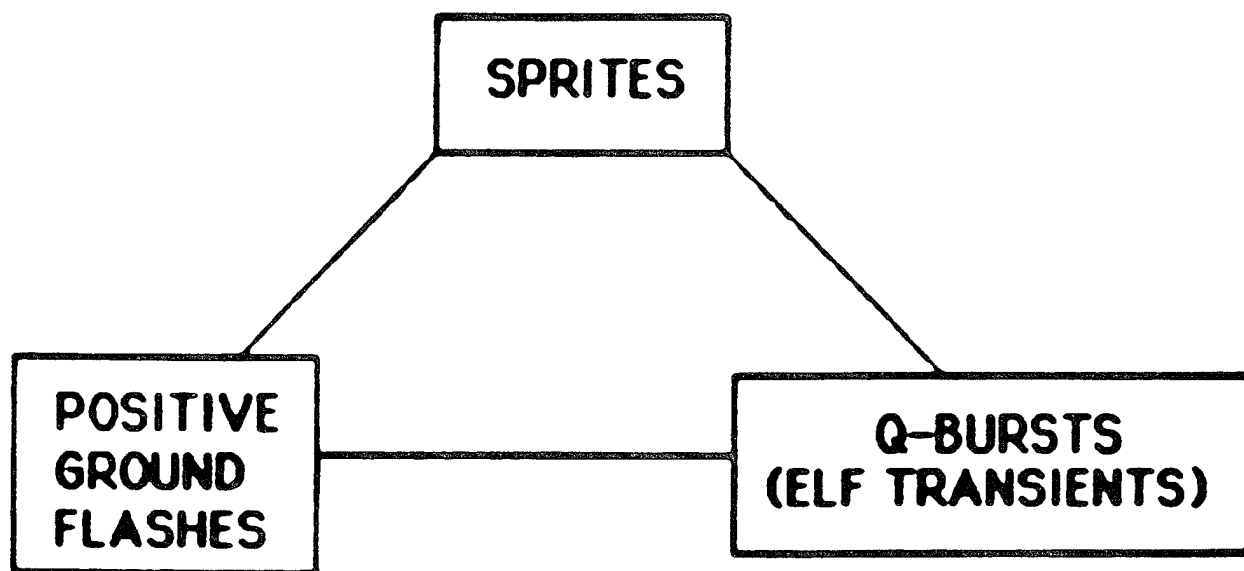
**Earle Williams**

**Massachusetts Institute of Technology**



# WORKING HYPOTHESES (BOCCIPPIO et al 1995)





1. WHY ONLY POSITIVES?

2. EXPLORATION OF SOURCE  
WITH SCHUMANN RESONANCE  
METHODS

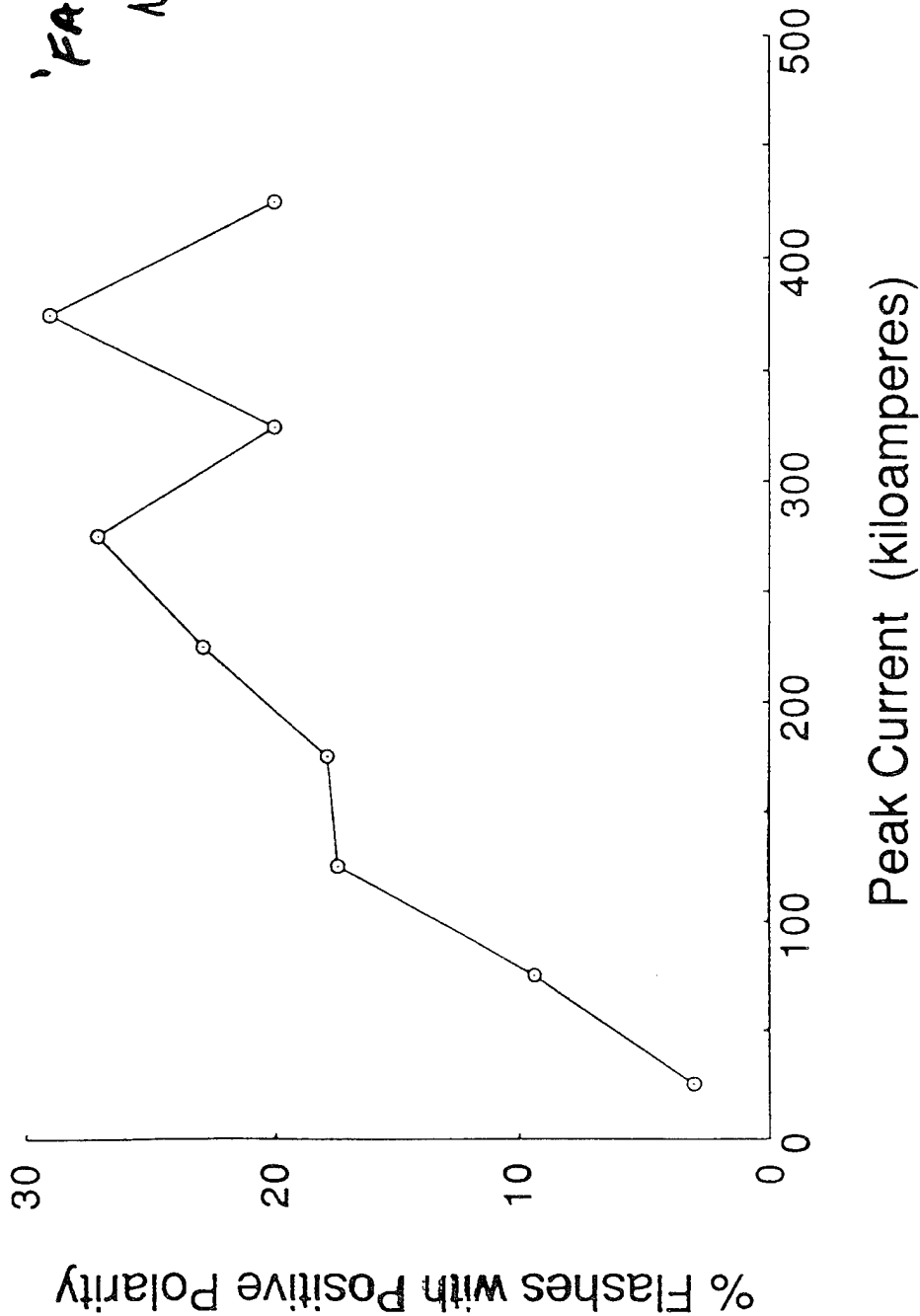
SPRITES ARE ASSOCIATED  
ALMOST EXCLUSIVELY BY  
POSITIVE CG's.

WHY CAN'T NEGATIVES DO IT?

ONE NEARLY BLACK-AND-WHITE  
DISTINCTION ALREADY KNOWN:

- THE MOST COMMON NEGATIVE CG IS A SINGLE STROKE CG BUT  $< 6\%$  HAVE CONTINUING CURRENT
- THE MOST COMMON POSITIVE CG IS A SINGLE STROKE CG BUT  $> 85\%$  HAVE LARGE CONTINUING CURRENT

PERCENTAGE OF GROUND FLASHES WITH POSITIVE POLARITY  
vs. PEAK CURRENT  
All events for 1992 NLDN

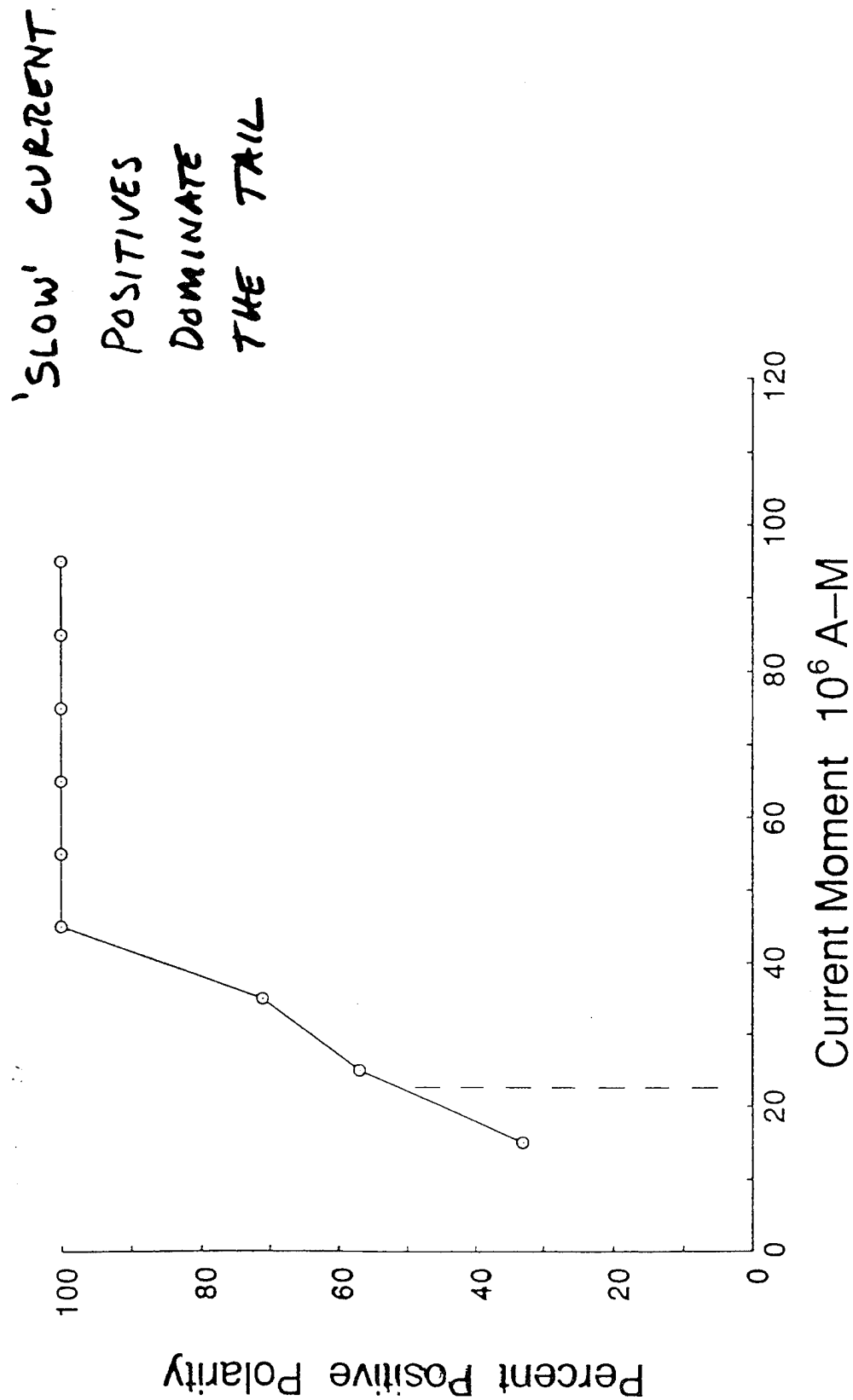




# FRACTION OF EVENTS WITH POSITIVE POLARITY

Burke and Jones (1995)

274 events total



100%

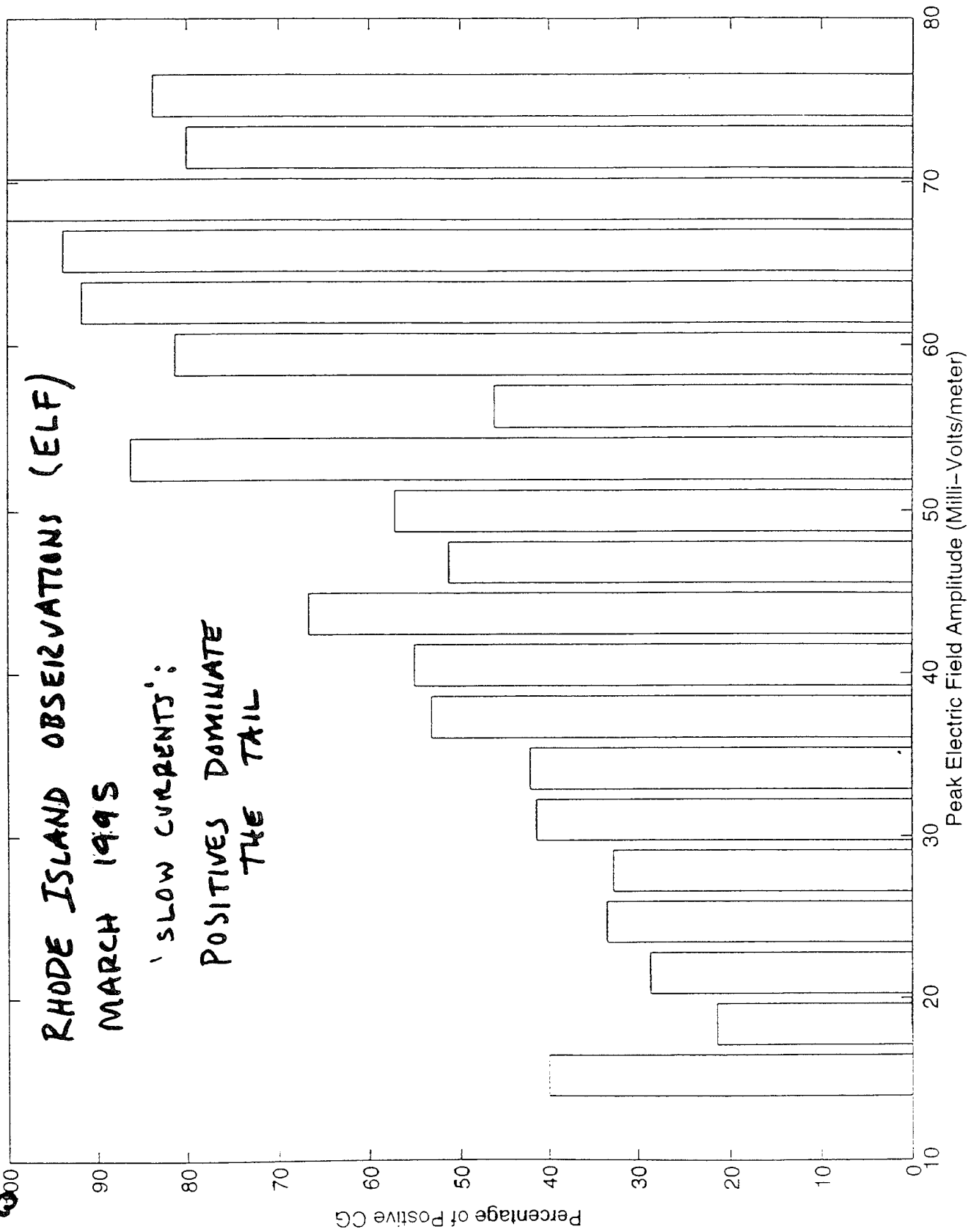
PERCENTAGE POSITIVES

Percentage of positive CG on 3-31-95 11:30-15:30GMT

RHODE ISLAND OBSERVATIONS (ELF)

MARCH 1995

'SLOW CURRENTS':  
POSITIVES DOMINATE  
THE TAIL



## NORMAL MODE EQUATIONS

(FINDING SPRITES WITH SCHUMANN RESONANCE)

### ELECTRIC FIELD

$$E(\omega) = i \frac{I ds(\omega) v (v+1) P_v^0(-\cos\theta)}{4\pi a^2 \epsilon_0 \omega h \sin(\pi v)}$$

### MAGNETIC FIELD

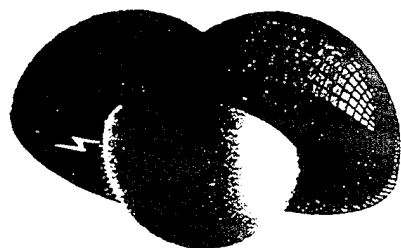
$$H(\omega) = \frac{-I ds(\omega) P_v^1(-\cos\theta)}{4ah \sin(\pi v)}$$

### WAVE IMPEDENCE

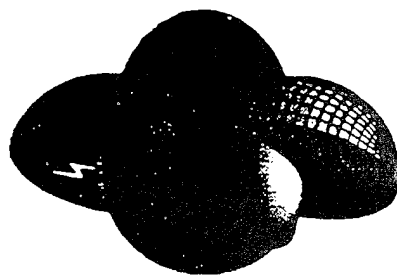
$$Z(\omega) = \frac{E(\omega)}{H(\omega)} = -i \frac{v (v+1) P_v^0(-\cos\theta)}{a \epsilon_0 \omega P_v^1(-\cos\theta)}$$

# Angular Distributions of Schumann Resonance Modes

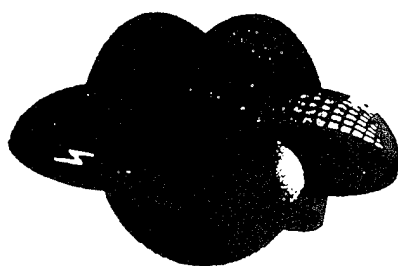
Electric



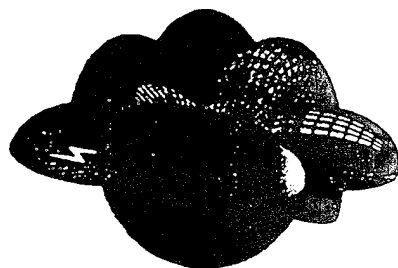
$n=1$



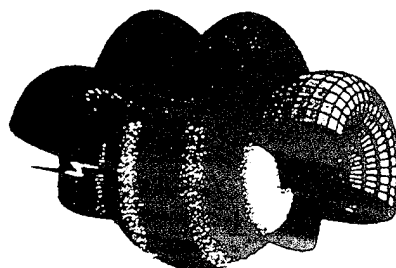
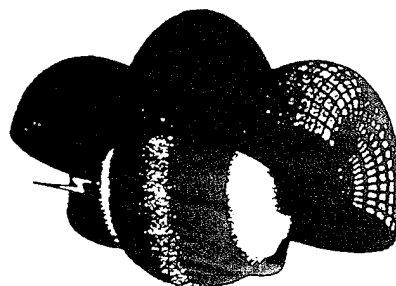
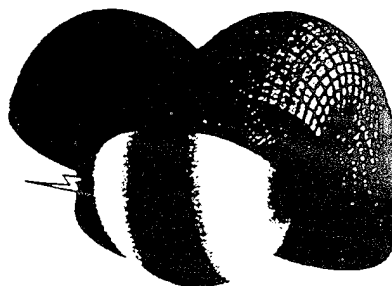
$n=2$



$n=3$



$n=4$



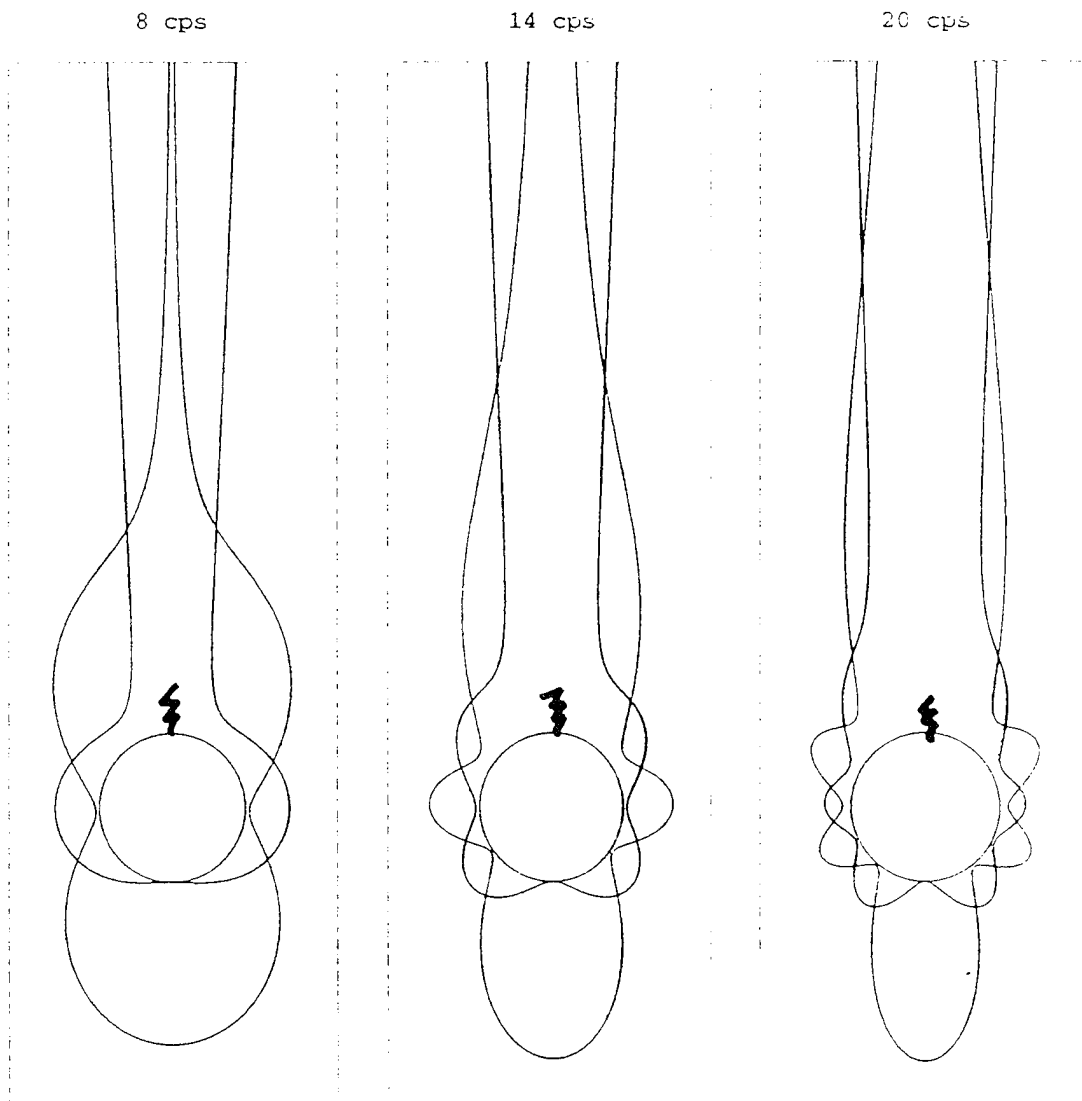
Magnetic  $14 \text{ Hz}$

$8 \text{ Hz}$

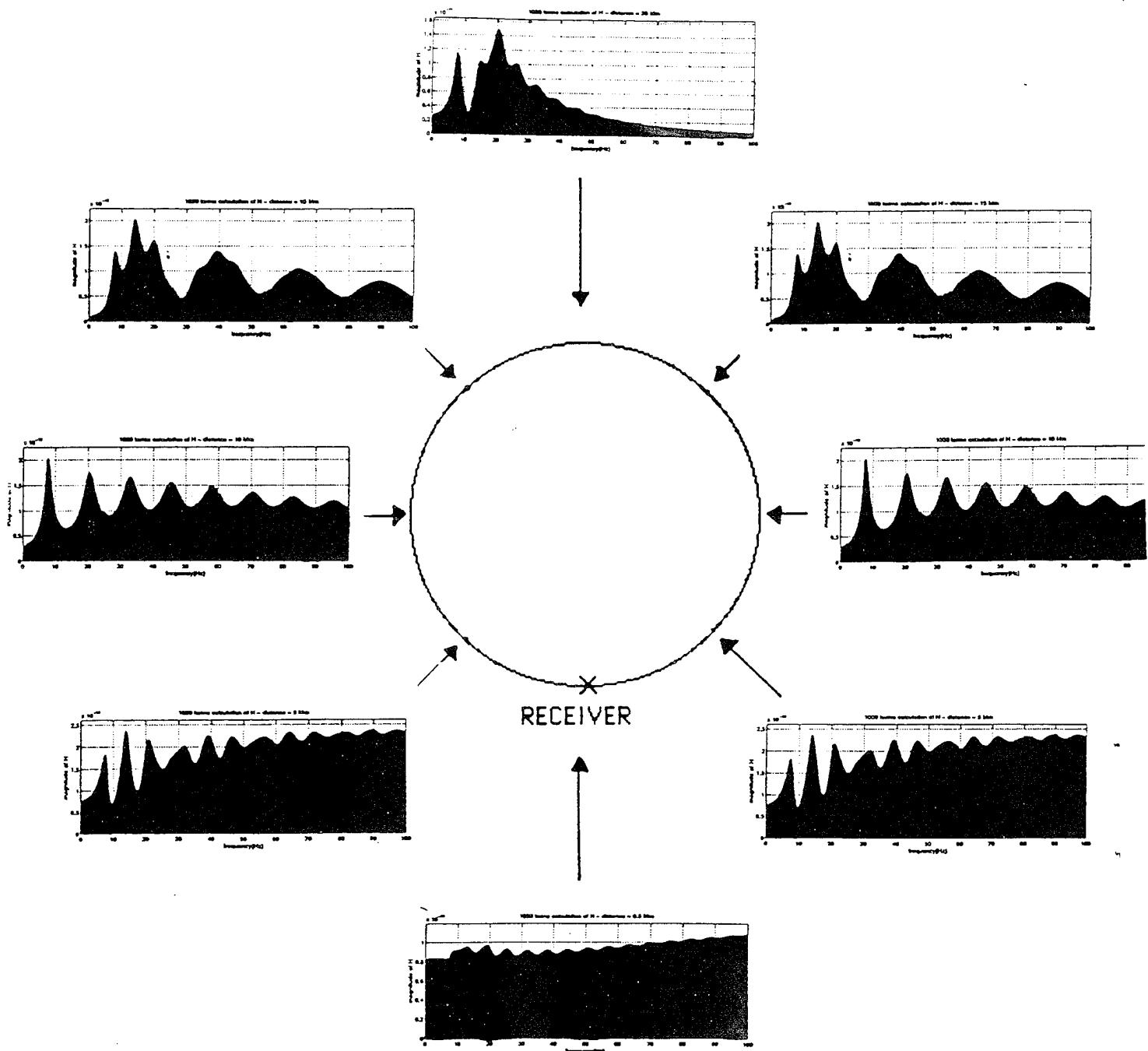
$20 \text{ Hz}$

$26 \text{ Hz}$

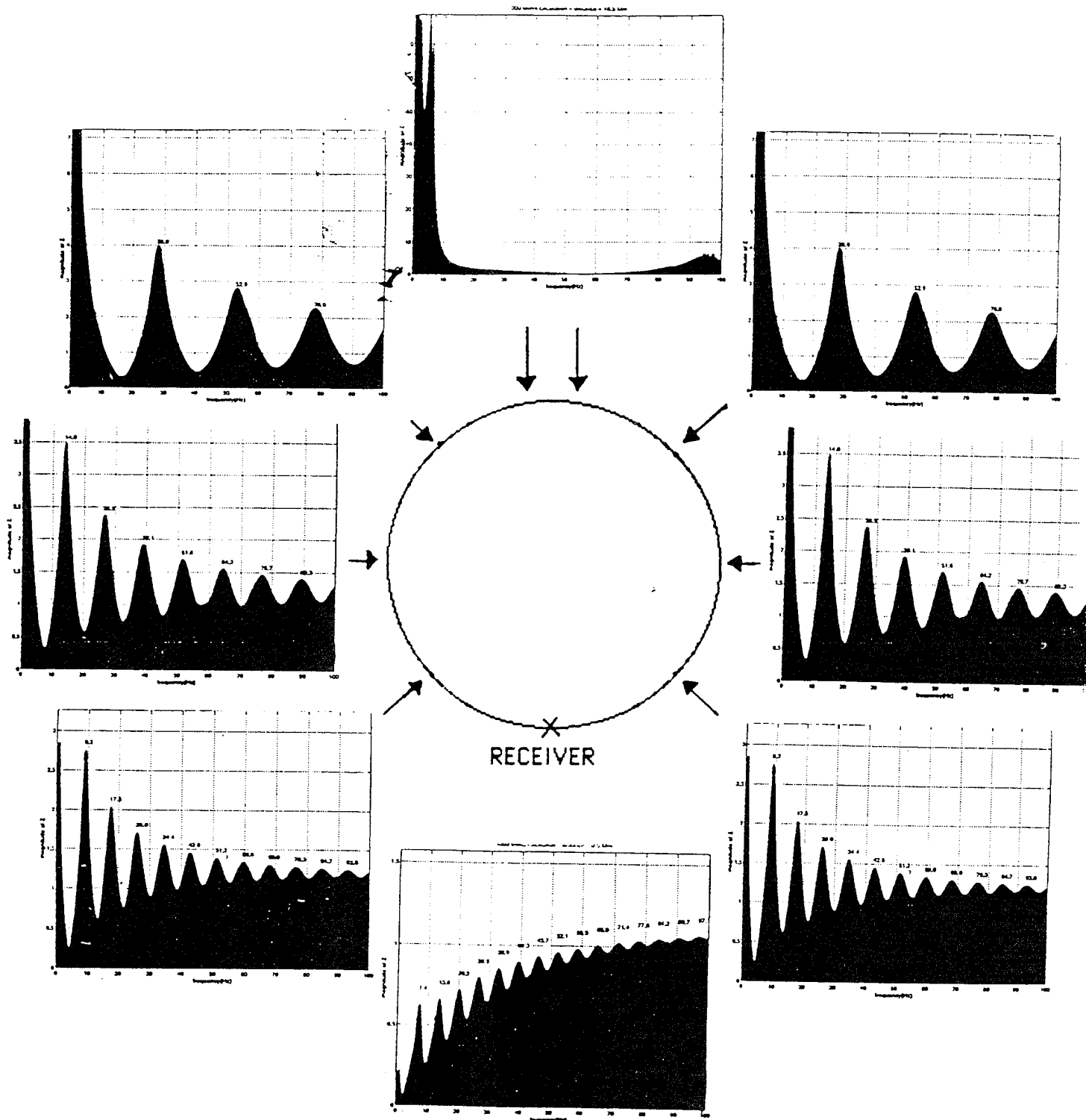
# SR MODE STRUCTURE (WITH REALISTIC ATTENUATION) FOR POINT SOURCE



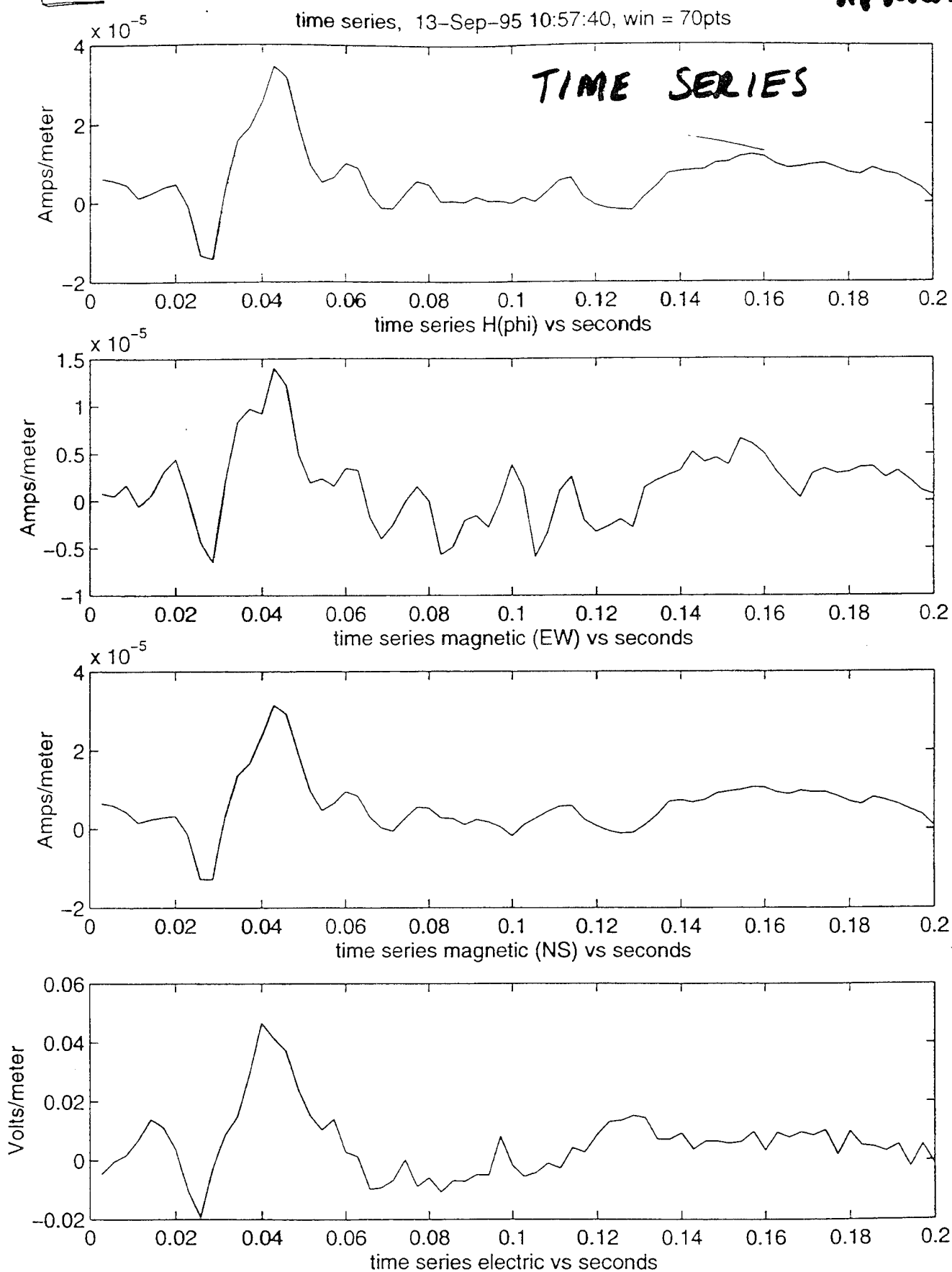
# MAGNETIC FIELD SPECTRA



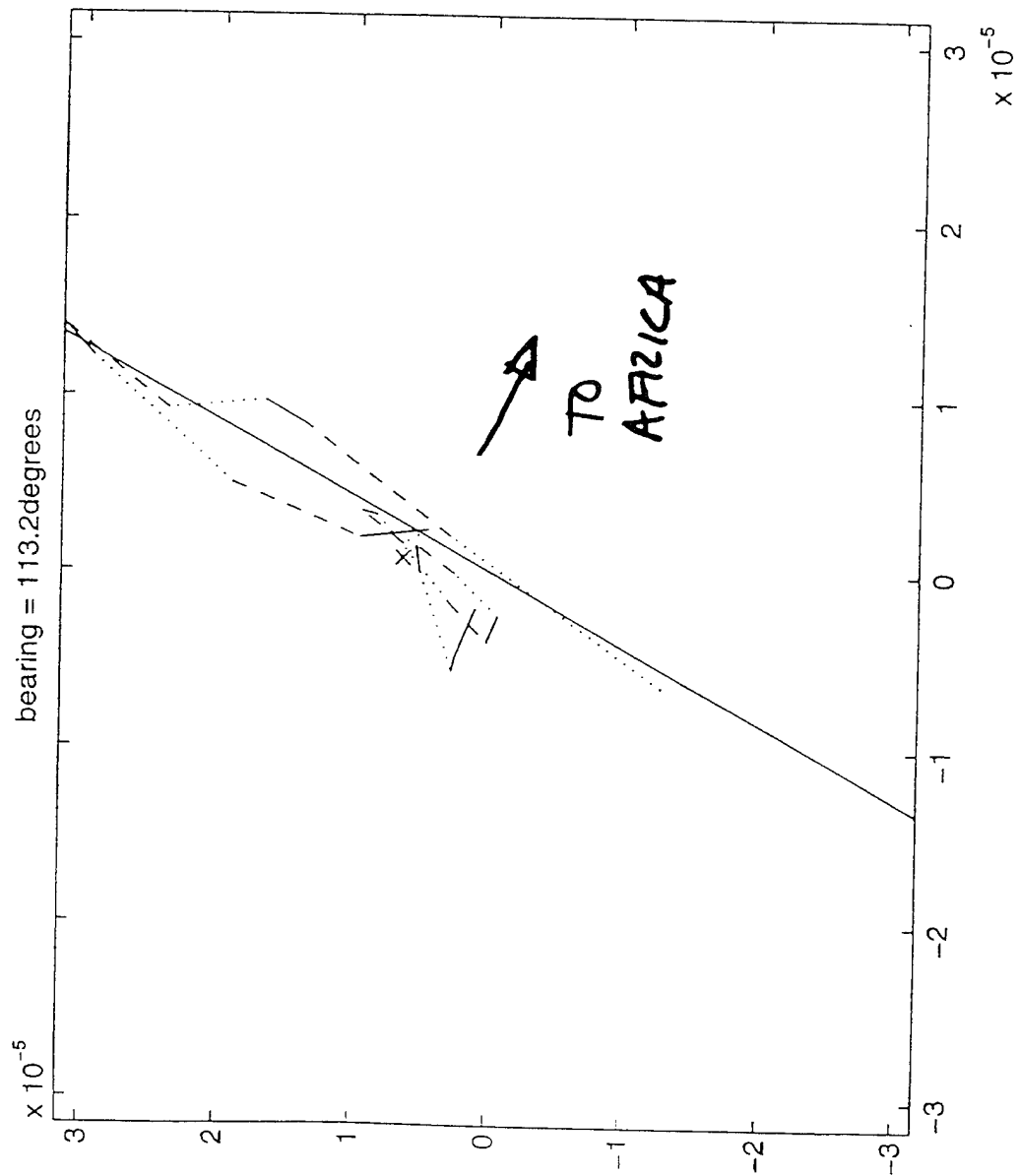
# IMPEDANCE SPECTRA



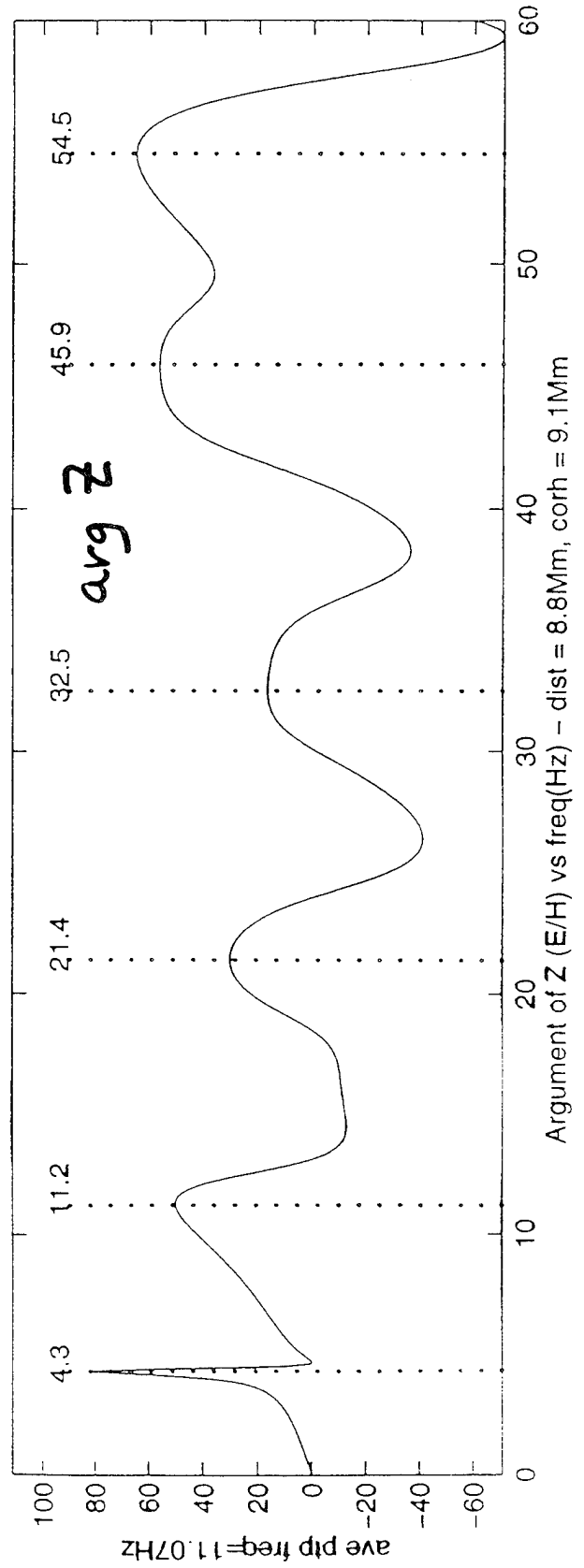
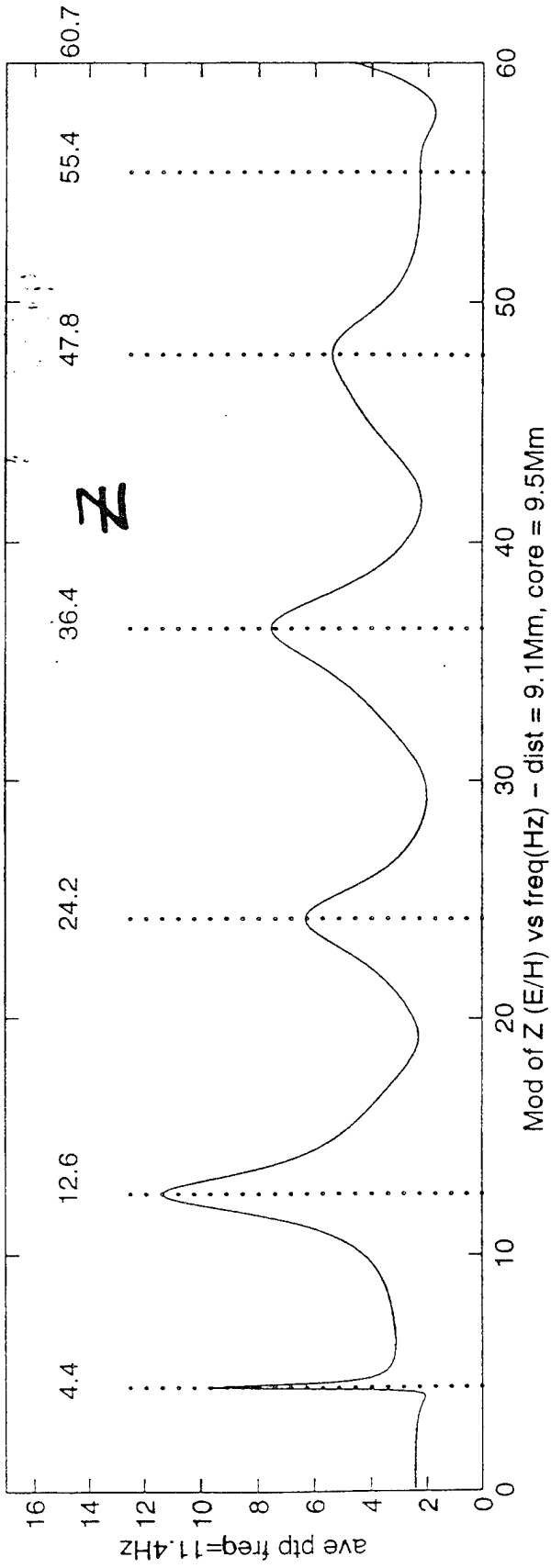
**AFRICA**

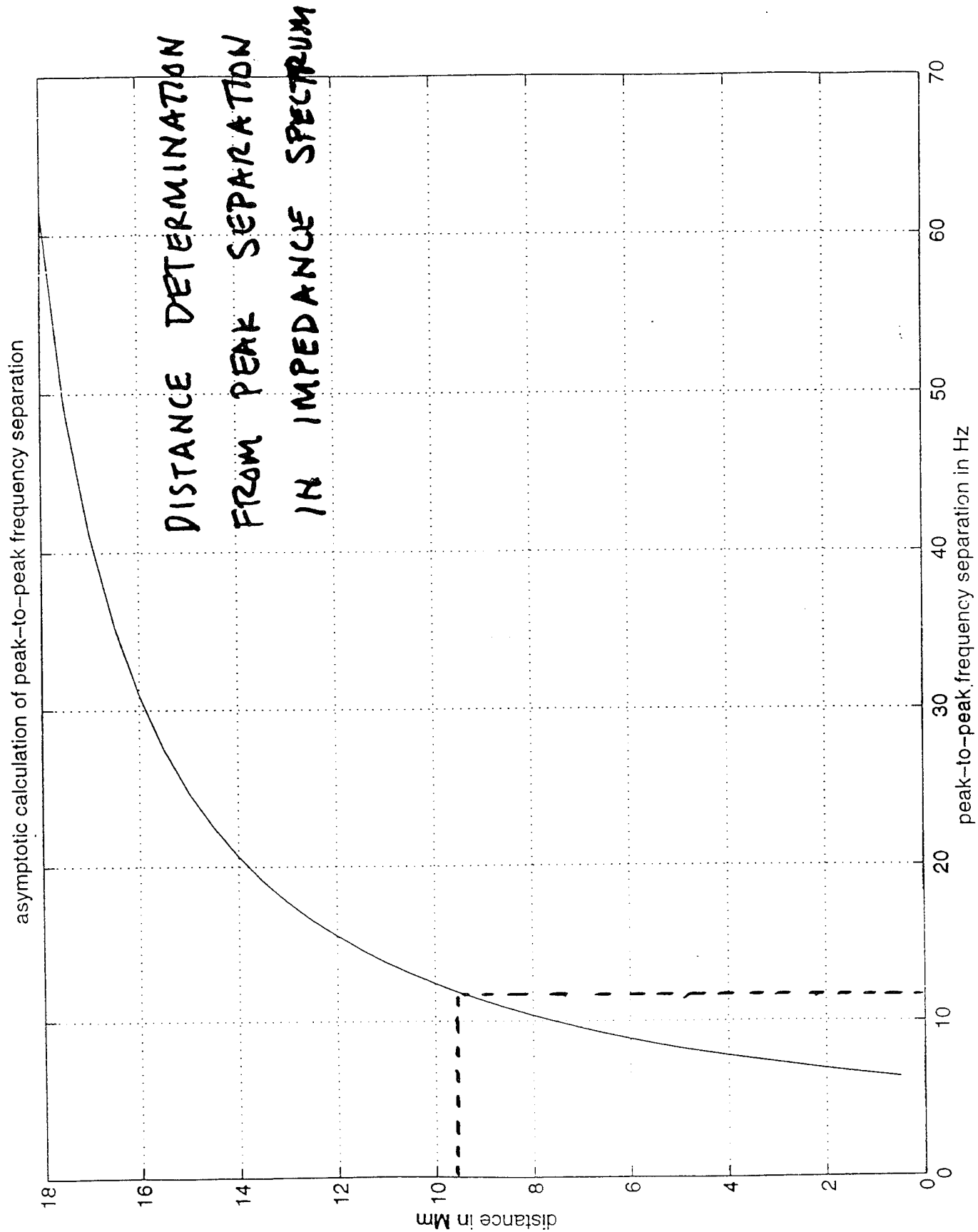




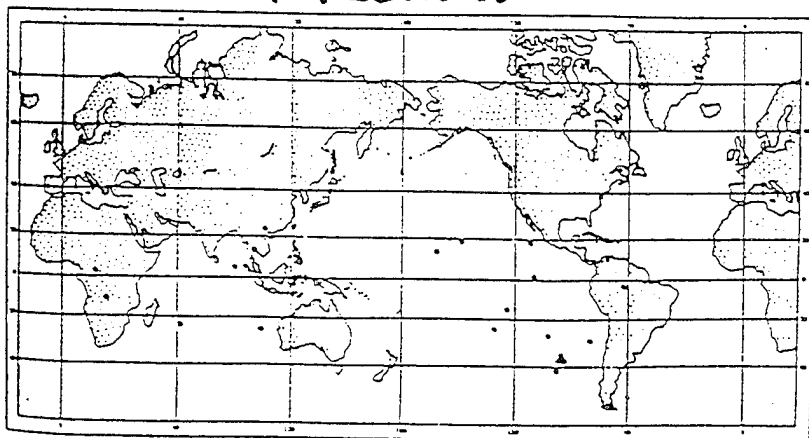


modulus plot, 13-Sep-95 10:57:40, win = 70pts

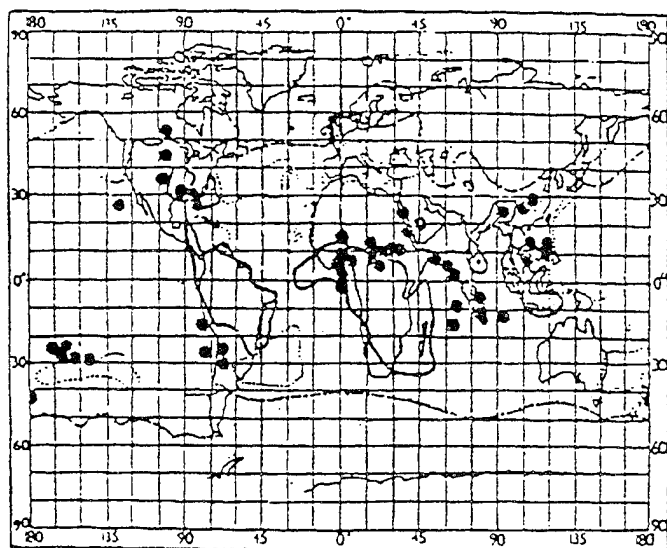




# NICKOLAEVSKO



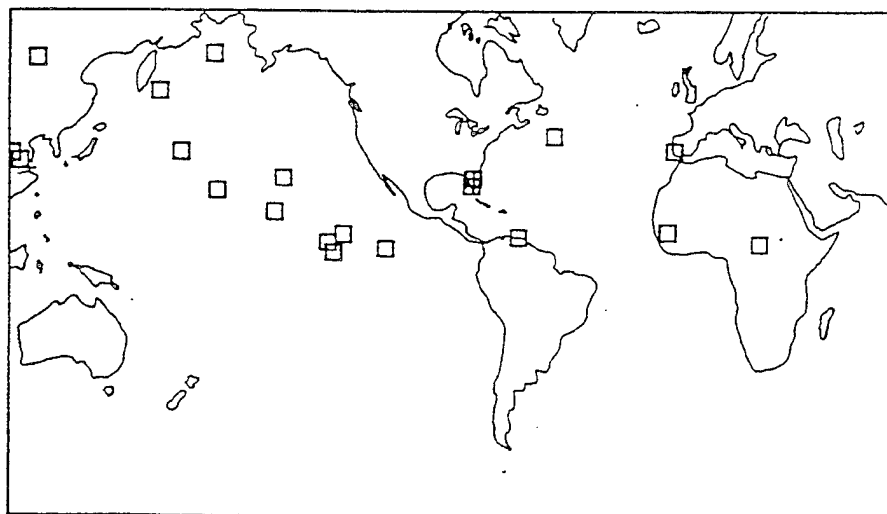
## KEMP



## BURKE AND JONES

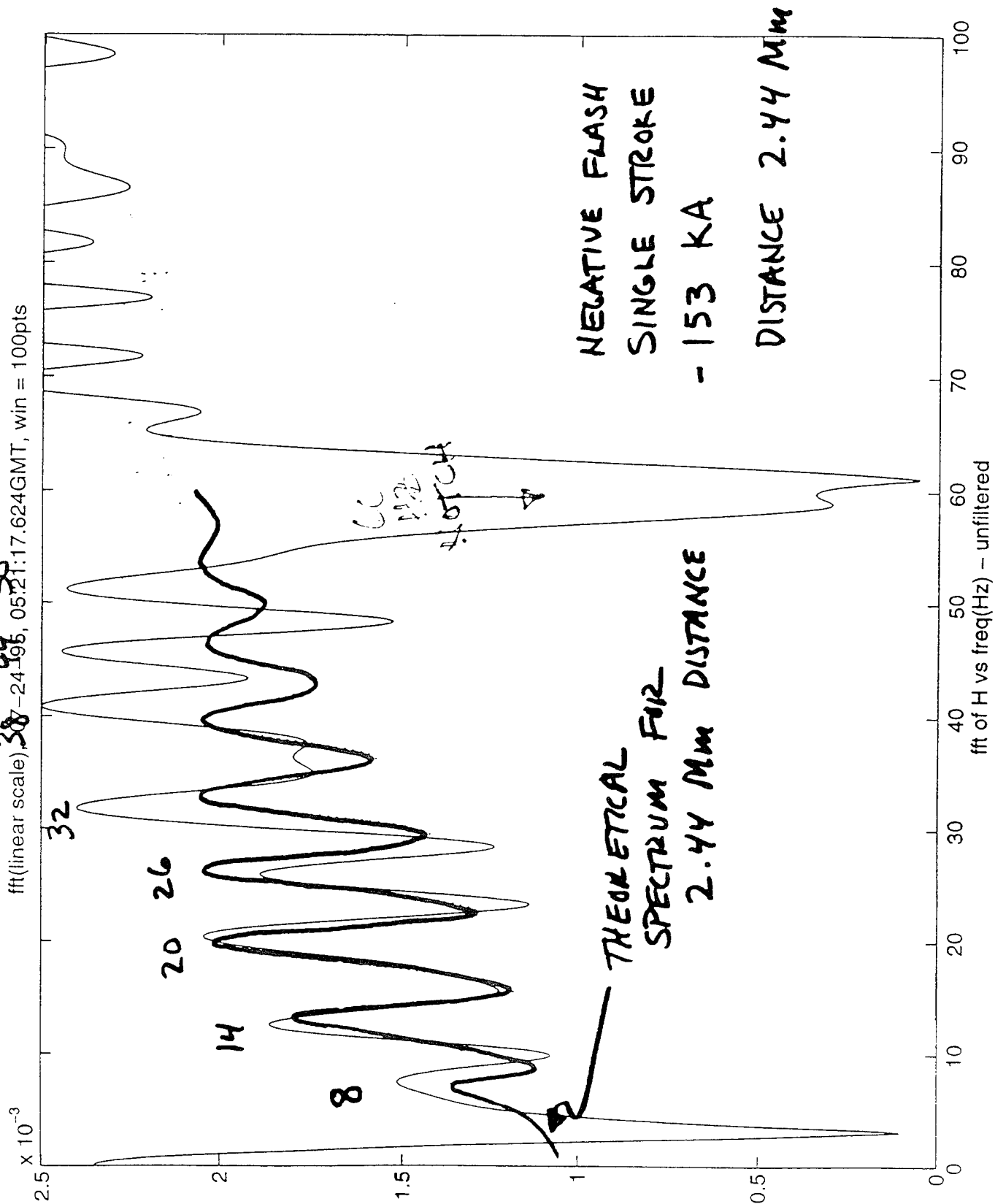


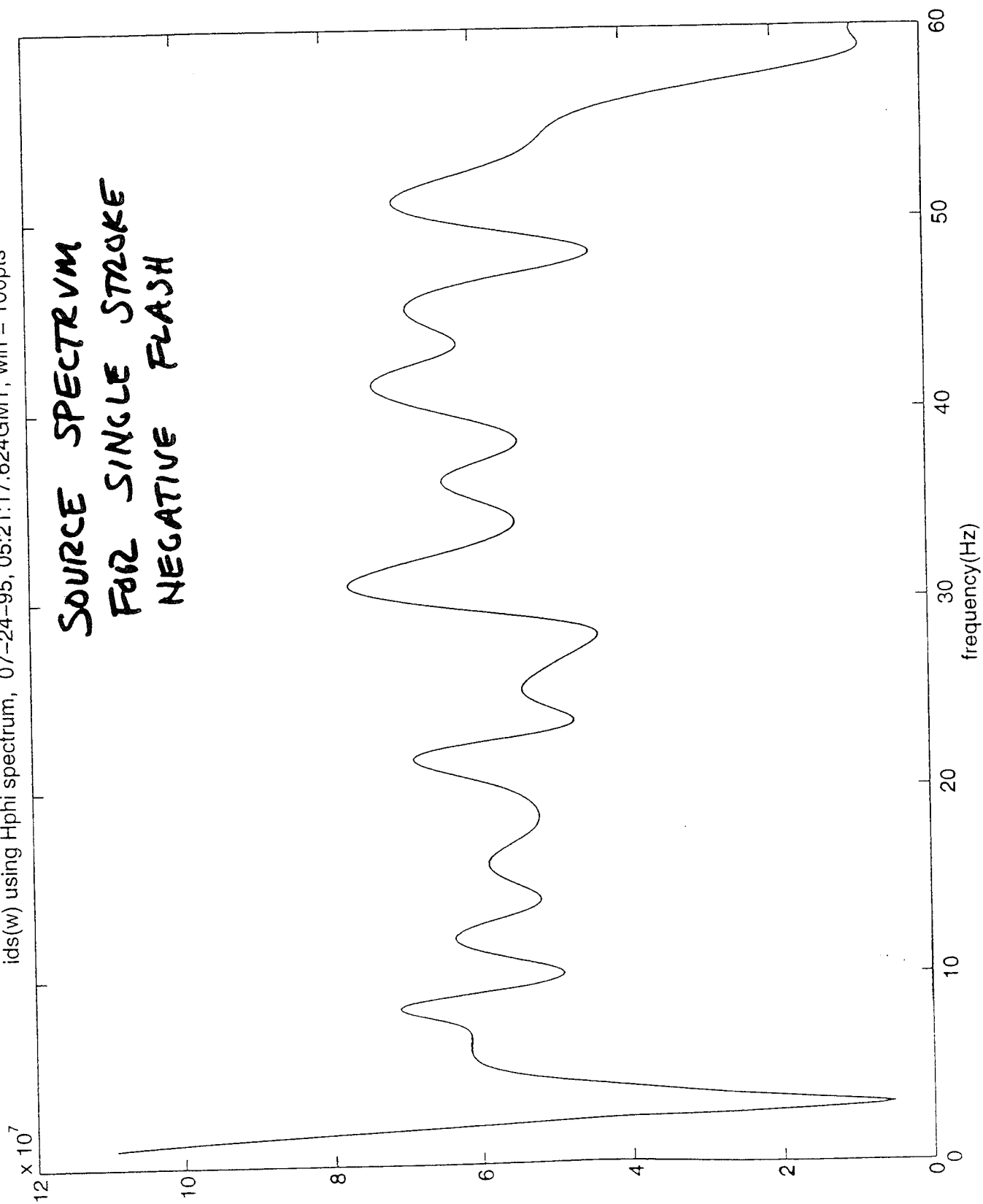
## SCHMIDT



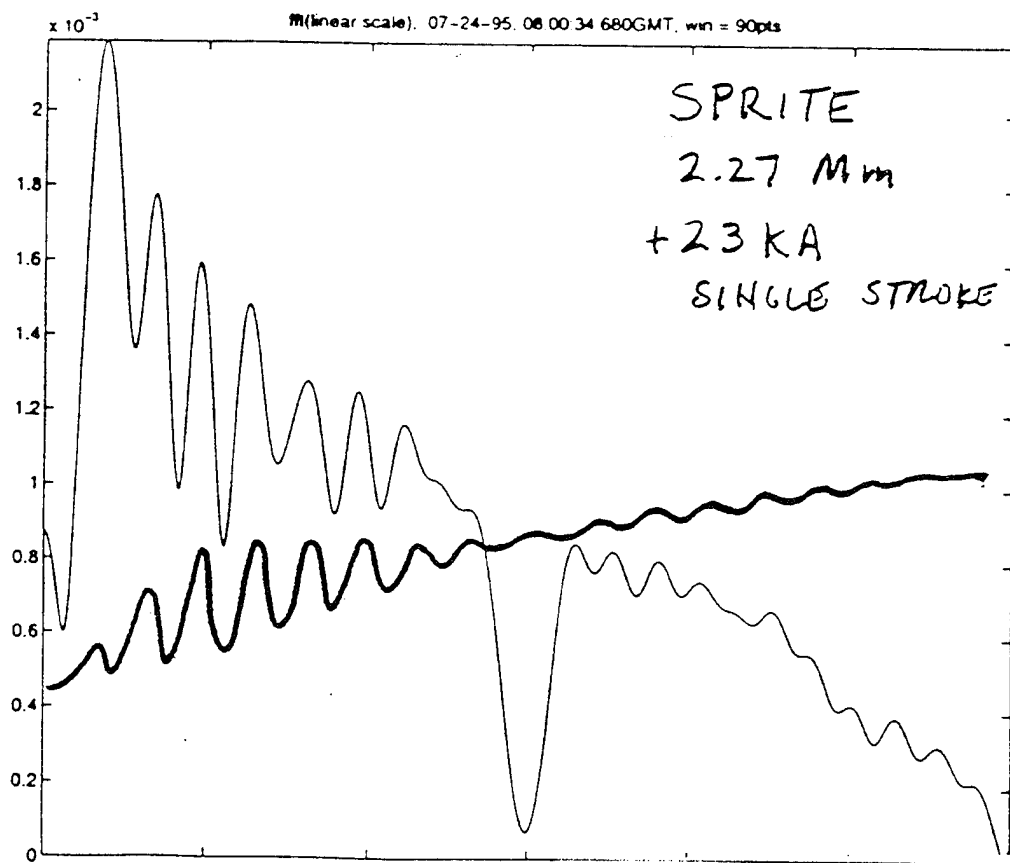
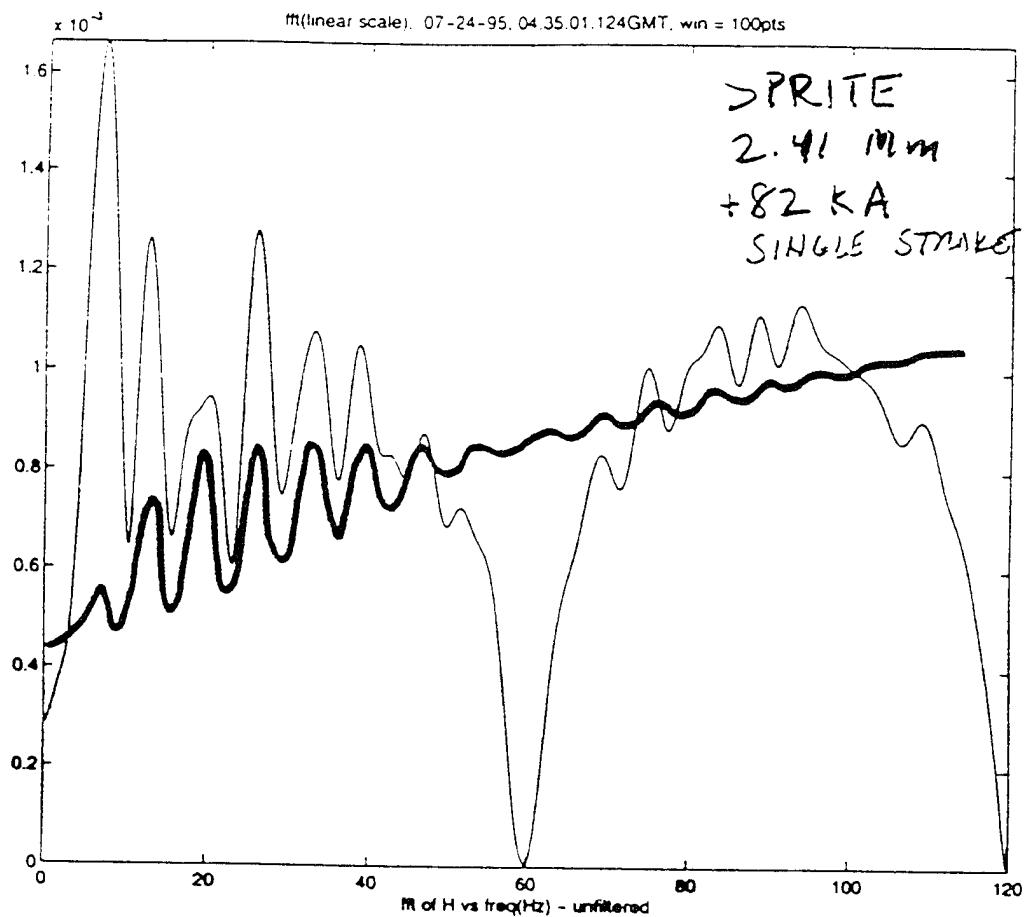
## Q-BURST MAPS

ftt(linear scale) 38-24 44 58 196, 05:21:17.624GMT, win = 100pts

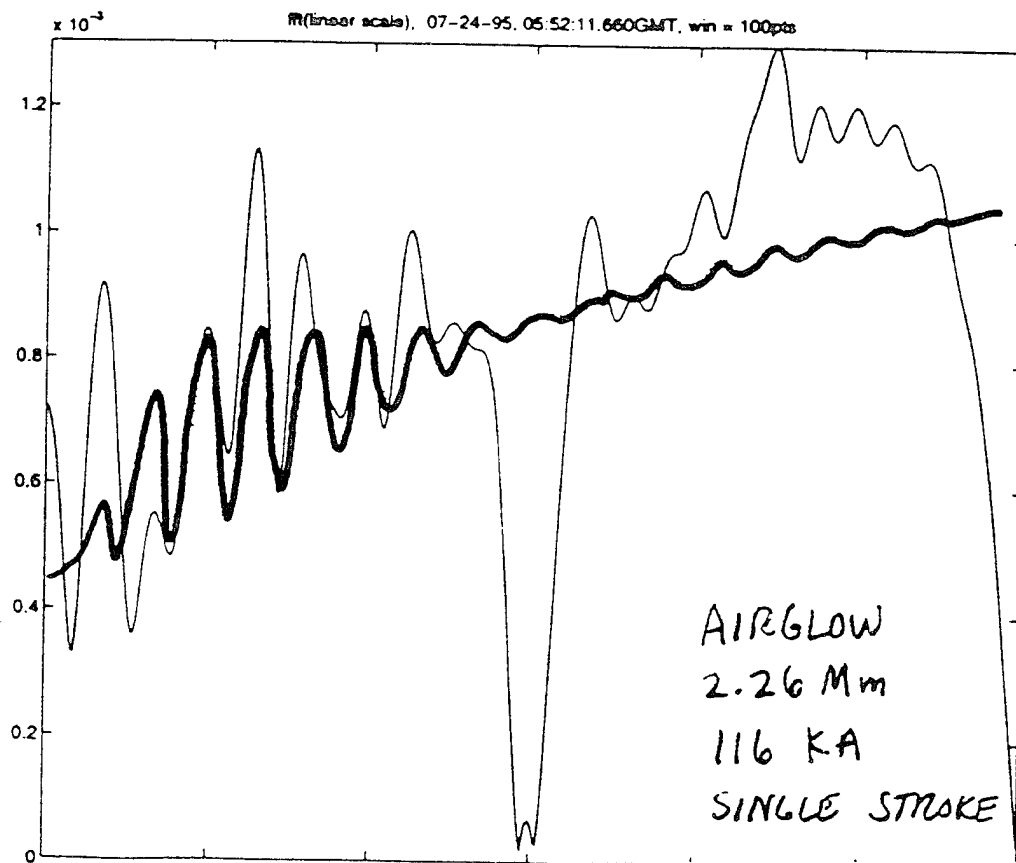
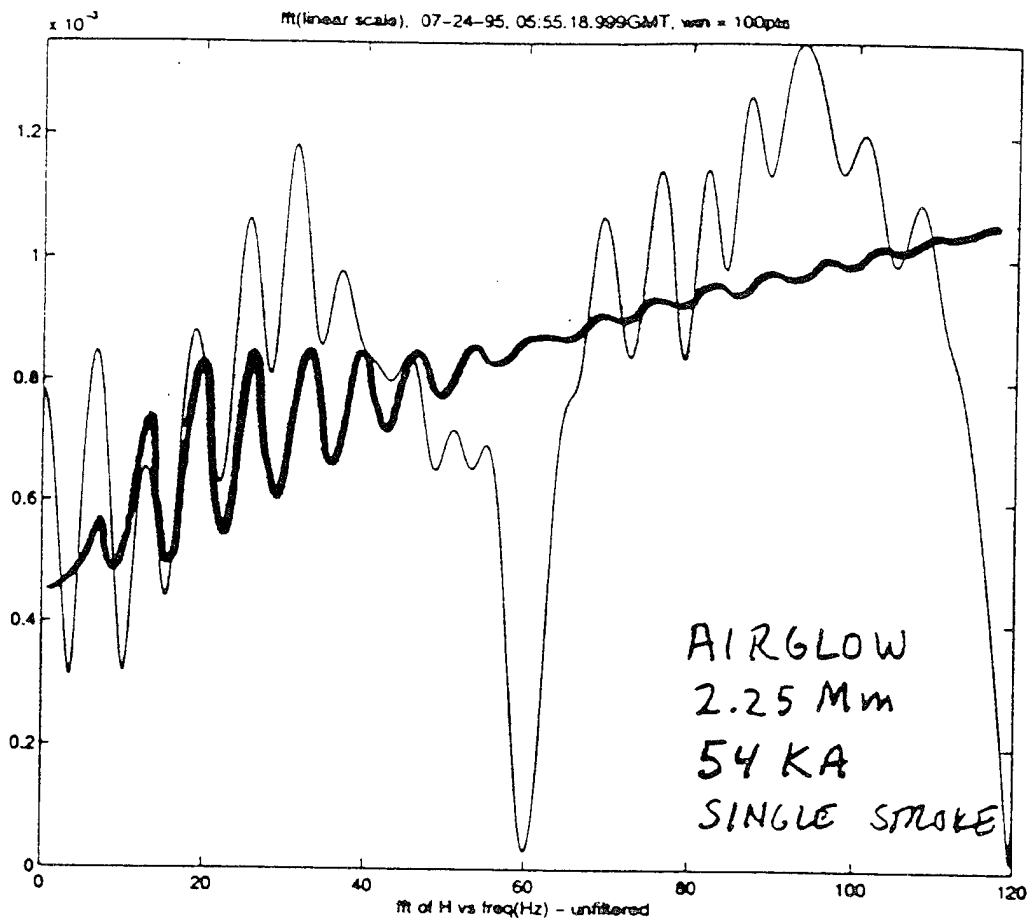




SPRITES

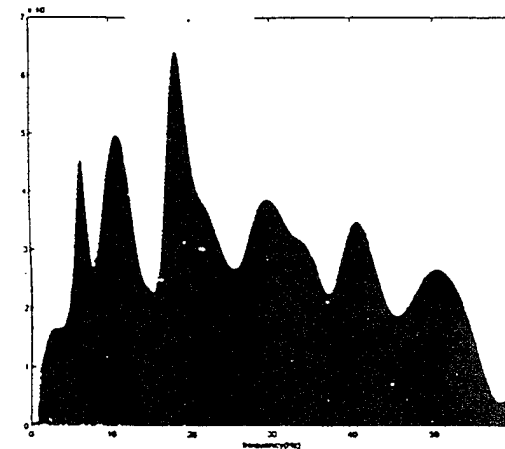
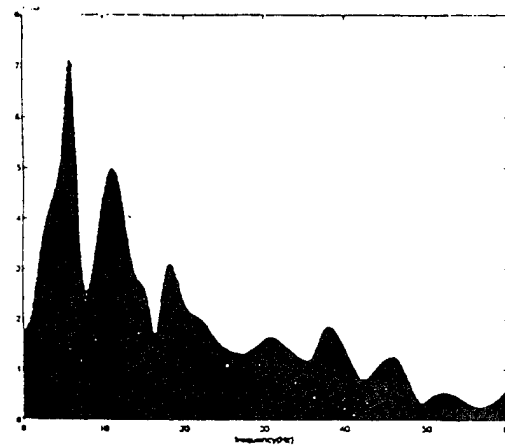
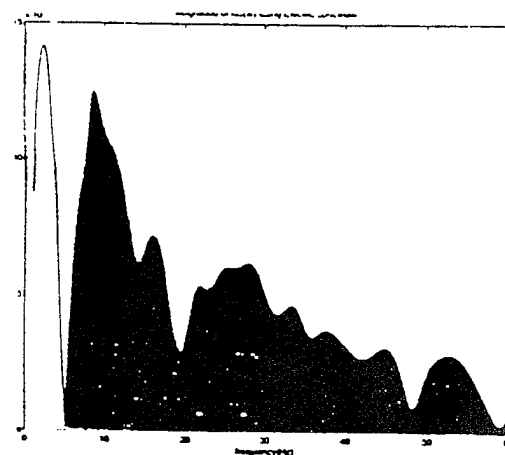
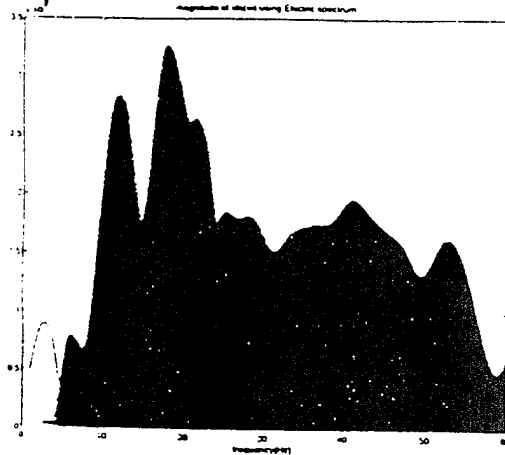


ELVES

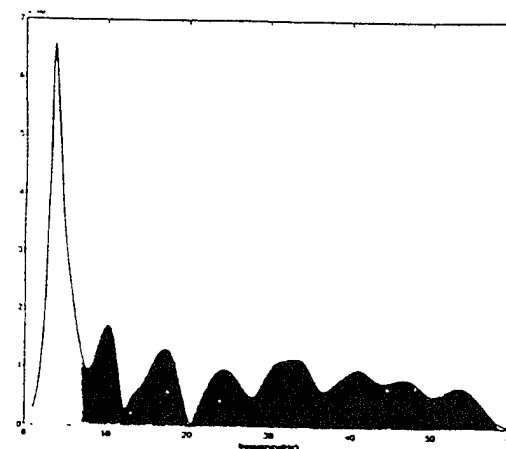
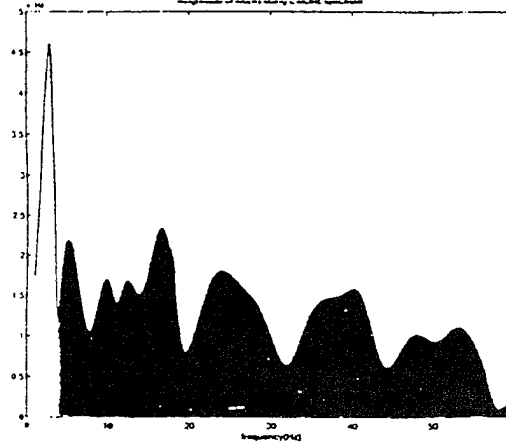
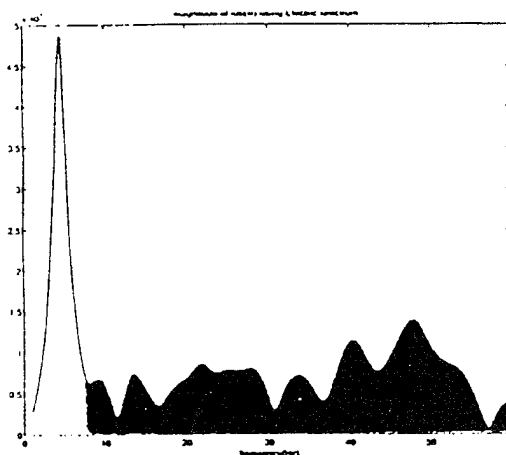
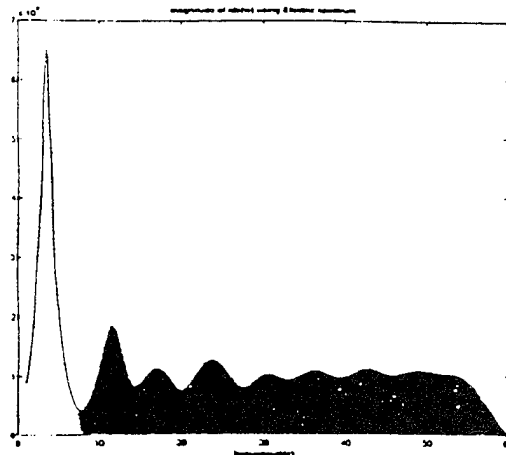


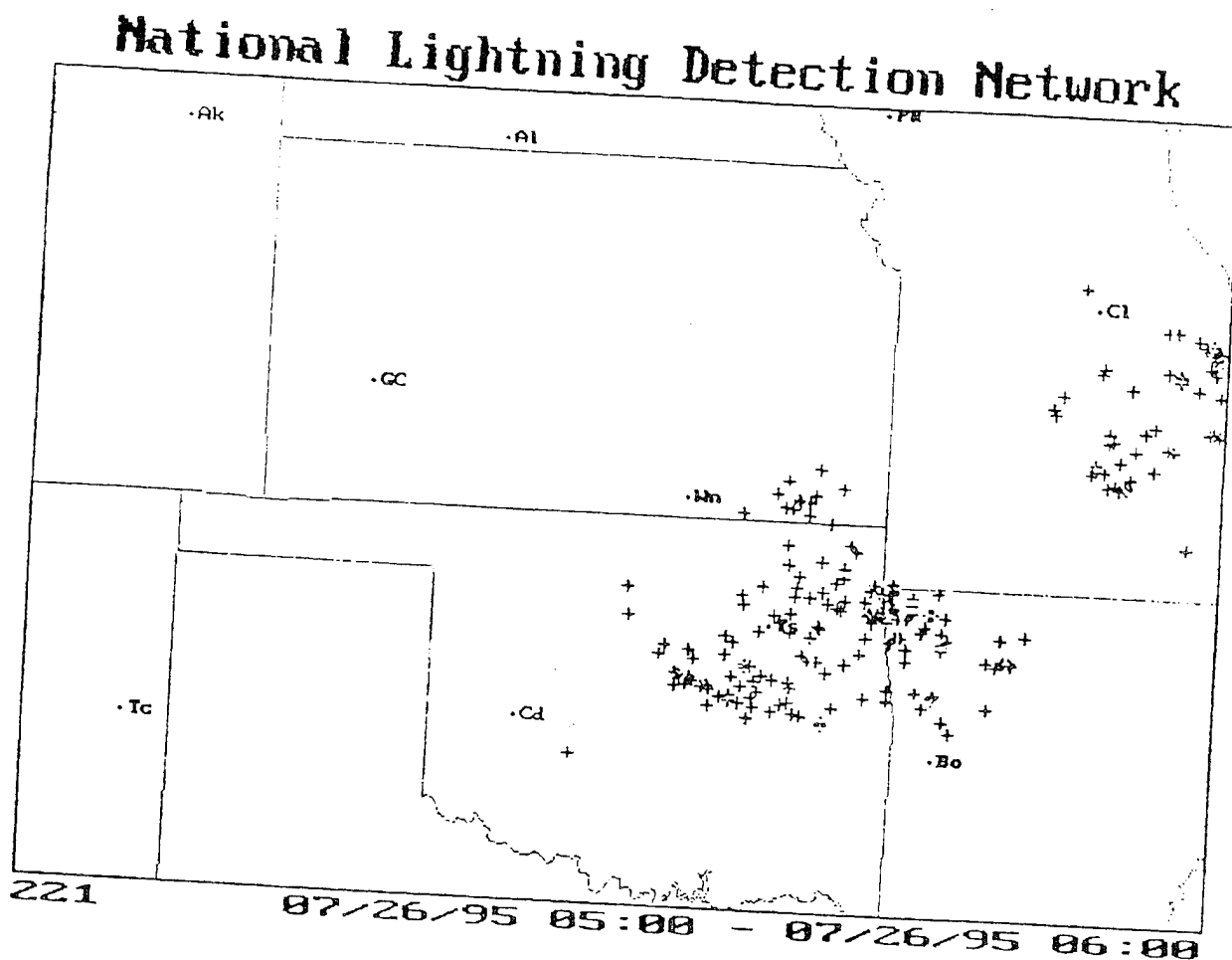


# POSITIVE CG's



# NEGATIVE CG's

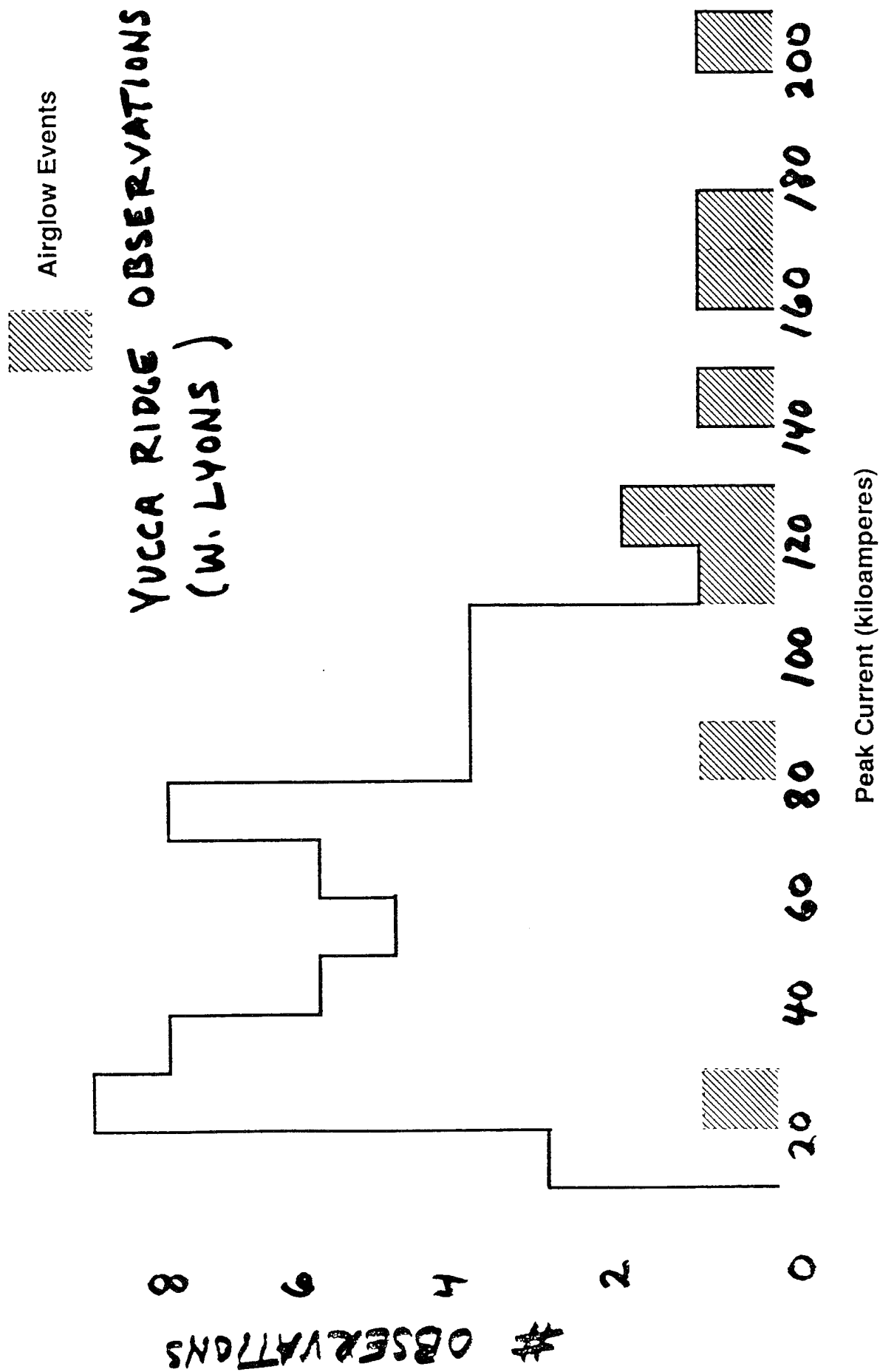




"last hour" -

Positives only -  
POSITIVE GROUND FLASHES  
SPRITES FROM YUCCA RIDGE  
Q-BURSTS IN RHODE ISLAND

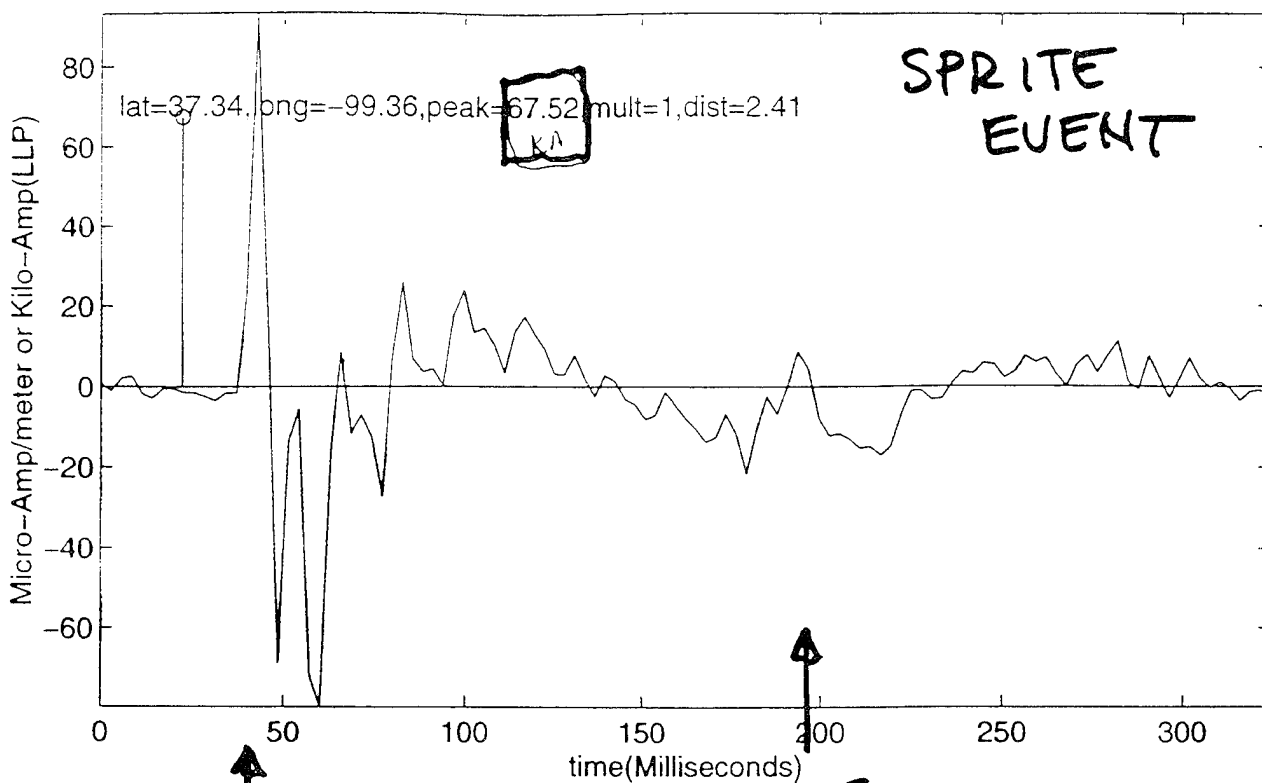
# July 25, 1995 Positive Peak Currents Associated with Sprite Events



$$LLP = 291/5 = 58.2$$

Sprite event  
red spectrum

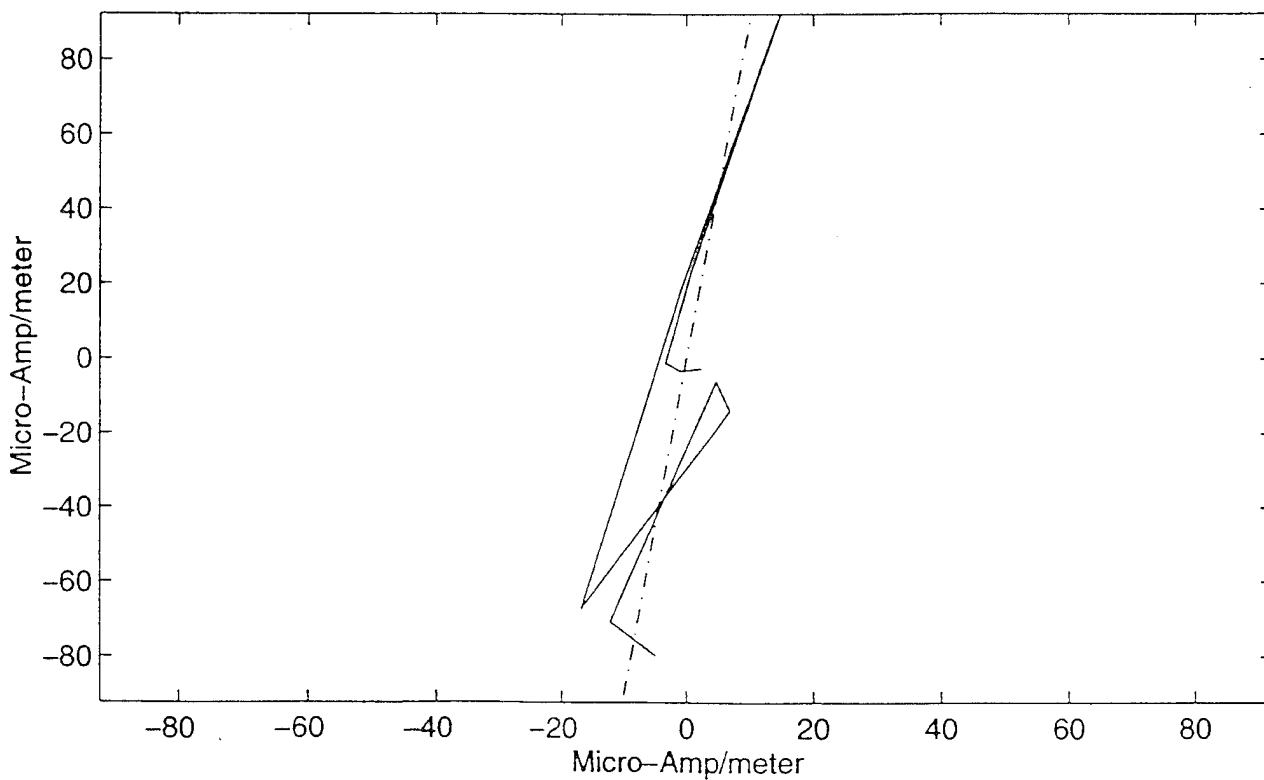
time=4:40:21.399, Bearing=267.8



↑  
INITIAL  
ARRIVAL

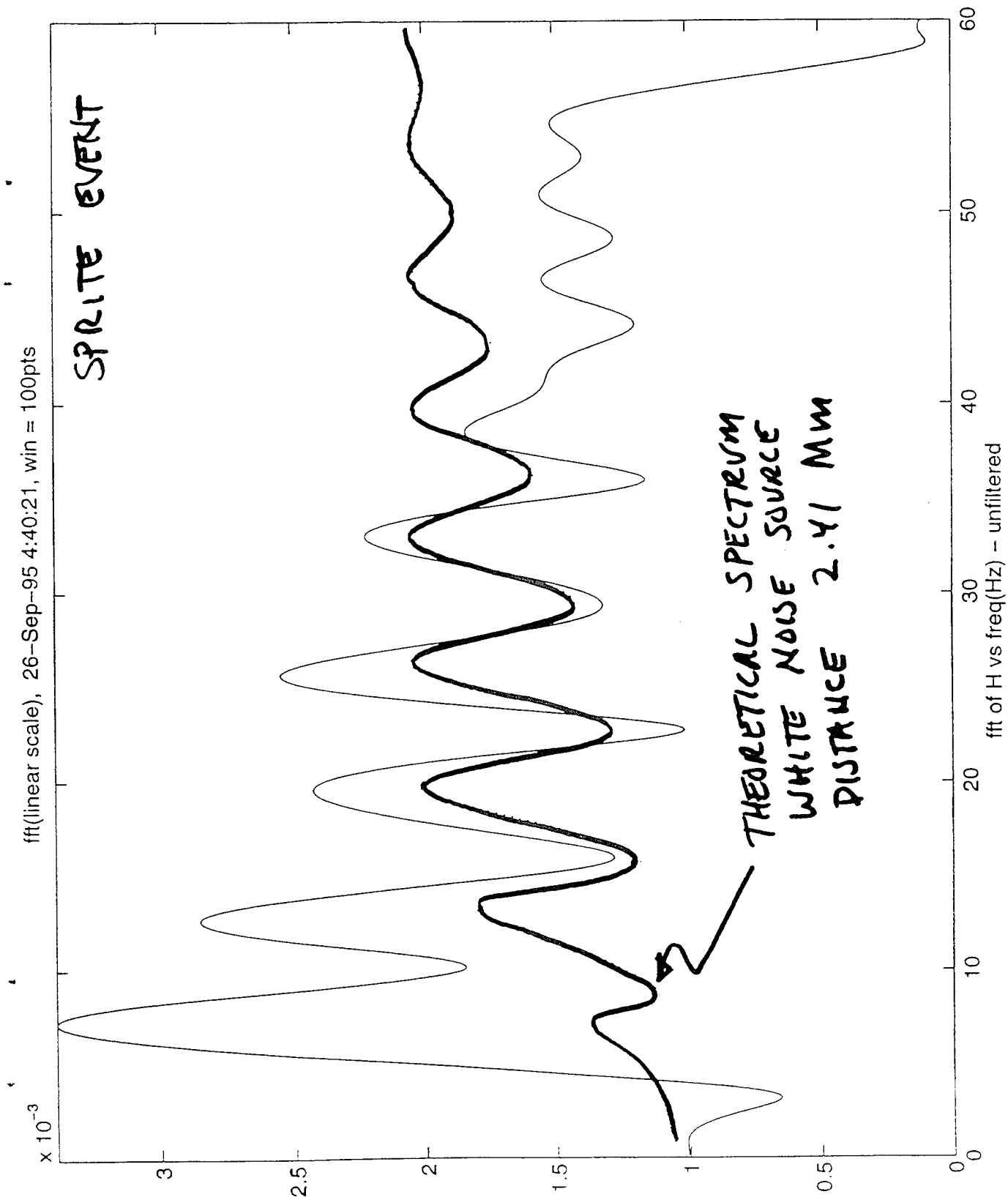
↑  
ONCE  
AROUND  
THE WORLD

bearing = 276.4

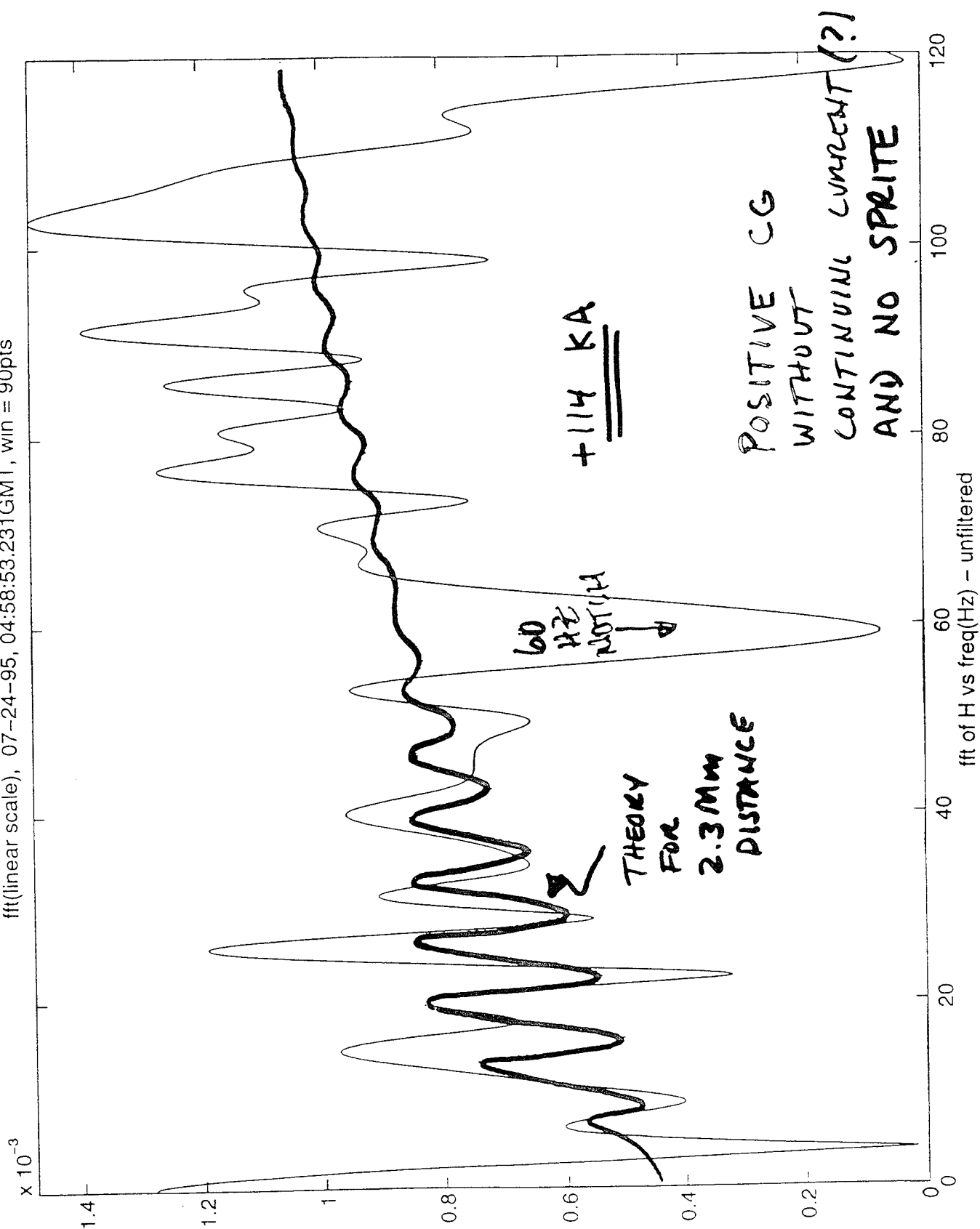


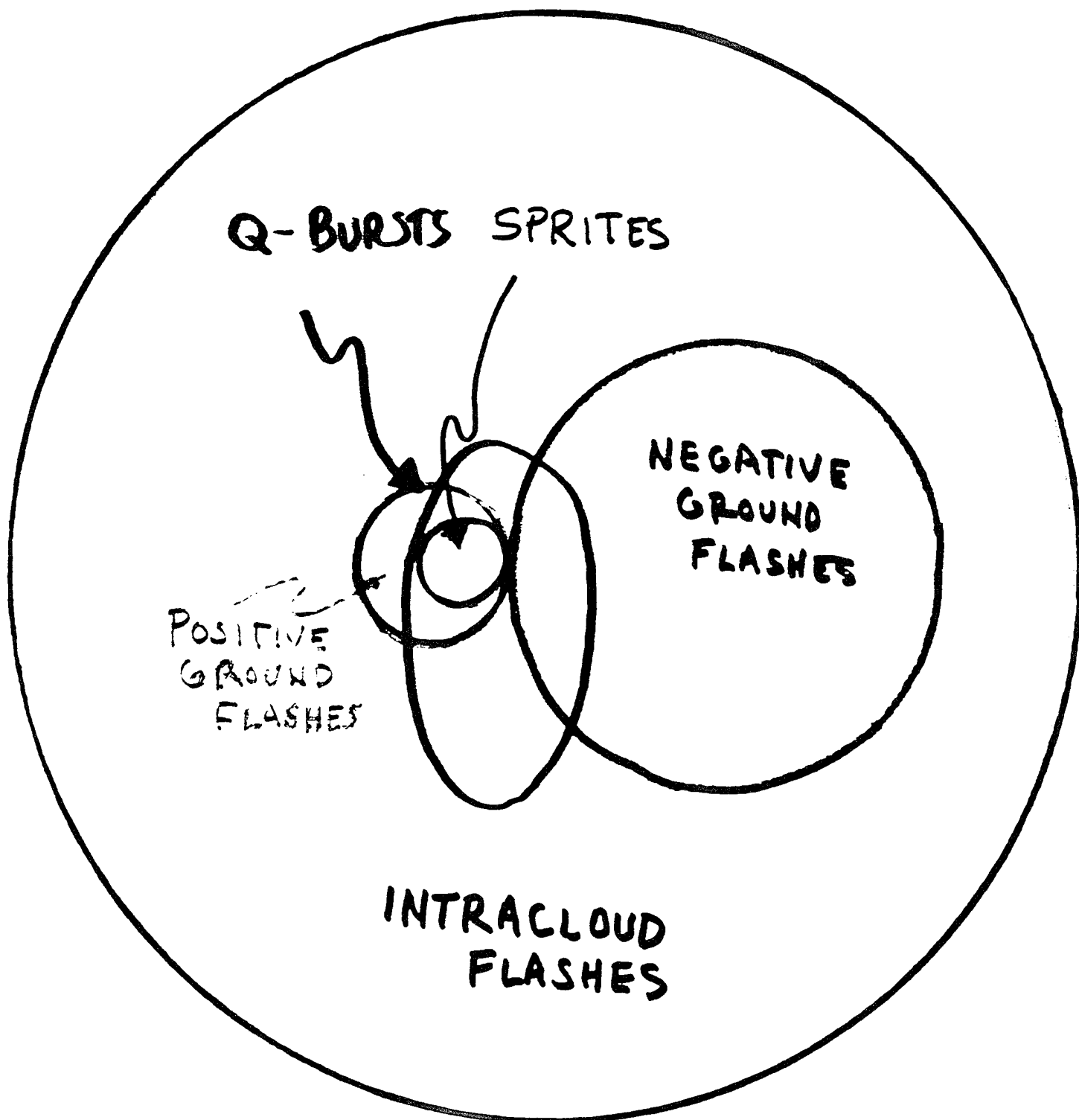
fft(linear scale), 26-Sep-95 4:40:21, win = 100pts

SPRITE EVENT

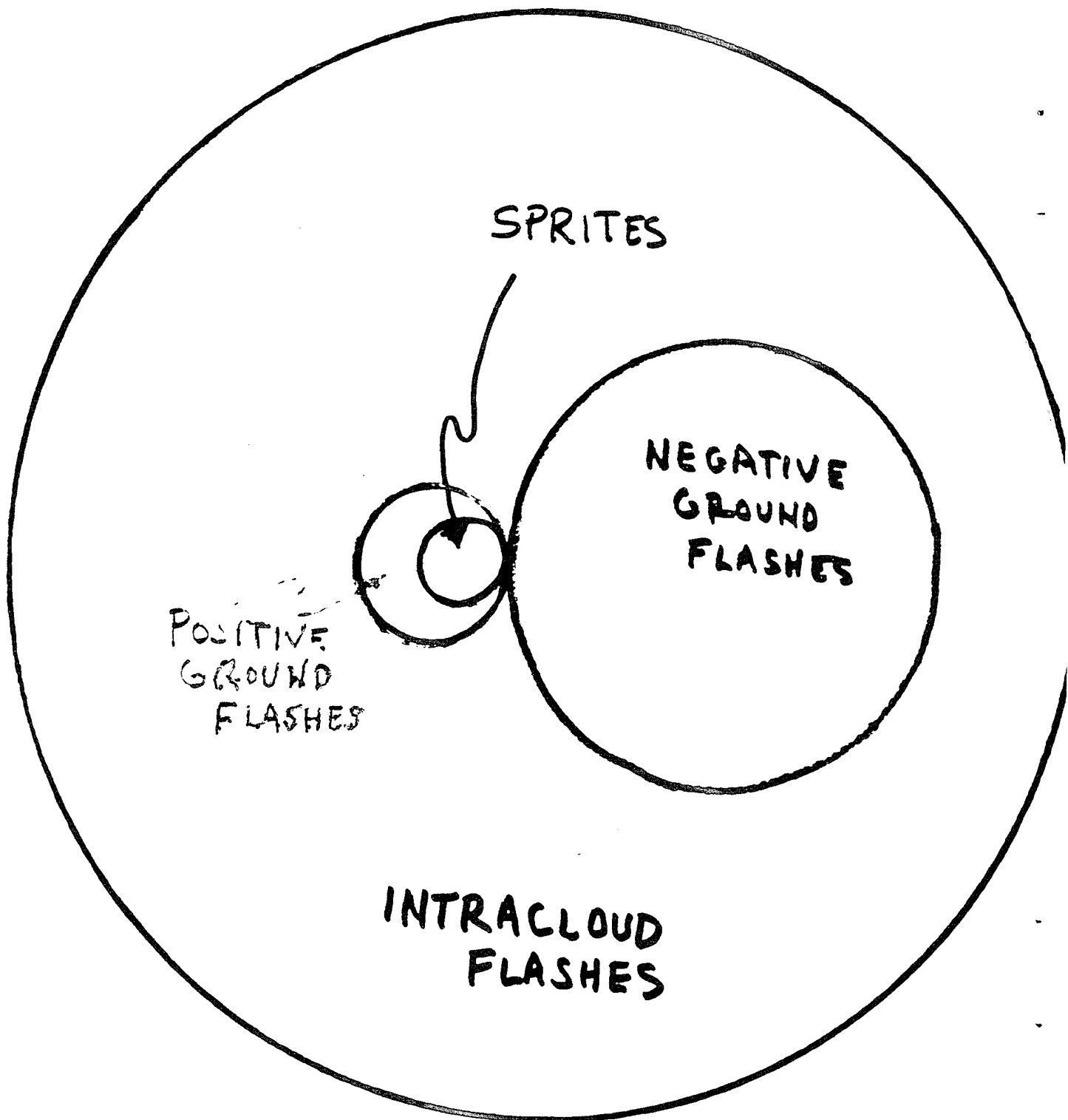


fft(linear scale), 07-24-95, 04:58:53.231GMT, win = 90pts





VENN DIAGRAM FOR LIGHTNING



VENN DIAGRAM FOR LIGHTNING



# RELAXATION TIME HALE (1985)

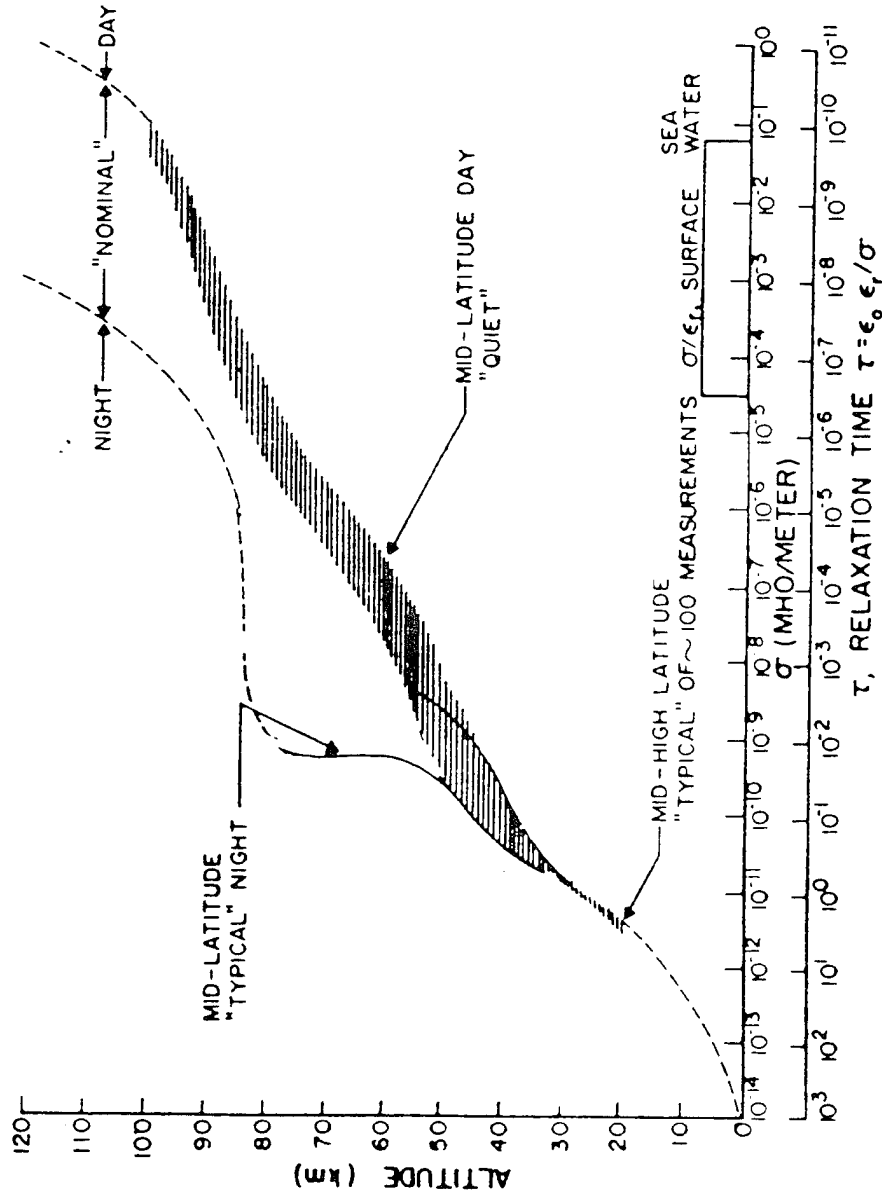
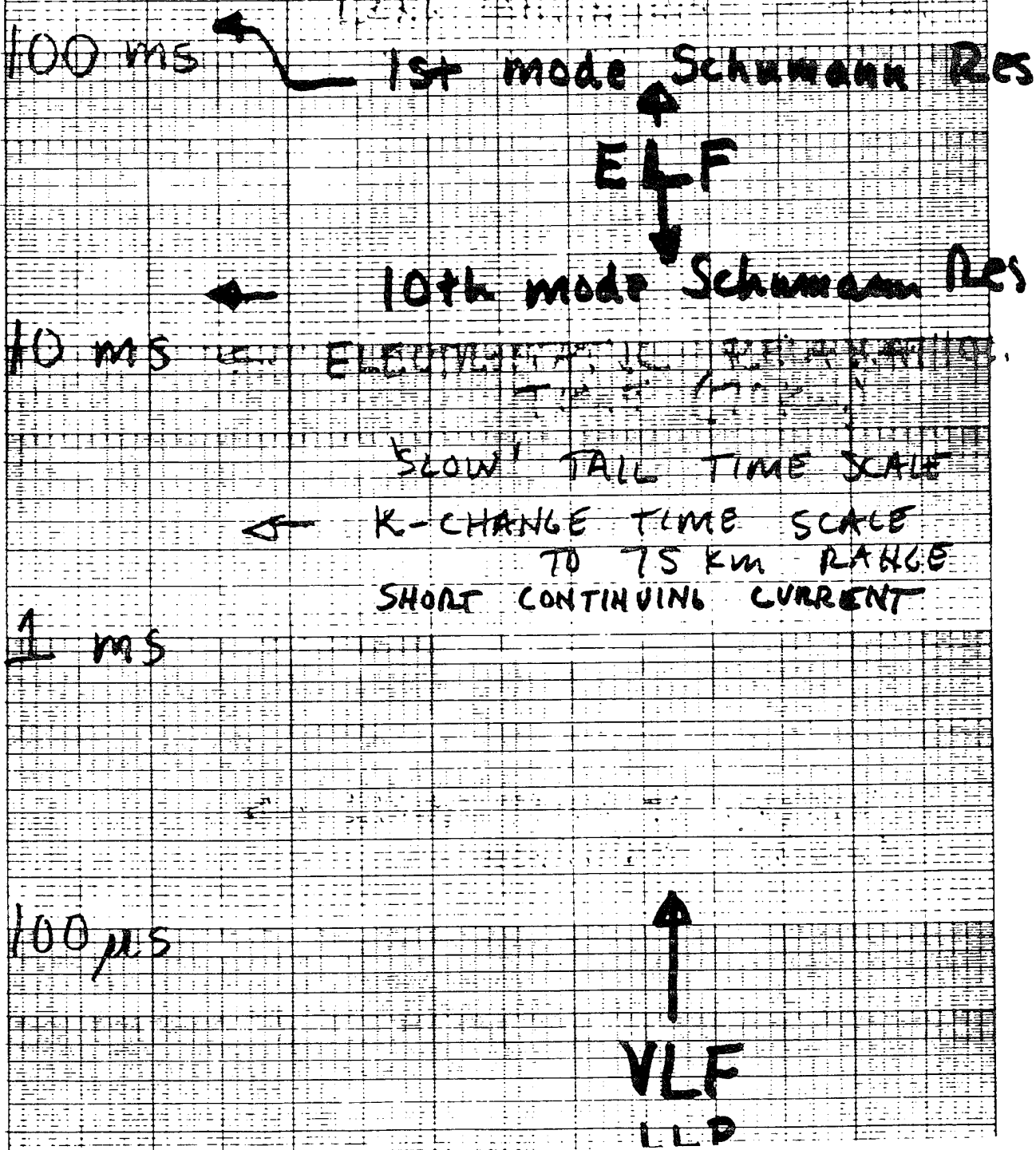


Fig. 3. Total conductivity and corresponding relaxation time under a variety of conditions.

# RELEVANT TIME SCALES (SPRITES & ELVES)



46 6210

K-E SEMI-LOGARITHMIC 5 CYCLES X 70 DIVISIONS  
KEUFEL & ESSER CO. MADE IN U.S.A.

# SUMMARY

SPRITE  
EVENTS

POSITIVE  
CG's

'RED' SPECTRA

AIRGLOW

POSITIVE  
CG's

'PINK' SPECTRA

NON SPRITE

NEGATIVE  
CG  
SINGLE STROKE

WHITE  
SPECTRUM

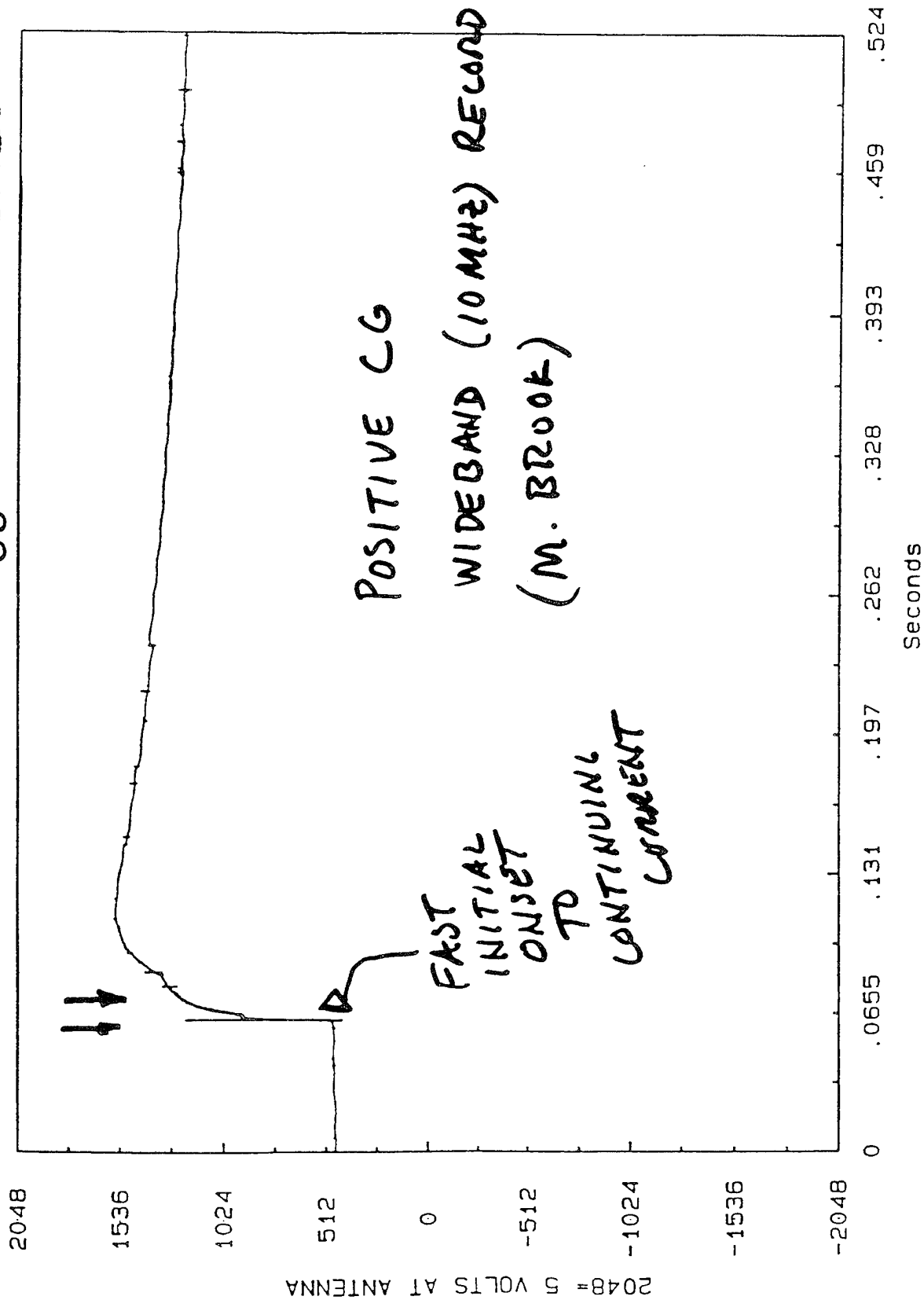
NON SPRITE

POSITIVE CG  
NO CONT.  
CURRENT

WHITE  
SPECTRUM

# COMPACTED PLOT

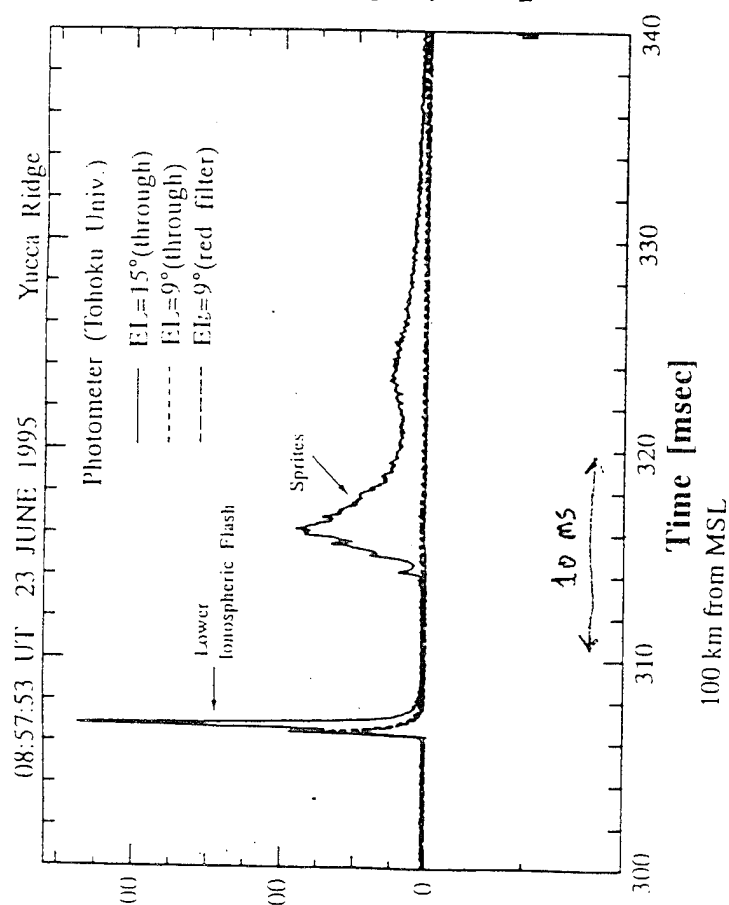
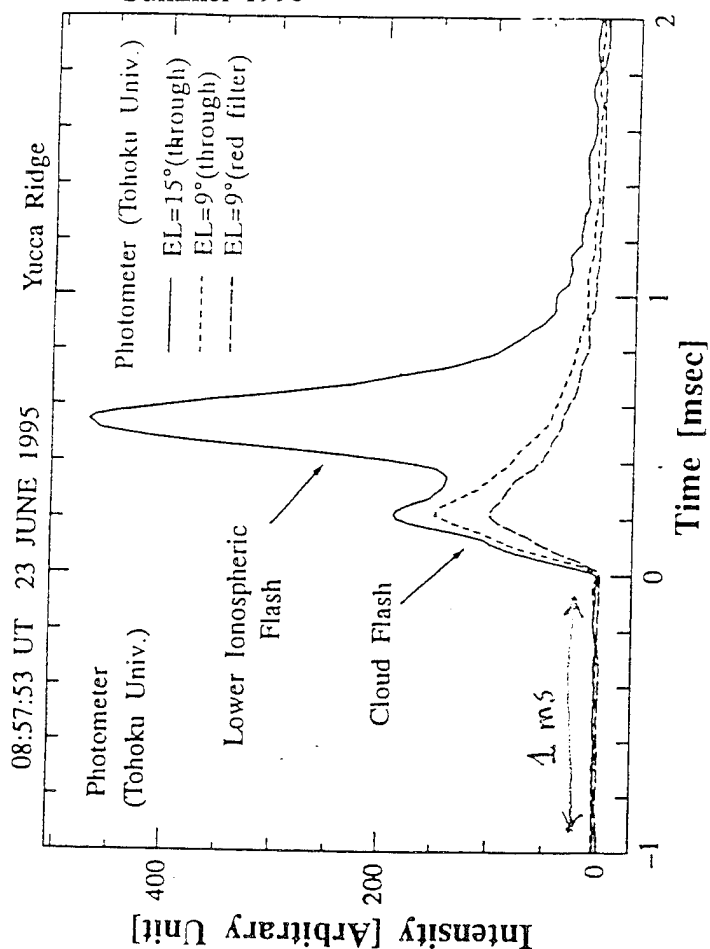
1990 139 57 21 27 29 3 64 5 2000 Trigger Time 21:27:29



**Sprites, Blue Jets, and High Altitude Optical Flashes  
Produced by Quasi-Electrostatic Thundercloud Fields  
and Lightning EMP**

**U.S. Inan  
Stanford University**

Description of the experiments of Fukunishi et al., carried out at Yucca Ridge during Summer 1995



07:27:16 UT 8 JULY 1995 Yucca Ridge

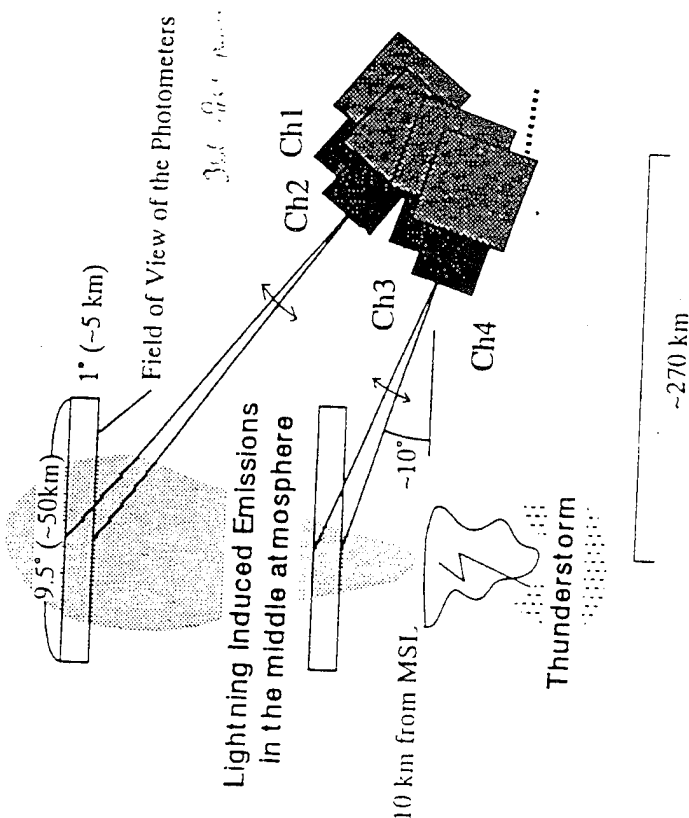
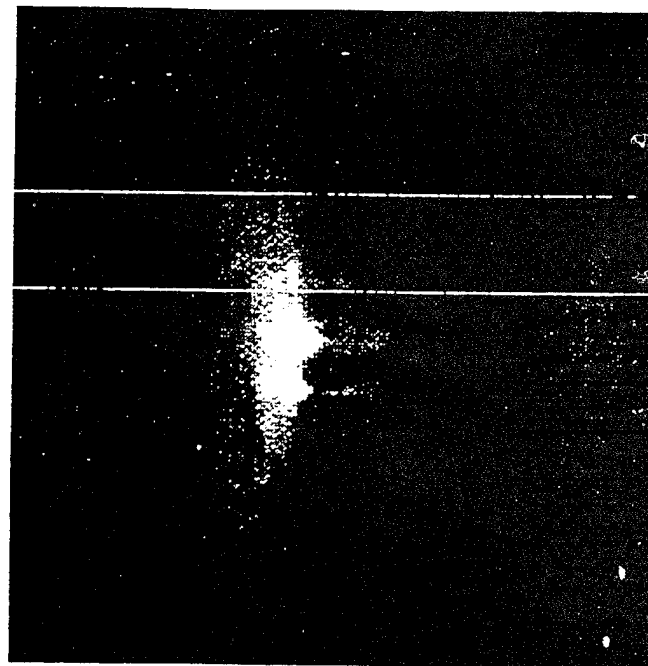
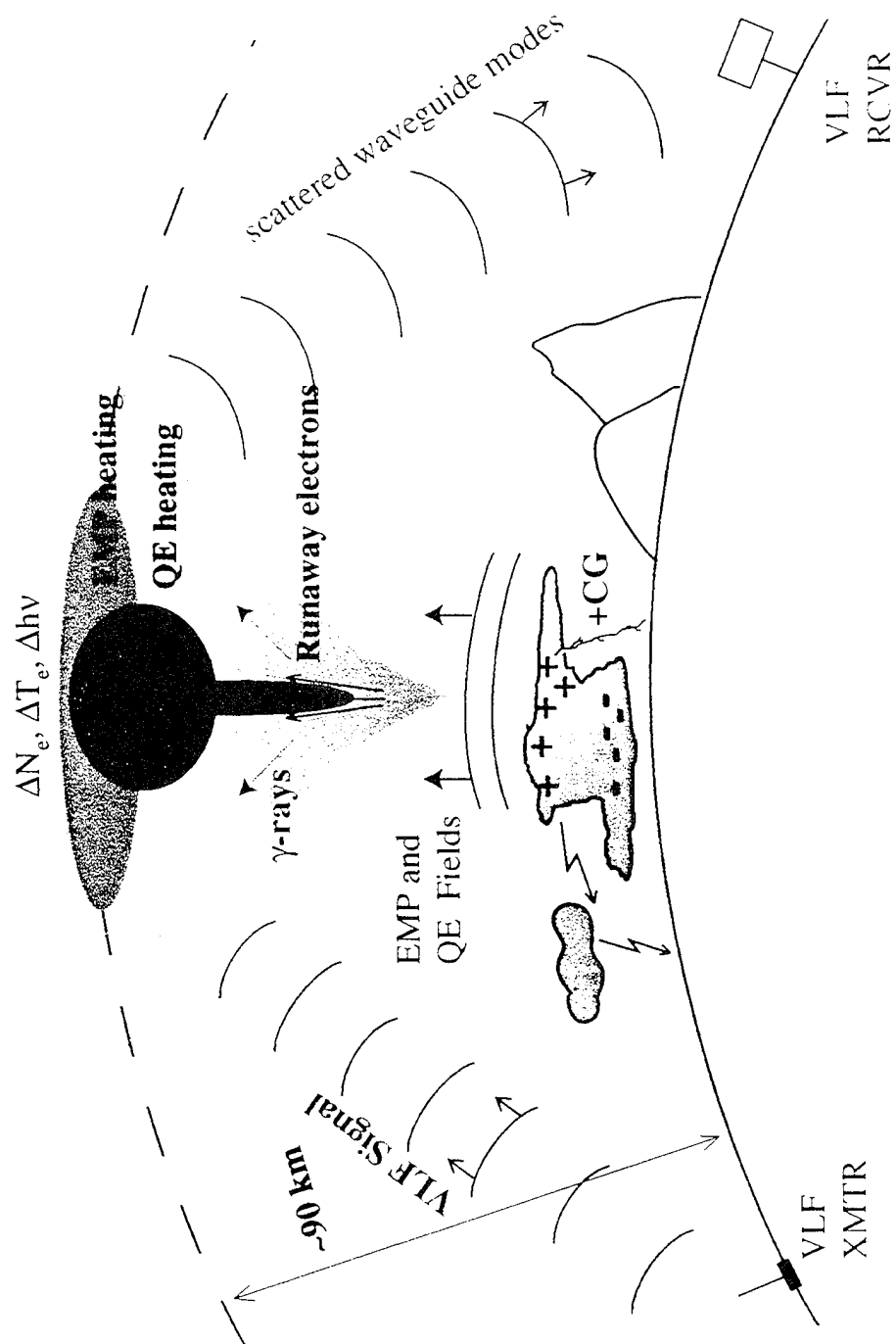
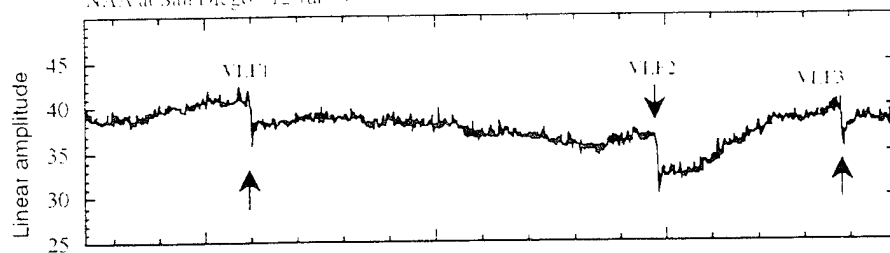


Illustration of different mechanisms operating at different altitude ranges and detection of the disturbances via the VLF-scattering method

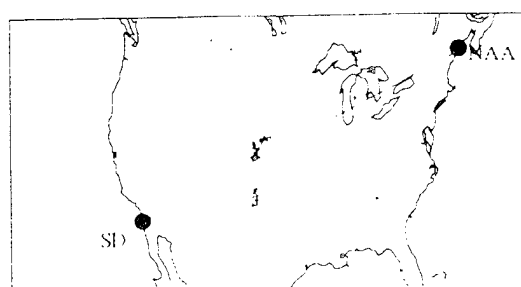
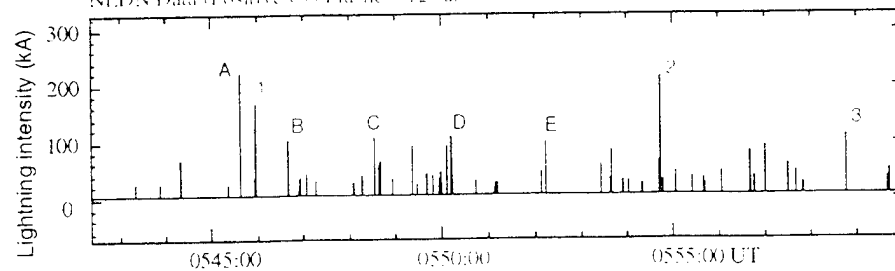


# VLF remote sensing of transient ionospheric disturbances from [Inan, Bell, Pasko, Sentman, Wescott, Lyons, in review at GRL, 1995]

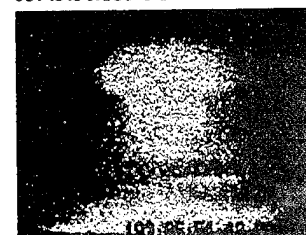
NAA at San Diego 12 Jul 94



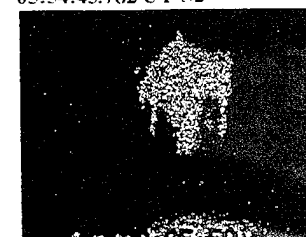
NLDN Data (Positive CG Flashes) 12 Jul 94



05:45:56.188 UT S1



05:54:43.782 UT S2



05:58:45.391 UT  
S3 "ANGEL"

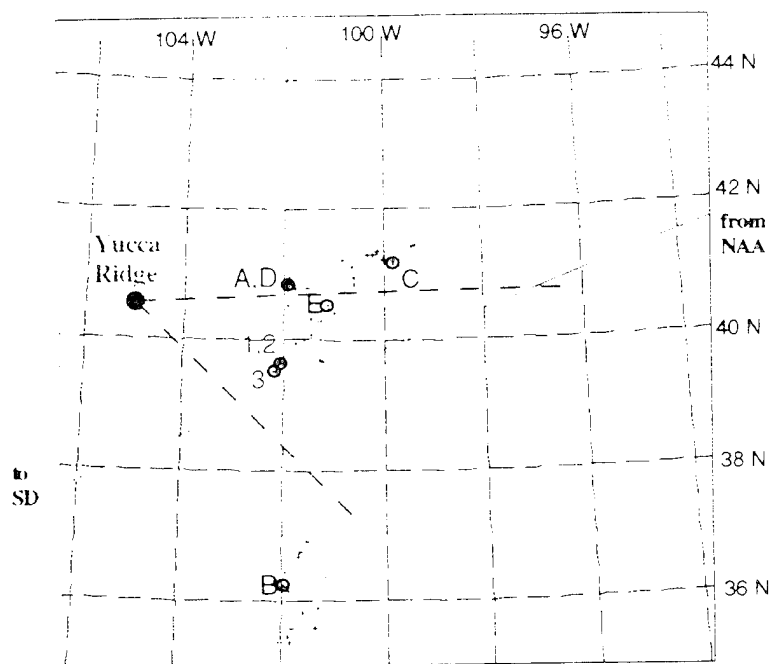
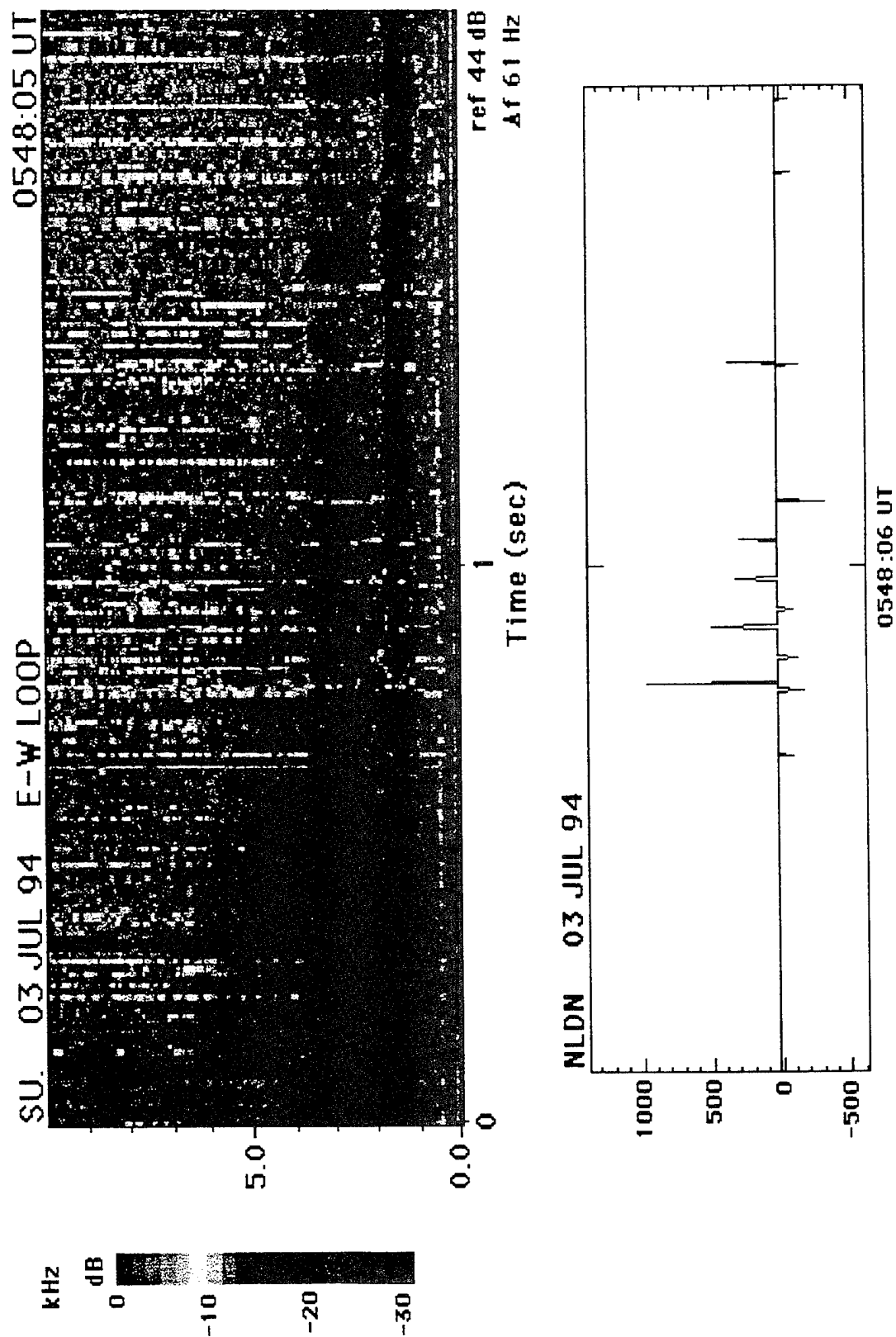


Figure 3



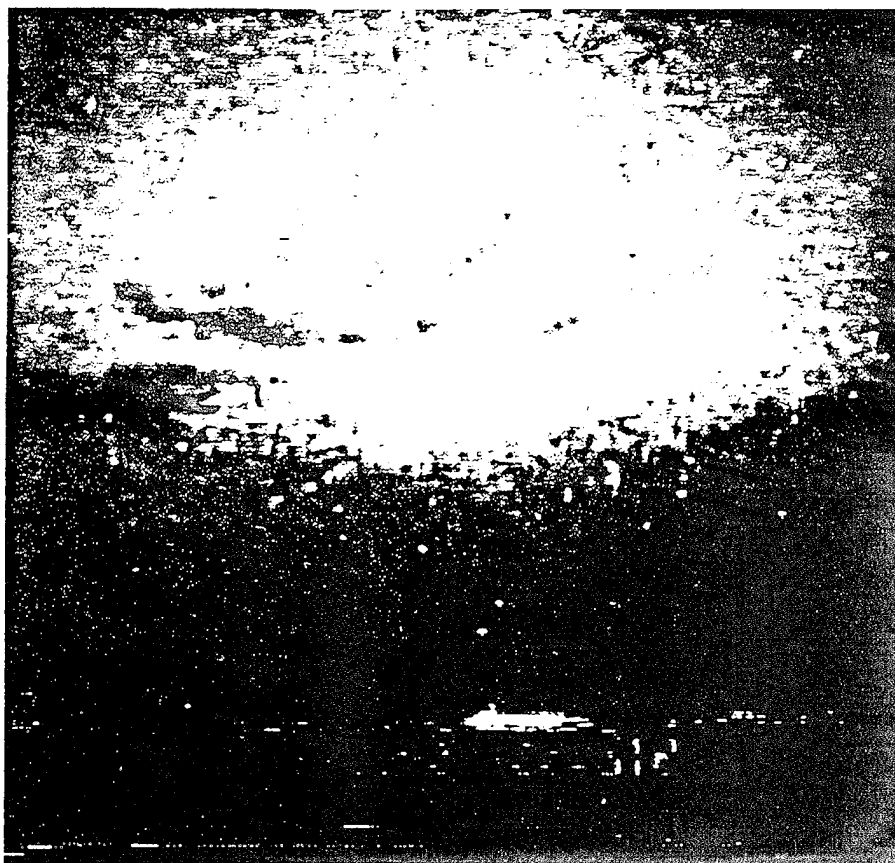
Characteristics of ELF/VLF sferics of CG lightning discharges producing sprites  
 from [Reising, Inan, Bell, to be presented at Fall AGU Meeting]



Intensity  
[Arbitrary Unit]  
234

95/06/23 08:57 UT (1)

10

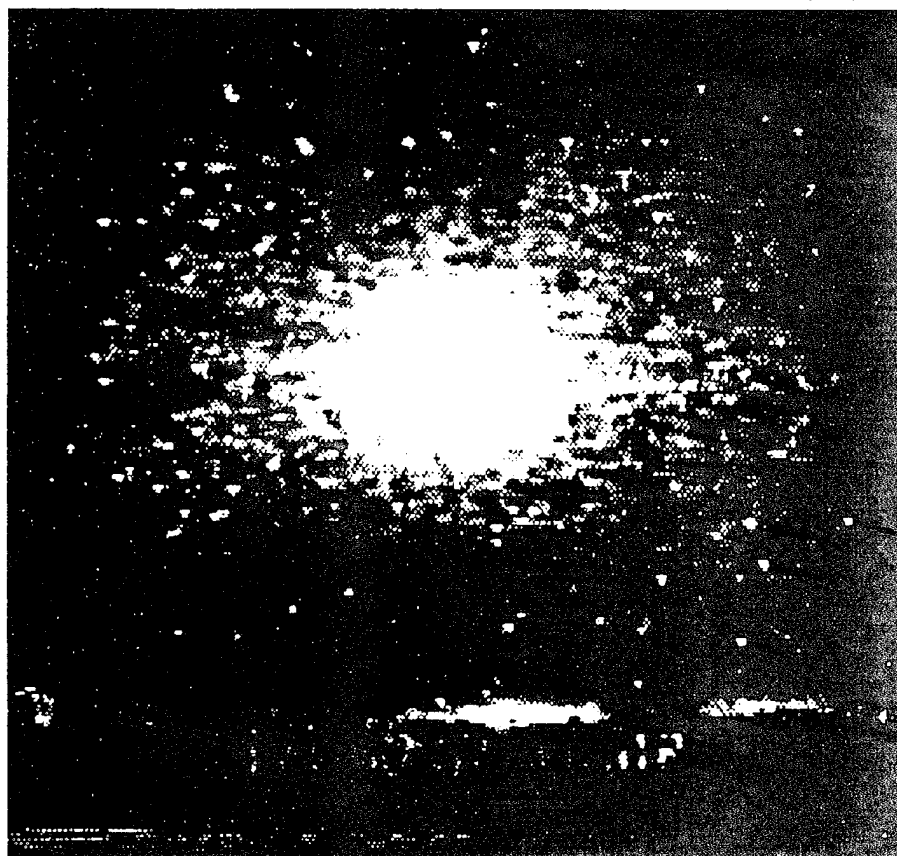


Images of lower ionospheric flashes (elves) and sprites  
from Fukunishi et al. [1995, paper in preparation for submission to Nature]

Intensity  
[Arbitrary Unit]  
201

95/06/23 08:57 UT (2)

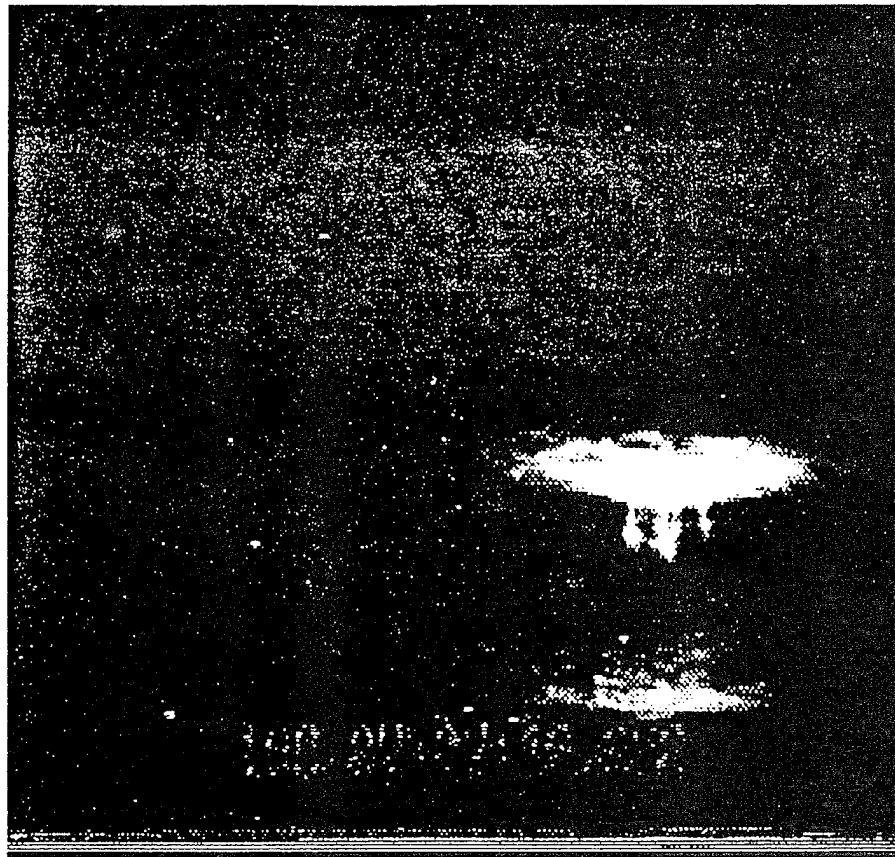
10



Intensity  
[Arbitrary Unit]  
247

95/07/08 07:27 UT (1)

10

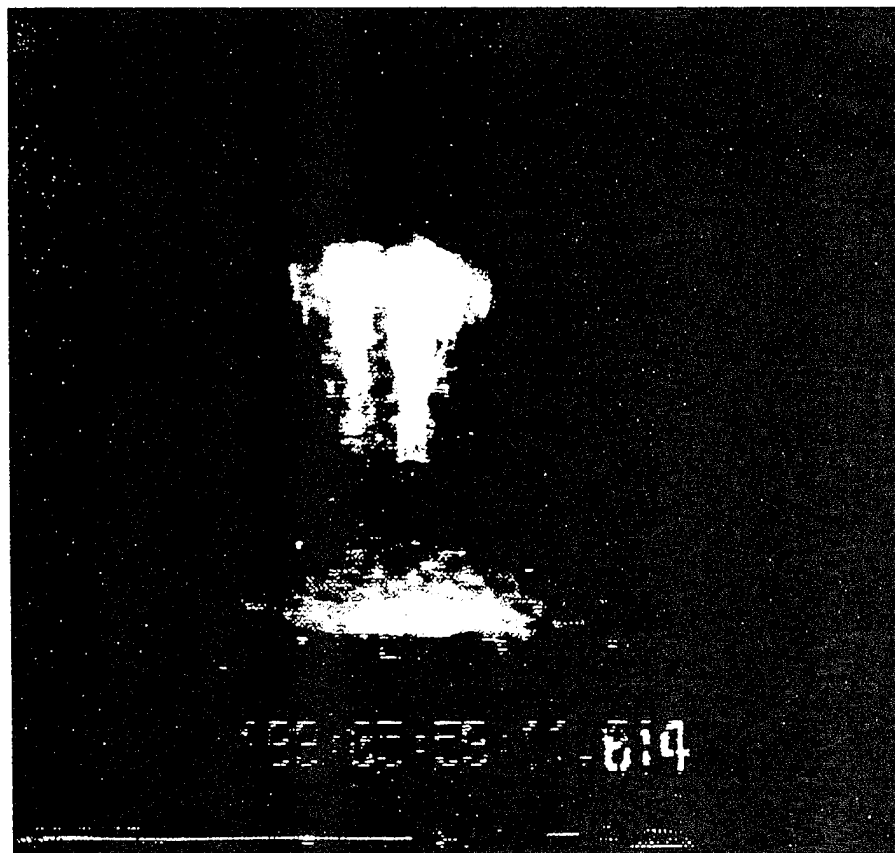


Images of lower ionospheric flashes (elves) and sprites  
from Fukunishi et al. [1995, paper in preparation for submission to Nature]

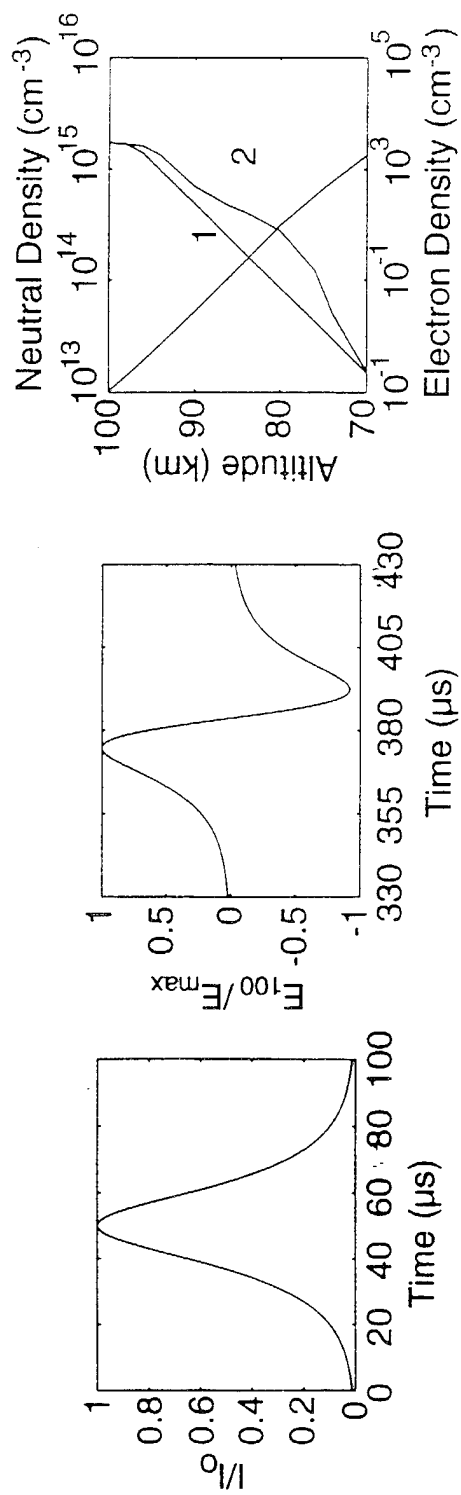
Intensity  
[Arbitrary Unit]  
210

95/07/08 05:59 UT (1)

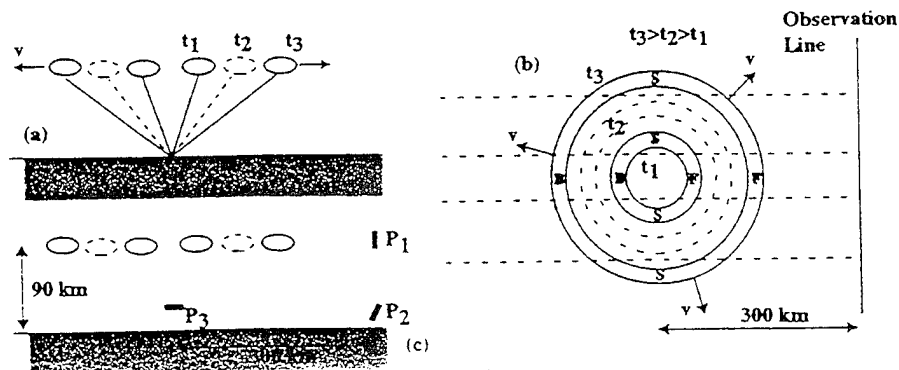
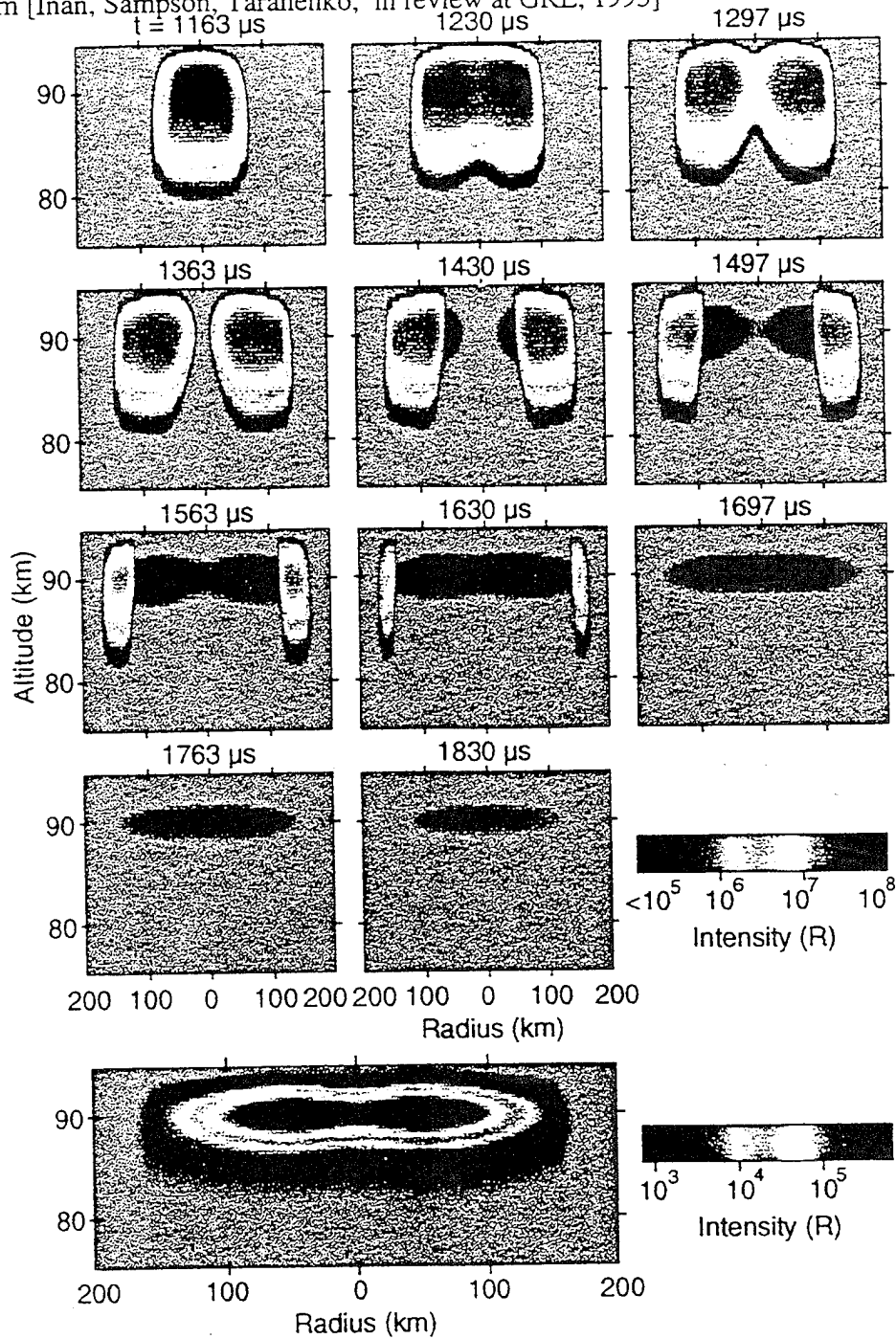
10



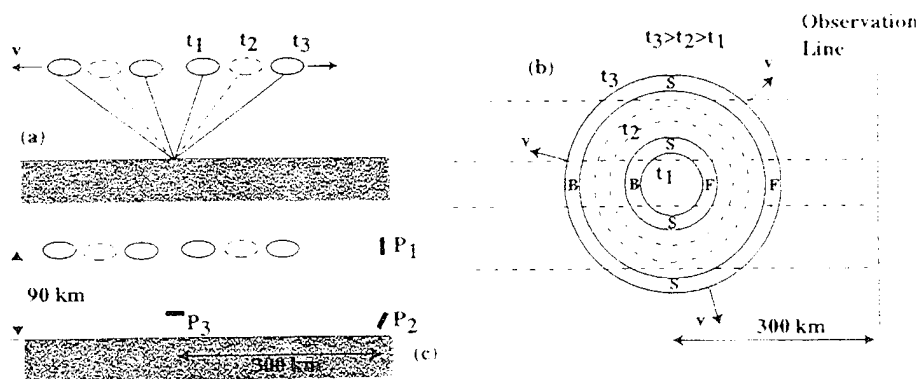
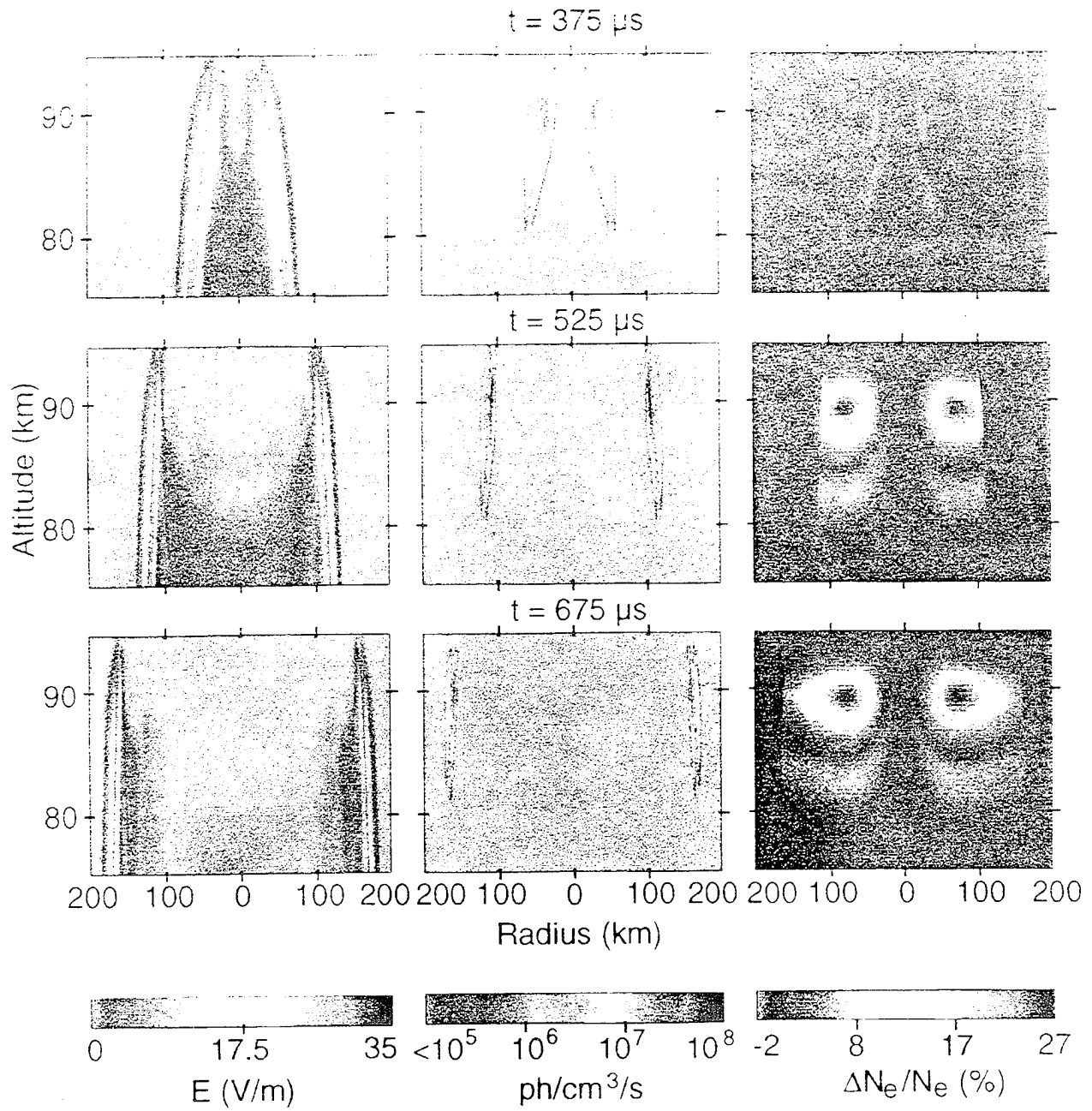
Results of a new 2-D model of EMP-ionosphere interaction  
[Inan, Sampson, Taranenko, in review at GRL, 1995]



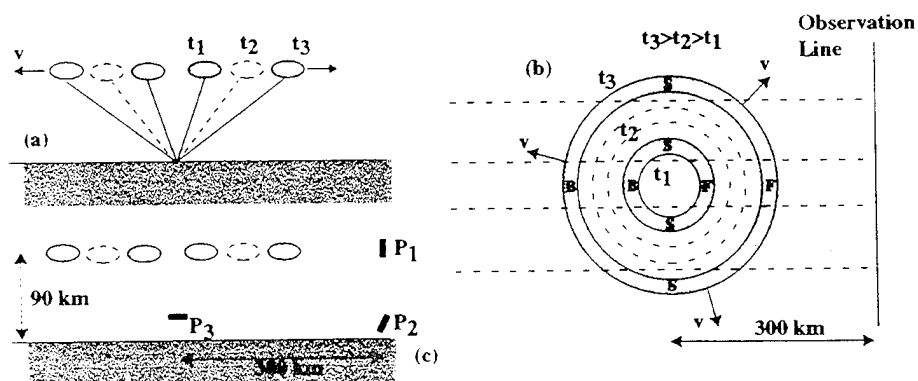
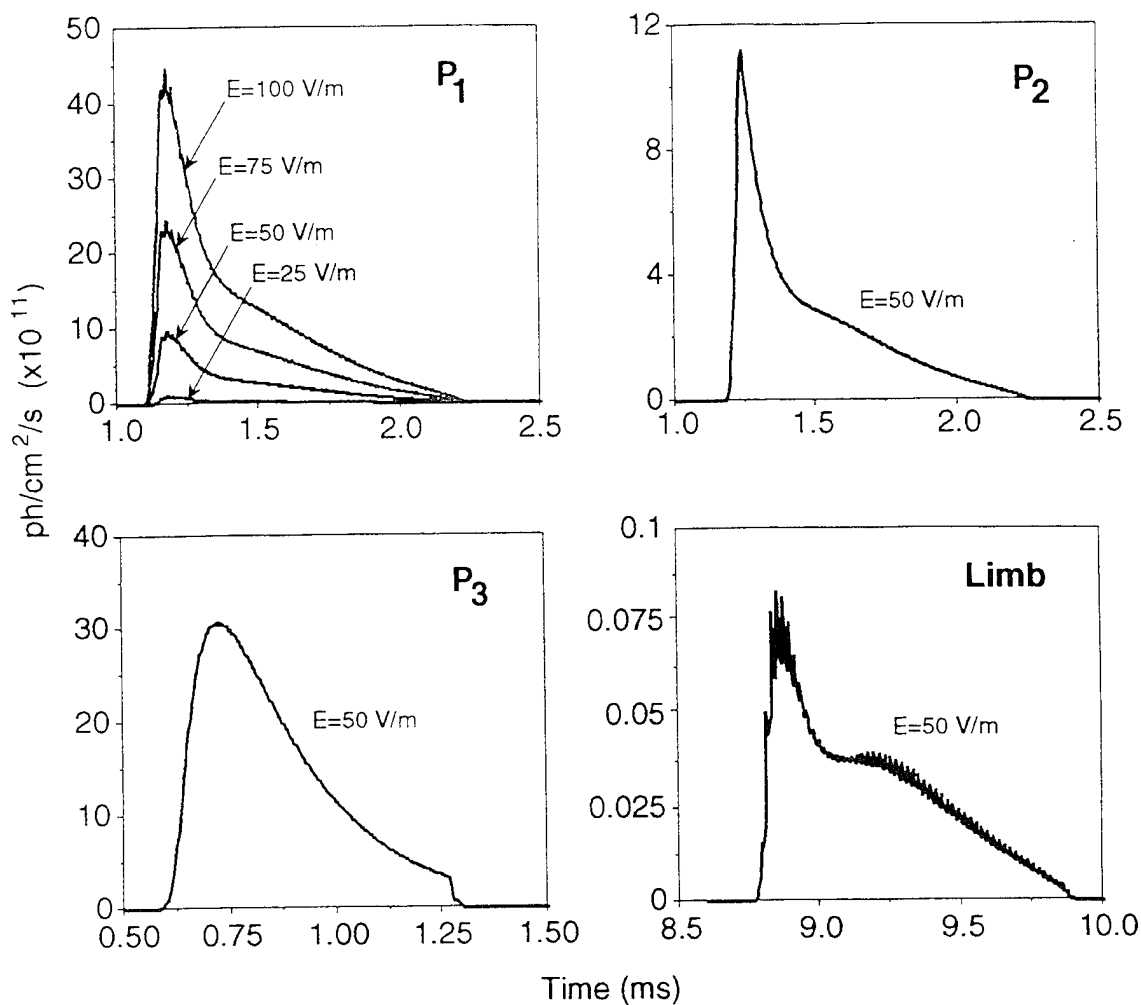
"A light show in the sky" produced by the interaction of the EMP with the ionosphere  
 from [Inan, Sampson, Taranenko, in review at GRL, 1995]



from 2-D EMP model (Ivan, Samsonov, Tarasenko, in review, JGR, 1995)

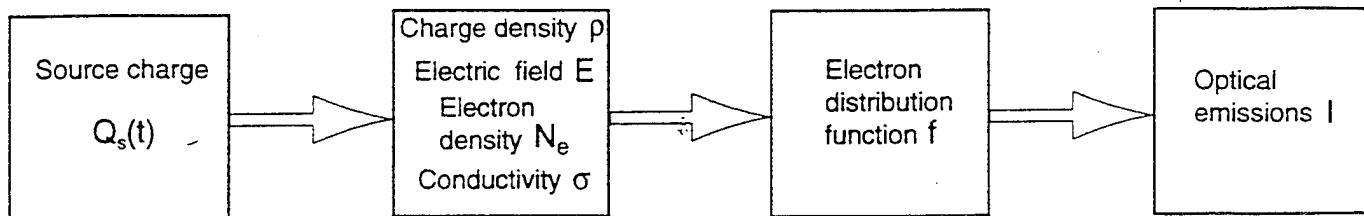
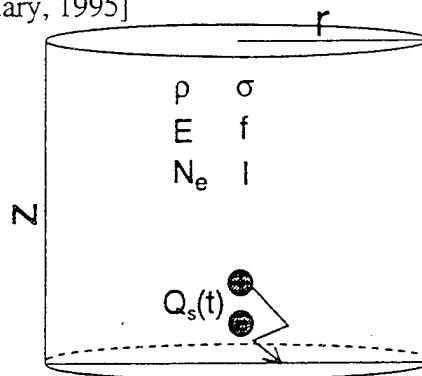


Theoretical predictions for photometric measurements from different vantage points from [Inan, Sampson, Taranenko, in review at GRL, 1995]



# 2-D Quasi-Electrostatic Model 2-D QE Model

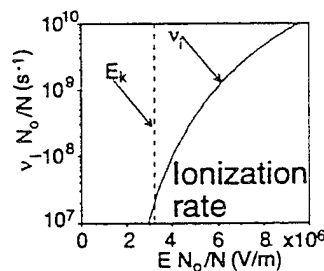
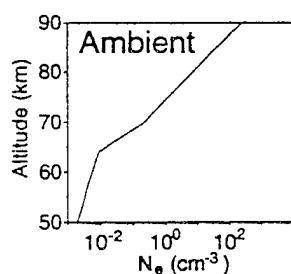
[Pasko et al., GRL, February, 1995]



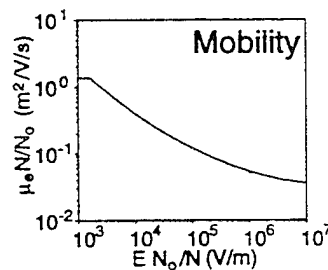
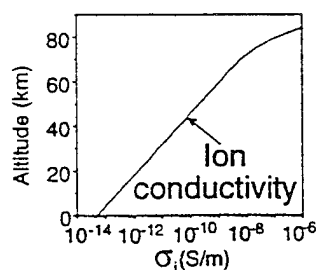
1 Charge density  $\rho$  :  $\frac{\partial \rho}{\partial t} + \frac{\sigma}{\epsilon_0} \rho + \nabla \cdot \vec{E} = 0$

2 Electric field  $E$  :  $\nabla \cdot \vec{E} = (\rho + \rho_s)/\epsilon_0$

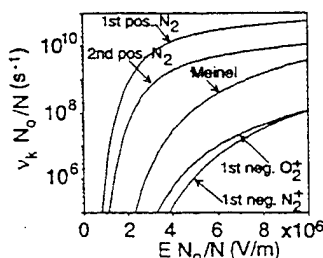
3 Electron number density  $N_e$  :  $\frac{dN_e}{dt} = \nu_i N_e - \alpha N_e^2$



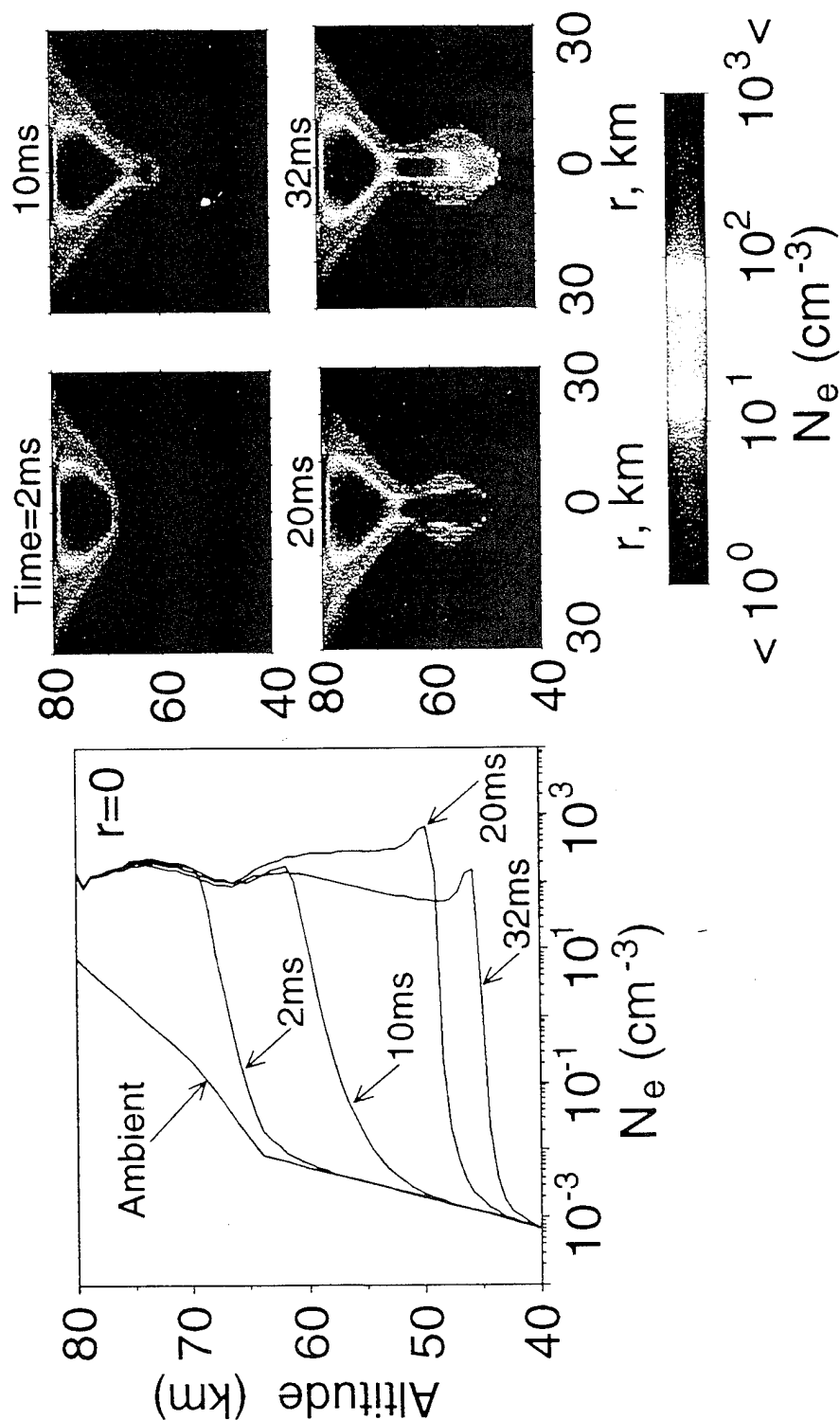
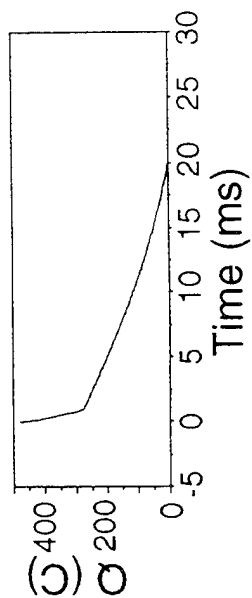
4 Conductivity  $\sigma$  :  $\sigma = \sigma_i + \sigma_e$  ;  $\sigma_e = \mu_e N_e e$



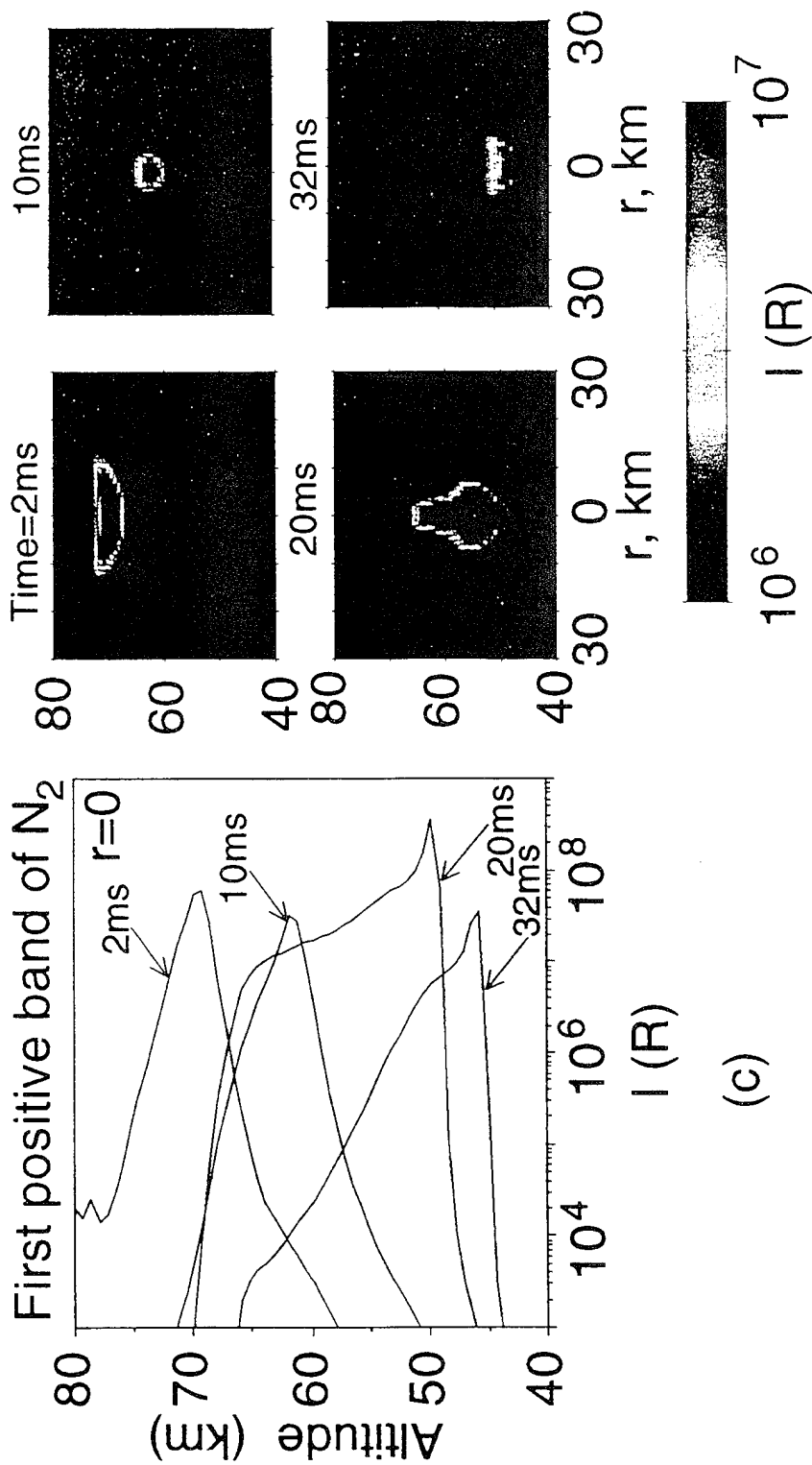
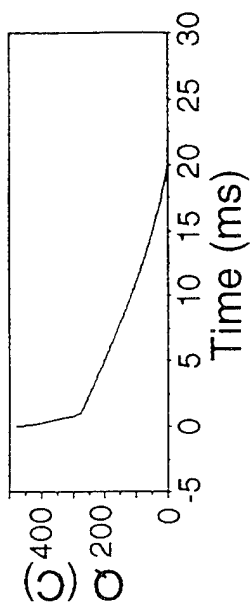
5 Optical emissions:





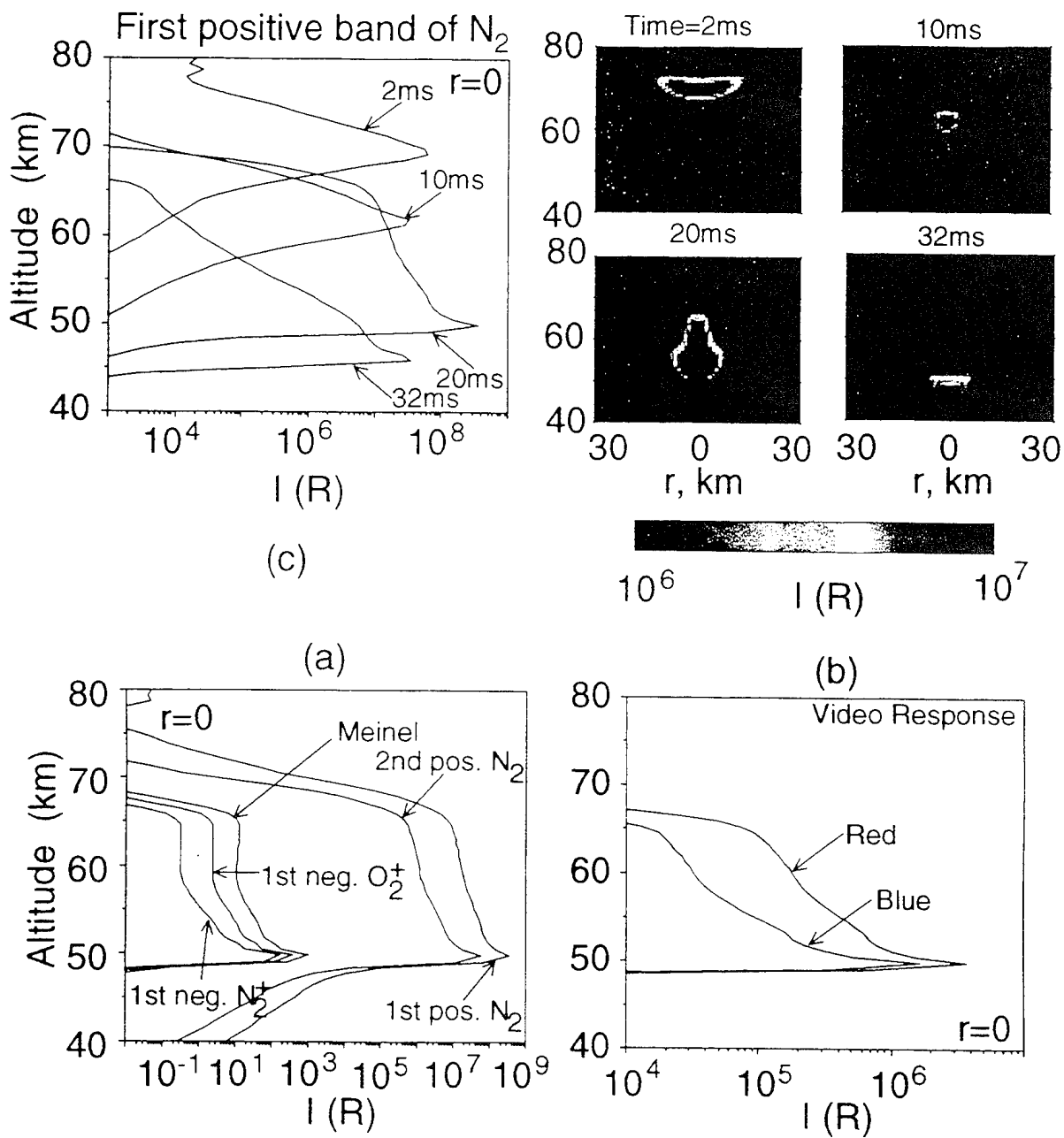


Predictions of a new paper on the formation of ionization columns and carrot-like structures [Pasko et al., 1995, in review at GRL]

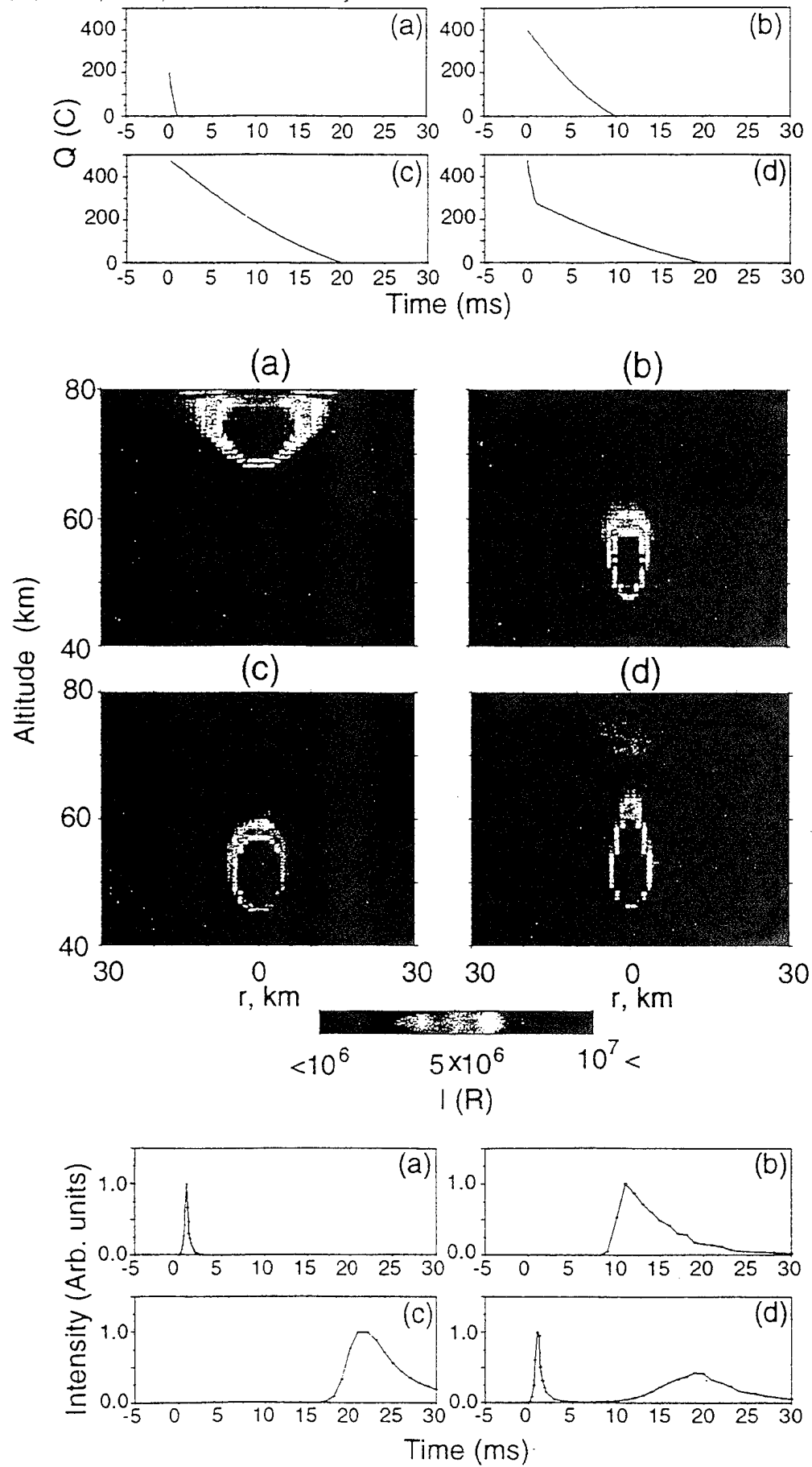


Predictions of a new paper on the formation of ionization columns and carrot-like structures [Pasko et al., 1995, in review at GRL]

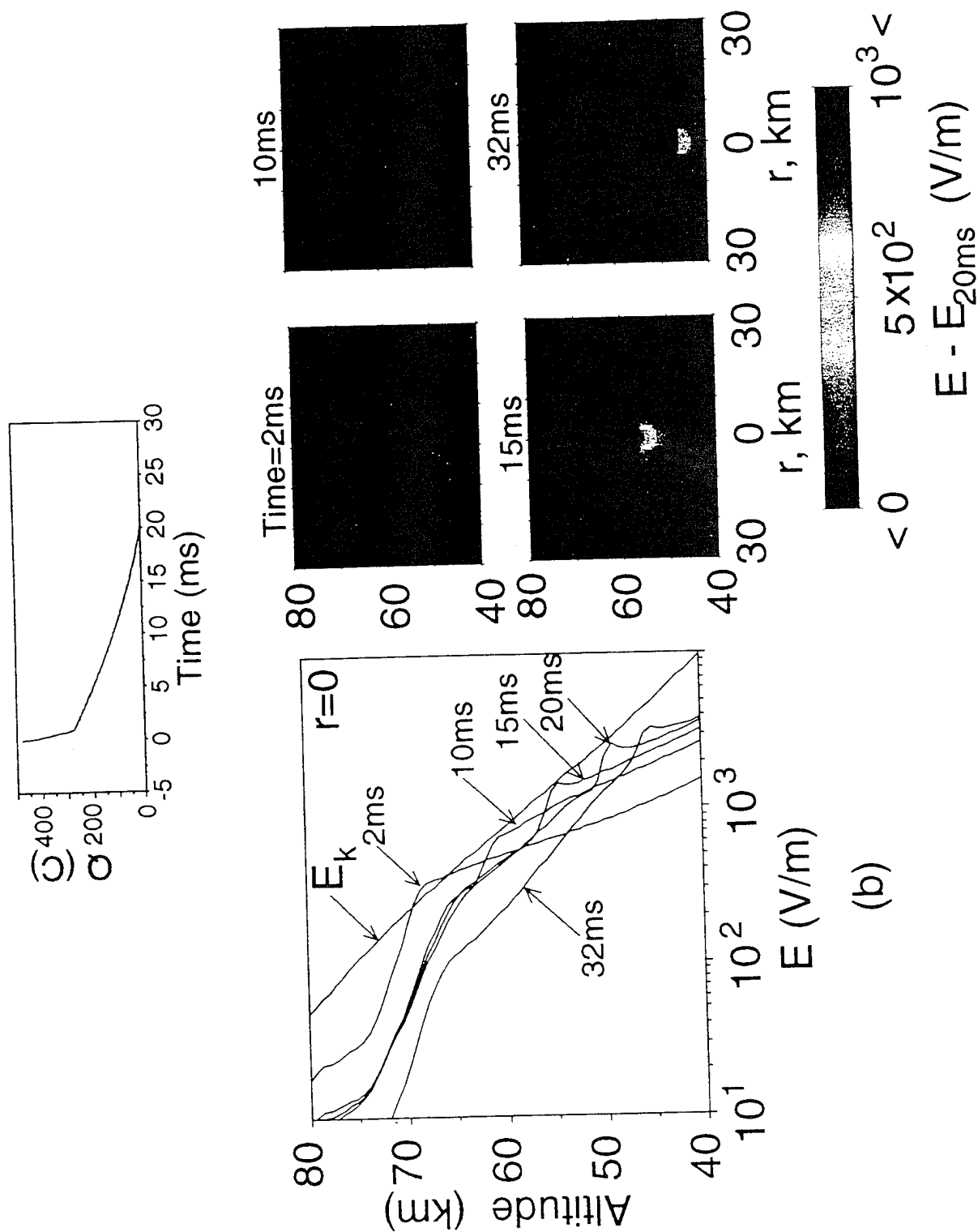
Predictions of a new paper on the formation of ionization columns and carrot-like structures [Pasko et al., 1995, in review at GRL]



Dependence of the sprite structure and "delay" on the rate of removal of charge  
from [Pasko et al., 1995, in review at GRL]

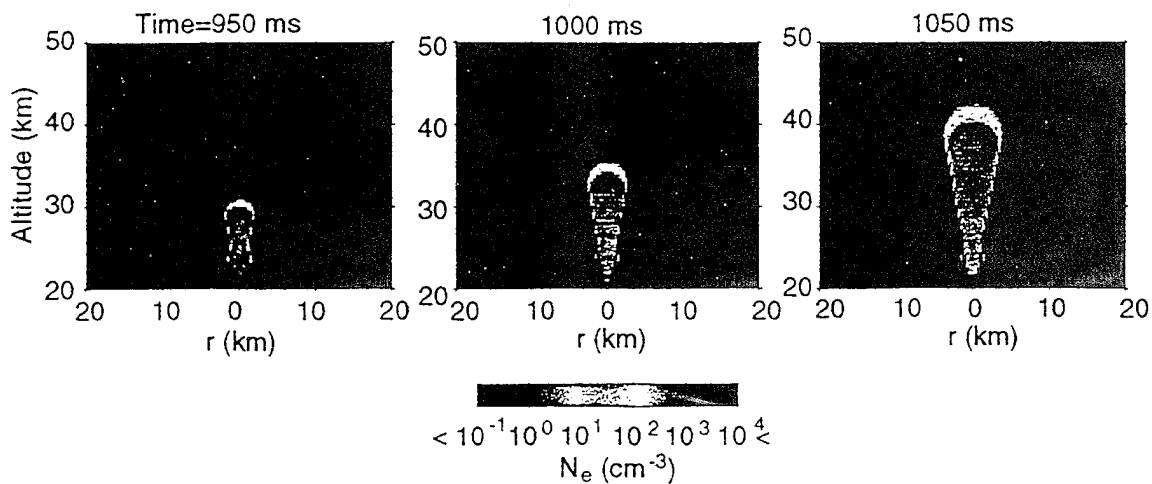


Predictions of a new paper on the formation of ionization columns and carrot-like structures [Pasko et al., 1995, in review at GRL]

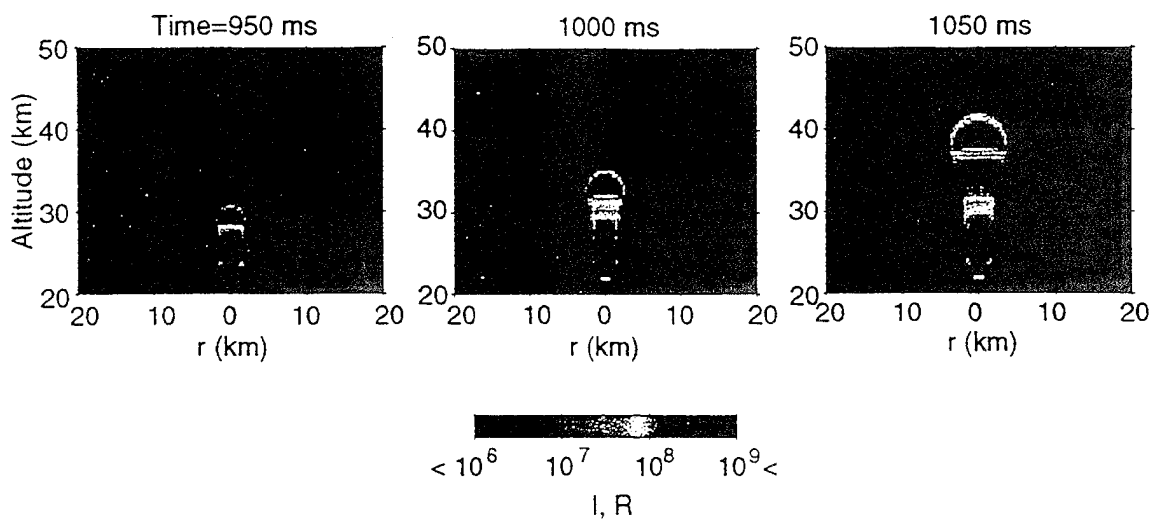


# Blue Jets

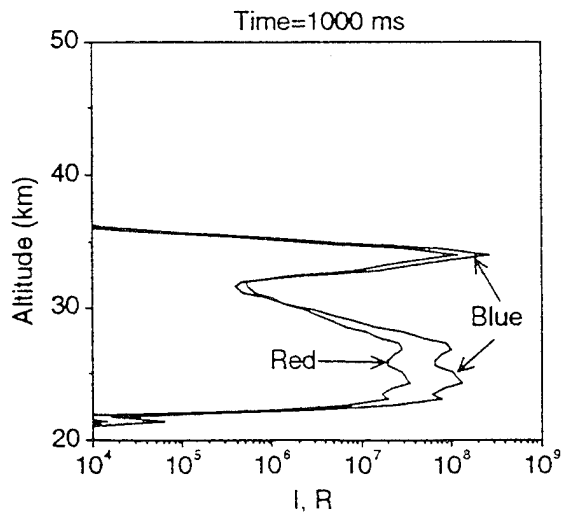
## Electron number density

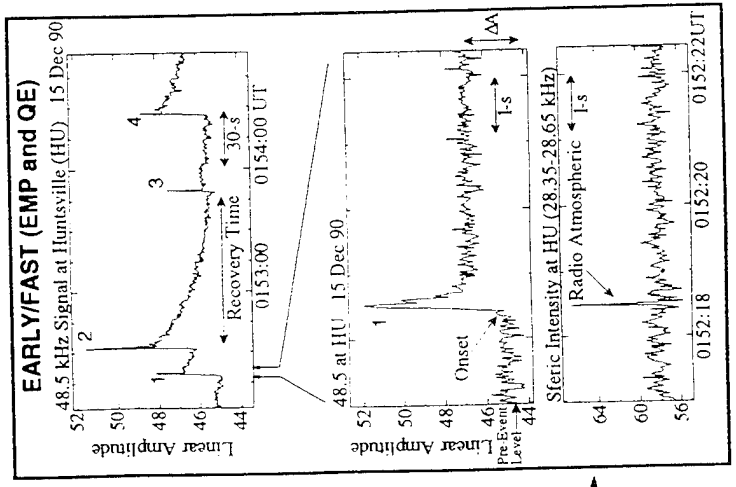
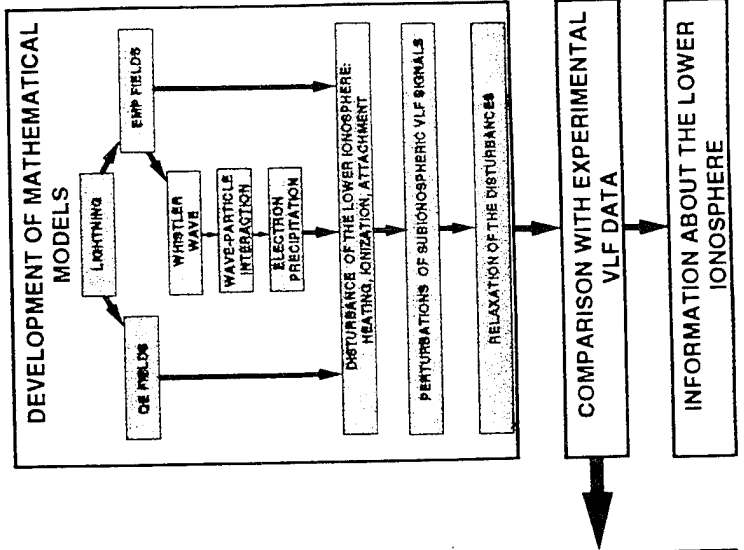
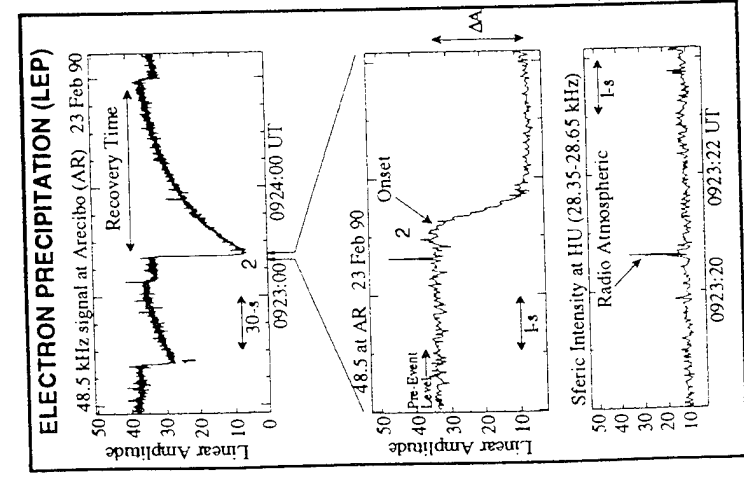
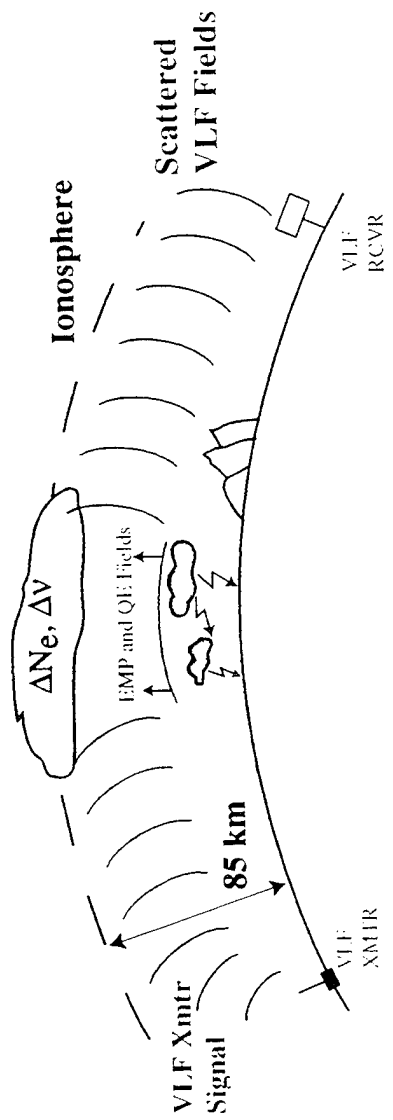
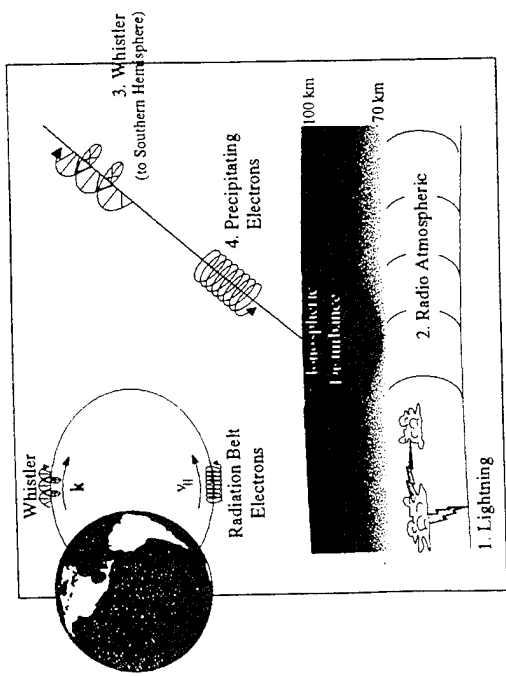


## 2nd positive band of $N_2$



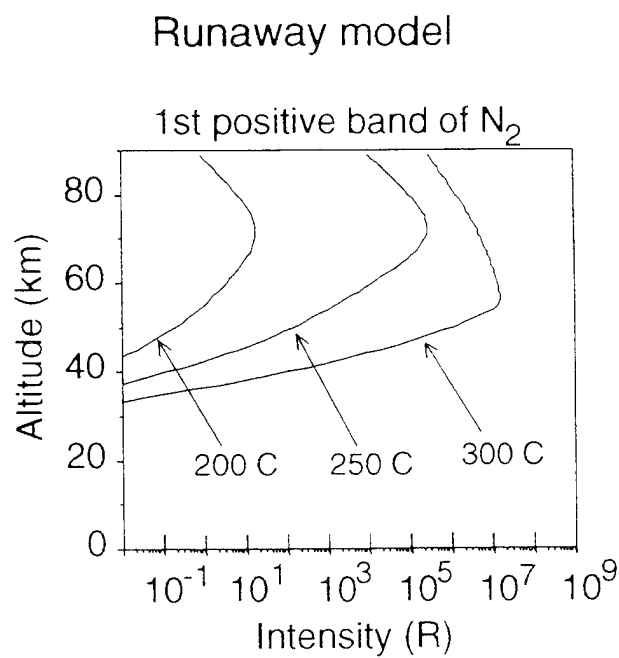
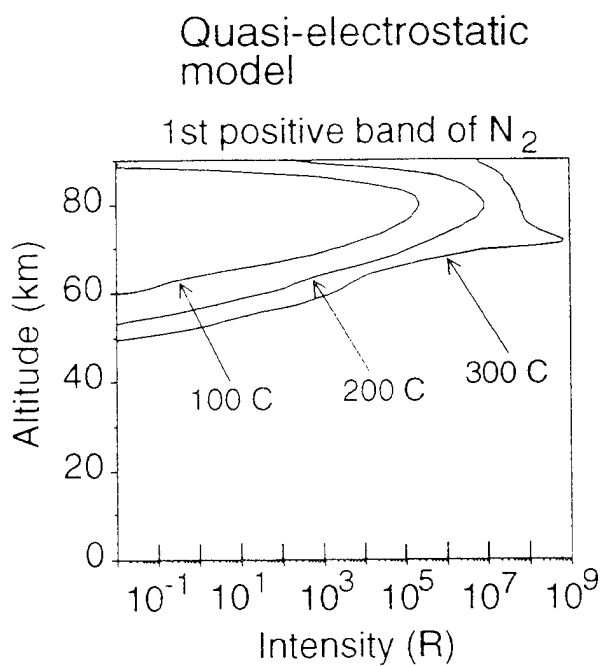
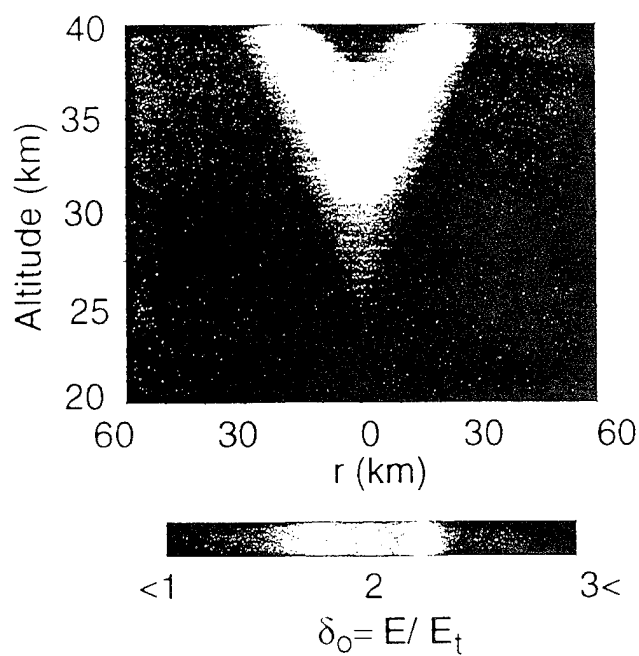
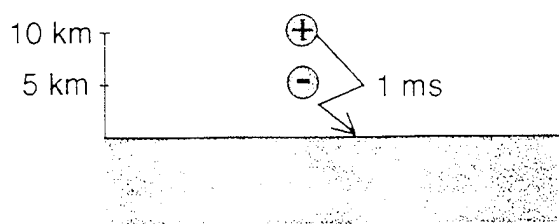
## Video response





VLF remote sensing of transient ionospheric disturbances from [Inan, Bell, Pasko, Sentman, Wescott, Lyons, in review at GRL, 1995]

Essentials of the runaway breakdown model [Bell et al., GRL, August, 1995]





VLF remote sensing of transient ionospheric disturbances  
from [Inan, Bell, Pasko, Sentman, Wescott, Lyons, in review at GRL, 1995]

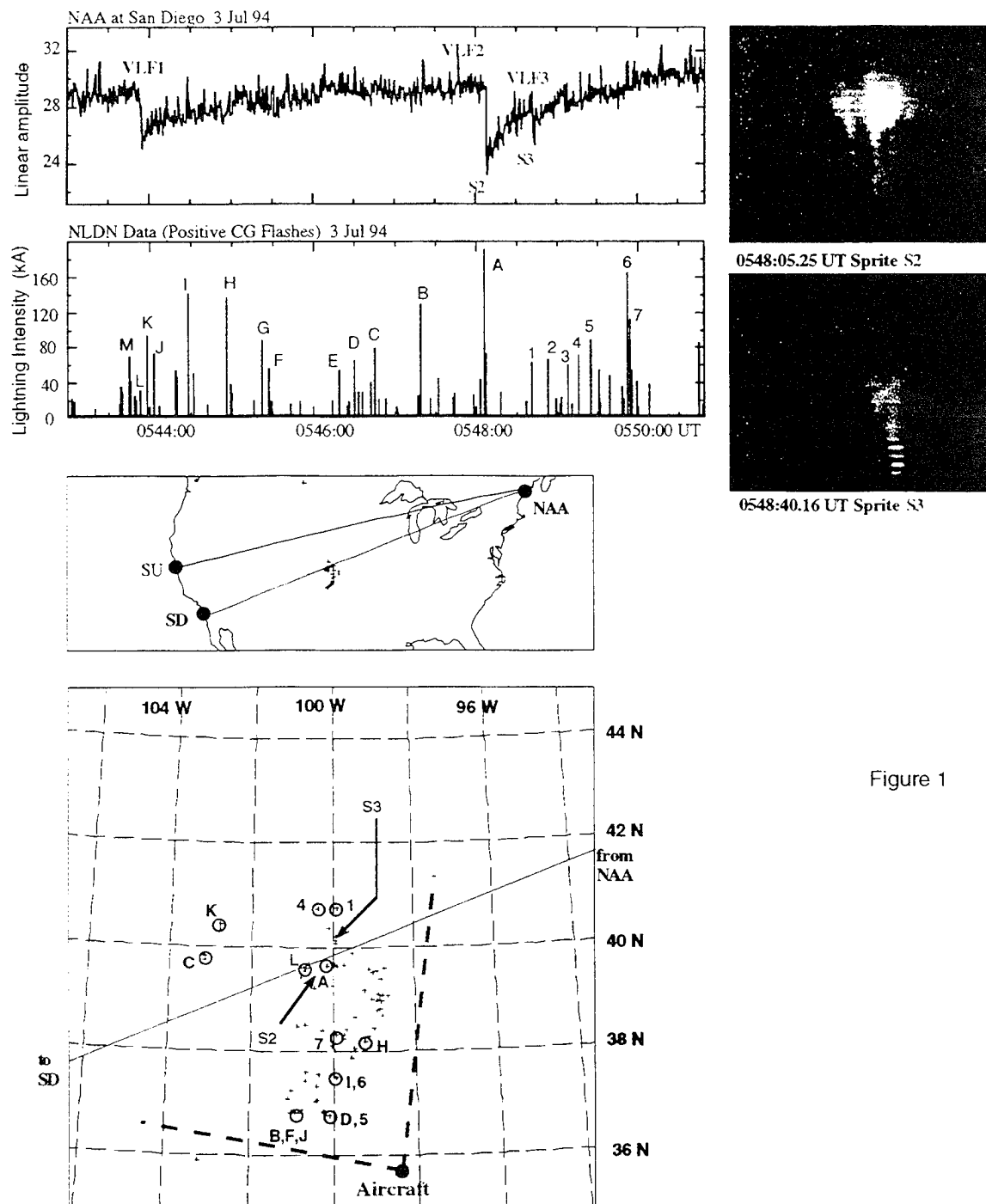


Figure 1

VLF remote sensing of transient ionospheric disturbances  
 from [Inan, Bell, Pasko, Sentman, Wescott, Lyons, in review at GRL, 1995]

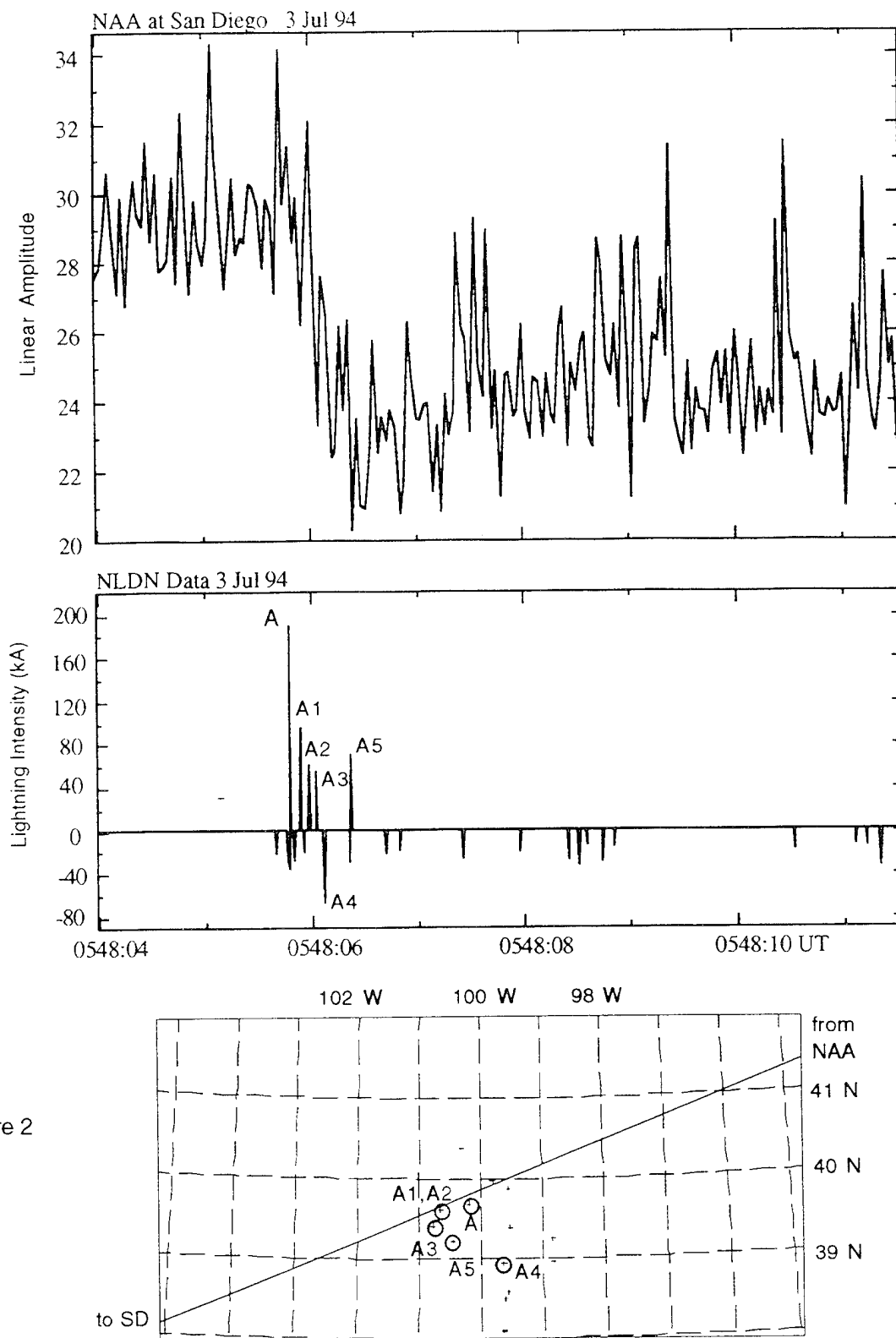
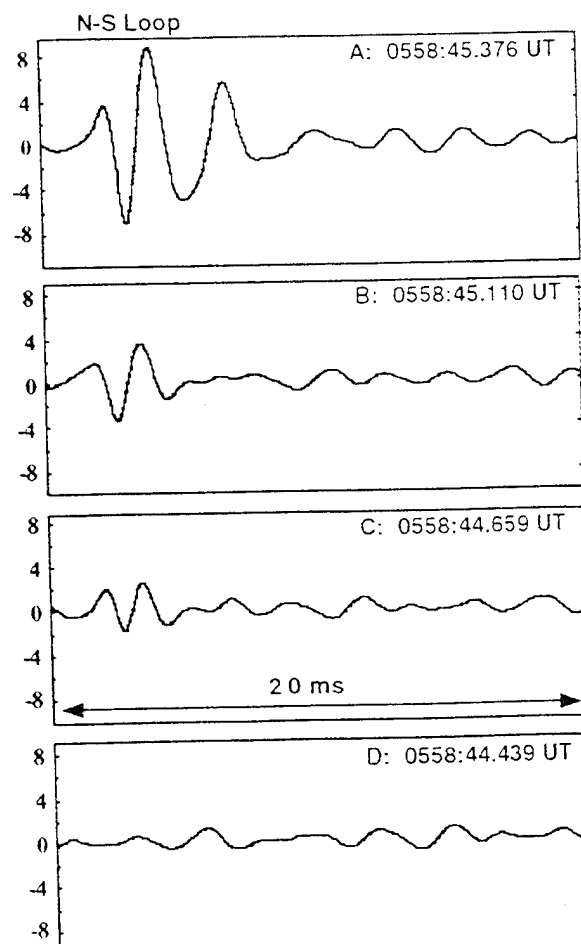
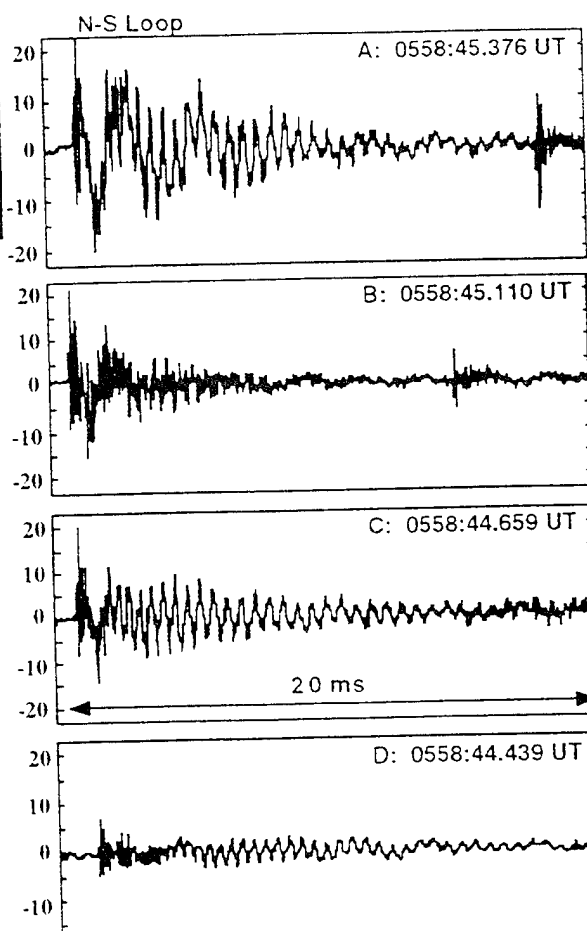
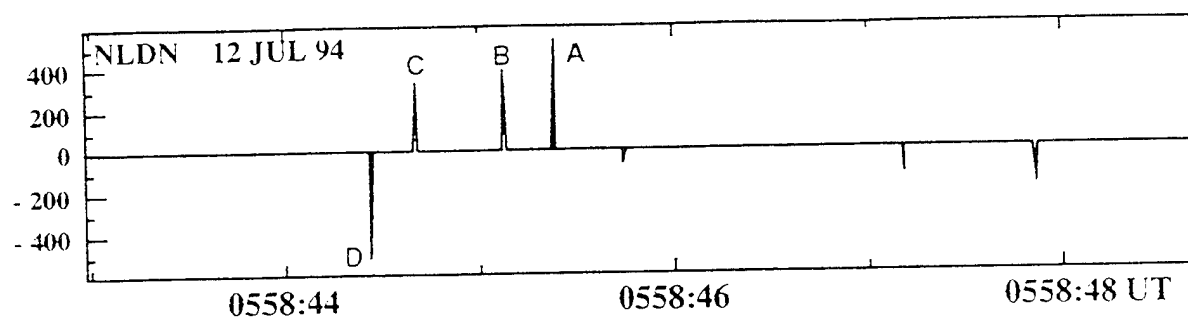
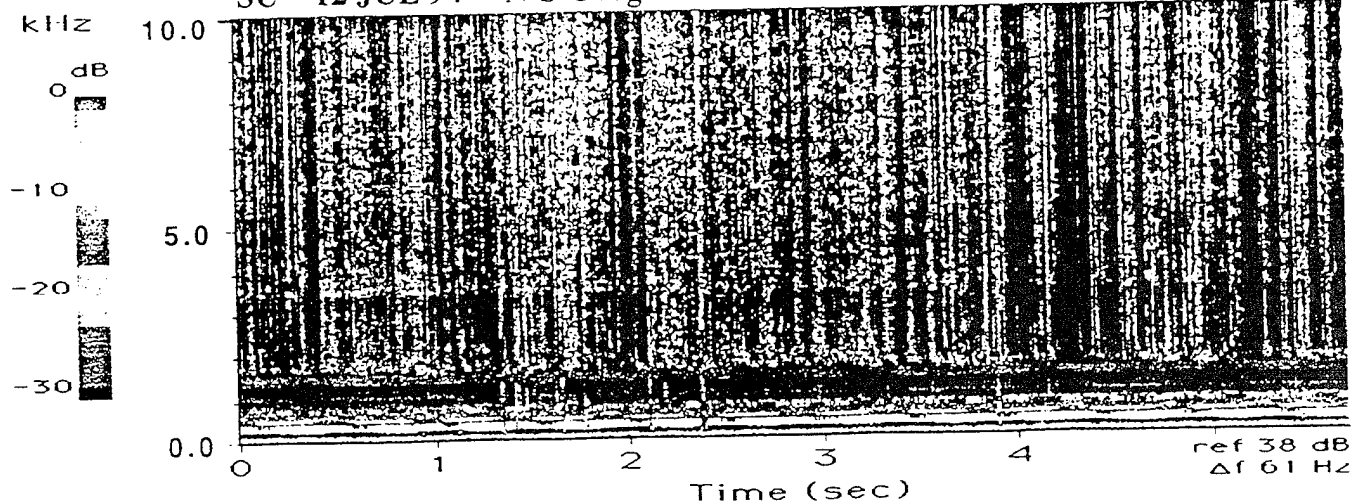


Figure 2

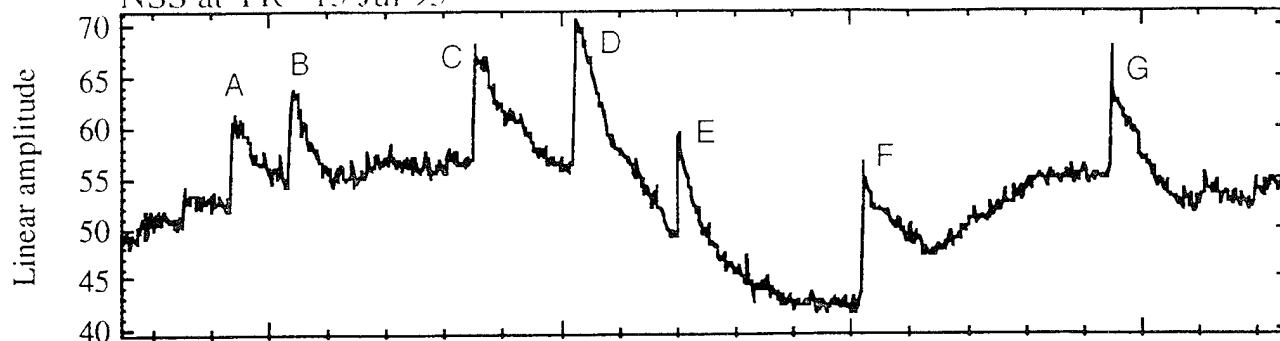
SU 12 JUL 94 N-S Geog.

0558:43 UT

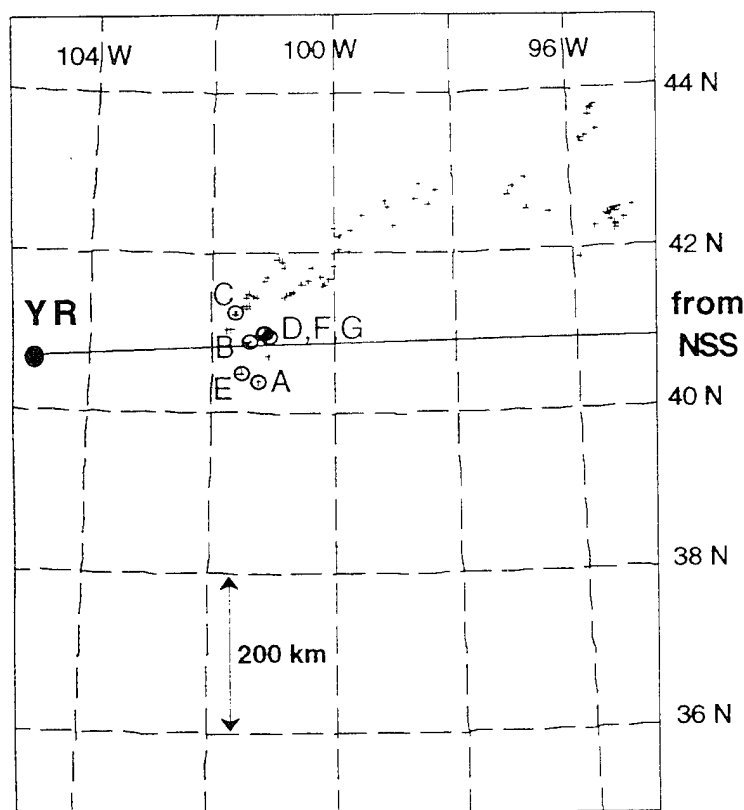
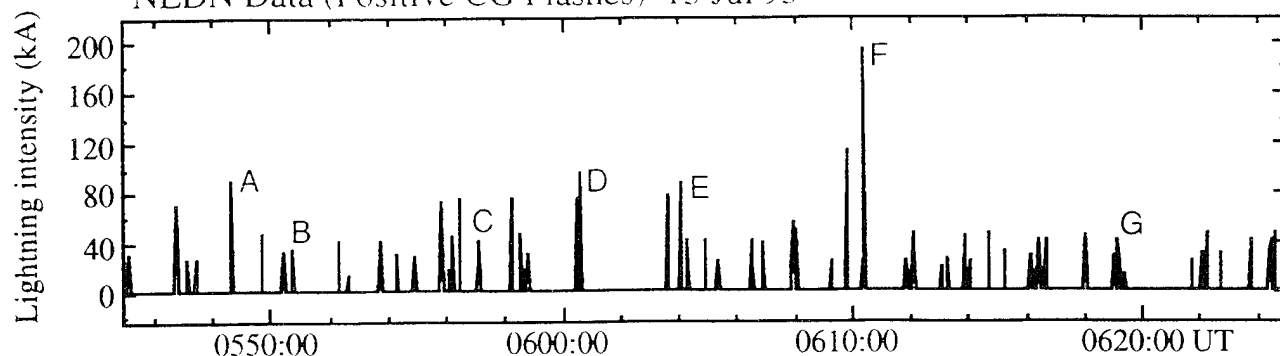


A spectacular example of association of VLF events and sprites  
from [Inan, Reising, Lyons, to be presented at Fall AGU, 1995]

NSS at YR 15 Jul 95

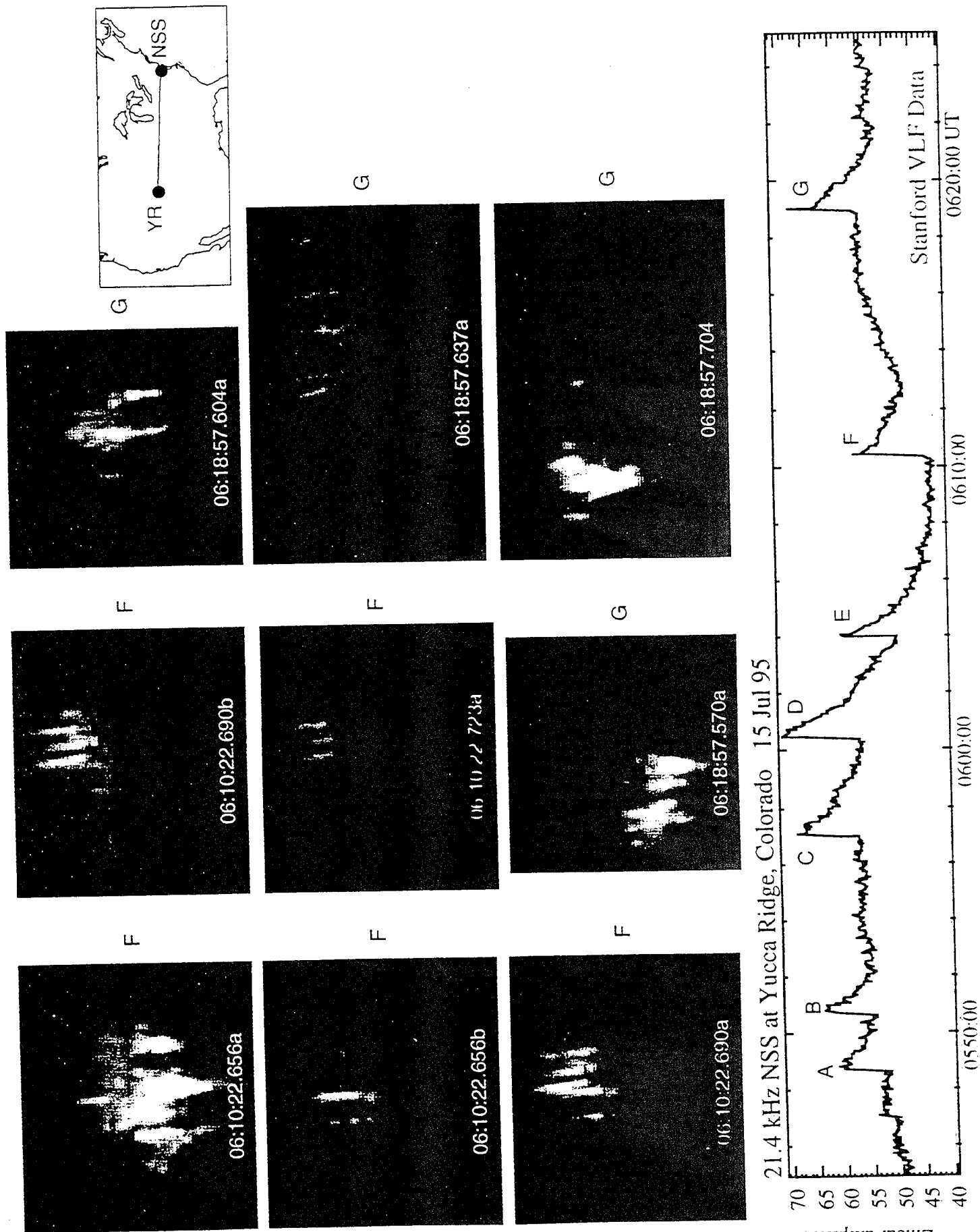


NLDN Data (Positive CG Flashes) 15 Jul 95

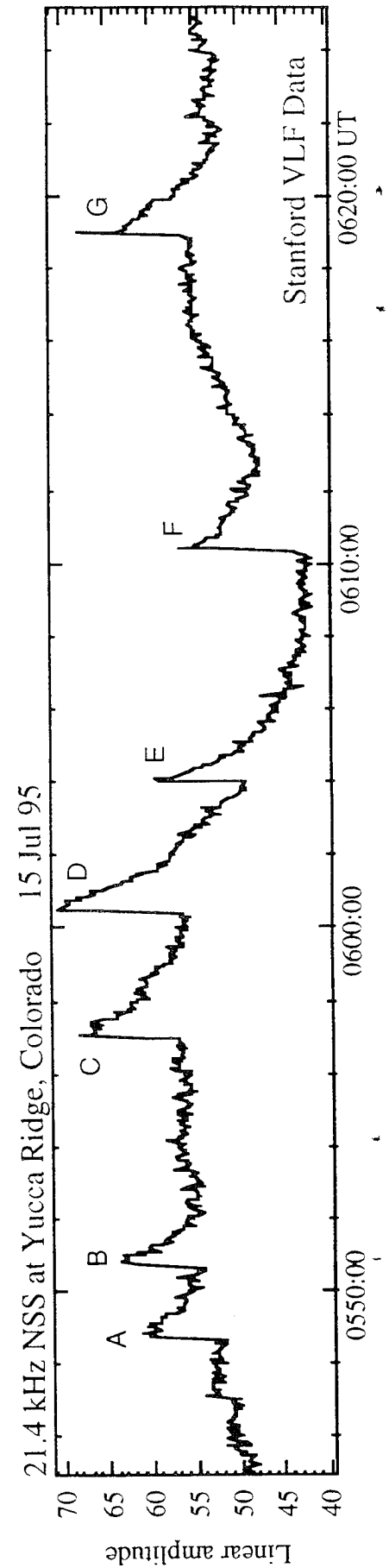
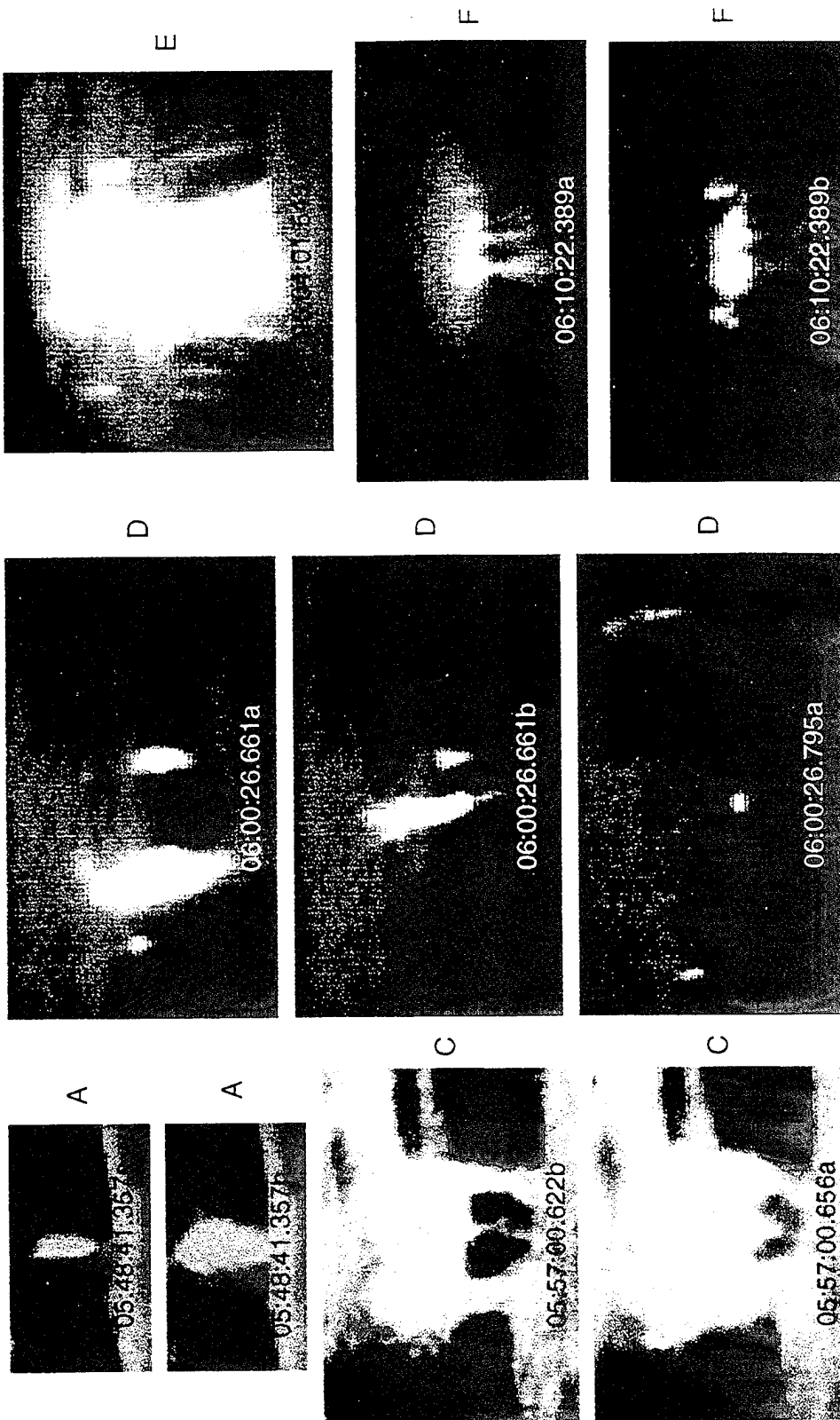


At least 6 of the 7 VLF perturbation events shown in the top panel were accompanied by well-defined, bright Sprites, as confirmed by optical ground measurements by the W. Lyons group. This figure shows the detailed association of VLF events observed on the NSS-YR signal with CG lightning discharges. The top panel shows the amplitude of the NSS (21.4 kHz) signal observed at Yucca Ridge showing seven large (> 1dB) amplitude perturbations. The positive CG flashes from this storm are shown in the middle panel. The CG flashes associated with the seven VLF events are denoted on the NLDN data, and the locations are shown on the map below.

A spectacular example of association of VLF events and sprites from [Inan, Reising, Lyons, to be presented at Fall AGU, 1995]

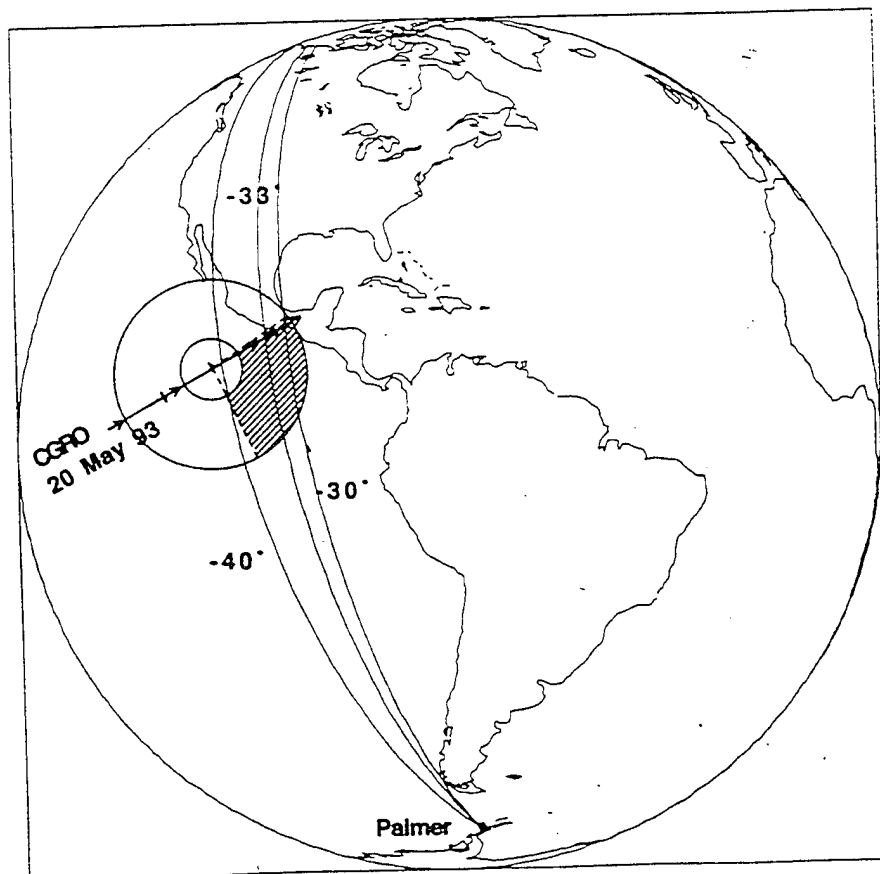
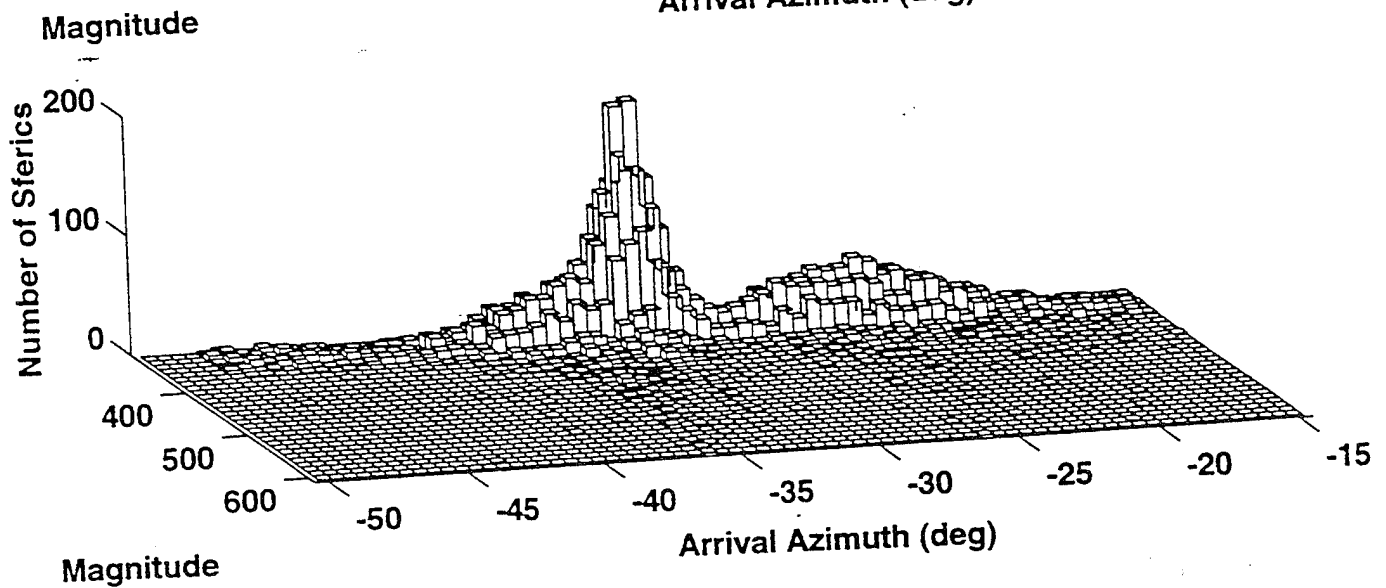
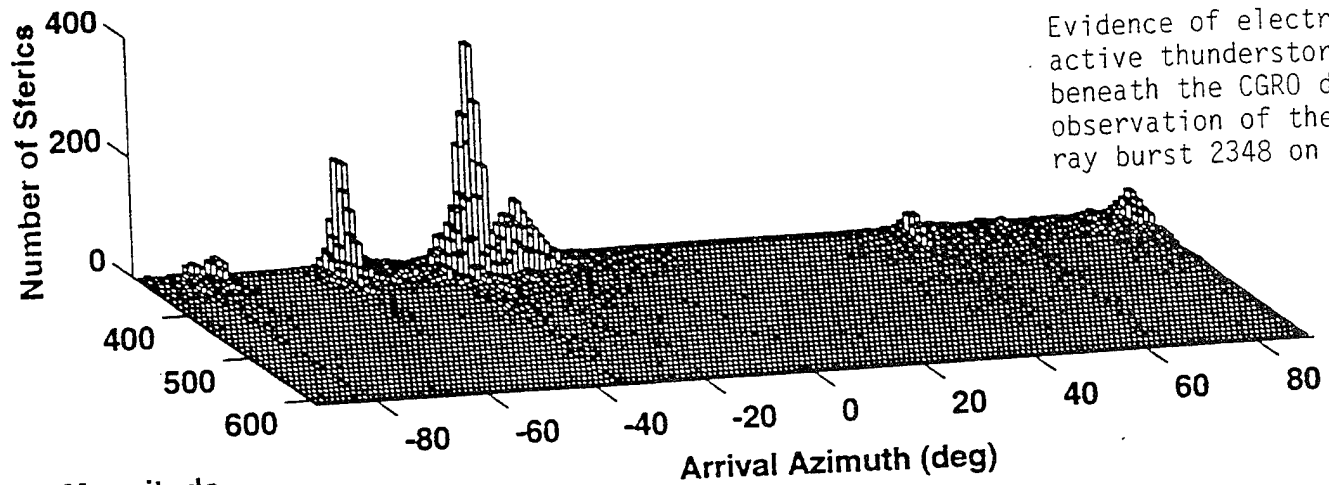


A spectacular example of association of VLF events and sprites from [Inan, Reising, Lyons, to be presented at Fall AGU, 1995]



# Sferic Histogram for PA, 20 May 93 0150-0220 UT, v. 3.2

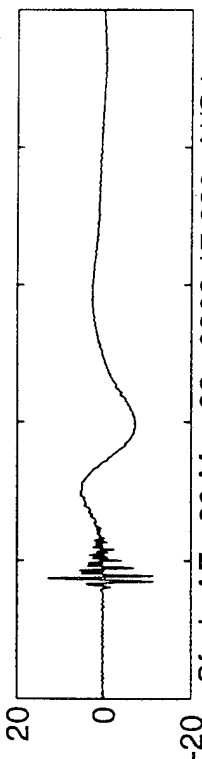
Evidence of electrically active thunderstorm beneath the CGRO during the observation of the gamma ray burst 2348 on 5/20/93.



The "smoking-gun" evidence of terrestrial gamma ray burst-lightning-sprite connection

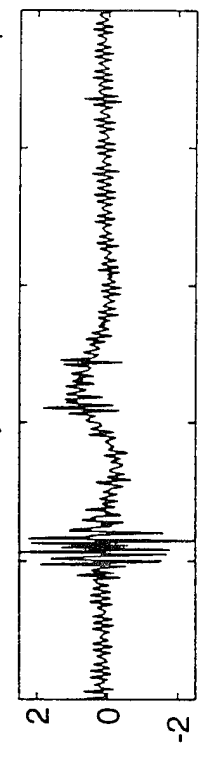
"Slow-tail" feature of these sferics as observed at PALMER STATION, ANTARCTICA indicates long enduring continuing currents

Sferic A1: 20 May 93, 0202:17.824, N/S loop



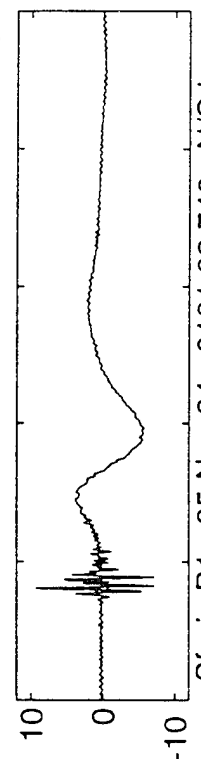
Large +ve flash with "slow-tail" from the storm under CGRO

Sferic AE: 20 May 93, 0202:17.680, N/S loop

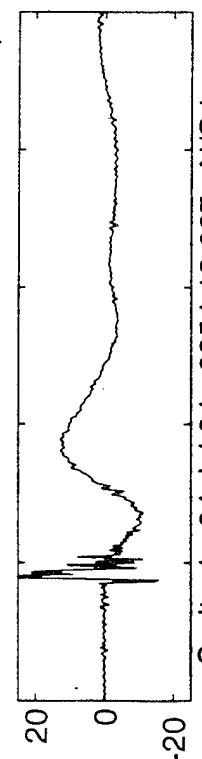


Sferic observed at Palmer within 1ms of the CGRO gamma ray burst

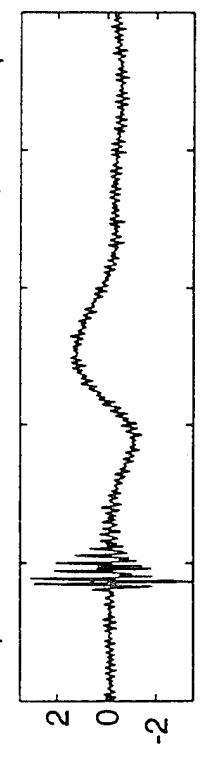
Sferic A3: 20 May 93, 0201:05.366, N/S loop



Sferic B1: 05 Nov 94, 0101:02.746, N/S loop

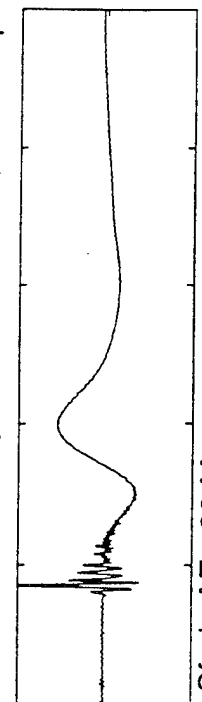


Sprite 1: 04 Jul 94, 0354:12.637, N/S loop

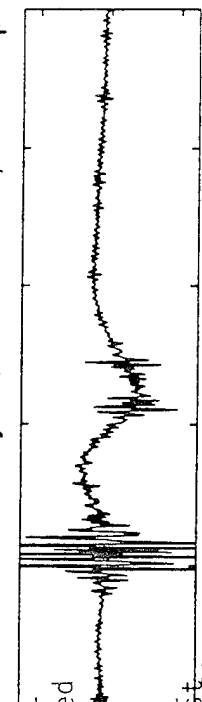


SPRITE producing lightning

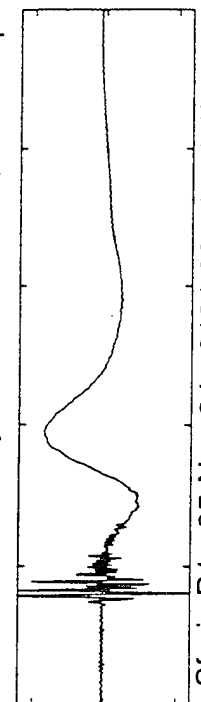
Sferic A1: 20 May 93, 0202:17.824, E/W loop



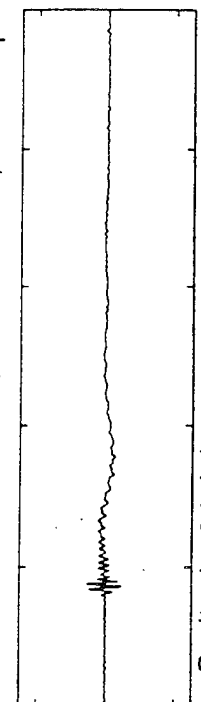
Sferic AE: 20 May 93, 0202:17.680, E/W loop



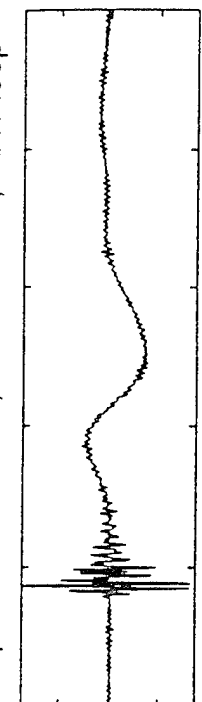
Sferic A3: 20 May 93, 0201:05.366, E/W loop



Sferic B1: 05 Nov 94, 0101:02.746, N/S loop



Sprite 1: 04 Jul 94, 0354:12.637, E/W loop



Time (msec)

Time (msec)



**AFOSR/PL WORKSHOP ON  
SPRITES AND BLUE JETS  
18-19 October 1995**

---

**RF Measurements of Lightning-induced  
Ionospheric Effects**

**K. M. Groves, J. V. Rodriguez, P. J. Erickson<sup>1</sup>  
J. M. Quinn, T. Arce<sup>2</sup> and M. Cox<sup>1</sup>**

**Ionospheric Effects Division, Phillips Laboratory  
Hanscom AFB, MA 01731**

**<sup>1</sup>MIT Haystack Observatory, Westford MA 01886**

**<sup>2</sup>Eng. and Theory Ctr, Cornell Univ., Ithaca NY 14853**

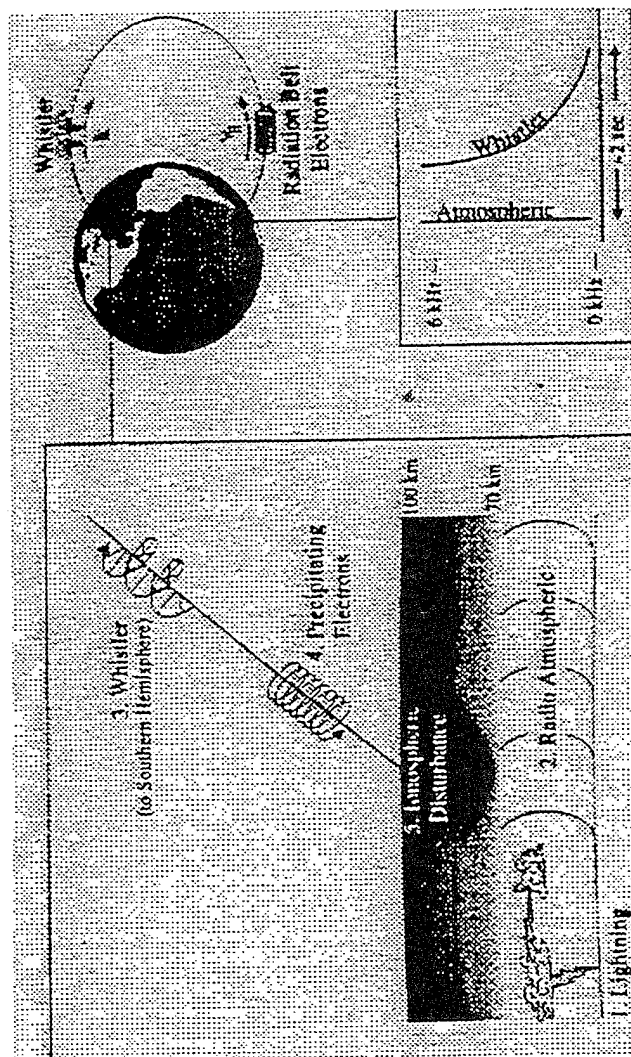
# Outline

---

- **Background Motivation**
  - Recent Developments in Atmospheric Electricity (“Direct” interactions; Sprites, etc.)
- **Measurement Techniques**
  - Multi-Diagnostics Observations
    - UHF Incoherent Scatter Radar
    - VLF Receiver, VHF Radar, Others
- **Preliminary Results**
- **Summary**

# Conventional Understanding of Lightning-Ionosphere Interaction

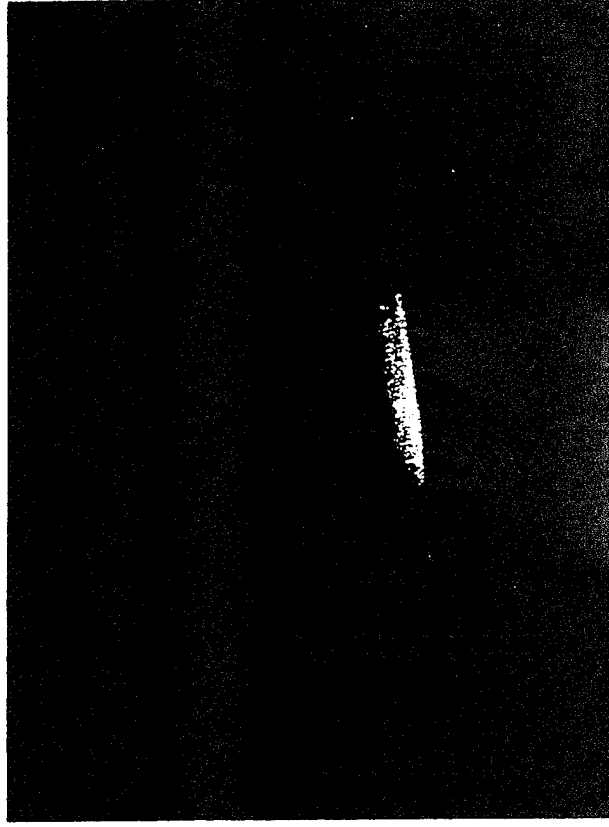
## VLF Wave Generation, Whistler Wave Propagation, Subsequent Interaction and Electron Precipitation



# Recent Evidence of “Direct” Interactions

---

- Upward Discharges (Sprites, Blue Jets)
- D-Region VLF Signatures: Heating, Ionization
- F-Region Wave Turbulence (Heating, E-fields, Irreg.)
- Excited Optical Emissions
- Link to Large Scale Structuring (e.g. Spread F)



[Sentman et al., 1995]

# Potential Lightning-Induced “Direct” Ionospheric Effects

| Effect           | Estimated           |           | Region Affected | Diagnostic(s)   |
|------------------|---------------------|-----------|-----------------|-----------------|
|                  | Magnitude           | Duration  |                 |                 |
| Heating          | 10s-100s K          | 1-1000 ms | D, E, F         | VLF, Radar      |
| Ionization       | $10^2$ - $10^4$ /cc | > 10 sec  | D               | VLF, Radar      |
| Plasma Waves     | 10s mV/m            | 1-10 ms   | E, F            | Radar           |
| Optical Emission | 10-50 kR            | 1-5 ms    | D               | low-light video |
| Irreg. Formation | ???                 | >100 sec  | F               | Scintillation   |
| Spread F         | ???                 | >100 sec  | F               | Digisonde       |
| Accel. Part.     | > 10 eV             | 1-1000 ms | D, E, F         | DMSP            |

# **Lightning-induced Ionospheric Effects (TRUTH95) Diagnostics**

---

- **Millstone Hill 440 MHz Incoherent Scatter Radar**
  - 2.5 MW Peak Power; 150' Steerable Dish (43 dB gain)
  - *D, E, F* region Plasma Parameters
- **VLF Receiver System**
  - *D* region Perturbations
  - Three Channel Phase/Amplitude; Multiple Simultaneous Paths
- **PL 50 MHz Coherent Backscatter Radar**
  - 50 kW Peak Power; Fixed Yagi Antenna Array (17 dB gain)
- **Additional Diagnostics**
  - Low-light Video; Digisonde; National Lightning Detection Network (NLDN)

\_\_\_\_\_



# TRUTH95

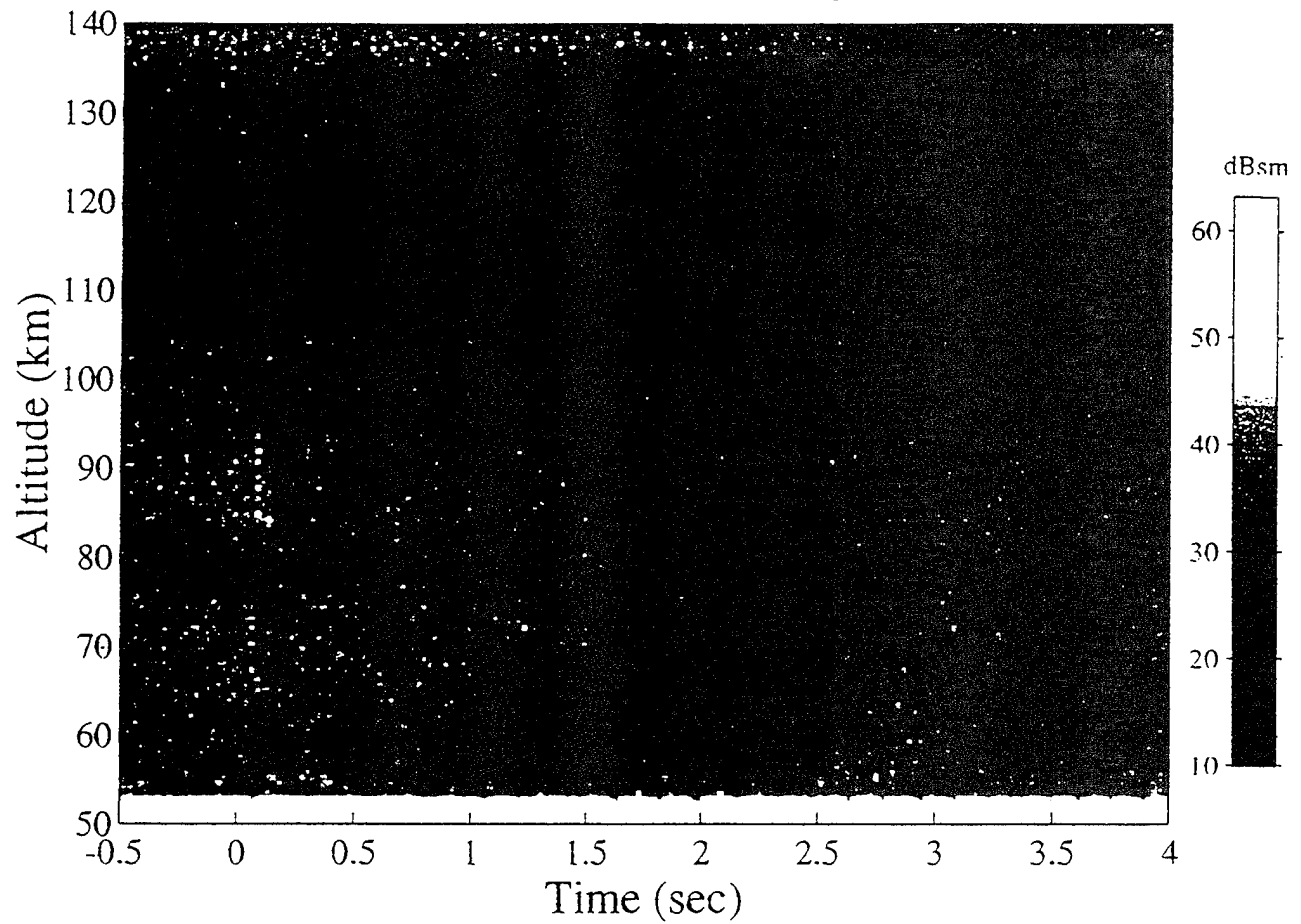
## Preliminary Results

---

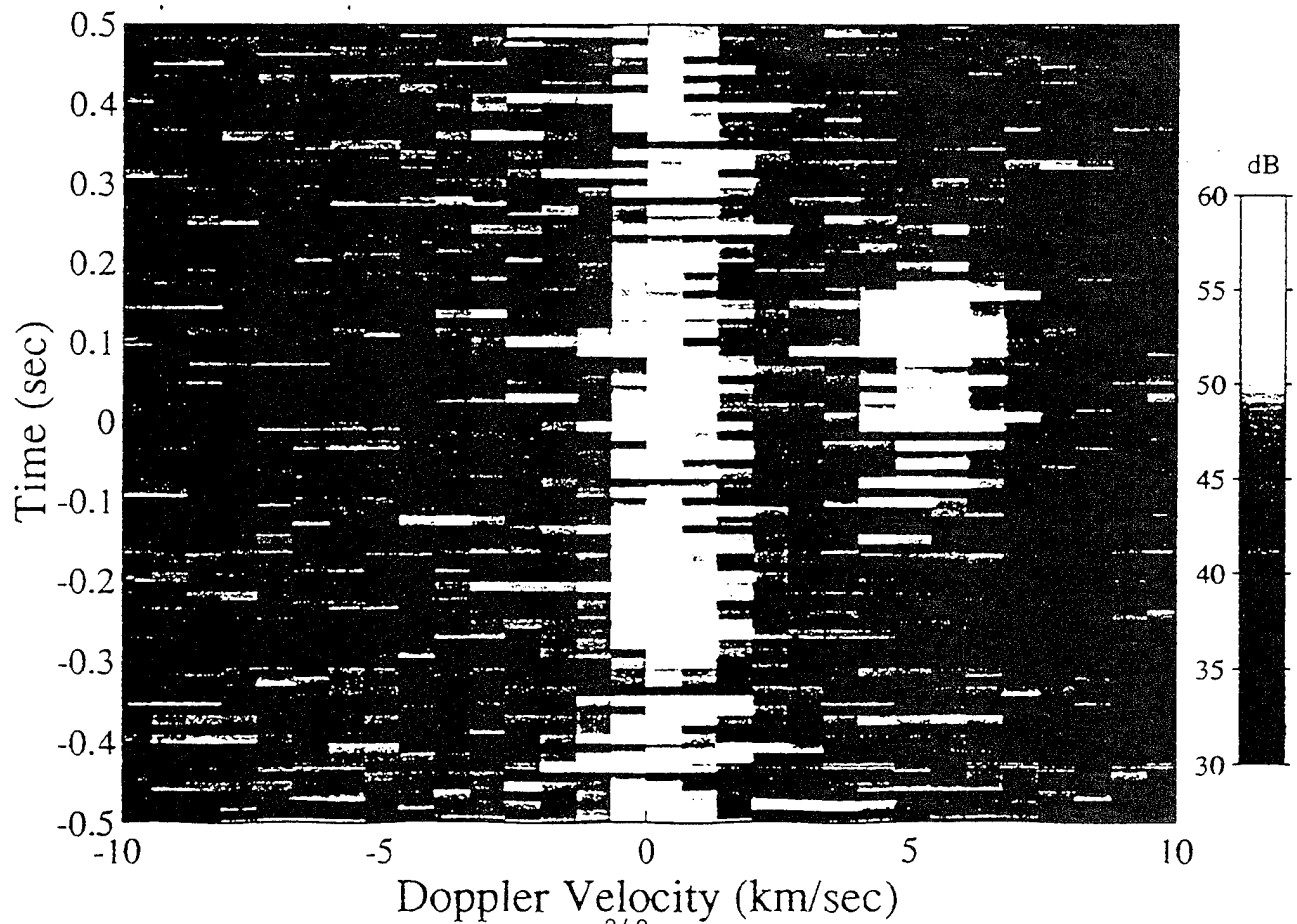
- MHR Data Collected on 8 Days; 3 Days Analyzed
  - 39 Positive CG Events observed with UHF Radar to date
  - Satellites/ambiguous returns
  - Peak currents below nominal Sprites threshold (~50 kA)
- VLF Signatures Confirm Direct Lightning Interactions
- Interference Issues with VHF Radar
  - Effective noise floor increased by ~6dB



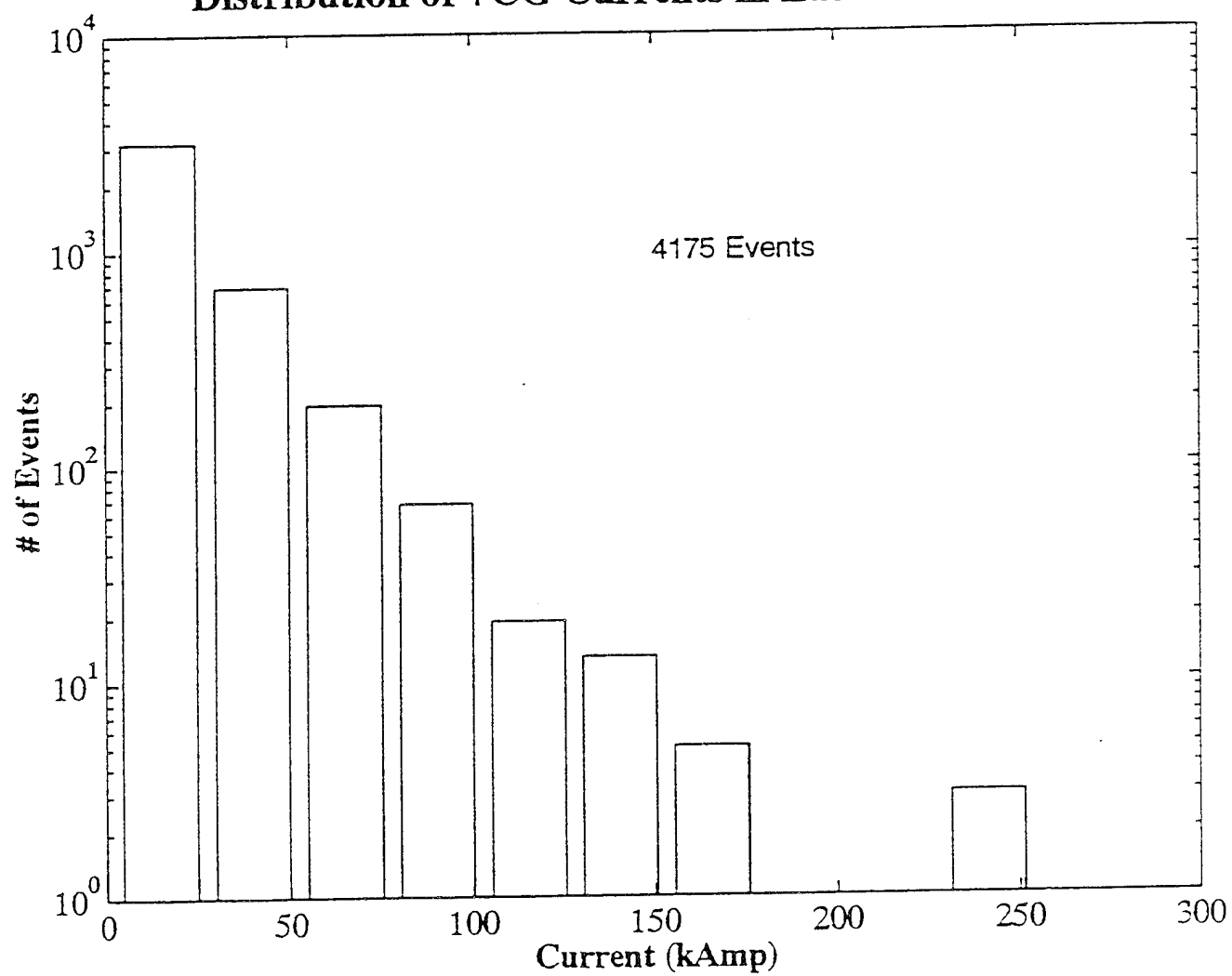
# Millstone UHF 27 July 1995



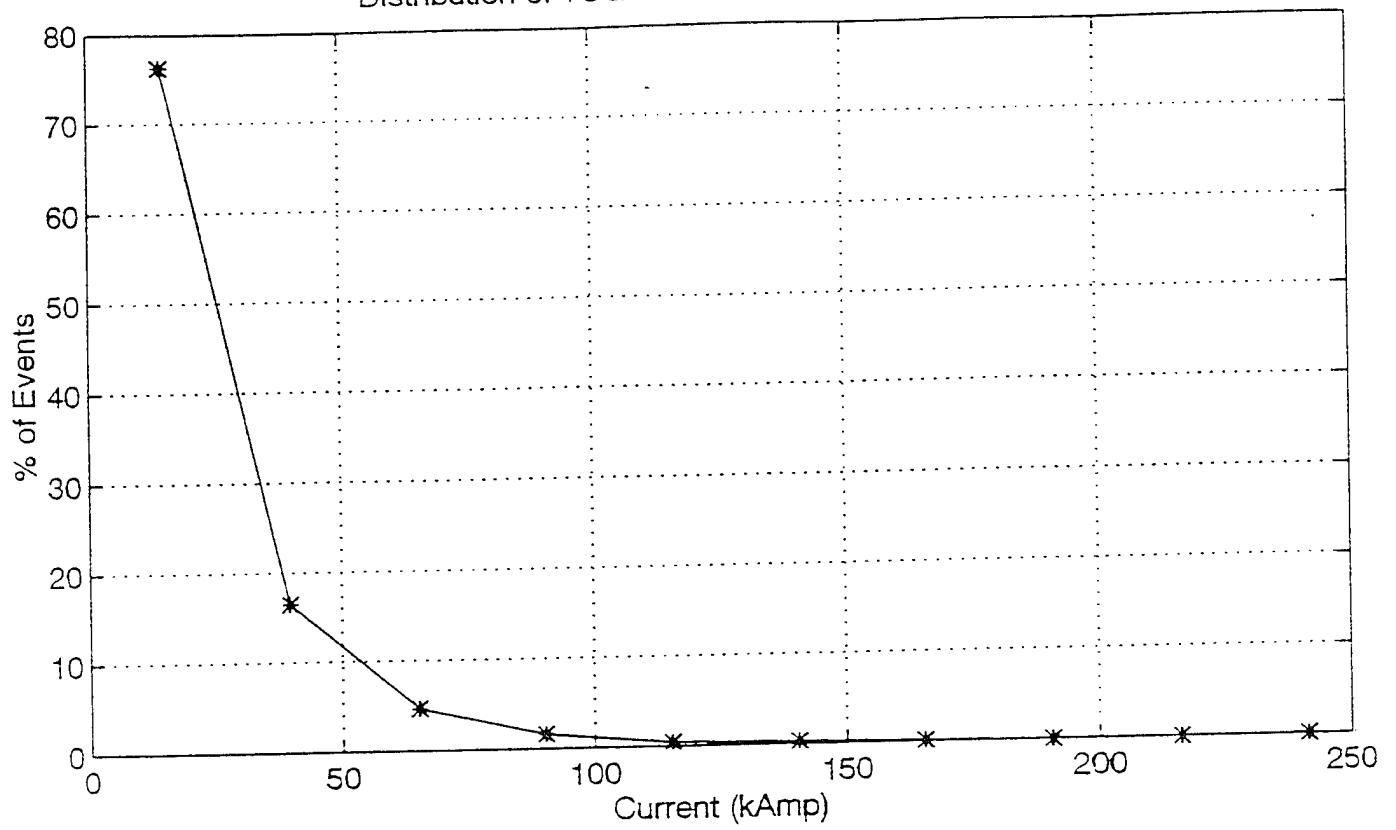
## 27JUL95 MHR UHF 23:16:47.8 UT



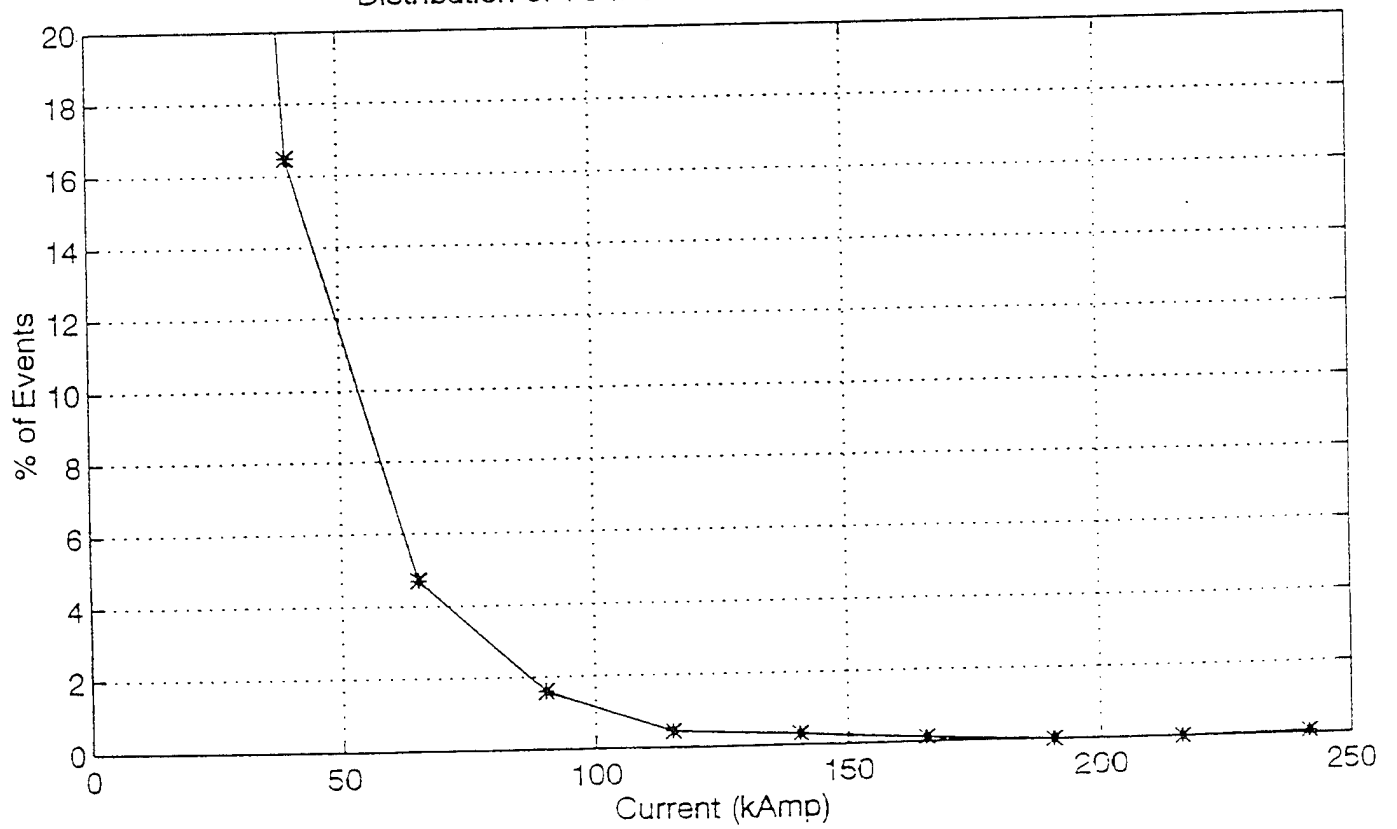
**Distribution of +CG Currents in East Coast Storms**



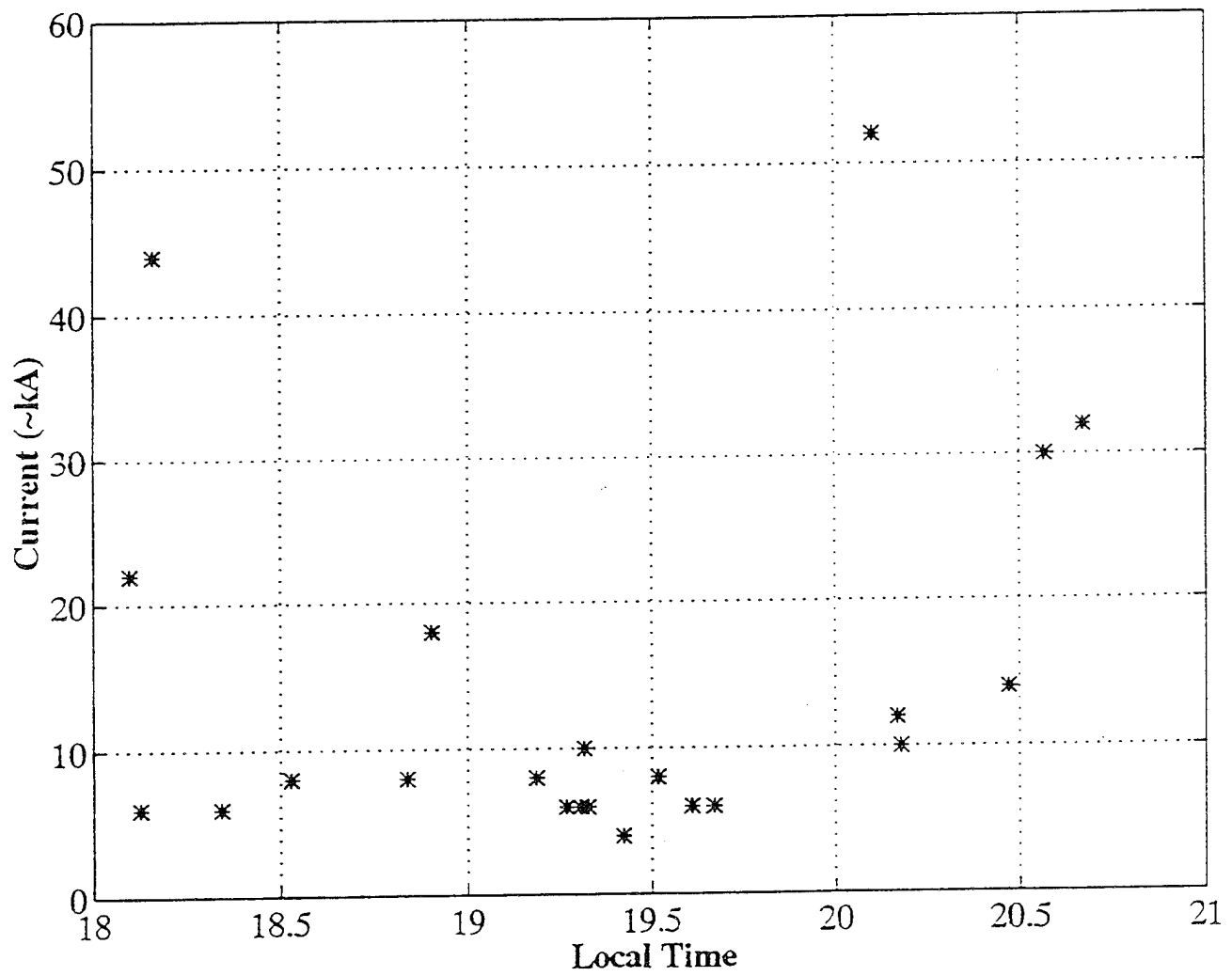
Distribution of +CG Currents in East Coast Storms



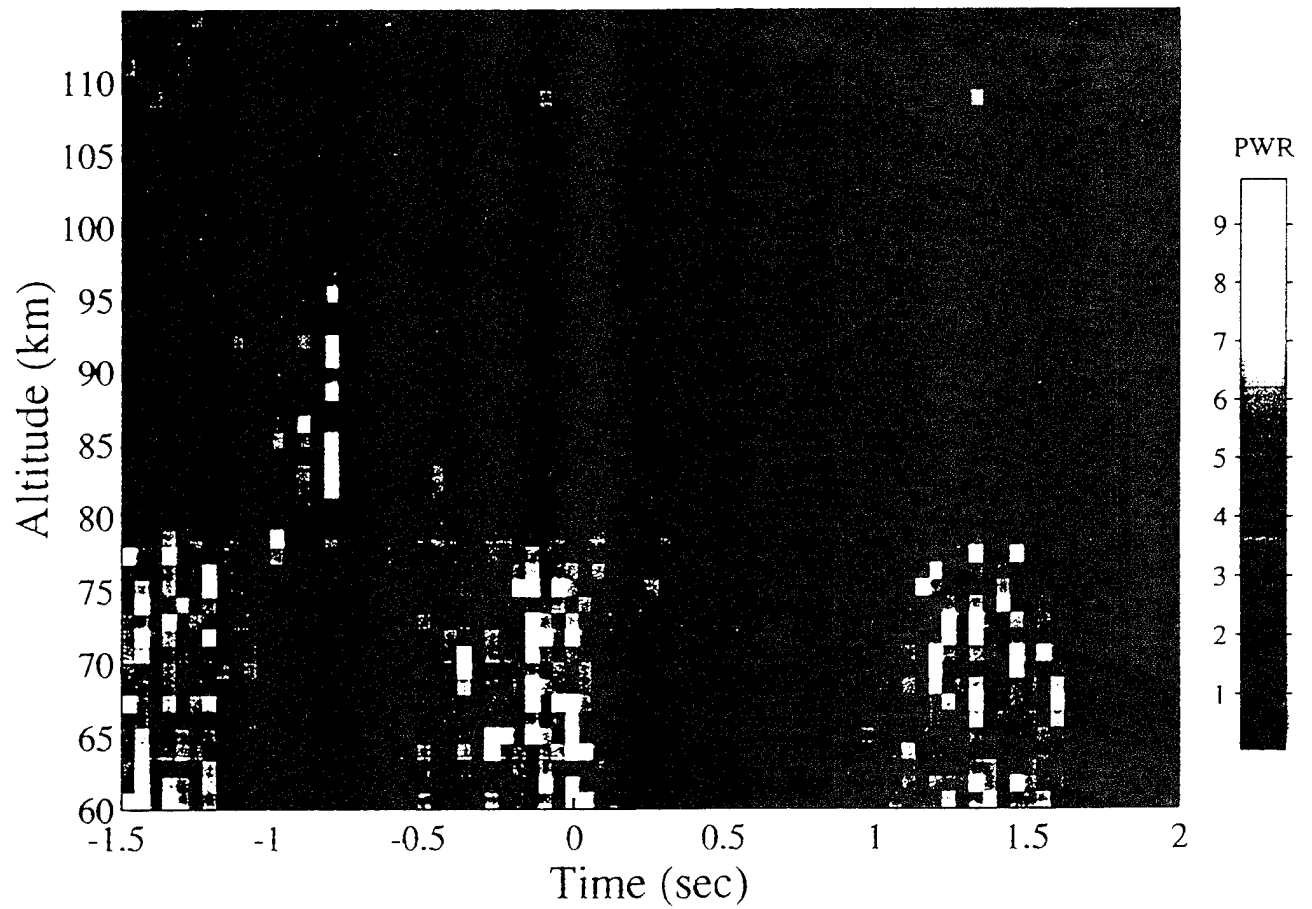
Distribution of +CG Currents in East Coast Storms



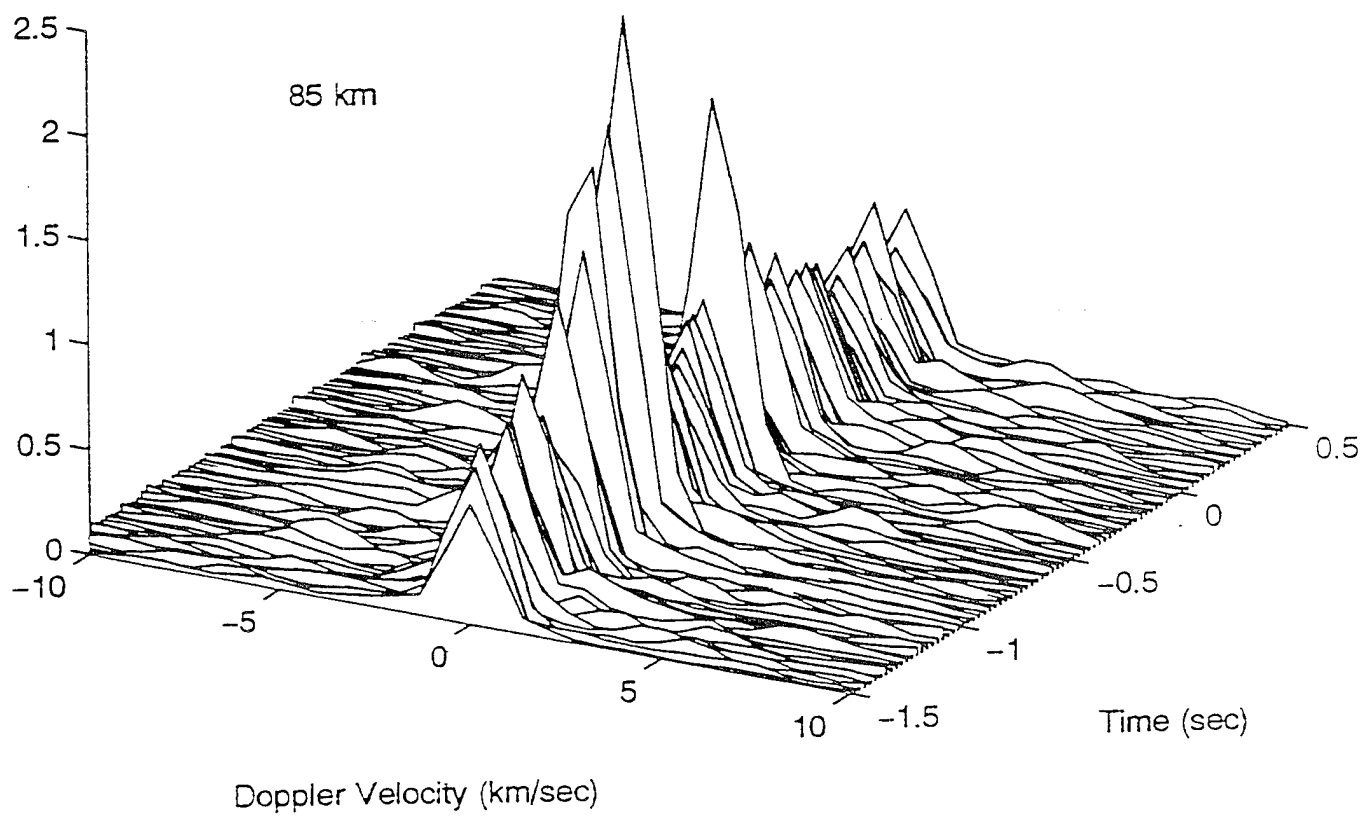
# 11AUG95 +CG in MHR Beam



# 11AUG95 MHR UHF 00:06:09



11AUG95 MHR UHF 00:06:09 UT



# Summary

---

- Preliminary RF Study of Sprites and Associated Phenomena

- UHF observations of weak +CG events ambiguous
- VLF signatures confirmed
- East Coast storms are suitable for investigation

## MORE ANALYSIS AND DATA NEEDED

- Effort Contributes to Expanded Investigation in 1996/97
  - Emphasize “Common Volume” Measurements
  - Systematic *D*, *E*, and *F* Region Observations
  - Bi-Static Measurements Planned
  - Need “Proof of Sprites” Data

# PULSED RADAR INVESTIGATIONS OF RED SPRITES

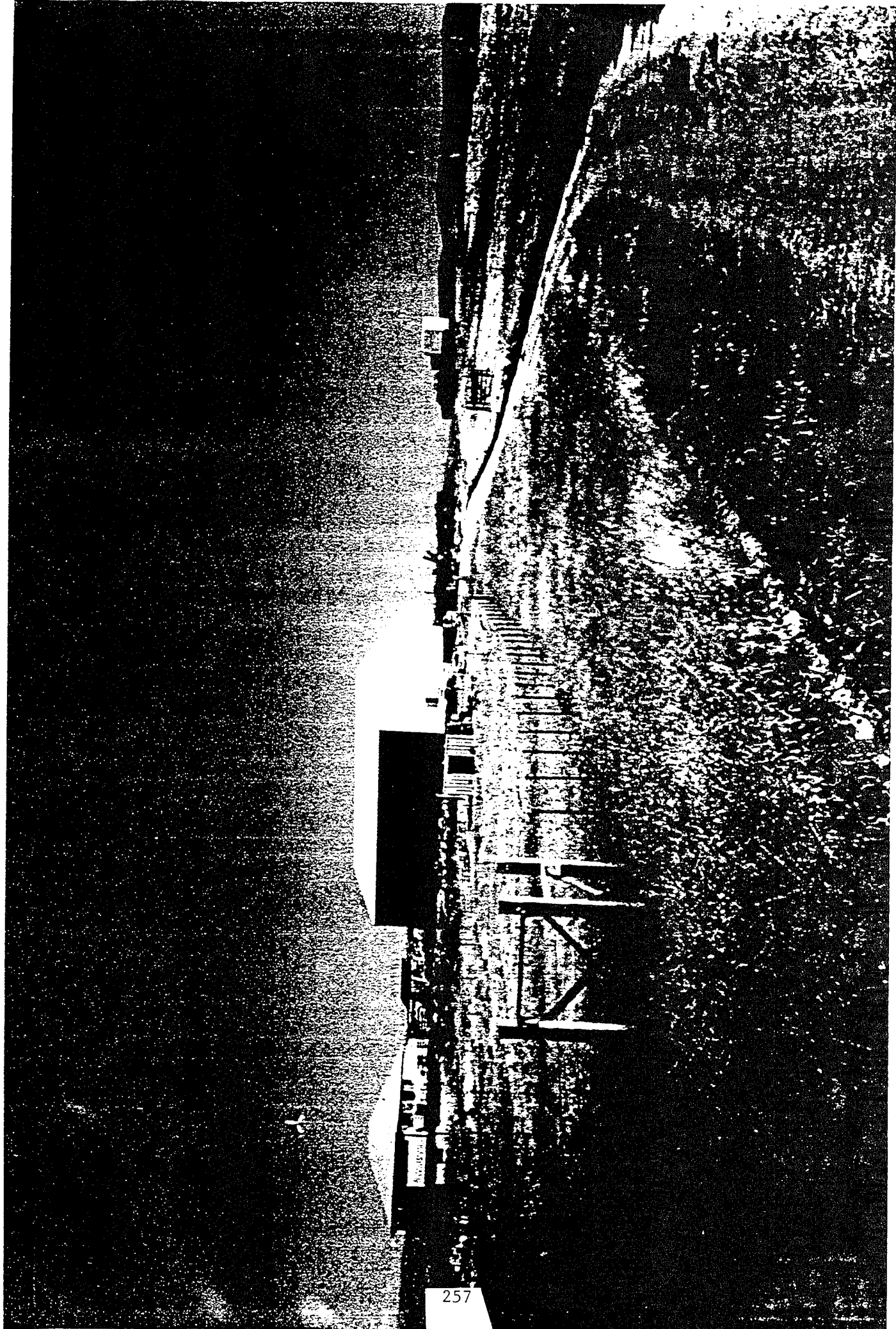
Roland T. Tsunoda  
Geoscience and Engineering Center  
SRI International  
Menlo Park, CA 94025

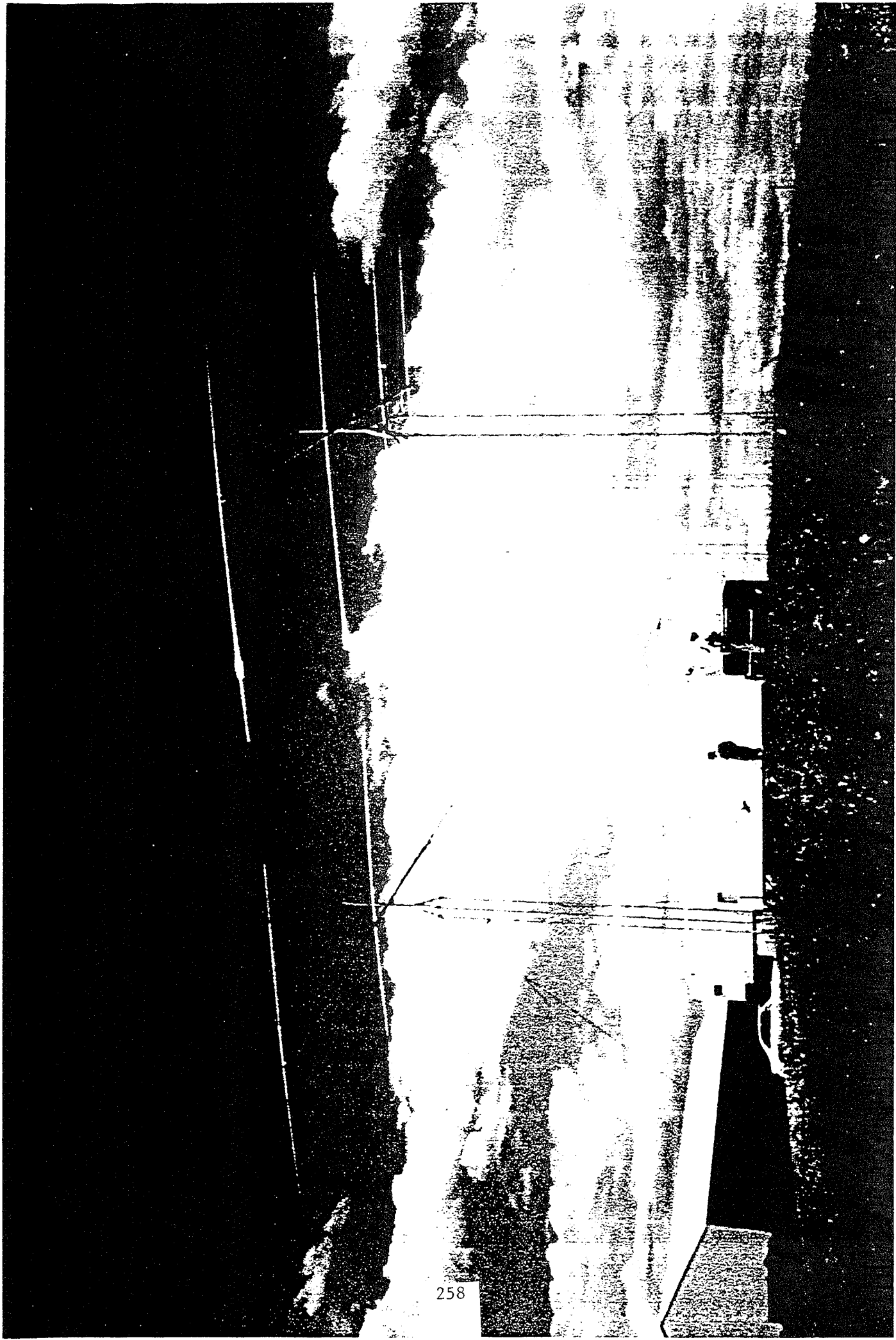
- Sponsored by National Science Foundation, Aeronomy Section
- Experiment: Yucca Ridge Field Station, Colorado  
Last week in July 1995
- Rationale
  - (1) Ionization anomalies associated with red sprites (e.g., VLF propagation effects)
  - (2) Increase in average ionization is likely to be small (e.g.,  $N \leq 10^4$  el/cm<sup>3</sup>)
  - (3) Ionization/electron heating likely to be impulsive and structured. Therefore, refractive index fluctuations could be large → Radar Backscatter
  - (4) If measurable, backscatter characteristics could shed light on plasma physics associated with red sprites.

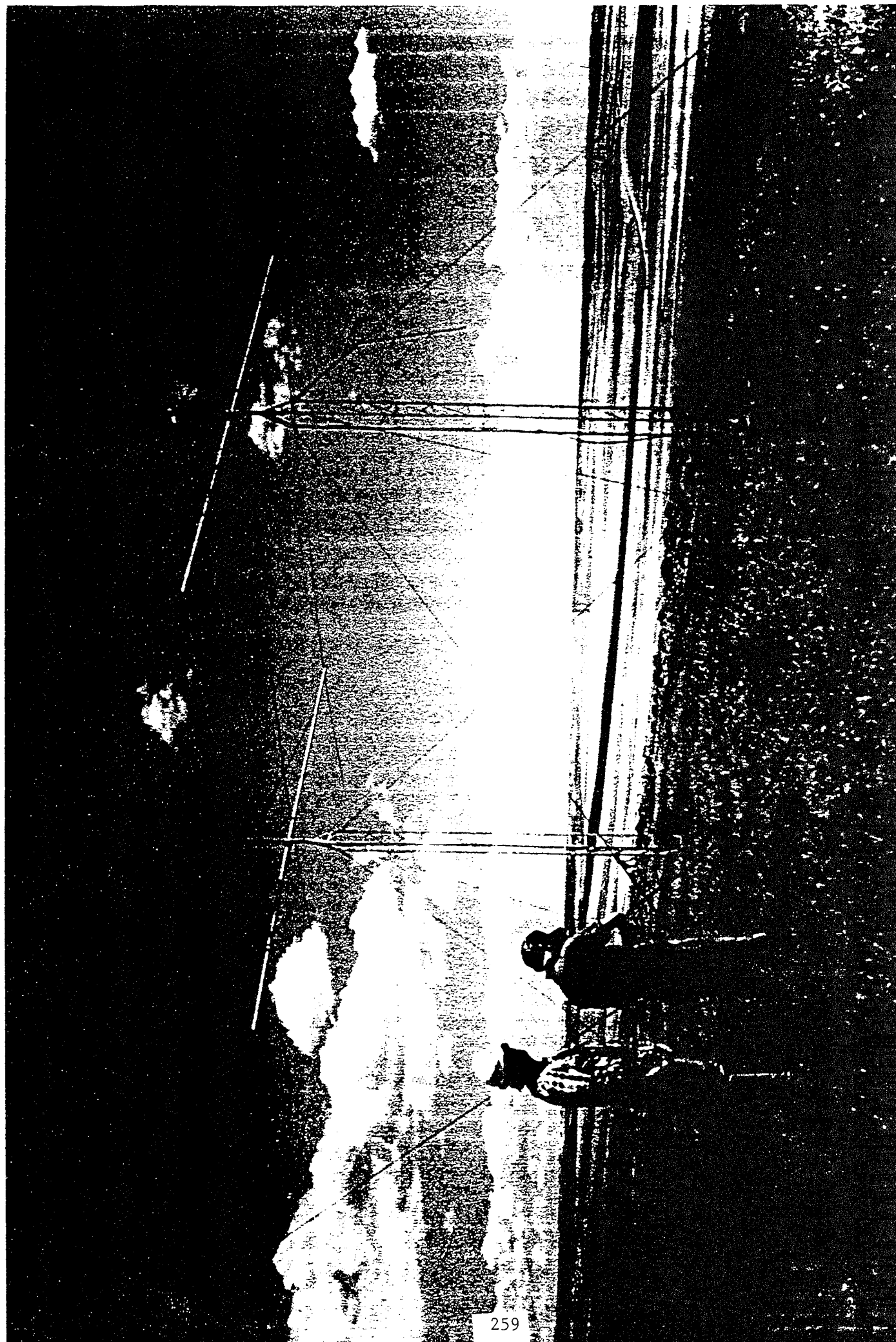
## EXPERIMENTAL APPROACH

- Use SRI High-Power Frequency-Agile Radar (FAR)
  - Pulsed system
  - Frequency range: 2 to 32 MHz
  - Peak power:  $4 \times 30$  kW (120 kW total)
  - Maximum duty cycle: 5 percent
- Reproduce Results by *Rumi* [1957]
- Make Measurements with Optical Sensors
  - compare and correlate radar echoes with red sprites

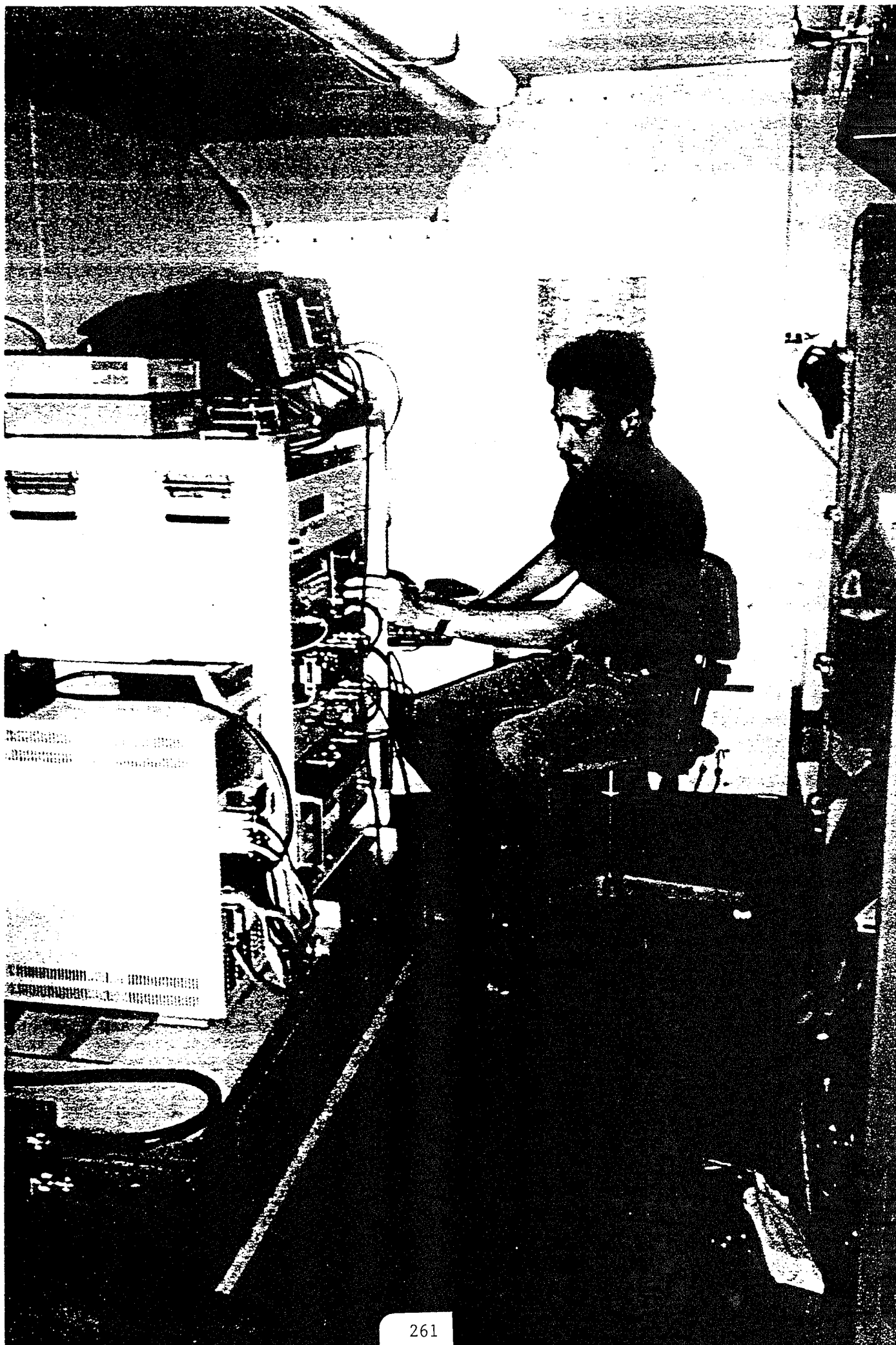










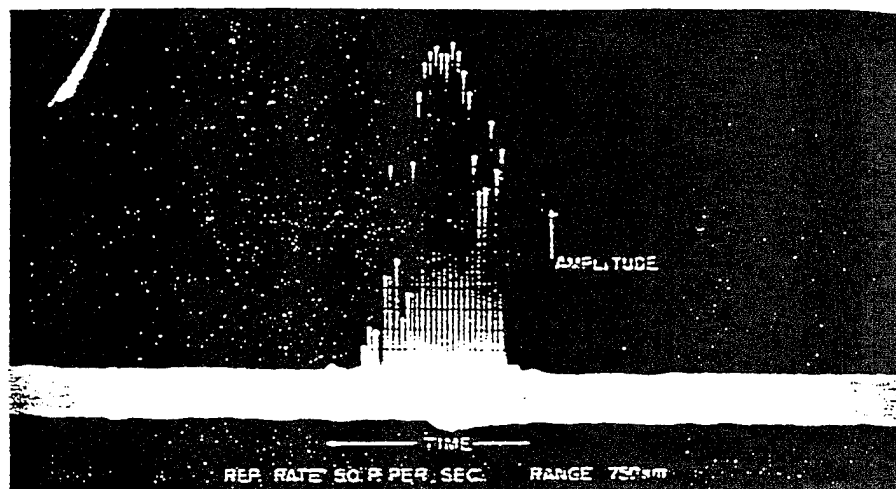


## Pulsed Radar Investigations of Red Sprites

| Radar Parameters       | <i>Rumi</i> [1957] | SRI                |
|------------------------|--------------------|--------------------|
| Radar frequency (MHz)  | 27.85              | 24.515             |
| Peak power (kW)        | 200                | 30                 |
| Pulse width ( $\mu$ s) | 40                 | 60                 |
| PRF ( $s^{-1}$ )       | 50                 | 100                |
| Antenna                | Vee                | two 4-element Yagi |

### Radar Echo Characteristics obtained by *Rumi* [1957]

- Echoes are discrete and last less than 0.5 s
- Echoes show no preferred range, out to 900 km
- Rise times (noise level to maximum) in 40 ms
- Decay times (from at least 7 dB SNR) in 100 ms; not exponential
- Sometimes have tendency to recur at the same range
- Occurrence favored  $\pm 1$  hour around midnight
- As many as 400 echoes occurred in 1 hour
- Occurred on more than half the nights during September-November 1955 (very few occurred in December)
- No correlation found with any known phenomena was established



Range = 750 km  
PRF = 50 s<sup>-1</sup>

Echo 156—Radar echo obtained at Ithaca, New York, on 27.55 Mc/sec, October 21, 1955, 2310-2415 hours EST

*Echo 150* is typical, not only for the steep rise, but also for the very flat horizontal top. It has to be emphasized that no saturation is limiting the amplitude. Indeed, the little rise at the left of the top indicates that there is still a possibility of increasing amplitude. Furthermore, a comparison with Echo 156 will show that larger pips with the same noise level can be recorded.



Range = 650 km  
PRF = 50 s<sup>-1</sup>

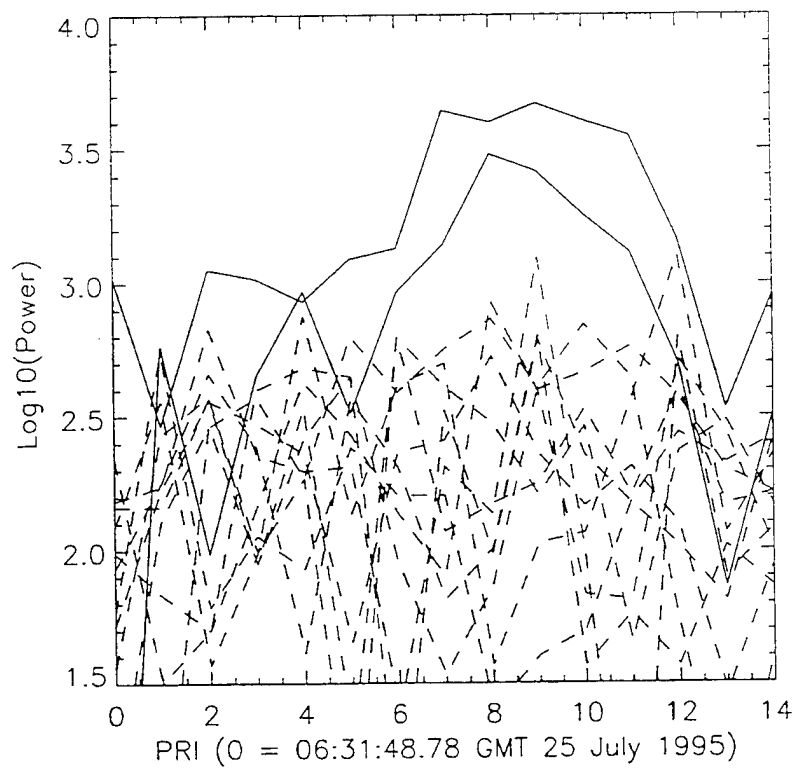
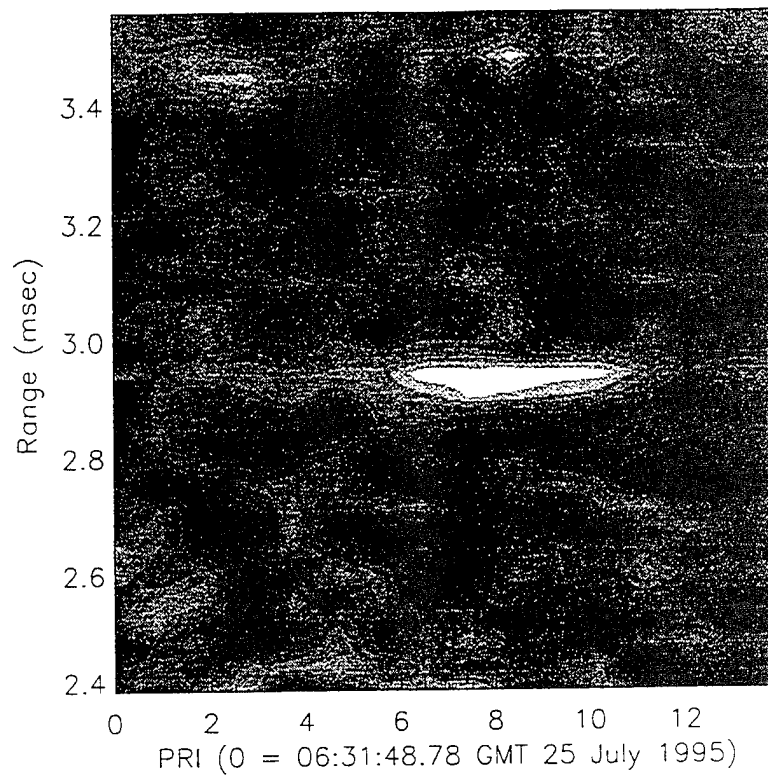
Echo 150—Radar echo obtained at Ithaca, New York, on 27.55 Mc/sec, October 21, 1955, 2310-2415 hours EST

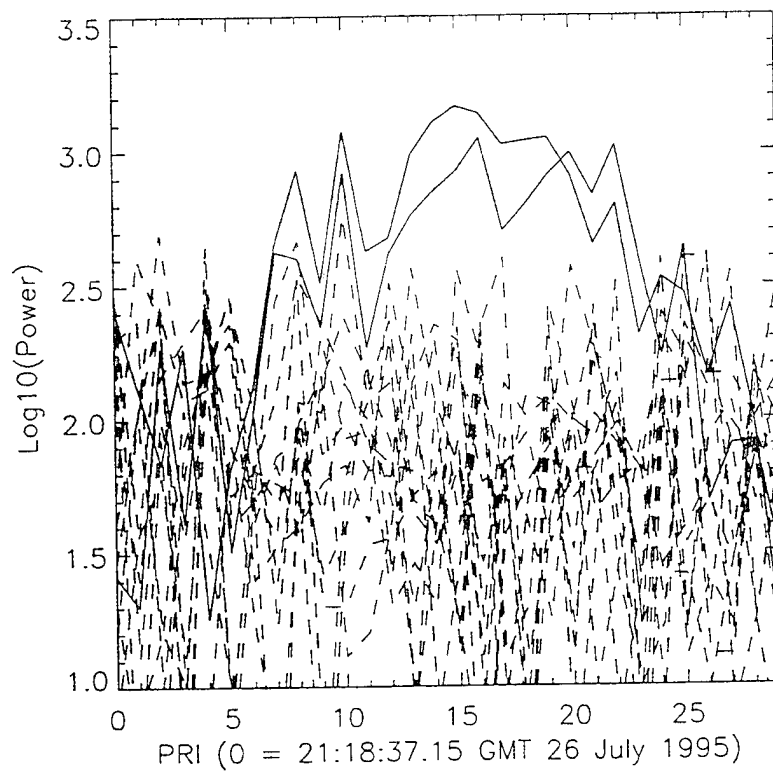
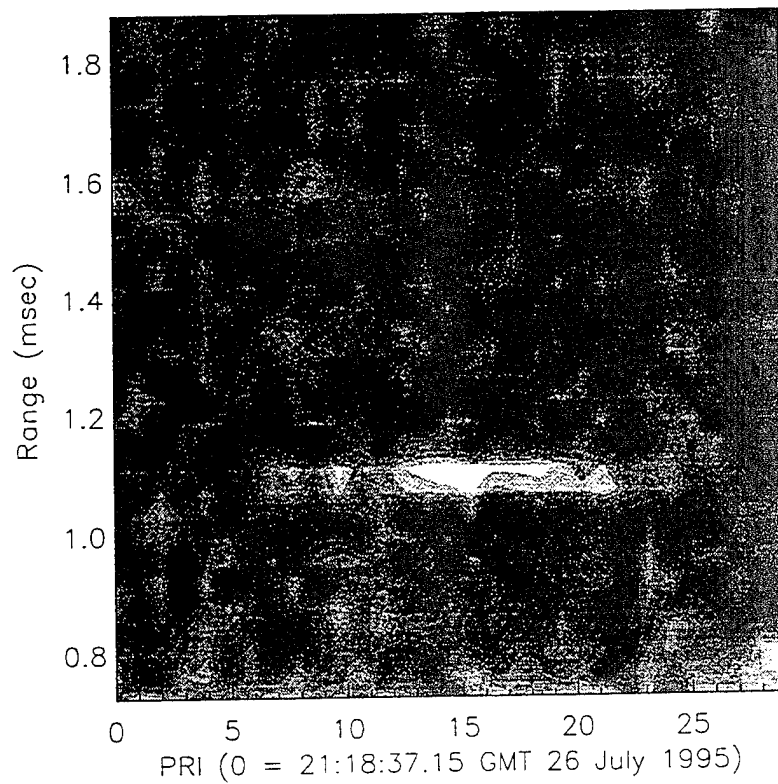


## QUICK-LOOK RESULTS

- RADAR ECHOES WERE OBSERVED THAT SEEM TO BE SIMILAR TO THOSE REPORTED BY RUMI [1957].
  - 1) Echo strength  $\leq 10$  dB (SNR)
  - 2) Range extent  $\sim 80 \mu\text{s}$
  - 3) Rise/fall times  $\sim 20$  ms
  - 4) Amplitude  $\sim$  constant
  - 5) Time duration: 70 - 200 ms
- RESULTS SUGGEST PRESENCE OF IONIZATION AND ROLE FOR  $\Delta T_e$







## RADAR BACKSCATTER FROM RED SPRITES

In the absence of magnetic-field effects, the refractive index (magneto-ionic theory) is given by

$$(\mu - i\chi)^2 = 1 - \frac{X}{1 - iZ} \quad (1)$$

where  $\mu$  and  $\chi$  are the real and imaginary parts,

$$X = \frac{\omega_p^2}{\omega^2} \quad \text{and} \quad Z = \frac{\nu_e}{\omega} \quad (2)$$

where  $\omega_p$  is the plasma frequency,  $\omega$  is the angular radio wave frequency, and  $\nu_e$  is the electron collision frequency. We can rewrite the real part of (1) as

$$\mu^2 = \frac{1}{2} \left\{ \left[ (1 - pX)^2 + (pXZ)^2 \right]^{1/2} + 1 - pX \right\} \quad (3)$$

where  $p = \frac{1}{1 + Z^2}$

For the case  $X \ll 1$  and  $Z^2 \gg 1$ , we have  $p \approx Z^{-2}$  and  $pX \ll 1$ , and (3) becomes

$$\mu^2 \approx 1 + \frac{1}{4} \left[ \frac{X}{Z} \right]^2 \quad (4)$$

Differentiating (4)

$$\Delta\mu \approx \frac{1}{2\mu} \frac{\omega_p^2}{\nu_e \omega} \left[ \frac{\Delta N}{N} - \frac{\Delta \nu_e}{\nu_e} \right] \quad (5)$$

where  $\omega_p^2 = 80.6N$  and  $N$  is the electron density. And from *Bostrom* [1964]

$$v_{en} = 1.5 \times 10^{-11} n_n T_e^{1/2} \quad (6)$$

$$\Delta v_{en} = 1.5 \times 10^{-11} n_n T_e^{-1/2} \Delta T_e \quad (7)$$

$$\frac{\Delta v_{en}}{v_{en}} = \frac{\Delta T_e}{T_e} \quad (8)$$

Substituting (6) and (8) into (5)

$$\Delta\mu \approx \frac{40.3}{1.5 \times 10^{-11} n_n T_e^{1/2} \omega} \left[ \frac{\Delta N}{N} - \frac{\Delta T_e}{T_e} \right] \quad (9)$$

For the Yucca Ridge experiment,  $f \approx 25$  MHz or  $\omega = 1.57 \times 10^8$ . If we assume that  $N \approx 10^{10} \text{ m}^{-3}$  and  $n_n \approx 10^{20} \text{ m}^{-3}$ , (9) becomes

$$\Delta\mu \approx \frac{1.7 \times 10^{-6}}{T_e^{1/2}} \left[ \frac{\Delta N}{N} - \frac{\Delta T_e}{T_e} \right] \quad (10)$$

We also note that  $X \approx 3.2 \times 10^{-5}$  and  $Y \approx 4.5 \times 10^{-2}$  for  $B = 0.4$  G.

## TO DO -- DATA ANALYSIS

- EXAMINE/ANALYZE LARGER DATA BASE.
- COMPARE RADAR ECHOES W/ RED SPRITES
- DETERMINE DOPPLER VELOCITIES

## TO DO -- NEXT EXPERIMENT

- MORE TIME OVERLAP W/OPTICAL SENSORS
- OBTAIN ANGLE OF ARRIVAL INFORMATION
  - azimuth: sprite direction
  - elevation: altitude of echo
- TWO OR MULTI-FREQUENCY MEASUREMENTS
  - characterize scattering mechanism
- POSSIBLY INCREASE SENSITIVITY  
(i.e., power-aperture product)

# On Runaway Breakdown and Upward Propagating Discharges

**Robert Roussel-Dupré, Yuri Taranenko**

*Space and Atmospheric Sciences  
Los Alamos National Laboratory  
Los Alamos, NM 87545*

*and*

**Alex Gurevich**

*P.N. Lebedev Institute of Physics  
Moscow 117924  
Russia*

**Los Alamos**

*Space & Atmospheric Sciences*

# Outline

- ⇧ Runaway Breakdown
- ⇧ Ingredients for an Upward Discharge
- ⇧ Models
- ⇧ Emissions
  - Optical
  - $\gamma$ -ray
  - VHF Radio
- ⇧ Summary

# Runaway Air Breakdown

- ⇧ Initiated by energetic ( $> 100$  keV) electron produced by cosmic rays
- ⇧ Avalanche proceeds when  $E > 218 (N/N_0)$  kV/m
- ⇧ Formation of collimated electron beam
- ⇧ Spatial scales at high altitudes
  - Avalanche lengths  $\sim > 100$  m - kms
  - Beam diameter  $\sim > 1$  km - tens of kms
- ⇧ Temporal Scales
  - Beam growth  $\sim > 3 \mu\text{s} - 100 \mu\text{s}$
  - Discharge duration  $\sim 100 - 150 \mu\text{s}$

**Los Alamos**

Space & Atmospheric Sciences



# Ingredients for Upward Discharge

## ⇨ Thunderstorm

- Large Mesoscale Convective system
- High flash rate (50-60 / minute)

## ⇨ Lightning stroke

- Intracloud or Positive cloud-to-ground
- High currents ( $> 100 \text{ kA}$ )
- Large charge neutralization ( $> 100 \text{ C}$ )

## ⇨ Low upper atmospheric conductivity

- Electrical relaxation time  $> 10 \text{ ms}$  up to  $70 \text{ km}$  altitude

---

**Los Alamos**

Space & Atmospheric Sciences

# Models of Upward Discharges

- 2-d hydrodynamic model
  - Primary electrons, secondary electrons, negative ions, positive ions
  - Avalanche of runaway electrons (based on kinetic calculations)
  - Ionization, recombination, attachment
  - Swarm model for secondary electrons
  - Quasi-electrostatic field model plus runaway and secondary currents
- Semi-empirical model
  - Use optical observations to constrain total energy in electron beam
  - Develop model of single equivalent discharge
  - Quasi-electrostatic field model, parameterization of beam in terms of  $\delta_0$

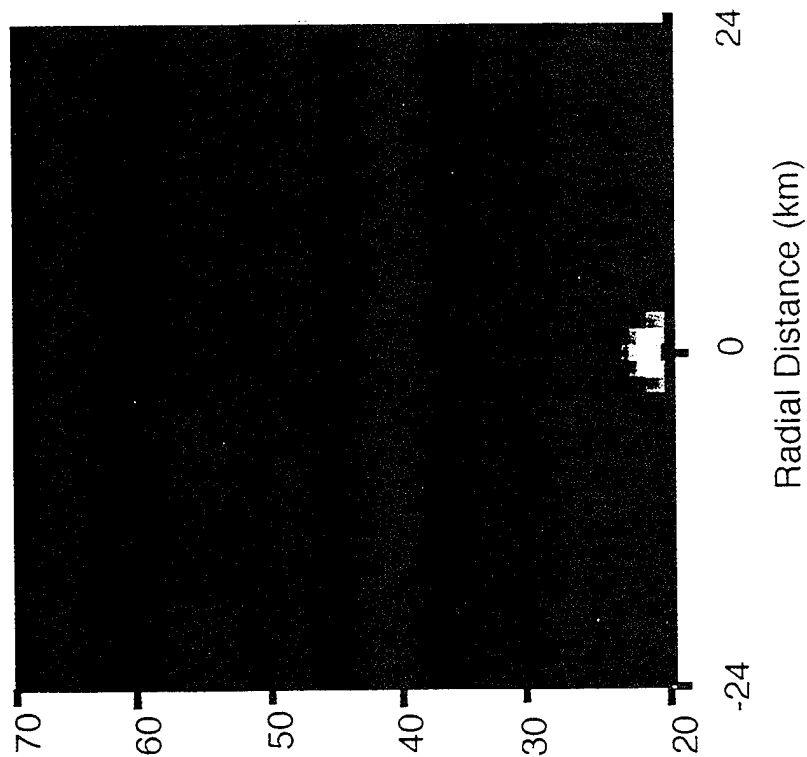
---

**Los Alamos**

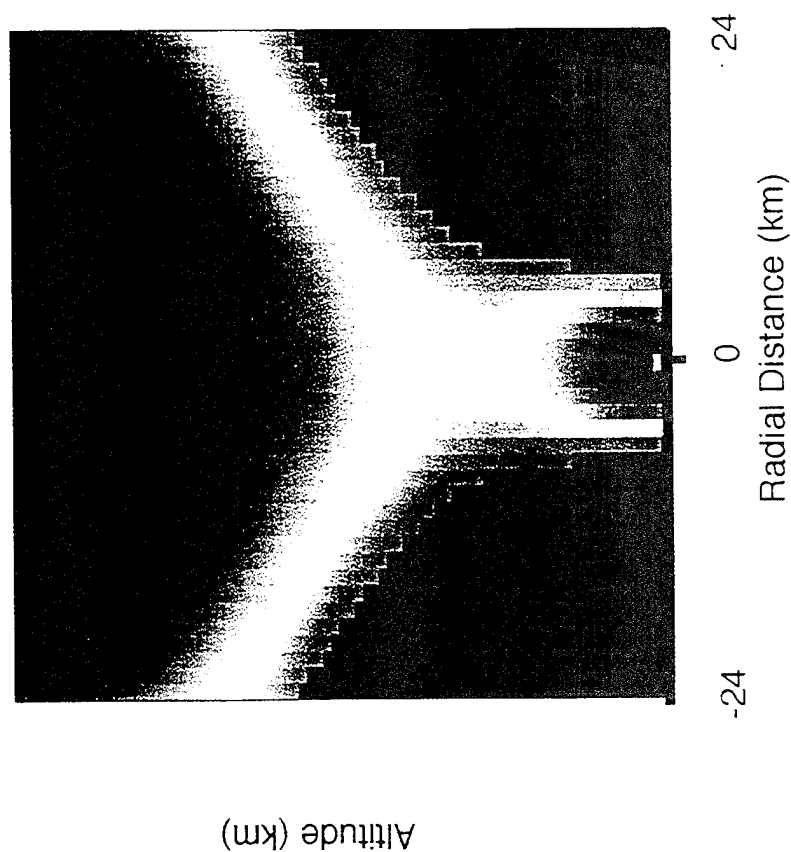
Space & Atmospheric Sciences

# NORMALIZED ELECTRIC FIELD

BEFORE



AFTERD



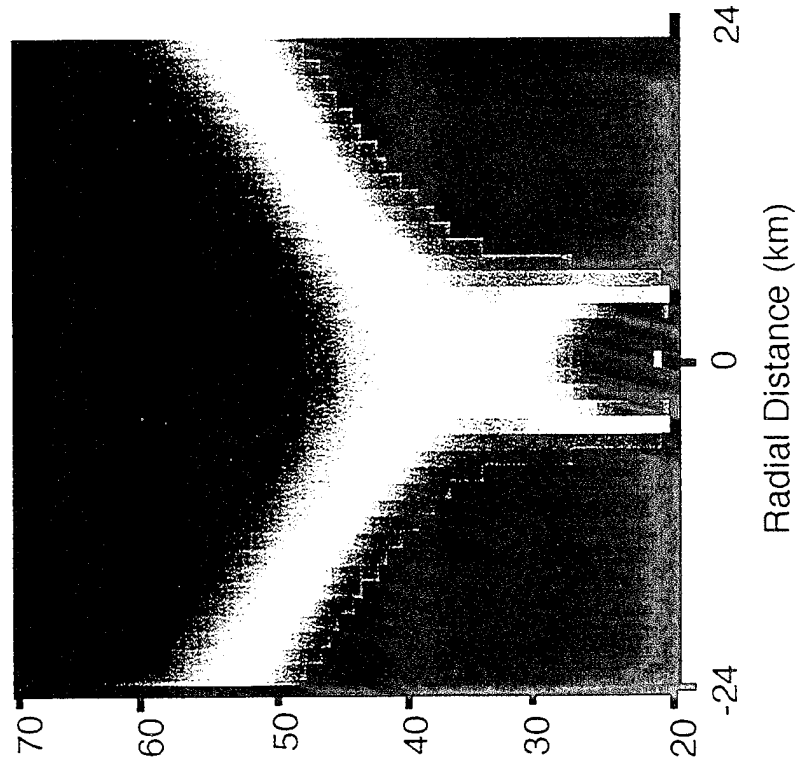
7

<1

Fig. 1

# NORMALIZED ELECTRIC FIELD

@ T=0



@ T=117  $\mu$ s

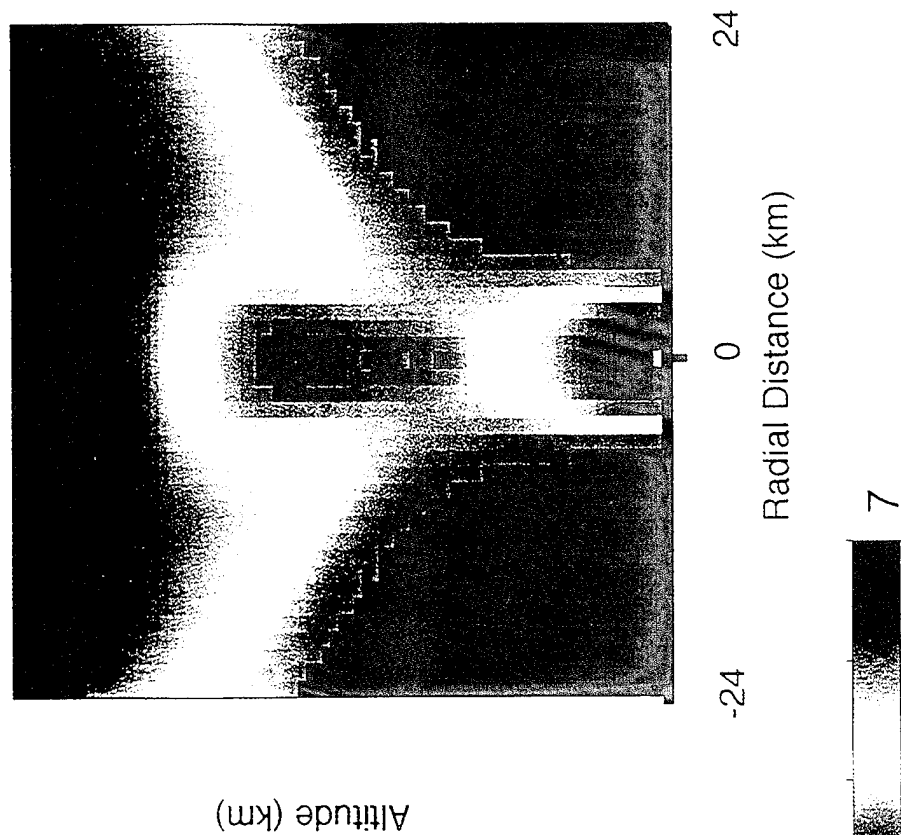


Fig. 5

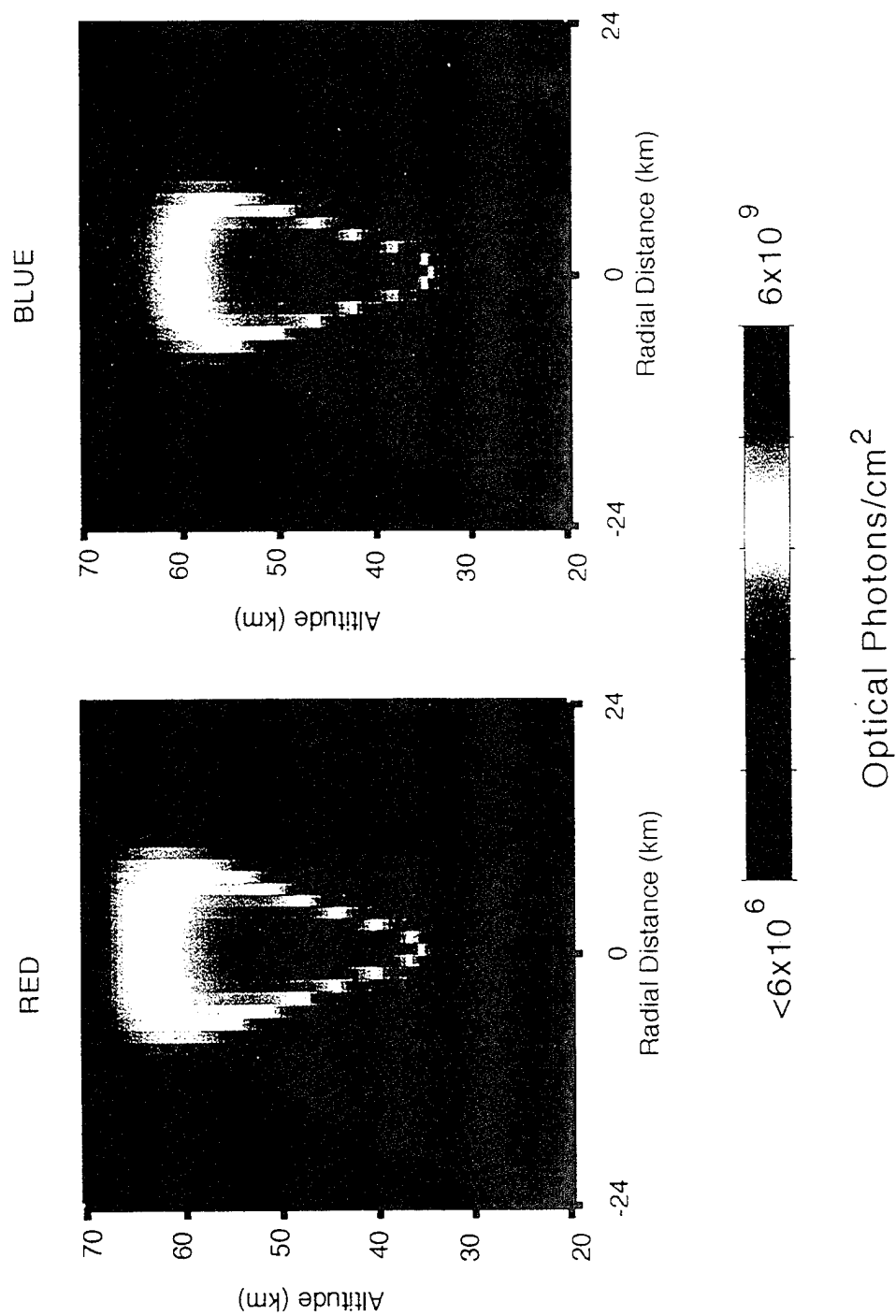
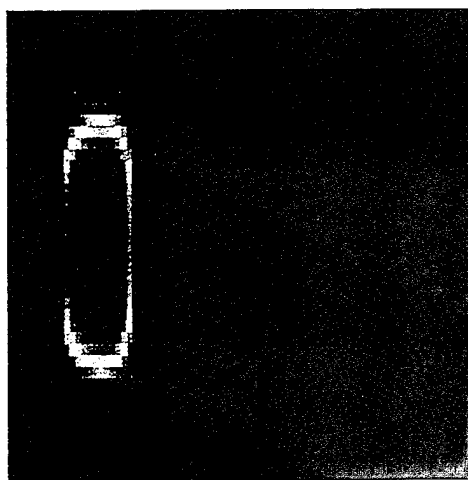


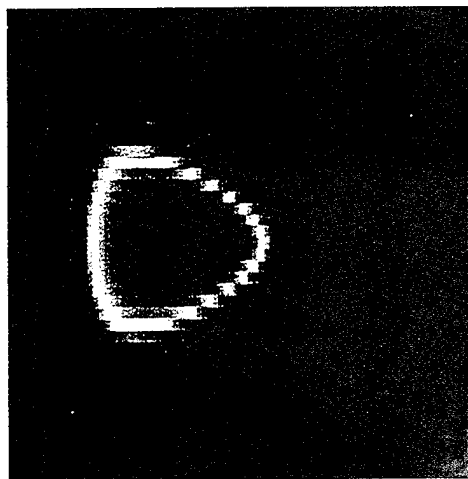
Fig. 4

PARTICLES @  $T=117\mu s$

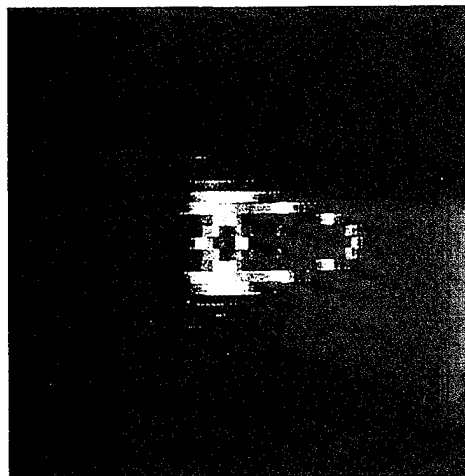
PRIMARIES



SECONDARIES



TOTAL CHARGES



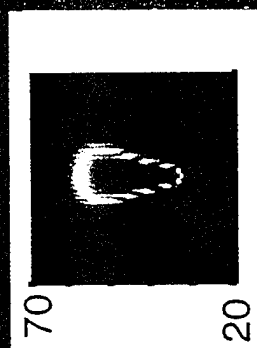
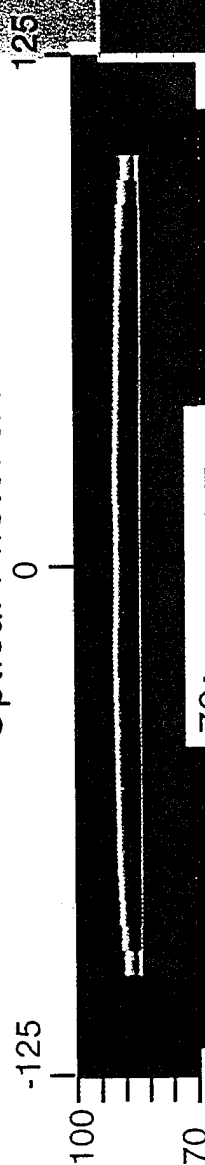
SIGN OF CHARGE



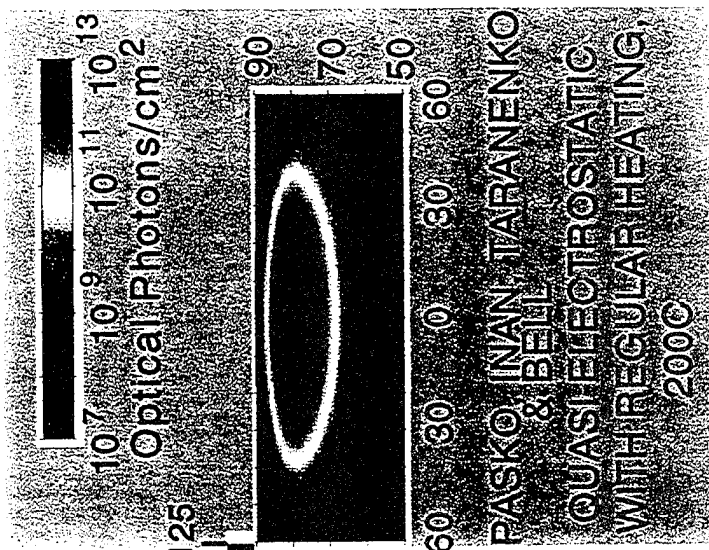
Fig. 4

# OPTICAL EMISSIONS OF DIFFERENT MODELS

PRESENT MODEL WITH REGULAR HEATING, EMP=20 V/M



Optical Photons/cm<sup>2</sup>



PASKO, INAN, TARANENKO  
& BELL  
QUASIELECTROSTATIC  
WITH REGULAR HEATING,  
2000

PASKO, INAN, TARANENKO, DUFRE  
QUASIELECTROSTATIC WITH  
HUNAWAY BREAKDOWN, 1000C

# Emissions

|                  | Model                                | Observations                               |
|------------------|--------------------------------------|--|
| Total Energy     | ~ 480 J                              | 100 J - several kJ                         |
| Intensity        | ~ 1 MR                               | ~ 1 MR                                     |
| Spectrum         | Red above 60 km and blue below 18 km | Red above 60 km and blue below 10 - 50 km  |
| Maximum Diameter |                                      |  |
| Source Region    | 30 - 70 km                           | 25 - 90 km                                 |
| Count Rate       | ~800 counts / burst                  | ~400 counts / burst                        |
| Rise-time        | ~ 0.15 ms                            | ~ 0.1 ms                                   |
| Duration         | ~ 0.3 ms                             | ~ 1-5 ms                                   |
| VHF Flux         | ~ $1.1 \times 10^{14} \text{ J/m}^2$ | median of $1 \times 10^{14} \text{ J/m}^2$ |
| Pulse Separation | tens of $\mu\text{s}$                | mean of 51 $\mu\text{s}$                   |
| Duration         | several $\mu\text{s}$                | mean of 5 $\mu\text{s}$                    |

Optical

$\gamma$ -rays

VHF above 25 MHz

Los Alamos

Space & Atmospheric Sciences



## Satellite Measurements of TlPPs

As seen from Blackbeard (low earth orbiting satellite in circular orbit at 800 km altitude and  $70^\circ$  inclination) in 25-75 MHz band

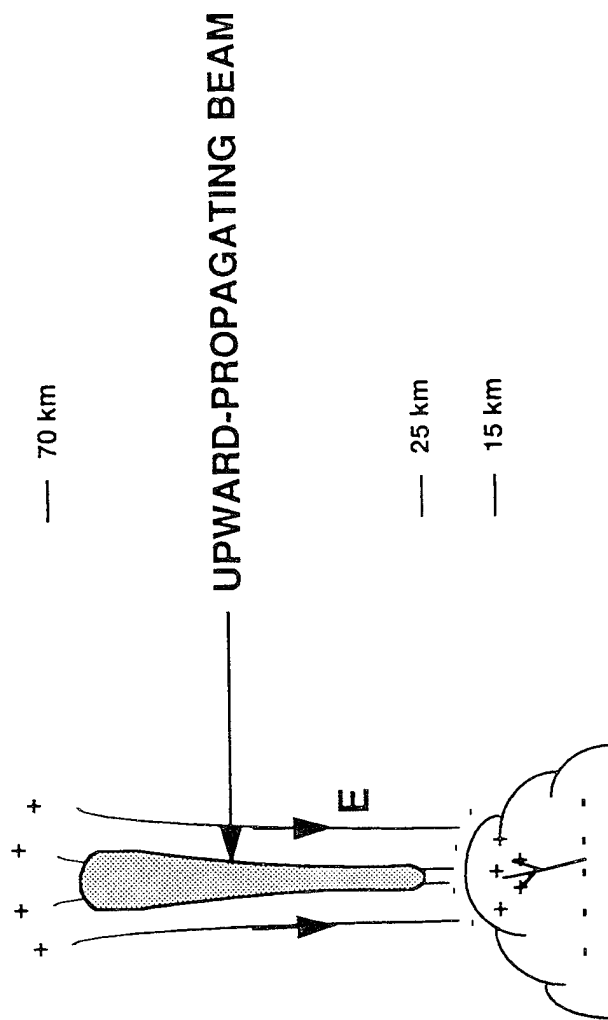
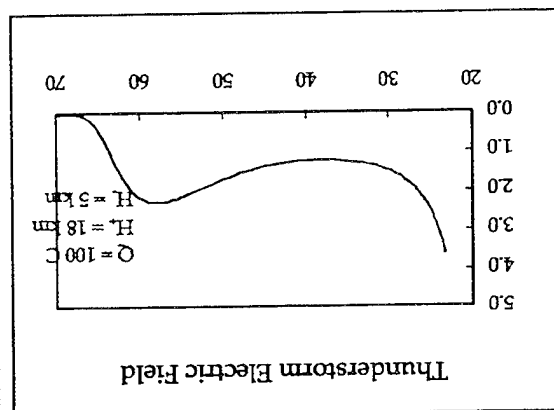
- ⇒ Intense pairs of pulses
- ⇒ Duration ranged from 0.5-14  $\mu\text{s}$  with a mean of 5  $\mu\text{s}$  and a median of 3.8  $\mu\text{s}$
- ⇒ Separation ranged from 7.5-102  $\mu\text{s}$  with a mean of 51  $\mu\text{s}$  and a median of 52  $\mu\text{s}$
- ⇒ Fluence ranged from  $2.5\text{-}170 \times 10^{-15}$  Joules/ $\text{m}^2$  with a median of  $10 \times 10^{-15}$ .

**Los Alamos**

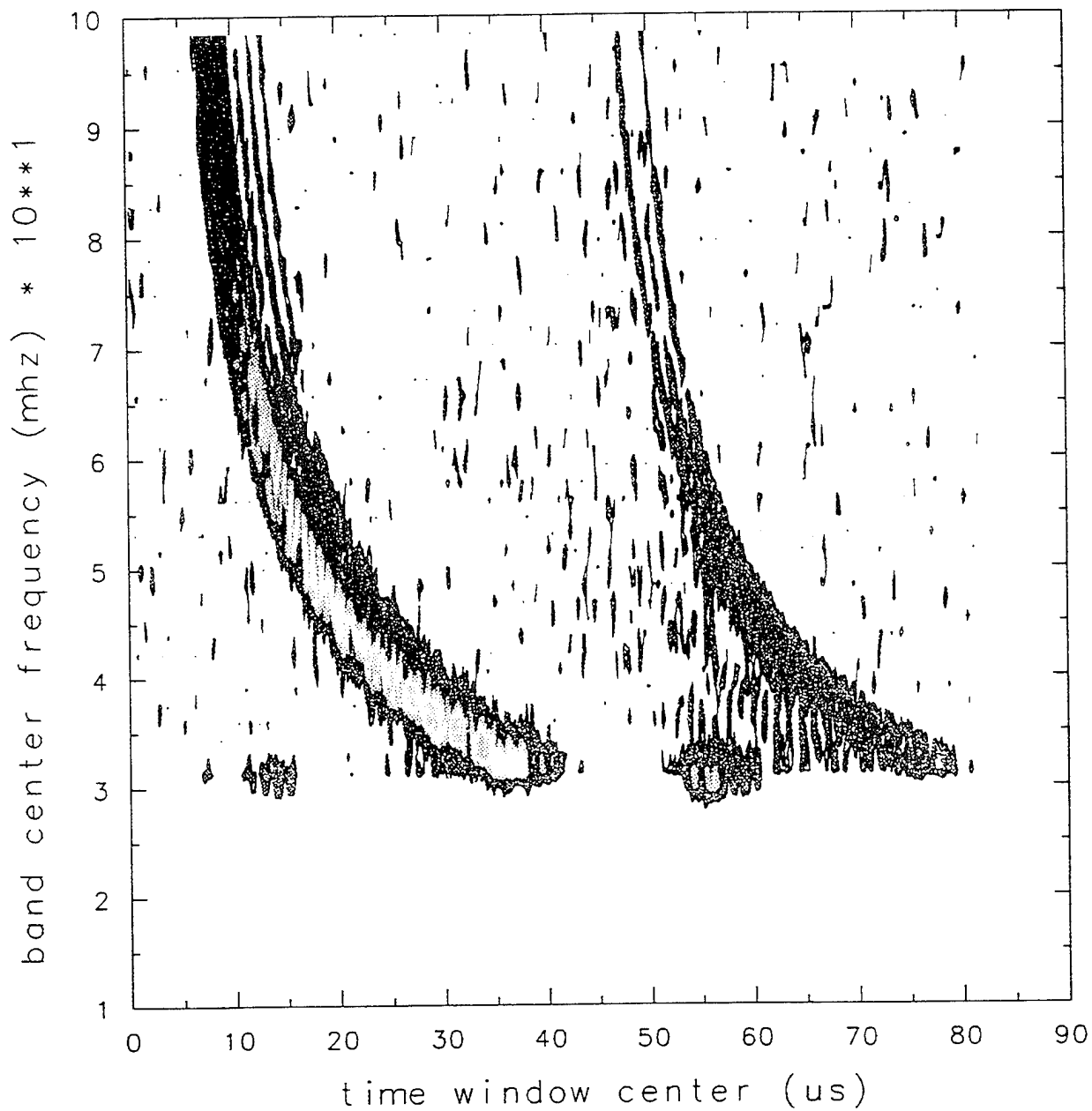
Space & Atmospheric Sciences

# TIPPS AND UPWARD DISCHARGES

Ionosphere



$10 \cdot \log_{10}((E/\text{MAX})^{**2})$ , MAX= 1.65E-03(V/MS-HZ)  
SPECTROGRAM GENERATED BY 128 POINT WELCH WINDOW



# Summary

- Runaway breakdown models reproduce
  - optical observations of upward discharges
  - $\gamma$ -ray measurements of BATSE
  - TIPP events measured by BLACKBEARD
- Needed Measurements
  - Simultaneous optical,  $\gamma$ , and rf
  - Atmospheric conductivity profiles
  - Thunderstorm electric fields, currents, and charge distribution
  - Energetic particle measurements
  - Experiment to validate theory of runaway breakdown

**Los Alamos**

Space & Atmospheric Sciences

Numerical Simulations of Lower  
Ionospheric Breakdown Caused by  
Lightning Generated Electric Fields

Harvey Rowland, Richard Fernsler,  
Carl Sieftring and Paul Bernhardt

Naval Research Lab

Sprite Workshop, Phillips Lab.  
Oct. 18, 1995

## Model

The code uses Maxwell's equations with the currents calculated by Ohm's law,  $\mathbf{j} = \sigma \mathbf{E}$ , where

$$\sigma = \begin{vmatrix} \sigma_P & \sigma_H & 0 \\ -\sigma_H & \sigma_P & 0 \\ 0 & 0 & \sigma_{\parallel} \end{vmatrix} \quad (1)$$

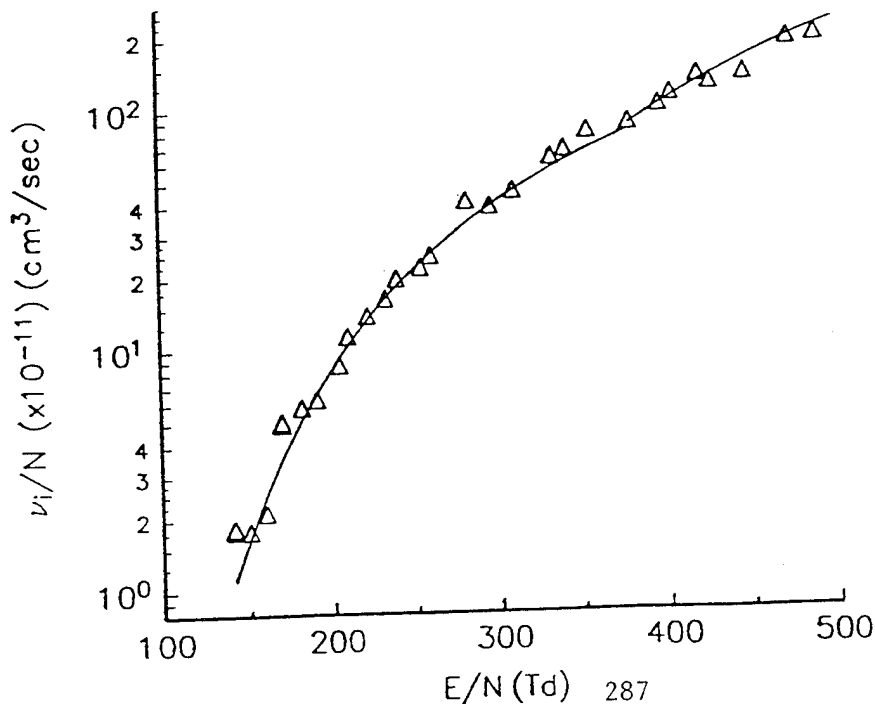
The conductivities are the Pedersen ( $\sigma_P$ ), Hall ( $\sigma_H$ ) and parallel ( $\sigma_{\parallel}$ ). The code has two spatial dimensions and the currents ( $x$ ,  $z$ ,  $j_x$ ,  $j_y$ , and  $j_z$ ). The earth's magnetic field is in the  $z$  direction.

## Ionization and Breakdown

We use a fit to laboratory data of ionization of air for the appropriate range of  $E/N$  values.

$$v_i \approx \begin{cases} 5 \times 10^{-8} N \exp(-1550N/E_{\text{eff}}) & E_{\text{eff}}/N > 370 \\ 10^{-8} N \exp(-960N/E_{\text{eff}}) & E_{\text{eff}}/N < 370 \end{cases} \quad (2)$$

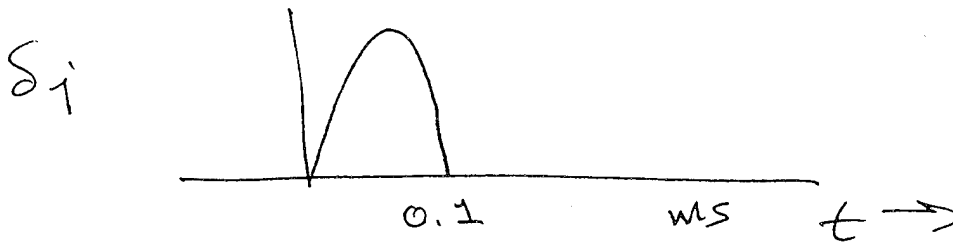
where the gas density  $N$  is in  $\text{cm}^{-3}$ ,  $v_i$  is in  $\text{sec}^{-1}$ , and  $E_{\text{eff}}/N$  is expressed in Td ( $1 \text{ Td} = 10^{-17} \text{ V-cm}^2$ ). the ionization rate is then used to update the conductivities.



## EMP Driven Breakdown

$$E_{EMP} \propto \frac{I}{r} \quad \text{while} \quad E_{QS} \propto \frac{Q}{r^3}$$

Use a discharge with large  $I_{\max}$  but no continuing current -- EMP dominates (Rowland, et al., GRL, 361, 1995).





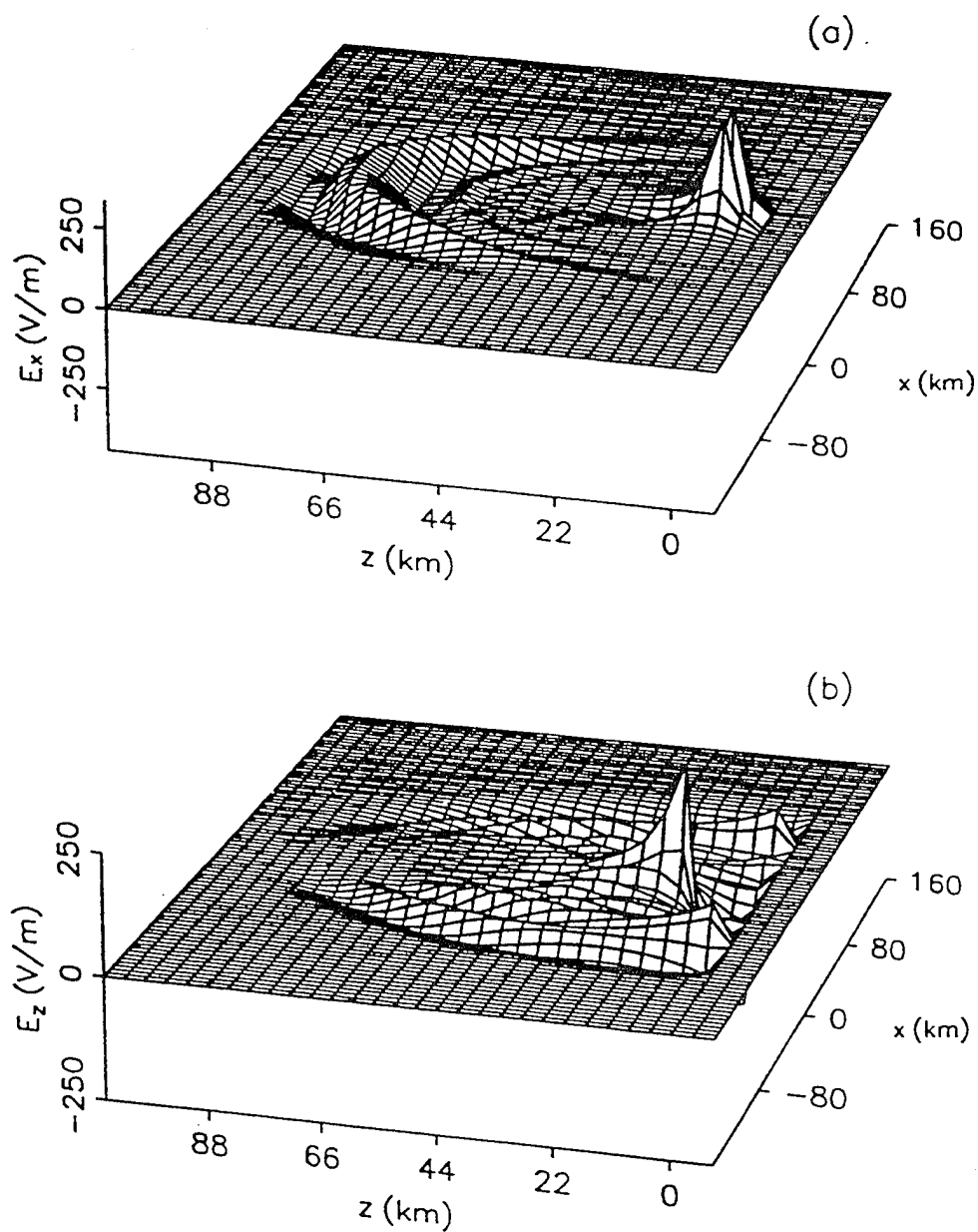


**Figure 1.** The electric fields generated by (a) a horizontal and by (b) a vertical discharge at 300  $\mu$ sec after the start of the discharge.

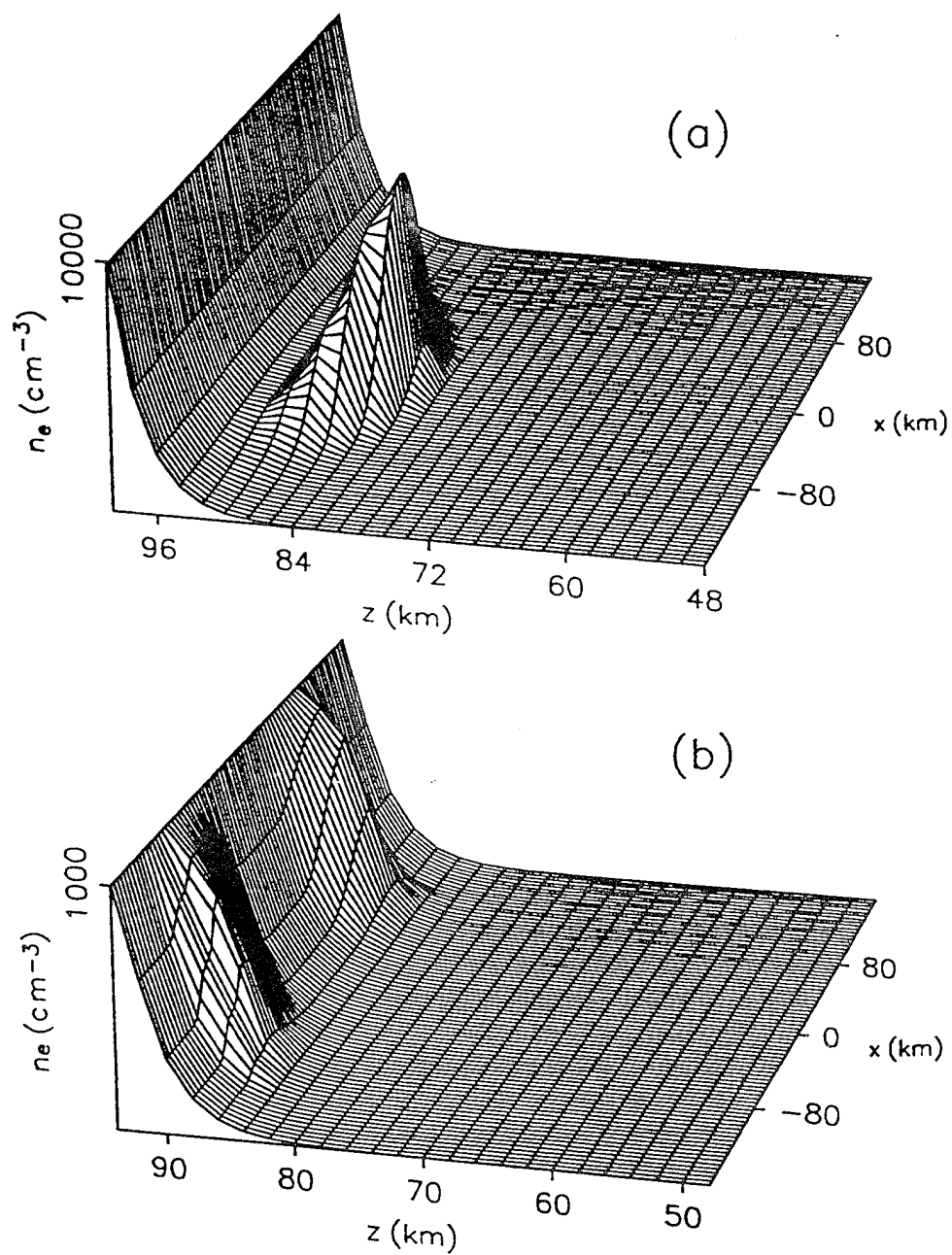
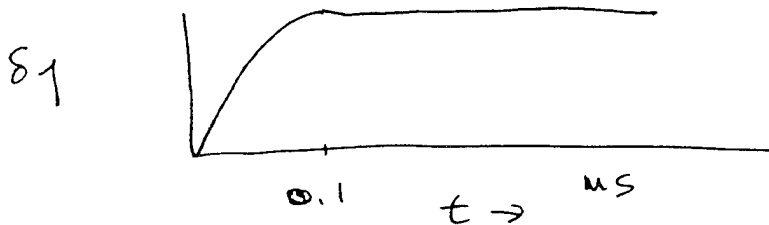


**Figure 2.** The ionospheric plasma density at 400  $\mu\text{sec}$  after the start of the discharge (a) for a horizontal and (b) for a vertical discharge with  $E_{100}=55 \text{ V/m}$ .

## Breakdown due to combined EMP and QS fields

$$E_{EMP} \propto \frac{I}{r} \quad \text{while} \quad E_{QS} \propto \frac{Q}{r^3} \quad \text{where} \quad Q = \int I dt$$



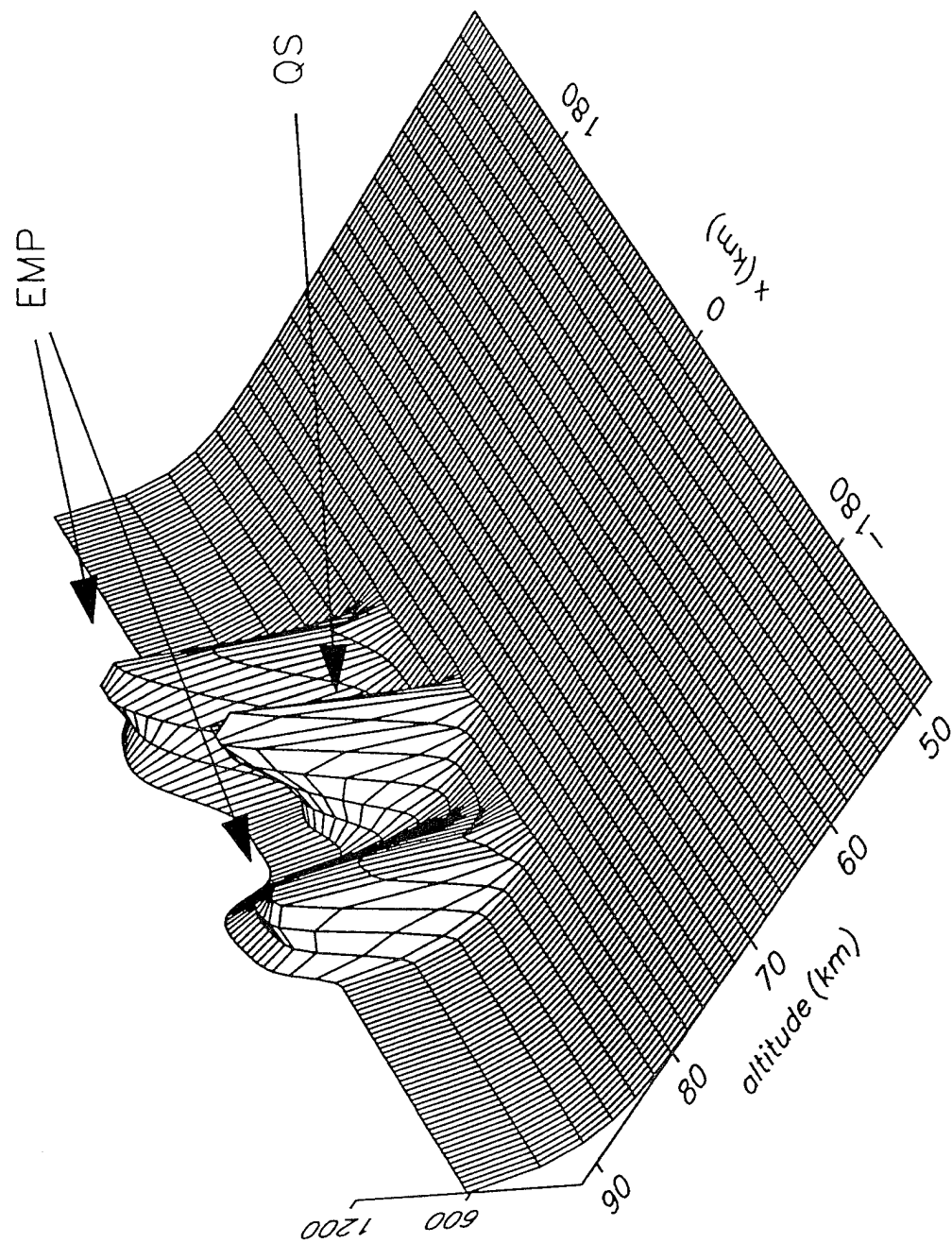
The same  $I_{\max}$  as in previous simulation but with a continuing current. When  $Q \approx 60C$ , breakdown from QS  $\approx$  EMP. As  $Q$  becomes larger, maximum ionization moves to lower altitude.

First, the EMP forms the broad (100's km), high altitude (70-90 km), sub-ms flash --ELVES.

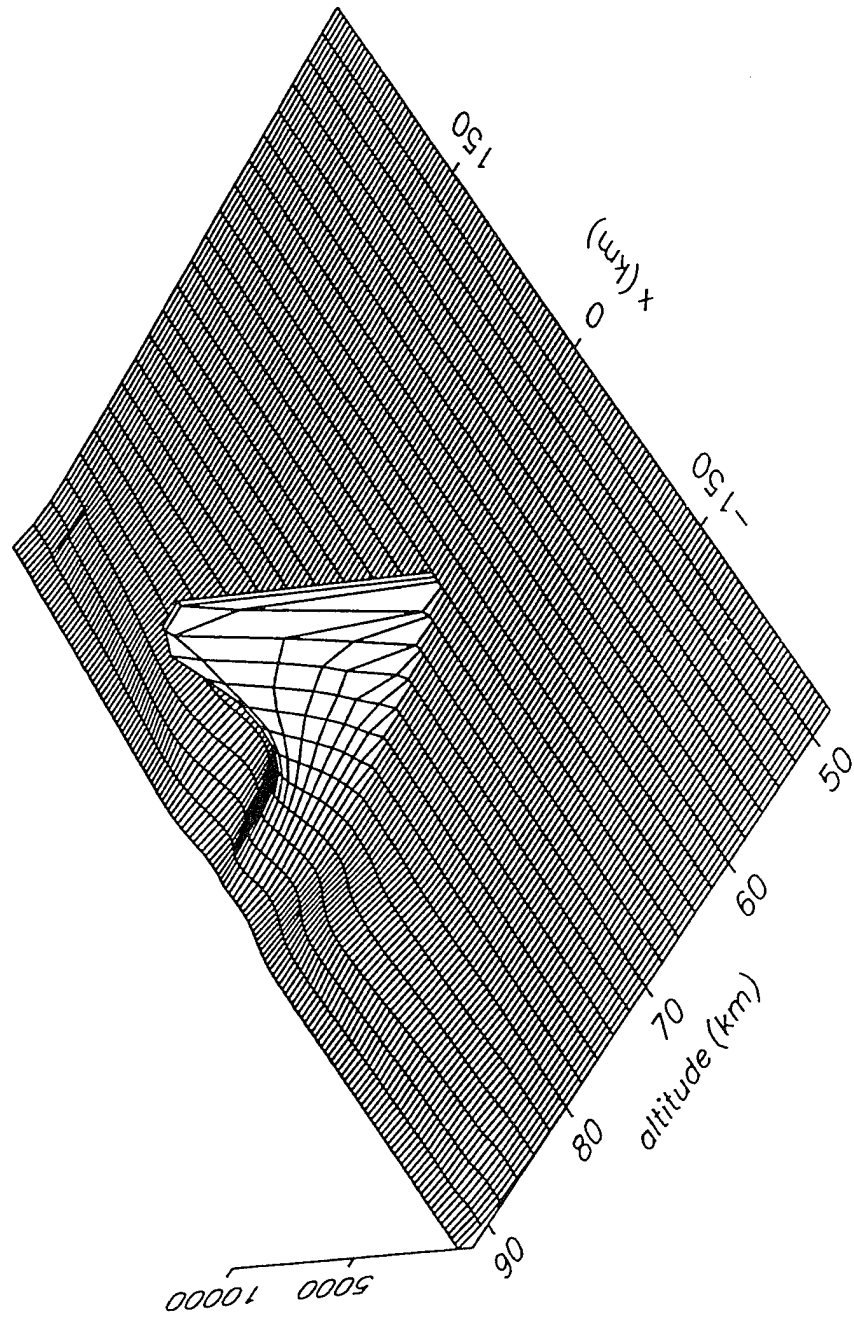
The QS can then form the narrow (10- 50 km), lower altitude (55-90 km), several msec flash --- SPRITES.

Raising the top of the discharge, increases ionization and lowers its altitude for same  $Q$ .

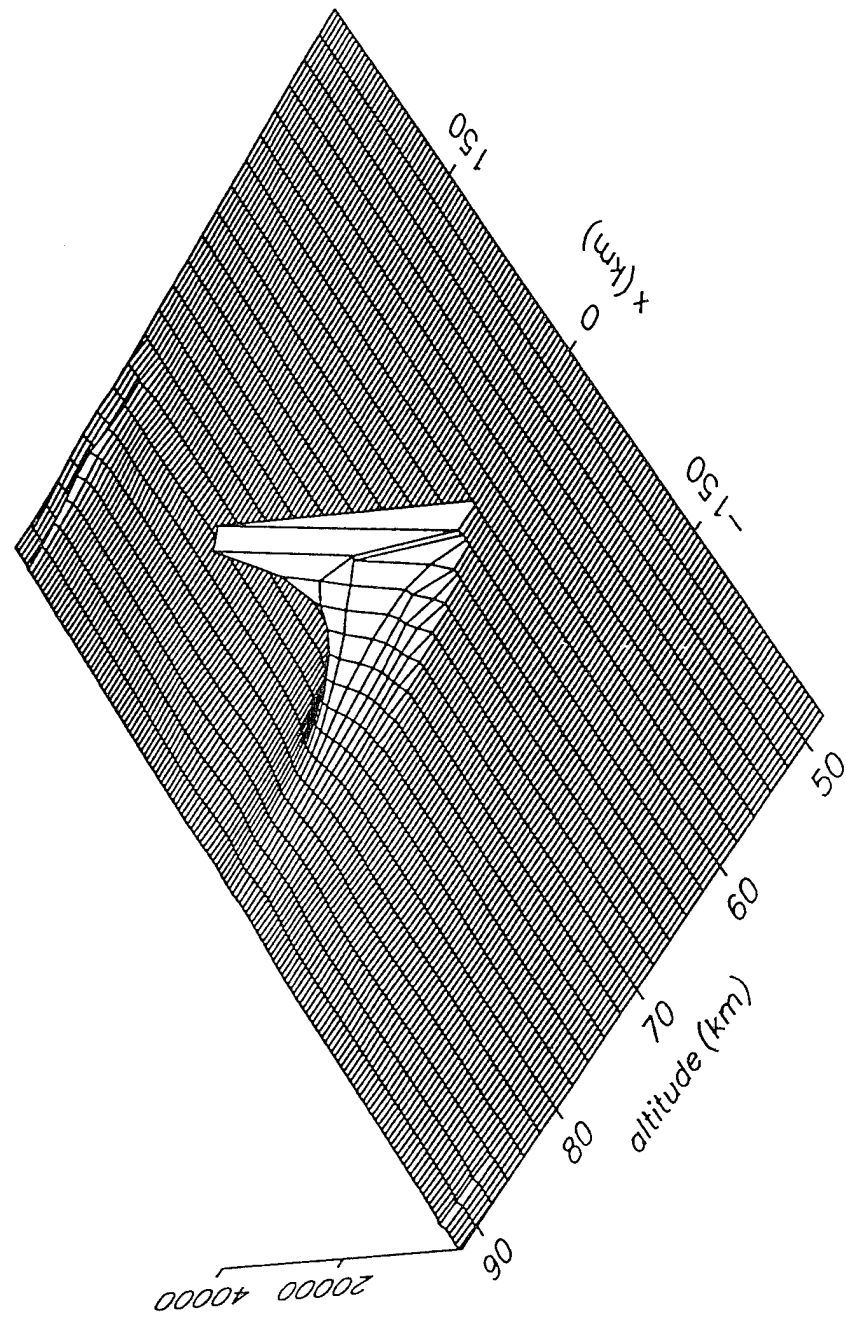
electron density  
 $E_{100} = 110 \text{ V/m}; t = 0.5 \text{ msec}; Q = 60 \text{ C}$



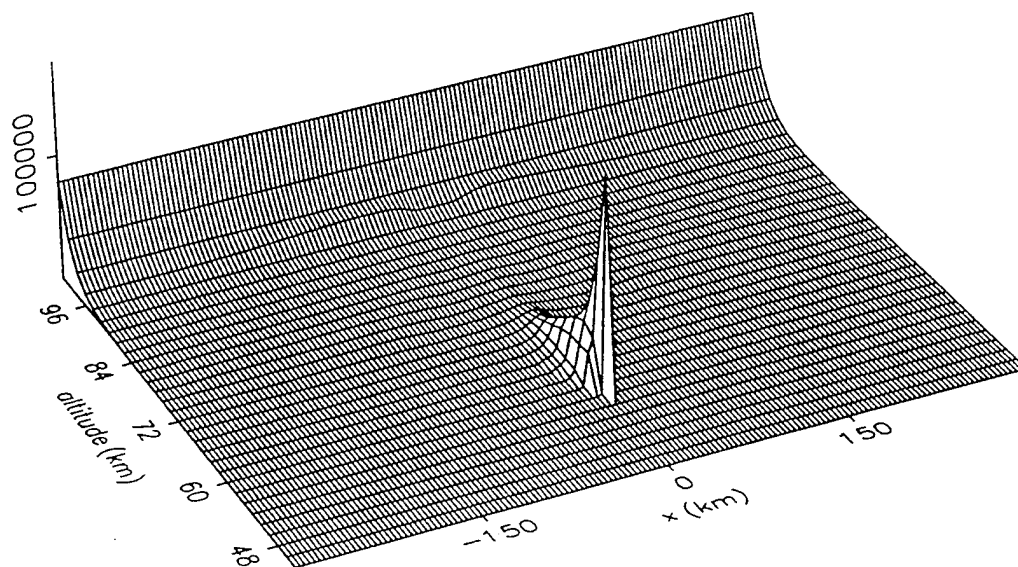
electron density  
 $E_{100} = 110 \text{ V/m}; t = 1 \text{ msec}; Q = 210 \text{ C}$



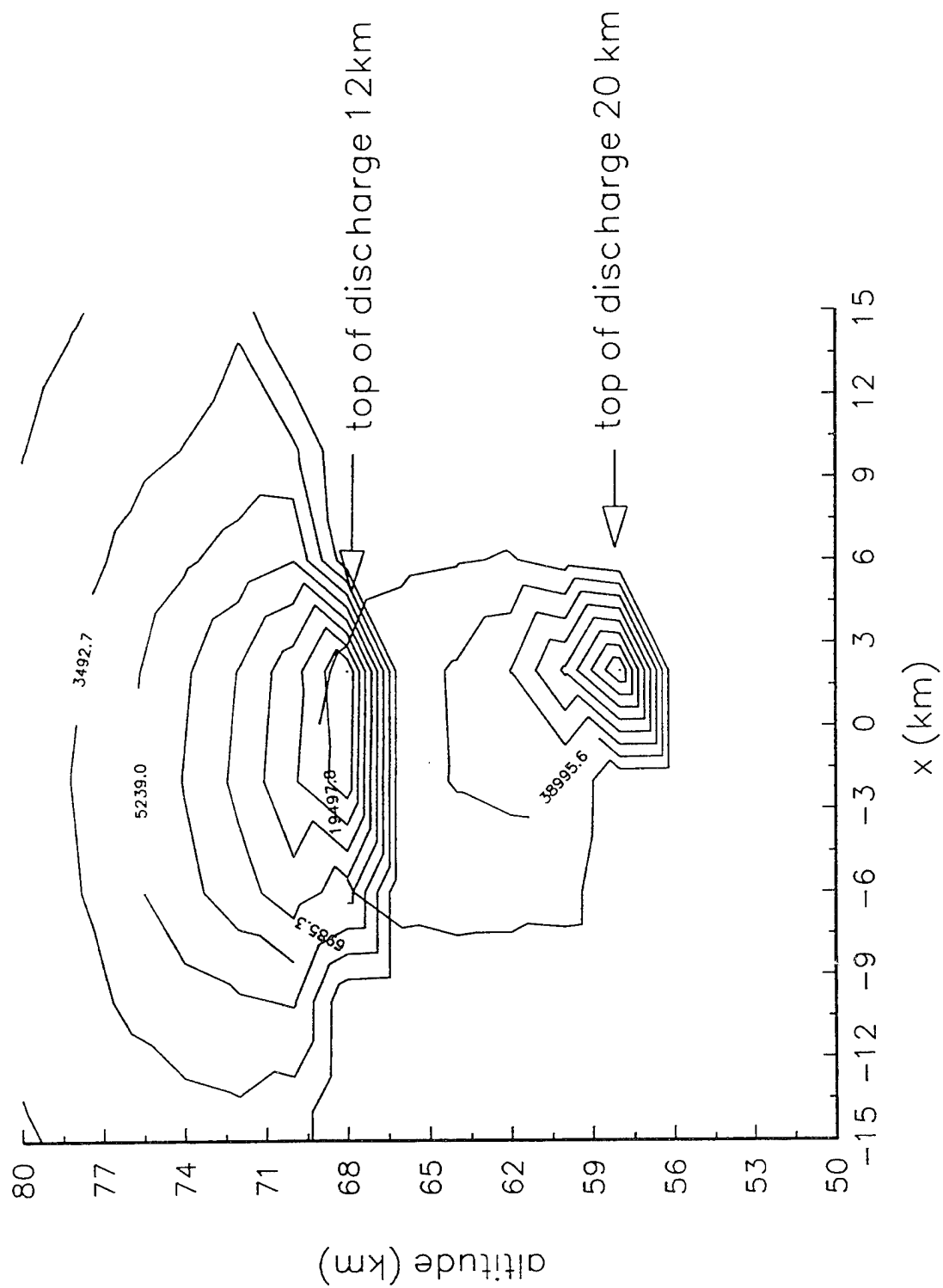
electron density  
 $E_{100} = 110 \text{ V/m}; t = 1.5 \text{ msec}; Q = 360 \text{ C}$



$n_e$   
continuing current;  $t = 1$  msec;  $Q = 210$  C



electron density  
 $E_{100} = 110 \text{ V/m}$ ;  $t = 1 \text{ msec}$ ;  $Q = 210 \text{ C}$





## Effects on the EMP and the QS fields

Breakdown modifies the conductivity and thus the propagation of the EMP. Fig. 5, 3, and 6 are for the horizontal discharge shown in Fig. 2a. By turning off ionization, one can compare the interaction with only the ambient, unmodified ionosphere.

Figure 7 and 8 show the effects of breakdown on the QS field for a cloud-to-ground discharge by comparing a simulation with breakdown to one with a fixed ambient ionosphere. The top figure shows the time history of the vertical electric field at 70 km directly above the discharge. As the ionization patch moves downward, the vertical field is initially enhanced. As it sweeps past, the increased conductivity shorts out the field. The bottom figure shows the spatial distribution of the vertical electric field at 1 msec. The bottom of the ionization is at 70 km at this time. In comparison to the simulation with a fixed ionosphere, the field is enhanced below 70 kilometers and reduced above.

Figure 9 shows a 2 D plot of the time integrated  $E_{rms}$  for the c-g discharge with no ionization (top) and ionization (bottom). This shows only the high altitude fields. The central fields are the QS fields and the left and right structures are the EMP. There is an absorbing strip along the left and right boundaries. One can see the notch cut into the QS fields by the ionization patch.

The enhanced E vertical is due to-

- focusing of the field because of the pointed shape of the ionization patch in the horizontal direction and,
- lowering the effective ionosphere bring closer together the charge at the top of the cloud and its image charge in the ionosphere.

The 50% enhancement is important, since this lowers the Q needed for breakdown.

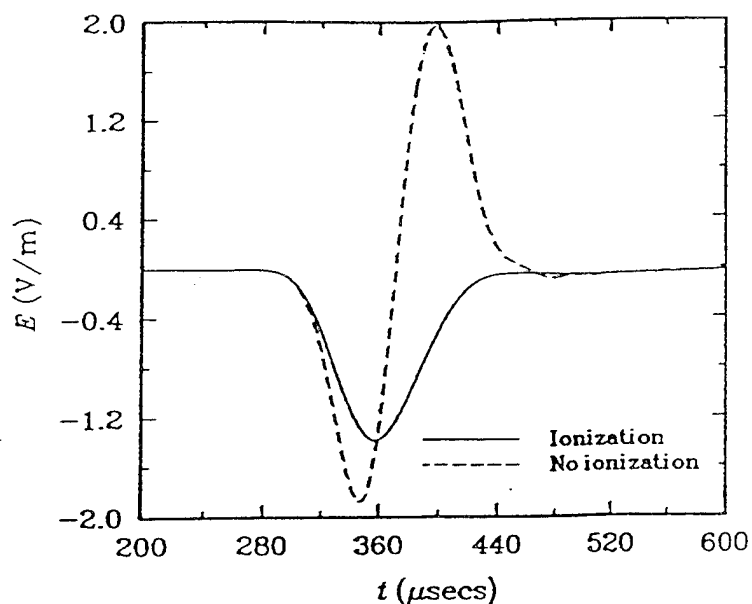


Figure 5.  $E$  versus time at 100 km altitude with ionization (solid line) and without ionization (dashed line). Only the leading edge propagates to higher altitude when an ionization patch forms.

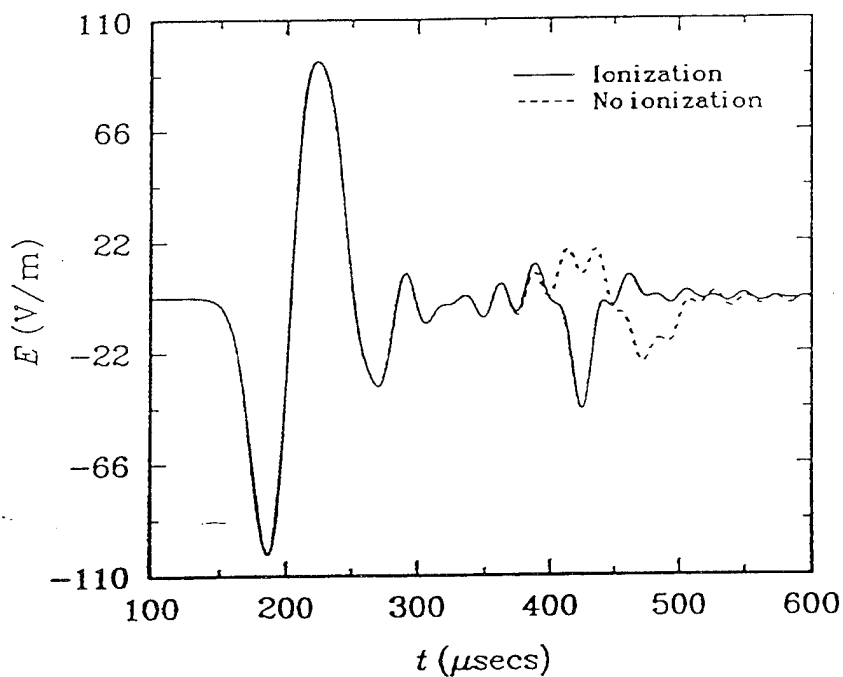


Figure 3.  $E_x$  versus time at 46 km altitude above the lightning discharge with (solid line) and without (dashed line) self consistent ionization. Enhanced ionization causes a strong reflected pulse from the trailing edge of the EMP.

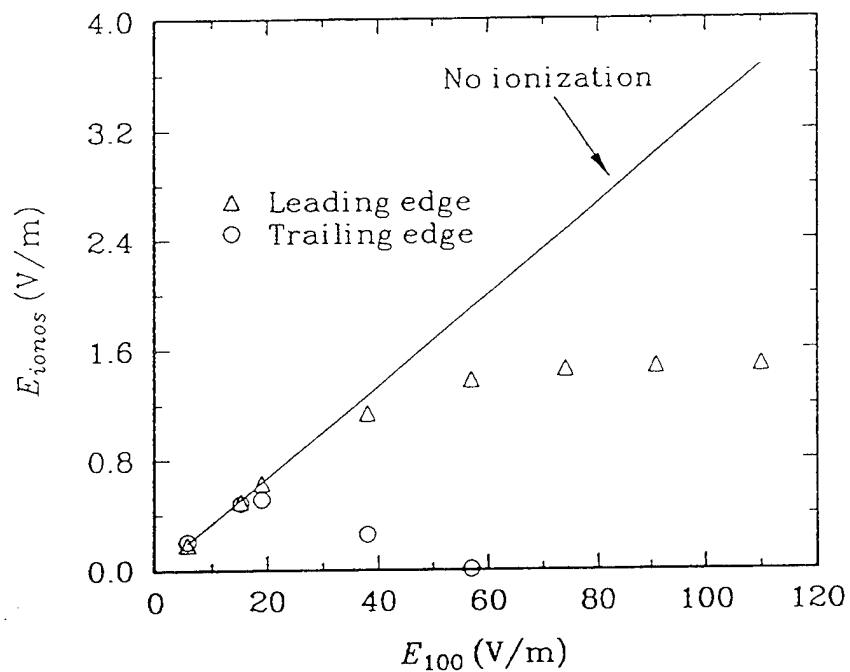


Figure 6. The amplitude of the leading edge of the EMP pulse (triangles) and the trailing edge (circles) as a function of normalized pulse strength. The straight line shows amplitude of the pulse with only initial ambient ionosphere. As the EMP exceeds breakdown threshold, first the trailing edge is reduced and then the leading edge reaches a maximum.

ABS ( $E_z$ )  
70 km altitude directly above discharge

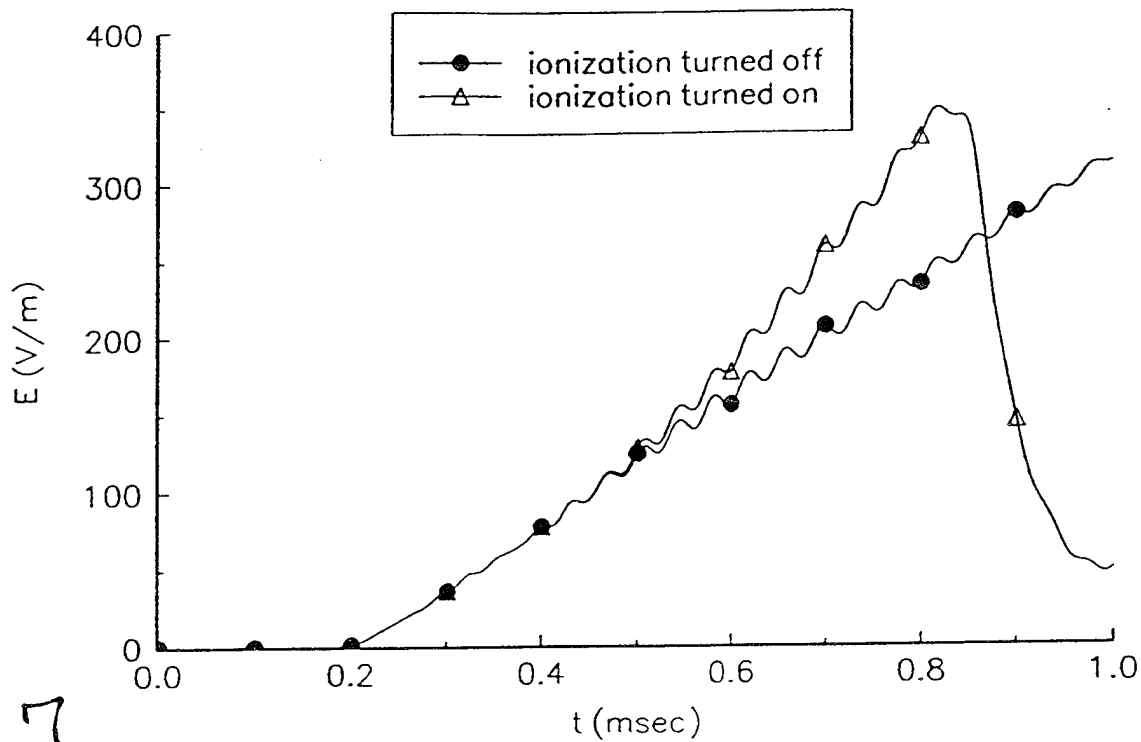


Fig 7

Vertical Electric Field Above Discharge  
 $t = 1$  msec;  $Q = 210$  C

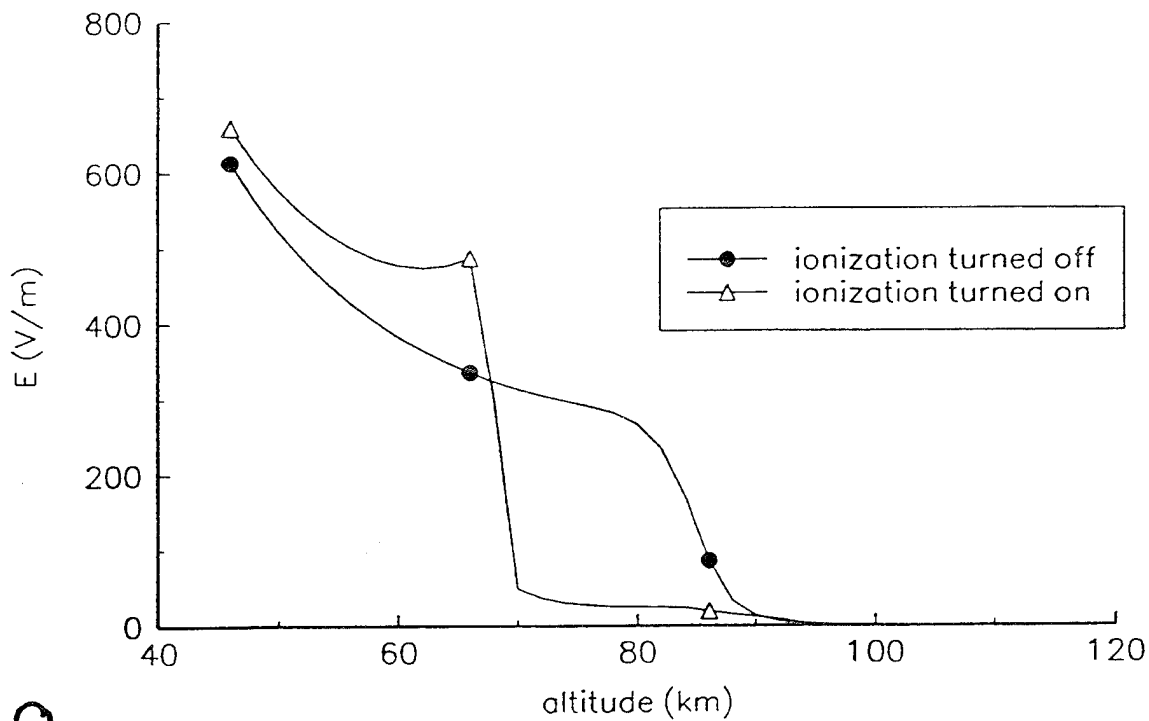
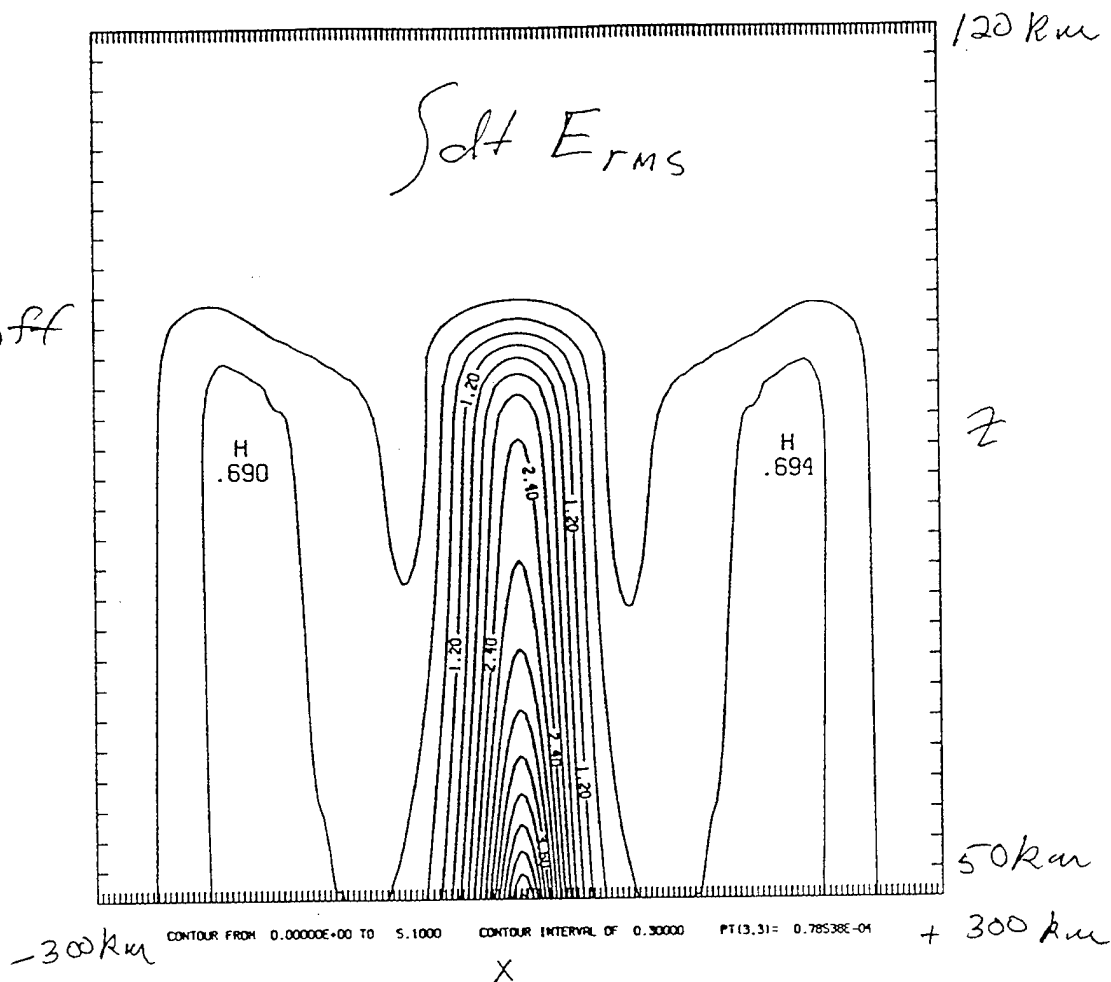


Fig 8

ionization  
turned off



ionization  
turned on

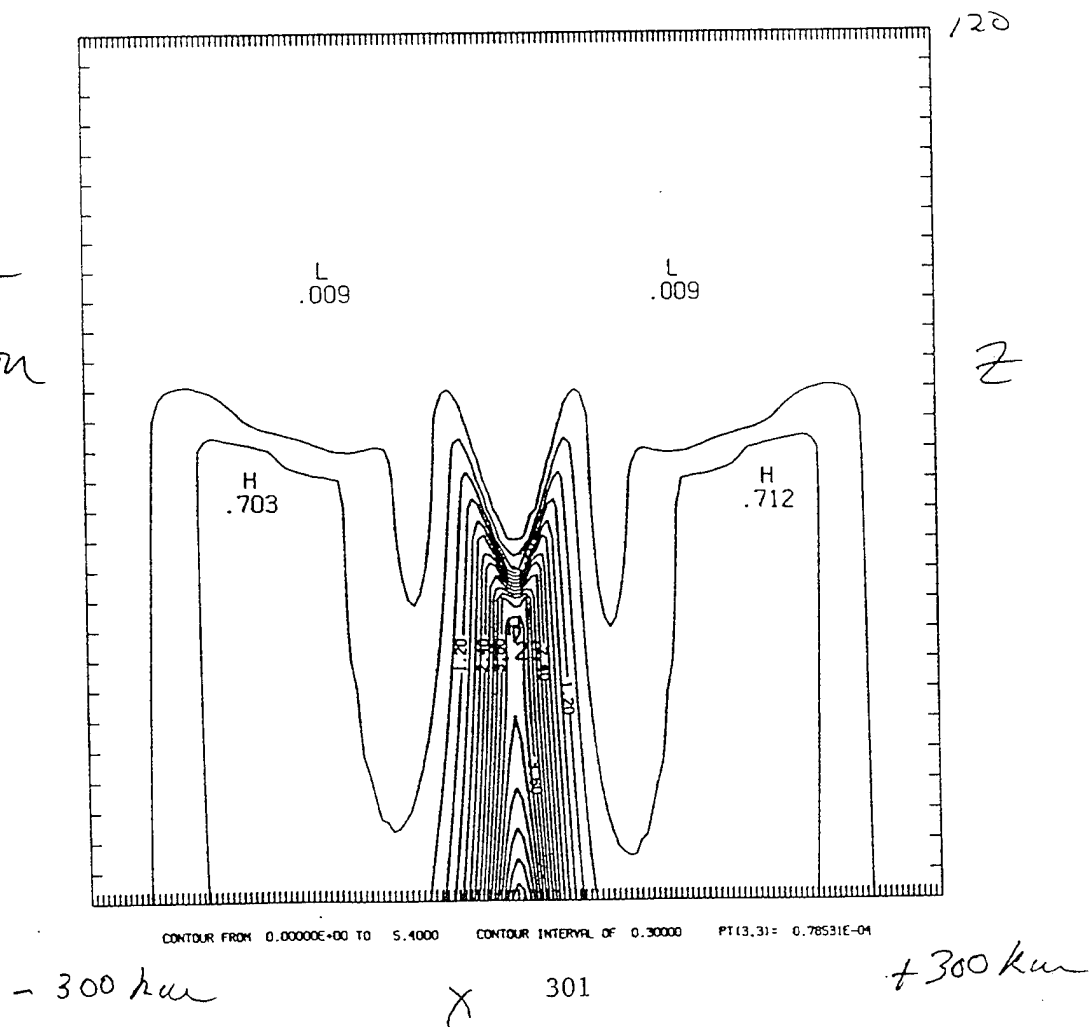
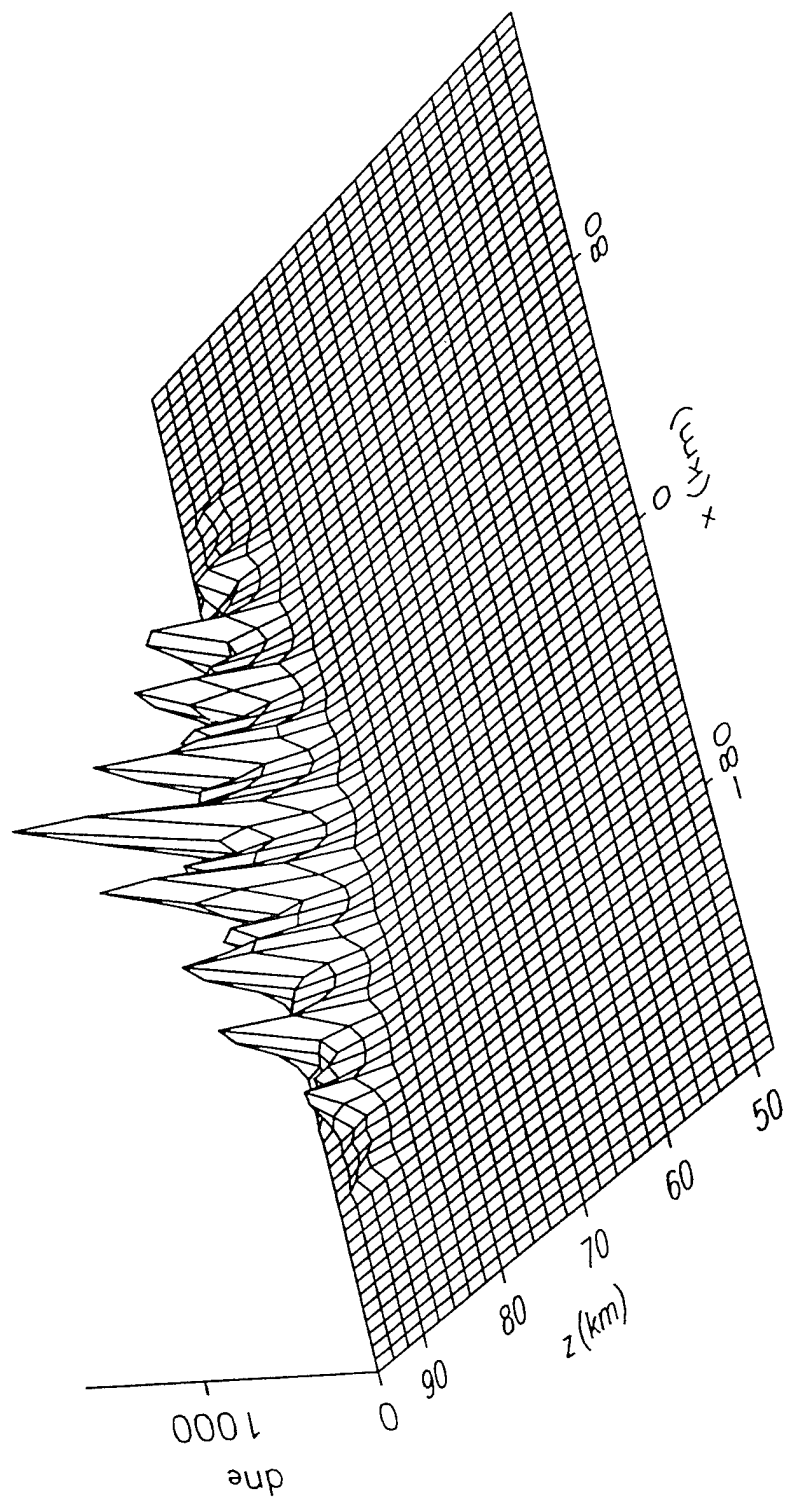


Fig 9

## Neutral density fluctuations

The ionization rate is sensitive to the neutral density. The ionization depends exponentially on the ionization rate which will amplify any neutral density variation. Therefore one possible source of the structure seen in elves and sprites may gravity waves. The following figure (Rowland, et al. submitted JGR, 1995) shows how a gravity wave (modelled as a horizontal sine wave) changes the ionization shown in 2a. The wavelength is determined by the wavelength of the gravity wave. For this example a 10% variation in the neutral density cause a variation between 3 and 4 in the ionized density .



## Conclusions

1) The EMP of the pulse forms ionization patches that are wide (100's km) in the horizontal direction and restricted in altitude between 70- 90 km (Rowland, et al. GRL, 361, 1995; Rowland, et al., submitted JGR, 1995). These characteristics fit ELVES.

Since the airglow only exists while the electric field is present, they are brief ( 0.1 msec). Because of the short lifetime, breakdown must occur to explain the strength of the airglow.

2) The QS fields grow if there is a continuing current. When  $Q > 60$  C, the maximum ionization due to the QS can become greater than that due to the EMP. The altitude of the QS ionization can extend slightly above the EMP ionization. As  $Q$  increases, the region of ionization extends to lower altitudes (55 km) and becomes narrower in the horizontal direction. In the simulations, the widths decrease to the cell size. The vertical altitude extends from 90 to 55 km. The horizontal size goes from 50 km at 80 km altitude down to a few km at 55 km altitude. These characteristics fit SPRITES.

As with the ELVES airglow, strong SPRITE airglow requires an E field. Since the enhanced conductivity shorts out the field internal to the SPRITE, it could be only the outer shell that radiates.

3) To form ELVES requires a large  $I_{\max}$ . This favors positive-to-ground discharges. Even if negative-to-ground and positive- to- ground discharges have the same  $\partial I/\partial t$ , the positive EMP will be longer in time and cause more ionization. Horizontal currents have a threshold current roughly half of that required for a vertical discharge. For a SPRITE to form requires a continuing current that can generate a large  $Q$ . This favors a positive-to-ground, vertical discharge.

Depending upon  $I_{\max}$ , the duration of the continuing current, and the orientation of the discharge, one can observe an ELF and a SPRITE or one and not the other. If both are present the ELF should appear first.



# **Runaway Breakdown in the Presence of Magnetic Field**

**A.V. Gurevich\*, J. A. Valdivia, G. M. Milikh, and K. Papadopoulos**

**Departments of Physics and Astronomy  
University of Maryland  
College Park, Maryland 20742**

**9 October 1995**

---

\*On leave from P.N. Lebedev Institute of Physics, Moscow 117924, Russia

—Observed  $\gamma$ -ray fluxes associated with runaway breakdown due to:

(i) Laminar electric fields following lightning discharges (Taranenko et al., 1993; Roussel-Dupre et al., 1994; Pasko et al., 1995)

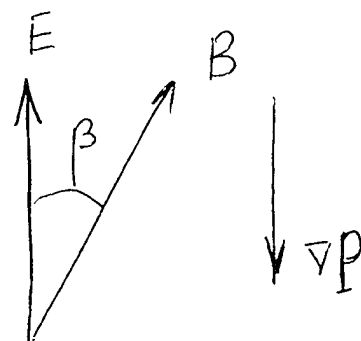
(ii) AC fields due to intracloud lightning discharges (Milikh et al., 1995; Rowland et al., 1995)

—Analysis up to day neglected the presence of  $B$ , and atmospheric density gradients.

—At high altitude the geomagnetic field could sufficiently influence the runaway process, since the gyrofrequency of high energy electrons becomes higher than their collision frequency.

—We present here analysis that includes the role of  $B$ . Restrict to-day to laminar fields. Analysis of AC fields ongoing.

## Main Results



—For  $80^\circ < \beta \leq 90^\circ$  the magnetic confinement occurs.

Runaway threshold is defined by the magnetic field.

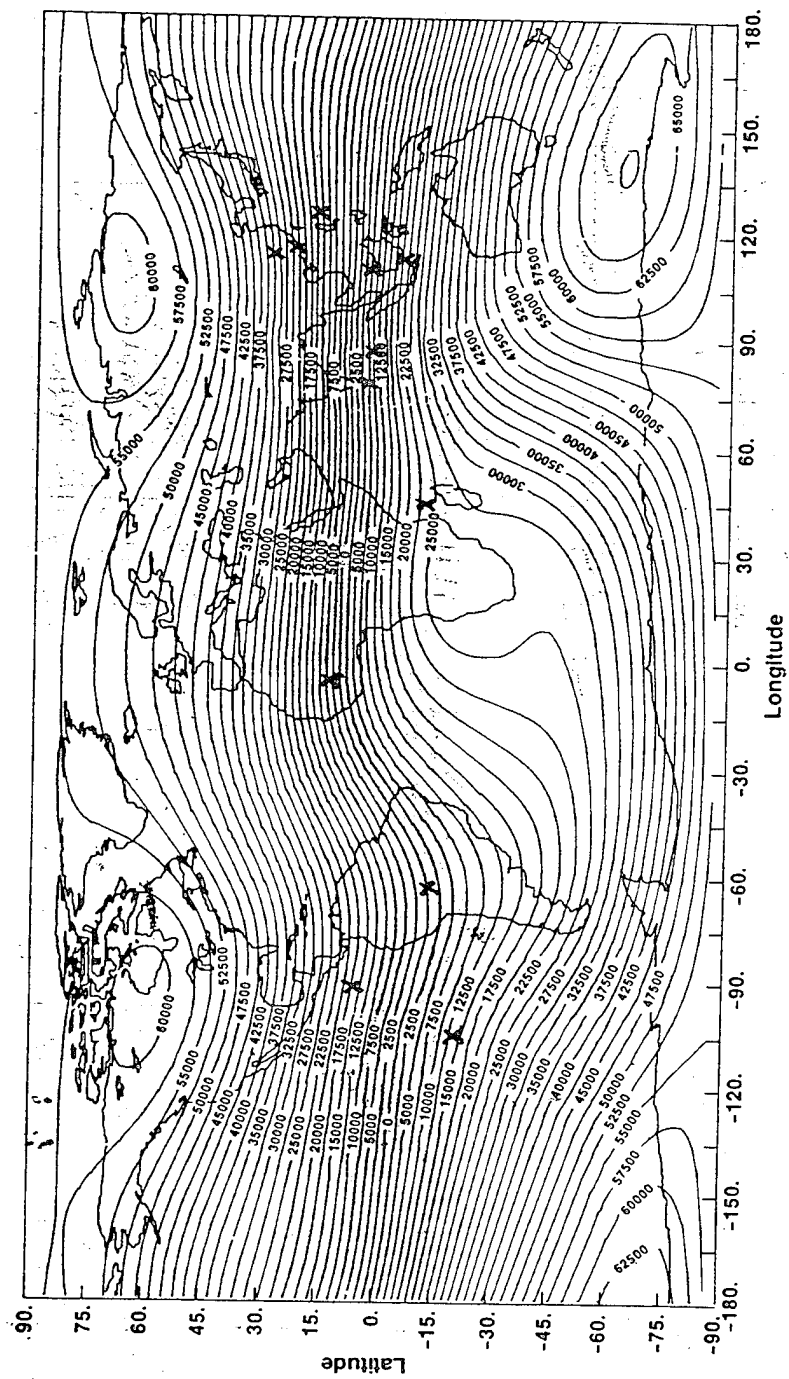
Process is independent on density gradient.

—For  $0 \leq \beta \leq 60^\circ$  the discharge is driven by the  $E \times \cos \beta$  component.

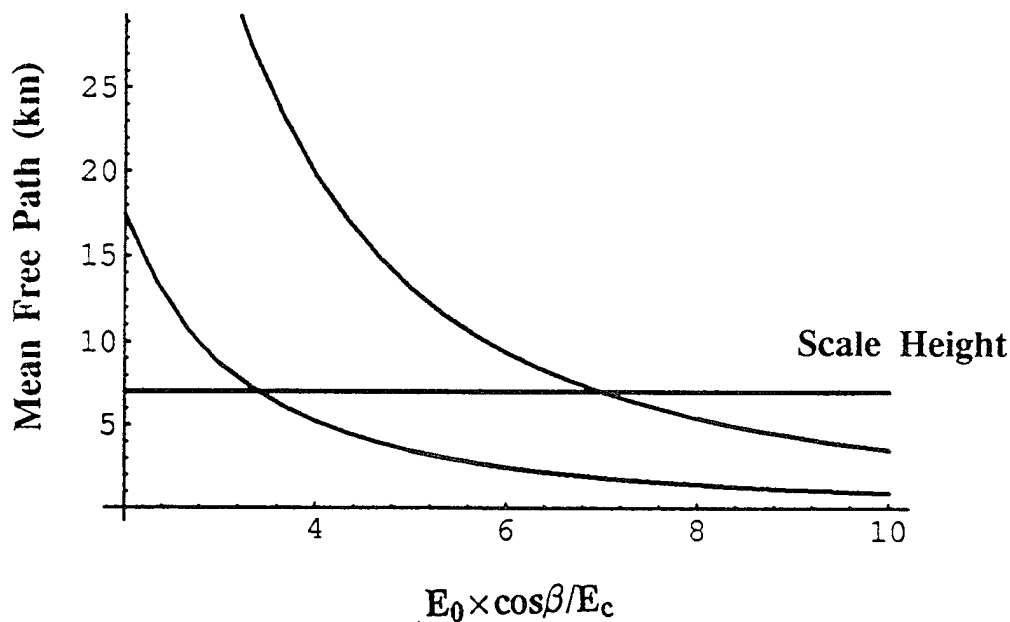
The magnetic field reduces cross-field diffusion of runaway electrons.

Filaments along E field could appear.

—For  $60^\circ < \beta \leq 80^\circ$  is the transient range.



Role of  $\nabla N$  on  $0 < \beta \leq 60^\circ$  case



Inhomogeneity increases threshold  
of the runaway breakdown at  $\geq 7150 \text{ km}$

## Runaway Acceleration

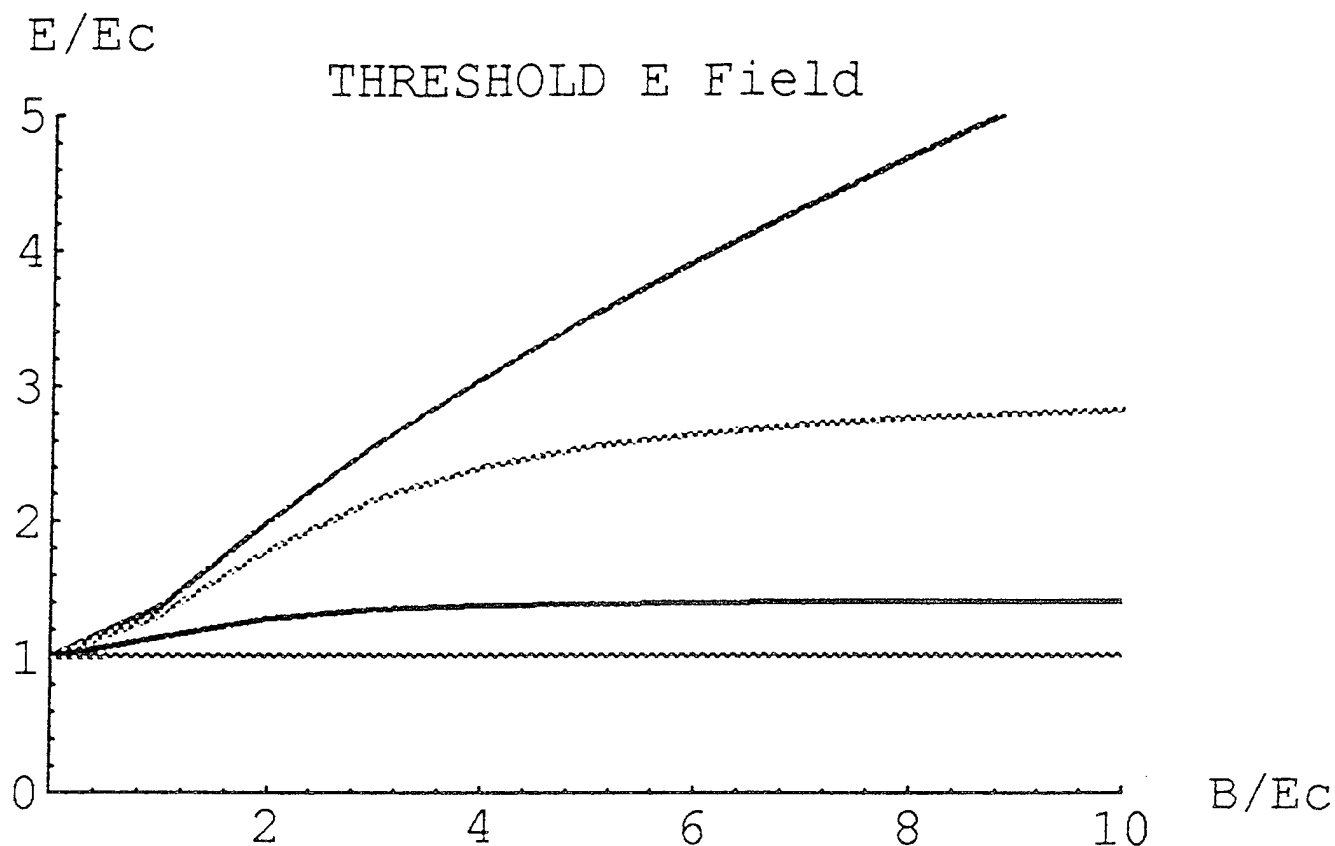
The equation of motion

$$\frac{d\mathbf{p}}{dt} = e\mathbf{E} - \mathbf{F}_D \quad B = 0$$

$$\frac{d\mathbf{p}}{dt} = e\mathbf{E} + \frac{e}{mc\gamma}(\mathbf{p} \times \mathbf{B}) - \mathbf{F}_D, \quad B \neq 0$$

$$\nu = F_D/p$$

- Obtain stationary solution and runaway threshold.
- Study phase space to find regions of runaway acceleration.
- Find ionization rate for runaway electrons.



The height at which the runaway breakdown increases to the point of conventional breakdown.

This happens when the value of the critical electric field  $\delta_{c0}(\eta_0)$  reaches the threshold of the conventional air breakdown  $\delta_{c0}(\eta_0) \simeq 10$ .

For instance, in  $E \perp B$  fields it corresponds to magnetic field  $B/Ec \simeq 27$ . In Gaussian units:

$$\frac{9 \text{ kV/m} \times B/0.3 \text{ G}}{220 \text{ kV/m} \times P(\text{atm})} = 27.$$

For a middle latitude  $B \simeq 0.3 \text{ G}$ , this gives  $p = 1.5 \times 10^{-3} \text{ atm}$ .

Thus at  $z > 65 \text{ km}$  the conventional breakdown dominates over the runaway if  $\beta > 80^\circ$ .

### 3. The Electron Runaway Boundary

Equation of the electron motion:

$$\frac{d\tilde{p}_x}{d\tau} = \delta_0 + \frac{\eta_0}{\gamma} \tilde{p}_y \sin \beta - \frac{\Phi(\gamma)}{\sqrt{\gamma^2 - 1}} \tilde{p}_x,$$

$$\frac{d\tilde{p}_y}{d\tau} = -\frac{\eta_0}{\gamma} \tilde{p}_x \sin \beta + \frac{\eta_0}{\gamma} \tilde{p}_z \cos \beta - \frac{\Phi(\gamma)}{\sqrt{\gamma^2 - 1}} \tilde{p}_y,$$

$$\frac{d\tilde{p}_z}{d\tau} = -\frac{\eta_0}{\gamma} \tilde{p}_y \cos \beta - \frac{\Phi(\gamma)}{\sqrt{\gamma^2 - 1}} \tilde{p}_z,$$

$$\gamma = \sqrt{1 + \tilde{p}_x^2 + \tilde{p}_y^2 + \tilde{p}_z^2},$$

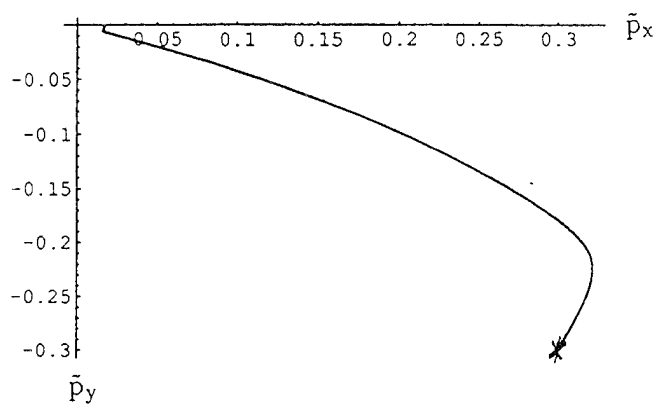
The dimensionless momentum  $\tilde{p}_{x,y,z} = p_{x,y,z}/mc$ ,  $\tau$  is the dimensionless time and  $\beta$  is the angle between **E** and **B**.

Equations were integrated numerically. Results of the computation are discussed separately for:

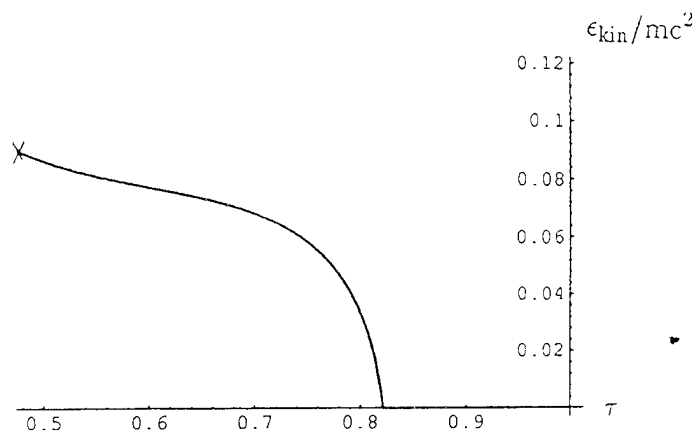
1.  $\mathbf{E} \perp \mathbf{B}$ , i.e.  $\beta=90^\circ$ . In this case the momentum is fading along the axes  $z$ , so essentially electrons are moving in the  $x$ - $y$  plane.

2.  $\mathbf{E} \parallel \mathbf{B}$ , i.e.  $\beta=0$ .

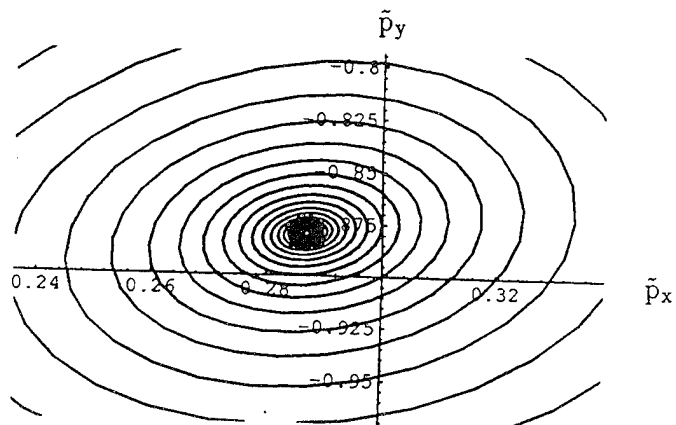
3. Arbitrary  $\beta$ .



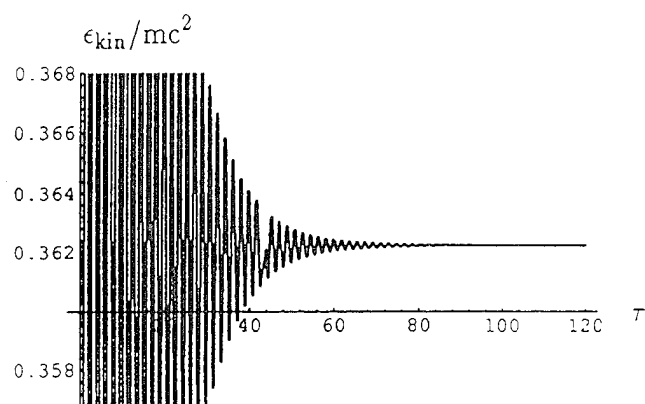
a)



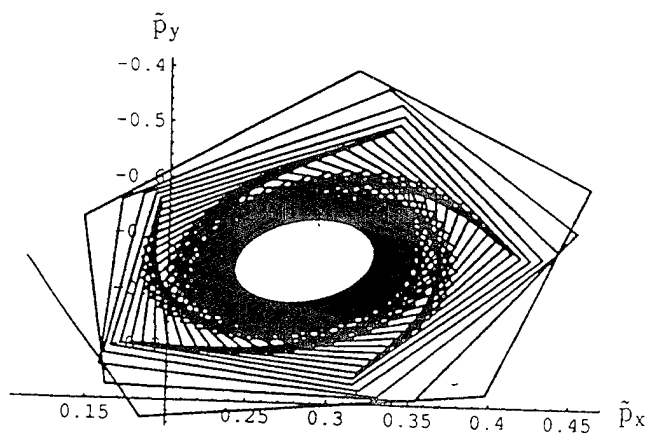
b)



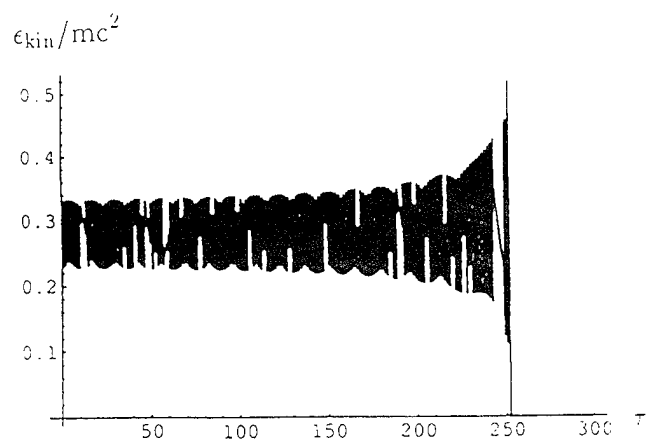
a)



b)



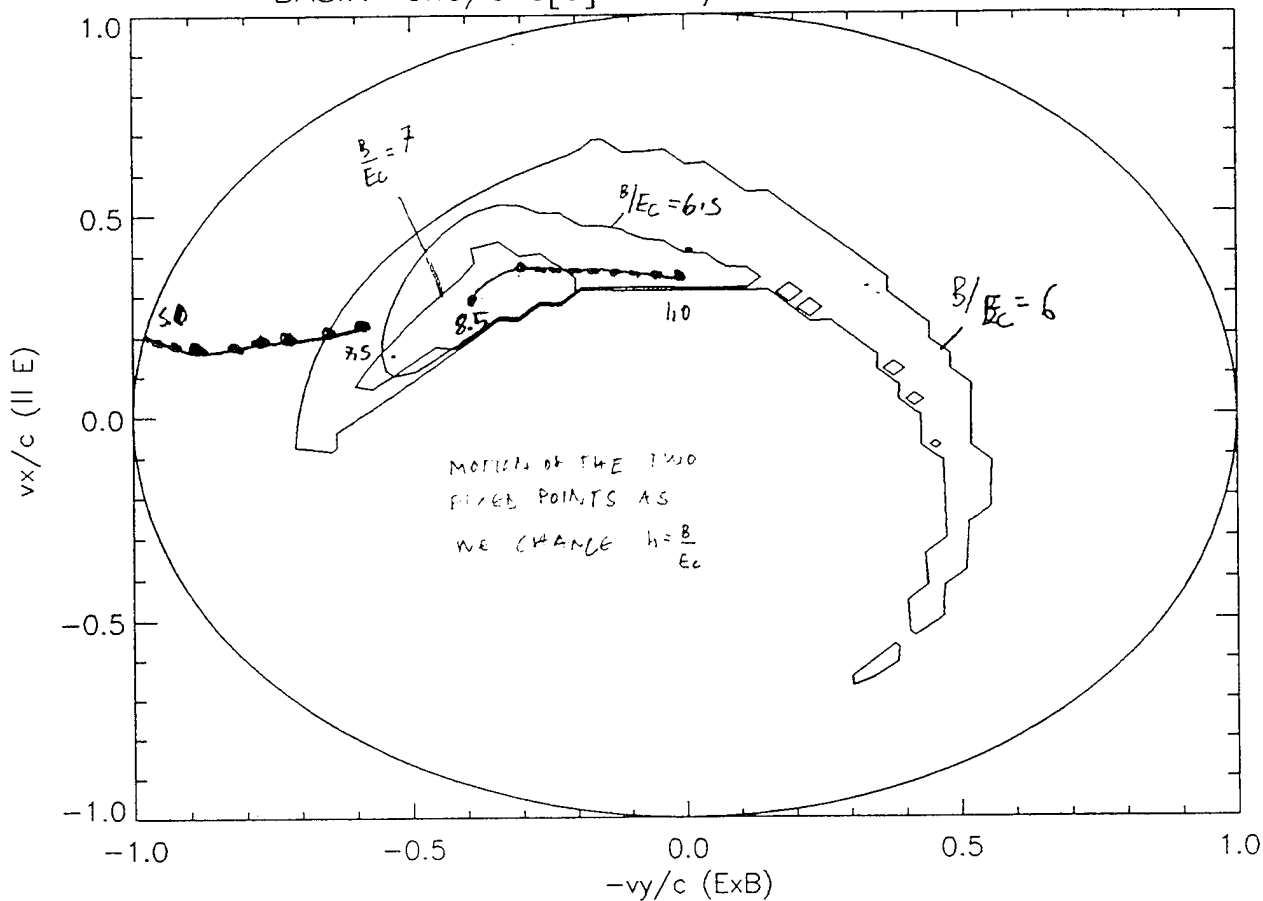
a)



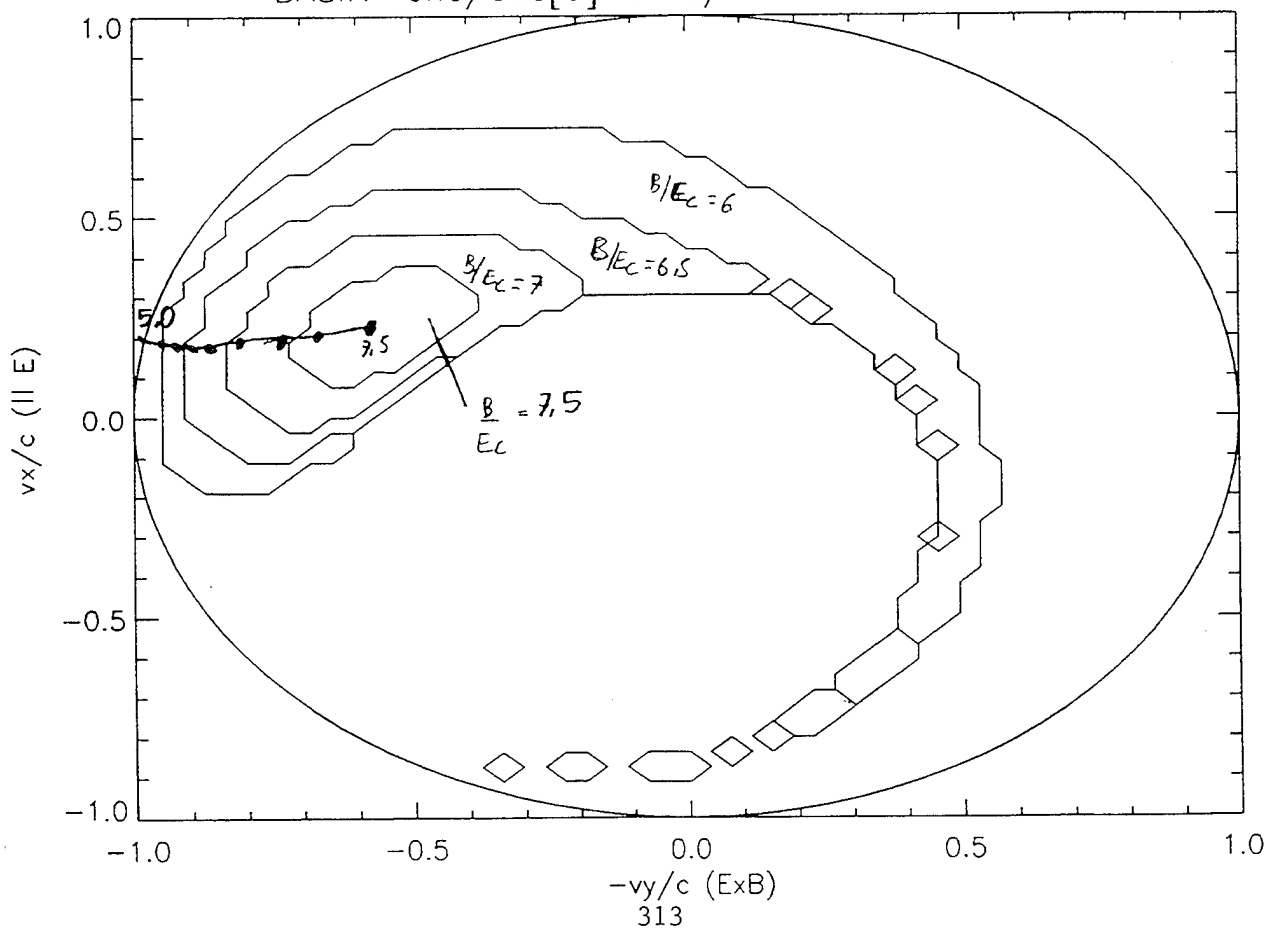
b)



BASIN ene/ene[0]=2 E/Ec= 5.00 tho= 90.



BASIN ene/ene[0]=0 E/Ec= 5.00 tho= 90.



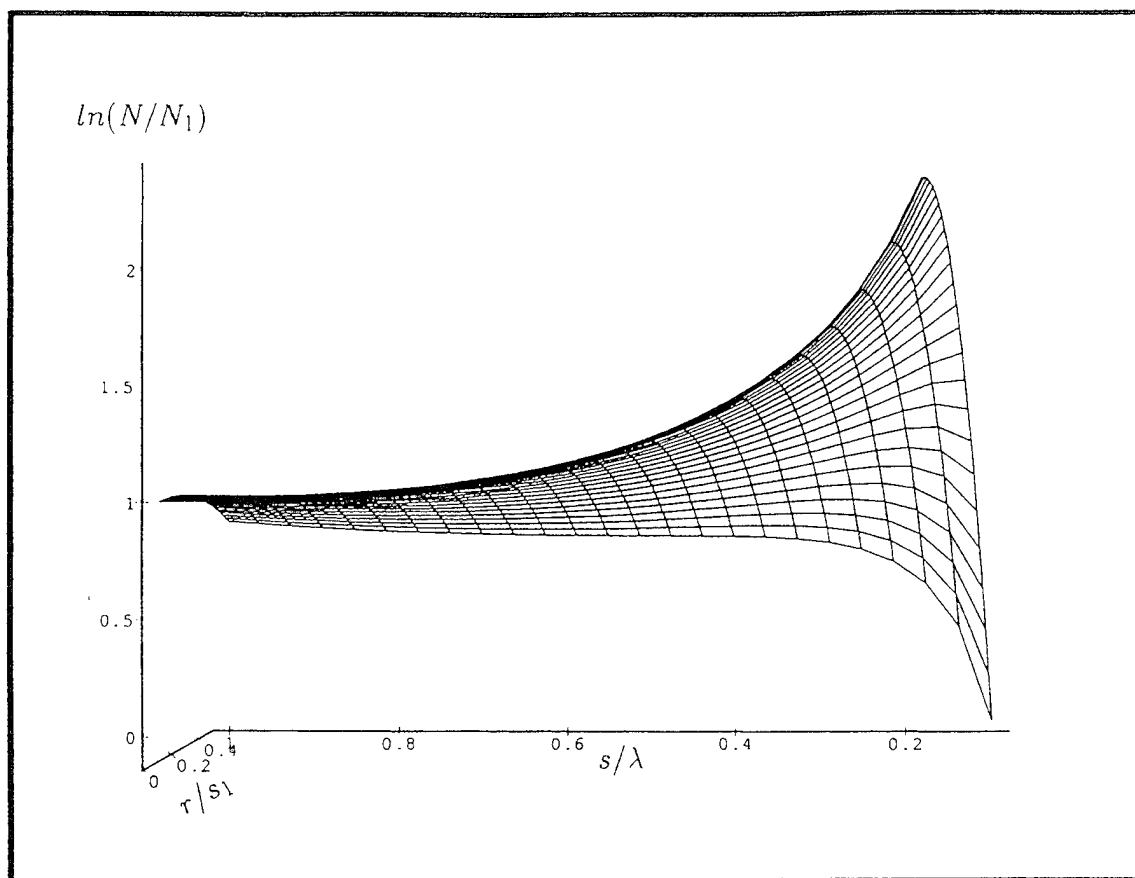
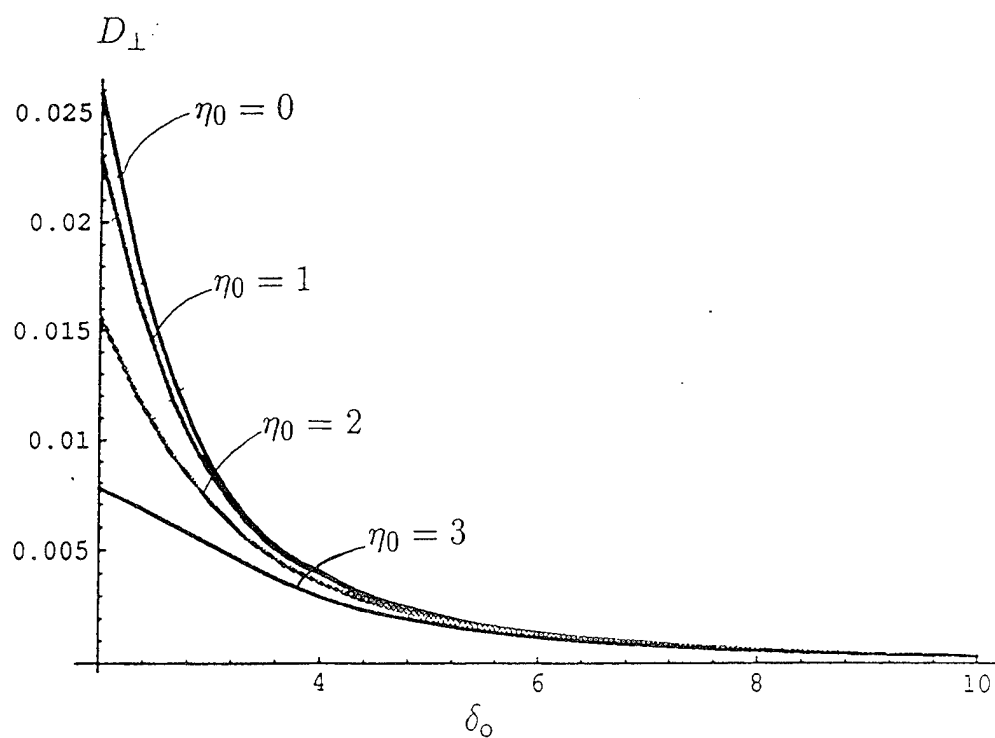
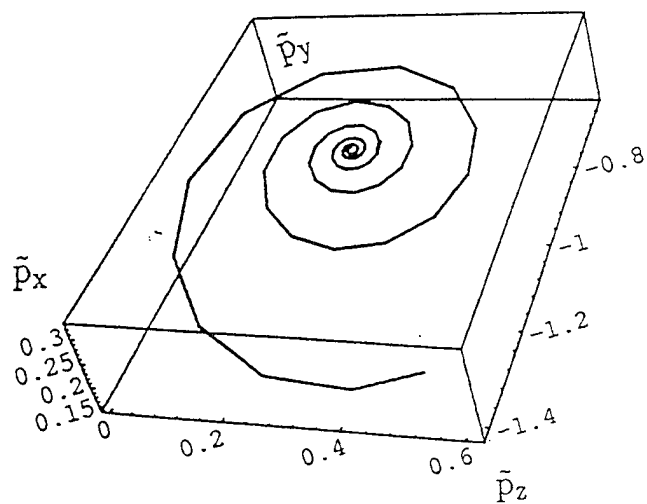


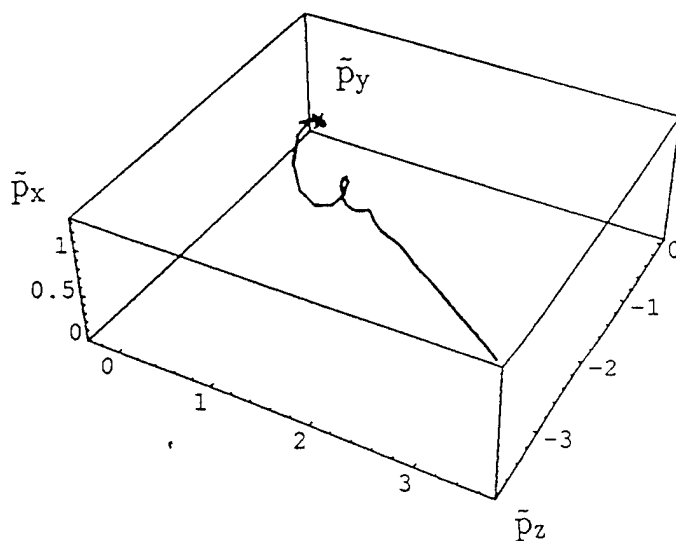
Fig 7





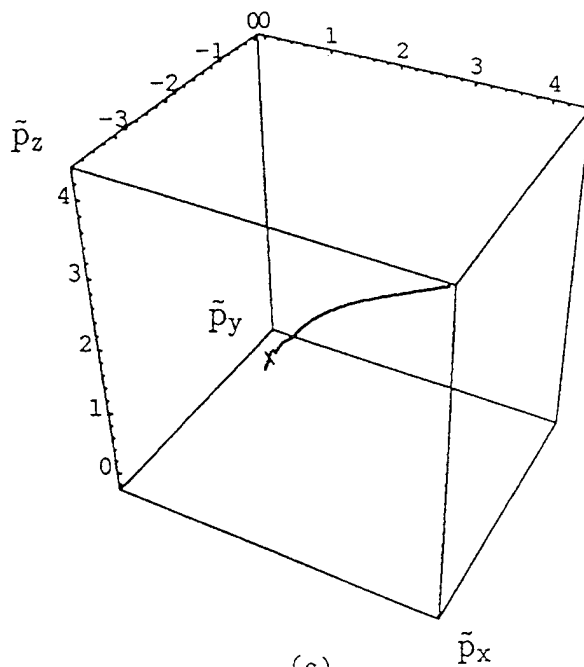
(a)

$$\beta = 85^\circ$$



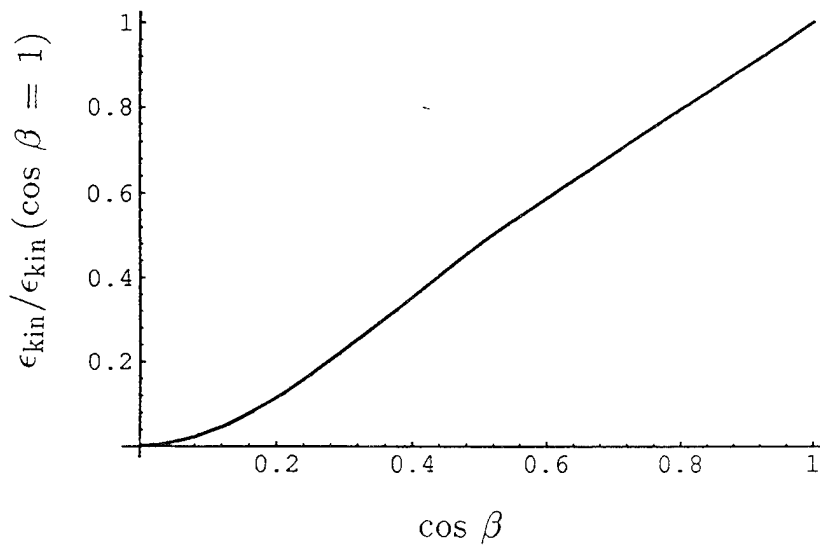
(b)

$$\beta = 80^\circ$$



(c)

$$\beta = 60^\circ$$



## Conclusions

- Physics of the runaway discharge in laminar E, B fields is determined by the angle  $\beta$  between E and B, and by their ratio E/B.

- Three different ranges of the angle  $\beta$  were distinguished:

$80^\circ < \beta \leq 90^\circ$  the runaway discharge develops only if the ratio E/B is less than a certain critical value; the runaway electrons reach a steady state. At high altitude the runaway discharge merges into conventional breakdown.

$0^\circ < \beta \leq 60^\circ$  the electrons moving along the direction of the magnetic field driven by a  $E \times \cos \beta$  component of the electric field, and gain the energy unlimitedly. The magnetic field manifests itself by pitching the runaway discharge.

$60^\circ < \beta \leq 80^\circ$  is the transient range. Electron trajectories are twisted by the magnetic field at low energy range. Electron then gains energy along a straight trajectory.

- Runaway separatrix is obtained, which separates momentum space into two regimes: those electrons which possess trajectories that take them into higher energies, and other electrons which possess trajectories leading to zero energy.

- Characteristic time required for the creation of a secondary runaway electron and the mean free path of the runaway electron are found.

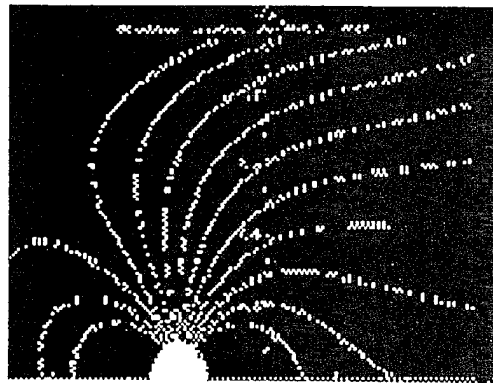
# On the Structure of the Red Sprites Lightning as a fractal antenna

J. Valdivia, K. Papadopoulos, G. M. Milikh

**S**PACE AND

**P**LASMA

**P**HYSICS



---

Dept. of Physics  
Dept. of Astronomy

UNIVERSITY OF MARYLAND, College Park, MD 20742

---

Supported by NSF grant

## HIGH ALTITUDE LIGHTNING

### OBSERVATIONS —> SPRITES!!

- Sentman et al. [1995]
- Winckler et al. [1994]
- Extreme structures
- Multiple scale lengths
- Resembles a fractal

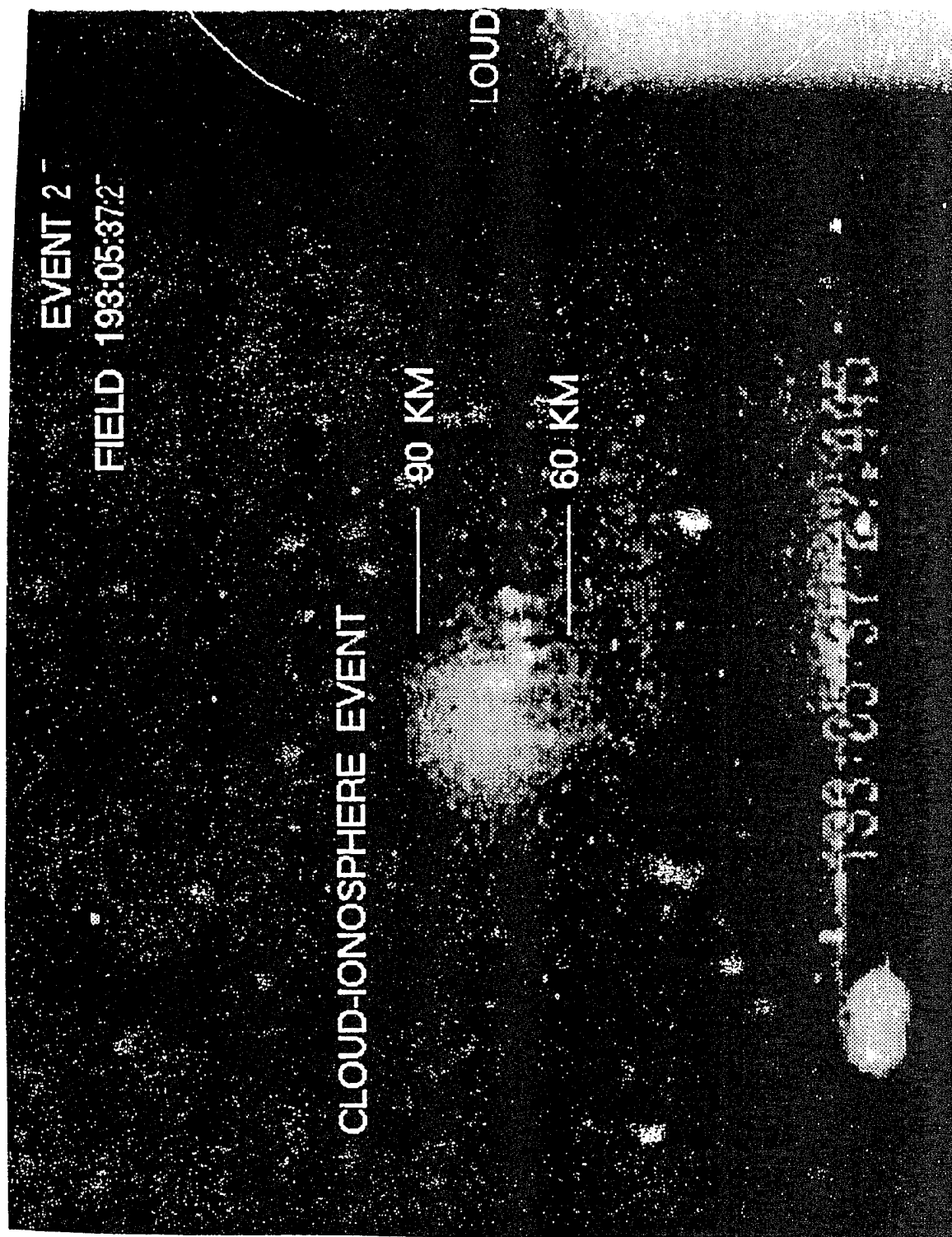
### THEORY —> SPRITES!!

G. Milikh, K. Papadopoulos, C. Chang, et al [1995]

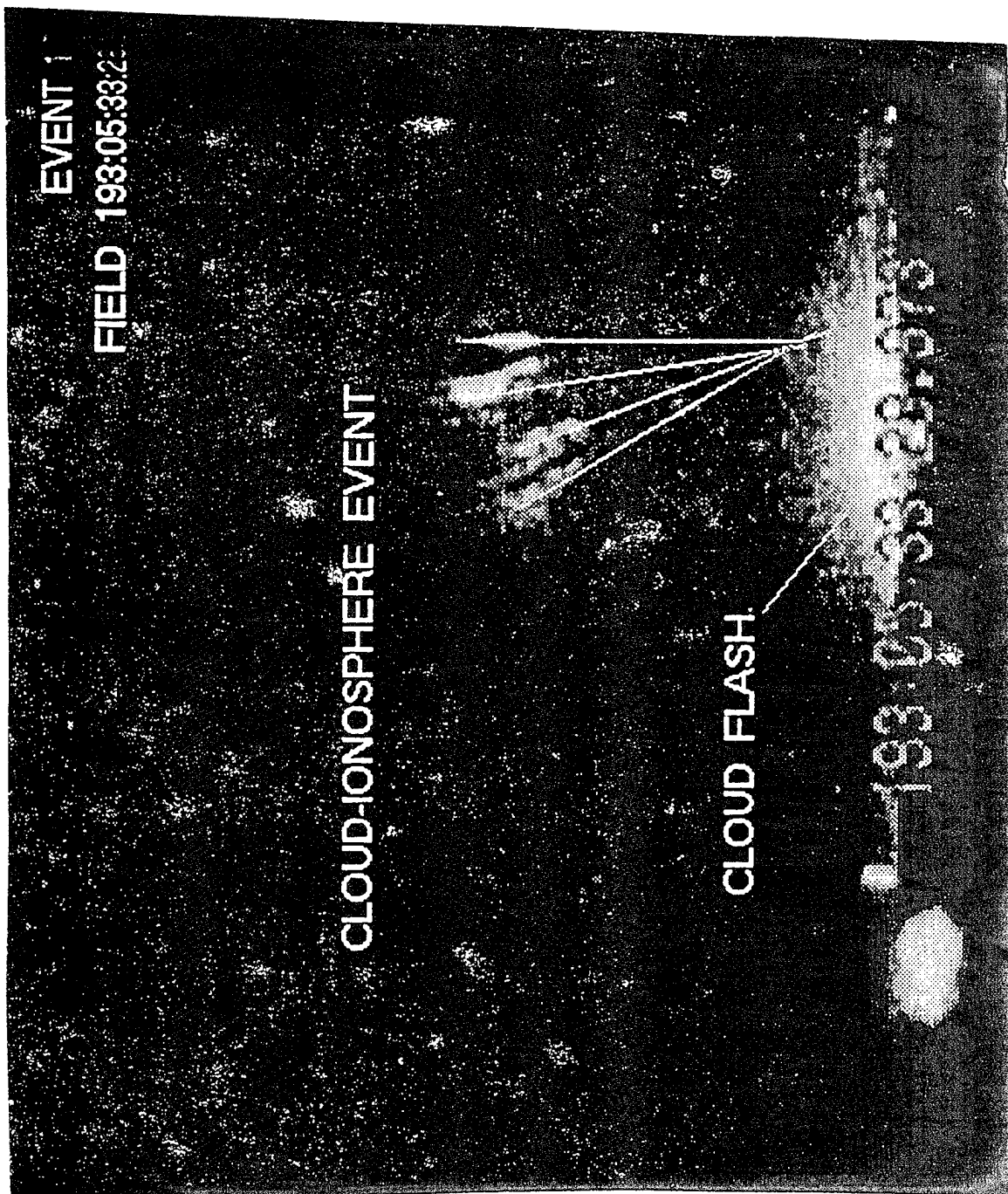
- Energetic tails of D-Region electrons
- Created by EMP fields due to

—> Horizontal intercloud discharge!!

(TWO CASES OF SPRITES)



- Winckler et al. [1994]



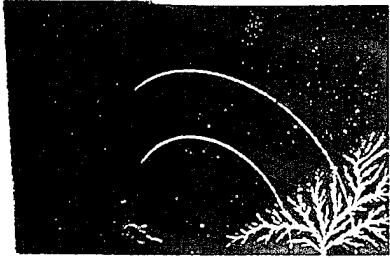
- Winckler et al. [1994]



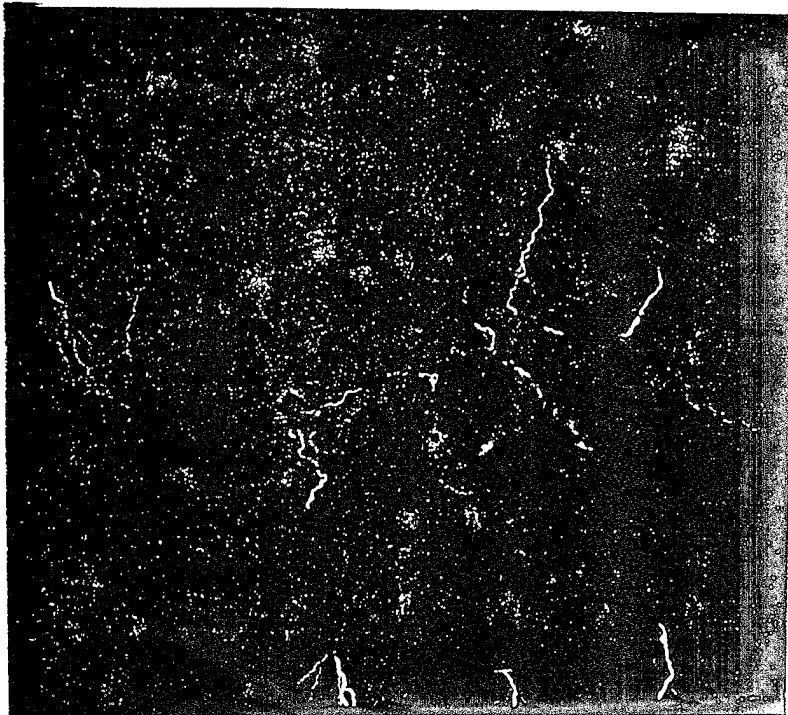
## HORIZONTAL DISCHARGES

- Spider Lightning
- Resemble Lichtenberg patterns
  - > Dielectric discharges
  - > Fractal with space filling properties
  - > Dimension  $\sim 2$

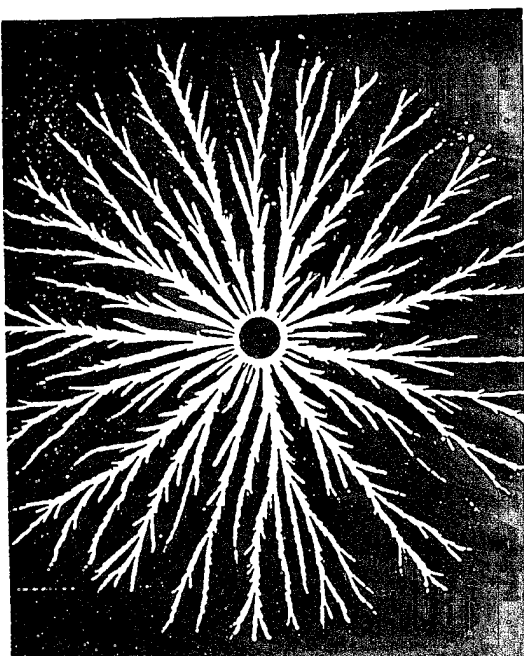
(LICHTENBERG PATTERN and LIGHTNING)



• Williams [1988]



• Williams [1988]



**LICHTENBERG**

What is the RELATION to cloud discharge?

- Discharge as a FRACTAL antenna array
- Characterization by a fractal dimension
- Radiation pattern depends on Dimension

Important gain

Fine scale structure

## RADIATION PATTERN

- Use hertz vector !

$$\Pi(x, w) = \sum_{\{\theta_o\}} \frac{i}{w} \int_0^L I(s, w) \frac{e^{ik\|x-r_r-l\|}}{\|x - r_r - l\|} dl \quad (1)$$

$$I(s, w) = I(w) e^{i\frac{w}{c}(r+l)}$$

$$B = -ik \nabla_x \Pi(x, w)$$

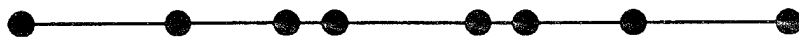
$$E = \nabla_x \nabla_x \Pi(x, w) \quad (2)$$

- Compute far field !
- Make a CANTOR set out of a ring  $\{\theta_o\}$

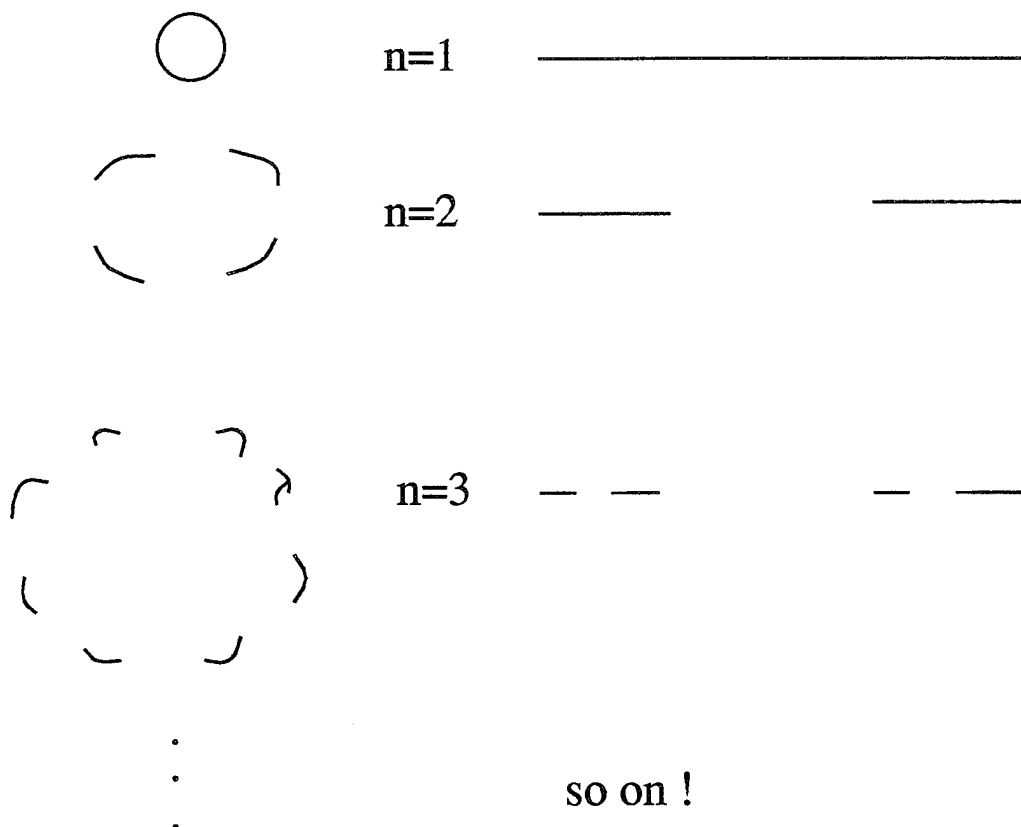
Specifies the dimension

Radially “peel” the cantor set

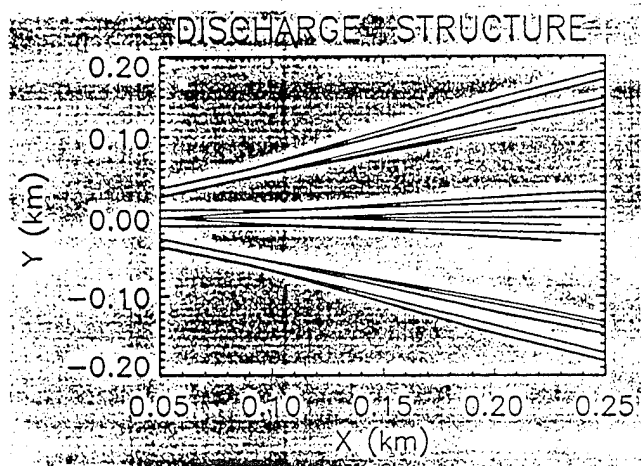
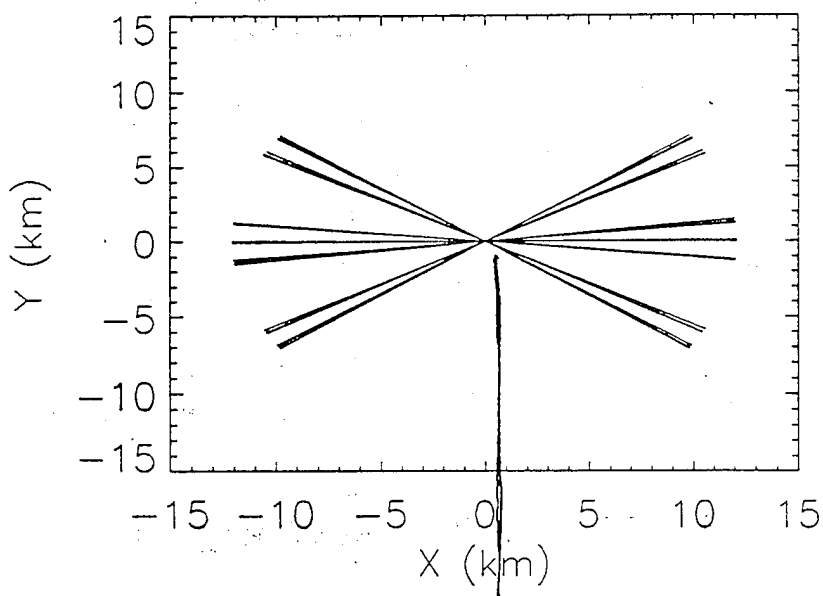
( CANTOR SET AND PEELING)



Line elements  $\rightarrow$  Fractal pattern  
Werner et al. [1995]

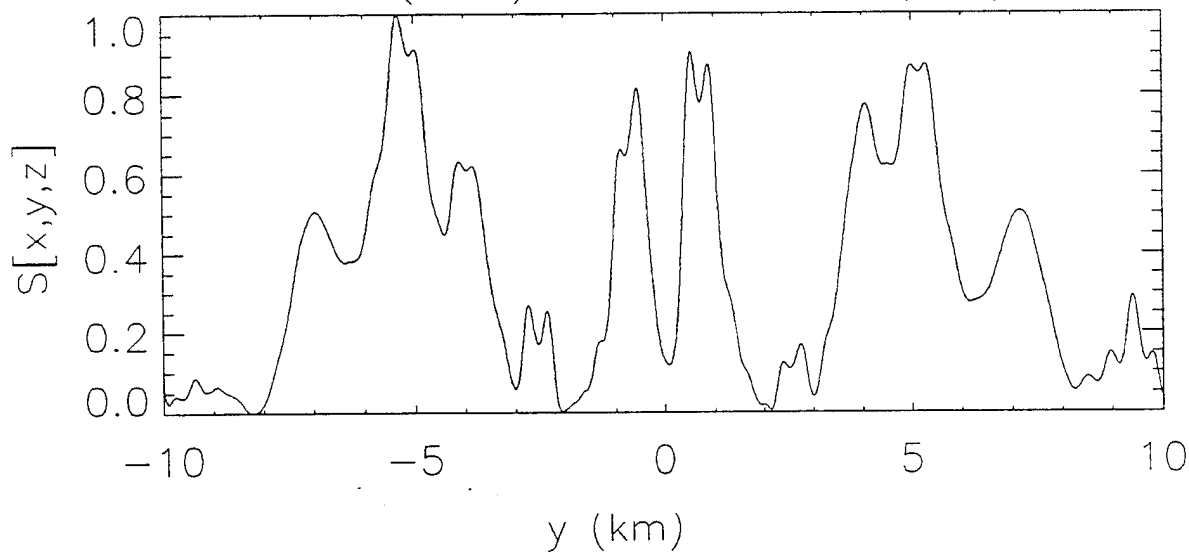


# DISCHARGE STRUCTURE

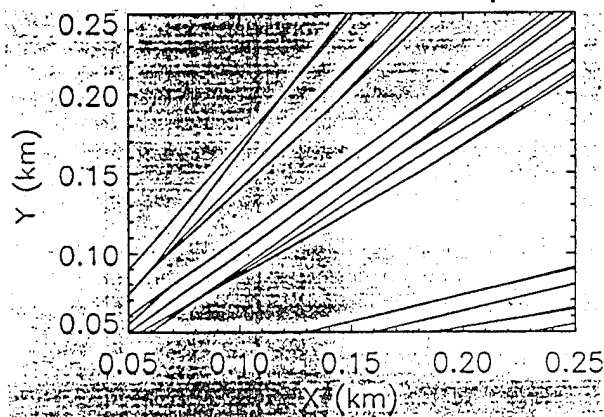
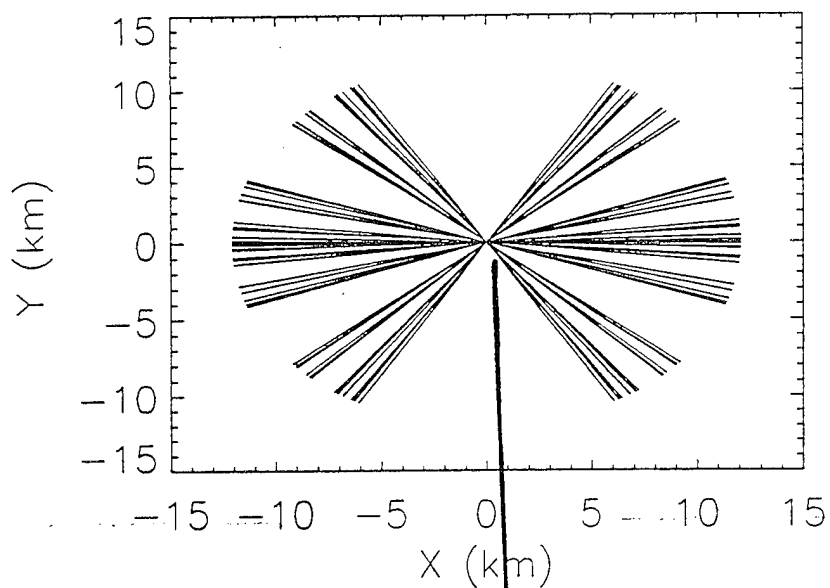


SMALL SCALE  
STRUCTURE

POINTING FLUX ( $E \times B$ )  $z=60. \text{ (km)}$   $x=4. \text{ (km)}$



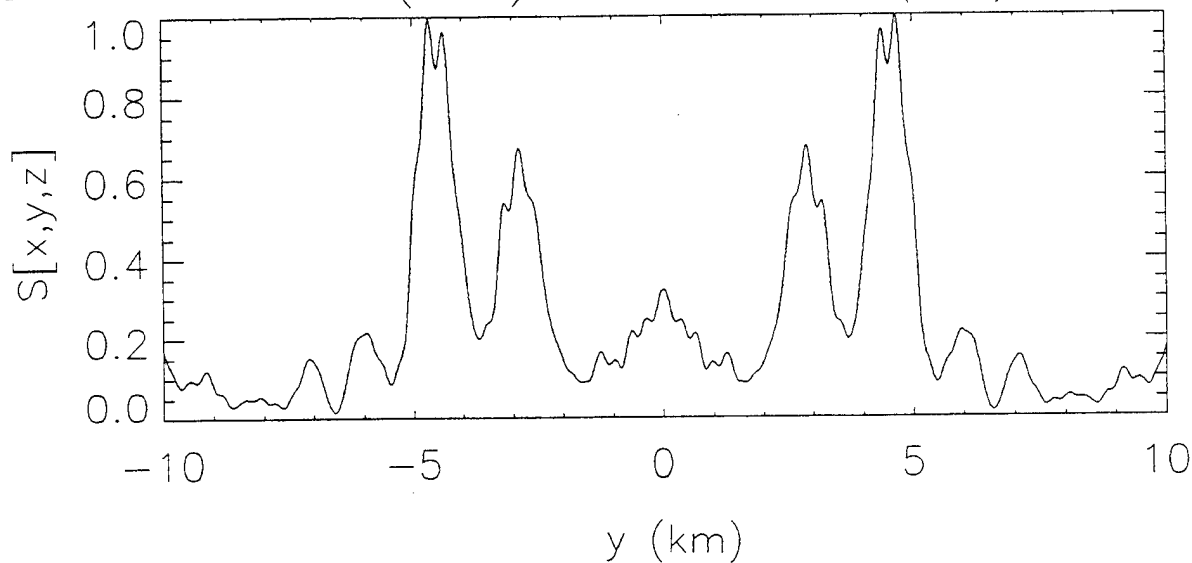
# DISCHARGE STRUCTURE



**SMALL SCALE  
STRUCTURE.**

POINTING FLUX ( $E \times B$ )

$z = 60. \text{ (km)}$   $x = 4. \text{ (km)}$



## DEPENDENCE ON DIMENSION

- Power density depends on dimension
- Gain depends on dimension

Large gain can be obtained

- Structure depends on dimension

Large scale

Small scale

- Large scale structure insensitive to details
- Controlled mainly by dimension  
—> General result !!

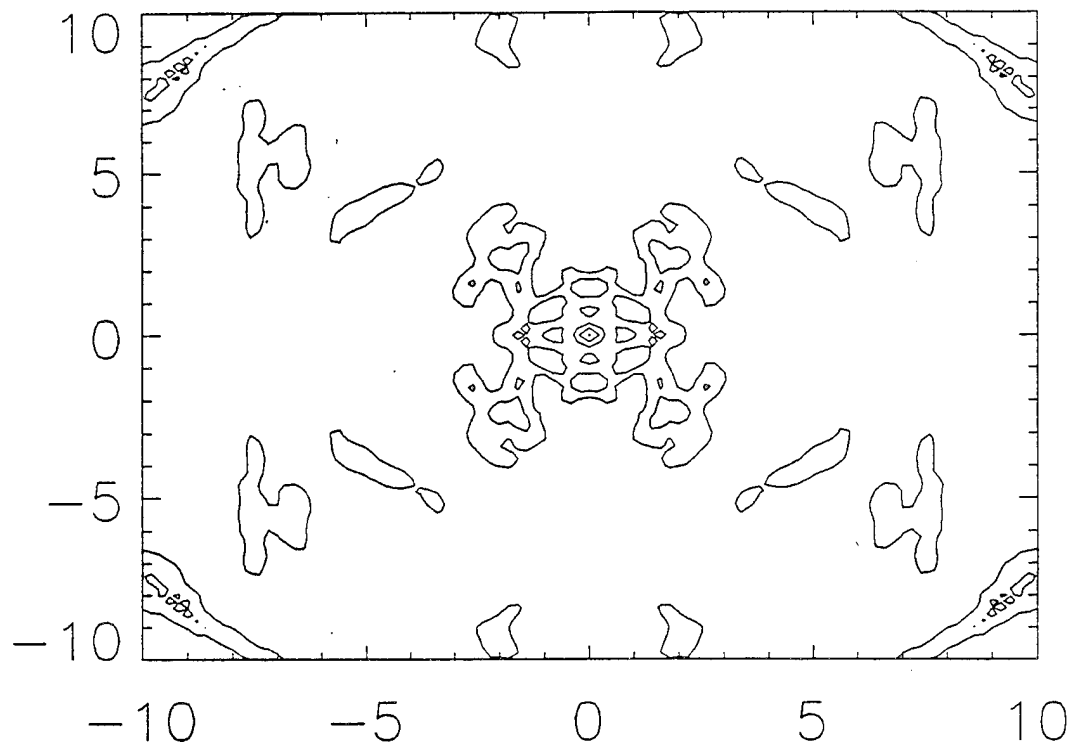
(CASES OF 2 DIMENSIONS with discharges)

POINTING FLUX ( $E \times B$ )

$z=60.$

$\alpha = 3/2$   
(CANTOR)

$y$  (km)

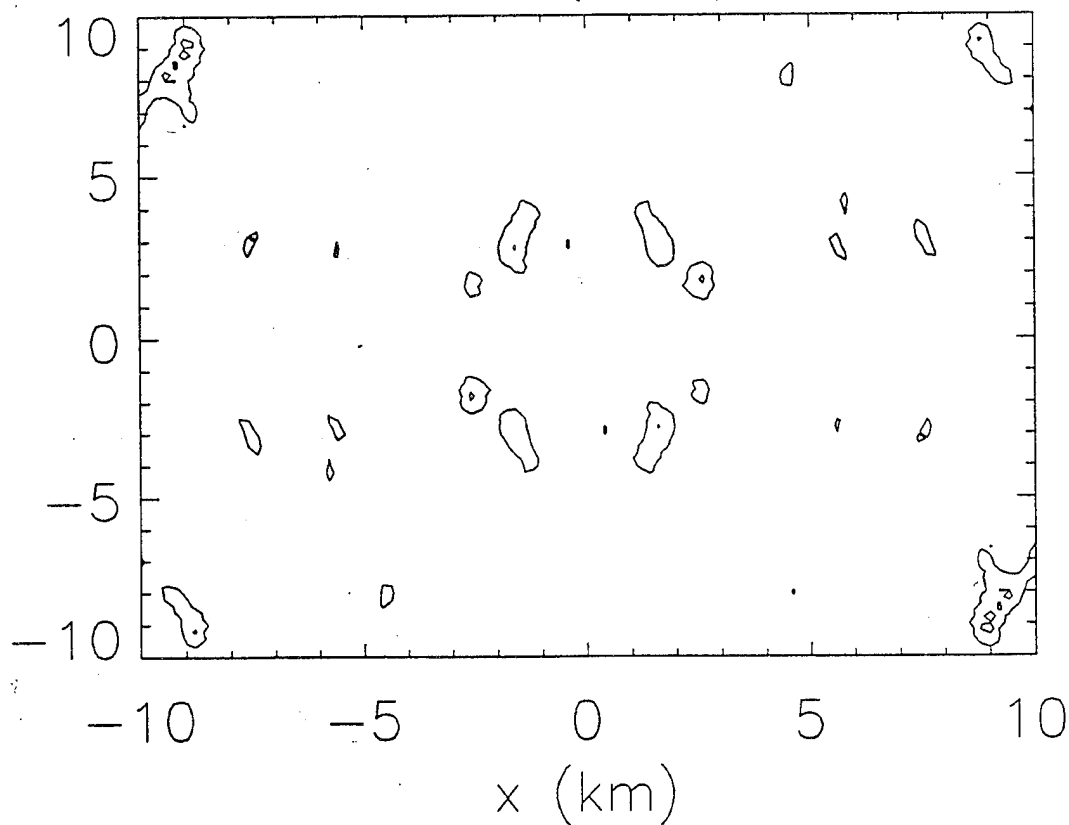


POINTING FLUX ( $E \times B$ )

$z=60.$

$\alpha = 5/2$

$y$  (km)





## HOW TO PROBE INTERCLOUD DISCHARGE?

- Direct correspondence between

Dimension of discharge  
radiation pattern that causes sprites

- Connection can be made concrete!!

FURTHER STUDY —> As a general problem

- study full spatio-temporal structures
- Match for near field also!
- Applications in communications

## CONCLUSIONS

- Radiation pattern due to horizontal discharge
- Associate with Sprites
- Dimension of discharge controls

Power gain

Large scale structure

- Large scale structure insensitive to details
- Only depends mainly on dimension
- Can be used as a probe to intercloud discharge

# Nonequilibrium Infrared Radiative Modeling - Application to Sprites

R.H. Picard, J.R. Winick, W.A.M. Blumberg, Phillips Laboratory / Geophysics,  
Bedford, Mass., USA

P.P. Wintersteiner, ARCON Corporation, Waltham, Mass., USA

R.A. Armstrong, J.A. Shorter, Mission Research Corporation, Nashua, N.H., USA

AFOSR / PL Workshop on Sprites & Blue Jets

Hanscom AFB

18-19 Oct 1995

## Nonequilibrium Infrared Radiative Modeling - Application to Sprites

R H Picard, J R Winick, W A M Blumberg (Phillips Laboratory, Geophysics Directorate,

Hanscom AFB, MA 01731)

P P Wintersteiner (ARCON Corporation, Waltham, MA 02154)

R.A. Armstrong, J.A. Shorter (Mission Research Corporation, Nashua, NH 03062)

Estimating infrared emission from atmospheric high-altitude lightning is complicated by the transient nature of the excitation process and by the multidimensionality of the ensuing radiative transfer. This is especially true for the 4.3- $\mu\text{m}$   $\text{CO}_2$   $v_3$ -mode rovibrational emission, due to a combination of the strength of the transitions, resulting in large opacities, and the slowness of the vibrational energy transfer to  $\text{CO}_2$  from the large  $\text{N}_2$  vibrational energy reservoir. Photon trapping occurs due to the self-absorption, lengthening the effective lifetimes of the radiating vibrationally-excited states and broadening the excitation region. As a result, the magnitude, the shape, and the effective relaxation time of the  $\text{CO}_2$  vibrational response vary strongly with altitude. We review briefly the nonequilibrium infrared radiative transfer problem in the quiescent and the disturbed atmosphere. Then we show how the ARC (Atmospheric Radiance Code) transient radiative model has been applied successfully to auroral emission data and indicate how it can be modified to predict 4.3- $\mu\text{m}$  emission from sprites. We discuss the input requirements to the radiative model, from data or from discharge models, and make preliminary predictions of 4.3- $\mu\text{m}$  spectral observations relevant to the forthcoming 1996 Summer Campaign.

## ***Outline -***

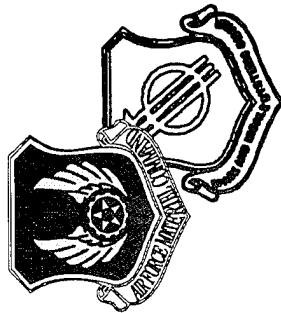
- Background
  - Infrared radiance models / codes
  - The nonequilibrium radiative transfer problem
  - CO<sub>2</sub> 4.3- $\mu$ m nonequilibrium radiance model
- Steady-state line-by-line model for quiescent atmosphere: CIRIS-1A earthlimb spectra
- Time-dependent band model for aurora - RBFWI auroral data
- Toward a sprites 4.3- $\mu$ m radiance model
  - Preliminary results
  - Implications for 1996 Summer Campaign
  - Model input needs
- Discussion / conclusions

## ***Application to Sprites***

- IR radiation modeling for sprites must deal with several complications:
  - Excitation process *transient*
  - *Multidimensional radiative transfer* (optically thick bands)
- These factors are most stressing for 4.3- $\mu\text{m}$   $\text{CO}_2(\nu_3)$  emission
  - Slow vibrational energy transfer from  $\text{N}_2(\nu)$  reservoir to  $\text{CO}_2(\nu_3)$
  - Large transition strength ---> large optical depths
- Consequences for 4.3- $\mu\text{m}$  sprites:
  - Time-dependent (*transient*) effects important
    - Steady-state band model (SSBM) not adequate
  - *Radiative transfer* affects both excitation & loss
    - Optically thin, opaque, & escape-function approximations (EFA) not adequate

# ***IR Emission from High-Altitude Discharges***

- Phillips Lab / Geophysics has extensive library of state-of-the-art IR radiation models/codes
- Models extensively validated against data for
  - LTE (local thermodynamic equilibrium) atmosphere
  - non-LTE quiescent atmosphere
  - non-LTE energetic-electron-disturbed atmosphere
    - aurora
    - artificial aurora
- These non-LTE models ideally suited to calculate IR radiance from sprites

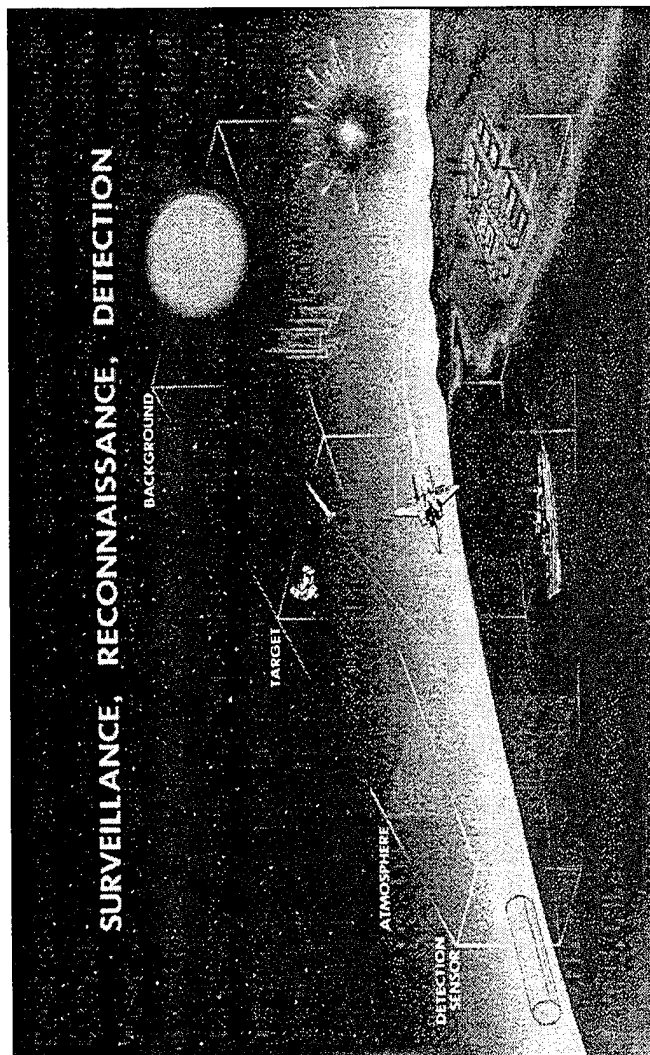


# PL Atmospheric and Celestial Background Effects Code Program



## Code Overview

- 1-D Spectral Radiance Codes
  - MODTRAN 3.0
  - MOSART 1.4
  - SHARC 3.0
  - SAMM 1.0
  - FASCODE 3.0
- 2-D Radiance Structure Codes
  - SHARC 4.0
  - SASS 1.0
  - SAMM 2.0
  - CBSD 2.0
- Integrated Codes
  - PLEXUS 2.0





## ***Non-LTE Models / Codes***

- ARC (Atmospheric Radiance Code) - First-principles non-LTE line-by-line (LBL) model, quiescent atmosphere
- AARC (Auroral Atmospheric Radiance Code) - First-principles non-LTE auroral radiance model
  - Line-of-sight radiance: LBL model
  - Radiative excitation: Simple band model, several varieties
- AARC-EFA (Escape-function approximation) - Emitted photons either reabsorbed locally or escape to space, no radiative coupling
- AARC-SSBM (Steady-state band model) - Solve rate equations in steady-state
- AARC-TDBM (Time-dependent band model) - Time-dependent solution of rate equations

# The Nonequilibrium (Non-LTE) Radiative Transfer Problem

- Solve coupled equations for monochromatic specific intensity of radiation and species / level population densities

- Equation of transfer:

$$\frac{dI(\nu)}{d\tau_\nu} = S(\nu) - I(\nu)$$

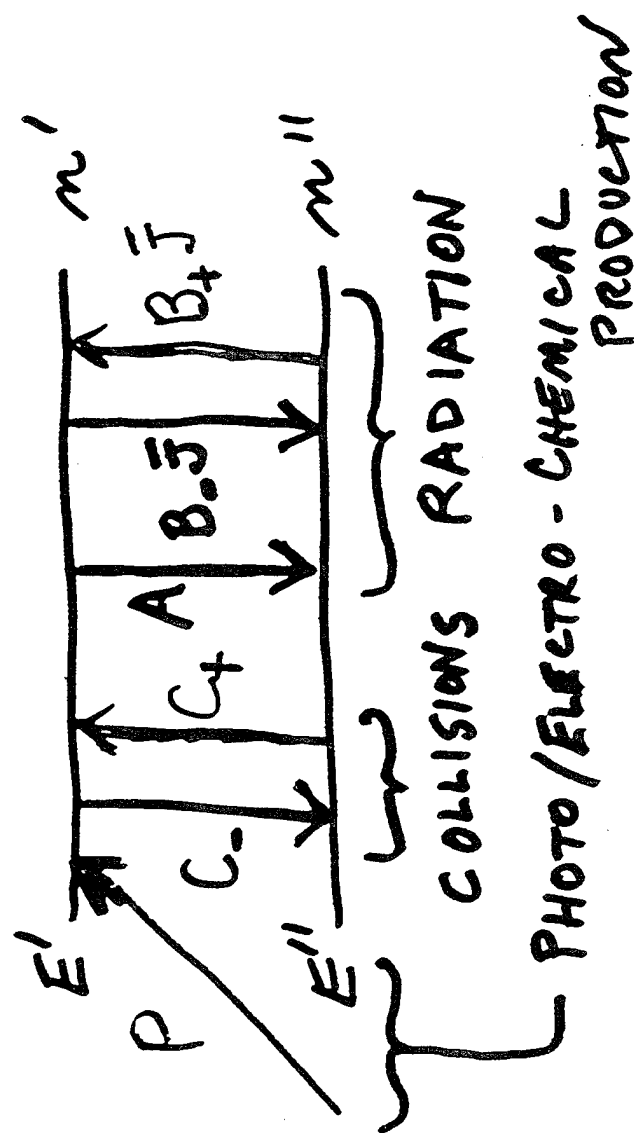
- Source function:

$$S = \frac{\frac{n'}{n}A}{B_+ - \frac{n'}{n}B_-}$$

- Rate equation:

$$\frac{dn'}{dt} = P + (C_- + B_+ \bar{J})n'' - (C_+ + A + B_- \bar{J})n'$$

$\bar{J}$  = integrated mean intensity = average of  $I(\nu)$  over absorption line and over solid angle



# CONCEPT OF VIBRATIONAL TEMPERATURE $T_{vib}$

$$\begin{array}{c} E' \\ \text{---} \uparrow \text{---} \\ T_{act} \\ \text{---} \downarrow \text{---} \\ E'' \end{array} \quad \begin{array}{c} n' \\ \\ n'' \end{array} \quad \begin{array}{c} \text{POPULATION RATIO} \\ \\ \\ \end{array} \quad \begin{array}{c} \frac{n'}{n''} \equiv \frac{g'}{g''} e^{-\frac{E' - E''}{k_B T_{vib}}} \end{array} \quad \uparrow$$

LTE:  $T_{vib} = T$  COLLISIONS DOMINATE

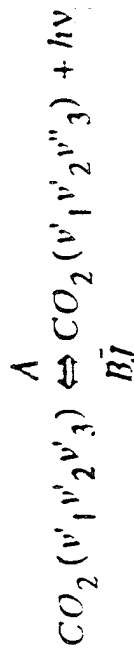
Non-LTE:  $T_{vib} \neq T$

$T_{vib} < T \Rightarrow$  NON-COLLISIONAL LOSS

$T_{vib} > T \Rightarrow$  NON-COLLISIONAL PRODUCTION

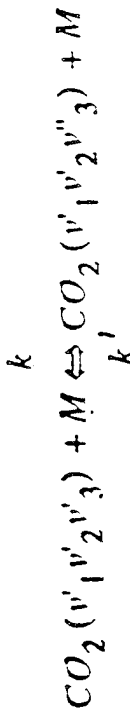
# Production & Loss Processes - $CO_2(v_3)$

## - Radiative (4.3 $\mu m$ )



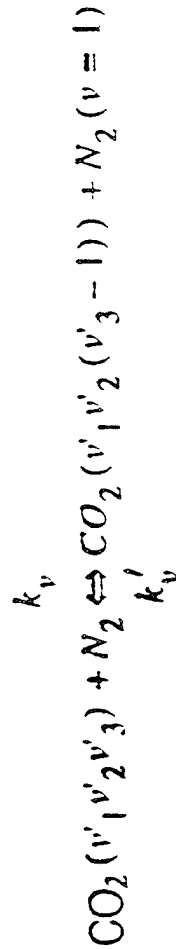
(solar and earthshine pumped; strong diurnal variation)

## - Collisional (V-T)



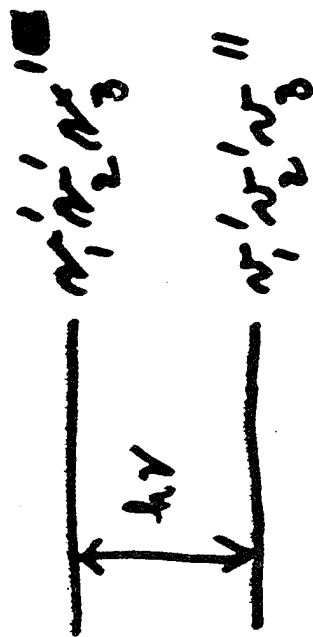
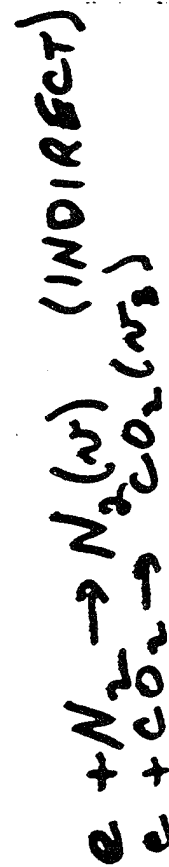
(M =  $N_2, O_2, O$ )

## - Vibrational transfer (V-V)

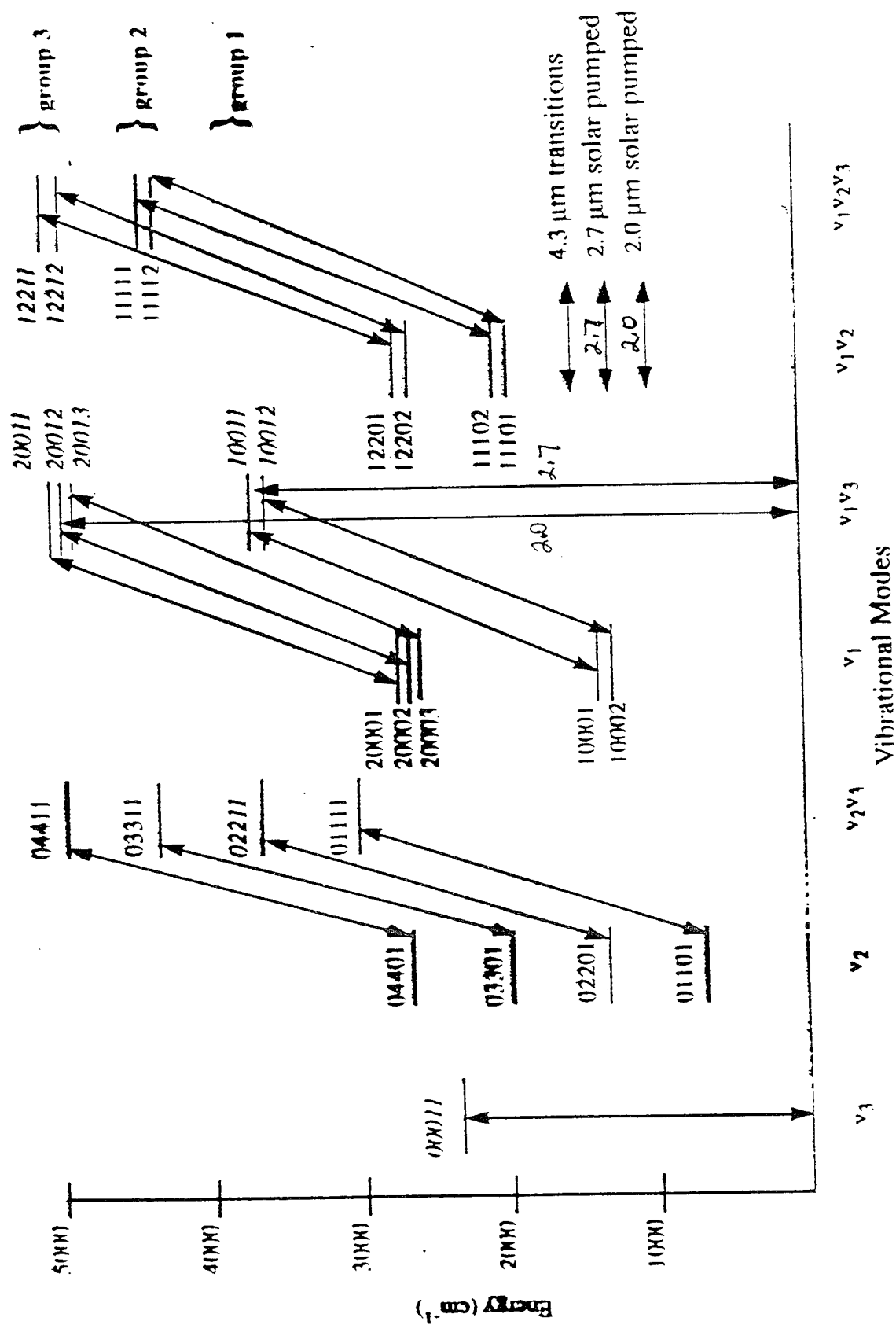


$$\Delta E = 19.2 \text{ cm}^{-1}; k_v = 5.0 \times 10^{-13} (300/T)^{0.5}$$

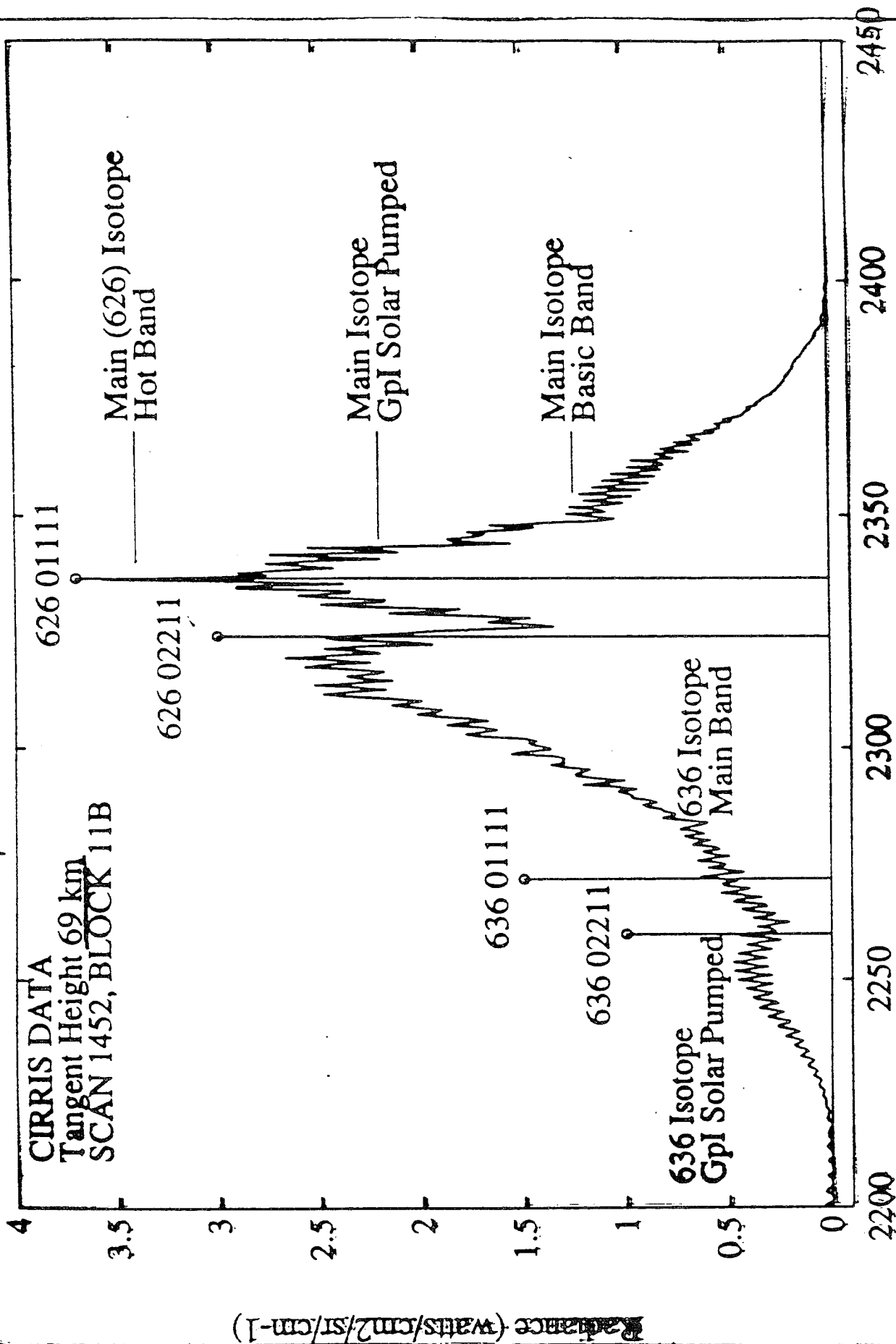
## - Electron excitation:

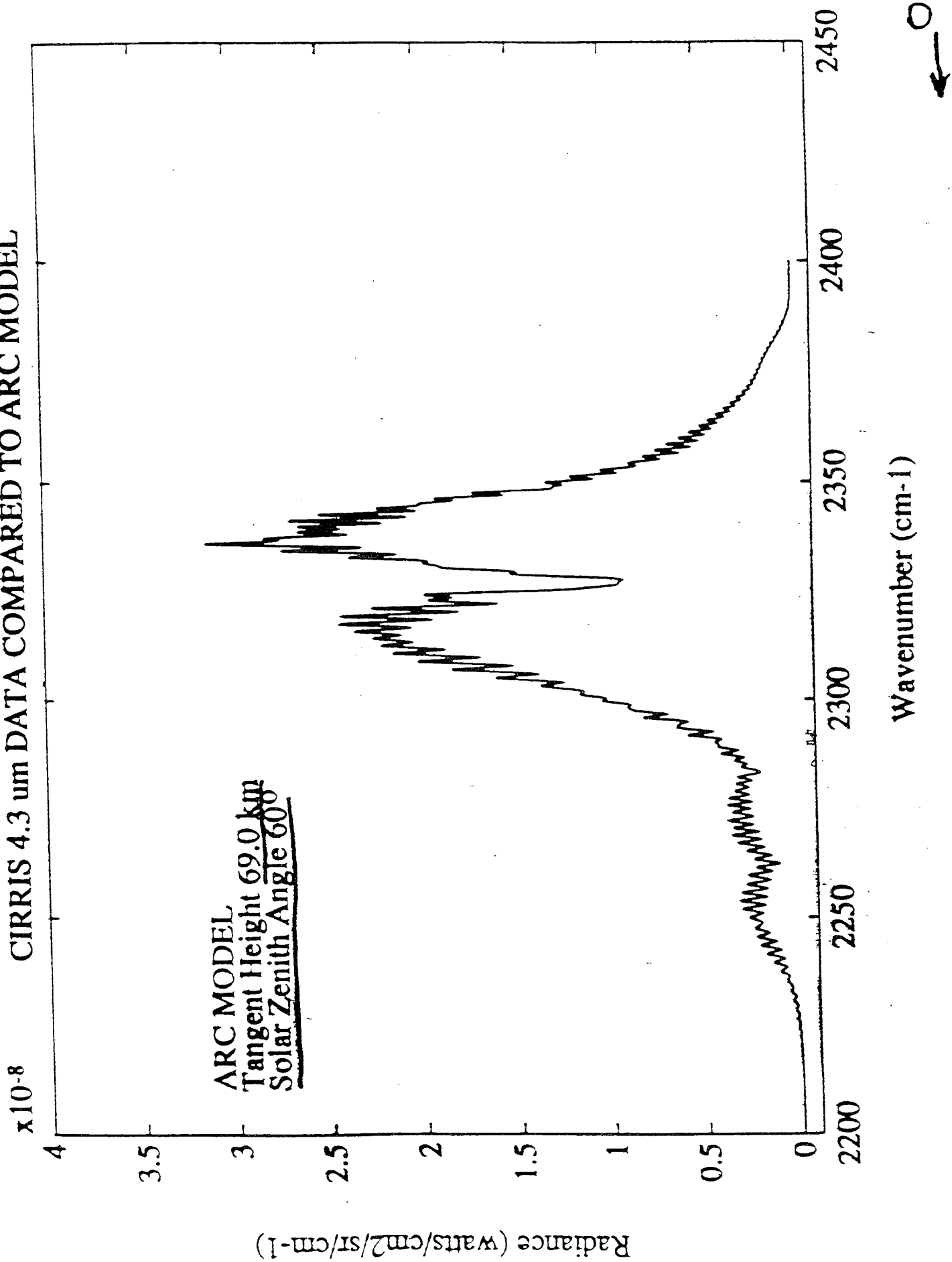


CO<sub>2</sub> Energy Diagram of 4.3  $\mu$ m States



**x10<sup>-8</sup> CIRIS 4.3 μm DATA COMPARED TO ARC MODEL (PRELIM.)**



CIRRIS 4.3  $\mu\text{m}$  DATA COMPARED TO ARC MODEL

# **Time-Dependent Band Model (TDBM)**

## **Assumptions (Currently)**

- Plane-parallel atmosphere - no horizontal radiative transport
- Weak Isotopic and hot bands assumed to have same vibrational temperature as main band
- No coupling to OH(v) and H<sub>2</sub>O(v)
- Includes correctly:
  - neutral collisional excitation / loss (V-T)
  - electron collisional excitation
  - radiative excitation / loss (-> vertical radiative diffusion)
  - N<sub>2</sub>-CO<sub>2</sub> resonant V-V transfer
  - transient (time-dependent) effects



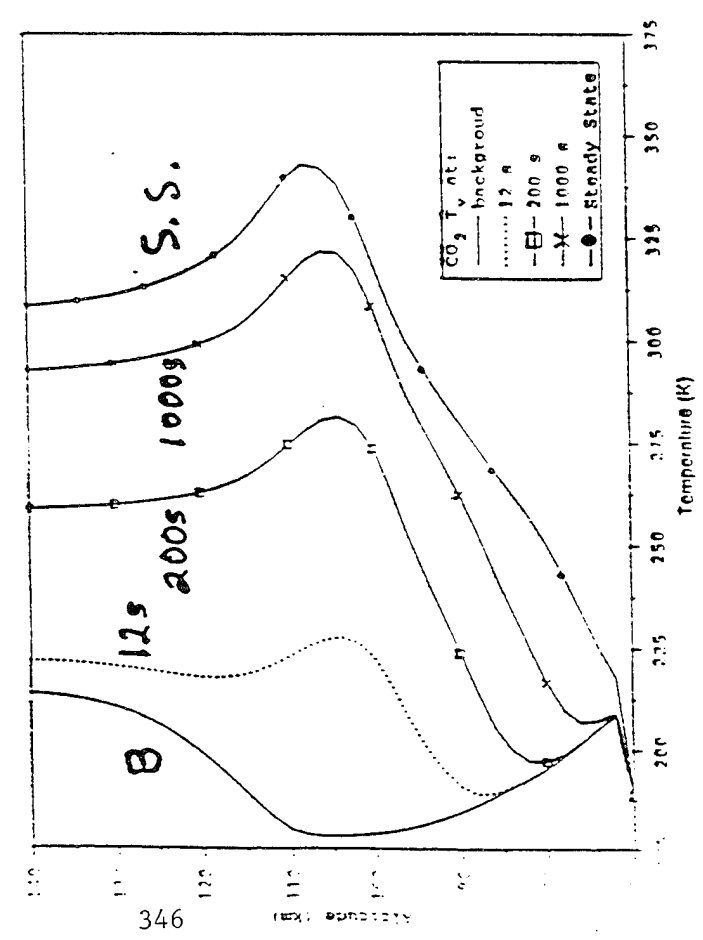
## ***Applications of TDBM***

- 4.3- $\mu$ m aurora -
  - IBC III aurora, sudden initiation, constant dosing
  - IBC II<sup>+</sup> aurora - RBFWI data
    - Only 1.3 kR 427.8 nm N<sub>2</sub><sup>+</sup> 1N at time of measurement, significant predosing 190 s earlier peaking at 8 kR 427.8 nm (52 kR 557.7 nm)
    - Moderately hard spectrum: Peak electron energy ~11 keV, altitude of peak dosing 103 km
- 4.3- $\mu$ m sprite
  - Vertical extent - 40-90 km
  - Horizontal extent - 40 km
  - Electron spectrum - Gaussian, Intensity 10<sup>8</sup> eV/cm<sup>3</sup>s, E<sub>0</sub>~2.5 eV,  $\Delta E/E_0 \sim 0.4$ , Gaussian

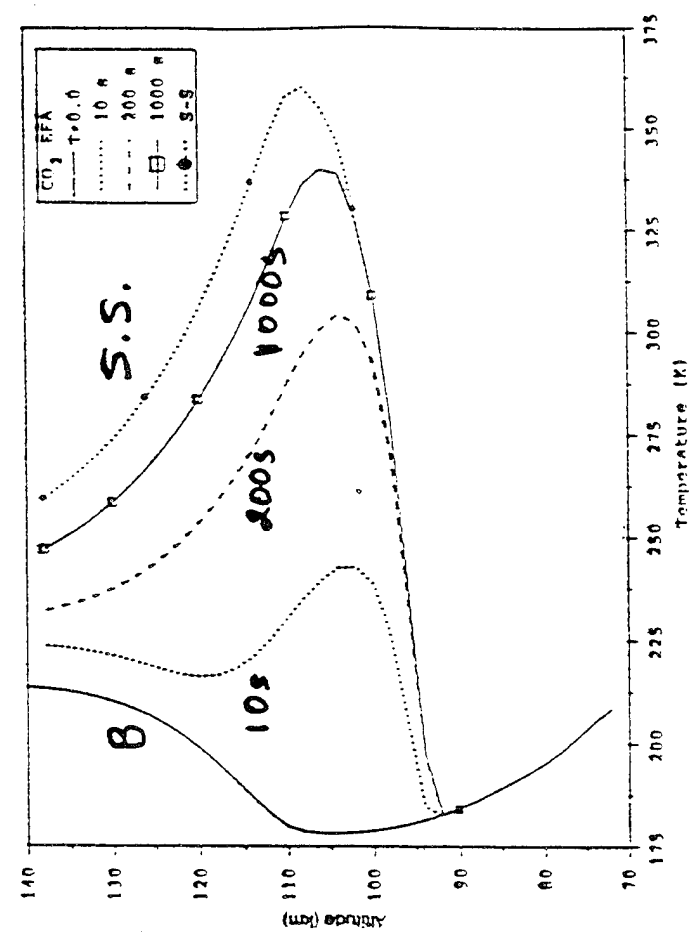
# COMPARISON OF CO<sub>2</sub> (00011) VIBRATIONAL TEMPERATURES FOR CONSTANT STRONG AURORA STARTING AT TIME=0 USING AARC-TDBM AND AARC-EFA

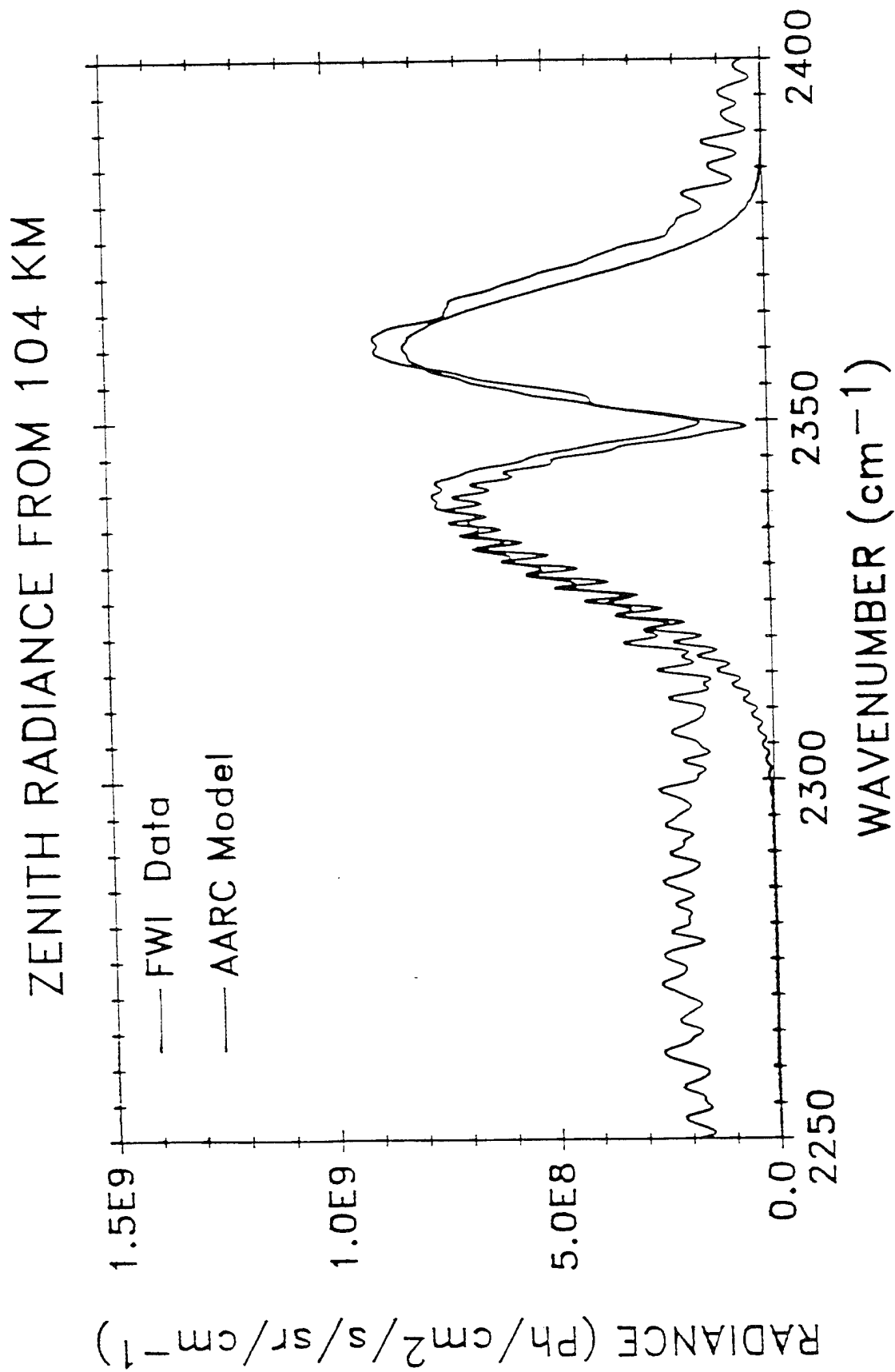
IBC III

AARC-TDBM

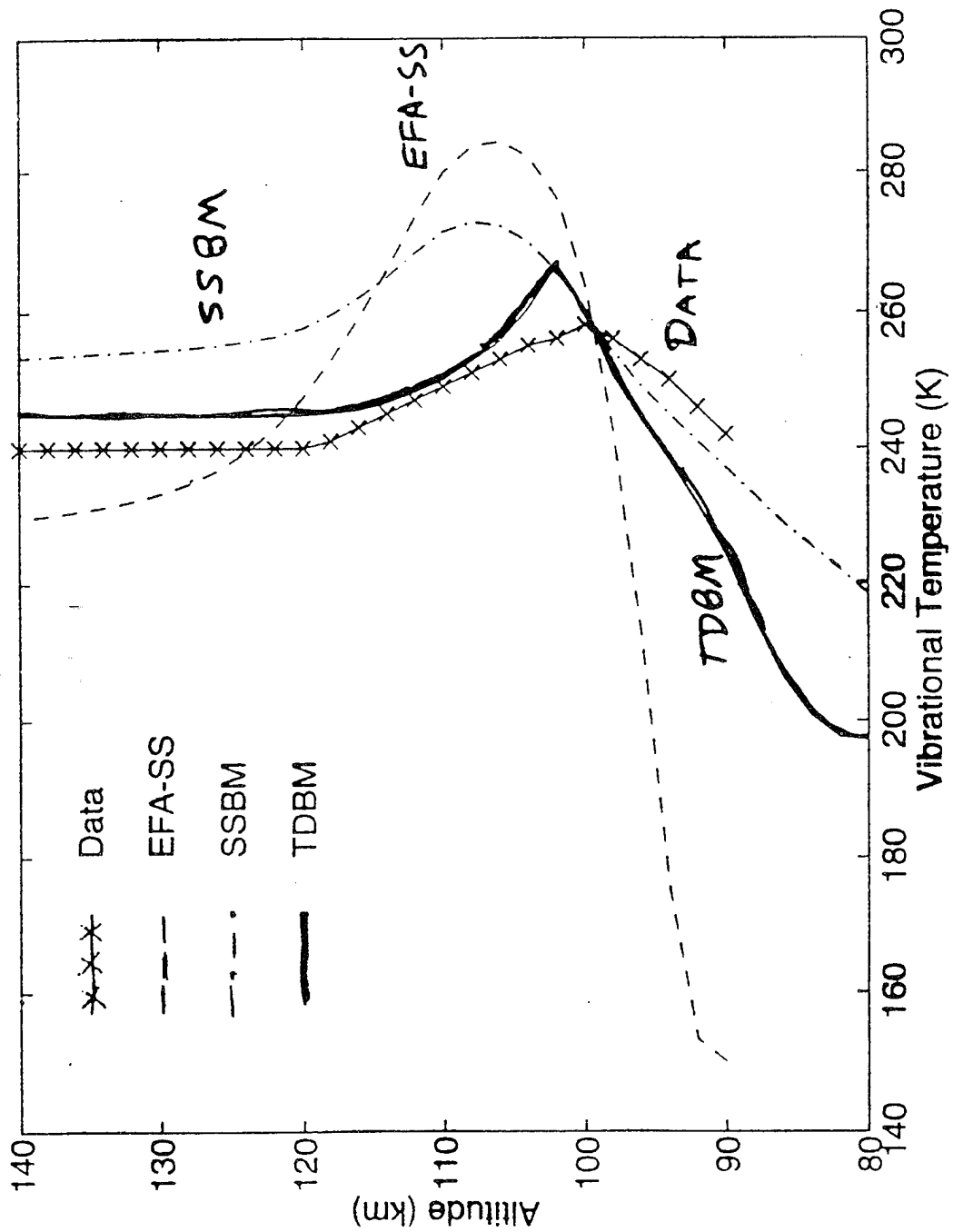


AARC-EFA

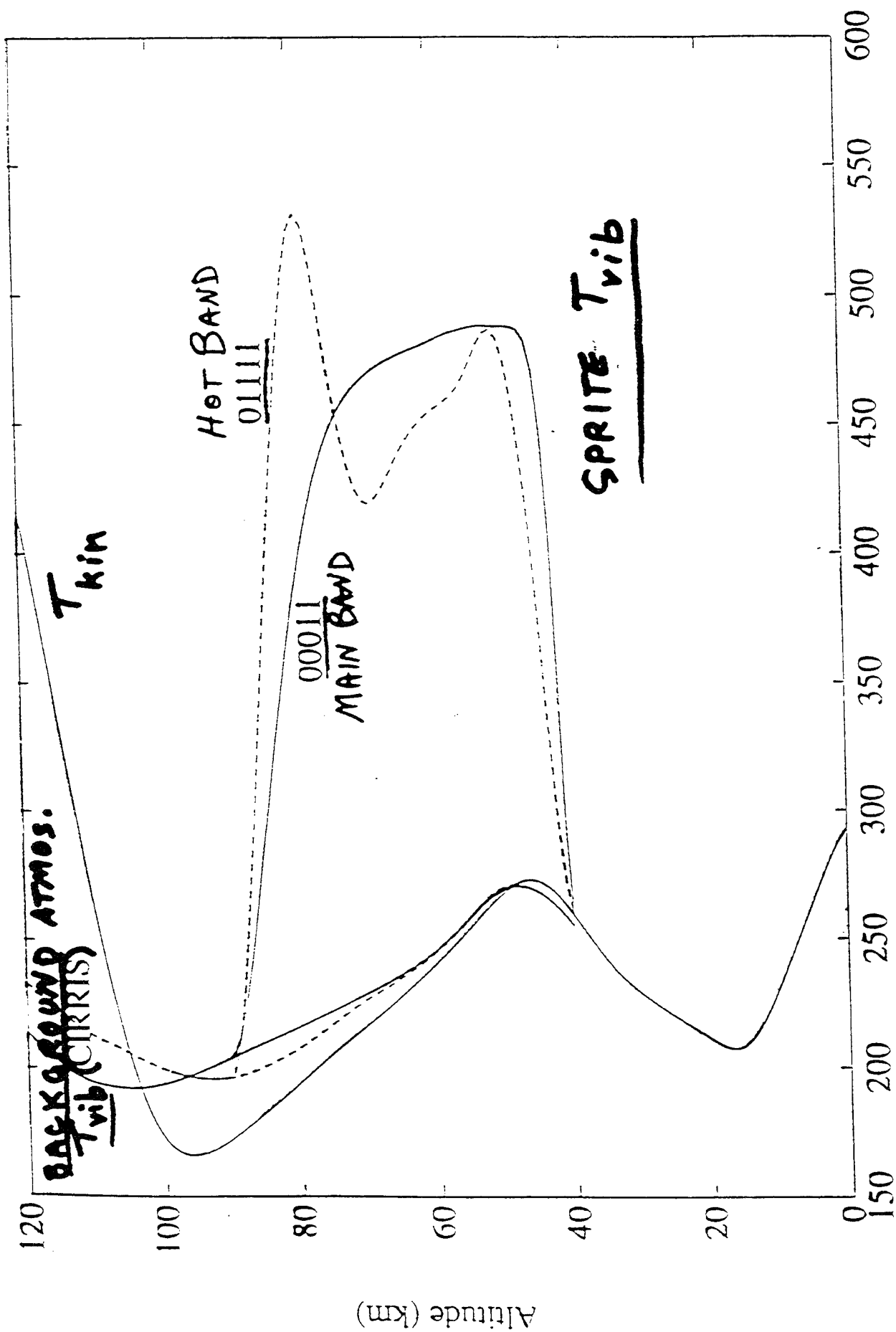




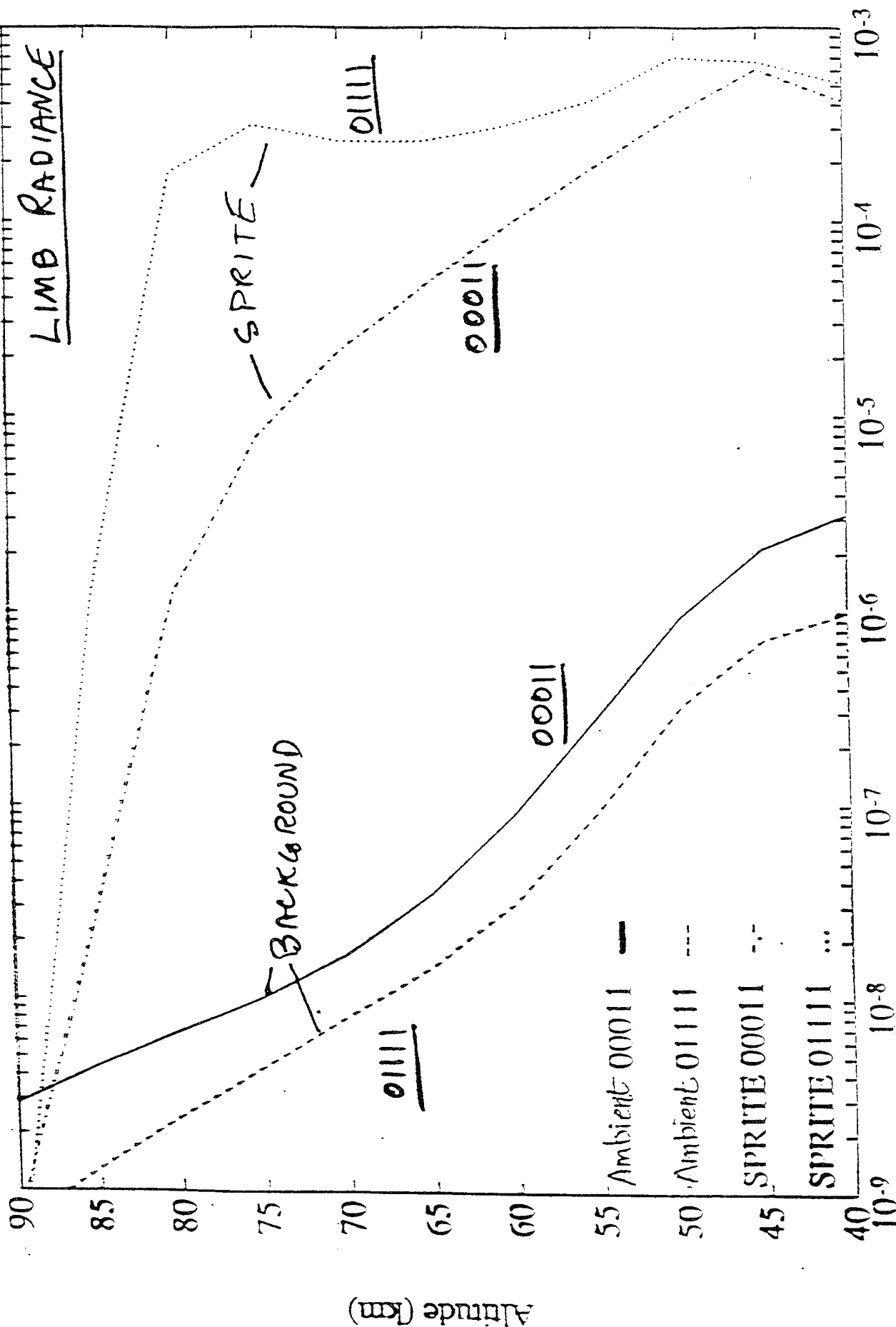
RBFWI April 1983 4.3  $\mu\text{m}$  CO<sub>2</sub>



SPRITE: Vibrational Temperature 10/17/95



# SPRITE: Limb Radiance (Individual)



Limb Radiance (W/cm² sr)

## **Observation of 4.3 $\mu\text{m}$ CO<sub>2</sub> Radiance in Sprites from Ground-based and Airborne Platforms - Case Study**

### **• Observation conditions-**

- Observer platform at ground (0 km), 35 kft (11 km), 60 kft (18 km), 110 kft (34 km)
- Line-of-sight intercepts sprite at 85 km altitude
- Slant range 400 km

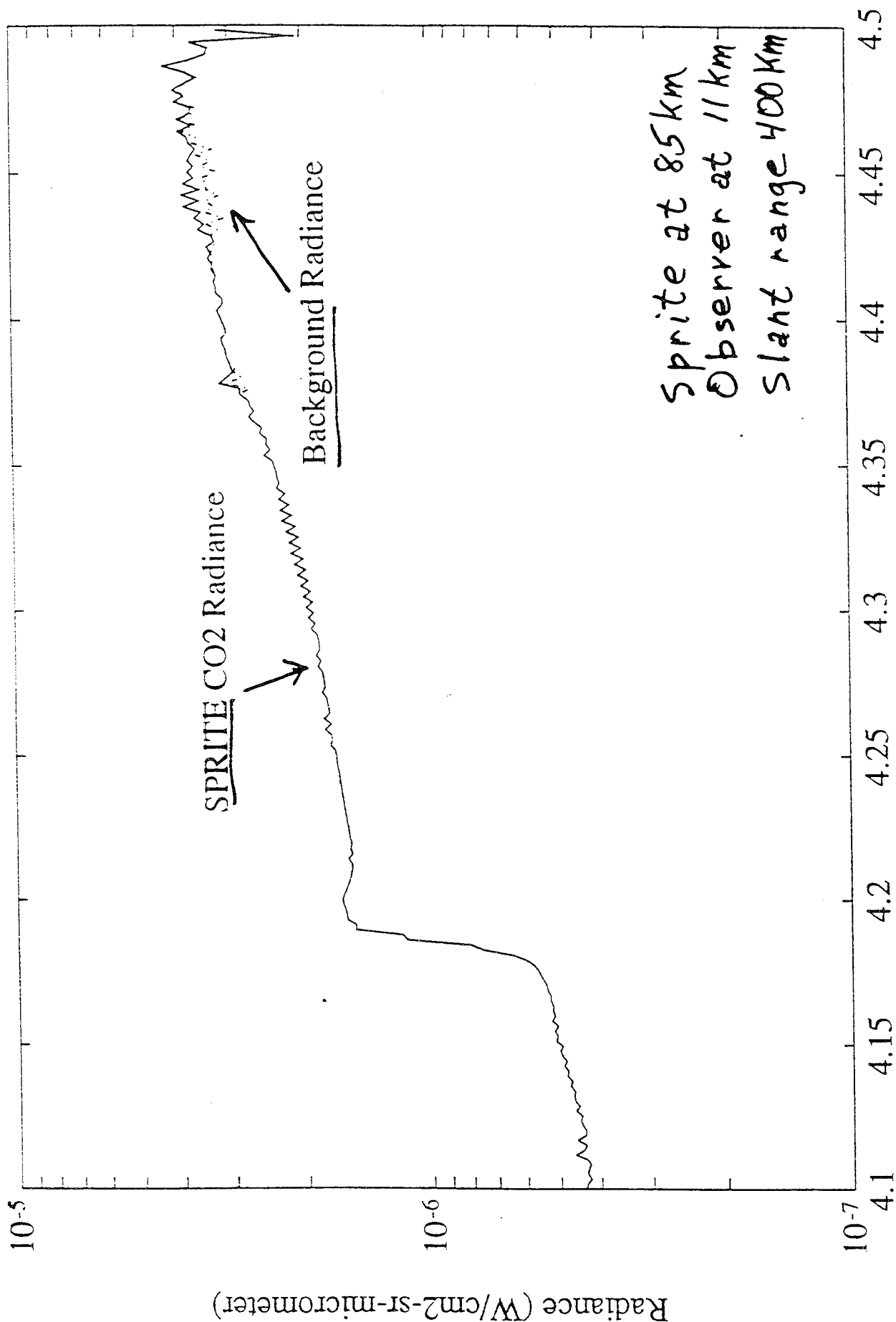
### **• Sprite model**

- Horizontal extent - 40 km
- Electron spectrum Gaussian - Flux  $10^8 \text{ eV/cm}^3\text{s}$ ,  $E_0 \sim 2.5 \text{ eV}$ ,  $\Delta E/E_0 \sim 0.4$

### **• Result**

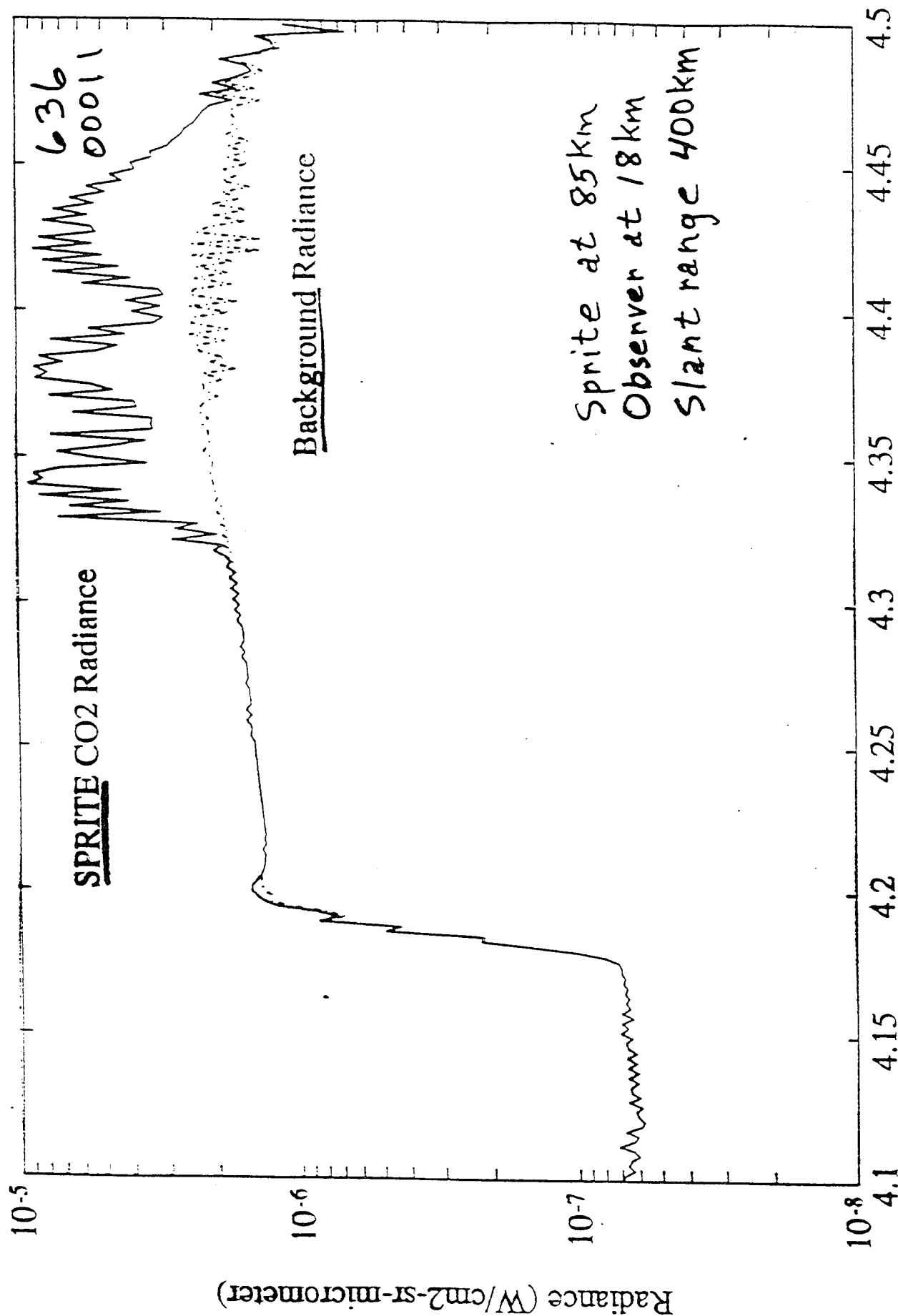
- Sprite only observable at 4.3  $\mu\text{m}$  from stratospheric aircraft and balloon platforms

SPRITE: 35,000 FT to 85 km, 400 km Slant Range

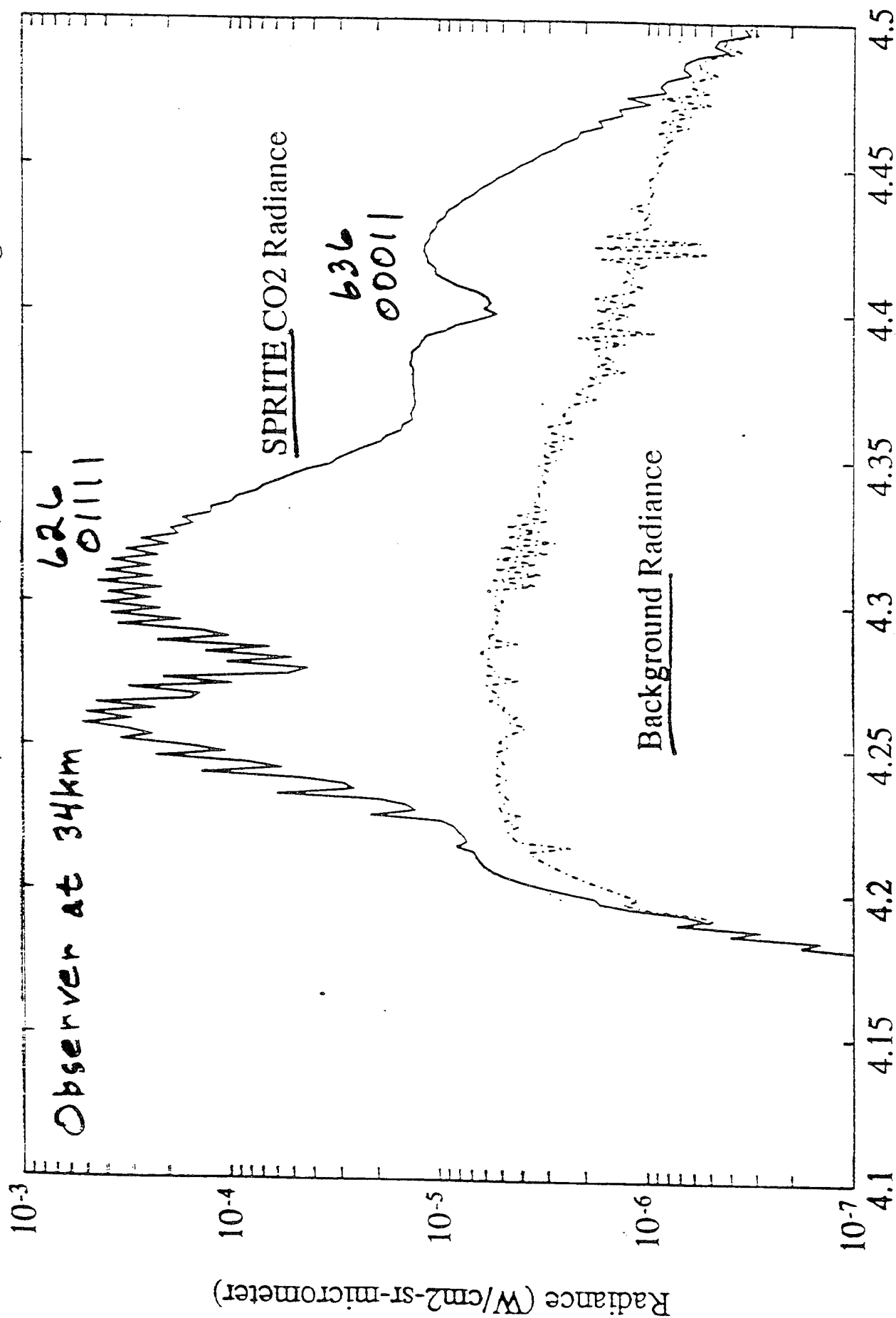




SPRITE: 60,000 FT to 85 km, 400 km Slant Range



SPRITE: 110,000 FT to 85 km, 400 km Slant Range



Wavelength (micrometer)

## ***IR Radiative Model Needs***

- Input:

- Spatial map of electron spectrum as a function of time required from *data* or from *model* - *most critical need*.
- Use to calculate production rate of  $\text{CO}_2(v_3)$  from e on  $\text{CO}_2$  and of  $\text{N}_2(v)$  from e on  $\text{N}_2$
- Background atmosphere:  $[\text{N}_2]$ ,  $[\text{O}_2]$ ,  $[\text{O}]$ ,  $[\text{CO}_2]$ , T versus altitude (from data or model)

- Validation:

- Spectral measurements of monochromatic specific intensity of radiation from sprites in *well-characterized* atmosphere
- Ancillary measurements of atmosphere and discharge important
- At  $4.3 \mu\text{m}$  airborne platform appears necessary

# ***Trapping & Diffusion Effects - Sprites***

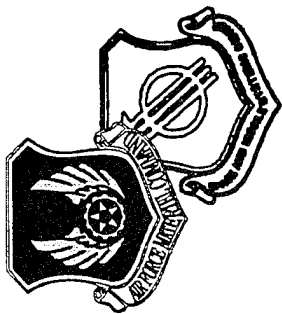
- Radiation transport: Repeated absorption & reemission  
---> radiation trapping - *Increases effective radiative lifetime to many times isolated  $\text{CO}_2(\nu_3)$  lifetime of 2.5 ms*
- > radiative diffusion - Extends production outside region of discharge, vertically & horizontally
- Resonant transfer: V-V transfer  $\text{N}_2(\nu) \leftrightarrow \text{CO}_2(\nu_3)$ 
  - Increases effective overall time constant because (a) not all  $\text{N}_2$  collisions of  $\text{CO}_2(\nu_3)$  --> quenching, (b)  $\text{N}_2(\nu)$  does not radiate  $\rightarrow$  *Energy storage mechanism*

## ***Conclusions - IR Radiation Models***

- Auroras & sprites can both lead to large enhancements in the 4.3- $\mu\text{m}$  emission from  $\text{CO}_2(\nu_3)$  above ambient
- Available tools, including transient radiative models, can model the IR radiation from the quiescent atmosphere, from aurora, and, somewhat modified, also from sprites
- A simple time-dependent band model (TDBM) is capable of accounting quantitatively for 4.3- $\mu\text{m}$  RBFWI auroral data
- Space-time maps of electron spectra are required for input to the TDBM to model IR sprites radiance
- Bright sprites emission at 4.3  $\mu\text{m}$  should be visible in satellite earthlimb observations & from high-altitude aircraft or balloon platforms

## ***Future Work - IR Radiative Models for Sprites***

- Incorporate diffusion model for horizontal transport into AARC-TDBM
- Obtain better electron spectral input to model
- Investigate how radiative transfer effects broaden the  $\text{CO}_2(\nu_3)$  excitation region
- Investigate how radiative transfer and resonant V-V trapping lengthen the effective lifetime of  $\text{CO}_2(\nu_3)$



# **AFOSR-PL Program**

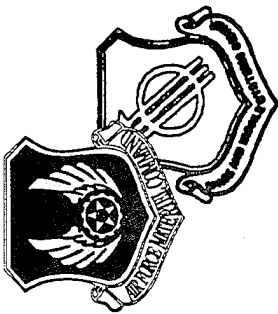


## **Infrared and Optical Signatures of High-Altitude Atmospheric Discharges**

**Presented To  
AFOSR-PL Workshop  
on Sprites and Blue Jets**

**Briefer  
Dr. Laila S. Jeong  
Phillips Laboratory  
Geophysics Directorate**

**19 October 1995**

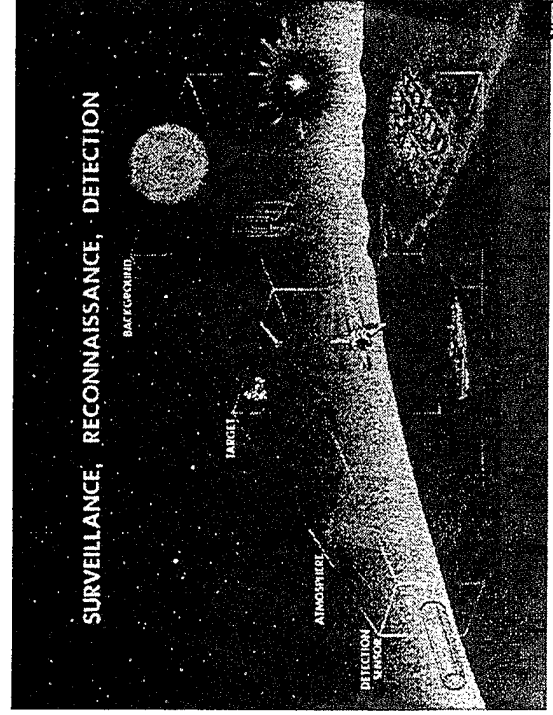


# Motivation



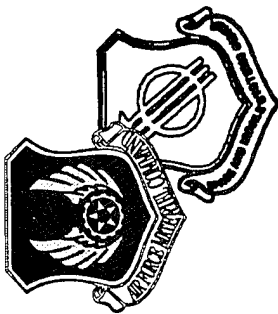
- Anomalous events observed by AF satellites
- Improved optical discrimination capability required for enhanced AF system performance

- Potential new source of persistent IR emission signatures
- Impact assessment required for next generation AF surveillance and tracking systems



1906095 .2  
10/17/95





# Objectives

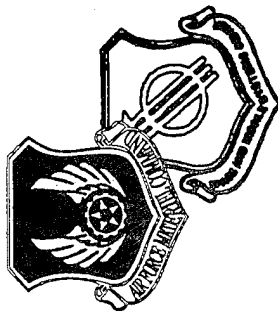


- Characterize enhancements in atmospheric radiance due to transient high-altitude atmospheric discharges
- Predict IR/UV/VIS signatures of elves, sprites, and blue jets
- Transition technical base to AF operational users

361

## Products and Payoffs

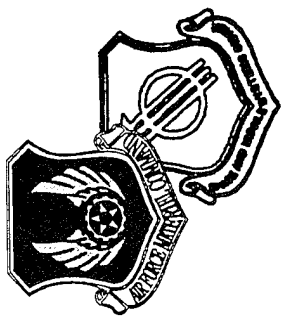
- Measured IR, UV, and VIS backgrounds from atmospheric discharge events
- Integrated Sprites Atmospheric Radiance Code (SPARC)
  - Electrodynamics/Chemistry/Radiation Transport
- Tailored capability to determine discharge-induced atmospheric background impacts in AF system simulations to optimize system performance



# Current Knowledge of High-Altitude Discharge Optical Emissions



- Sprite morphology determined (Sentman & Westcott)
- Sprite red emission identified as  $N_2$  First Positive (Sentman & Westcott, Mende)
- Sprite and blue jet ranges of brightness determined from image data (Sentman & Westcott)
- Sprite blue emission measured at 427.8 nm due to  $N_2^+$  First Negative (Armstrong)
- Ultra-bright precursor flash (elf) identified (Fukunishi, Lyons)



# Key Technical Deficiencies



- Spectral/spatial/temporal data of enhanced background emissions

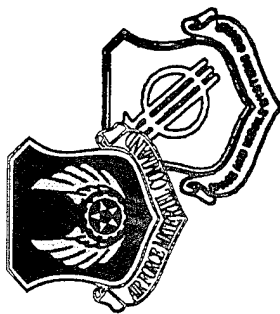
## IR

CO<sub>2</sub> 4.3 micron band  
NO 2.7 micron band

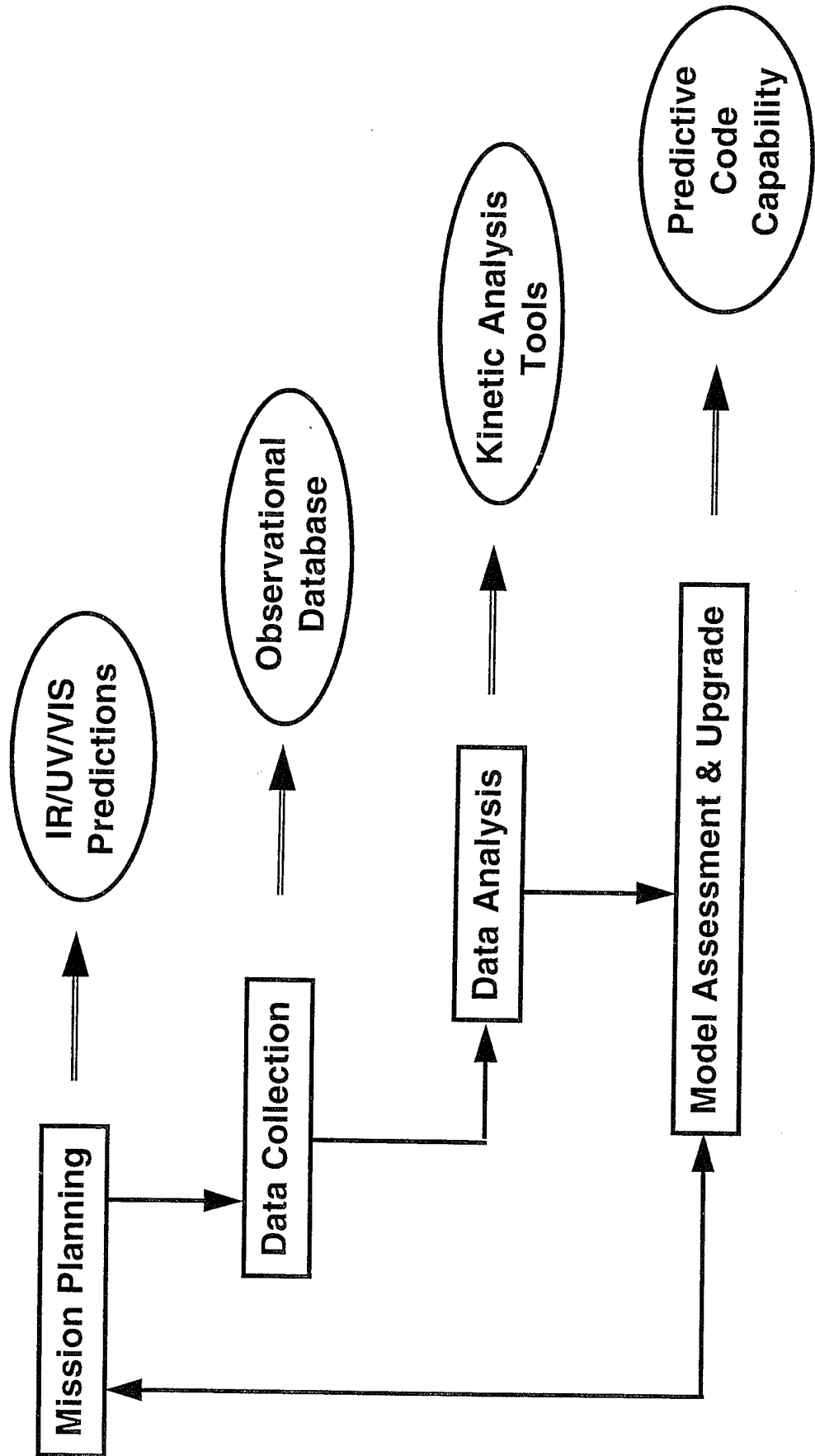
## UV/VIS

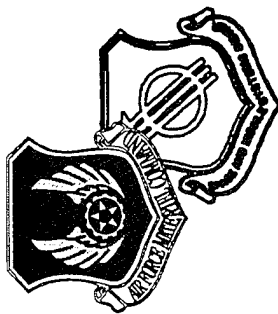
N<sub>2</sub><sup>+</sup> First Negative  
(391.4 nm, 427.8 nm)

- Electron density/energy distribution
  - Temporal dependence
  - Altitude dependence
- Fundamental understanding of discharge dynamics (electro-, chemical)



# Overall Approach

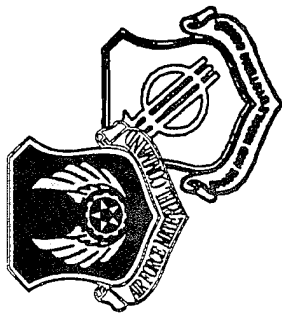




# Mission Planning



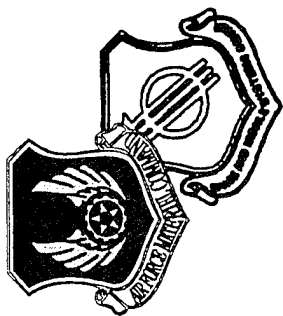
- Review current database and define technical baseline
  - October '95 Workshop
  - Spectral Fitting
  - Kinetic Assessments
- Conduct kinetic analysis of new data from Summer '95 Campaign
- Develop modeling tools to predict UV/VIS/IR signatures for data collects
  - Modified high-altitude atmospheric radiance code



# Mission Planning



- Predict UV/VIS/IR signatures to optimize data collects for Summer '96 Campaign
  - Radiance calculations for aircraft sensor bands and viewing geometries
- Define aircraft data collection requirements and mission operations
  - Aircraft mission requirements document and mission operations plan
- Identify satellite data collection events for sprite measurements
  - Add-on to automated data processing software to flag atmospheric discharge events and analyze emissions

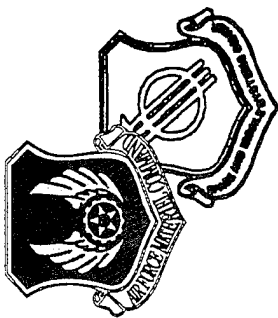


# Data Collection

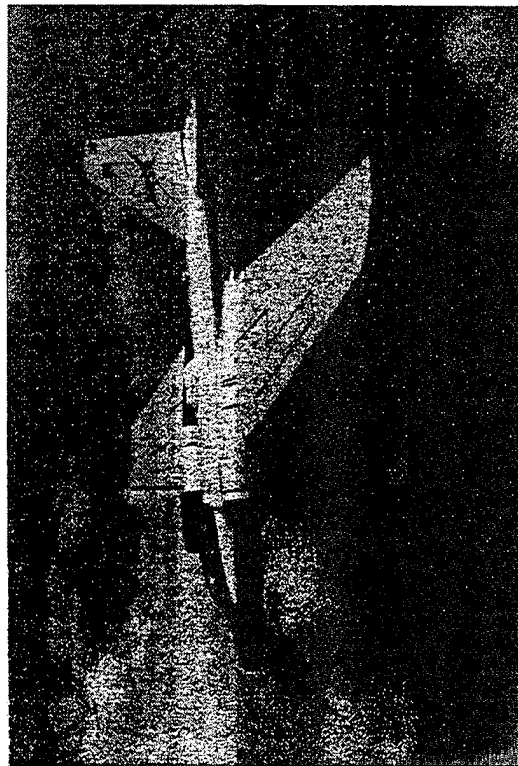


| Platform               | IR Signature Measurements                       | UV/VIS Signature Measurements | Radar Measurements               |
|------------------------|---|-------------------------------|----------------------------------|
| ARES Aircraft (SAFSP)  | Radiometer<br>Imaging Spectrometer<br>IR Camera | Visible Cameras               |                                  |
| MSX Satellite (BMDO)   | Radiometer<br>Interferometer                    | Imaging Spectrometer          |                                  |
| MSTI-3 Satellite (SMC) | Imaging Radiometer                              |                               |                                  |
| Ground-Based (PL)      |   | Radiometer                    | Portable Radar<br>Millstone Hill |

- Data Reduction ----> Calibrated Data Sets

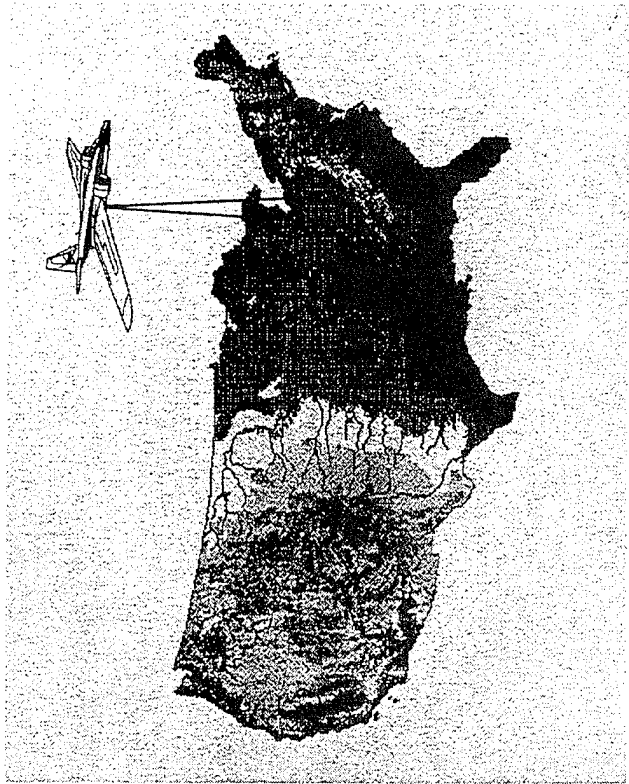


# Airborne Remote Earth Sensing (ARES)

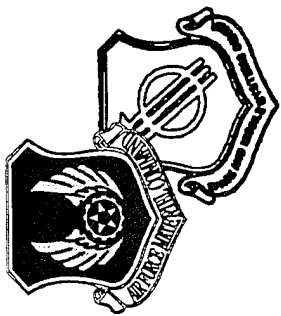


- Two Visible Cameras
- IR Camera (2.0 x 3.2 microns)
- 4-Band Radiometer (2.2 - 4.6 microns)
- Imaging Spectrometer (2-6 microns)

- RESPO Controlling Agency
- RB-57F Aircraft
- 65 kft Altitude
- 2,500 NM Range



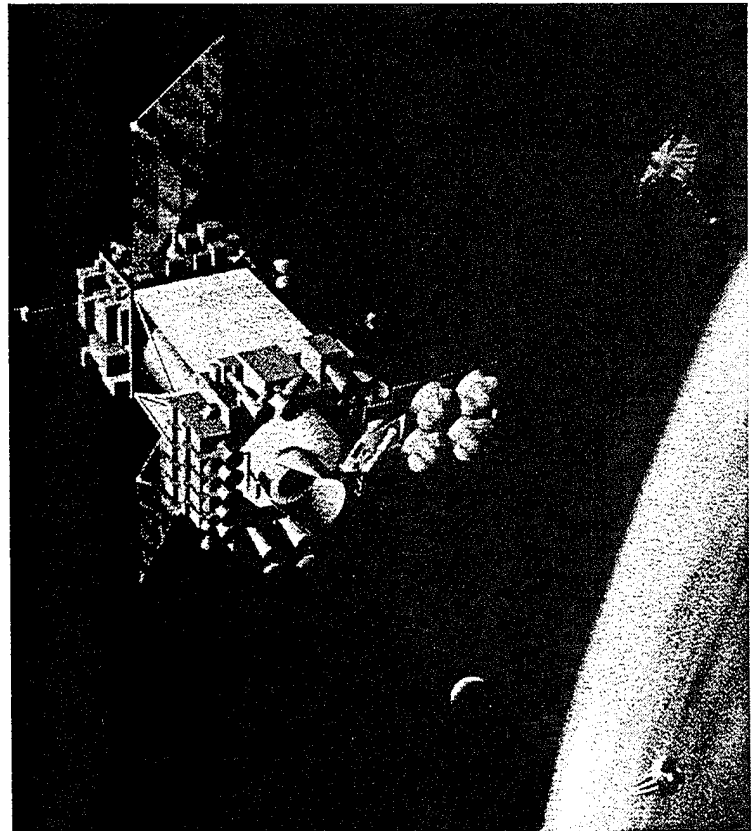




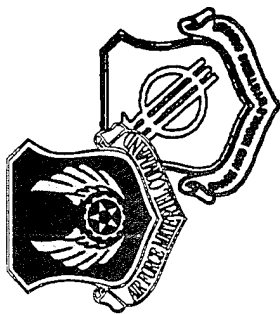
# Midcourse Space Experiment (MSX)



Provide multi-band and multi-LOS scene data of earth, earthlimb, and celestial backgrounds



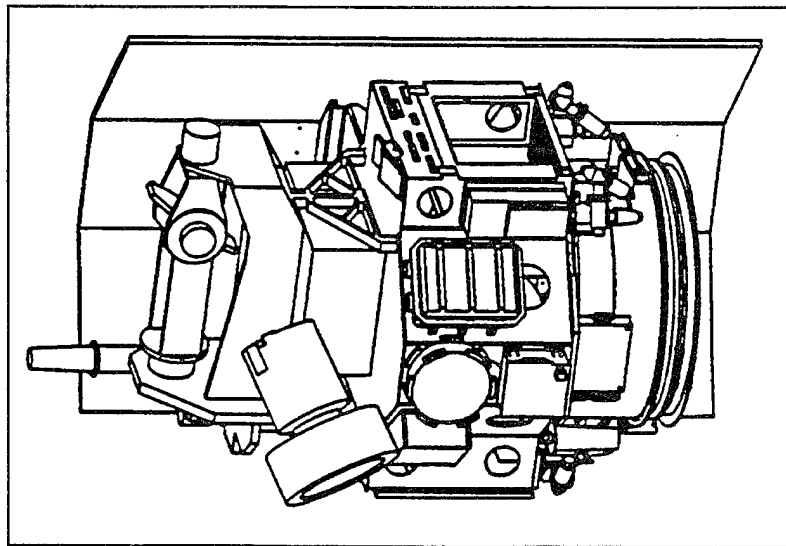
- Sun-synchronous polar orbit at 800 km altitude
- Spatial Infrared Imaging Telescope (SPIRIT III) covering MWIR-VLWIR:
  - 5-band scanning radiometer
  - 6-channel Fourier transform spectrometer
- UV/VIS Imaging and Spectrographic Imaging Sensor System covering far UV to near IR:
  - 5 spectrographic imagers
  - 4 imagers
- March '96 launch date



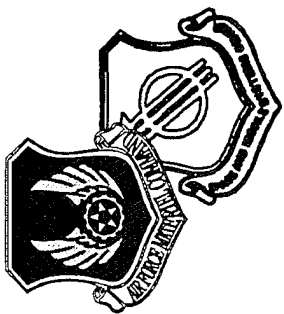
# Miniature Sensor Technology Integration (MSTI-3)



Provide high-spatial resolution SWIR/MWIR imagery  
of atmospheric backgrounds



- Sun-synchronous polar orbit at 425 km altitude
- Suite of three sensors
  - MWIR camera with 7 narrow-band filters
  - SWIR camera with 7 narrow-band filters
  - VIS imager
- April '96 launch date



# Ground-Based Optical and Radar Measurements



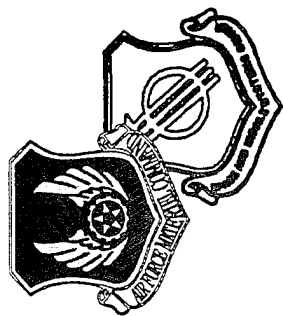
371

## Objective

- Characterize ionization enhancements in high-altitude discharge glows

## Approach

- Characterize spectral/spatial/temporal UV/VIS emissions using co-aligned imaging spectrometer/radiometer
- Determine D-region effects using 28 and 50 MHz portable radar systems
- Determine D-F region effects using UHF (430 MHz) incoherent scatter radar and other diagnostics at Millstone Hill



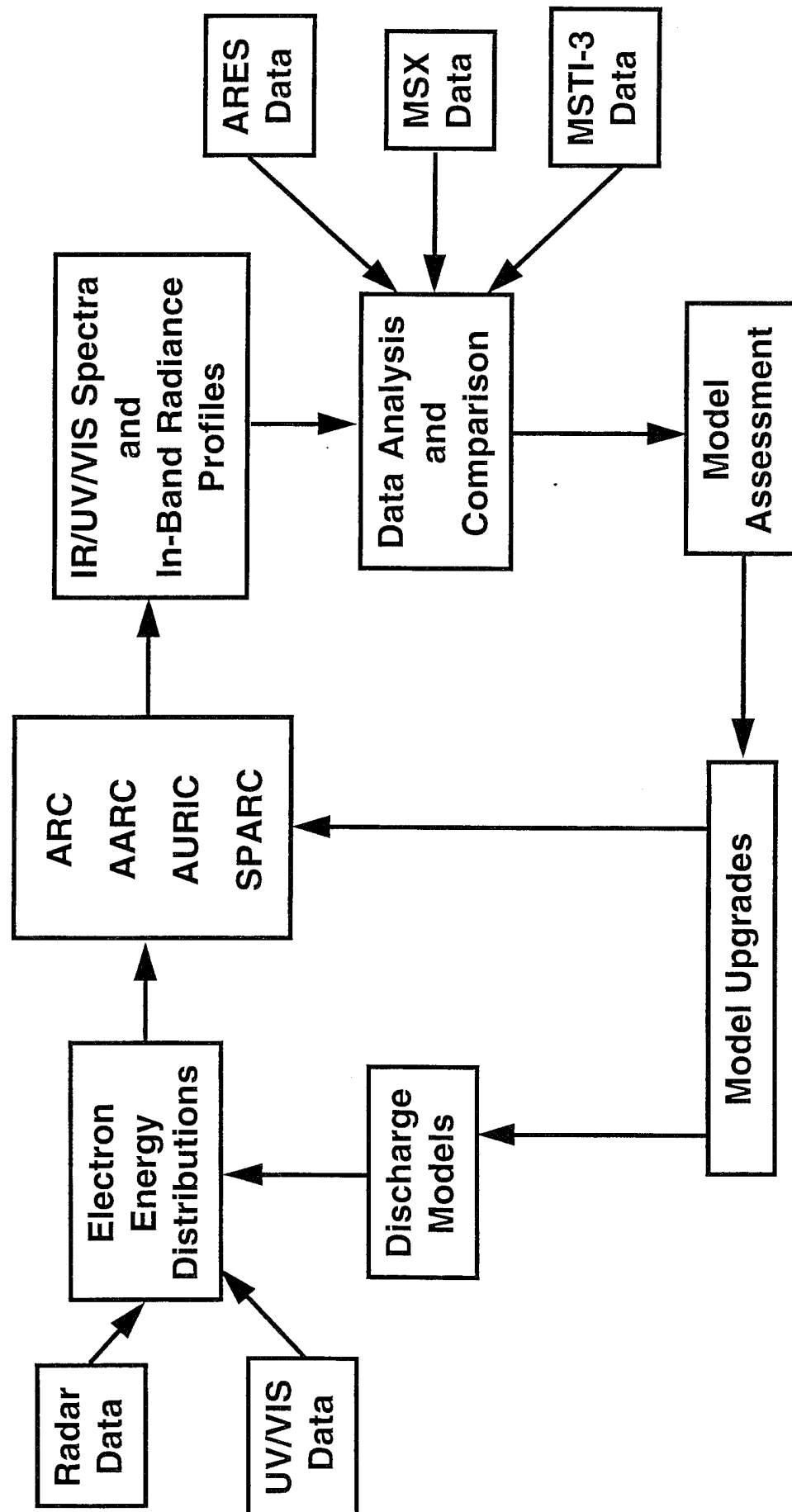
# Infrared and Optical Background Measurement Data Analysis

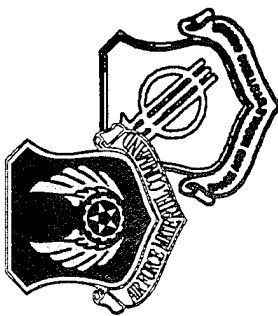


- Spectral Fitting
  - Determine excited-state species number density
  - Interband comparisons
- Kinetic Analysis
  - Model excited-state excitation and relaxation dynamics



# Atmospheric Background Model Assessment





# High-Altitude Atmospheric Radiance Codes

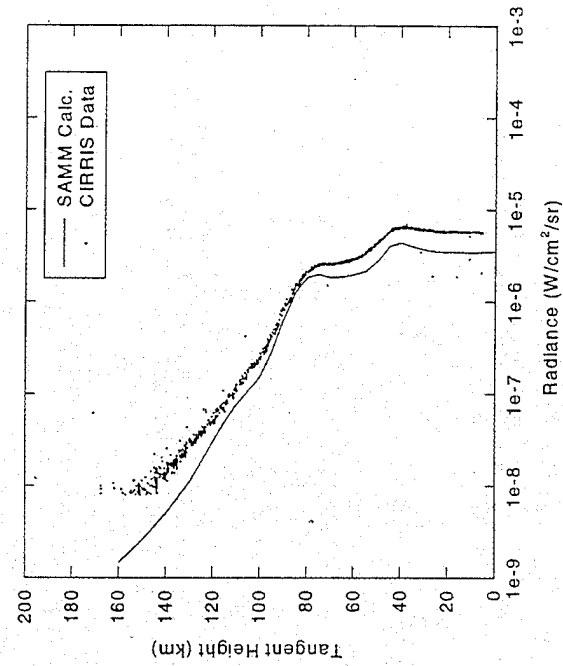


- ARC - Quiescent IR Backgrounds
- AARC - Auroral IR Backgrounds
- AURIC - UV/VIS Backgrounds

374

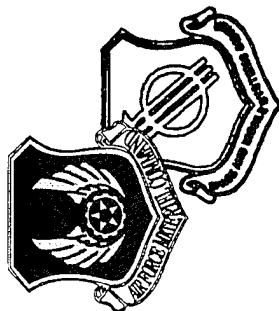
## Capabilities

- Calculate high-altitude atmospheric radiance backgrounds
- Model NLTE atmospheric emission and photoexcitation processes
- Support arbitrary viewing geometries
- Extensively validated using field data



## 4.3 Micron Band Radiance Profiles

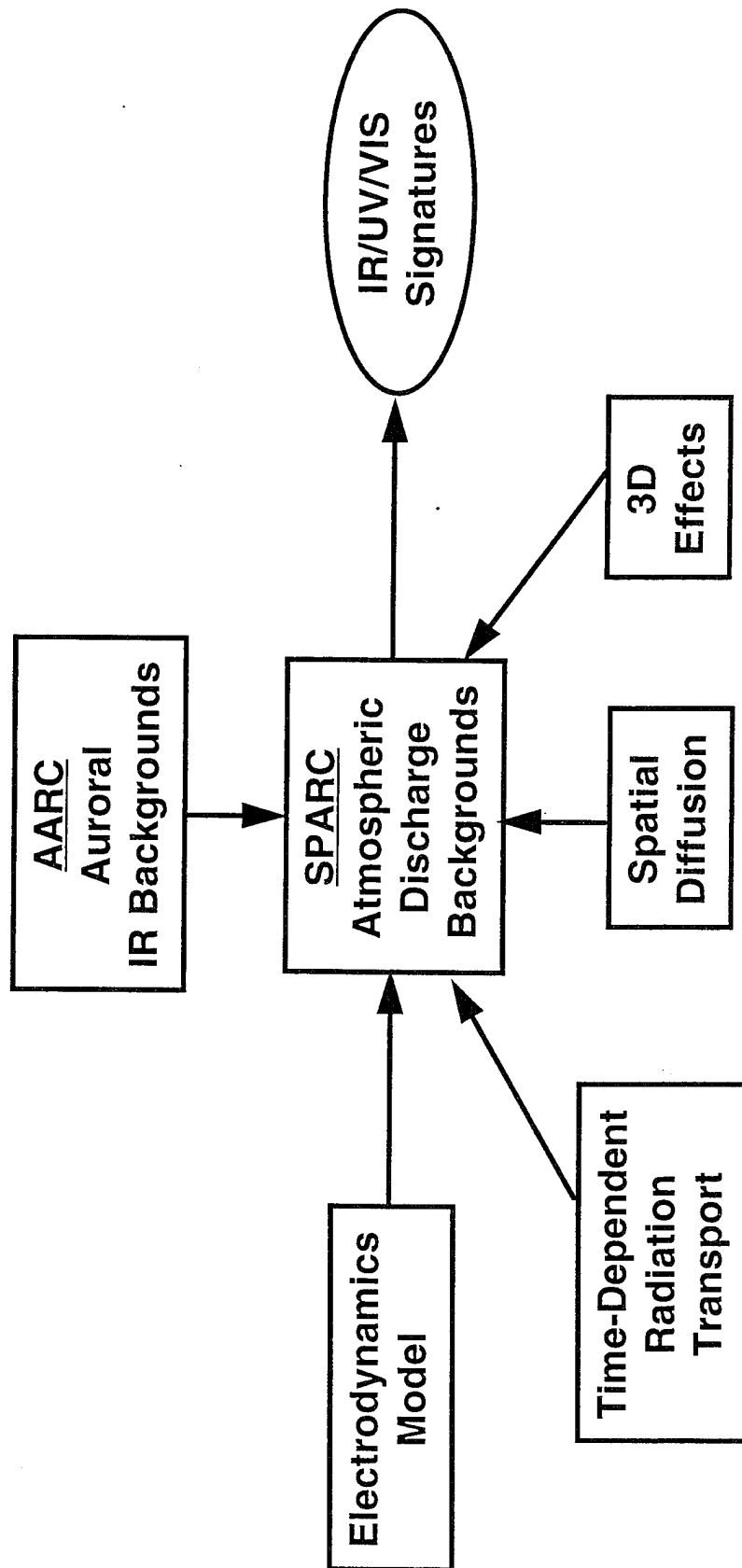
19oct95 .16  
10/17/95

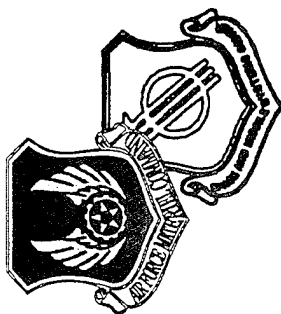


# Sprites Atmospheric Radiance Code (SPARC)



## New Modeling Capability for High-Altitude Atmospheric Discharge Backgrounds





# Summary



- Focused research program to measure and model IR/UV/VIS signatures of high-altitude atmospheric glow discharges
- Goal to integrate Air Force program with other agency programs to support coordinated Summer '96 Campaign with multiple assets





# AN AIRBORNE IMAGING SPECTROMETER IN OPERATION AND AVAILABLE FOR COLLECTIONS

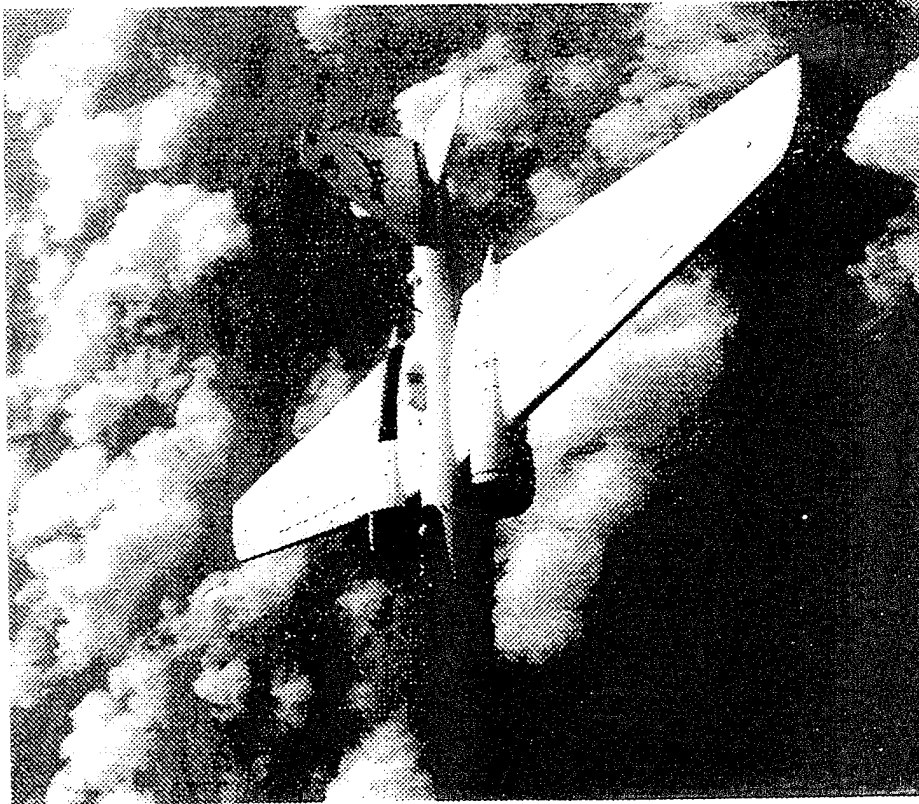
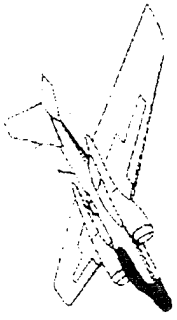
P. Kupferman  
Aerospace Corporation

- AIRBORNE REMOTE EARTH SENSING PROGRAM (ARES)
- NASA WB-57F AIRCRAFT PLATFORM
- 75 CHANNEL IMAGING SPECTROMETER
- UPLOOK AND DOWNLOOK CONFIGURATIONS
- PROGRAM MANAGED BY DoD REMOTE EARTH SENSING PROGRAM OFFICE, CAPT. TILTON
- EXPERIENCED TEAM (10+ YEARS)  
PROVIDES MISSION PLANNING, OPERATIONS,  
ANALYSIS AND DATA DISTRIBUTION





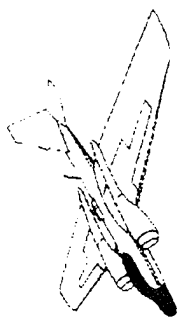
## ARES PROGRAM



- PROVIDES HIGHLY CALIBRATED RADIONOMETRIC AND SPECTROMETRIC S/MWIR DATA (2-6  $\mu\text{m}$ )
- CONTINUE DATA COLLECTION TO SUPPORT:
  - SPACEBORNE IR SYSTEM CONCEPT DEFINITION
  - DEVELOPMENT OF IMAGERY FOR REFINEMENT OF MULTISPECTRAL EXPLOITATION TECHNIQUES
  - NATIONAL SECURITY REQUIREMENTS
  - MILITARY REQUIREMENTS
  - ENVIRONMENTAL COMMUNITY RESEARCH REQUIREMENTS



# Location of ARES Program Facilities and Operation Sites



Also Planning FY 95 continental  
measurement series for NSF  
from 70° S to 70° N latitude

Lead Sensor Contractor /  
Integrator - Lockheed RDSB  
Palo Alto, CA

SAFSP/RESPO  
Headquarters  
Fairfax, VA

Chesapeake Bay

Wright-Patterson  
AFB, OH

Eastern Range, FL

Hamlet's Cove  
Eglin AFB, FL

Cloud Physics  
(Central Texas)

Aircraft Hangar Facilities /  
Flight Operations Headquarters  
Houston, TX

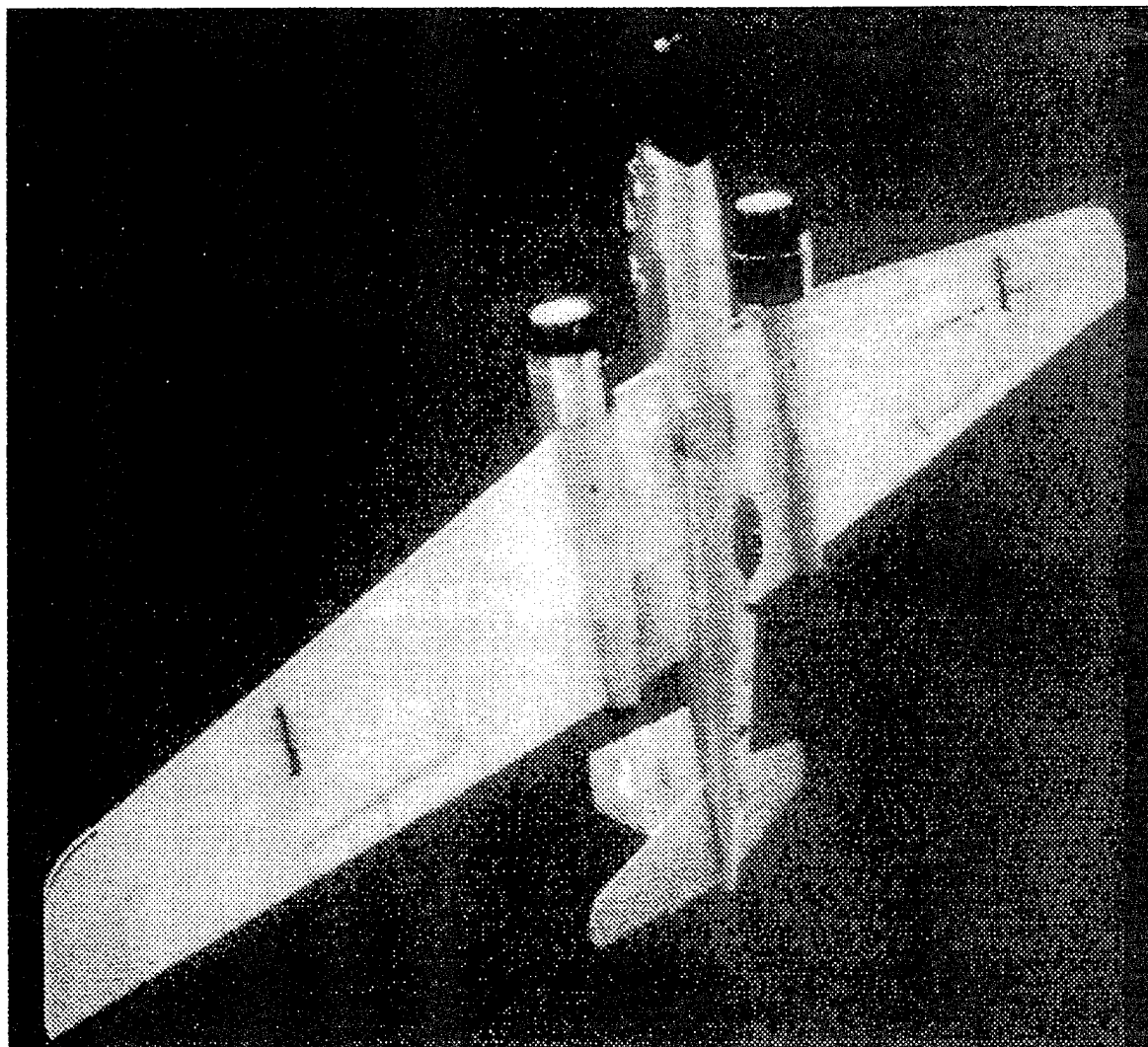
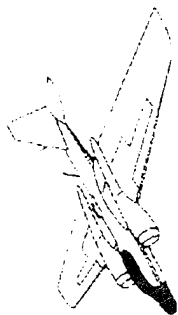
Atmospheric  
Radiation  
Measurements (ARM)  
Program Site  
Lamont, OK

White Sands Missile  
Range, NM

Western Range, CA



# RB-57F



ALTITUDE

65,000 FT+

RANGE

2,500 NMI

ENDURANCE

6 HOURS+

PAYLOAD

4,000 LB+

VOLUME

250 FT<sup>3</sup>

POWER

40 KVA/GENERATOR

SPEED

400 KTS

RUNWAY

6,000 FT

CROSSWIND

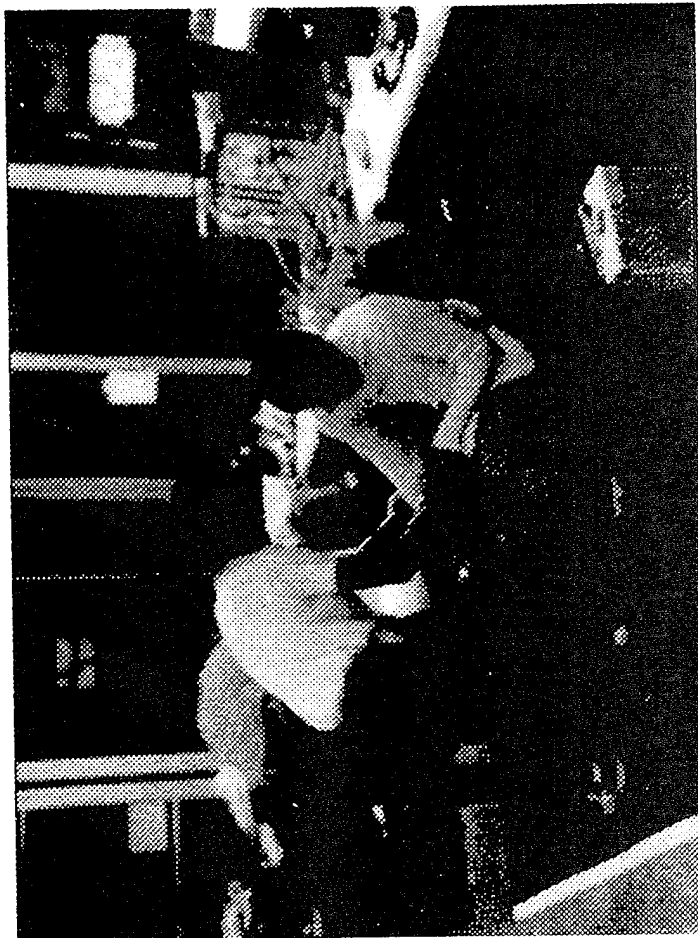
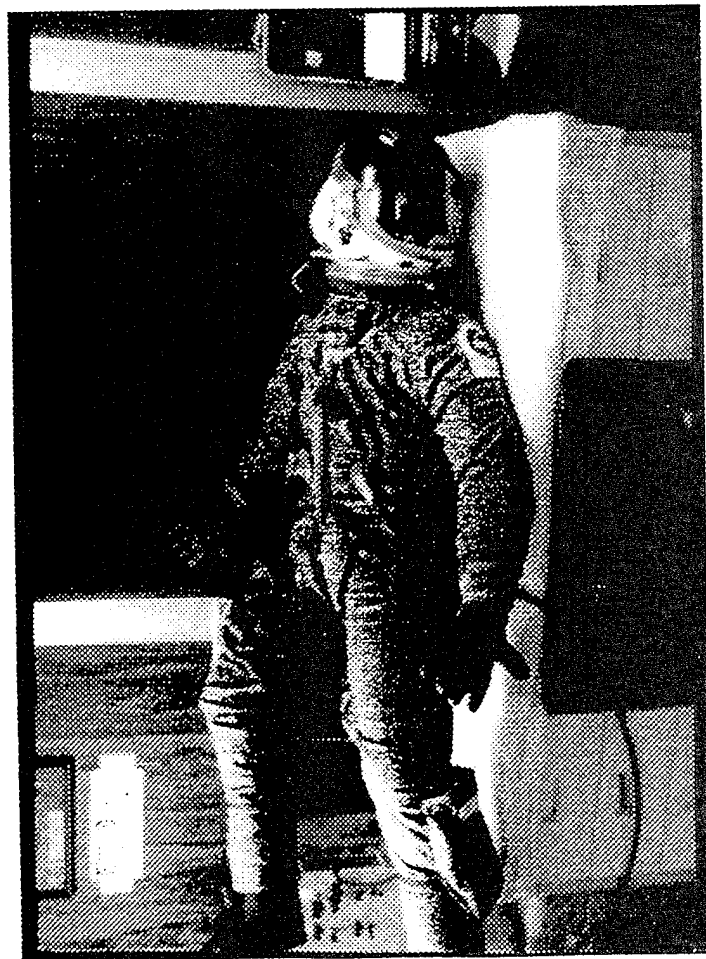
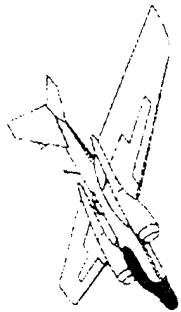
15 KTS

NAVIGATION

INS/ONS/LORAN



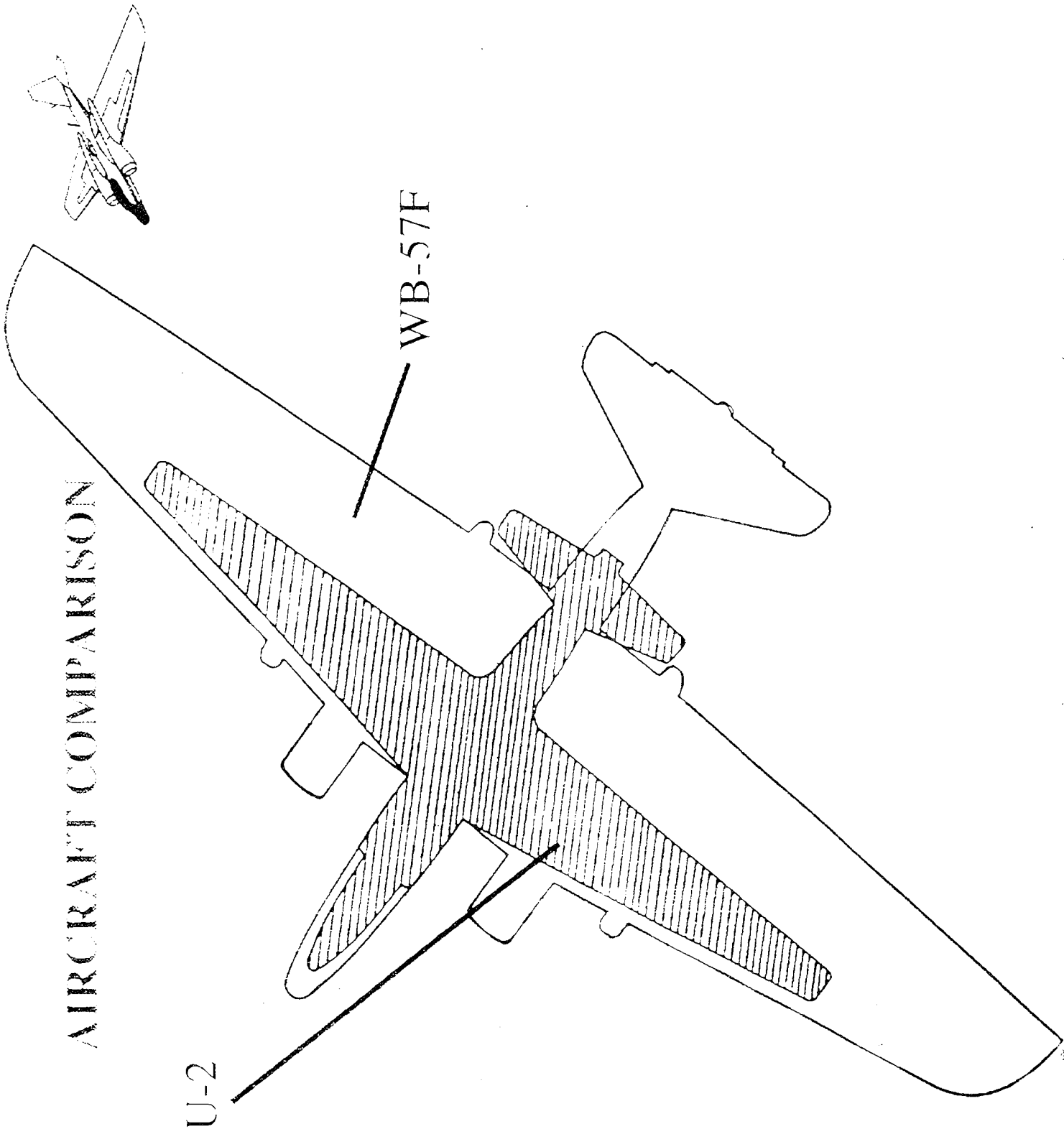
# PRESSURE SUITS FOR HIGH ALTITUDE



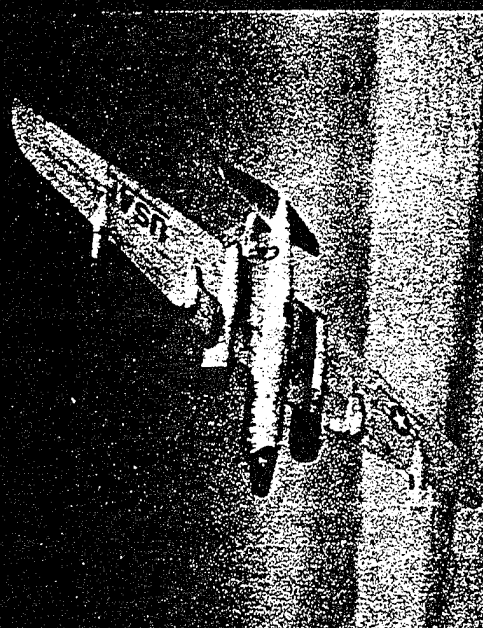
Program Fully compliant with DoD and  
FAA regulations for High Altitude Flight



# AIRCRAFT COMPARISON



Sample Data Collection





## Geology (Vulcanology)

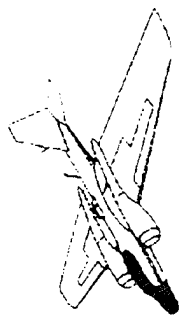


4.5 km x 12.5 km mosaic image formed from seven multispectral flightlines over Kilauea volcano (Hawaii), depicting extensive subsurface lava tube network, ocean thermal plumes.





# PAYLOAD INSTRUMENTS



## TWO VISIBLE CAMERAS

{  
FOV 1  
FOV 2

10.4° x 7.5°

1.6° x 1.9°

FOV

1.8° x 1.4°

## IR CAMERA

BANDPASS

2.0 X 3.2  $\mu$ m

}  
CAN BE UTILIZED WITH  
TRACKER (CENTROID/  
EDGE/CORRELATION)

## IR FPA 45 X 45

FIELD OF REGARD 2.6° x 2.6°

PIXEL RESOLUTION: 1.0 mrad x 1.0 mrad  
20m x 20m @ 20KM

## -- RADIONETER:

BANDS

FULL WIDTH - HALF MAX ( $\mu$ m)

2.205 - 2.259

2.716 - 2.972

3.723 - 3.843

4.406 - 4.553

## -- SPECTROMETER:

IMAGING SLIT

FOV 2.6° x 0.36°

20m x 2.8m @ 20KM

2.0 - 6.0  $\mu$ m/75 CHANNELS

BANDPASS RANGE 26 - 69 NM

## RECORDERS: TWO 12 BIT A & D

(ALL FPA DATA DIGITALLY RECORDED)

(ALL INS DATA DIGITALLY RECORDED)

56 MINUTES TOTAL DATA RECORDING TIME

## THREE VHS FLIGHT RECORDERS

COCKPIT VIDEO MONITOR (INCLUDES AUDIO)

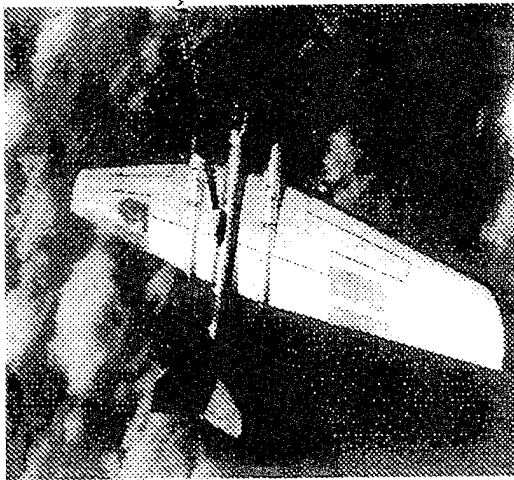
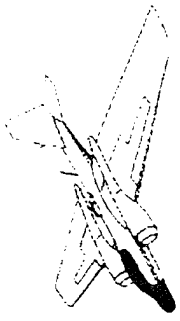
IR CAMERA

REAL TIME DISPLAY SYSTEM (RTDS)

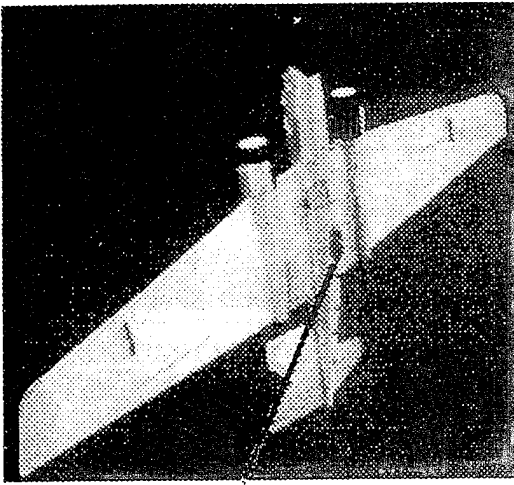


# PAYLOAD INSTALLATION

WB-57F

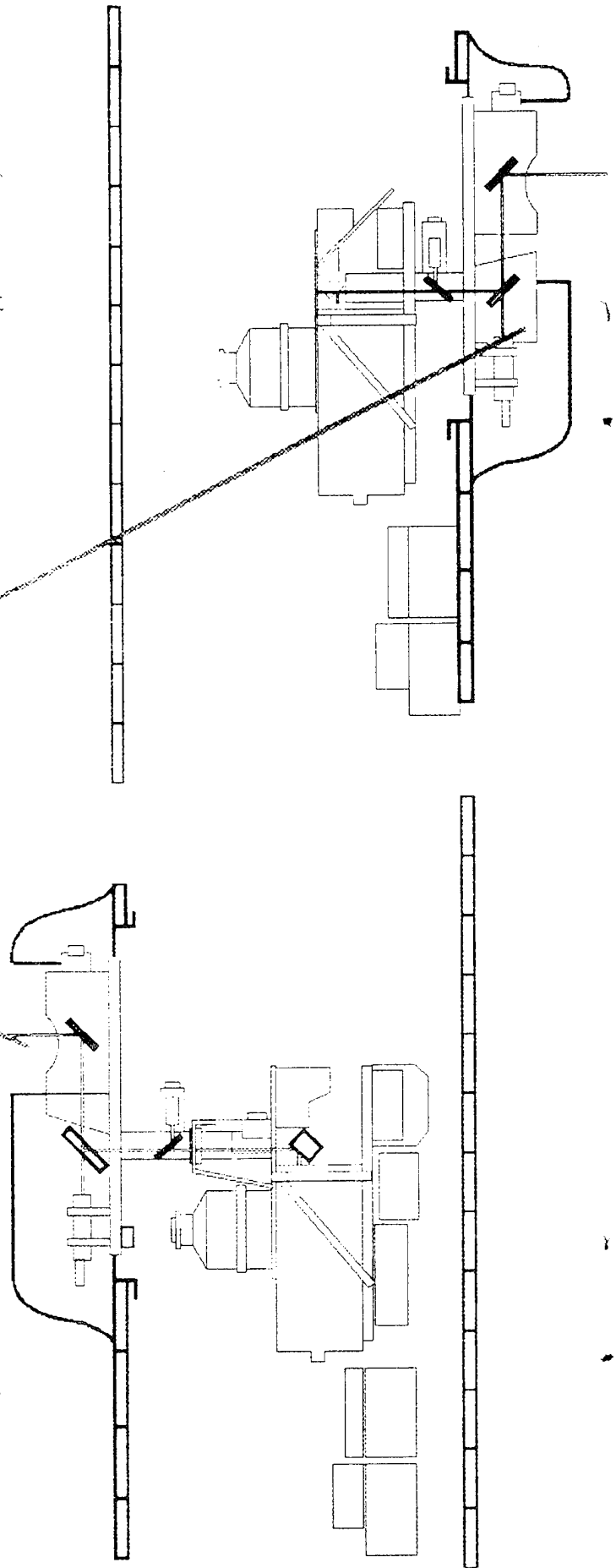


(Up-Look Configuration)



(Down Look Configuration)

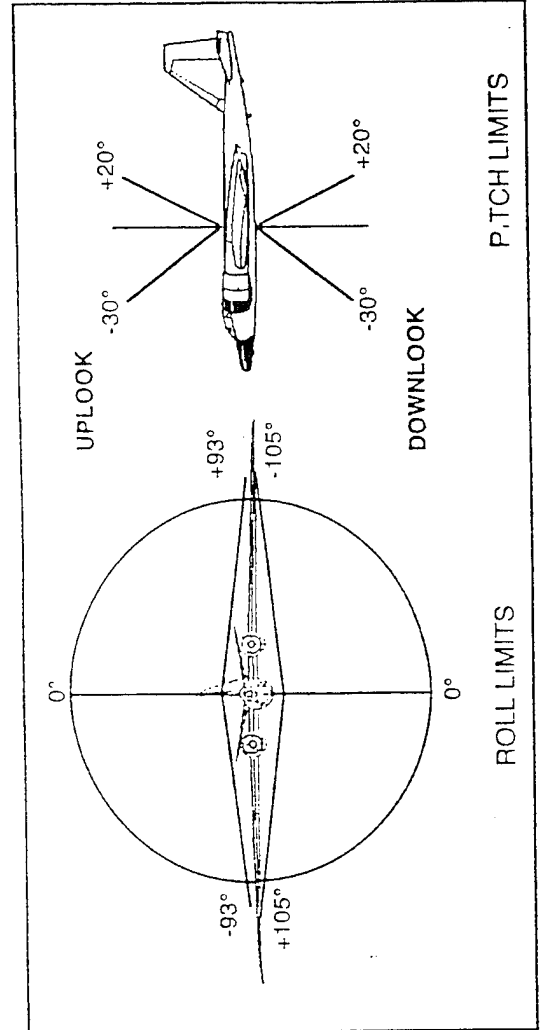
Telescope port





## Sensor Basic Capabilities - Continued -

- Total Spectral Bandwidth: 2.0 - 6.5 $\mu$ m (Optics Limited)
- Resolution
  - Spectral: 25 - 70nm
  - Spatial: 1.17mrad
  - Temporal: 10 - 80Hz
- Field-of-View: 53mrad Square, 53mrad x Scar/Sweep
- Field-of-Regard





## Sensor Basic Capabilities (Currently Available)

---

- Optics
  - 2.0" Aperture
  - Multi-Element 3.8" Focal Length Imager (F1.9)
  - Afocal Reflective Slit Spectrometer Telescope
  - 2 Element Ge-MgO Prism Assembly
  - Two 5 - Position Motor Driven Filter Wheels
  - Internal Optics Vacuum/Cryo-Cooled (77° K)
  - External Scanning Mirror System
  - External Pointing Mirror
  - On-Board Blackbody Cal Sources (3)
- Pointing and Tracking Capabilities
  - Accuracy: .25° - .5°
    - » Within 4x4 Pixels in Radiometer Mode; Total - 45x45 Pixels
  - Types of pointing: Computer, Manual
  - Types of tracking: Correlation, Edge, Centroid



## SENSOR BASIC CAPABILITIES

- Continued -

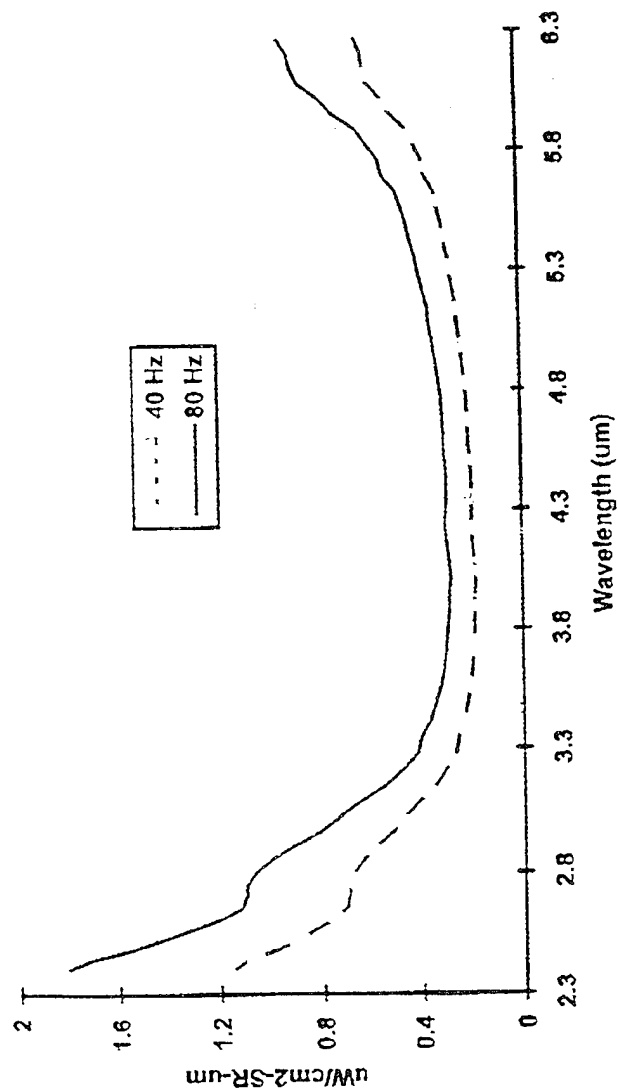
- Detector Characteristics
  - 45 x 90 Element 2-D Array
  - Si:In Photoconductive Detector Material
  - Hybrid w/ Si CCD Readout Structure
  - Spectral Range 2 - 7 $\mu$ m
  - Selectable 10 - 80Hz Integration Time
  - Vacuum/Cryo-Cooled to 24° K
  - 12-Bit A/D Conversion
  - Readout Noise: 1 Count out of 4096
  - 100 $\mu$ m Detector Pitch
- Dynamic Range
  - 12 Bit Digital (Selectable Dynamic Range Over 3 Orders of Magnitude Using IL Filter Wheel)
- Calibration Accuracy
  - <10% Absolute Traceable to NIST Standards
  - <2% Relative Spectrometric Accuracy Band-to-Band
  - <1% Relative Radiometric Accuracy  $\lambda/\lambda$  in a Spectral Band



## SENSOR BASIC CAPABILITIES

- Continued -

- Data handling
  - Recording: Digital
  - Reduction
  - Distribution/Archival: Archival Package @ LMSC
- Stereoscopic Imaging Capability
- Sensitivity





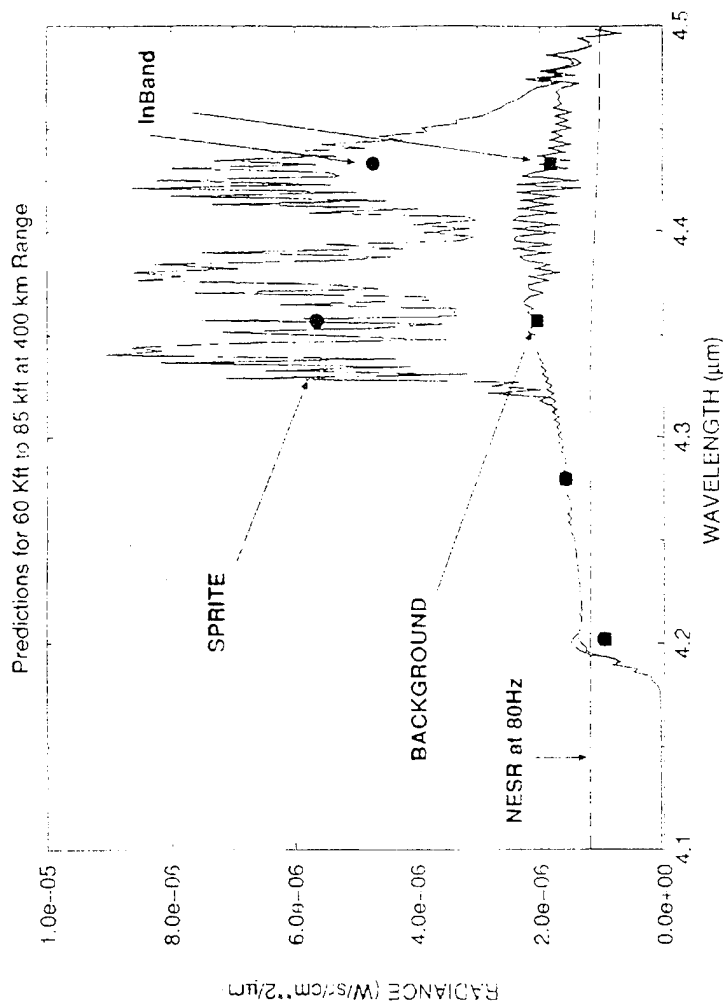
# SENSITIVITY OF ARES SPECTROMETER SUFFICIENT FOR SPRITE MEASUREMENTS

• PREDICTIONS PROVIDED BY L. JEONG, 10/13/95

• PREDICTIONS INTEGRATED INTO SAMPLE  
ARES SPECTRAL BANDS

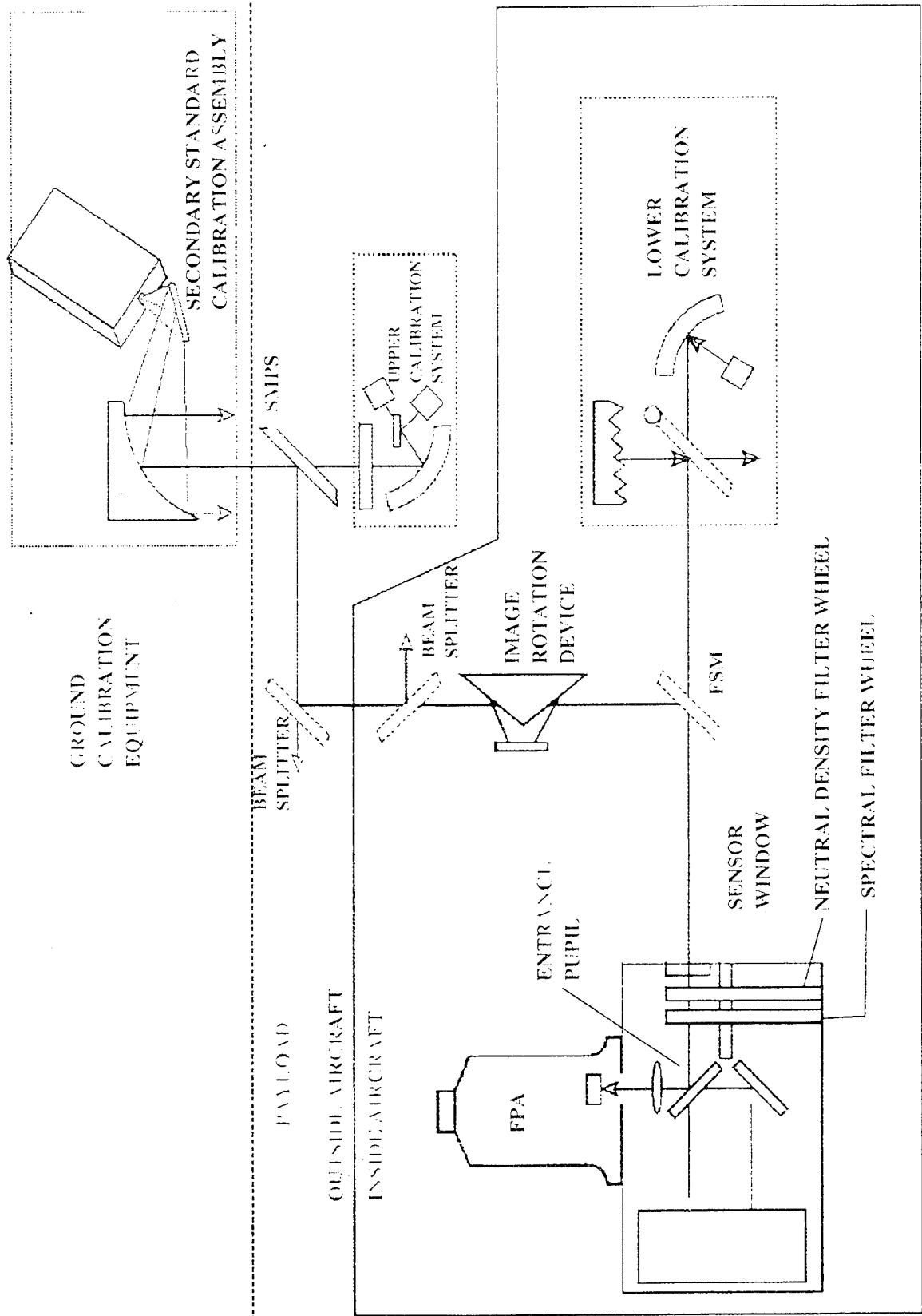
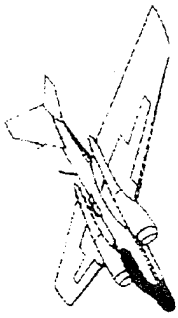
• NESR FROM PREVIOUS OPERATION AND  
SHOULD IMPROVE

• SPECTROMETER OPERATION AT 40, 20, OR  
10 Hz WILL IMPROVE NESR, DEPENDING ON  
SPRITE DURATION





# CALIBRATION SCHEMATIC





SPECTRAL FITTING OF MENDE'S SPRITE SPECTRUM

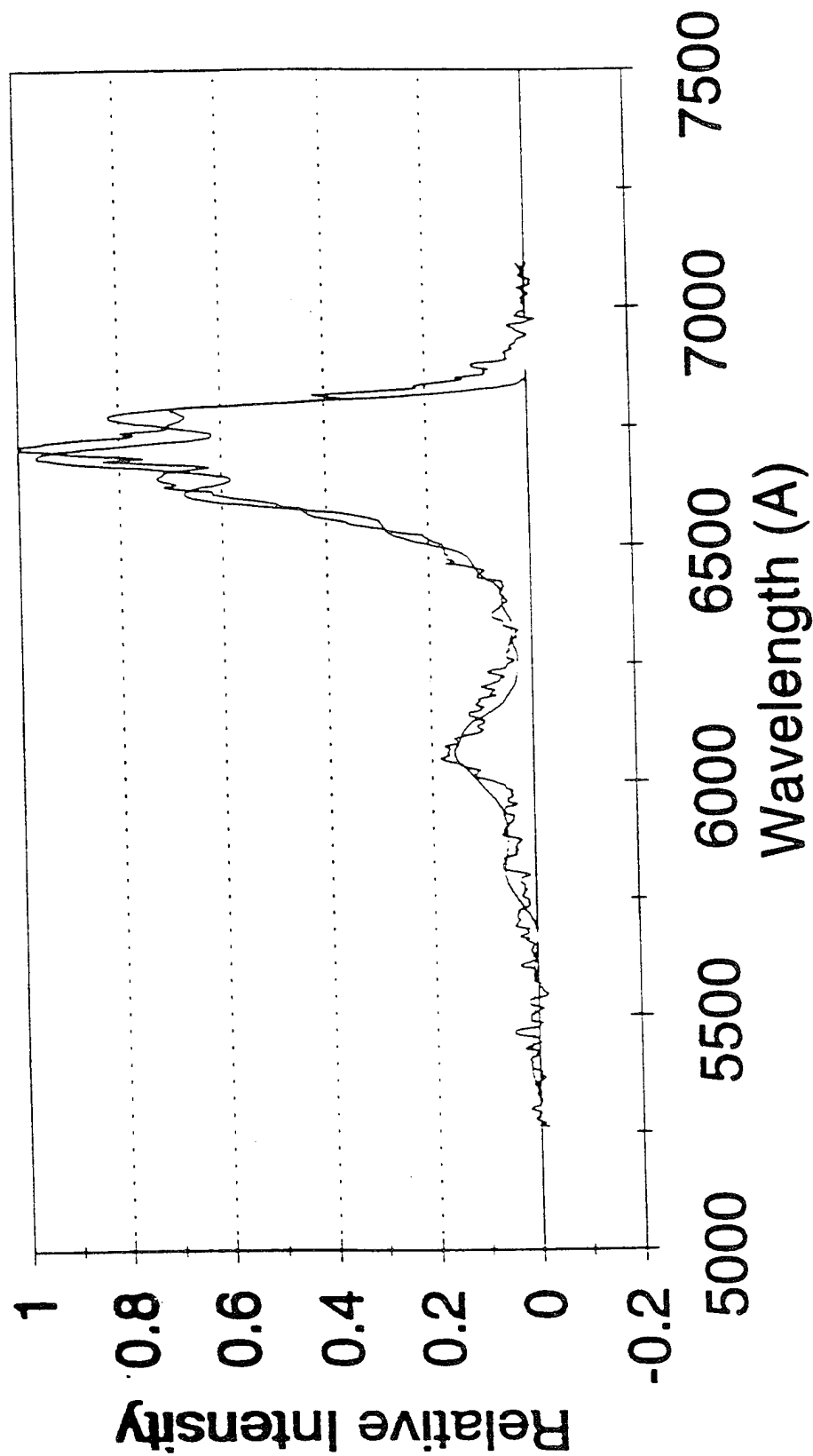
MARK FRASER, DAVID GREEN AND TERRY RAWLINS  
PHYSICAL SCIENCES INC.  
ANDOVER MA 01810

PH: 508-689-0003 FAX: 508-689-3232 EMAIL: green@psicorp.com

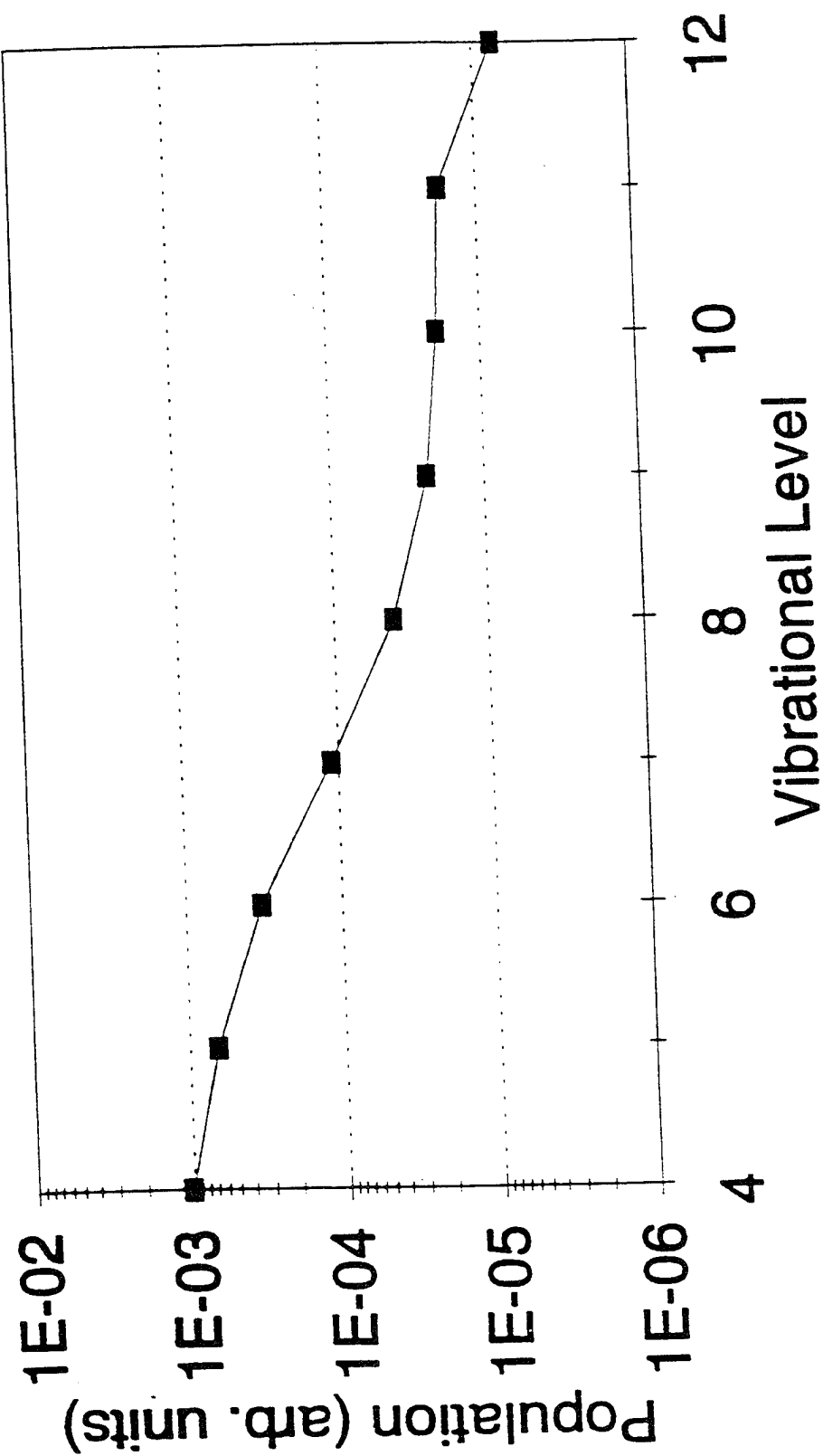
PRESENTED AT THE SPRITES WORKSHOP AT PL GEOPHYSICS  
19 OCTOBER 1995

# N21P Fit to Sprite Data

50A resol.,  $v=2-12$ ,  $\lambda < 7100 \text{ \AA}$

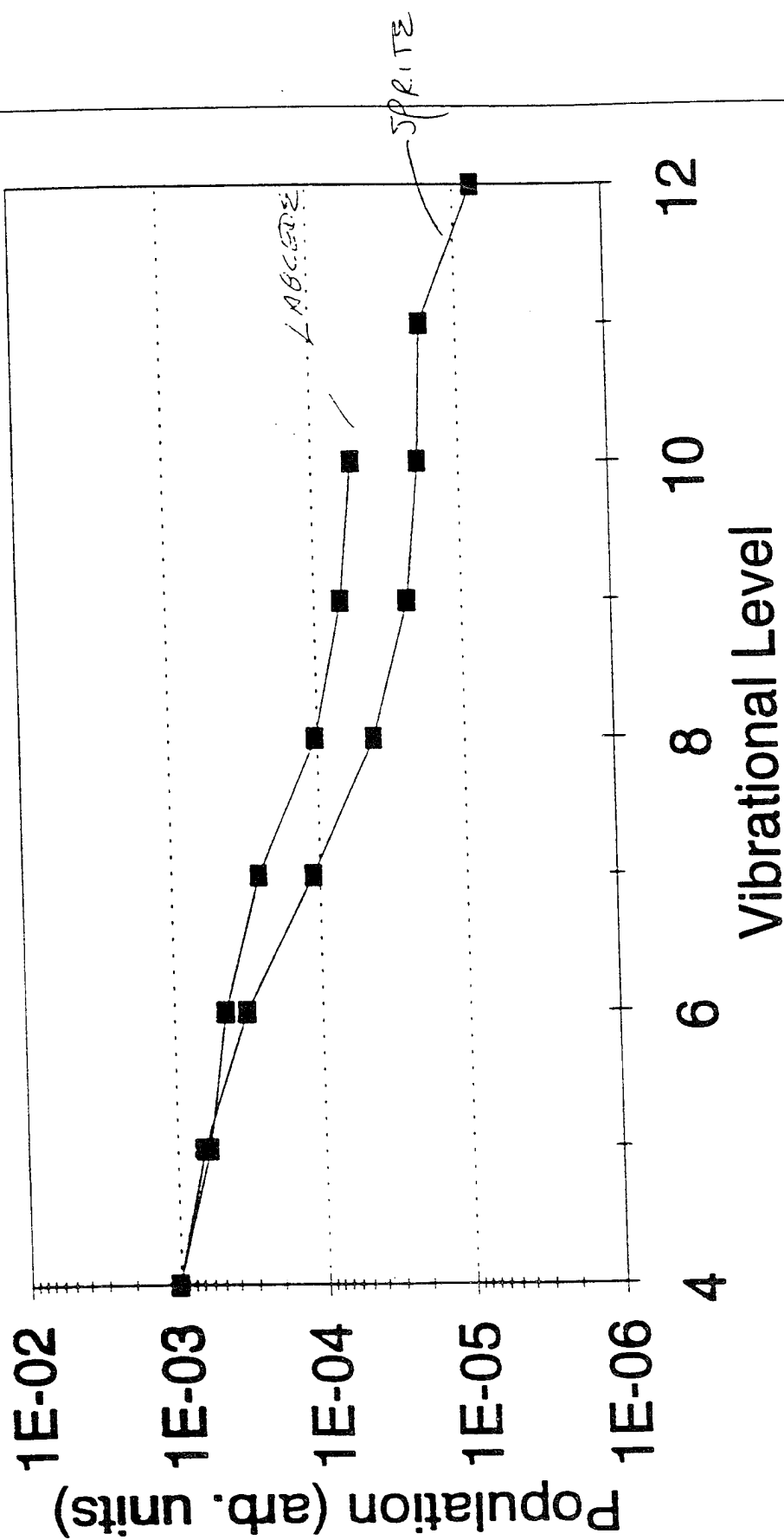


# N21P Vibrational Populations



# N21P Vibrational Populations

$v=4-10$  Labcede 68 km Data



# STATED CONCLUSIONS

- DATA NOT RESPONSE CORRECTED SO CONCLUSIONS VERY PRELIMINARY
- OBSERVE  $N_2$  B STATE LEVELS UP TO DISSOCIATION LIMIT
  - 15 eV ELECTRONS REQUIRED TO PRODUCE THESE STATES
  - ATOMS LIKELY FORMED
  - AT IONIZATION POTENTIAL, WITHIN FEW eV OF THRESHOLD
  - \* ATOMS AND IONS TURN ON CHEMISTRY
- RELATIVE BRIGHTNESS OF  $N_2^+$  1st NEGATIVE TO  $N_2$  1st POSITIVE PROVIDES INSIGHT INTO ELECTRON ENERGY DISTRIBUTION
- OBSERVED SPRITE DISTRIBUTION VIBRATIONALLY COLDER THAN THAT OBSERVED IN LAB keV ELECTRON IRRADIATED  $N_2$  AT PRESSURES CORRESPONDING TO 68km
- IF THIS CONCLUSIONS HOLDS UP IN RESPONSE CORRECTED DATA, IMPLIES EXCITATION ELECTRONS LESS ENERGETIC THAN AURORAL, LESS THAN 100 eV
- OPTICAL EMISSIONS CAN PROVIDE INSIGHT INTO MECHANISMS AND THRESHOLDS VIA ELECTRON ENERGY SPECTRUM

## Discussion of Major Research Issues and Experiments for Sprites '96 Campaign

- Altitude-dependent measurements of  $N_2^+(1N)/N_2(1P)$  ratio
- Gamma rays (local)
  - High-altitude balloons
- Horizontal Luminosity
  - Temporal/spatial structure (neutral)
  - Gravity wave coupling
  - Elf-Gravity wave
  - Discharge dynamics
  - Coupling to neutrals
- Atmospheric monitoring of jets
  - Optical/IR spectra
- High frame rate optical measurements (2000 frames/second)
  - Add multi-spectral
- High-speed photometers (<0.5 ms)
  - NIR (atomic, ion lines)
- Co-aligned photometer/spectrometer
- Low-light cameras
  - Blue sensitive
- UHF/VHF
  - Compare with TIPPS
- Causative lightning
  - Optical
  - RF
  - new NLDN sensors (waveforms)
- Additional optical stations
  - Triangulation
- VLF/ELF signals
  - GPS clock
  - Sync with "anomalous events"
- 20 km balloons
  - Electric fields/charge distributions

- Cosmic rays
- CO<sub>2</sub>/NO characterization
  - Ground-based
- VLF remote sensing
  - Ionization
- Mesoscale structure of lightning
- Radar
  - Temperature data
  - Scattering data
  - Other possible outputs
- IR signatures
  - ARES measurements
- Relativistic electrons
  - Important?
- Threshold
  - Why not more sprites?
- Relationship to +CG's
- Correlations with ELF
- Potential Locations/Dates
  - Last week June - Mid July
  - Midwest
  - Moon down (July 15 - new moon)
  - Local midnight
  - Coordinate with ARM, OK, and other sites
- Potential Aircraft/Balloon Platforms
  - FISTA
  - ARES (Petersen AFB, Tinker AFB)
  - NCAR (Jefferson County Airport)
  - NASA ER2
  - Balloons - LANL, OK
  - Sounding rockets
  - Drop sondes
- Potential Ground-Based Assets
  - NLDN
  - Chase vans
  - Electric field mills (MIT/LL)
  - Multiple sites ("long baseline") - NM, Univ. of Wyoming

**Groups Interested in  
Sprites, Blue Jets, and Elves**

Russ Armstrong  
Mission Research Corporation  
Atmospheric Sciences  
One Tara Boulevard  
Suite 302  
Nashua, NH 03062-2801  
Telephone: (603) 891-0070, Ext. 203  
Fax: (603) 891-0088  
Email: @lanl.gov:rarmstrong@mrcnh.com

Grant Aufderhaar  
Aerospace  
Telephone: (703) 318-5421.

Sunanda Basu  
National Science Foundation  
Division of Atmospheric Sciences  
4201 Wilson Boulevard  
Room 790  
Arlington, VA 22230  
Telephone: (703) 306-1529  
Fax: (703) 306-0849  
Email: sbasu@nsf.gov

William Beasley  
University of Oklahoma  
School of Meteorology  
Norman, OK 73019-0470  
Telephone: (405) 325-6561  
Fax: (405) 325-7689  
Email: wbeasley@uoknor.edu

Paul Bernhardt  
Naval Research Laboratory  
Beam Physics Branch  
MC 4780 1PB  
Washington, DC 20375-5320  
Telephone: (202) 767-0196  
Fax: (202) 767-0631  
Email: bern@ppd.nrl.navy.mil

Dennis Boccippio  
NASA Marshall Space Flight Center  
ES44  
Huntsville, AL 35812  
Telephone: (205) 922-5909  
Fax: (205) 922-5723  
Email: djboccip@cirrus.mit.edu

William Boeck  
Niagara University  
Department of Physics  
CIS  
Niagara, NY 14109  
Telephone: (716) 285-1212  
Fax: (716) 286-8254  
Email: boeck@niagara.edu

Bob Boldi  
MIT/Lincoln Laboratory  
Group 43  
S1-613 (L Lab)  
Lexington, MA 02173-9108  
Telephone: (617) 981-2293  
Email: bobb@ll.mit.edu

Eric Bucsela  
Naval Research Laboratory  
4555 Overlook SW  
Washington, DC 20375  
Telephone: (202) 767-6166  
Email: bucsela@uap.nrl.navy.mil

Lin Callis  
NASA Langley Research Center  
Atmospheric Sciences Division  
Hampton, VA 23681  
Telephone: (804) 864-5843  
Fax: (804) 864-6326  
Email: lbc@jaguar.larc.nasa.gov

Hugh Christian  
NASA Marshall Space Flight Center  
Global Hydrology and Climate Center  
977 Explorer Blvd.  
ES 43, Room B210  
Huntsville, AL 35806  
Telephone: (205) 922-5828  
Fax: (205) 922-5723  
Email: hugh.christian@msfc.nasa.gov



Michael Desch  
NASA Goddard Space Flight Center  
LEP  
Code 695  
Greenbelt, MD 20771  
Telephone: (301) 286-8222  
Fax: (301) 286-1683  
Email: ysmdd@lepmdd.gsfc.nasa.gov

Capt. David Desrocher  
National Test Facility  
730 Irwin Ave.  
NTF/WE  
Falcon AFB, CO 80912-7300  
Telephone: (719) 567-9450  
Fax: (719) 567-9464  
Email: ddesroch@inet.ntf1.af.mil

Eric Dors  
University of New Hampshire  
Space Science Center - 254 Morse Hall  
39 College Road  
Durham, NH 03824  
Telephone: (603) 862-3751  
Email: eric.dors@unh.edu

Frank Djuth  
GeoSpace Research Inc.  
550 North Continental Blvd.  
Suite 110  
El Segundo, CA 90245  
Telephone: (310) 322-1160  
Fax: (310) 322-2596

Ken Eack  
University of Oklahoma  
Department of Physics and Astronomy  
Norman, OK 73019  
Email: keack@uoknor.edu

Philip Erickson  
MIT Haystack Observatory  
Atmospheric Science Group  
Westford, MA 01886  
Telephone: (617) 981-5769  
Email: pje@hyperion.haystack.edu

Jim Ernstmeyer  
Massachusetts Institute of Technology & RL  
Department of Electrical Engineering  
Telephone: (617) 377-8977  
Email: imjay@mit.edu

Gerald Fishman  
NASA Marshall Space Flight Center  
Space Science Laboratory  
Code ES81  
Huntsville, AL 35812  
Telephone: (205) 544-7691  
Fax: (205) 544-5800  
Email: fishman@ssl.msfc.nasa.gov

John Foster  
MIT Haystack Observatory  
Atmospheric Sciences  
Route 40  
Westford, MA 01886  
Telephone: (617) 981-5621  
Email: jef@hyperion.haystack.edu

Marv Frandsen  
HQ AFTAC/TXC  
Advanced Systems Directorate  
1030 South Highway A1A  
Patrick AFB, FL 32925-3002  
Telephone: (407) 494-4178  
Fax: (407) 494-5501  
Email: frandsen@crusher.aftac.gov

Richard Goldberg  
NASA Goddard Space Flight Center  
Laboratory for Extraterrestrial Physics  
Code 690  
Greenbelt, MD 20771  
Telephone: (301) 286-8603  
Fax: (301) 286-1648  
Email: goldberg@nssdca.gsfc.nasa.gov

Steve Goodman  
NASA Marshall Space Flight Center  
Global Hydrology and Climate Center  
977 Explorer Blvd.  
ES-43, Room C11  
Huntsville, AL 35806  
Telephone: (205) 922-5891  
Fax: (205) 922-5723  
Email: steven.goodman@msfc.nasa.gov

Dave Green  
Physical Sciences Inc.  
20 New England Business Center  
Andover, MA 01810  
Telephone: (508) 689-0003  
Fax: (508) 689-3232  
Email: green@psicorp.com

John Ground  
Phillips Laboratory  
PL/SX  
3550 Aberdeen Ave. SE  
Kirtland AFB, NM 87117-5776  
Email: groundj@plk.af.mil

Leslie Hale  
Pennsylvania State University  
Communications and Space Sciences  
Laboratory  
316 Electrical Engineering East  
University Park, PA 16802-2707  
Telephone: (814) 865-2361  
Fax: (814) 863-8457  
Email: leshale@psu.edu

Bob Harris  
NASA Headquarters  
Code YS  
300 E Street S.W.  
Washington, DC 20546-0001

Al Hurd  
Visidyne Inc.  
10 Corporate Place  
South Bedford St.  
Burlington, MA 01803  
Telephone: (617) 273-2820

Dan Holden  
Los Alamos National Laboratory  
Mail Stop D466  
Los Alamos, NM 87545  
Telephone: (505) 667-3406  
Fax: (505) 665-7395  
Email: dh@transio.lanl.gov

Rick Howard  
NASA Headquarters  
Space Physics  
300 E Street S.W.  
Code SS  
Washington, DC 20546-0001  
Telephone: (202) 358-0898  
Fax: (202) 358-3987  
Email: rhoward@hq.nasa.gov

Robert Huffman  
Phillips Laboratory  
GP Representative at PL/KAFB  
29 Randolph Road  
PL/GPI  
Hanscom AFB, MA 01731-3010  
Telephone: (505) 846-0298  
Fax: (505) 846-2282  
Email: huffman@plk.af.mil

Umrans Inan  
Stanford University  
Department of Electrical Engineering  
STAR Laboratory  
Durand 321, MC-4055  
Stanford, CA 94305  
Telephone: (415) 723-4994  
Fax: (415) 723-9251  
Email: inan@nova.stanford.edu

Laila Jeong  
Phillips Laboratory  
Optical Environment Division  
29 Randolph Road  
PL/GPOS  
Hanscom AFB, MA 01731-3010  
Telephone: (617) 377-3671  
Fax: (617) 377-8900  
Email: jeong@plh.af.mil

Dikshitulu Kalluri  
Univ. of MA at Lowell  
Electrical Engineering Department  
1 University Avenue  
Lowell, MA 01856  
Telephone: (508) 934-3318  
Fax: (508) 934-3027  
Email: kallurid@woods.uml.edu

Craig Kletzing  
University of New Hampshire  
Space Science Center - Morse Hall  
39 College Road  
Durham, NH 03824  
Telephone: (603) 862-3187  
Fax: (603) 862-1915  
Email: kletzing@unhedi2.unh.edu

Maj James Kroll  
Air Force Office of Scientific Research  
110 Duncan Avenue  
Bolling AFB, DC 20332-0001  
Telephone: (202) 767-7900  
Fax: (202) 404-7496  
Email: kroll@afosr.af.mil

Peter Kupferman  
Aerospace Corp.  
Hallmark Bldg.  
13873 Park Ct Rd.  
Herndon, VA 22071  
Telephone: (703) 318-1659  
Fax: (703) 318-5409  
Email: peter.n.kupferman@aero.org

Min-Chang Lee  
Massachusetts Institute of Technology  
Plasma Fusion Center (NW 16-240)  
167 Albany Street  
Cambridge, MA 02139  
Telephone: (617) 253-5956  
Fax: (617) 253-0448  
Email: mclee@pfc.mit.edu

Carl Lennon  
NASA JFK Space Center  
TE-CID-3  
Kennedy Space Center, FL 32899  
Telephone: (407) 867-4042  
Fax: (407) 867-2848

Walter Lyons  
ASTER Division/Mission Research  
Corporation  
Yucca Ridge Field Station  
46050 Weld County Road 13  
Ft Collins, CO 80524  
Telephone: (970) 568-7664  
Fax: (303) 482-8627  
Email: lyonsccm@csn.org

Sam Makhoul  
Utah State University  
Stewart Radiance Laboratory  
139 Great Road  
Bedford, MA 01730  
Telephone: (617) 377-4903  
Email: makhoul@pldac.plh.af.mil

Lee Marshall  
Penn State  
Electrical Engineering  
332 EE East  
State College, PA 16802  
Telephone: (814) 865-2361  
Email: lhm100@psu.edu

Stephen Mende  
Lockheed Martin Palo Alto Research  
Laboratory  
Dept. 91 20 Bldg. 255  
3251 Hanover St.  
Palo Alto, CA 94304  
Telephone: (415) 424-3282  
Fax: (415) 424-3333  
Email: mende@sag.space.lockheed.com

Gennady Milikh  
University of Maryland  
Department of Physics and Astronomy  
College Park, MD 20850  
Telephone: (301) 405-1558  
Fax: (301) 405-9966  
Email: milikh@avl.umd.edu

John Molitoris  
Lawrence Livermore National Laboratory  
Regional Atmospheric Sciences Division  
700 East Ave.  
P.O. Box 808, L-262  
Livermore, CA 94551-9900  
Telephone: (510) 423-3496  
Fax: (510) 422-5844  
Email: molitoris1@llnl.gov

Jeff Morrill  
Naval Research Laboratory  
4555 Overlook SW  
Code 760  
Washington, DC 20375-5352  
Telephone: (202) 404-7826  
Fax: (202) 767-5636

Dean Morss  
Creighton University  
Department of Atmospheric Sciences  
Omaha, NE 68178-0114  
Telephone: (402) 280-5759  
Fax: (402) 280-1731  
Email: damorss@creighton.edu

K. Papadopoulos  
University of Maryland  
Department of Physics and Astronomy  
College Park, MD 20742  
Telephone: (301) 454-6810  
Fax: (301) 314-9067  
Email: kp@astro.umd.edu

Larry Radke  
NCAR  
P.O. Box 3000  
Boulder, CO 80397-3000  
Telephone: (303) 497-1032  
Fax: (303) 497-1092  
Email: radke@atd.ucar.edu

Terry Rawlins  
Physical Sciences Inc.  
20 New England Business Center  
Andover, MA 01810  
Telephone: (508) 689-0003  
Fax: (508) 689-3232  
Email: rawlins@psicorp.com

Jean Reazer  
NAIC/DXDR  
4115 Hebble Creek Rd.  
Suite 6  
Wright Patterson ARB, OH 45433-5610  
Telephone: (513) 257-0992  
Fax: (513) 257-9888

Bill Roder  
45th Weather Sq  
1201 Minuteman St.  
Patrick AFB, FL 32925-3238

Robert Roussel-Dupre  
Los Alamos National Laboratory  
Space and Atmospheric Sciences Group  
NIS-1, Mail Stop D466  
Los Alamos, NM 87545  
Telephone: (505) 667-9228  
Email: rroussel-dupre@lanl.gov

Harvey Rowland  
Naval Research Laboratory  
Plasma Physics  
4555 Overlook SW  
Washington, DC 20375  
Telephone: (202) 767-6644  
Email: rowland@ppd.nrl.navy.mil

David Rust  
National Severe Storms Lab  
1313 Halley Circle  
Norman, OK 73069  
Telephone: (405) 366-0404  
Fax: (405) 366-0472  
Email: rust@nssl.uoknor.edu

Phil Schwartz  
Naval Research Laboratory  
4555 Overlook SW  
Washington, DC 20375

Davis Sentman  
University of Alaska  
Geophysical Institute  
903 Koyukuk Drive  
P.O. Box 757320  
Fairbanks, AK 99775-7320  
Telephone: (907) 474-6442  
Fax: (907) 474-7290  
Email: rocket@geewiz.gi.alaska.edu

Orr Sheperd  
Visidyne Inc.  
10 Corporate Place  
South Bedford St.  
Burlington, MA 01803  
Telephone: (617) 273-2820  
Fax: (617) 272-1068  
Email: sheperd@bur.visidyne.com

Jeff Shorter  
Mission Research Corporation  
One Tara Boulevard  
Nashua, NH 03062  
Telephone: (603) 891-0070  
Fax: (603) 891-0088

Carl Sieftring  
Naval Research Laboratory  
Plasma Physics Division  
4555 Overlook SW  
Space Experiments Section/Code 6755  
Washington, DC 20375  
Telephone: (202) 767-2467  
Fax: (202) 404-7082  
Email: sieftring@nrlfs1.nrl.navy.mil

Tom Slanger  
SRI International  
333 Ravenswood Avenue  
Menlo Park, CA 94025-3493  
Telephone: (415) 859-2764  
Fax: (415) 859-6196  
Email: slanger@mplvax.com

Cdr Steve Smolinski  
Naval Research Laboratory  
4555 Overlook SW  
Washington, DC 20375  
Email: smolinsk@sgate.com

Dick Spalding  
Sandia Laboratory  
ORG 5909  
MS 0978  
Albuquerque, NM 87185  
Telephone: (505) 844-5934  
Fax: (505) 844-2057  
Email: respald@sandia.gov

Eugene Symbalist  
Los Alamos National Laboratory  
NIS-1  
Los Alamos, NM 87545  
Telephone: (505) 667-9670  
Fax: (505) 665-7398  
Email: esymalisty@lanl.gov

Yuri Taranenko  
Los Alamos National Laboratory  
Space and Atmospheric Sciences Group  
MS D466  
Los Alamos, NM 87545  
Fax: (505) 665-3332  
Email: ytaranenko@lanl.gov

Micheal Taylor  
Utah State University  
Science Division  
Space Dynamics Laboratory  
Engineering Building, Room 241  
Logan, UT 84322-4145  
Telephone: (801) 797-3919  
Fax: (801) 797-4044  
Email: taylor@psi.sci.sdl.usu.edu

Barry Tilton  
SAFSP/RESPO  
11782 Lee-Jackson Hwy  
Oakwood Center, Suite 500  
Fairfax, VA 22033  
Telephone: Pager: (800) 759-8255 (PIN:  
2832955)

Roland Tsunoda  
SRI International  
Geoscience and Engineering Center  
333 Ravenswood Avenue  
Menlo Park, CA 94025-3493  
Telephone: (415) 859-3124  
Fax: (415) 322-2318  
Email: tsunoda@unix.sri.com

James Ulwick  
Stewart Radiance Laboratory  
Utah State University  
139 Great Road  
Bedford, MA 01730  
Telephone: (617) 275-8273  
Fax: (617) 271-0535  
Email: ulwick@plh.af.mil

Otha Vaughan, Jr.  
NASA Marshall Space Flight Center  
Global Hydology & Climate Center  
977 Explorer Blvd.  
ES-44  
Huntsville, AL 35812  
Telephone: (205) 922-5893  
Fax: (205) 922-5723  
Email: skeet@sferic.msfc.nasa.gov

Susan Voss  
Los Alamos National Laboratory  
NIS-1 Space and Atmospheric Science  
MS D466  
Los Alamos, NM 87545  
Telephone: (505) 665-5520  
Fax: (505) 665-7395  
Email: svoss@lanl.gov

Mark Weber  
MIT/Lincoln Laboratory  
244 Wood Street  
Lexington, MA 02173-9108  
Telephone: (617) 981-7434  
Fax: (617) 981-0632

Jeff West  
Phillips Laboratory  
PL/SX  
3550 Aberdeen Ave. SE  
Kirtland AFB, NM 87117-5776  
Telephone: (505) 846-1411  
Fax: (505) 846-4143

Gene Wescott  
University of Alaska  
Geophysical Institute  
903 Koyukuk Drive  
P.O. Box 757320  
Fairbanks, AK 99709  
Telephone: (907) 474-7576  
Fax: (907) 474-7290  
Email: rocket@giuaf.gi.alaska.edu

Earl Williams  
Massachusetts Institute of Technology  
Parsons Lab  
77 Massachusetts Ave.  
MIT 48-211  
Cambridge, MA 02139-4307  
Telephone: (617) 253-2459  
Fax: (617) 253-6208  
Email: earlew@ll.mit.edu

Jack Winckler  
University of Minnesota  
School of Physics and Astronomy  
Minneapolis, MN  
Telephone: (612) 624-5086  
Fax: (612) 624-4578

Peter Wintersteiner  
ARCON Corp.  
260 Bear Hill Rd.  
Waltham, MA 02154  
Fax: (617) 890-5189  
Email: winters@arcon.com

Charles Wong  
Massachusetts Institute of Technology  
77 Massachusetts Ave.  
Cambridge, MA 02139-4307